INSTITUT POLYTECHNIQUE DE PARIS

NNT :

Thèse de doctorat

ÉCOLE POLYTECHNIQUE

IP PARIS

Large macroeconomic fluctuations

Self-organized criticality in firm networks, agent-based models and random matrices

Thèse de doctorat de l'Institut Polytechnique de Paris
préparée à l'Ecole Polytechnique

École doctorale n°626 École doctorale de l'Institut Polytechnique de Paris (EDIPP)
Spécialité de doctorat : Physique

Thèse présentée et soutenue à Paris, le 12 Octobre 2022, par

THÉO DESSERTAINE

Composition du Jury :

Herbert Dawid Universität Bielefeld	Rapporteur
Francesco Zamponi ENS Ulm	Rapporteur
Isabelle Mejean Science Po Paris	Examinatrice
Grégory Schehr Sorbonne Université	Examinateur
Jean-Pierre Nadal EHESS	Examinateur
Michael Benzaquen Ecole polytechnique	Directeur de thèse
Jean-Philippe Bouchaud Capital Fund Management	Co-directeur de thèse
Alan Kirman EHESS	Invité

À Albane

Remerciements

J'aimerais commencer par remercier mes directeurs de thèse, Michaël Benzaquen et Jean-Philippe Bouchaud, de m'avoir accompagné tout au long de ces trois années de doctorat. Tout au long de la thèse, ils ont toujours été disponibles pour m'orienter et me suivre dans mes différents projets, tout en me conférant le juste degré d'autonomie dès mon arrivée en stage. Je leur suis reconnaissant de m'avoir prodigué leur soutien sans faille pour tous les aspects de ma thèse, c'est une réelle chance d'avoir pu être leur étudiant. Cela a été pour moi un plaisir de discuter et d'interagir avec eux au grè de nos réunions (et en dehors) tant leur expertise est vaste.

J'aimerais en particulier remercier Michaël de m'avoir fait confiance en me donnant l'opportunité d'être chargé des travaux dirigés pour deux de ses cours. L'enseignement a été pour moi une expérience particulièrement enrichissante et appréciable.

Je souhaiterais exprimer ma plus grande gratitude envers José Moran qui m'a pris sous son aile lors de mes débuts en stage. Son expertise dans un si grand nombre de domaines a toujours été pour moi une source d'admiration, et je suis très heureux d'avoir pu collaborer avec lui.

J'adresserai aussi mes remerciements aux différents membres de mon jury de doctorat Alan Kirman, Isabelle Méjean, Grégory Schehr, Jean-Pierre Nadal, Herbert Dawid et Francesco Zamponi. J'aimerais en particulier remercier Francesco Zamponi et Herbert Dawid pour avoir accepté d'être rapporteurs de ma thèse.

J'ai aussi eu la chance de pouvoir faire partie de la chaire d'Econophysique et Systèmes Complexes dès ses débuts. Un grand merci à tous les membres de l'équipe Antoine, José, Medhi, Pierre, Federico, Cécilia, Jérome, Samy, Salma, Elia, Gianluca, Swann.

Je tenais à adresser en particulier mes remerciements aux personnes avec qui j'ai pu collaborer sur des projets publiés ou non Johannes, Camille, Prachi, Elia, ainsi que Claude Godrèche.

Un grand merci aux relecteurs de ce manuscrit qui m'ont été d'une aide précieuse Jean-Philippe, Michaël, Jérôme, Cécilia, Albane ainsi que ma mère.

Un immense merci à ma mère qui a toujours su trouver les mots justes dans les moments où la motivation venait à me manquer. Elle n'a cessé, dès mon plus jeune âge, de nourrir ma curiosité et m'encourager dans mes études.

Finalement, j'aimerais remercier Albane, à qui je dédie ce manuscrit. Elle a été à mes côtés depuis le premier jour de cette thèse et m'a soutenu tout au long de cette aventure de trois ans. Ses encouragements ont été une vraie source de motivation, sans laquelle ces trois années seraient probablement passées plus lentement.

Résumé

Quelle est l'origine des fluctuations macroéconomiques ? À la fin du xxe siècle, Ben Bernanke introduisait pour la première fois ce qu'il appela le puzzle des "small shocks, large business cycles" faisant référence à l'apparente incompatibilité entre les petites fluctuations observées au niveau granulaire de l'économie ("small shocks") et les larges fluctuations macroéconomiques ("large business cycles"). Par exemple, le PIB des États-Unis montre un taux moyen de croissance annuelle stable autour de 3% mais présente des fluctuations atteignant 2.7%. L'énigme réside dans le fait que la plupart de cette volatilité en excès ne peut être liée à des crises *exogènes* connues, comme les chocs pétroliers ou la crise financière de 2008, et doit donc être d'origine *endogène*, c'est-à-dire générée par l'économie elle-même. De nombreuses explications ont vu le jour, les plus connues impliquant la distribution en loi de puissance des tailles d'entreprises qui se répercuterait au niveau agrégé de l'économie, ou bien des effets de réseaux responsables de l'amplification des chocs microscopiques. En revanche, ces explications reposent sur des modèles économiques à l'équilibre représentant le monde comme une succession d'états équilibrés atteints instantanément et sans frictions, et qui, tautologiquement, ne prennent pas en compte les effets hors équilibres. Dans cette thèse, les deux premières parties sont consacrées à la recherche de mécanismes hors équilibres pouvant expliquer la volatilité en excès. La troisième partie est dédiée à l'étude plus générale des systèmes linéaires par cônes, omniprésents en économie.

Nous commençons par montrer que l'équilibre au sens économique n'existe pas toujours dans les réseaux d'entreprises. Cela a plusieurs conséquences. Premièrement, comme l'équilibre n'est pas toujours bien défini, les modèles économiques devraient être principalement conçus *hors-equilibre*. Deuxièmement, proposant un modèle dynamique minimal et comportemental pour l'ajustement des prix et productions dans un contexte d'interactions inter-entreprises, nous montrons que l'économie subit un *ralentissement critique* au voisinage du point de non-existence de l'équilibre caractérisé par une divergence du temps de relaxation et une accumulation des chocs dans le réseau générant naturellement de la volatilité en excès. Troisièmement, nous argumentons, dans le même esprit que Bak et al., que les économies actuelles sont proches du point de non-existence de l'équilibre à cause du phénomène dit de *criticalité auto-organisée*.

Dans la deuxième partie, nous nous éloignons du modèle minimal et proposons un modèle basé agents pleinement cohérent prenant en considération des éléments économiques plus réalistes. Nous montrons que la multitude de boucles de rétroactions, engendrées par les interactions entre entreprises, génère des oscillations endogènes pour des valeurs économiquement cohérentes des paramètres gouvernant le modèle, donnant alors une autre piste pour expliquer la volatilité en excès. En outre, une étude analytique du modèle révèle que la dynamique reste non triviale au niveau linéaire : la dépendance linéaire des entrées et sorties économiques peut elle-même varier en fonction de la forme des entrées. Ces systèmes, appelés linéaires par cônes, génèrent aisément, même dans les cas les plus simples, des paternes de crises ainsi que des oscillations et sont omniprésents en économie.

Cela mène naturellement à la dernière partie de cette thèse où nous nous intéressons aux propriétés de stabilité de ces systèmes dans un contexte plus général de matrices aléatoires. Nous montrons que les systèmes linéaires par cônes peuvent exhiber des propriétés hautement non triviales comme l'absence de concentration de la mesure de l'exposant de Lyapunov maximum qui gouverne la stabilité du système.

Abstract

What is the origin of macroeconomic fluctuations? In the late XXth century, Ben Bernanke first introduced the so-called "small shocks, large business cycles" puzzle as the seeming incompatibility between small fluctuations observed at granular levels of the economy (small shocks) and large macroeconomic fluctuations (large business cycles). As an example, the Unites States' GDP displays a steady average yearly growth rate of around 3% but with fluctuations reaching 2.7%. The conundrum is that most of this volatility cannot be linked to known *exogeneous* crises, such as oil shocks or the 2008 financial crisis, and must therefore be of *endogeneous* origin, i.e. generated by the economy itself. Numerous explanations have been proposed, the most famous of which involve the power-law distribution of firms' sizes, rippling out at aggregate levels of the economy, or network effects responsible for amplifying micro-level shocks. However, these explanations rely on equilibrium-only economic models which picture the world as a succession of equilibria instantaneously reached without friction, and which tautologically do not account for out-of-equilibrium effects. In this thesis, the first two parts are devoted to finding mechanisms accounting for the excess volatility through those overlooked out-of-equilibrium effects. The third part is dedicated to studying more general properties of so-called conewise linear systems, which are ubiquitous in economics.

We start by showing that, in firm networks, economic equilibrium does not always exist. This has several consequences. First, since equilibrium can be ill-defined, economic models should be chiefly devised *out-of-equilibrium*. Second, upon proposing a minimal behavioral dynamical model of prices and productions' adjustment with inter-firms interactions, we show that at the onset of equilibrium non-existence, the economy experiences a *critical slow-down* where the relaxation time diverges and shocks start accumulating in the network, naturally generating excess volatility. Third, in the same spirit as Bak et al., we argue that economies generically sit close to the non-existence point through a phenomenon called *self-organized criticality*.

In the second part, we depart from the first minimal model and devise a fully consistent Agent-Based Model by factoring in some more realistic economic features. We show that, because of the multiple feedbacks stemming from the interactions between firms, our model is able to generate sustained endogenous business cycles for economically sound values of the parameters governing the model, giving yet another avenue for explaining excess volatility at aggregate levels. Furthemore, an analytical study of the model reveals a non-trivial dynamics even at linear level: the linear dependency between economic inputs and outputs can vary depending on the inputs themselves. Such systems, called conewise linear, can easily generate crises-like patterns and oscillations even in the simplest cases and naturally come to play in economics.

This naturally leads to the last part of this thesis, where we investigate more general stability properties of conewise linear systems in a random matrix theory setting. We show that such system can exhibit highly non-trivial properties, such as the non-self-averaging of the maximal Lyapunov exponent governing the system's stability.

List of papers and scientific contributions presented in this thesis

[1] Théo Dessertaine, José Moran, Michael Benzaquen, and Jean-Philippe Bouchaud. *Out-of-equilibrium dynamics and excess volatility in firm networks*. Journal of Economic Dynamics and Control, 138:104362, 2022.

[2] Théo Dessertaine and Jean-Philippe Bouchaud. *Non-self-averaging Lyapunov exponent in random conewise linear systems*. Phys. Rev. E, 105:L052104, May 2022.

[3] Théo Dessertaine, Claude Godrèche, and Jean-Philippe Bouchaud. *Occupation time of a renewal process coupled to a discrete Markov chain*. Journal of Statistical Mechanics: Theory and Experiment, 2022(6):063204, jun 2022.

[4] Théo Dessertaine and Jean-Philippe Bouchaud. *Explicit computation of mixed-moments of real Gaussian elliptic random matrices*. In preparation.

[5] Théo Dessertaine. Network agent based model web application. `https://yakari.polytechnique.fr/dash`

Table of contents

Table of contents **vii**

Introduction **1**
1 Small shocks, large business cycles: a macroeconomic conundrum 1
2 Main proposition and outline of the manuscript 3

Part I Critical network-economies **15**

I Equilibrium network-economies **19**
1 Firm networks, production functions and household 19
2 Competitive equilibrium 24
3 Positive equilibrium and Hawkins-Simons condition 28
4 Self-organized criticality in firm networks 32
5 Conclusion 33
Appendices 35

II Weakly out-of-equilibrium economies **41**
1 Reduced-form differential equations: the Goodwin model 41
2 Adjustment processes through behavioral rules of thumb 43
3 Dynamical system for Leontief economies 45
4 Linear study and marginal stability at the onset of feasibility 50
5 Excess volatility 57
6 Conclusion 59
Appendices 63

III Dynamical mean-field theory: the proverbial firm **75**
1 Dynamical mean-field theory 75
2 Mean-field Hawkins-Simons transition 78
3 DMFT for firm networks 81
4 Conclusion 86
Appendices 87

Part II Macroeconomic agent based modelling **99**

IV A simplified approach **103**
1 A causal mass-conserving economy . . . 103
2 Short numerical survey . . . 109
3 Conewise dynamics and geometric study . . . 112
4 Conclusion . . . 124
Appendices . . . 128

V Out-of-equilibrium dynamics and excess volatility in firm networks **133**
1 A fully consistent approach . . . 133
2 A numerical study . . . 141
3 Real world networks . . . 161
4 Conclusion . . . 162
Appendices . . . 166

VI Summary, discussion and extensions **185**
1 Summary and discussion . . . 185
2 Extensions . . . 191

Part III Complex interactions and random matrices **197**

VII Random conewise linear systems **201**
1 Introduction . . . 201
2 Persistence and intra-cone behavior . . . 203
3 Switch process and distribution of the maximal Lyapunov exponent . . . 206
4 Finite N effects . . . 209
5 Conclusion and extensions . . . 210
Appendices . . . 213

VIII Renewal processes and Markov chains **229**
1 Introduction . . . 229
2 Renewal processes: a brief reminder . . . 233
3 Distribution of the sum S_t when $\alpha_1, \alpha_2, \ldots$ are IID random variables . . . 234
4 Distribution of the sum S_t for a Markov renewal process . . . 238
5 Moments . . . 242
6 Discussion . . . 246
Appendices . . . 248

IX Mixed-moments of Gaussian elliptic matrices **253**
1 Introduction . . . 253
2 Gaussian elliptic matrices . . . 254
3 General formula for the mixed-moments . . . 255
4 Explicit formula for $\tau\left(\mathbb{X}^t(\mathbb{X}^\top)^s\right)$ . . . 256

5 Asymptotics of $\tau\left(\mathbb{X}^t(\mathbb{X}^\top)^s\right)$ as $t, s \to \infty$ 262
6 Conclusion 265
Appendices 267

Conclusion **271**

Bibliography **273**

Introduction

1 Small shocks, large business cycles: a macroeconomic conundrum

One of the most empirically well-identified stylized fact of economic time-series is the persistence of large deviations from economic trends at the aggregate levels of large economies. For instance, take the Gross Domestic Product (GDP) of the United States, whose rolling yearly growth rate is represented on Figure 1 starting in 1948. On average, the United States' GDP has grown by 3.13% each year, but one observes very large fluctuations around the average growth. Some of these fluctuations can be linked to known crises such as the 2008 financial crisis or the Covid-19 pandemic, that has been hitting the globe since 2020 and whose consequences are still unraveling. However, long periods of times seemingly unaffected by known crises still display wild fluctuations, which, all things considered, result in a standard deviation of the yearly growth rate around 2.7%, i.e. of the same order of magnitude as the average.

Understanding the origin of these large fluctuations has puzzled economists for a long time. The first attempt at understanding their origin dates back to the XIXth century. As large crises account for some of the volatility of the United States' economy, one could naively try to explain the remaining fluctuations by searching for *hidden* crises or events. Jevons proposed in 1875 his "sunspot theory" [7], linking weather fluctuations and solar activity to the seasonal variations of the price of corn. Even though more than a century old, his explanation is still very prominent nowadays: fluctuations are thought to be chiefly driven by *exogenous events*, i.e. events hitting economies from the outside, some of which are clearly visible (the Covid-19 pandemic for instance), and some others are not (the solar activity of Jevons).

The idea that economic fluctuations are mainly driven by exogenous events is deeply intertwined with the idea of economic equilibrium. Textbook macroeconomic models picture the world as a succession of equilibria where markets clear perfectly and firms maximize their profits. Each equilibrium is characterized by a different level of productivity or household preferences, themselves driven by exogenous shocks, which are the primary cause of fluctuations. Drawing an analogy from physics, one may call such an approach "adiabatic", in the sense that the time needed for the system to reach equilibrium is much shorter than the time over which the environment changes, so *out-of-equilibrium* effects can be neglected. The time evolution of the economy is then slaved to the time evolution

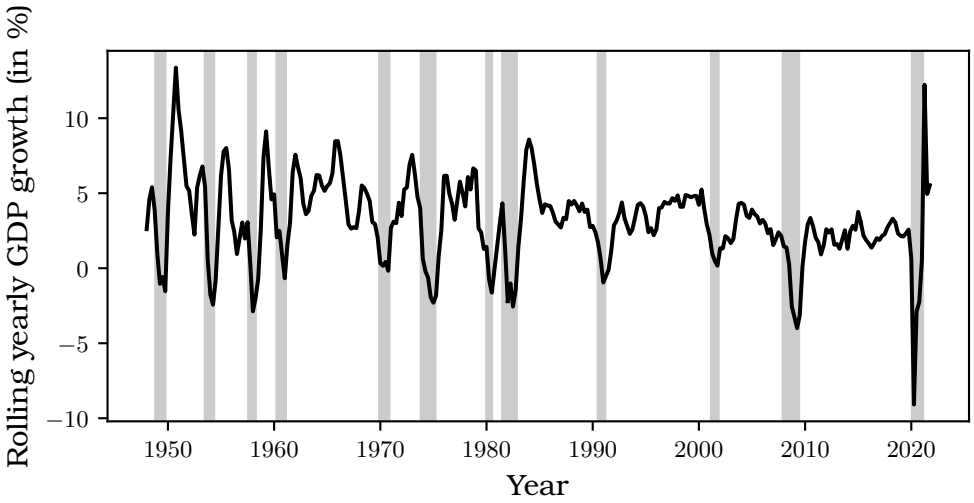


Figure 1: Rolling yearly GDP growth rate (in %) from January 1st, 1948 to October 1st, 2021. Gray areas represent the time span over which effects of well identified external shocks or crises were dominant. Source Bureau for Economic Analysis (BEA) [6].

of the exogenous parameters. Such assumptions along with using representative agents are at the core of the so-called "Dynamic Stochastic General Equilibrium" models used by central banks, which completely failed when the world's banking system nearly collapsed in 2008. As put by Willem Buiter in 2009 [8]: "*Standard macroeconomic theory did not help foresee the crisis, nor has it helped understand it or craft solutions. [...] both the New Classical and New Keynesian complete markets macroeconomic theories not only did not allow the key questions about insolvency and illiquidity to be answered. They did not allow such questions to be asked. A new paradigm is needed.*"

In the late 1990s, Cochrane [9] and then Bernanke [10] first pointed out what Bernanke later referred to as the "small shocks, large business cycles puzzle": exogenous shocks undergone at granular levels of the economy cannot alone account for the aggregate volatility observed. The remainder of the volatility should therefore be of *endogenous* origin, i.e. generated within the economy itself, but this could not be understood within equilibrium-only representative-agent frameworks prominent at the time (hence the "puzzle"). As an illustration, consider an economy of N representative firms, with production at time t given by $y_i(t)$ and assume that, initially, $y_i(0)$ is distributed according to some narrow distribution such that $y_i(0) \approx y(0)$. We further define total production as $Y(t) = \sum_i y_i(t)$. Assume now that production follows a multiplicative growth model from one year to the other, i.e.

$$y_i(t+1) = (1 + m + \sigma\xi_i(t))y_i(t), \tag{1}$$

where m represents a constant growth rate and $\sigma\xi_i(t)$ exogenous shocks, modeled by IID Gaussian random variables, that account for the fluctuations around the constant growth.

If macroeconomic fluctuations originate from the aggregation of micro-level shocks, one should expect the yearly growth rate of total production $Y(t)$ to display large fluctuations. For small times t, we can consider the distribution of $y_i(t)$ to still be narrow enough such that

$$\frac{Y(t+1)}{Y(t)} \approx 1 + m + \frac{\sigma}{\sqrt{N}}\xi(t), \tag{2}$$

with $\xi(t)$ a unit-variance Gaussian random variable. We therefore see that, within this framework, aggregate fluctuations around the average growth should decrease as $1/\sqrt{N}$, which should be completely negligible as the U.S. economy comprises around 5 million firms. This simple computation illustrates that large macroeconomic fluctuations need a much richer modelling framework than the representative one to be understood. Note however, that the previous reasoning is only valid at small times since it is known that multiplicative growth models can yield distributions with broad tails if one waits long enough. Therefore, the previous naive reasoning breaks down, and one must consider more general arguments such as the granularity arguments presented below.

As understanding the mechanisms responsible for this excess volatility is crucial for policy-making, this conundrum stemmed numerous seminal works and explanations. The first notable one is due to Xavier Gabaix [11], and known as the *granularity hypothesis*. A statistically robust stylized fact about firms is that the probability distribution P of their sizes S displays a power-law behavior $P(s) \sim_{s\to\infty} s^{-\mu}$ [12] with an exponent μ close to 1. Consequently, firms cannot be thought of as identical since their size can vary widely thanks to the power-law distribution, rendering invalid the naive reasoning of the last paragraph. Because of the fat-tailedness of firms' sizes, fluctuations of the aggregate sales are dominated by fluctuations undergone by the largest firms, which typically do not average out. The CLT-like reasoning must be traded for its generalized version, where aggregate fluctuations take the form of Lévy-stable distributions with infinite variance. The second notable explanation is due to Daron Acemoglu [13] whose mechanism favors the effects due to the network of interactions between firms. In Gabaix's explanation, firms remain independent, which is of course not realistic. Since firms interact on a supplier-buyer network, shocks can propagate up or down the supply chain and successively affect other firms. This contagion effect can amplify micro-level shocks into long-lived perturbations shaking the entire network and contributing at aggregate levels.

2 Main proposition and outline of the manuscript

Even though previous explanations are appealing and certainly reflect relevant mechanisms at hand, they still rely on equilibrium-only descriptions of the economy. We believe that such descriptions, especially as a foundation for policy-making, can widely underestimate the effects of shocks and therefore favor fragility over resilience. At the time of writing of this manuscript, the world stood in horror witnessing Russia's vicious invasion over Ukraine. European political leaders, reluctant to engage in a direct military intervention to help Ukraine that could lead to a global conflict, imposed a string of stringent economic, political and cultural sanctions against Russia. An important sanction concerned the

European Union (EU) oil imports from Russia. Up until the end of May 2022, EU states had been importing "2.2 million barrels per day (bpd) of crude oil from Russia and 1.2 million bpd of oil products" according to the BBC [14]. EU nations agreed to ban all sea-imported oil from Russia, thus cutting Russian exports to the EU by about two-thirds. Of course, some anxiety about the price of energy followed this decision, since most European countries depended to some extent on Russian oil. In Germany, a study from March 2022 [15] showed that a sudden drop of Russian oil imports would affect German GDP down by only 0.3% (at most 3% which they compare to the 4.5% drop caused by Covid-19 in 2020), which in turn would affect German households by 120€. An even lower figure (54€) is obtained for France [16] (in French). Such low numbers of course go in the sense of dropping oil imports, but could very well minimize the effects on European economies. Indeed, the economic models used for these studies assume that the economies will "quickly" converge back to equilibrium and equilibrium descriptions can therefore be used. However, a physicist would ask what is the meaning of "quickly" and how big a drop can we expect during this "quick" equilibrating time. These models completely neglect the behavior of the economy in this transient phase and therefore could miss GDP drops much direr than the expected 0.3% (see [17] in French).

The central proposition of this manuscript is that large macroeconomic fluctuations can chiefly be explained through *out-of-equilibrium* effects where, in such situations, the dynamics is mostly of endogenous origin. We argue that, rather than on initial and final economic states (which can be equilibria), economic modelling should focus on the path (possibly paths plural) linking these two states. Furthermore, we also argue that such path is not a collection of quasi-equilibria (as if the evolution followed the "quasi-static" idea from physics) but can be arbitrarily far from equilibrium and, in fact, remain far for arbitrarily large times. Finally, we place ourselves within the network framework of Acemoglu [18, 13] where firms interact on a supplier-buyer network. We will argue that the equilibrating time of the economy depends on the network and that interactions, which are too often neglected in economic modelling, are an integral part of large macroeconomic fluctuations.

This manuscript is organized in three parts. The first two parts are entirely devoted to economic modelling in an *out-of-equilibrium* framework. In the first part, entitled "Critical network-economies", we propose a fully non-linear evolution of prices and productions using behavioral rules, and show that, through a process called *self-organized criticality*, large economies are prone to being far from equilibrium and fluctuating widely. In the second part, entitled "Macroeconomic agent-based modelling", we propose a hybrid approach between standard economic thinking (where firms attempt to optimize profits in a competitive environment, and households optimize their utility function to balance consumption and labor) and Agent-Based Models (ABM), where simplified behavioral assumptions allow one to specify the decision-making process of firms. The third and last part, entitled "Complex interactions and random matrices", deals with idealizations of systems that naturally arise in economic models: conewise linear systems. The closely related question of occupation time is also discussed. Even though related to economic modelling, this part will more appeal to the theoretical physicist readership.

Finally, the first two parts account (almost in chronological order) for the different steps building up to the publication of [1]. We of course added some additional results, analytical derivation and intuitions, but the reader will find the same general outline. For the last part, the reader will surely notice a change in style as we decided to expose the results on conewise linear systems, occupation time and elliptic random matrices as they are published [2, 3] or in their "in preparation" version [4]. The reader will however see that [2] has been reworked and augmented for this manuscript. We also chose to provide technical appendices at the end of each corresponding chapter. We changed both font color and size to indicate that, although appendices should provide details and insights about computations, they are not fundamental for the understanding of the overall manuscript.

2.1 Critical network-economies

> The behavior of large assemblies of interacting individuals cannot be understood as a simple extrapolation of the properties of isolated individuals. Instead, entirely new, unanticipated behaviors may appear and their understanding requires new ideas and methods. Statistical physics has developed tools to describe these "collective phenomena", pertaining to crowds and not to any of its single constituents. Small changes at the individual level can trigger dramatic effects at the collective level - for the better or for the worse.
>
> Philip Warren Anderson, adapted from *More is Different*, Science 1972

2.1.1 From local to global: self-organized criticality in firm networks

The study of large assemblies of particles has led to the development of statistical physics. From the kinetic theory of gases by Ludwig Boltzmann in the XIXth century to the study of active biological particles and spin-glasses, statistical physics increasingly showed that large interacting systems could not be understood solely by extrapolating individual behaviors: macroscopic properties *emerge* from interactions. The concept of *phase transition* is central in statistical physics: small variations of parameters can trigger dramatic changes in the macroscopic phase of the system. Take water, for instance. Below $0°$, solid ice is the stable state. Increasing the temperature, the ice will melt into liquid water at $0°$ and vaporize at $100°$. The nature of water molecules and of their interaction has not changed in the process, but the system did however undergo two macroscopic phase transitions. Nearing *critical points* where phase transition occurs, interacting systems are prone to *scale-free behaviors*, i.e. subsystems sharing the same macroscopic property can be found at all scales. When systems get closer to phase transitions, the correlation length diverges, thus creating global fluctuations from local interactions.

Since economic systems are large highly complex interacting systems, it is quite naturally that Bak et al. [19] proposed the criticality explanation to account for macroeconomic fluctuations. However, economies cannot be tuned by a few parameters such as

temperature, and the concept of economic phase transition, let alone economic critical points, is hard to define. In [20], Bak proposes a general mechanism, called *self-organized criticality* [1] (SOC), explaining that complex systems naturally organize towards critical points. If applied to economic systems, SOC would nip in the bud the questions about defining economic critical points.

As an introduction to the concept of SOC, let us present a model of sandpiles: the Bak–Tang–Wiesenfeld model (BTW) [23]. A sandpile is literally a pile of sand, which is of course idealized in the BTW model. Consider an $L \times L$ grid where for each square cell (x, y) we associate the height $Z(x, y)$ of the sandpile in this cell. As put by Per Bak in [20], the sand is a "theoretical physicist's sand" here, i.e. modeled as regular cube of unit sides. Now, one can define a dynamical process for adding sand to the pile. At each time step, choose a site (x, y) at random and add a grain of sand at this cell

$$Z(x, y) \to Z(x, y) + 1.$$

If the height of the pile at this site is low enough $Z(x, y) \leq Z_c$, then nothing happens. If, however, the height exceeds the threshold $Z(x, y) > Z_c$, the sandpile topples on the four neighboring sites

$$\begin{aligned} Z(x, y) &\to Z(x, y) - 4 \\ Z(x \pm 1, y) &\to Z(x \pm 1, y) + 1 \\ Z(x, y \pm 1) &\to Z(x, y \pm 1) + 1. \end{aligned}$$

If toppling occurs near the edges of the grid, the sand simply leaves the system.

The state with the lowest energy of this sandpile is the flat state, since one would need to add energy to the system to create heaps. However, due to the friction of the sand, i.e. the pile topples only above a certain threshold, the system will not revert to the ground state whenever one stops adding sand. Consequently, a sandpile naturally displays local heaps with associated local slopes. When these slopes are relatively low, i.e. the sandpile is not very high, the grains of sand tend not to topple, and, when they do, create only local disturbances on the pile without much communication between different heaps. However, upon increasing the global height of the pile, adding sand may cause avalanches which spread throughout the entire pile. Indeed, assume that one only adds sand at the center cell. At some point, the global slope cannot increase any further, since the entering sand is perfectly balanced by the grains exiting at the edges. The system reaches a stationary state of balance between entering and leaving grains that requires communication throughout the entire system (between center and edges). Such state, called *self-organized critical*, is prone to very large avalanches that span throughout the entire system. Even though the process of adding sand is local, the SOC state has global dynamics.

[1] The term *self-organization* is actually due to Wiliam Ashby in 1947 [21, 22] in the context of cybernetics. It refers to the natural tendency of (complex) systems to evolve towards states of high *complexity*.

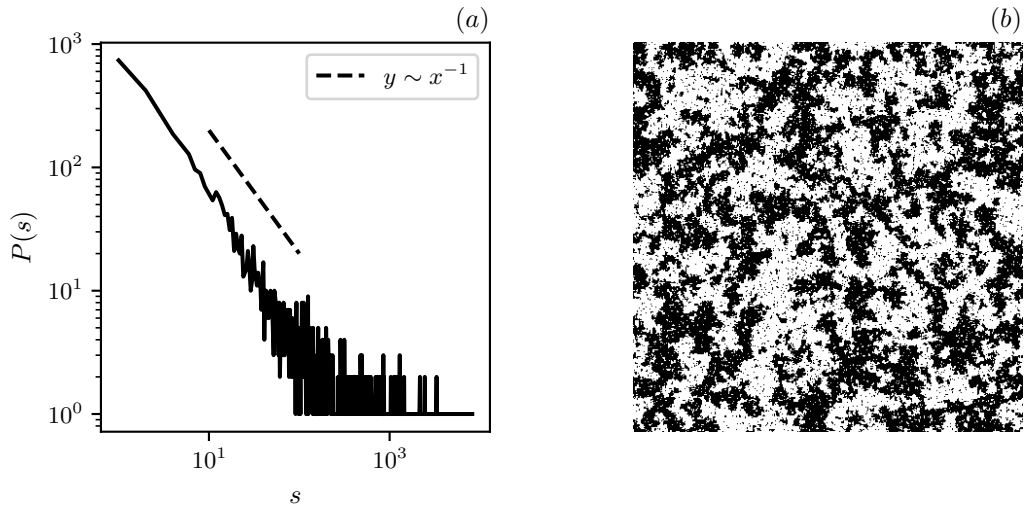


Figure 2: (a) Distribution $P(s)$ of avalanche sizes s in the BTW sandpile model. We see a power-law decay indicating scale-free behavior (disregarding finite-size effects). (b) Two-dimensional Ising model on a 400×400 lattice with periodic boundary conditions. The system is quenched at the critical temperature $T = T_c$ which separates paramagnetic (high temperature, no global order) and ferromagnetic (low temperature, global order) macroscopic behaviors. The system evolves according to a Glauber dynamics. We see the emergence of large structures of correlated spins which illustrate the divergence of the correlation length at the critical point. Both figures are obtained using software from the NetLogo App [25, 26, 27].

As we said, Bak et al. [19] proposed the criticality explanation to account for large macroeconomic fluctuations. They argued that economic networks are typically in SOC states which make them prone to large contagion/avalanche effects that amplify exogenous shocks, therefore leading to large fluctuations. This idea was revisited in [24], where authors exploit the Hawkins-Simons transition to define a critical point in firm networks (see Chapter I), and argue in favor of SOC states. However, they remained within the equilibrium framework from which we will depart by endowing classical firm networks with some dynamics. Close to the economic critical point (reached through a SOC mechanism), such dynamics should be able to generate large fluctuations from local interactions (see an illustration of this phenomenon on Figure 2).

2.1.2 Economies as dynamical systems

Past literature in macroeconomics (see e.g. [28, 29, 30, 31, 32, 33] and [34]) has been mainly concerned with "disequilibrium" effects, which in that context means studying the impact of price or wage frictions and rigidities that prevent the economy from reaching full equilibrium. In a sense, these models postulate economies that are not able to reach an idealized state of equilibrium because of certain imperfections, but they still mostly deal

with the *static* properties of such economies, with no particular focus on their dynamics or on how said state is reached. Effectively, the dynamics that are studied through these models are those in which the agents in the economy are all capable of optimizing their behavior, exchanging goods and coordinating between themselves instantly. The main source of fluctuations is therefore given by *external* shocks to the economy. This is, for example, the case of [35] and [36], despite their common acknowledgment of the need to take into account the "time to build" in the economy, which we choose to interpret too as the time required for all the agents to coordinate and exchange enough information to reach equilibrium.

In Chapter II we go beyond *disequilibrium* and propose an *out-of-equilibrium* economic description. We draw onto the concept of *toy-modelling* dear to physicists. With toy-models, physicists try to strip away as much complexity as possible while still being able to capture the mechanisms responsible for particular empirical observations. In a way, toy-models aim for the most minimal non-trivial empirically relevant models. Most of the time, they rely on heuristics rather than precise microscopic descriptions. Some have advocated for the use of heuristics in socioeconomic modelling [37, 38] arguing that people tend to make decisions under "bounded rationality" (a term coined by Herbert Simon [39, 40]): only partial information is available, threshold effects drive decision-making etc. We therefore propose a minimal set of heuristic rules for prices and productions adjustments in firm networks. Such models have recently become popular as a way to generate excess aggregate volatility, as shocks may propagate through the input-output network. However, the seminal papers of [35], and of [13], are studied within the "adiabatic" framework in which the system instantaneously adapts to productivity shocks (for a recent enlightening review of these models, see [41]). We therefore propose a dynamical description that is based on the assumption that economic agents react to observables rather than optimizing their behavior. Firms interact on a supplier-buyer network, but we do not assume any coordination *a priori*, i.e. equilibrium is not the constitutive state of the system but rather one of the possible dynamical outcomes.

A strand of the economic literature considers "reduced-form" differential equations that describe the coupled evolution of a set of aggregate variables (for example employment, wage and output in the original model by Goodwin [42] and revived in [43]). These low-dimensional dynamical equations can generate various types of dynamics, such as business cycles in the Goodwin model, which is equivalent to the classic Lotka-Volterra (or predator-prey) model of [44, 45]. Note also that [46] establish a system of coupled dynamical equations whose dynamics are determined by certain matrices that describe the production network. This is, in a way, a similar approach to ours, but our *toy-model* considers a fully non-linear description with a *linearized* evolution governed by a production-network determined matrix that is only valid close to equilibrium. In a sense, our model can be seen as a multidimensional, discrete time version of the reduced-form differential equations *à la* Goodwin [42] and followers, that also lead to oscillatory dynamics. The main difference is that we describe the dynamics of the economy at a highly granular level (that of firms), which is an important aspect in view of the amount of microdata now available to calibrate such models.

2.2 Macroeconomic agent-based modelling

> The atomistic, optimizing agents underlying existing models do not capture behavior during a crisis period. We need to deal better with heterogeneity across agents and the interaction among those heterogeneous agents. We need to entertain alternative motivations for economic choices. [...] Agent-based modelling dispenses with the optimization assumption and allows for more complex interactions between agents. Such approaches are worthy of our attention.
>
> Jean-Claude Trichet, *Opening address at the ECB Central Banking Conference Frankfurt*, 18 November 2010

2.2.1 From cellular automata to agent-based models: numerical simulations as a new paradigm

Even though the appeal of toy-modelling is quite clear (models are often simple and sometimes analytically tractable), these models are not usually designed to be predictive as they aim for a more qualitative understanding of the phenomenon at hand. However, the idea that simple enough rules can create very complex behaviors has been at the heart of the development of computational physics and more generally the tools for numerical simulations.

In the 1940s, John Von Neumann and Stanislaw Ulam (working respectively on self-replicating machines and crystal growth) introduced the concept of *cellular automaton* (CA) [47]. It was not until the 1960s that the concept was recognized as significant when John Conway simplified the initial complicated CA of Von Neumann [2] into what is now called the "Game of Life" (LIFE) [48]. A CA is a *discrete-time model* on a grid of *cells* that can occupy different *states*. From an initial condition of states at $t = 0$, a new generation is created using a set of rules determining the future state of each cell depending on the current state of the cell itself and of its neighbors. The model then carries out, evolving into new generations according to the same rules. For instance, in Conway's LIFE, cells can be either dead or alive, and the evolution rules are: (a) any live cell with two or three live neighbors survives; (b) any dead cell with three live neighbors becomes a live cell; (c) all other live cells die in the next generation and all other dead cells stay dead. This simple set of rules can lead to intricately complex phenomena in the grid: it has been shown that LIFE contains self-replicating patterns, is undecidable and Turing complete [3] [49, 50, 51].

[2] Working on self-replicating machines, Von Neumann designed a CA where cells (the constitutive entities) could be in 29 different states. He finally found a self-replicating pattern that occupied 200000 cells.

[3] The last two concepts are actually related. *Undecidability* has to be understood in Gödel's sense: there is no algorithm that can predict whether some pattern will emerge starting from a given initial layout. *Turing completeness* indicates that a universal Turing machine, i.e. a machine capable of performing arbitrary finite computations, can be built within LIFE. It is proven that Turing completeness implies undecidability.

Even though this historical detour through cellular automata might seem like a digression, the study of CA actually created a new paradigm: not only complex structures can emerge from very simple rules, but, more importantly, these rules can and must be simulated. With the increase of computational power over the last decades, this paradigm is at the base of what is now known as Multi-Agent Systems, or more precisely in the context of this manuscript Agent-Based Models (ABM). Such models are built upon the same general principles as CA. They are discrete time systems composed of constitutive entities called *agents* (the evolution of Conway's cells) which can be heterogeneous. To go one step forward in time, agents undertake some *actions* (the evolution of Conway's rule) based on other agents, themselves, the general environment etc. Of course, the agents are not described by a binary state anymore but rather by a collection of continuous variables (in the context of economic modelling prices, productions, debts...). The actions are also much more complex, usually involving non-linearities and intricate interactions. The general principle however is not different from that of cellular automata. Note that this approach has been advocated for economic modelling by Holland and Miller in [52]. They consider *complex adaptive systems* [4] as the right framework for studying economic system and they especially insist on the notion of *emergence* [53].

2.2.2 Macroeconomic modelling and policy-making

The use of agent-based modelling in economics seems to be a right avenue to explore, since economic systems comprise heterogeneous agents which interact in a complex manner. It is therefore natural that in the second part of this thesis, we moved towards an ABM description of our network economies. ABMs are explicitly dynamical models (which goes in the way of our general proposition), in the sense described by [54]: decision rules lead to actions (buy/sell, produce, update prices and wages, etc.) that move the economy one step forward in time. As argued in [55] in the context of financial markets, ABMs are very well suited to understand non-linear behaviors such as bubbles or crises.

Some macroeconomic ABMs have emerged in the last years [56, 57, 58, 59, 60, 61, 62, 62, 63, 64, 65, 66] to account for various macroeconomic aspects. In [58], authors describe the Eurace@Unibi Model with three types of agents (firms, household, banks) spatially arranged and interacting. The decision rules attempt at describing as closely as possible actual behaviors observed in the real economy. In [61, 62], the Mark0 model (a simplification of the MarkI family of models elaborated in [57]) is described along with its use for the understanding of different macroeconomic aspects such as monetary policies in [62] for instance. The work in [63, 64] describes an ABM based on the general framework of constraint satisfaction problems (studied at length in theoretical physics and mathematics) and more specifically on the *perceptron* model.

In [61, 62] (see also [67] in a DSGE-ABM crossover framework), the authors also provide a classification in *phases* of the possible dynamical outcomes depending on the

[4] Complex adaptive systems are characterized by (*i*) a network of interacting agents, (*ii*) a dynamic aggregate behavior emerging from the individual agents, (*iii*) the fact that the aggregate behavior may be characterized without detailed knowledge of the behavior of individual agents.

parameters of the model. This physics-inspired approach highlights one of the main proposition in this manuscript: depending on the parameters of the model, the economy may not reach equilibrium. The use of phase diagrams is, in our opinion, not only an excellent way to gain a deeper understanding of the model itself, but could also allow for better decision-making in macroeconomic policies. Establishing the phase diagram on the parameters targeted by some specific policy might help understanding the effect of said policy on the economy. Furthermore, the dynamical aspect of the model allows for *in silico* experiments to track the effects of policies over time.

This long-term *in silico* monitoring goes along with voices advocating in favor of more *scenario-based* macroeconomic [68, 69]. One aspect of macroeconomic modelling is its propensity to try and forecast very short-term trends. Scenario-based policies or macroeconomics advocate for the understanding of more general and long-term trends along with the possible factors influencing these trends. As an example, climate change cannot be understood by trying to forecast tomorrow's weather, but rather by identifying the causes that make the world's average temperature rise. The understanding of long-term trends and tipping points from one scenario to another should make systems more resilient. We will use this approach in the manuscript by proposing phase diagrams which classify possible outcomes of the economy (along with mechanisms accounting for these outcomes) rather than looking at economic time-series on short-term scales.

The approach of ABMs, although very prolific, has been heavily criticized by those who argue in favor of "micro-founded" models where agents are forward-looking and optimize inter-temporal utility functions. However, whenever interactions are complex, involving non-linearities for instance, analytic treatment becomes a fool's errand and must give way to numerical assessment. During the Covid-19 pandemics, a lot of difficult political decisions about lock-downs and vaccinations were made using projections from ABMs [70, 71, 72]. Maybe this recent use for political decision making in time of crisis will make this approach more palatable for economic policy-making.

2.3 Complex interactions and random matrices

> Not only in research, but also in the everyday world of politics and economics, we would all be better off if more people realized that simple nonlinear systems do not necessarily possess simple dynamical properties.
>
> Robert M. May, *Simple mathematical models with very complicated dynamics*, Nature 1976

In the second part of the manuscript, the study of our network-economy ABM naturally leads to a class of dynamical systems called *conewise linear*. In such systems, the relationship between inputs and outputs is linear, but the linear transformation depends on the direction of the vector of inputs in state space. Take a sequence of numbers $U(t)$ such that $U(t+1) = aU(t)$ if $U(t) > 0$ and $U(t+1) = bU(t)$ otherwise. Depending on the relative signs of $U(0)$, a and b, this sequence will have very different evolution. Of course, when the dimension of the space increases, things get more complicated as the

matrices governing the linear evolution do not commute as real numbers do. Even though each individual step forward is linear, the overall evolution is actually very complex and does not possess simple dynamical properties. Very little is known about these systems, let alone analytical methods to solve them.

Chapter VII is devoted to the study of such systems by considering linear evolution governed by *random matrices* in the large-dimensional limit. Replacing complex interactions by random elements is a trick that is well-known in high-energy physics. Eugene Wigner came up with this idea upon studying the energy levels of large atoms nuclei. The Hamiltonian of these systems was so complex that diagonalizing it to find the energy levels revealed too formidable a task. Wigner suggested rephrasing the question in statistical terms, i.e. what is the probability to find the atom in such or such level spacing? He therefore proposed to abandon the deterministic description of the Hamiltonian and replace it with random Hermitian matrices drawn from the same ensemble. The underlying idea was that, to some extent whenever interactions are complex enough and the system large enough, the overall spectrum does not depend on the precise system (i.e. the precise Hamiltonian) but is rather universally described through a few key parameters. This simple and rather bold idea is at the base of what is called Random Matrix Theory, which has been a very prolific field in both mathematics and physics over the past few decades.

In the case of the conewise systems resulting from the ABMs of Part II, the choice to try to move to a randomized description was quite natural. As it will be demonstrated in the manuscript, the dimension of state space is actually of order $\mathcal{O}(N^2)$ where N is the number of firms involved in the economy. Furthermore, the network of interaction can be very complex and intricate, and we usually choose it random anyway. Of course, the resulting model of Chapter VII is a crude idealization of the systems of Part II, but it highlights the level of complexity at hand. The seemingly simple question "will the system be stable?" does not have a straightforward answer. Depending on the initial perturbation and the time of observation, one may find that the system is stable or unstable.

The last part of this manuscript also addresses questions that one naturally asks when studying conewise linear systems. For instance, since each step forward is linear, one can ask for how long the system is governed by the same linear evolution. This question falls into the study of *occupation time* of stochastic processes, where one studies for how long a given process keeps some property (for instance positivity in the case of Chapter VII). Actually, these kinds of questions directly relate to economic concerns. As the Covid-19 crisis was unraveling in 2020, the word *resilience* was thrown around a lot when speaking about the economy. Even though elusive, the concept of economic resilience refers to the inherent capacity of the economy to recover and heal itself after a shock. The real question though is how much time will this process take, i.e. for how long will the economy feel the aftermaths of said shock. In the ABM framework of Part II, this question amounts to understanding for how long firms can be, for instance under producing before the economy stabilizes or collapses, and therefore relates to occupation time issues.

Even though the last part of the manuscript can be read almost independently, it

still relates to the main proposition of this work: understanding the path from initial to final state is crucial, all the while accepting that the economy can occupy a state that will never allow it to converge back towards equilibrium.

Part I

Critical network-economies

Foreword

The first part of this thesis is devoted to a study regarding *out-of-equilibrium* dynamics in firm networks. We will show that excess volatility can be created by network-induced amplification of shocks through a process called *self-organized criticality*.

In Chapter I, we lay the foundation on which Part I and Part II are based. The reader will become familiar with the framework of firm networks along with basics from the theory of production functions. We will also introduce the household sector as another constitutive entity of our model. We will then define economic equilibrium and show that, in the context of firm networks, it can be ill-defined which will motivate moving towards a fully *out-of-equilibrium* description of the economy. Furthermore, we will see that economic equilibrium exists provided the economy fulfills the Hawkins-Simons (HS) conditions, and we will argue that real economies tend to *self-organize* right at the point where these conditions are only marginally satisfied.

The out-of-equilibrium economic description is provided in Chapter II where we propose a set of behavioral rules to set prices and productions. Rather than optimizing at every time-steps, firms react to imbalances such as excess of production and try to correct them. This description will naturally lead to a *non-linear* dynamical system for prices and productions adjustments. In the same spirit as [35], we linearize this system around economic equilibrium and show that, at the onset of violating the HS conditions, the economy experiences a *critical slow-down*. As a consequence, the economy will take an increasingly large amount of time to converge back to equilibrium, rendering it dynamically unattainable in effects. Furthermore, another consequence of the critical slow-down is that exogenous shocks will accumulate and linger in the network, creating excess volatility.

Finally, some features of this model are still unsatisfactory since, for instance, we could not find any bounded trajectory whenever the HS conditions are violated and economic equilibrium ceases to exist. We show this feature in Chapter III using the framework of Dynamical Mean-Field Theories from statistical physics. This inconsistency below the HS threshold will be our motivation to refine the model in the second part of the manuscript.

CHAPTER I

Equilibrium network-economies

Abstract

In this introductory chapter, we present the building blocks on which the work presented in this manuscript is based. We introduce the different agents that will be interacting throughout Part I and Part II along with the general framework of firm networks as introduced by Acemoglu et al. [13]. We also introduce the notion of economic equilibrium, but we depart from the standard definition by drawing closer to ideas from physics, i.e. keeping in mind that equilibrium is the result of a dynamical adjustment process. Furthermore, we give conditions for equilibrium to be economically admissible (with positive prices and productions) and uncover a transition on the "feasibility" of the economy known as the Hawkins-Simons transition. Finally, we link this transition to the idea by Bak et al. [19] that excess volatility at aggregate levels comes from the proximity of the economy to a critical point, which corresponds here to the Hawkins-Simons transition point.

1 Firm networks, production functions and household

1.1 Firm networks

One of the central ideas in our work is that microscopic shocks can amplify through interactions between firms and account to some extent for the excess volatility observed at aggregate levels[13]. One of the vectors for these interactions is the supplier-buyer network (or input-output network) describing fluxes of goods between firms. Schematically, if one firm produces cars it will need raw materials such as steel. A link will therefore be formed from a steel-supplying firm to the car-producing one. The resulting interaction structure is therefore a graph J whose nodes are firms with directed links $j \to i$ describing the relation "j supplies to i". Such links can be weighted if one is interested in the actual amount supplied.

Firm networks have drawn a lot of attention in the past decades since they display rather non-trivial topological features. A central well-established stylized fact is that the empirical distribution of the number of in and out links (denoted by $k_{in/out}$) displays a

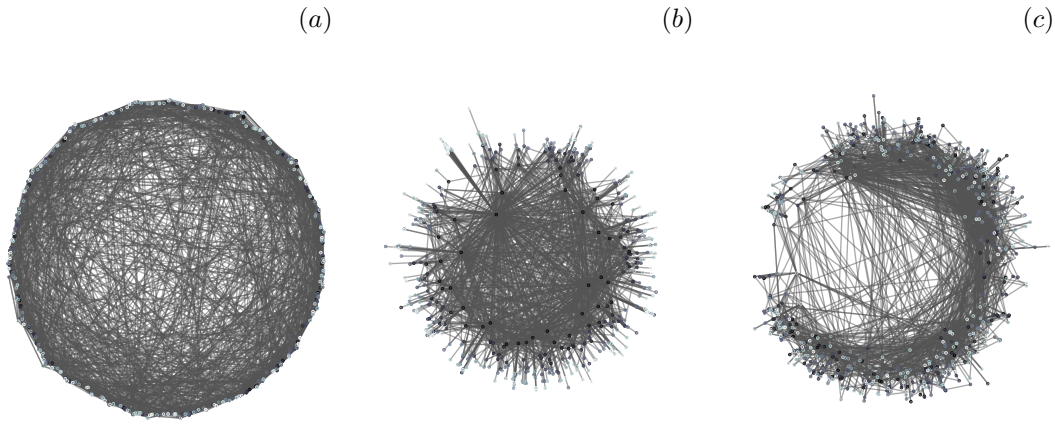


Figure I.1: Different types of networks. The original networks are directed but we omitted links' directions for clarity. (a) Random 4-regular network on $n = 500$ firms. The number of in and out links is fixed to $d = 4$. (b) Scale-free network on $n = 500$ firms. The number of in and out links follows a Pareto distribution with parameter $\mu_{in} = 1.29$ and $\mu_{out} = 1.25$ (power-law exponents from [75]). (c) Input-output network over $n = 660$ firms inferred from the FACTSET data-set [76]. Links correspond to an existing supplier-buyer relationship between 2012 and 2015. These networks are represented with an embedding described in [77].

truncated power-law behavior

$$\mathbb{P}(k_{in/out} = q) \underset{q\to\infty}{\propto} \frac{e^{-q/Q_{in/out}}}{q^{1+\mu_{in/out}}}. \tag{I.1}$$

Even if the power-law exponents $\mu_{in/out}$ or the truncation may vary from country-to-country, this general form seems to be universal. Note that this scale-free behavior of sizes $q \ll Q_{in/out}$ supports the granularity hypothesis [11] for excess volatility of aggregate outputs. While microscopic shocks might originate from a sparsely-connected firm, it can propagate towards central firm, and therefore ripple out on a large part of the network. For a complete overview of the features of firm networks beyond scale-free behavior, see [73, 74, 41]. Figure I.1 shows a visual comparison between synthetic and real-world input-output networks.

Finally, firm networks are not static in time. New firms can enter the network, while existing firms can go bankrupt. New contracts can also be negotiated and change links in the network. This calls for a dynamic description of the network itself. We will discuss this point at the end of Part II but we will consider throughout Part I and Part II that the network is fixed in time. We implicitly assume that the evolution of the network occurs on time-scales much slower than those underlying the adjustment process of firms' prices and productions. For dynamical networks, we refer the reader to [73] where authors present a model for network creation aiming at reproducing empirical features of firm networks.

1.2 Production functions

The production function gives the quantity y_i of goods produced by firm i as a function of input goods, labor and the intrinsic, possibly time dependent, productivity of the firm z_i (i.e. its efficiency in converting a given amount of inputs into outputs). The production function is mathematically described by a relationship of the type

$$y_i = z_i f_i(\{x_{ij}\}_{j=0,\dots,N}) := z_i \gamma_i, \tag{I.2}$$

where x_{ij} denotes the amount of good j (or labor $x_{i0} := \ell_i$ if $j = 0$) available to i, and where we defined the level of production γ_i of firm i as the purely input-dependent part of the production, i.e.

$$\gamma_i := f_i(\{x_{ij}\}_{j=0,\dots,N}). \tag{I.3}$$

1.2.1 Constant Elasticity of Substitution

Although many types of production functions exist, we present here a specific family of functions called the Constant Elasticity of Substitution (CES) family. We generalize the standard CES production function [78] as [1]

$$\gamma_i := \left(a_{i0} \left(\frac{\ell_i}{J_{i0}} \right)^{-1/q} + \sum_{j=1}^{N} a_{ij} \left(\frac{x_{ij}}{J_{ij}} \right)^{-1/q} \right)^{-bq}, \tag{I.4}$$

where $J_{ij} \geq 0$ and $a_{ij} \geq 0$ are link variables that measure the importance of good j in the production of i. The a_{ij} are normalized such that

$$\forall i, \sum_{\substack{j=1 \\ J_{ij} \neq 0}}^{N} a_{ij} + a_{i0} = 1.$$

Note that although for all values of $q \in]0, \infty[$, the J_{ij}s can be absorbed into the a_{ij}, our specification allows for consistent limits when $q = 0$ (Leontief) and $q = \infty$ (Cobb-Douglas).

The parameter q measures the substitutability of inputs. For example, when $q \to 0^+$ we get the Leontief production function, corresponding to the case where production falls to zero if a single input is missing

$$\gamma_i = \left(\min \left[\frac{\ell_i}{J_{i0}}, \min_j \left(\frac{x_{ij}}{J_{ij}} \right) \right] \right)^b. \tag{I.5}$$

The link variable J_{ij} can therefore be interpreted as the amount of good j that i would need to achieve a level of production equal to z_i. The Leontief production function corresponds to an economy where firms only keep a small, very optimized portfolio of suppliers that does not allow for redundancy.

[1] The standard CES function corresponds to all J_{ij} set to unity.

If $q \to +\infty$, we get the Cobb-Douglas production function

$$\gamma_i = \left(\left(\frac{\ell_i}{J_{i0}} \right)^{a_{i0}} \prod_{j=1}^{N} \left(\frac{x_{ij}}{J_{ij}} \right)^{a_{ij}} \right)^b , \tag{I.6}$$

for which some amount of substitutability is present. Indeed, halving the quantity x_{ik} of input k can be compensated by multiplying the input of ℓ by $2^{a_{ik}/a_{i\ell}}$, where the a_{ij} describes the amount of substitutability between goods for the production of i.

Finally, one can also extend the domain of validity of q to include the interval $]-1, 0[$. For $q = -1$, we recover a linear production function

$$\gamma_i = \left(a_{i0} \frac{\ell_i}{J_{i0}} + \sum_{j=1}^{N} a_{ij} \frac{x_{ij}}{J_{ij}} \right)^b . \tag{I.7}$$

As in the Cobb-Douglas case, substitutability is present but in an additive way. Reducing input k by a quantity r_{ik} can be compensated by augmenting input ℓ by $r'_{i\ell} = r_{ik}(a_{ik} J_{i\ell})/(a_{i\ell} J_{ik})$.

Finally, the parameter b sets the return to scale: if all inputs and labor are multiplied by a factor λ, then the total output is multiplied by λ^b. For example, for increasing return to scales $b > 1$, $\lambda^b > 1$ which means that outputs increase if the firm aggregate more inputs. This situation can reflect economies of scale made by firms upon buying larger quantities of inputs (see [79] for a detailed account).

1.2.2 Hybrid and nested production functions

CES production functions assume that there is a certain extent of substitutability among inputs. However, we can imagine that some inputs are more crucial than others and therefore not subsitutable, while others could be interchangeable. We can therefore write hybrid production functions with – say – Leontief and Cobb-Douglas parts

$$\gamma_i = \left(\min_{j \in S_l} \left(\frac{x_{ij}}{J_{ij}} \right) \right)^b \left(\prod_{j \in S_{cb}} \left(\frac{x_{ij}}{J_{ij}} \right)^{a_{ij}} \right)^b , \quad S_l \cup S_{cb} = \{1, \ldots, N\},$$

where we omitted labor for conciseness and where S_l and S_{cb} refer to the subsets of firms belonging to the Leontief or Cobb-Douglas classes respectively.

Another generalization would be that of nested production functions. These functions appear where production is carried out through different aggregation levels. As an example, these nested functions are used to estimate the amount of substitutability between capital, labor and energy for countries. Calling K, L and E these different variables, an intermediate aggregate X is defined as

$$X = \left(\alpha K^{-1/\sigma} + (1 - \alpha) L^{-1/\sigma} \right)^{-\sigma} , \tag{I.8}$$

and used in the final output Y

$$Y = \left(\beta X^{-1/\theta} + (1-\beta)E^{-1/\theta}\right)^{-\theta}, \tag{I.9}$$

see for instance [80] where authors use this structure to estimate elasticity of substitutions between capital labor and energy in the Chinese economy.

1.3 Household

As we anticipated in the previous section, another agent is present in the network. Throughout this manuscript, we will consider the household to be representative, i.e. the coarse grained version of in-homogeneous real households. We do not specify the coarse-graining procedure but see Chapter III for an example of such procedure applied to firms. A more realistic description is of course possible by introducing M different households and a household interaction network that could measure the degree of influence between individuals on consumption, for instance. For the case of a representative firm and a network of households, see [67] that studies consumption crises and confidence collapse in a DSGE framework.

As it is standard in the economic literature, the household interacts with firms by consuming goods and providing work. Consumption and labor supply are set through the optimization of a *separable utility function* that measures the "happiness" of the household depending on the amount consumed and worked. Usually, the utility function is written as

$$\mathcal{U} = f(\{C_i\}_{i=1,\dots,N}) + g(\{\ell_i\}_{i=1,\dots,N}), \tag{I.10}$$

where C_i and ℓ_i denote the amount of good i consumed and working hours provided to firm i respectively. The functions f and g can virtually be any reasonable functions that account for the fact that people tend to be happier when consuming more and working less. In this manuscript, we will restrict ourselves to the following rather standard utility function

$$\mathcal{U} = \sum_j \theta_j \log C_j - \frac{\Gamma}{1+\varphi}\left(\frac{L}{L_0}\right)^{1+\varphi}, \tag{I.11}$$

where $L(t) = \sum_j \ell_j(t)$ is the total amount of work provided by the representative household and θ_i is the preference for good i. The Frisch elasticity index φ, after the eponymous author of [81], gives a measure of the convexity of the disutility of work, L_0 is the scale of the amount of work that the household is able to provide and Γ is a parameter that can be set to one without loss of generality. In the limit $\varphi \to \infty$, households are indifferent to the amount of work provided $L < L_0$, but refuse to work more than L_0. We restrict to a "myopic" optimization here, that does not take into account the long-term forecasts and desires of the household. Intertemporal effects would require to add interest rates, which we do not consider in the work presented in this manuscript.

The household therefore optimizes the previous utility while assuming that the entirety of its budget B will be used for consumption. This budget comes from the wage

p_0 earned by working for the different firms, i.e. $B = p_0 L$. The optimization procedure can therefore be written as

$$(C_i, L) = \begin{cases} \underset{(C_i,L)}{\arg\max} \sum_j \theta_j \log C_j - \frac{\Gamma}{1+\varphi} \left(\frac{L}{L_0}\right)^{1+\varphi} \\ \text{subject to } p_0 L = \sum_i p_i C_i \end{cases}, \tag{I.12}$$

leading to

$$\begin{aligned} C_i &= L_0 \frac{\theta_i}{\mu} \frac{p_0}{p_i} \\ L &= L_0 \mu^{1/\varphi}, \end{aligned} \tag{I.13}$$

with $\mu = (\sum_i \theta_i)^{\varphi/(1+\varphi)}$. Rewriting consumption as $C_i = \frac{\theta_i}{\sum_j \theta_j} \frac{B}{p_i}$ allows us to see that the household partitions its budget with respect to preferences and prices, luxurious goods being consumed less.

1.4 Modelling framework

Following the descriptions of [35, 13, 66] and [41], we model the economy as consisting of N firms which interact with one another and with a single representative household providing labor and consuming goods. The economy is described by a "technology network", namely a directed graph where each node $i = 1, \ldots, N$ represents a firm and where the link $j \to i$ exists if i uses the good produced by j for its own production. The node conventionally labelled $i = 0$ represents households. Each edge in the graph $j \to i$ carries a "weight" J_{ij} that is a measure of the number of j goods needed to make a unit of i. Figure I.2 shows a schematic representation of a firm network augmented by one representative household.

2 Competitive equilibrium

Equilibrium in physics corresponds to the balancing of forces leading to idle or constant-velocity bodies. In economics, these forces are replaced by fluxes of goods that should be balanced at equilibrium. The first equilibrium condition is known as *market clearing*: at equilibrium, the entirety of production must be sold either to other firms or to the household. The second condition is that of *maximum profits*: at equilibrium, firms maximize their profits under the market clearing condition. Note that this second condition is not equivalent to null profits at equilibrium (which would balance money fluxes) except when return to scales are constant. In the present manuscript, and in the worked we published in [1], we propose a different definition of equilibrium having in mind the possible dynamical processes needed to reach it, along with the idea that forces must balance at equilibrium.

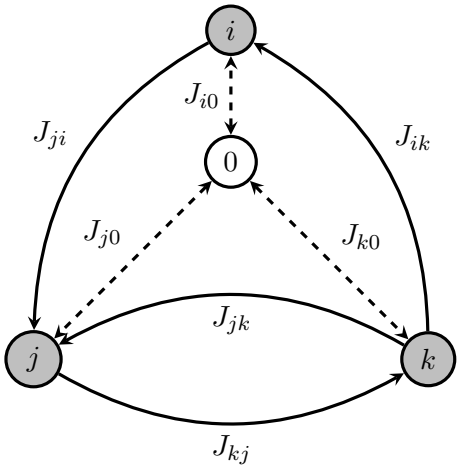


Figure I.2: Schematic representation of a network of 3 firms and one household. The household supplies work and consumes goods through the links $f \dashleftarrow\dashrightarrow 0$, $f \in \{i, j, k\}$. The coefficient J_{f0} measures the amount of working hours needed by firm f in its production. Firms can also buy goods from each other through the links $f \longleftarrow f'$, and the coefficient $J_{ff'}$ measures the amount of goods f' needed by f for production.

2.1 Competitive equilibrium under uncertainty

Given prices p_i of the goods and wage p_0, the profit π_i of firm i can be written as

$$\pi_i = \sum_{j=0}^{N} x_{ji} p_i - \sum_{j=0}^{N} x_{ij} p_j \equiv \mathscr{G}_i - \sum_{j=0}^{N} x_{ij} p_j, \tag{I.14}$$

where $\mathscr{G}_i$ denotes the total proceeds of the future sales ("gains"), $x_{i0} := \ell_i$ the working hours provided by the household and $x_{0i} := C_i$ is the consumption of good i by the households. Now, the textbook protocol at this stage is to impose that firms maximize their profit *assuming* that markets will clear, so that all that is produced will be sold, hence

$$\mathscr{G}_i \equiv y_i p_i. \tag{I.15}$$

Using the production function (I.4), profit maximization by firm i then leads to the optimal quantities of input goods x_{ij} and optimal production $z_i \gamma_i$. Note that when $b = 1$, the corresponding solution leads to profits that are zero in equilibrium, but they are strictly positive when $b < 1$, corresponding to imperfect competition in that case.

We take another stance and depart from the standard definition of equilibrium in two ways:

1. Since we do not assume that markets clear at each time step, firms can only compute the optimal input quantities $\widehat{x}_{ij}$ required to reach a certain production target $\widehat{y}_i := z_i \widehat{\gamma}_i$. Since firms do not know in advance how much of their production they will be able to sell (and consequently how much they will earn), the only lever

on which they can act is the cost term that they attempt to minimize. The process yielding the specific target value $\widehat{\gamma}_i$ will be specified in Part II.

2. We assume that our firm network is competitive in the sense that enough firms sell similar goods to drive profits down to zero at equilibrium. An explicit description of such a competitive process would entail introducing a time dependent network where firms rewire towards cheaper suppliers. We will also briefly discuss this process in Part II.

2.1.1 Step 1: Cost-minimizing inputs

More explicitly, the cost-minimizing input quantities are such that

$$\widehat{x}_{ij} = \begin{cases} \underset{x_{ij}}{\arg\min} \sum_{j=0}^{N} x_{ij} p_j \\ \text{subject to } \left(\sum_{j=0}^{N} a_{ij} \left(\frac{x_{ij}}{J_{ij}} \right)^{-1/q} \right)^{-bq} = \widehat{\gamma}_i. \end{cases} \tag{I.16}$$

Within the CES framework, this leads to

$$\widehat{x}_{ik} = a_{ik}^{q\zeta} J_{ik}^{\zeta} \left(\sum_j a_{ij}^{q\zeta} J_{ij}^{\zeta} \left(\frac{p_j}{p_k} \right)^{\zeta} \right)^{q} \widehat{\gamma}_i^{1/b}, \tag{I.17}$$

with $\zeta = (1+q)^{-1}$. In the Leontief case with $b = 1$, this boils down to

$$\widehat{x}_{ik} = J_{ik} \widehat{\gamma}_i, \tag{I.18}$$

which amounts to buying no more than the minimum amount needed to reach the target. In the Cobb-Douglas case with $b = 1$, we get

$$\widehat{x}_{ik} = a_{ik} p_k^{-1} \prod_{\substack{j=0 \\ J_{ij} \neq 0}}^{N} \left(\frac{J_{ij}}{a_{ij}} p_j \right) \hat{\gamma}_i, \tag{I.19}$$

where substitutability is measured through the ratios p/a. For any value of q and b, we see that cost-minimizing input quantities can be expressed through the $2N$ variables p_i and $\widehat{\gamma}_i$.

2.1.2 Step 2: Market clearing and competitive prices

We then obtain equilibrium prices and productions by assuming perfect competition, i.e. null profits $\pi_i = 0$ for all firms (step 2), and perfect market clearing. These conditions can be written for each firm i as

$$\sum_{j=0}^{N} x_{eq,ji} p_{\mathrm{eq},i} - \sum_{j=0}^{N} x_{eq,ij} p_{\mathrm{eq},j} = 0, \tag{I.20a}$$

$$y_{\mathrm{eq},i} - C_{\mathrm{eq},i} - \sum_{j=1}^{N} x_{\mathrm{eq},ji} = 0, \tag{I.20b}$$

where C_i is the household demand for good i. They furnish $2N$ equations on the $2N$ variables $p_{\mathrm{eq},i}$ and $\gamma_{\mathrm{eq},i} := \widehat{\gamma}_{eq,i}$ [2] if one uses the relationships derived above for $x_{eq,ij} = \widehat{x}_{eq,ij}$ [2].

Except when return to scales are constant ($b = 1$), the above two-step procedure is *not* equivalent to the standard profit maximization where market clearing is assumed from the start, which allows firms to know their gains in advance and include them in the optimization program. Indeed, the standard definition of competitive equilibrium requires *maximum profits*. Whenever $b \neq 1$, this maximum is different from 0 since one maximizes a functional of y_i consisting in a sum of a concave or convex part (depending on whether return to scales are decreasing or increasing) and a linear part.

Finally, consumption *a priori* depends on prices. As long as the consumption is only a function of prices, the specific relationship is not important to establish the equilibrium equations, but we will assume that it takes the form of Eq. (I.13).

2.1.3 Equilibrium conditions on prices and productions

Imposing market clearing, production target and real production must be equal at equilibrium. This allows us to write closed form equations on prices and productions for $q < \infty$ (see Appendix B for a derivation)

$$\begin{aligned} \mathbf{M}{\mathbf{p}_{\mathrm{eq}}}^{\zeta} &= \mathbf{V} + \mathbf{z}^{\zeta} \circ {\mathbf{p}_{\mathrm{eq}}}^{\zeta} \circ \left(1 - {\boldsymbol{\gamma}_{\mathrm{eq}}}^{\zeta \frac{b-1}{b}}\right) \\ \mathbf{M}^{\top} \boldsymbol{\Delta} \left(\mathbf{z}^{q\zeta} {\mathbf{p}_{\mathrm{eq}}}^{q\zeta}\right) {\boldsymbol{\gamma}_{\mathrm{eq}}}^{\zeta \frac{bq+1}{b}} &= \mathbf{C}_{\mathrm{eq}} + \mathbf{z} \circ {\mathbf{p}_{\mathrm{eq}}}^{q\zeta} \circ {\boldsymbol{\gamma}_{\mathrm{eq}}}^{\zeta \frac{bq+1}{b}} \left(1 - {\boldsymbol{\gamma}_{\mathrm{eq}}}^{\zeta \frac{b-1}{b}}\right), \end{aligned} \tag{I.21}$$

where $\zeta = (1+q)^{-1}$, $V_i = p_0 J_{i0}$ and $\circ$ denotes the term-wise (Hadamard) vector or matrix product. The Cobb-Douglas case requires more care and a better specification of the relationships between consumption and prices (see Appendix B for a derivation in the case of an inverse relationship between prices and consumption). We also introduced a matrix $\mathbf{M}$ that we will call the *network matrix* and which is expressed by

$$M_{ij} = z_i^{\zeta} \delta_{ij} - a_{ij}^{q\zeta} J_{ij}^{\zeta}. \tag{I.22}$$

This matrix relates the ability of firms to convert inputs into outputs (through productivity factors z_i) with the network needs J_{ij} weighted by substitutability factors. In the Leontief case, the matrix is simpler and reads

$$M_{ij} = z_i \delta_{ij} - J_{ij},$$

which only takes into account the network needs, while in the Cobb-Douglas case, substitutability prevails

$$M_{ij} = \delta_{ij} - a_{ij}.$$

[2] At equilibrium, market clearing implies perfect balance between supply and demand, between work supply and work demand as well as between consumption and budget. No shortages of any kind occur at equilibrium which implies that cost-minimizing inputs are equal to actually exchanged quantities, i.e. $x_{eq,ij} = \widehat{x}_{eq,ij}$. As a corollary, production targets are reached, i.e. $\gamma_{\mathrm{eq},i} := \widehat{\gamma}_{eq,i}$.

3 Positive equilibrium and Hawkins-Simons condition

Whether the economy is at equilibrium or evolving according to some dynamical process, prices and productions must remain positive to make sense. This positivity condition is not obviously guaranteed by Eqs. (I.21) and this section is devoted to the conditions under which an admissible positive equilibrium exists.

3.1 Constant return to scales

The first and easiest situation to look at is that of constant return to scale $b = 1$. We will also focus on the Leontief limit $q \to 0^+$ since results are qualitatively similar in the CES case (see [24]). In this limit, equilibrium equations become linear

$$\begin{aligned} \mathbf{M}\mathbf{p}_{\text{eq}} &= \mathbf{V} \\ \mathbf{M}^\top \boldsymbol{\gamma}_{\text{eq}} &= \mathbf{C}_{\text{eq}}. \end{aligned} \tag{I.23}$$

Regardless of the relationship between prices and consumption (once again as long as consumption is only price dependent), these equations can be solved in cascade, i.e. solving the first one and injecting the results into the second one. As long as $\mathbf{M}$ is invertible, the solutions are straightforward and read

$$\begin{aligned} \mathbf{p}_{\text{eq}} &= \mathbf{M}^{-1}\mathbf{V} \\ \boldsymbol{\gamma}_{\text{eq}} &= \left(\mathbf{M}^\top\right)^{-1} \mathbf{C}_{\text{eq}}. \end{aligned} \tag{I.24}$$

The positivity condition is guaranteed if the matrix $\mathbf{M}$ is a so-called *M-matrix*. Our network matrix has negative off-diagonal elements $-J_{ij}$ ($-a_{ij}^{q\zeta} J_{ij}^{\zeta}$ in the general case) and positive diagonal elements z_i (z_i^{ζ} in the general case). Owing to this particular shape, $\mathbf{M}$ is an M-matrix if and only if all of its eigenvalues have positive real parts (see [82]). Furthermore, we can also use a theorem paramount to that of Perron-Frobenius to show that the smallest eigenvalue (in modulus) of $\mathbf{M}$ is real, simple and associated to a full positive eigenvector. Calling ε this eigenvalue, the positivity condition can be rewritten as

$$\mathbf{p}_{\text{eq}},\, \boldsymbol{\gamma}_{\text{eq}} > 0 \iff \varepsilon > 0. \tag{I.25}$$

The different results about M-matrices are reported in [82] and the previous condition is known as the Hawkins-Simons (HS) condition [83] in economics. Eq. I.25 is the equivalent of the HS condition in the context of network economies which has been revisited in [24].

To understand this condition, we give the following example. Consider an economy where productivity factors are homogeneous $z_i := z$ and where the number of in/out links is fixed to some value d (the subsequent network is called d-regular). The network matrix is therefore

$$\mathbf{M} = z\mathbf{I}_N - \mathbf{J},$$

where $\mathbf{I}_N$ is the identity matrix. Assuming unit weights, we have $\sum_{j=1}^{N} J_{ij} = d$ since the number of in links is fixed to d. Therefore, d is an eigenvalue of $\mathbf{J}$ associated to the

eigenvector $\mathbf{e} = (1, \dots, 1)^\top$. This eigenvalue is the top eigenvalue of $\mathbf{J}$ and we can use it to express ε

$$\varepsilon = z - d.$$

The HS condition then translates into $z > d$: firms' ability to transform inputs into outputs (the productivity factor z) must be large enough with respect to input needs (here the connectivity d).

As a consequence, as soon as $\varepsilon \leq 0$, admissible economic equilibrium ceases to exist, rendering invalid one of the founding hypothesis of standard economics. Furthermore, one defining feature of the economy (the equilibrium) is dramatically different whether the economy is above or below the point $\varepsilon_c = 0$. This points therefore constitutes an *economic critical point*, and we retrieve the instability point theorized by Bak et al. [19] that we mentioned in the introduction and whose implications will be discussed in Section 4.

3.2 Non-constant return to scales

Of course, the picture is a lot more complex when dealing with non-constant return to scales $b \neq 1$. In the general case, Eqs. (I.21) constitute a set of $2N$ non-linear coupled algebraic equations about which very little can be said. Although some conditions could be found in [84] for instance, a complete characterization of the solutions is not possible yet.

3.2.1 Large productivity regime

A first interesting limit to consider is the large productivity limit $\varepsilon \to \infty$. This limit coincides with very large productivity factors or equivalently negligible network effects. To express prices and productions in this limit, we therefore set $J_{ij} = 0$ in Eqs. (I.21) and get for all i

$$z_i^\zeta p_{\mathrm{eq},i}^\zeta \gamma_{\mathrm{eq},i}^{\zeta\frac{b-1}{b}} = V_i \tag{I.26a}$$

$$z_i p_{\mathrm{eq},i}^{q\zeta} \gamma_{\mathrm{eq},i}^{1/b} = C_{eq,i}. \tag{I.26b}$$

Using the relationship $C_{eq,i} = \kappa_i / p_{\mathrm{eq},i}$ where κ_i depends on the parameters of the utility function, we therefore get the solutions

$$p_{\mathrm{eq},i} = \frac{V_i^{x/\zeta}}{z_i \kappa_i^{b-1}} \tag{I.27a}$$

$$\gamma_{\mathrm{eq},i} = \left(\frac{\kappa_i}{V_i}\right)^b, \tag{I.27b}$$

with $x = 1 - \zeta(b-1)(q-1)$. In this regime, regardless of the values of the elasticity of substitution q or return to scale b, equilibrium is always positive. This reinforces the point made in the previous section: interactions are a vector of instabilities in network economies.

3.2.2 Linear shift to the Hawkins-Simons transition

A second interesting limit is $b = 1 - \delta$ with $|\delta| \ll 1$, i.e. return to scales close to constant but not quite. We expect that the transition from existence to non-existence of equilibrium gets shifted with δ. To illustrate this shift, let us consider homogeneous productivity factors $z_i = z$ along with a symmetric network J_{ij} (for a more general computation, see Chapter II). We denote by $(\rho_\nu)_{\nu=1,\dots,N}$ the eigenvalues of $\mathbf{J}$ ordered such that ρ_N corresponds to the top Perron-Frobenius eigenvalue. Eigenvectors are denoted by $\mathbf{e}_\nu$ with $\mathbf{e}_N$ full, i.e. without elements equal to zero, and positive. Finally, the relationship between prices and production is given by

$$C_i = \frac{\mu_i}{p_i}, \tag{I.28}$$

which results from the maximization of a log-utility function by the household (see Chapter II).

Writing $\mathbf{x}_{eq} = \mathbf{x}_{eq}^{(0)} + \delta\, \mathbf{x}_{eq}^{(1)}$ for any quantity $\mathbf{x}$, we can δ-expand the equation on prices from (I.21) to get

$$\mathbf{M}\mathbf{p}_{\rm eq}^{(1)} = z\mathbf{p}_{\rm eq}^{(0)} \log \boldsymbol{\gamma}_{\rm eq}^{(0)}, \tag{I.29}$$

where any function of a vector is to be understood as acting component-wise. Now, we need to take the limit $\varepsilon = z - \rho_N \to 0^+$ in the previous equation to assess the shift introduced by δ in the positivity of $\mathbf{p}_{\rm eq}$. It is easy to see that

$$\mathbf{M}^{-1} \underset{\varepsilon\to 0}{\sim} \frac{1}{\varepsilon}\mathbf{e}_N\mathbf{e}_N^\top \tag{I.30}$$

resulting into

$$\mathbf{p}_{\rm eq}^{(0)} \underset{\varepsilon\to 0}{\sim} \frac{1}{\varepsilon}(\mathbf{e}_N^\top\mathbf{V})\mathbf{e}_N \tag{I.31}$$

$$\boldsymbol{\gamma}_{\rm eq}^{(0)} \underset{\varepsilon\to 0}{\sim} \frac{\mathbf{e}_N}{(\mathbf{e}_N^\top\mathbf{V})}. \tag{I.32}$$

Injecting these into Eq. (I.29), we get for $\mathbf{p}_{\rm eq}^{(1)}$

$$\mathbf{p}_{\rm eq}^{(1)} \underset{\varepsilon\to 0}{\sim} (\mathbf{e}_N^\top\mathbf{V})\frac{\rho_N}{\varepsilon^2}\left(\sum_{i=1}^N e_{N,i}\ln\frac{e_{N,i}}{\mathbf{e}_N^\top\mathbf{V}}\right)\mathbf{e}_N. \tag{I.33}$$

A first order condition for the positivity of prices can be obtained by equating $\mathbf{p}_{\rm eq}^{(0)} + \delta\mathbf{p}_{\rm eq}^{(1)}$ to 0 and yields

$$\varepsilon_c(\delta) \underset{\delta\to 0}{\sim} -\delta\rho_N\left(\sum_{i=1}^N e_{N,i}^2\ln\frac{e_{N,i}}{\mathbf{e}_N^\top\mathbf{V}}\right). \tag{I.34}$$

In the case where $\mathbf{J}$ accounts for a symmetric d-regular network, we get the simple condition

$$\varepsilon_c(\delta) \underset{\delta\to 0}{\sim} \delta d\ln\sum_{i=1}^N V_i,$$

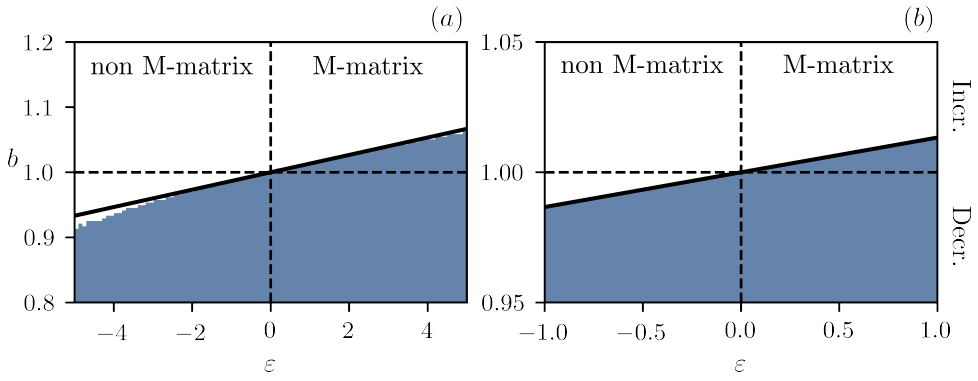


Figure I.3: (a) Region of existence of an admissible economic equilibrium for a directed 15-regular network on $N = 50$ firms as a function of return to scale b and ε. The work vector V_i is uniformly drawn between 1 and 5. The region where $p_{\mathrm{eq},i}, \gamma_{\mathrm{eq},i} > 0$ for all i is represented in blue-gray. (b) shows a close-up of (a) onto the regions $b \sim 1$ and $\varepsilon \sim 0$. The black line shows the linear approximation from Eq. (I.34) which aligns with numerical simulations. Finally, note that if $b = 1$, an admissible equilibrium exists whenever $\mathbf{M}$ is an M-matrix, i.e. whenever $\varepsilon > 0$ as expected.

which is reported in Figure I.3. Decreasing return to scale ($\delta < 0$) lowers the threshold below which equilibrium disappears and therefore stabilizes the network. At least at linear level, b does not qualitatively change the HS transition, and we will therefore restrict ourselves to $b = 1$ in the following, except when stated otherwise.

3.3 Parallel with ecological equilibria

The existence of an admissible positive equilibrium relates to the broader question of the existence of positive solutions to a set of equations. Whenever the equations are non-linear, very little is known except in some specific cases [84]. The linear case (corresponding to constant return to scales $b = 1$ in our case) has drawn a lot of attention in the context of ecological equilibria. Consider the generalized Lotka-Volterra equations that account for the dynamics of the populations $N_i(t)$ of interacting species, namely

$$\frac{\mathrm{d}N_i}{\mathrm{d}t} = N_i \left(1 - N_i - \sum_{j \neq i} \alpha_{ij} N_j \right). \tag{I.35}$$

The interaction matrix $\boldsymbol{\alpha}$ describes how species may cooperate $\alpha_{ij} > 0$ or hinder $\alpha_{ij} < 0$ one another. Equilibrium is reached whenever species populations reach stationary values $N_i^\star$ that are obtained through

$$(\mathbf{I}_N + \boldsymbol{\alpha})\, \mathbf{N}^\star = \mathbf{e}, \tag{I.36}$$

with $\mathbf{e} = (1, \ldots, 1)^\top$. A realizable equilibrium requires that $N_i^\star \geq 0$ which amounts to $\mathbf{I}_N + \alpha$ being an M-matrix. Since interactions between species are hard to capture, α

is usually considered random to allow statistical treatment (an idea first introduced by Wigner and Dyson to explain the level spacing of heavy nuclei [85, 86]). Depending on its properties (distribution of elements, sparsity...) positive solutions may or may not exist leading to interesting phase transitions, see for instance [87].

4 Self-organized criticality in firm networks

The idea of Bak et al. [19] that economies sit close to a point of instability can prompt criticisms. In light of the previous section, the instability point in question would be the $\varepsilon_c = 0$ threshold around which economic equilibrium exists or not. A natural question would be: why would the economy sit close to such a point, since virtually any value of ε is possible? This question is actually more general. In any complex systems, critical phenomena occur at very specific values in parameter space, and it is not at all obvious why parameters should be close to these instability points.

To assess this criticism, we must turn to a dynamical framework where parameters are allowed to evolve. With simple heuristics, one is generally able to explain why some systems should *self-organize* such that the relevant parameters are drawn towards instability points. In the context of network economies, an in depth discussion of this point can be found in [24] but we expose in this section an intuitive argument pointing towards a self-organization around $\varepsilon_c = 0$.

Consider an economy comprising N firms with productivity factors z_i interacting on a network J_{ij}. Let us introduce a new firm with productivity factor $z_\star$ and in/out links $J_{\star i}, J_{i\star}$. One can write the equilibrium condition on $p_\star$

$$p_\star = \frac{V_\star}{z_\star} + \sum_{i=1}^{N} \frac{J_{\star j}}{z_\star} p_j,$$

and plug this equation into the equilibrium equation for the N original firms. With some rearranging, we get

$$\left(z_i - \frac{J_{i\star} J_{\star i}}{z_\star} \right) p_i - \sum_{j=1}^{N} \left(J_{ij} + \frac{J_{i\star} J_{\star j}}{z_\star} \right) p_j = V_i + \frac{J_{i\star} V_\star}{z_\star}. \tag{I.37}$$

Effectively, original productivity factors decrease $z_i \to z_i - \frac{J_{i\star} J_{\star i}}{z_\star}$ while network needs increase $J_{ij} \to J_{ij} + \frac{J_{i\star} J_{\star j}}{z_\star}$. This leads to a decrease in ε which pushes the economy towards the critical point. As a consequence, growing economies can only be drawn towards the instability point with time. Similar arguments can be crafted regarding an increase in the connectivity of the most connected firms of the network (which renders the economy more unstable); or regarding the increase of the global interconnectivity of the network [88]. These arguments rely on dynamical processes underlying network formation. As we mentioned before, such processes will be briefly discussed in Part II but is not at the heart of the work discussed in this manuscript.

5 Conclusion

The key point of this chapter is the notion of feasible and unfeasible economies. Whenever economies are inefficient in converting inputs into outputs, an equilibrium with positive prices and productions ceases to exist. In the case of constant return to scale, the sign of the smallest eigenvalue ε of the network matrix

$$M_{ij} = z_i^\zeta \delta_{ij} - a_{ij}^{q\zeta} J_{ij}^\zeta, \tag{I.38}$$

determines whether economies are feasible ($\varepsilon > 0$) or not ($\varepsilon < 0$). This transition is the analogous to the Hawkins-Simons transition in the context of network economies [24].

Furthermore, heuristic arguments concerning the modifications of links in firm networks allow us to surmise that large economies sit close to the critical value $\varepsilon_c = 0$: adding extra firms or increasing connectivity tend to lower ε. With real economies containing numerous firms (around 5 million in the US, for instance) and with power-law distribution for in/out-links degree, the idea of *self-organized criticality* seems to be a good avenue to follow in order to account for excess volatility at aggregate levels. Indeed, as we will see in the next chapters, the HS transition translates into a dynamical transition that increases the volatility of outputs.

Finally, this transition is yet another example that a standard hypothesis in economic textbooks is actually invalid: equilibrium might not exist and equilibrium economies therefore cannot make sense in the general case. This calls for an *out-of-equilibrium* description of economies that we will attempt in the following chapters of this manuscript.

Key takeaways

- **Firms** produce a single good in quantity y_i and sells it at price p_i. They transform input quantities x_{ij} into outputs through the production function

$$y_i = z_i \left(\min \left[\frac{\ell_i}{J_{i0}}, \min_j \left(\frac{x_{ij}}{J_{ij}} \right) \right] \right)^b,$$

  where z_i is the productivity factor and J_{ij} the weighted input-output network elements measuring the need of good j in i's production.

- **Households** are considered representative. They consume a quantity C_i and work ℓ_i for each firm. Labor market clearing imposes that $\sum_i \ell_i = L_0$ where L_0 is the total amount of work supplied (and fixed) by the household. Consumption is then obtained through utility maximization, upon imposing a constraint on budget.

- **The Hawkins-Simons transition (network setting)** refers to the existence (or not) of positive prices and productions at competitive equilibrium. For constant return to scale, positive solutions to the equilibrium equations exist whenever

$$\varepsilon > 0,$$

  with ε the smallest eigenvalue of the network matrix $M_{ij} = z_i \delta_{ij} - J_{ij}$. Small enough increasing or decreasing return to scale $b = 1 \pm \delta$, linearly shifts the value of the threshold ε_c.

- **Self-organized criticality** refers to the capacity of complex systems to drive themselves towards a critical point. For firm networks, the value of ε decreases as both the number of firms and their connectivity increases. Large economies are therefore prone to being unstable.

A Optimizations

In this appendix, we detail the computations leading to the optimal quantities $\widehat{x}_{ik}$ of Eq. (I.17) as well as consumption and labor Eqs. (I.13).

A.1 Household

The household maximizes the utility function (I.11) under the budget constraint $p_0 L = \sum_i p_i C_i$. Introducing the Lagrange multiplier $\mu/(p_0 L_0)$, we differentiate $\mathcal{U}$ we respect to both C_i and L

$$\begin{aligned}\frac{\partial \mathcal{U}}{\partial C_i} &= \frac{\theta_i}{C_i} - \mu p_i \\ \frac{\partial \mathcal{U}}{\partial L} &= -L_0^{-1-\varphi} L^{\varphi} + \mu/L_0.\end{aligned}$$

Setting both partial derivative to zero then yields

$$\begin{aligned}C_i &= L_0 \frac{\theta_i p_0}{\mu p_i} \\ L &= L_0 \mu^{1/\varphi}.\end{aligned}$$

The parameter μ can be found using the budget constraint and reads

$$\mu = \sum_j \theta_j.$$

A.2 Firms

Using the same reasoning as in the previous section, we introduce a Lagrange multiplier λ enforcing the constraint

$$\widehat{\gamma}_i = \gamma_i := \left(\sum_j a_{ij} \left(\frac{x_{ij}}{J_{ij}} \right)^{-1/q} \right)^{-bq}.$$

We compute the partial derivatives of the cost terms $\mathcal{C}_i$ with respect to input quantities

$$\frac{\partial \mathcal{C}_i}{\partial x_{ik}} = p_k - \lambda b a_{ik} J_{ik}^{1/q} x_{ik}^{-1/q\zeta} \gamma_i^{(bq+1)/bq}.$$

Setting the left-hand side to zero, we get

$$\widehat{x}_{ik} = \left(\frac{b\lambda a_i k}{p_k J_{ik}^{-1/q}} \right)^{q\zeta} \widehat{\gamma}_i^{\zeta(bq+1)/b}.$$

Finally, we use the constraint to express λ

$$\widehat{\gamma}_i = \left(\sum_j a_{ij} J_{ij}^{-1/q} \left(\frac{b\lambda a_{ij}}{p_j J_{ij}^{-1/q}} \right)^{-\zeta} \widehat{\gamma}_i^{-\zeta(bq+1)/bq} \right)^{-bq},$$

leading to

$$b\lambda = \left(\sum_j a_{ij}^{q\zeta} J_{ij}^{\zeta} p_j^{\zeta} \right)^{1/\zeta} \widehat{\gamma}_i^{(1-b)/b},$$

and finally

$$\widehat{x}_{ik} = a_{ik}^{q\zeta} J_{ik}^{\zeta} p_k^{-q\zeta} \left(\sum_j a_{ij}^{q\zeta} J_{ij}^{\zeta} p_j^{\zeta} \right)^{q} \widehat{\gamma}_i^{1/b}.$$

B General equilibrium conditions

In this appendix, we show the computations that lead to the equilibrium equations on prices and production levels in the case of a general CES production function and a non-constant return to scale b. To alleviate notations, we will denote by Λ_{ij} the matrix elements

$$\Lambda_{ij} = a_{ij}^{q\zeta} J_{ij}^{\zeta}, \quad M_{ij} = z_i^{\zeta} \delta_{ij} - \Lambda_{ij} \tag{I.39}$$

Note that matrix elements Λ_{ij} extend for $j = 0$ to account for labor. Finally, we will consider that consumption is inversely proportional to prices

$$C_i(t) = \frac{\mu_i}{p_i(t)}, \tag{I.40}$$

where μ_i are coefficients depending on the form of the log-utility function from which one deduces the inverse proportionality relationship. Remember that at equilibrium we have $\gamma_{\mathrm{eq},i} = \widehat{\gamma}_{eq,i}$ such that optimal quantities, given by Eq. (I.17)

$$\widehat{x}_{eq,ik} = \Lambda_{ik} p_{\mathrm{eq},k}^{-q\zeta} \left(\sum_j \Lambda_{ij} p_{\mathrm{eq},j}^{\zeta} \right)^{q} \widehat{\gamma}_{eq,i}^{1/b},$$

are equal to quantities that are actually exchanged, i.e. $x_{eq,ik} = \widehat{x}_{eq,ik}$. Finally, we will set the wage p_0 to 1 which amounts to rescaling all prices.

Since markets clear at equilibrium, i.e.

$$z_i \gamma_{\mathrm{eq},i} = \sum_{j=1}^{N} x_{\mathrm{eq},ji} + C_{\mathrm{eq},i}, \tag{I.41}$$

the gains realized by firm i are simply given by $z_i \gamma_{\mathrm{eq},i} p_{\mathrm{eq},i}$. The zero profit condition can therefore be rewritten as

$$z_i \gamma_{\mathrm{eq},i} p_{\mathrm{eq},i} = \sum_j x_{eq,ij} p_{\mathrm{eq},j}. \tag{I.42}$$

Eqs. (I.41)-(I.42) will be our starting point to compute the equilibrium conditions on prices and productions.

B.1 Case $q < +\infty$: Leontief and general CES

At equilibrium, we can deduce a nicer expression for the quantity $p^{\text{net}}_{\text{eq},i} = \sum_{j=0}^{N} \Lambda_{ij} p^{\zeta}_{\text{eq},j}$ intervening in (I.17). Using (I.42) we have

$$z_i p_{\text{eq},i} \gamma_{\text{eq},i} = \sum_j \Lambda_{ij} p^{\zeta}_{\text{eq},j} \left(p^{\text{net}}_{\text{eq},i}\right)^q \gamma^{1/b}_{\text{eq},i}$$

We can extract both $p^{\text{net}}_{\text{eq},i}$ and $\gamma^{1/b}_{\text{eq},i}$ from the sum and, after some rearanging, get

$$p^{\text{net}}_{\text{eq},i} = \left(z_i p_{\text{eq},i} \gamma^{\frac{b-1}{b}}_{\text{eq},i}\right)^{\zeta}.$$

Plugging this expression into (I.17), we deduce a neater expression for the exchanged quantities

$$x^{eq}_{ij} = z_i^{q\zeta} \Lambda_{ij} \left(\frac{p_{\text{eq},i}}{p_{\text{eq},j}}\right)^{q\zeta} \gamma^{\zeta \frac{bq+1}{b}}_{\text{eq},i}. \tag{I.43}$$

We express (I.43) back into the the zero profit condition to retrieve the first equilibrium equation

$$\begin{aligned}
&\forall i,\ z_i p_{\text{eq},i} \gamma_{\text{eq},i} - \sum_{j=1}^{N} p_{\text{eq},j} z_i^{q\zeta} \Lambda_{ij} \left(\frac{p_{\text{eq},i}}{p_{\text{eq},j}}\right)^{q\zeta} \gamma^{\zeta \frac{bq+1}{b}}_{\text{eq},i} = z_i^{q\zeta} \Lambda_{i0} p^{q\zeta}_{\text{eq},i} \gamma^{\zeta \frac{bq+1}{b}}_{\text{eq},i} \\
\iff &\forall i,\ z_i^{\zeta} p^{\zeta}_{\text{eq},i} \gamma^{\zeta \frac{b-1}{b}}_{\text{eq},i} - \sum_{j=1}^{N} \Lambda_{ij} p^{\zeta}_{\text{eq},j} = \Lambda_{i0} \\
\iff &\forall i,\ z_i^{\zeta} p^{\zeta}_{\text{eq},i} - \sum_{j=1}^{N} \Lambda_{ij} p^{\zeta}_{\text{eq},j} = \Lambda_{i0} + z_i^{\zeta} p^{\zeta}_{\text{eq},i} \left(1 - \gamma^{\zeta \frac{b-1}{b}}_{\text{eq},i}\right) \\
\iff &\mathbf{M} {\mathbf{p}_{\text{eq}}}^{\zeta} = \mathbf{V} + \mathbf{z}^{\zeta} \circ {\mathbf{p}_{\text{eq}}}^{\zeta} \circ \left(1 - {\boldsymbol{\gamma}_{\text{eq}}}^{\zeta \frac{b-1}{b}}\right),
\end{aligned}$$

and then in the market clearing condition to retrieve the second equilibrium equation

$$\begin{aligned}
&\forall i,\ z_i \gamma_{\text{eq},i} - \sum_{j=1}^{N} z_j^{q\zeta} \Lambda_{ji} \left(\frac{p_{\text{eq},j}}{p_{\text{eq},i}}\right)^{q\zeta} \gamma^{\zeta \frac{bq+1}{b}}_{\text{eq},j} = \frac{\kappa_i}{p_{\text{eq},i}} \\
\iff &\forall i,\ z_i \gamma_{\text{eq},i} p^{q\zeta}_{\text{eq},i} - \sum_{j=1}^{N} z_j^{q\zeta} \Lambda_{ji} p^{q\zeta}_{\text{eq},j} \gamma^{\zeta \frac{bq+1}{b}}_{\text{eq},j} = \frac{\kappa_i}{p^{\zeta}_{\text{eq},i}} \\
\iff &\forall i,\ z_i^{\zeta} \gamma_{\text{eq},i} z_i^{q\zeta} p^{q\zeta}_{\text{eq},i} - \sum_{j=1}^{N} \Lambda_{ji} z_j^{q\zeta} p^{q\zeta}_{\text{eq},j} \gamma^{\zeta \frac{bq+1}{b}}_{\text{eq},j} = \frac{\kappa_i}{p^{\zeta}_{\text{eq},i}} \\
\iff &\forall i,\ z_i^{\zeta} \gamma^{\zeta \frac{bq+1}{b}}_{\text{eq},i} z_i^{q\zeta} p^{q\zeta}_{\text{eq},i} - \sum_{j=1}^{N} \Lambda_{ji} z_j^{q\zeta} p^{q\zeta}_{\text{eq},j} \gamma^{\zeta \frac{bq+1}{b}}_{\text{eq},j} = \frac{\kappa_i}{p^{\zeta}_{\text{eq},i}} + z_i p^{q\zeta}_{\text{eq},i} \gamma^{\zeta \frac{bq+1}{b}}_{\text{eq},i} \left(1 - \boldsymbol{\gamma}^{\zeta \frac{b-1}{b}}_{\text{eq}}\right) \\
\iff &\mathbf{M}^{\top} \boldsymbol{\Delta} \left(\mathbf{z}^{q\zeta} {\mathbf{p}_{\text{eq}}}^{q\zeta}\right) {\boldsymbol{\gamma}_{\text{eq}}}^{\zeta \frac{bq+1}{b}} = \frac{\boldsymbol{\kappa}}{{\mathbf{p}_{\text{eq}}}^{\zeta}} + \mathbf{z} \circ {\mathbf{p}_{\text{eq}}}^{q\zeta} \circ {\boldsymbol{\gamma}_{\text{eq}}}^{\zeta \frac{bq+1}{b}} \left(1 - {\boldsymbol{\gamma}_{\text{eq}}}^{\zeta \frac{b-1}{b}}\right).
\end{aligned}$$

In the case where $q \to 0^+$ and $b = 1$, one can check that one retrieves Eq. (I.23).

B.2 Case $q = +\infty$: Cobb-Douglas

To get the equilibrium equations in the case $q = +\infty$, we need to first take this limit in (I.17). It yields

$$\begin{aligned}
\widehat{x}_{il} &= a_{il}^{q\zeta} J_{il}^{\zeta} p_l^{-q\zeta} \left(\sum_{j=0}^{N} a_{ij}^{q\zeta} J_{ij}^{\zeta} p_j^{\zeta} \right)^{q} \hat{\gamma}_i^{1/b} \\
&= a_{il}^{q\zeta} J_{il}^{\zeta} p_l^{-q\zeta} \left(\sum_{\substack{j=0 \\ J_{ij}\neq 0}}^{N} a_{ij}^{q\zeta} J_{ij}^{\zeta} p_j^{\zeta} \right)^{q} \hat{\gamma}_i^{1/b} \\
&\underset{q\to+\infty}{\approx} a_{il} p_l \hat{\gamma}_i^{1/b} \exp\left\{ q \ln \left(\sum_{\substack{j=0 \\ J_{ij}\neq 0}}^{N} a_{ij} \exp \zeta \ln \left[\frac{J_{ij}}{a_{ij}} p_j \right] \right) \right\} \\
&\underset{q\to+\infty}{\approx} a_{il} p_l^{-1} \hat{\gamma}_i^{1/b} \exp\left\{ q \ln \left(\sum_{\substack{j=0 \\ J_{ij}\neq 0}}^{N} a_{ij} + \zeta \sum_{\substack{j=0 \\ J_{ij}\neq 0}}^{N} \ln \left[\frac{J_{ij}}{a_{ij}} p_j \right] \right) \right\} \\
&\underset{q\to+\infty}{\approx} a_{il} p_l^{-1} \hat{\gamma}_i^{1/b} \exp\left\{ q \ln \left(1 + \zeta \sum_{\substack{j=0 \\ J_{ij}\neq 0}}^{N} \ln \left[\frac{J_{ij}}{a_{ij}} p_j \right] \right) \right\} \\
&\underset{q\to+\infty}{\approx} a_{il} p_l^{-1} \hat{\gamma}_i^{1/b} \exp\left\{ q\zeta \sum_{\substack{j=0 \\ J_{ij}\neq 0}}^{N} \ln \left[\frac{J_{ij}}{a_{ij}} p_j \right] \right\} \\
&\underset{q\to+\infty}{\approx} a_{il} p_l^{-1} \hat{\gamma}_i^{1/b} \prod_{\substack{j=0 \\ J_{ij}\neq 0}}^{N} \left(\frac{J_{ij}}{a_{ij}} p_j \right).
\end{aligned}$$

We can then express the quantity $z_i \gamma_{\mathrm{eq},i}^{\frac{b-1}{b}} p_{\mathrm{eq},i}$ through the zero profit condition as

$$z_i \gamma_{\mathrm{eq},i}^{\frac{b-1}{b}} p_{\mathrm{eq},i} = \prod_{\substack{j=0 \\ J_{ij}\neq 0}}^{N} \left(\frac{J_{ij}}{a_{ij}} p_{\mathrm{eq},j} \right). \tag{I.44}$$

Using the market clearing condition, we get the first equilibrium equation in the Cobb-Douglas

case

$$\begin{aligned}
&\forall i,\ z_i\gamma_{\mathrm{eq},i} = \frac{\kappa_i}{p_{\mathrm{eq},i}} + \sum_j a_{ji} p_{\mathrm{eq},i}^{-1} \gamma_{\mathrm{eq},j}^{1/b} \prod_{\substack{j=0\\ J_{ij}\neq 0}}^{N} \left(\frac{J_{ij}}{a_{ij}} p_{\mathrm{eq},j}\right) \\
\iff &\forall i,\ z_i\gamma_{\mathrm{eq},i}p_{\mathrm{eq},i} = \kappa_i + \sum_j a_{ji} z_j \gamma_{\mathrm{eq},j} p_{\mathrm{eq},j} \\
\iff &\left(\mathbf{I}_N - \mathbf{a}^\top\right) \mathbf{z} \circ \boldsymbol{\gamma}_{\mathrm{eq}} \circ \mathbf{p}_{\mathrm{eq}} = \boldsymbol{\kappa} \\
\iff &\mathbf{z} \circ \boldsymbol{\gamma}_{\mathrm{eq}} \circ \mathbf{p}_{\mathrm{eq}} = \left(\mathbf{I}_N - \mathbf{a}^\top\right)^{-1} \boldsymbol{\kappa}.
\end{aligned}$$

To get the second equation, we inject the previous result into Eq. (I.44) and take the logarithm. It reads

$$\begin{aligned}
&\forall i,\ \ln z_i\gamma_{\mathrm{eq},i}p_{\mathrm{eq},i} - \frac{1}{b}\ln\gamma_{\mathrm{eq},i} = \sum_{\substack{l=1\\ J_{il}\neq 0}}^{N} a_{il} \ln\frac{J_{il}}{a_{il}} + \sum_{\substack{l=1\\ J_{il}\neq 0}}^{N} a_{il}\ln p_{\mathrm{eq},i} \\
\iff &\forall i,\ \frac{b-1}{b}\ln\left[\left(\mathbf{I}_N - \mathbf{a}^\top\right)^{-1}\boldsymbol{\kappa}\right]_i + \frac{1}{b}\ln p_{\mathrm{eq},i} + \frac{1}{b}\ln z_i = \sum_{\substack{l=1\\ J_{il}\neq 0}}^{N} a_{il} \ln\frac{J_{il}}{a_{il}} + \sum_{\substack{l=1\\ J_{il}\neq 0}}^{N} a_{il}\ln p_{\mathrm{eq},i} \\
\iff &\left(\frac{1}{b}\mathbf{I}_N - \mathbf{a}\right)\ln\mathbf{p}_{\mathrm{eq}} = \frac{1-b}{b}\ln\left(\mathbf{I}_N - \mathbf{a}^\top\right)^{-1}\boldsymbol{\kappa} - \frac{1}{b}\ln\mathbf{z} + \mathbf{h}.
\end{aligned}$$

where $h_i = \sum_{\substack{l=1\\ J_{il}\neq 0}}^{N} a_{il}\ln\frac{J_{il}}{a_{il}}$.

In the Cobb-Douglas case, a positive equilibrium for prices and productions always exists. Indeed, looking at the second equation, one sees that a solution generically exists (except in the very specific case where b^{-1} is an eigenvalue of $\mathbf{a}$) for $\ln\mathbf{p}_{\mathrm{eq}}$. Exponentiating this solutions shows that $\mathbf{p}_{\mathrm{eq}}$ will always be positive. For the first equation, the matrix $\mathbf{I}_N - \mathbf{a}$ is always invertible since the eigenvalues λ of $\mathbf{a}$ are such that $|\lambda - a_{00}| = |\lambda| \leq \sum_{j=1}^{N} a_{ij} = 1 - a_{i0} < 1$ thanks to Gershgorin's theorem. This also proves that $\mathbf{I}_N - \mathbf{a}$ is in fact an M-matrix, which makes the solution of this equation positive, implying in turn that $\boldsymbol{\gamma}_{\mathrm{eq}}$ is also positive.

CHAPTER II

Weakly out-of-equilibrium economies

Abstract

This chapter reports our first attempt at endowing classical firm networks with out-of-equilibrium dynamics. A strand of the literature considers low-dimensional dynamical systems on a set of aggregate variables that are able to generate non trivial behavior, see [42, 43]. We propose here a more granular view with a set of reduced-form non-linear differential equations on prices and productions directly. They follow a set of heuristic rules which aim at reducing imbalances with respect to equilibrium. As it is the case with the Goodwin model [42], our equations are closely related to generalized Lotka-Volterra dynamics. The model displays a marginally stable dynamics as the economy reaches the Hawkins-Simons transition. The relaxation time of the system, i.e the time needed to reach back equilibrium (provided it exists) after a perturbation, becomes infinite close to the transition. This behavior increases the instabilities in the system as shocks can accumulate and therefore create excess volatility.

Adapted from: [1] Théo Dessertaine, José Moran, Michael Benzaquen, and Jean-Philippe Bouchaud. *Out-of-equilibrium dynamics and excess volatility in firm networks.* Journal of Economic Dynamics and Control, 138:104362, 2022.

1 Reduced-form differential equations: the Goodwin model

As an introduction to this chapter and to reduced-form differential equations, we begin with the well-known Goodwin model. This model was first introduced by Richard Goodwin in 1967 [42]. It aims at explaining economic fluctuations and cycles through redistribution of capital. Goodwin considered an economy with two agents: capitalists, which possess capital $k(t)$ at time t, and n workers, supplying a quantity $\ell(t)$ of work at time t. The production $y(t)$ is driven by both work and capital through

$$y(t) = \min(a(t)\ell(t), k(t)/\sigma),$$

where a and σ represent productivity of work and capital-to-production ratio respectively. Goodwin assumed that capital is used in its entirety at each time-step, therefore implying $k(t)/\sigma = a\ell(t) = y(t)$. Goodwin then considered a constant growth rate β of population, which allows to write an evolution equation for the share of employment $v = \ell/n$

$$\frac{\dot{v}}{v} = \frac{\dot{\ell}}{\ell} - \beta,$$

where $\dot{b} = db/dt$, for any time-dependent quantity b. In the same way, assuming constant growth rate α for productivity a yields

$$\frac{\dot{\ell}}{\ell} = \frac{\dot{y}}{y} - \alpha.$$

Furthermore, he also postulated that wages w are given by a Philips-curve-type relationship [89]

$$\frac{\dot{w}}{w} = \rho v - \gamma,$$

where ρ and γ are constant, and which also allows one to write the evolution of the share of workers in production $u = w\ell/y$

$$\frac{\dot{u}}{u} = \frac{\dot{w}}{w} - \alpha.$$

Finally, workers consume their entire salary, capital owners save a fraction s of their profits while capital is depreciated at rate δ. One can therefore write a final equation on capital

$$\frac{\dot{k}}{k} = s(1-u)y/k - \delta.$$

A lot of the previous equations are actually redundant and the model can be summarized through two constitutive equations

$$\dot{v} = v\left(\frac{s}{\sigma}(1-u) - \delta - \alpha - \beta\right) \tag{II.1}$$

$$\dot{u} = u\left(\rho v - \gamma - \alpha\right). \tag{II.2}$$

Interestingly, these equations are *mutatis-mutandi* Lotka-Volterra equations in the context of prey-predator dynamics. The simple Goodwin model is actually able to generate limit-cycles and *endogenous* economic fluctuations. The origin of these cycles is as follows: whenever labor share in production is low, investments – which is this case are comparable to profits – still allow for a steady growth, therefore increasing employment. As employment reaches its cap of available workers in the economy, salaries start to increase and profits increasingly go towards workers. Capital therefore decreases slowing down investment and overall growth which makes employment plummet. Therefore a cycle is generated through the interplay between capital owners, workers and the redistribution process.

Even though this model is simple and stylized, it sheds light on a mechanism that, not only surely happens in the real economy but can also be responsible for economic cycles. In physics, *toy-modelling* refers to this exact approach. Upon devising a model, one tries to strip away as much complexity as possible while still being able to observe some key mechanisms. In the following, we will take this stance by proposing a minimal model that can endogenously amplify economic fluctuations whenever close to the Hawkins-Simons transition.

2 Adjustment processes through behavioral rules of thumb

In this section, we introduce the set of rules that is the core of the different models that are described in this section and later in the manuscript. The equations we postulate are based on reasonable "rules of thumb" that firms are likely to use in real life conditions, see [90, 91, 37]. We draw inspiration from what physicists call "phenomenological approaches", based on symmetry, plausibility and dimensional arguments. As we have learnt from physics, general arguments can often be used to write down correct equations before the underlying foundations have been worked out. For example, the Navier-Stokes equations for fluid motion have been postulated in the XIXth century based on general arguments, 50 years before Boltzmann's statistical theory of molecular motion gave a solid, first principle justification of these equations.

2.1 Forces restoring equilibrium

Whereas in the economic equilibrium, as defined in the Chapter I, profits are zero and markets clear, out-of-equilibrium situations tautologically imply non zero profits and/or excess supply or demand. So we naturally introduce, for each firm, two indicators that measure the distance from equilibrium: $\mathscr{E}_i(t)$ is the excess production at time t (interpreted as unsatisfied demand if $\mathscr{E}_i(t) < 0$), and $\pi_i(t)$ the instantaneous profits or losses of the firm at time t.

Prices and productions must then adapt through some kind of adjustment process to reduce these imbalances:

- Faced with excess production, firms will lower prices to prop up demand, and/or reduce production to limit losses.
- Faced with excess demand, on the other hand, firms can consider increasing prices and/or increase production.
- Similarly, when profits are positive, firms may be tempted to increase production but at the same time competition, attracted by the prospect of a profit, should put pressure on prices.
- If profits are negative, firms will try to adapt by lowering production and increase prices, with the hope of better compensating production costs.

All these rules are common sense and it is hard to argue that they do not play a crucial role in real economies with boundedly rational agents. What is more debatable, however, is how to model them quantitatively. Throughout the manuscript, we further assume that restoring forces are all *linear* in $\mathscr{E}_i(t), \pi_i(t)$, at least when these imbalances are small enough. For the point that we want to make in this section, higher order terms would in any case be irrelevant since we will perform a linear analysis.

If only for dimensional reasons, all quantities determining price and production relative changes must appear as relative, non-dimensional quantities, i.e. ratios of $\mathscr{E}_i(t)$ to total production $y_i(t)$ and $\pi_i(t)$ to total possible sales $y_i(t)p_i(t)$. Hence we posit the following adjustment rules for prices and production

$$\log\left(\frac{p_i(t+\delta t)}{p_i(t)}\right) = \left(-\alpha\frac{\mathscr{E}_i(t)}{y_i(t)} - \alpha'\frac{\pi_i(t)}{p_i(t)y_i(t)}\right)\delta t \tag{II.3a}$$

$$\log\left(\frac{y_i(t+\delta t)}{y_i(t)}\right) = \left(\beta\frac{\pi_i(t)}{p_i(t)y_i(t)} - \beta'\frac{\mathscr{E}_i(t)}{y_i(t)}\right)\delta t, \tag{II.3b}$$

where δt is an elementary time step, and the parameters α, α', β, β' characterize the speed of adjustment in the face of imbalances. From our general arguments above, we expect that all these parameters are non-negative, i.e. that firm policies and market forces tend to dampen imbalances.

Of course, these parameters could depend on the firm i, with some firms choosing to be more aggressive than others in their adjustment policy. Throughout the present work we will stick to time-independent and firm-independent values for α, α', β, β'. Furthermore, one could imagine a version of the model where firms attempt to *learn* optimal values of these adjustment parameters, adding an extra level of complexity in the dynamical rules. The simple rules of Eqs. (II.3a, II.3b) are very similar in spirit to those used in several well studied Agent-Based Models – see [57, 61]. Note that $\alpha' > 0$ reflects our hypothesis that competition is at play in the economy, pushing prices down when profits are positive.

2.2 Competitive equilibrium as dynamical equilibrium

Although null profits and market clearing obviously imply from Eqs. (II.3a, II.3b) that prices and productions are time invariant, the converse is more subtle. Assume indeed that there exists quantities $p_i^\star$, $y_i^\star$, $\mathscr{E}_i^\star$ and $\pi_i^\star$ towards which prices, productions, and imbalances converge under the dynamics (II.3a, II.3b). These values should satisfy

$$\begin{aligned} -\alpha\frac{\mathscr{E}_i^\star}{y_i^\star} - \alpha'\frac{\pi_i^\star}{p_i^\star y_i^\star} &= 0 \\ -\beta'\frac{\mathscr{E}_i^\star}{y_i^\star} + \beta\frac{\pi_i^\star}{p_i^\star y_i^\star} &= 0 \end{aligned} \iff \begin{pmatrix} \alpha & \alpha' \\ \beta' & -\beta \end{pmatrix} \begin{pmatrix} \dfrac{\mathscr{E}_i^\star}{y_i^\star} \\ \dfrac{\pi_i^\star}{p_i^\star y_i^\star} \end{pmatrix} = \begin{pmatrix} 0 \\ 0 \end{pmatrix}. \tag{II.4}$$

If the matrix comprising adjustment speeds is non-singular, then the only solution is trivial and $\mathscr{E}_i^\star = \pi_i^\star = 0$ which coincides with the equilibrium defined in the previous section. The only way through which this matrix can be singular is by having $\alpha\beta + \alpha'\beta' = 0$.

Since α, α', β, β' are chosen to be positive, this happens only when at least one of the pairs (α, α'), (β, β'), (α, β') or (α', β) is equal to $(0, 0)$. In the first two cases, prices or productions are frozen in time, making the dynamical rules moot. In the last two cases, prices and productions are driven either only by profits or only be production surplus. The dynamics will converge towards a partial competitive equilibrium with only one of the two conditions of null profits or market clearing fulfilled. This is again not a satisfying choice of parameters, because it implies no reaction from the firms to either supply/demand imbalances or to profits/losses. Therefore, the stationary solutions associated with our dynamical rules coincide with competitive equilibrium for generic cases. Note that this is true even if Eqs.(I.21) have multiple solutions: the resting point of our behavioral rules would then coincide with one of them.

3 Dynamical system for Leontief economies

3.1 Expressing surplus and profits

Eqs. (II.3a, II.3b) may now be closed by expressing imbalances in terms of prices p_i and productions y_i, as

$$\pi_i(t) = p_i(t) \sum_{j=1}^{N} x_{ji}(t) + p_i(t) C_i(t) - \sum_{j=1}^{N} x_{ij}(t) p_j(t) - p_0(t) \ell_i(t) \tag{II.5a}$$

$$\mathscr{E}_i^c(t) = y_i(t) - \sum_{j=1}^{N} x_{ji}(t) - C_i(t), \tag{II.5b}$$

where once again $C_i(t)$ is the consumption of households, $\ell_i(t)$ the quantity of labor, and where we recall that we have restricted our analysis to constant return to scale Leontief production functions.

Note that here, we discard possible shortages in both work and supply. For instance firm i still supplies fully even if demands are too great. Accounting for shortages would require modifying the exchanged quantities in Eq. (II.5a) as

$$x_{ik}(t) \to x_{ik}(t) \min\left(1, \frac{y_k(t)}{\sum_{\ell=1}^{N} x_{\ell k}(t) + C_k(t)}\right),$$

for example [1]. We will not account for this point here but we will come back to it in Part II.

[1] As it will be discussed in Part II, this choice accounts for a proportional redistribution of goods whenever a firm is faced with defaulting supply. One could devise more general redistribution rules of the form

$$x_{ik}(t) \to x_{ik}(t)\, g_k\left(\frac{y_k(t)}{\sum_{\ell=1}^{N} x_{\ell k}(t) + C_k(t)}\right),$$

where g_k is a firm-dependent function such that $g_k(u) = 1$ whenever $u \geq 1$ and $g_k(u) < 1$ whenever $u < 1$.

We use a Leontief production function to express exchanged quantities $x_{ij} = J_{ij}\gamma_i$ and further express profits and surplus

$$\pi_i(t) = p_i(t)\sum_{j=1}^{N} J_{ji}\gamma_j(t) + p_i(t)C_i(t) - \sum_{j=1}^{N} J_{ij}\gamma_i(t)p_j(t) - V_i\gamma_i(t), \tag{II.6a}$$

$$\mathscr{E}_i(t) = z_i\gamma_i(t) - \sum_{j=1}^{N} J_{ji}\gamma_j(t) - C_i(t), \tag{II.6b}$$

where we recall that $V_i = J_{i0}p_0(t)$. Here again there is an inconsistency. Firms use goods $x_{ij}(t)$ bought at time t to produce $y_i(t)$. However, this production is also sold at time t to other firms. Causality is therefore violated since in principle goods cannot be sold before produced or vice versa. We will come back to this point at the end of the chapter and introduce a causal framework in Part II. Studying these equations is of course still enlightening since the fine-grained causal structure of the equations may not matter if one studies the system on longer time-scales.

We finally express both profits and surplus with the network matrix $M_{ij} = z_i\delta_{ij} - J_{ij}$

$$\pi_i(t) = \gamma_i(t)\left(\sum_{j=1}^{N} M_{ij}p_j(t) - V_i\right) - p_i(t)\left(\sum_{j=1}^{N} M_{ji}\gamma_j(t) - C_i(t)\right), \tag{II.7a}$$

$$\mathscr{E}_i(t) = \sum_{j=1}^{N} M_{ji}\gamma_j(t) - C_i(t), \tag{II.7b}$$

and one recognizes distances to equilibrium $\sum_j M_{ij}p_j(t) - V_i$ and $\sum_j M_{ji}\gamma_j(t) - C_i(t)$.

One must too model the consumption of households. For simplicity, we assume that households work full time, i.e. with Frisch index $\varphi = \infty$, and denote by L_0 the total amount of available labor supplied by the household. Consumption is obtained by saturating the current budget $p_0(t)L_0$ [2] to maximize a log-consumption utility, i.e.

$$\max_{C_i(t)} \sum_i \theta_i \log C_i(t) \qquad \text{with} \qquad \sum_i p_i(t)C_i(t) = p_0(t)L_0, \tag{II.8}$$

where θ_i is the preference for good i. The optimal consumption is then

$$C_i(t) = L_0\theta_i/\mu(t)p_i(t)$$

with $\mu(t) = \sum_i \theta_i/p_0(t)$ as we saw in Chapter I. For simplicity, we will assume constant unit wages (which amounts to a rescaling of prices at any time) along with $L_0 = 1$.

[2] Note that, in the absence of market clearing, the budget should be $p_0(t)\sum_i \ell_i(t)$ since $/sum_i\ell_i \neq L_0$ *a priori*.

Putting all these ingredients together and taking the continuous time limit $\delta t \to 0$ in (II.3) yields the following system of coupled non-linear ordinary differential equations

$$\frac{\mathrm{d}p_i}{\mathrm{d}t} = -(\alpha - \alpha')\frac{p_i(t)}{z_i\gamma_i(t)}\left(\sum_j M_{ji}\gamma_j(t) - C_i(t)\right) - \frac{\alpha'}{z_i}\left(\sum_j M_{ij}p_j(t) - V_i\right) \tag{II.9a}$$

$$\frac{\mathrm{d}\gamma_i}{\mathrm{d}t} = \beta\frac{\gamma_i(t)}{z_i p_i(t)}\left(\sum_j M_{ij}p_j(t) - V_i\right) - \frac{\beta + \beta'}{z_i}\left(\sum_j M_{ji}\gamma_j(t) - C_i(t)\right). \tag{II.9b}$$

These equations are slightly different from the ones presented in our article [1]. Indeed, in the published version, we assume that profits take their market clearing form

$$\pi_i(t) = p_i(t)y_i(t) - \sum_{j=1}^{N} x_{ij}(t)p_j(t),$$

which amounts to a redefinition of time-scales

$$\frac{\mathrm{d}p_i}{\mathrm{d}t} = -\widetilde{\alpha}\frac{p_i(t)}{z_i\gamma_i(t)}\left(\sum_j M_{ji}\gamma_j(t) - C_i(t)\right) - \frac{\widetilde{\alpha}'}{z_i}\left(\sum_j M_{ij}p_j(t) - V_i\right) \tag{II.10a}$$

$$\frac{\mathrm{d}\gamma_i}{\mathrm{d}t} = \widetilde{\beta}\frac{\gamma_i(t)}{z_i p_i(t)}\left(\sum_j M_{ij}p_j(t) - V_i\right) - \frac{\widetilde{\beta}'}{z_i}\left(\sum_j M_{ji}\gamma_j(t) - C_i(t)\right). \tag{II.10b}$$

In the following, we will consider this set of equations but we will omit the $\widetilde{(\cdot)}$ on time-scales for clarity. This set of reduced-form dynamical equations will be a naive candidate for weakly out-of-equilibrium dynamics in firm networks. Since they are non-linear and coupled, very few things can be said about their behavior and we will resort to numerical simulations in order to characterize them.

3.2 Simulations

Figure II.1 shows time-series for different values of time-scales α, β, α', β', network stability ε and initial conditions $p_i(0), \gamma_i(0)$. The most striking feature is the difference between large and low values of ε. As ε decreases, relaxation towards equilibrium seems to slow down for given values of α, β, α', β'. Furthermore, outputs seem to rapidly synchronize onto a single mode of oscillations or exponential dampening. As we will see, this is due to a separation of time-scales in the behavior of the stability matrix of the system as $\varepsilon \to 0$. Both features hint at a relationship between fading feasibility of the economy and diverging relaxation time which we are going to prove further down in this chapter. In addition, the relative value of time-scales seem to affect whether the subsequent dynamics will be oscillatory or not. Initial conditions, though affecting the aspect of time-series, do not seem to affect the outputs qualitatively. Very large initial conditions can however lead to diverging outputs.

As the Hawkins-Simons transition gets violated, i.e. $\varepsilon < 0$, no bounded trajectories have been found numerically. The associated non-economically-sound equilibrium is negative and the system, confined within the region of positive prices and outputs, blows up exponentially. This point is not satisfying and will be discussed further down in this chapter. We do not show the time-series since they bear little relevant information.

One must be particularly careful about spurious numerical effects when simulating Eqs. (II.9). Indeed, such differential equations fall into the category of so called *stiff* ordinary differential equations (ODE). They are characterized by an evolution governed by two (or more) very different timescales. For a dynamical system of the form of Eq. II.11, i.e.

$$\frac{\mathrm{d}\mathbf{U}(t)}{\mathrm{d}t} = \mathbb{D}\mathbf{U}(t),$$

we denote by σ_ν the eigenvalues of the matrix $\mathbb{D}$ (as in Appendix B). We call $\overline{\sigma}$ and $\underline{\sigma}$ the two eigenvalues such that

$$\forall \nu, \left|\mathfrak{Re}\left(\overline{\sigma}\right)\right| \geq \left|\mathfrak{Re}\left(\sigma_\nu\right)\right| \geq \left|\mathfrak{Re}\left(\underline{\sigma}\right)\right|,$$

i.e. respectively the *fastest* and *slowest* timescales of the system. The stiffness ratio is defined as

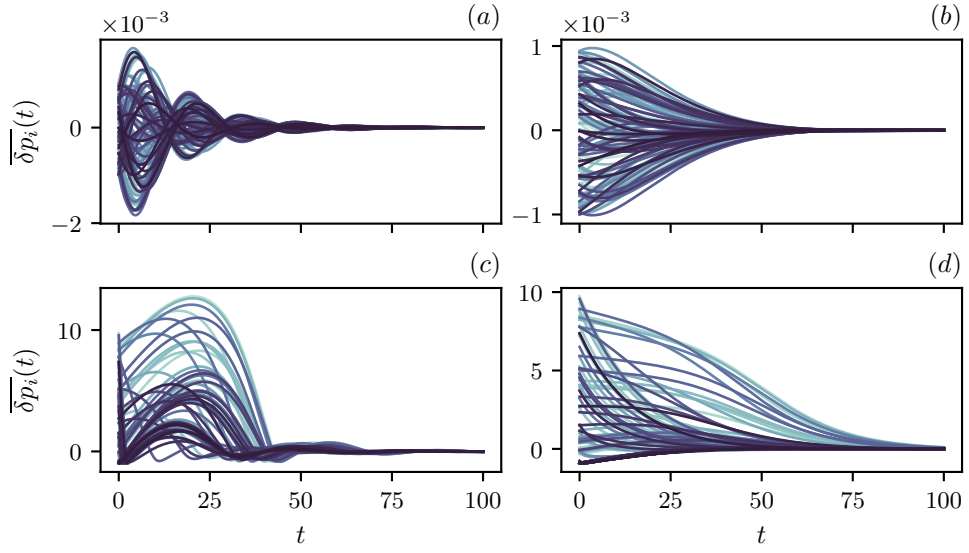
$$r = \frac{\left|\mathfrak{Re}\left(\overline{\sigma}\right)\right|}{\left|\mathfrak{Re}\left(\underline{\sigma}\right)\right|},$$

and the system is said to be stiff if this ratio is large. In our case, as $\varepsilon \to 0$, $\overline{\sigma}$ will remain finite whereas $\underline{\sigma}$ is of order ε making the stiffness ratio $r \sim \varepsilon^{-1}$ divergent (see Appendix B). Stiff ODEs require special care for their simulation. More precisely, one cannot use simple explicit integration routines with fixed step-size but rather implicit schemes such as Radau integration (see [92]).

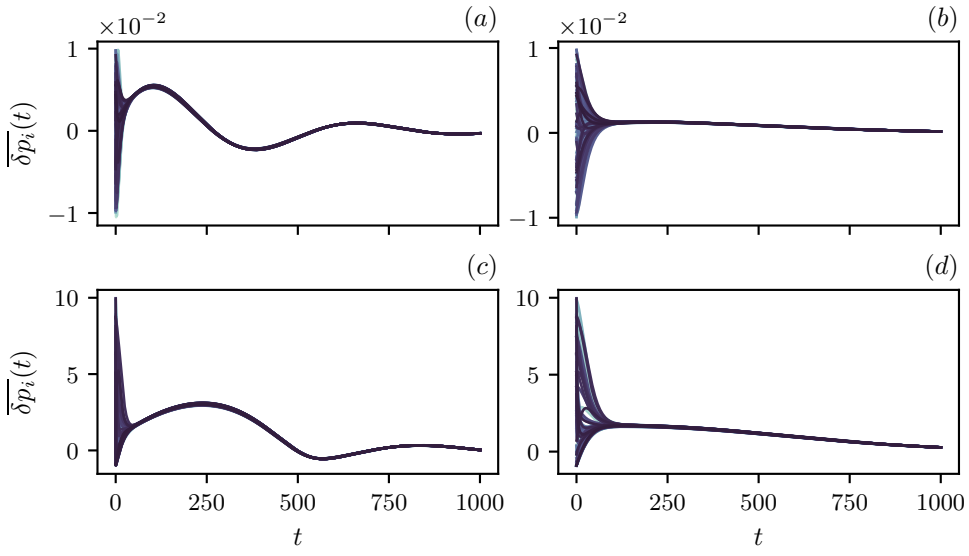
3.3 Parallel with generalized Lotka-Volterra equations

As mentioned previously, these equations bear a strong resemblance to generalized Lotka-Volterra models used in theoretical ecology by [93], where an ecosystem self-organizes into a configuration that is highly susceptible to amplify external perturbations. Newer extensions to such models, along the lines of [94], show that they can also explain anomalous, persistent fluctuations in the populations of the different species that make up an ecosystem. The different analogies linking the study of firm networks and ecosystem have also been fruitful in linking the notion of trophic levels, namely the position of a species along the food web, to the "upstreamness" of a firm along the supply chain, as done by [95], and in the work of [96] where these concepts are used to study the properties of production networks. Interesting parallels between these two domains could also arise when studying the impact of technological innovation or biological evolution within these models.

The economic intuition behind the analogy with Lotka-Volterra equations is the following: when dealing with a complex assembly of interacting entities, be it an ecosystem with species having attained a certain evolutionary level or an economy with firms capable



(i) $\varepsilon = 100$



(ii) $\varepsilon = 0.001$

Figure II.1: Simulated trajectories of relative price difference from equilibrium $\overline{\delta p_i}(t) = (p_i(t) - p_{\mathrm{eq},i})/p_{\mathrm{eq},i}$ for (i) $\varepsilon = 100$, $t_{\max} = 100$ and (ii) $\varepsilon = 0.001$, $t_{\max} = 1000$. We do not show the time-series of $\overline{\delta\gamma_i}(t)$ since they are qualitatively similar. The network is Gaussian with $J_{ij} \hookrightarrow N^{-1}\,|\mathsf{N}\,(0,1)|$. Parameters: $\alpha = 0.01$, $\beta = 0.01$, $\beta' = 0.1$. $(a) - (c)$ $\alpha' = 0.5$, $(b) - (d)$ $\alpha' = 0.05$. $(a) - (b)$ Initial conditions $\overline{\delta p_i}(0), \overline{\delta\gamma_i}(0) \in]-0.001, 0.001[$, $(c) - (d)$ Initial conditions $\overline{\delta p_i}(0), \overline{\delta\gamma_i}(0) \in]-0.9, 10[$.

of using certain technologies, one is considering a complex system with a large amount of feedback loops. The different entities depend on one another in a way that creates feedback loops that can lead to very volatile oscillatory behavior or even chaos, and in general to crises where certain firms or certain species must become "extinct" to re-stabilize the system, a point that was made by [24] and [19] arguing in favor of "self-organized criticality". Although the analogy with ecology is chosen here because it is easy to understand, we stress that we believe this is a generic characteristic of a large class of systems with a large number of inter-dependencies, as is the case for firm networks.

4 Linear study and marginal stability at the onset of feasibility

Equations (II.10) are our "naive" candidate equations for the out-of-equilibrium dynamics of the firm network model, the limitations of which will be discussed below. As we mentioned previously, very little can be said about these equations in their fully non-linear form. We resort to a linear analysis, which turns out to be enough for the point we want to make about excess volatility generated by network effects.

Writing $p_i(t) = p_{\mathrm{eq},i} + \delta p_i(t)$ and $\gamma_i(t) = \gamma_{\mathrm{eq},i} + \delta\gamma_i(t)$ and keeping only terms of order 1 in $\delta(.)$, one finds a linear evolution equation for a $2N$ dimensional vector $\mathbf{U} = (\delta\mathbf{p}, \delta\boldsymbol{\gamma})^\top$, of the form

$$\frac{\mathrm{d}\mathbf{U}(t)}{\mathrm{d}t} = \mathbb{D}\mathbf{U}(t). \tag{II.11}$$

The stability matrix $\mathbb{D}$ is written in the following block form

$$\frac{\mathrm{d}\mathbf{U}}{\mathrm{d}t} = \begin{pmatrix} \mathbf{D}_1 & \mathbf{D}_2 \\ \mathbf{D}_3 & \mathbf{D}_4 \end{pmatrix} \mathbf{U}(t) := \mathbb{D}\mathbf{U}(t), \tag{II.12}$$

where the different blocks of the matrix are

$$\begin{aligned} \mathbf{D}_1 &= -\alpha\boldsymbol{\Delta}\left(\frac{\mu\theta_i}{z_i\gamma_{\mathrm{eq},i}p_{\mathrm{eq},i}}\right) - \alpha'\boldsymbol{\Delta}\left(z_i^{-1}\right)\mathbf{M} \qquad & \mathbf{D}_2 &= -\alpha\boldsymbol{\Delta}\left(\frac{p_{\mathrm{eq},i}}{z_i\gamma_{\mathrm{eq},i}}\right)\mathbf{M}^\top \\ \mathbf{D}_3 &= \beta\boldsymbol{\Delta}\left(\frac{\gamma_{\mathrm{eq},i}}{z_i p_{\mathrm{eq},i}}\right)\mathbf{M} - \beta'\boldsymbol{\Delta}\left(\frac{\mu\theta_i}{z_i p_{\mathrm{eq},i}^2}\right) & \mathbf{D}_4 &= -\beta'\boldsymbol{\Delta}\left(z_i^{-1}\right)\mathbf{M}^\top, \end{aligned} \tag{II.13}$$

with $\boldsymbol{\Delta}(v_i)$ the diagonal matrix with entries v_i.

It is well known that the eigenvalues of the matrix $\mathbb{D}$ dictate whether the system is stable, i.e, whether it will be able to reach equilibrium back after a small perturbation. As long as the real parts of the eigenvalues are negative, equilibrium will be stable. They also dictate the speed at which the relaxation will occur. Calling σ_+^N the eigenvalue whose real part is closest to zero, the relaxation time τ_r of the system is approximately

$$\tau_r \approx \frac{1}{|\mathfrak{Re}\left(\sigma_N^+\right)|}. \tag{II.14}$$

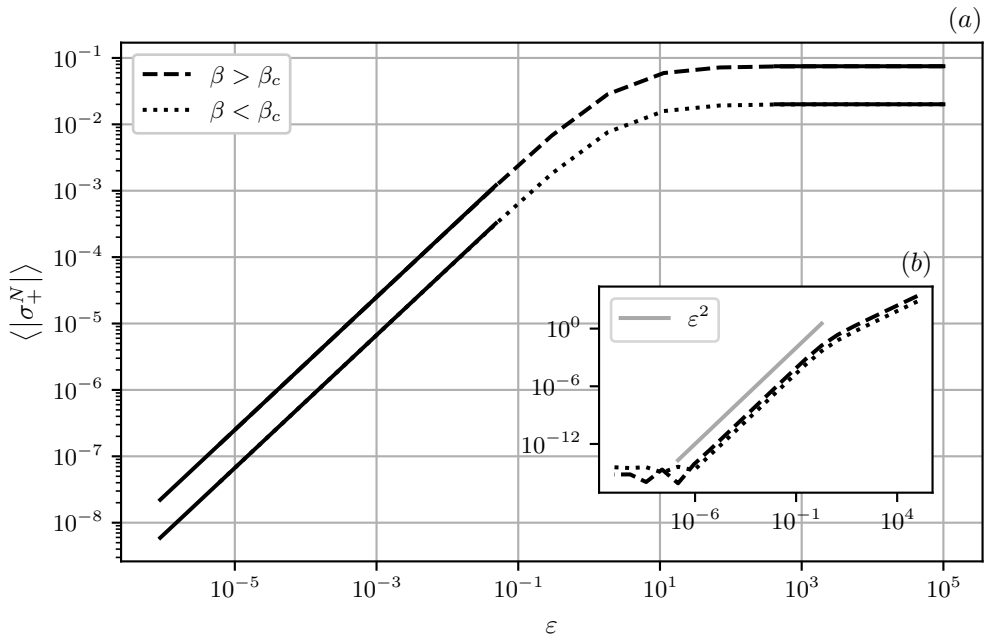


Figure II.2: (a) Modulus of the largest eigenvalue of $\mathbb{D}$ for economies on $N = 100$ firms on a 3-regular undirected network with unit weights. We generate 50 such economies and average out the eigenvalue of $\mathbb{D}$ closest to 0 in real part. Plain dark lines give the linear estimate when $\varepsilon \to 0$ (as given by Eq. (II.29)) and the plateaus as $\varepsilon \to \infty$ (corresponding to the values of Eq. (II.27)). Finally, β_c (defined in Eq. (II.18)) gives the threshold on β such that the linearized dynamics is oscillatory and dampening ($\beta \leq \beta_c$) or purely exponentially dampening ($\beta > \beta_c$). (b) Absolute error between the linear estimate from Eq. (II.29) and the simulated eigenvalue. We see that the error decays as ε^2 (as it should be) before numerical accuracy becomes limiting.

It can be interpreted as follows: at time $t \ll \tau_r \sim 1/\left|\mathfrak{Re}\left(\sigma_+^N\right)\right|$ after the perturbation, the system is still relatively far away from equilibrium whereas it is close to it for times $t \gg \tau_r$. As τ_r increases, the initial perturbation will take longer and longer to be absorbed by the system. This notion of relaxation time, which is central in physics, can be related to the *resilience* of economies: the faster shocks are absorbed by economies, the more resilient they are.

On Figure II.2, we show the evolution of the modulus of the eigenvalue σ_N^+ of the matrix $\mathbb{D}$ as a function of the distance to the Hawkins-Simons transition. We can clearly see two regimes: whenever $\varepsilon \to \infty$, i.e, far-away from the transition, this eigenvalue, and therefore the relaxation time, reaches a strictly positive plateau; however, as $\varepsilon \to 0$, $|\sigma_N^+| \propto \varepsilon$ which indicates a diverging relaxation time $\tau_r \underset{\varepsilon \to 0^+}{\sim} \varepsilon^{-1}$. In the following, we will give an analytical justification of the observations displayed on Figure II.2.

4.1 Relaxation time in the high productivity regime

In this section, we assume that the productivity factors are large enough to ignore interactions between firms: firms are so efficient that the actual amount of inputs does not matter in the final production. This regime $z_i \to \infty$ corresponds to an economy far-away from the HS transition, i.e. $\varepsilon \to \infty$. We can therefore give approximate expressions for the equilibrium prices and productions

$$p_{\mathrm{eq},i} = \frac{V_i}{z_i} \tag{II.15a}$$

$$\gamma_{\mathrm{eq},i} = \frac{\mu\theta_i}{V_i}, \tag{II.15b}$$

which are equivalent to Eqs. (I.27) in Chapter I for $q = 0$ and $b = 1$, i.e. Leontief production function with constant return to scale.

Similarly, we can approximate each block of the stability matrix

$$\begin{aligned} \mathbf{D}_1 &\underset{z_i\to\infty}{\approx} -(\alpha+\alpha')\mathbf{I}_N & \mathbf{D}_2 &\underset{z_i\to\infty}{\approx} -\alpha\boldsymbol{\Delta}\left(\frac{V_i^2}{z_i\mu\theta_i}\right) \\ \mathbf{D}_3 &\underset{z_i\to\infty}{\approx} (\beta-\beta')\boldsymbol{\Delta}\left(\frac{z_i\mu\theta_i}{V_i^2}\right) & \mathbf{D}_4 &\underset{z_i\to\infty}{\approx} -\beta'\mathbf{I}_N, \end{aligned} \tag{II.16}$$

and deduce the spectrum of matrix $\mathbb{D}$ by computing its characteristic polynomial and setting it to 0

$$\begin{aligned} \det\left(\sigma\mathbf{I}_{2N} - \mathbb{D}\right) &= \begin{vmatrix} \sigma\mathbf{I}_N - \mathbf{D}_1 & -\mathbf{D}_2 \\ -\mathbf{D}_3 & \sigma\mathbf{I}_N - \mathbf{D}_4 \end{vmatrix} \\ &\underset{z_i\to\infty}{\approx} \det\left(\left(\sigma+\alpha+\alpha'\right)\left(\sigma+\beta'\right)\mathbf{I}_N + \alpha(\beta-\beta')\mathbf{I}_N\right) \\ &= \left(\sigma^2 + \sigma(\alpha+\alpha'+\beta') + \alpha\beta + \alpha'\beta'\right)^N \\ &= 0. \end{aligned}$$

Solving this equation yields two eigenvalues $\sigma_\pm$ degenerated N times reading

$$\sigma_\pm = \frac{1}{2} \times \begin{cases} -\alpha'-\beta'-\alpha \pm \sqrt{(\alpha'+\beta'+\alpha)^2 - 4(\alpha\beta+\alpha'\beta')} & \text{if} \quad \beta_c > \beta \\ -\alpha'-\beta'-\alpha \pm i\sqrt{4(\alpha\beta+\alpha'\beta') - (\alpha'+\beta'+\alpha)^2} & \text{if} \quad \beta_c \leq \beta \end{cases}, \tag{II.17}$$

with

$$\beta_c = \frac{(\alpha+\alpha'+\beta')^2 - 4\alpha'\beta'}{4\alpha}. \tag{II.18}$$

We see here that the dynamics can be oscillatory with exponential hull or purely exponentially dampening, depending on the magnitude of β with respect to β_c. In any case, since time-scales are chosen positive, equilibrium remains stable in that limit. Furthermore, as we saw in Chapter I, network effects are negligible in the large productivity limit: firms behave independently from one another which accounts for the degeneracy of the eigenvalues $\sigma_\pm$. The slowest eigenvalue σ_+^N of $\mathbb{D}$ plotted on Figure II.2 is therefore none

other than σ_+ and we see that it reaches the plateau defined by Eq. (II.27). Finally, considering the case $\beta \leq \beta_c$ for simplicity, the relaxation time is

$$\tau_r = \frac{2}{\alpha' + \alpha + \beta'}, \tag{II.19}$$

which is finite and of the same order as the time-scale of prices and productions adjustment. In this limit, firms efficiently cope with shocks and the economy is resilient.

4.2 Marginal stability and Hawkins-Simons transition

As a toy example, Eqs. (II.10) can be solved in the case where $\alpha = 0$, i.e. when prices are only driven by competition and inelastic to production surplus. In this case, prices read

$$\mathbf{p}(t) = \mathbf{p}_{\text{eq}} + e^{-\alpha' \mathbf{\Delta}\left(z_i^{-1}\right)\mathbf{M}t} \left(\mathbf{p}(0) - \mathbf{p}_{\text{eq}}\right). \tag{II.20}$$

Since we chose $\alpha' > 0$, as long as a feasible equilibrium exists, i.e. $\mathfrak{Re}\left(\text{Sp}\left(\mathbf{M}\right)\right) > 0$, the exponential factor is dampening and prices will reach their equilibrium value. However, as $\varepsilon \to 0^+$, the dynamics on prices will become slower and slower. Taking homogeneous productivity factors for simplicity $z_i := z$, the slowest mode of $\mathbf{\Delta}\left(z_i^{-1}\right)\mathbf{M}$ will be approximately $\frac{\varepsilon}{\rho_N} \boldsymbol{r}\boldsymbol{\ell}^\top$ with $\boldsymbol{r}, \boldsymbol{\ell}$ the right and left eigenvectors associated to the largest eigenvalue $\rho_N > 0$ of $\mathbf{J}$. Consequently, for an initial perturbation around equilibrium of magnitude $\boldsymbol{\delta}$, i.e. $\mathbf{p}(0) = \mathbf{p}_{\text{eq}} \circ (1 + \boldsymbol{\delta})$, the relative distance to equilibrium will behave as

$$\frac{p_i(t) - p_{\text{eq},i}}{p_{\text{eq},i}} = \left(\boldsymbol{\ell}^\top \boldsymbol{\delta}\right) r_i e^{-\alpha' \varepsilon t/\rho_N}. \tag{II.21}$$

The time needed to converge back to equilibrium will therefore be of order $\varepsilon^{-1} \to \infty$. More generally, this behavior is known as *marginal stability* in linear systems: the matrix $\mathbb{D}$ governing the evolution is Hurwitz (all eigenvalues negative) except for one eigenvalue which is exactly 0. Such systems are frozen in time since the mode associated to the null eigenvalue yields a forever non-vanishing contribution. In this toy example, marginal stability comes together with the violation of the Hawkins-Simons condition and we will see that this is actually a general feature of these equations, as was hinted by the behavior of σ_+^N as $\varepsilon \to 0$ on Figure II.2.

4.2.1 Perturbation expansion in ε for $\mathbb{D}$

Studying the behavior of $\mathbb{D}$ as $\varepsilon \to 0^+$ requires understanding the behavior of $\mathbf{M}$, $\mathbf{p}_{eq}$ and $\boldsymbol{\gamma}_{eq}$ in that limit. We now introduce the matrix $\widetilde{\mathbf{J}} = \mathbf{\Delta}\left(z_{\max} - z_i\right) + \mathbf{J}$ and denote by ρ_ν (resp. $|r_\nu\rangle$, $\langle \ell_\nu|$) [3] its eigenvalues (resp. right/left eigenvectors) ordered by their real parts. The Perron-Frobenius theorem implies that the top eigenvalue ρ_N is real, simple and associated to a full and positive eigenvector. We then use the following spectral representation of the matrix $\mathbf{M}$

[3] We use here Dirac bra-ket notation, where $|v\rangle$ represents a column vector and $\langle v|$ a row vector.

$$\mathbf{M} = \left(\rho_N \mathbf{I}_N - \widetilde{\mathbf{J}}\right) + \varepsilon \mathbf{I}_N \tag{II.22}$$

$$\begin{aligned}\mathbf{M}^{-1} &= \frac{1}{\varepsilon} |r_N\rangle \langle \ell_N| + \sum_{\nu=1}^{N-1} \frac{1}{\rho_N - \rho_\nu + \varepsilon} |r_\nu\rangle \langle \ell_\nu| \\ &= \frac{1}{\varepsilon} |r_N\rangle \langle \ell_N| + \sum_{k=0}^{\infty} (-\varepsilon)^k \sum_{\nu=1}^{N-1} \frac{1}{(\rho_N - \rho_\nu)^{k+1}} |r_\nu\rangle \langle \ell_\nu| ,\end{aligned} \tag{II.23}$$

which allows us to express the equilibrium prices and outputs as well as $\mathbb{D}$ in terms of ε. We also use the notation $\mathbf{M}_0$ to refer to the network matrix when $\varepsilon = 0$. This matrix is singular and verifies

$$\mathbf{M}_0 |r_N\rangle = 0 \quad , \quad \mathbf{M}_0^\top |\ell_N\rangle = 0. \tag{II.24}$$

Expanding in ε and neglecting factors of order $\mathcal{O}\left(\varepsilon^4\right)$ and higher gives the following form for the blocks of the stability matrix

$$\begin{aligned}&\mathbf{D}_1 = \mathbf{D}_1^{(0)} + \varepsilon \mathbf{D}_1^{(1)} + \varepsilon^2 \mathbf{D}_1^{(2)} + \varepsilon^3 \mathbf{D}_1^{(3)} && \mathbf{D}_2 = \frac{1}{\varepsilon}\mathbf{D}_2^{(-1)} + \mathbf{D}_2^{(0)} + \varepsilon \mathbf{D}_2^{(1)} + \varepsilon^2 \mathbf{D}_2^{(2)} + \varepsilon^3 \mathbf{D}_2^{(3)} \\ &\mathbf{D}_3 = \varepsilon \mathbf{D}_3^{(1)} + \varepsilon^2 \mathbf{D}_3^{(2)} + \varepsilon^3 \mathbf{D}_3^{(3)} && \mathbf{D}_4 = \mathbf{D}_4^{(0)} + \varepsilon \mathbf{D}_4^{(1)} + \varepsilon^2 \mathbf{D}_4^{(2)} + \varepsilon^3 \mathbf{D}_4^{(3)},\end{aligned} \tag{II.25}$$

where the exact values of the perturbation terms $\mathbf{D}_i^{(l)}$ are given in Appendix A. To ease computations and give closed-form results, we consider an undirected network (symmetric $\mathbf{M}$) with homogeneous productivity factors. The qualitative results are however unchanged when considering more general networks. In this setting, the right and left eigenvectors of $\mathbf{M}$ are the same and we denote them by $|e_\nu\rangle$.

4.2.2 Marginal stability for $\varepsilon = 0$

Interestingly enough, although the upper-right block of $\mathbb{D}$ diverges as $\varepsilon \to 0$, its spectrum converges to a finite limit. To see this, we use the block determinant formula

$$\begin{vmatrix} \mathbf{A} & \mathbf{B} \\ \mathbf{C} & \mathbf{D} \end{vmatrix} = \det\left(\mathbf{AD} - \mathbf{BC}\right),$$

for same-size matrices, where the commutator $[\mathbf{C},\mathbf{D}] = \mathbf{CD} - \mathbf{DC} = 0$. In our case, we need $[\mathbf{D}_3, \mathbf{D}_4] = 0$ which is true only in the limit $\varepsilon = 0$. We can then write [4]

$$\begin{aligned}
\det\left(\sigma\mathbf{I}_{2N} - \mathbb{D}\right) &\underset{\varepsilon\to 0}{\approx} \det\left(\left(\sigma\mathbf{I}_N - \mathbf{D}_1^{(0)}\right)\left(\sigma\mathbf{I}_N - \mathbf{D}_4^{(0)}\right) - \mathbf{D}_2^{(-1)}\mathbf{D}_3^{(1)}\right) \\
&= \det\left(\left(\sigma\mathbf{I}_N + \frac{\alpha'}{\rho_N}\mathbf{M}_0\right)\left(\sigma\mathbf{I}_N + \frac{\beta'}{\rho_N}\mathbf{M}_0\right) + \frac{\alpha\beta}{\rho_N^2}\mathbf{M}_0^2\right) \\
&= \det\left(\sigma^2\mathbf{I}_N + \sigma\frac{\alpha'+\beta'}{\rho_N}\mathbf{M}_0 + \frac{\alpha\beta+\alpha'\beta'}{\rho_N^2}\mathbf{M}_0^2\right) \\
&= \prod_{\nu=1}^{N}\left(\sigma^2 + \sigma\frac{\alpha'+\beta'}{\rho_N}(\rho_N - \rho_\nu) + \frac{\alpha\beta+\alpha'\beta'}{\rho_N^2}(\rho_N-\rho_\nu)^2\right) \\
&= \sigma^2\prod_{\nu\neq N}\left(\sigma^2 + \sigma(\alpha'+\beta')\left(1-\frac{\rho_\nu}{\rho_N}\right) + (\alpha\beta+\alpha'\beta')\left(1-\frac{\rho_\nu}{\rho_N}\right)^2\right).
\end{aligned}$$

Each factor ν in the product yields two eigenvalues

- If $(\alpha'-\beta')^2 > 4\alpha\beta$ then

$$\sigma_\pm^\nu = \frac{1}{2}\left(-\alpha'-\beta' \pm \sqrt{(\alpha'+\beta')^2 - 4(\alpha\beta+\alpha'\beta')}\right)\left(1-\frac{\rho_\nu}{\rho_N}\right), \tag{II.26}$$

- If $(\alpha'-\beta')^2 < 4\alpha\beta$ then

$$\sigma_\pm^\nu = \frac{1}{2}\left(-\alpha'-\beta' \pm i\sqrt{4(\alpha\beta+\alpha'\beta') - (\alpha'+\beta')^2}\right)\left(1-\frac{\rho_\nu}{\rho_N}\right), \tag{II.27}$$

- If $(\alpha'-\beta')^2 = 4\alpha\beta$ then

$$\sigma_0^\nu = -\frac{\alpha'+\beta'}{2}\left(1-\frac{\rho_\nu}{\rho_N}\right). \tag{II.28}$$

Since $\rho_\nu \leq \rho_N$ and $\alpha, \beta' > 0$, we see that $\mathbb{D}$ has only eigenvalues with negative real part and the system remains stable whenever $\varepsilon = 0$. However, we also see that $\sigma_\pm^N = 0$ such that, as anticipated, the system exhibits marginal stability in this limit. Figure II.3 shows the empirical distribution of eigenvalues of $\mathbb{D}$ for $\varepsilon = 0$ and the corresponding theoretical predictions given by Eqs. (II.27,II.26,II.28).

[4] We do not need to consider terms of order one in the commutator because $\left[\mathbf{D}_3^{(1)}, \mathbf{D}_4^{(0)}\right] = 0$, see Appendix A.

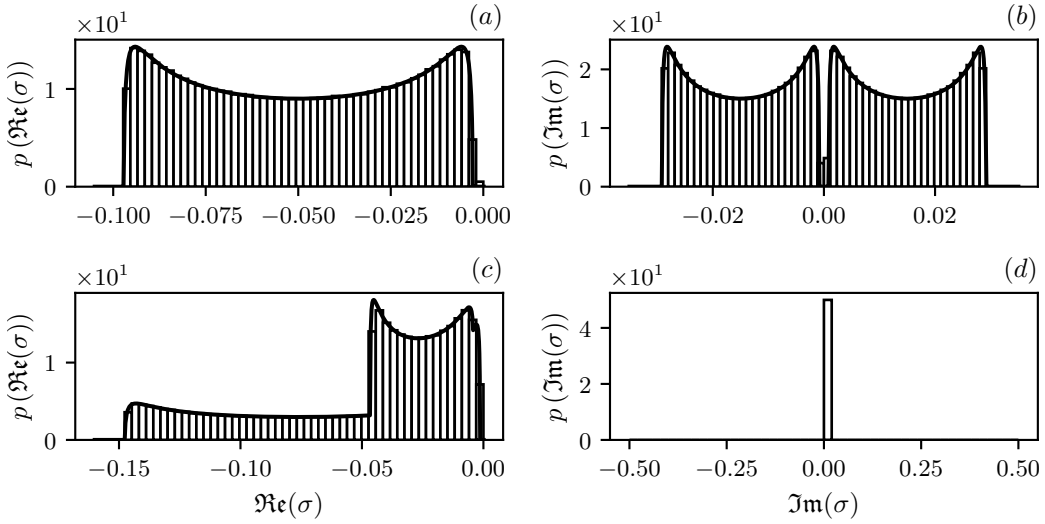


Figure II.3: $(a)-(b)$ Empirical probability distribution of the real part (a) and imaginary part (b) or eigenvalues in the case $(\alpha'-\beta')^2 < 4\alpha\beta$. $(c)-(d)$ Empirical probability distribution of the real part (c) and imaginary part (d) or eigenvalues in the case $(\alpha'-\beta')^2 > 4\alpha\beta$. The black line is the thermodynamic computation accounting for (II.27) and (II.26) using the McKay density for the eigenvalues of a random 3-regular graph [97] over $N \gg 1$ nodes. One can notice spikes at 0 accounting for the case $\nu = N$ in Eqs. (II.27, II.26).

4.2.3 Diverging relaxation time

For $\varepsilon = 0$, the equilibrium equations do not have any solutions and the linearized system (II.11) is ill-defined. Therefore, it makes more sense to study the spectrum of $\mathbb{D}$ as $\varepsilon \to 0^+$, i.e. close to the HS transition but with a well-defined equilibrium. In this limit, we can show that the slowest eigenvalue σ_+^N of $\mathbb{D}$ is proportional to ε. Since the computation is rather long and cumbersome, we only give the results here but see Appendix B for a full derivation. As the Hawkins-Simons condition is on the verge of being violated, we find that

$$\sigma_+^N \underset{\varepsilon\to 0}{\approx} \frac{\varepsilon}{2\rho_N} \times \begin{cases} -\alpha'-\beta'-\alpha \pm \sqrt{(\alpha'+\beta'+\alpha)^2 - 4(\alpha\beta+\alpha'\beta')} & \text{if} \quad \beta < \beta_c \\ -\alpha'-\beta'-\alpha \pm i\sqrt{4(\alpha\beta+\alpha'\beta') - (\alpha'+\beta'+\alpha)^2} & \text{if} \quad \beta > \beta_c \\ -\alpha'-\beta'-\alpha & \text{if} \quad \beta = \beta_c \end{cases}. \tag{II.29}$$

We reported this theoretical prediction on Figure II.2 and one can see a very good agreement with simulated values of σ_+^N. As a consequence, the relaxation time reads

$$\tau_r \approx \frac{2\rho_N}{\varepsilon} \times \begin{cases} \left(\alpha'+\beta'+\alpha - \sqrt{(\alpha'+\beta'+\alpha)^2 - 4(\alpha\beta+\alpha'\beta')}\right)^{-1} & \text{if} \quad \beta_c > \beta \\ (\alpha'+\beta'+\alpha)^{-1} & \text{if} \quad \beta_c \leq \beta. \end{cases} \tag{II.30}$$

When $\varepsilon \to 0$, the relaxation time of the system diverges, i.e. it takes an infinitely long time to reach equilibrium. This point is very important: even though equilibrium exists, it may never be reached effectively since changes in the technologies and in the network structure will happen before relaxation is complete. The existence of equilibrium therefore does not imply that the economy will sit anywhere close to it, or that it is always resilient to shocks.

5 Excess volatility

5.1 Marginally stable linear stochastic ODEs

In this section, we consider a general evolution for a vector $\mathbf{U}(t)$ given by a linear stochastic equation

$$\frac{\mathrm{d}\mathbf{U}(t)}{\mathrm{d}t} = \mathbb{A}\mathbf{U}(t) + \boldsymbol{\xi}(t), \tag{II.31}$$

where $\mathbb{A}$ is a real $N \times N$ matrix and $\xi(t)$ is a Gaussian correlated noise such that

$$\langle \xi_i(t) \rangle = 0 \tag{II.32}$$

$$\langle \xi_i(t)\xi_j(s) \rangle = 2\sigma^2 \delta_{ij} G\left(|t-s|\right). \tag{II.33}$$

We assume the dynamical matrix $\mathbb{A}$ to be diagonalizable with real eigenvalues [5] such that

$$\lambda_1 \leq \lambda_2 \leq \cdots \leq \lambda_{N-1} < \lambda_N := -\varepsilon < 0.$$

Negative eigenvalues mean that the system is stable, i.e. $\langle \|\mathbf{U}(t)\| \rangle \to 0$ as $t \to \infty$ for any initial condition. Let us assume that $\varepsilon \to 0$ and show that the volatility of $\mathbf{U}(t)$ increases as $\varepsilon^{-1/2}$. We introduce the eigenvectors $\mathbf{e}_\nu$ associated to λ_ν and we express $\mathbf{U}$ into the diagonal basis

$$\mathbf{U}(t) = \sum_{\nu=1}^{N} u_\nu \mathbf{e}_\nu. \tag{II.34}$$

Injecting this expression into (II.31), we get and evolution equation for the components of $\mathbf{U}(t)$ in the diagonal basis

$$\frac{\mathrm{d}}{\mathrm{d}t} u_\nu = \lambda_\nu u_\nu + \boldsymbol{\xi}(t) \cdot \mathbf{e}_\nu. \tag{II.35}$$

We can give an explicit solution for these components

$$u_\nu(t) = e^{\lambda_\nu t} \left[u_\nu(0) + \int_0^t ds\, e^{-\lambda_\nu s} \boldsymbol{\xi}(t) \cdot \mathbf{e}_\nu \right], \tag{II.36}$$

[5] The case with complex eigenvalues leads to the same conclusion. One must only take into account the fact that, since $\mathbb{A}$ is real, eigenvalues and eigenvectors will be conjugated so that there are two eigenvalues that are smallest in real parts. We can make the same ordering of eigenvalues replacing the λ's by their real parts.

and focus on u_N since this is the component yielding the $\mathcal{O}(\varepsilon^{-1/2})$ volatility. To show this, we compute the average value of $u_N(t)^2 - \langle u_N(t)\rangle^2$

$$\begin{aligned}
\left\langle u_N(t)^2 - \langle u_N(t)\rangle^2 \right\rangle &= e^{-2\varepsilon t}\left\langle \left[u_N(0) + \int_0^t ds\, e^{\varepsilon s}\boldsymbol{\xi}(s)\cdot\mathbf{e}_N\right]^2\right\rangle - u_N(0)^2 e^{-\varepsilon t} \\
&= e^{-2\varepsilon t}\left[u_N(0)^2 + 2u_N(0)\int_0^t ds\, e^{\varepsilon s}\left\langle\boldsymbol{\xi}(s)\cdot\mathbf{e}_N\right\rangle\right. \\
&\qquad \left. + \int dsds'\, e^{\varepsilon(s+s')}\left\langle(\boldsymbol{\xi}(s)\cdot\mathbf{e}_N)(\boldsymbol{\xi}(s')\cdot\mathbf{e}_N)\right\rangle\right] - u_N(0)^2 e^{-\varepsilon t} \\
&= e^{-\varepsilon t}\sum_{j,k} e_{N,j}e_{N,k}\int dsds'\, e^{\varepsilon(s+s')}\left\langle\xi_j(s)\xi_k(s')\right\rangle \\
&= 2\sigma^2\|\mathbf{e}_N\|^2 e^{-\varepsilon t}\int dsds'\, e^{\varepsilon(s+s')}G(|s'-s|).
\end{aligned}$$

Using $\|\mathbf{e}_N\| = 1$, we substitute $\tau = s' - s$ in the s integral to get

$$\left\langle u_N(t)^2 - \langle u_N(t)\rangle^2 \right\rangle = 2\sigma^2 e^{-\varepsilon t}\int_0^t ds'\, e^{2\varepsilon s'}\int_0^{s'-t} d\tau e^{-\varepsilon\tau}G(\tau).$$

Using the quick decay of the exponential term in the τ integral, we can expand the integration domain such that

$$\left\langle u_N(t)^2 - \langle u_N(t)\rangle^2 \right\rangle \approx 2\sigma^2 e^{-\varepsilon t}\int_0^t ds'\, e^{2\varepsilon s'}\int_0^{\infty} d\tau e^{-\varepsilon\tau}G(\tau),$$

and perform the integration over s' with an approximately vanishing exponential remainder

$$\left\langle u_N(t)^2 - \langle u_N(t)\rangle^2 \right\rangle \approx \frac{\sigma^2}{\varepsilon}\int_0^{\infty} d\tau e^{-\varepsilon\tau}G(\tau).$$

Denoting be τ_ξ the typical correlation time of G, we see that:

- if $\varepsilon\tau_\xi \ll 1$ (meaning that $\xi_i(t)$ is correlated on short time-scales) then $G(\tau) \sim \delta(0)$ such that
$$\int_0^{\infty} d\tau e^{-\varepsilon\tau}G(\tau) \approx 1,$$
- if $\varepsilon\tau_\xi \gg 1$ (meaning that $\xi_i(t)$ is correlated on long time-scales) then $G(\tau) \sim G(0)$ on the decay time of the exponential such that
$$\int_0^{\infty} d\tau e^{-\varepsilon\tau}G(\tau) \approx \frac{G(0)}{\varepsilon}.$$

Finally, the volatility of $\mathbf{U}(t)$ behaves as

$$\sqrt{\left\langle u_N(t)^2 - \langle u_N(t)\rangle^2 \right\rangle} \propto \begin{cases} \varepsilon^{-1/2} & \text{if} \quad \varepsilon\tau_\xi \ll 1 \\ \varepsilon^{-1} & \text{if} \quad \varepsilon\tau_\xi \gg 1 \end{cases}. \tag{II.37}$$

In both cases, the volatility of $\mathbf{U}(t)$, induced by the volatility of $u_N(t)$, increases as the matrix $\mathbb{A}$ gets closer to marginal stability. We will apply this generic feature in the case of our economic system.

Note also that this result generalizes to discrete time processes

$$\mathbf{U}_{t+1} = \mathbb{D}\mathbf{U}_t + \boldsymbol{\xi}_t, \tag{II.38}$$

for which the marginal stability condition can be written as $\lambda_N = 1 - \varepsilon$ [6] with $\varepsilon \to 0$. We can carry out the same kind of computation and derive the same result depending on the behavior of the quantity $\sum_{\tau\geq 0}(1-\varepsilon)^\tau G(\tau)$.

5.2 Shock accumulation

Now, suppose that the parameters describing the economic equilibrium (such as productivity factors or household preferences, etc.) are changing over time, the dynamical equation governing economic fluctuations, Eq. (II.11), becomes:

$$\frac{\mathrm{d}\mathbf{U}(t)}{\mathrm{d}t} = \mathbb{D}\mathbf{U}(t) + \xi(t), \tag{II.39}$$

where $\xi(t)$ represents the (weak) exogenous shocks to the economy modeled by a Gaussian white noise. As we saw in the previous section in the limit $\varepsilon \to 0$, the volatility of prices and output is proportional to $\varepsilon^{-1/2}$, and can thus be much larger than the variance of the exogenous shocks when the system approaches the limit of stability. The intuitive reason is that past shocks linger a very long time (comparable to τ_r) in the system and aggregate with more recent shocks, leading to a much larger overall perturbation.

Hence, the proximity to the point of instability is a natural candidate to explain the "small shocks, large business cycle" paradox (see [66] for a related discussion). An illustration of this phenomenon for our model is given in Figure II.4 for small Gaussian shocks on productivity factors.

6 Conclusion

The above results suggest that, although "naive", our equations already provide an interesting generic scenario for anomalous fluctuations of output, namely the proximity of an instability. Note that the dynamics we have described is directly linked to a large body of work concerned with the stability of large complex systems (see the historical precursors [98, 22], and [99] and [100] for recent general approaches), using random matrix

[6] Or more generally for complex eigenvalues $\lambda_N = r_N e^{i\theta_N}$ with $r_N = 1 - \varepsilon$.

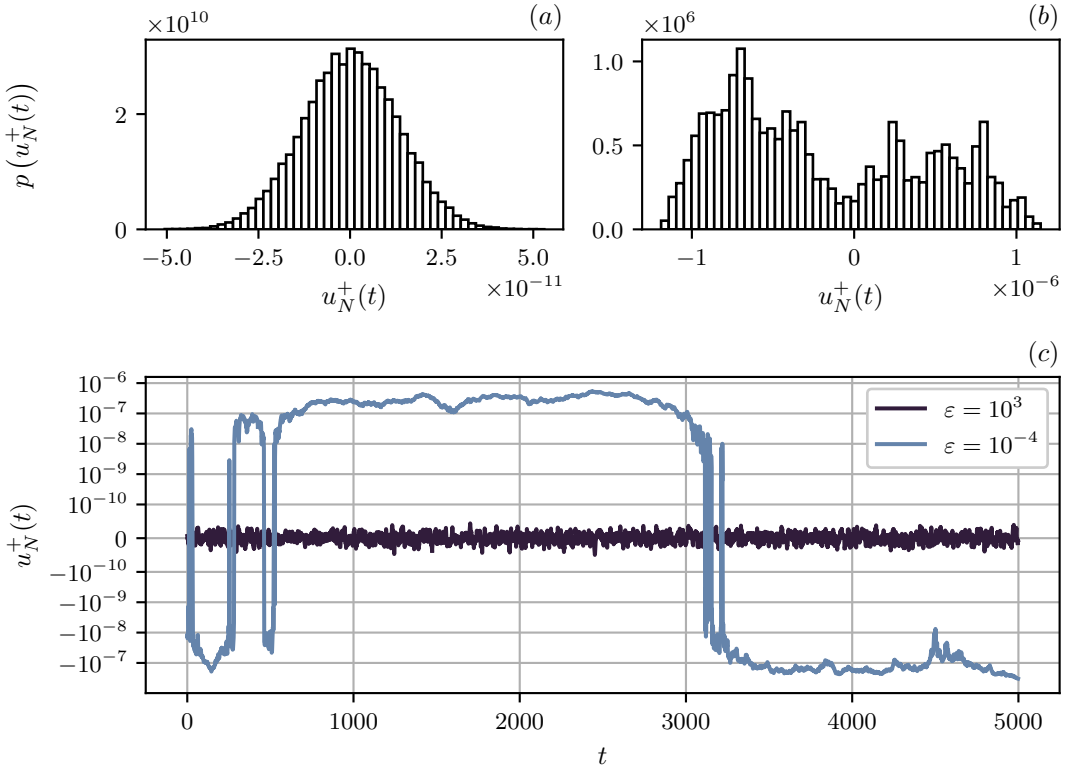


Figure II.4: $(a) - (b)$ Empirical distribution of the projection $u_N^+(t)$ of $(\delta \mathbf{p}/\mathbf{p}_{\text{eq}}, \delta\boldsymbol{\gamma}/\boldsymbol{\gamma}_{\text{eq}})$ onto the eigenvector associated to the marginal eigenvalue after productivity shocks with volatility $\sigma = 10^{-8}$ for (a) $\varepsilon = 10^3$ and (b) $\varepsilon = 10^{-4}$. Note that we rescaled price and production fluctuations by the equilibrium value to retrieve a square-root volatility (see Appendix C): for $\varepsilon = 10^{-4}$, the volatility of output and prices is of the order of 10^{-6} (vs 10^{-11} on (a)), i.e. 100 times larger than σ, as expected. The bi-modality on (b) is not a defining feature and only comes from the particular time-series that we chose. (c) Time-series of $u_N^+(t)$ on a symlog scale to accentuate the difference of behaviors between $\varepsilon = 10^{-4}$ and $\varepsilon = 10^3$.

techniques to represent generic interactions. These papers highlight the importance of studying the eigenvectors and eigenvalues of large random matrices for understanding complex systems, with other noteworthy contributions by [101, 102] and [103].

However, the naive approach above sweeps under the rug important constraints that, although irrelevant at equilibrium, turn out to be essential out-of-equilibrium:

- Causality: firms must plan production *before* they know how much they will manage to sell.
- Supply/demand imbalances (which are zero if markets clear): when supply exceeds demand, inventories accumulate, whereas when demand exceeds supply (including

inventories) involuntary savings increase. These extra variables should play a role in the out-of-equilibrium evolution of the economy, but are totally absent from Eqs.(II.9). Furthermore, if some input goods is missing, Eqs.(II.5b) incorrectly account for imbalances.

In Part II, we will propose a minimal, fully consistent model that allows one to account for both causality and imbalances. Interestingly, we will see that hard constraints – such as the impossibility to consume more than what is available – lead to intrinsically non-linear dynamics, even for small perturbations close to equilibrium. As a consequence, limit cycles or chaotic behavior will spontaneously emerge, when Eqs. (II.9) can only lead to damped oscillations converging to equilibrium. Such generalized equations in fact allow one to obtain legitimate dynamics even in the region where the equilibrium is no longer defined, i.e. when $\varepsilon < 0$, whereas Eqs. (II.9) cease to make sense in this case (prices and productions are are always dragged below zero).

Finally, another question that one might ask is: what is the good level of aggregation to look at in these models? This is of course a rather broad question and the answer is not straightforward. When looking at the Goodwin model of the first section, every agent is actually representative: capital owners are described by an aggregate variable and so are workers. In the model we presented throughout this section, firms are granular but workers still aggregate. Another natural question is: can we really consider representative agents? If yes, how can we model this *representativeness* properly? It seems that on account of such questioning, economic sciences do not provide answers. Statistical physics however has provided methods to bridge the gap between the micro and macro worlds. In the next chapter, we will present one of these methods called *dynamical mean-field*, which aims at properly taking the "representative limit".

Key takeaways

- **Toy-modelling** provides minimal models that properly identify key aspects to explain a particular phenomenon.
- **Behavioral rules** are used by firms to adjust their productions and prices according to *deviations* from equilibrium, measured in terms of production surplus $\mathscr{E}_i(t)$ and profits $\pi_i(t)$. We model this adjustment process as

$$\log\left(\frac{p_i(t+\delta t)}{p_i(t)}\right) = \left(-\alpha\frac{\mathscr{E}_i(t)}{y_i(t)} - \alpha'\frac{\pi_i(t)}{p_i(t)y_i(t)}\right)\delta t$$
$$\log\left(\frac{y_i(t+\delta t)}{y_i(t)}\right) = \left(\beta\frac{\pi_i(t)}{p_i(t)y_i(t)} - \beta'\frac{\mathscr{E}_i(t)}{y_i(t)}\right)\delta t,$$

  where α, α', β, β' are inverse time-scales measuring the feedback strength of the adjustments.
- **The Hawkins-Simons transition (dynamical setting)** translates into a dynamical transition. Linearizing previous rules around equilibrium, we can show that the stability matrix $\mathbb{D}$ of the system exhibits marginal stability on the verge of violating the HS conditions, i.e.

$$\min \mathfrak{Re}\left(\mathrm{Sp}\left(\mathbb{D}\right)\right) \underset{\varepsilon\to 0}{\propto} -\varepsilon.$$

  Therefore, the time needed to reach equilibrium diverges as ε^{-1} whenever the economy gets closer to unfeasibility.
- **Economic fluctuations and excess volatility** are driven by the minimum eigenvalue of $\mathbb{D}$ and increase as $\varepsilon^{-1/2}$ when the economy gets closer to unfeasibility. Intuitively, the increasingly long time needed to reach back equilibrium allows for an accumulation and lingering of shocks in the network, which increases volatility. This process, which corresponds to that of Bak et al. [19] is a natural candidate for shock amplification in firm networks.

A Blocks of the stability matrix

In this section, we give the values of the perturbation terms $\mathbf{D}_i^{(l)}$ for the blocks of the stability matrix. We introduce several notations for quantities that simplify in the case of an undirected network with homogeneous productivity factors. Finally, we use the bra (resp. ket) notation to refer to a row (resp. column) vector $|v\rangle$ (resp. $\langle v|$) and we denote by v_i its ith component. We also use the perturbation expansion of the matrix $\mathbf{M}$ from Eqs. (II.23).

A.1 Perturbation of $\mathbf{p_{eq}}$ and $\boldsymbol{\gamma_{eq}}$

Equilibrium prices are easily obtained by applying $\mathbf{M}^{-1}$ to the vector $|V\rangle$, which yields

$$\begin{aligned} p_{eq,j} &= \frac{1}{\varepsilon}\langle \ell_N \mid V\rangle\, r_{N,j} + \sum_{\nu=1}^{N-1} \frac{\langle l_\nu \mid V\rangle}{\rho_N-\rho_\nu} r_{\nu,j} - \varepsilon \sum_{\nu=1}^{N-1} \frac{\langle l_\nu \mid V\rangle}{(\rho_N-\rho_\nu)^2} r_{\nu,j} \\ &\quad + \varepsilon^2 \sum_{\nu=1}^{N-1} \frac{\langle l_\nu \mid V\rangle}{(\rho_N-\rho_\nu)^3} r_{\nu,j} - \varepsilon^3 \sum_{\nu=1}^{N-1} \frac{\langle l_\nu \mid V\rangle}{(\rho_N-\rho_\nu)^4} r_{\nu,j} \\ &:= \frac{1}{\varepsilon}\pi_{-1}^l(V)_j + \pi_0^l(V)_j - \varepsilon\pi_1^l(V)_j + \varepsilon^2\pi_2^l(V)_j - \varepsilon^3\pi_3^l(V)_j, \end{aligned} \tag{1.a}$$

and where we introduced (for $i \geq 0$)

$$\pi_{-1}^l(V) = \langle \ell_N \mid V\rangle\, |r_N\rangle \ , \ \pi_i^l(V) = \sum_{\nu=1}^{N-1} \frac{\langle l_\nu \mid V\rangle}{(\rho_N-\rho_\nu)^{i+1}}\, |r_\nu\rangle\,.$$

Equilibrium productions can be a little trickier to obtain. We first derive three useful identities to simplify computations. For $s = 1, \ldots, n$, we have

$$\begin{aligned} \frac{1}{\varepsilon p_{eq,s}} &= \frac{1}{\pi_{-1}^l(V)_s} - \varepsilon\frac{\pi_0^l(V)_s}{\left(\pi_{-1}^l(V)_s\right)^2} + \frac{\varepsilon^2}{\pi_{-1}^l(V)_s}\left(\frac{\pi_1^l(V)_s}{\pi_{-1}^l(V)_s} + \left(\frac{\pi_0^l(V)_s}{\pi_{-1}^l(V)_s}\right)^2\right) \\ &\quad - \frac{\varepsilon^3}{\pi_{-1}^l(V)_s}\left(\frac{\pi_2^l(V)_s}{\pi_{-1}^l(V)_s} + 2\frac{\pi_0^l(V)_s\pi_1^l(V)_s}{\pi_{-1}^l(V)_s} + \left(\frac{\pi_0^l(V)_s}{\pi_{-1}^l(V)_s}\right)^3\right) \end{aligned} \tag{i}$$

$$\frac{1}{p_{eq,s}} = \frac{\varepsilon}{\pi_{-1}^l(V)_s} - \varepsilon^2\frac{\pi_0^l(V)_s}{\left(\pi_{-1}^l(V)_s\right)^2} + \frac{\varepsilon^3}{\pi_{-1}^l(V)_s}\left(\frac{\pi_1^l(V)_s}{\pi_{-1}^l(V)_s} + \left(\frac{\pi_0^l(V)_s}{\pi_{-1}^l(V)_s}\right)^2\right) \tag{ii}$$

$$\frac{\varepsilon}{p_{eq,s}} = \frac{\varepsilon^2}{\pi_{-1}^l(V)_s} - \varepsilon^3\frac{\pi_0^l(V)_s}{\left(\pi_{-1}^l(V)_s\right)^2} \tag{iii}$$

$$\frac{\varepsilon^2}{peq_s} = \frac{\varepsilon^3}{\pi_{-1}^l(V)_s} \tag{iv}$$

$$\frac{\varepsilon^3}{peq_s} = o(\varepsilon^3). \tag{v}$$

Introducing $\psi_{eq,i} = \frac{\mu\theta_i}{p_{\mathrm{eq},i}}$, previous results allow to write the equilibrium productions

$$\begin{aligned}
\gamma_{eq,j} &= \frac{\mu}{\varepsilon}\left\langle r_N \mid \psi_{eq}\right\rangle l_{N,j} + \mu\sum_{\nu=1}^{N-1}\frac{\left\langle r_\nu \mid \psi_{eq}\right\rangle}{\rho_N-\rho_\nu}l_{\nu,j} - \varepsilon\mu\sum_{\nu=1}^{N-1}\frac{\left\langle r_\nu \mid \psi_{eq}\right\rangle}{(\rho_N-\rho_\nu)^2}l_{\nu,j} \\
&\quad + \varepsilon^2\mu\sum_{\nu=1}^{N-1}\frac{\left\langle r_\nu \mid \psi_{eq}\right\rangle}{(\rho_N-\rho_\nu)^3}l_{\nu,j} - \varepsilon^3\mu\sum_{\nu=1}^{N-1}\frac{\left\langle r_\nu \mid \psi_{eq}\right\rangle}{(\rho_N-\rho_\nu)^4}l_{\nu,j} \\
&= \mu l_{N,j}\sum_{s=1}^{n}\frac{r_{n,s}\theta_s}{\pi^l_{-1}(V)_s} + \varepsilon\mu\sum_{s=1}^{n}\left\{\sum_{\nu=1}^{N-1}\frac{l_{\nu,j}r_{\nu,s}\theta_s}{(\rho_N-\rho_\nu)\pi^l_{-1}(V)_s} - \frac{l_{N,j}r_{n,s}\theta_s\pi^l_0(V)_s}{\pi^l_{-1}(V)_s^2}\right\} \\
&\quad + \varepsilon^2\mu\sum_{s=1}^{n}\left\{\frac{\pi^l_1(V)_s}{\pi^l_{-1}(V)_s} + \left(\frac{\pi^l_0(V)_s}{\pi^l_{-1}(V)_s}\right)^2 - \sum_{\nu=1}^{N-1}\frac{l_{\nu,j}r_{\nu,s}\theta_s}{(\rho_N-\rho_\nu)\pi^l_{-1}(V)_s}\left(\frac{1}{\rho_N-\rho_\nu} + \frac{\pi^l_0(V)_s}{\pi^l_{-1}(V)_s}\right)\right\} \\
&\quad + \varepsilon^3\mu\sum_{s=1}^{n}\left\{\sum_{\nu=1}^{N-1}\frac{l_{\nu,j}r_{\nu,s}\theta_s}{(\rho_N-\rho_\nu)\pi^l_{-1}(V)_s}\left(\frac{\pi^l_1(V)_s}{\pi^l_{-1}(V)_s} + \left(\frac{\pi^l_0(V)_s}{\pi^l_{-1}(V)_s}\right)^2 + \frac{\pi^l_0(V)_s}{(\rho_N-\rho_\nu)\pi^l_{-1}(V)_s}\right.\right. \\
&\qquad\qquad \left.\left. + \frac{1}{(\rho_N-\rho_\nu)^3\pi^l_{-1}(V)_s}\right)\right\} \\
&:= \mu f_{0,j} + \varepsilon\mu f_{1,j} + \varepsilon^2\mu f_{2,j} + \varepsilon^3\mu f_{3,j}, \qquad \text{(1.b)}
\end{aligned}$$

where factors $f_{l,j}$ are obtained through straightforward identification.

A.2 Stability blocks

The next step is to perturb the stability matrix itself. This yields no particular difficulty, but computations are a bit lengthy so that we only give the results for the different blocks. We denote by τg_k the coefficients of the expansion of $z\gamma$ where $\tau_i = \rho_N e_{N,i}/\left\langle e_N \mid V\right\rangle$ for an undirected network. We have

$$\begin{aligned}
(D_1^{(0)})_{ij} &= -\alpha'\frac{1}{\rho_N}M_{ij} \\
(D_1^{(1)})_{ij} &= -\alpha\mu\frac{\theta_i}{\tau_i\pi^l_{-1}(V)_i}\delta_{ij} + \frac{\alpha'}{\rho_N^2}M_{ij} - \frac{\alpha'}{\rho_N}\delta_{ij} \\
(D_1^{(2)})_{ij} &= +\alpha\mu\frac{\theta_i}{\tau_i\pi^l_{-1}(V)_i}\left(g_{1,i} + \frac{\pi^l_0(V)_i}{\pi^l_{-1}(V)_i}\right)\delta_{ij} - \frac{\alpha'}{\rho_N^3}M_{ij} + \frac{\alpha'}{\rho_N^2}\delta_{ij} \\
(D_1^{(3)})_{ij} &= -\alpha\mu\varepsilon\frac{\theta_i}{\tau_i\pi^l_{-1}(V)_i}\left(g_{1,i}^2 - g_{2,i} + \frac{\pi^l_0(V)_i}{\pi^l_{-1}(V)_i}g_{1,i} + \frac{\pi^l_1(V)_i}{\pi^l_{-1}(V)_i} + \left(\frac{\pi^l_0(V)_i}{\pi^l_{-1}(V)_i}\right)^2\right)\delta_{ij} \\
&\quad + \frac{\alpha'}{\rho_N^4}M_{ij} - \frac{\alpha'}{\rho_N^3}\delta_{ij},
\end{aligned}$$

$$
\begin{aligned}
(D_2^{(-1)})_{ij} &= -\alpha \frac{\pi_{-1}^l(V)_i}{\tau_i} M_{ji} \\
(D_2^{(0)})_{ij} &= \frac{\alpha}{\tau_i} \left[M_{ji} \left(\pi_{-1}^l(V)_i g_{1,i} - \pi_0^l(V)_i \right) - \pi_{-1}^l(V)_i \delta_{ij} \right] \\
(D_2^{(1)})_{ij} &= \frac{\alpha}{\tau_i} \left[M_{ji} \left(\pi_{-1}^l(V)_i g_{1,i}^2 + 2\pi_{-1}^l(V)_i g_{1,i} g_{2,i} + \pi_0^l(V)_i g_{1,i} - \pi_{-1}^l(V)_i g_{2,i} - \pi_1^l(V)_i \right) \right. \\
&\quad \left. + \left(\pi_{-1}^l(V)_i g_{1,i} - \pi_0^l(V)_i \right) \delta_{ij} \right] \\
(D_2^{(2)})_{ij} &= \frac{\alpha}{\tau_i} \left[M_{ji} \left(\pi_1^l(V)_i g_{1,i} + \pi_2^l(V)_i - \pi_{-1}^l(V)_i \left(g_{3,i} + g_{1,i}^3 \right) + \pi_0^l(V)_i \left(g_{1,i}^2 - g_{2,i} \right) \right) \right. \\
&\quad \left. + \left(\pi_{-1}^l(V)_i \left(g_{1,i}^2 - g_{2,i} \right) - \pi_0^l(V)_i g_{1,i} - \pi_1^l(V)_i \right) \delta_{ij} \right],
\end{aligned}
$$

$$
\begin{aligned}
(D_3^{(1)})_{ij} &= \frac{\mu \beta f_{0,i}}{\rho_N \pi_{-1}^l(V)_i} M_{ij} \\
(D_3^{(2)})_{ij} &= \frac{\mu \beta f_{0,i}}{\rho_N} \left[\left(\frac{g_{1,i}}{\pi_{-1}^l(V)_i} - \frac{\pi_0^l(V)_i}{(\pi_{-1}^l(V)_i)^2} + \frac{g_{1,i}}{\rho_N} - \frac{\pi_0^l(V)_i}{\rho_N \pi_{-1}^l(V)_i} \right) M_{ij} + \frac{1}{\pi_{-1}^l(V)_i} \delta_{ij} \right] \\
&\quad - \beta' \frac{\mu \theta_i}{\rho_N \pi_{-1}^l(V)_i^2} \delta_{ij} \\
(D_3^{(3)})_{ij} &= \frac{\mu \beta f_{0,i}}{\rho_N} \left[M_{ij} \left(\frac{\pi_1^l(V)_i}{(\pi_{-1}^l(V)_i)^2} + \frac{(\pi_0^l(V)_i)^2}{(\pi_{-1}^l(V)_i)^3} - \frac{\pi_0^l(V)_i}{(\pi_{-1}^l(V)_i)^2} g_{1,i} + \frac{g_{1,i}}{\rho_N \pi_{-1}^l(V)_i} - \frac{\pi_0^l(V)_i}{\rho_N (\pi_{-1}^l(V)_i)^2} \right) \right. \\
&\quad \left. + \left(\frac{g_{1,i}}{\pi_{-1}^l(V)_i} - \frac{\pi_0^l(V)_i}{(\pi_{-1}^l(V)_i)^2} + \frac{1}{\rho_N} \left(g_{1,i} - \frac{\pi_0^l(V)_i}{\pi_{-1}^l(V)_i} \right) \right) \delta_{ij} \right] \\
&\quad + \beta' \frac{\mu \theta_i}{\rho_N \pi_{-1}^l(V)_i^2} \left(\frac{2\pi_0^l(V)_i}{\pi_{-1}^l(V)_i} + \frac{1}{\rho_N} \right) \delta_{ij},
\end{aligned}
$$

$$
\begin{aligned}
(D_4^{(0)})_{ij} &= -\beta' \frac{1}{\rho_N} M_{ij} \\
(D_4^{(1)})_{ij} &= \frac{\beta'}{\rho_N^2} M_{ij} - \frac{\beta'}{\rho_N} \delta_{ij} \\
(D_4^{(2)})_{ij} &= -\frac{\beta'}{\rho_N^3} M_{ij} + \frac{\beta'}{\rho_N^2} \delta_{ij} \\
(D_4^{(3)})_{ij} &= \frac{\beta'}{\rho_N^4} M_{ij} - \frac{\beta'}{\rho_N^3} \delta_{ij}.
\end{aligned}
$$

B Relaxation time in the limit $\varepsilon \to 0$

We have shown in Section 4.2.2 that our system exhibits marginal stability at $\varepsilon = 0$. We now prove that the relaxation time of the system behaves as $\tau_r \sim \varepsilon^{-1}$. To this end, we use analytical perturbation theory as described in [104], which in our setting reduces to the ε-perturbation of the characteristic polynomial of $\mathbb{D}(\varepsilon = 0)$ [7] as ε goes away from 0. Some elements of analytical

[7] We have done a slight abuse of notation, since $\mathbb{D}(\varepsilon = 0)$ is not formally defined because of the diverging upper right block.

perturbation theory are reported in Appendix D for completeness. This characteristic polynomial is given by

$$\chi(\sigma,0)=\sigma^2\prod_{\nu=1}^{N}\left(\sigma-\sigma_+^\nu\right)\left(\sigma-\sigma_-^\nu\right), \tag{II.40}$$

with $\sigma_\pm^\nu$ given in the Section 4.2.2.

We now try to find a perturbation of the σ^2 term to retrieve the perturbation on $\sigma_\pm^N=0$. Using analytical perturbation theory, we see that $(\varepsilon,\sigma)=(0,0)$ is a splitting point under the perturbation $\mathbb{D}(\varepsilon)$ ($\varepsilon=0$ is a multiple point – since $\mathbb{D}$ has at least one multiple root for $\varepsilon=0$ – and $\sigma_\pm^N=0$ is a multiple root.) In this setting, $\sigma_\pm^N=0$ splits under the perturbation $\mathbb{D}(\varepsilon)$ to give 2 perturbed eigenvalues. Henceforth, for small enough ε, the prime factor σ^2 of $\chi(\sigma,0)$ is expressed as a second order polynomial whose coefficients depend on ε.

We may write

$$p_0(\sigma):=\sigma^2\xrightarrow{\mathbb{D}(\varepsilon)}p_0(\sigma,\varepsilon):=\sigma^2(1+a_2^{(1)}\varepsilon+a_2^{(2)}\varepsilon^2+\cdots)+\sigma(a_1^{(1)}\varepsilon+a_1^{(2)}\varepsilon^2+\cdots)\\+a_0^{(1)}\varepsilon+a_0^{(2)}\varepsilon^2+\cdots.$$

This expansion makes sure that $p_0(\sigma,\varepsilon)\underset{\varepsilon\to0}{\longrightarrow}p_0(\sigma)$. Moreover, at least one of the $a_0^{(i)}$ is non-zero. Otherwise we would be able to factor out σ in $p_0(\sigma,\varepsilon)$, meaning that for small enough (but non zero) ε, $0\in\mathrm{Sp}\left(\mathbb{D}(\varepsilon)\right)$ which we know is not correct since the system is stable for $\varepsilon>0$.

Furthermore, we know that the splitting behavior of $\sigma_\pm^N=0$ is imposed, ensuring that the discriminant of $p_0(\sigma,\varepsilon)$ cannot vanish (leading to a multiple root), which yields another condition on the coefficients. Finally, since we are looking at complex roots in general, $p_0(\sigma,\varepsilon)$ will always factor into two irreducible and normalized polynomials of degree 1. This ensures that $\forall\, i\geq1,\ a_2^{(i)}=0$ and that $a_0^{(1)}=0$.

This last point is not so straightforward and warrants an explanation. From [104], the Puiseux series for the perturbed eigenvalues $\sigma_\pm^N(\varepsilon)$ can be written as

$$\sigma_\pm^N(\varepsilon)=\sum_{x=1}^{\infty}b_{\pm,x}^N\varepsilon^{x/g_{N,\pm}}$$

where $g_{N,\pm}$ is the degree of the polynomial from which the root $\sigma_\pm^N$ is extracted. In our setting $g_{N,\pm}=1$ meaning that the first perturbation to $\sigma_\pm^N$ is of order ε. Now, we also know that $\sigma_\pm^N$ is obtained by solving the second order equation $p_0(\sigma,\varepsilon)=0$. This means that both roots read

$$\sigma_\pm^N=o(\varepsilon)+\kappa_\pm\sqrt{\Delta},$$

with Δ the discriminant of $p_0(\sigma,\varepsilon)$. We may write Δ as

$$\Delta=o(\varepsilon^2)-4a_0^{(1)}\varepsilon,$$

so that, if $a_0^{(1)}\neq0$, the dominant term of $\sigma_\pm^N$ will be of order $o(\sqrt{\varepsilon})$ which contradicts the previous analysis.

Finally, we can look for a perturbation resembling

$$p_0(\sigma):=\sigma^2\xrightarrow{\mathbb{D}(\varepsilon)}p_0(\sigma,\varepsilon):=\sigma^2+\sigma(a_1^{(1)}\varepsilon+a_1^{(2)}\varepsilon^2+\cdots)+a_0^{(2)}\varepsilon^2+\cdots.$$

To determine the different terms in this expansion, we use the determinant computation from Section 4.2.2, but now keeping terms up to order ε^2. This yields

$$\begin{aligned}
\det\left(\sigma\mathbf{I}_{2N}-\mathbb{D}\right) &= \begin{vmatrix}\sigma\mathbf{I}_N-\mathbf{D}_1 & -\mathbf{D}_2\\ -\mathbf{D}_3 & \sigma\mathbf{I}_N-\mathbf{D}_4\end{vmatrix}\\
&\underset{\varepsilon\to 0}{\approx} \det\left((\sigma\mathbf{I}_N-\mathbf{D}_1)(\sigma\mathbf{I}_N-\mathbf{D}_4)-\mathbf{D}_2\mathbf{D}_3\right)\\
&= \det\left[\boldsymbol{\Sigma}^{(0)}(\sigma)+\varepsilon\boldsymbol{\Sigma}^{(1)}(\sigma)\varepsilon^2\boldsymbol{\Sigma}^{(2)}(\sigma)\right]\\
&\underset{\varepsilon\to 0}{\approx} \det\boldsymbol{\Sigma}^{(0)}(\sigma)+\varepsilon\mathrm{Tr}\left(\mathrm{Com}\left(\boldsymbol{\Sigma}^{(0)}\right)^{\top}\boldsymbol{\Sigma}^{(1)}(\sigma)\right)\\
&\quad+\varepsilon^2\mathrm{Tr}\left(\mathrm{Com}\left(\boldsymbol{\Sigma}^{(0)}\right)^{\top}(\sigma)\boldsymbol{\Sigma}^{(2)}(\sigma)\right)\\
&\quad+\varepsilon^2\frac{\left(\mathrm{Tr}\left(\mathrm{Com}\left(\boldsymbol{\Sigma}^{(0)}\right)^{\top}(\sigma)\boldsymbol{\Sigma}^{(1)}(\sigma)\right)\right)^2-\mathrm{Tr}\left(\left(\mathrm{Com}\left(\boldsymbol{\Sigma}^{(0)}\right)^{\top}(\sigma)\boldsymbol{\Sigma}^{(1)}(\sigma)\right)^2\right)}{2\det\boldsymbol{\Sigma}^{(0)}(\sigma)}.
\end{aligned}$$

where

$$\begin{aligned}
\boldsymbol{\Sigma}^{(0)}(\sigma) &= \sigma^2\mathbf{I}_N-\sigma\left(\mathbf{D}_1^{(0)}+\mathbf{D}_4^{(0)}\right)+\mathbf{D}_1^{(0)}\mathbf{D}_4^{(0)}-\mathbf{D}_2^{(-1)}\mathbf{D}_3^{(1)}\\
\boldsymbol{\Sigma}^{(1)}(\sigma) &= -\sigma(\mathbf{D}_1^{(1)}+\mathbf{D}_4^{(1)})+\mathbf{D}_1^{(0)}\mathbf{D}_4^{(1)}+\mathbf{D}_1^{(1)}\mathbf{D}_4^{(0)}-\mathbf{D}_2^{(-1)}\mathbf{D}_3^{(2)}-\mathbf{D}_2^{(0)}\mathbf{D}_3^{(1)}\\
\boldsymbol{\Sigma}^{(2)}(\sigma) &= -\sigma(\mathbf{D}_1^{(2)}+\mathbf{D}_4^{(2)})+\mathbf{D}_1^{(0)}\mathbf{D}_4^{(2)}+\mathbf{D}_1^{(1)}\mathbf{D}_4^{(1)}+\mathbf{D}_1^{(0)}\mathbf{D}_4^{(1)}-\mathbf{D}_2^{(-1)}\mathbf{D}_3^{(3)}\\
&\quad-\mathbf{D}_2^{(0)}\mathbf{D}_3^{(2)}-\mathbf{D}_2^{(1)}\mathbf{D}_3^{(1)}
\end{aligned}$$

The constant term $\det\boldsymbol{\Sigma}^{(0)}(\sigma)$ is the characteristic polynomial of $\mathbb{D}$ for $\varepsilon=0$, so that $\det\boldsymbol{\Sigma}^{(0)}(\sigma)=\chi(\sigma,0)$. Furthermore, it is easy to prove that, for a diagonalizable matrix $\mathbf{A}$ with eigenvalues λ and associated eigenvectors $|\lambda\rangle$, the matrix $\mathrm{Com}\,(\mathbf{A})$ can be diagonalized in the same basis and reads

$$\mathrm{Com}\,(\mathbf{A})=\sum_{\lambda}\left(\prod_{\lambda'\neq\lambda}\lambda'\right)|\lambda\rangle\langle\lambda|\,. \tag{II.41}$$

Using this lemma, we can write

$$\begin{aligned}
\mathrm{Com}\left(\boldsymbol{\Sigma}^{(0)}(\sigma)\right) &= \left(\prod_{\nu\neq N}\left(\sigma-\sigma_+^{\nu}\right)\left(\sigma-\sigma_-^{\nu}\right)\right)|e_N\rangle\langle e_N|\\
&\quad+\sum_{\nu\neq N}\left(\sigma^2\prod_{\mu\neq\nu,N}\left(\sigma-\sigma_+^{\mu}\right)\left(\sigma-\sigma_-^{\mu}\right)\right)|e_\nu\rangle\langle e_\nu|\,.
\end{aligned} \tag{II.42}$$

We now develop each trace term onto the eigenbasis of $\mathrm{Com}\left(\boldsymbol{\Sigma}^{(0)}(\sigma)\right)$. From now on and, we drop the σ dependencies of the $\boldsymbol{\Sigma}$ matrices for clarity, but bear in mind that these matrices are polynomials of order one in σ. The first trace reads

$$\begin{aligned}
\mathrm{Tr}\left(\mathrm{Com}\left(\boldsymbol{\Sigma}^{(0)}\right)^{\top}\boldsymbol{\Sigma}^{(1)}\right) &= \left(\prod_{\nu\neq N}\left(\sigma-\sigma_+^{\nu}\right)\left(\sigma-\sigma_-^{\nu}\right)\right)\langle e_N|\,\boldsymbol{\Sigma}^{(1)}\,|e_N\rangle\\
&\quad+\sum_{\nu\neq N}\left(\sigma^2\prod_{\mu\neq\nu,N}\left(\sigma-\sigma_+^{\mu}\right)\left(\sigma-\sigma_-^{\mu}\right)\right)\langle e_\nu|\,\boldsymbol{\Sigma}^{(1)}\,|e_\nu\rangle\,.
\end{aligned}$$

Only the first term is of interest for us and we can use the explicit forms of the blocks of $\mathbb{D}$ to find

$$\begin{aligned}\langle e_N|\,\mathbf{\Sigma}^{(1)}\,|e_N\rangle &= \sigma\,\langle e_N|\left(\mathbf{D}_1^{(1)}+\mathbf{D}_4^{(1)}\right)|e_N\rangle\\ &= -\frac{\sigma}{\rho_N}(\alpha+\alpha'+\beta').\end{aligned}$$

The same computation can be carried out for the second trace term,

$$\begin{aligned}\langle e_N|\,\mathbf{\Sigma}^{(2)}\,|e_N\rangle &= \sigma\,\langle e_N|\left(\mathbf{D}_1^{(2)}+\mathbf{D}_4^{(2)}\right)|e_N\rangle + \langle e_N|\,\mathbf{D}_1^{(1)}\mathbf{D}_4^{(1)}\,|e_N\rangle - \langle e_N|\,\mathbf{D}_2^{(0)}\mathbf{D}_3^{(2)}\,|e_N\rangle\\ &= \frac{\sigma}{\rho_N^2}(\alpha'+\beta') - \frac{\alpha'\beta'+\alpha\beta}{\rho_N^2}+\sigma\kappa,\end{aligned}$$

with $\kappa = \langle e_N|\,\mathbf{D}_1^{(2)}\,|e_N\rangle$ which we do not need to compute.

The square trace terms are very complicated, and we only sketch out their computation. The terms that could have entered in the perturbation of $p_0(\sigma)$ cancel out (these are sums of square terms). The terms that are rational fractions of polynomials (and could be pathological since we look for a polynomial perturbation) cancel out as well. The other terms do not enter the perturbation of $p_0(\sigma)$ and are non-pathological.

Finally the perturbation of $p_0(\sigma)$ reads

$$p_0(\sigma) := \sigma^2 \xrightarrow{\mathbb{D}(\varepsilon)} p_0(\sigma,\varepsilon) \approx \sigma^2 + \sigma\left(\varepsilon\frac{\alpha+\alpha'+\beta'}{\rho_N} - \varepsilon^2\frac{\alpha'+\beta'}{\rho_N^2} - \varepsilon^2\kappa\right) + \varepsilon^2\frac{\alpha'\beta'+\alpha\beta}{\rho_N^2}.$$

We now write the discriminant of this polynomial at second order to get

$$\Delta(\varepsilon) = \frac{\varepsilon^2}{\rho_N^2}\left((\alpha+\alpha'+\beta')^2 - 4(\alpha\beta+\alpha'\beta')\right).$$

We retrieve the formula from Section 4.2.3. Denoting by $\beta_c = \frac{(\alpha+\alpha'+\beta')^2-4\alpha'\beta'}{4\alpha}$, we have at order one in ε

$$\sigma_\pm^N \underset{\varepsilon\to 0}{\approx} \frac{\varepsilon}{2\rho_N}\times\begin{cases}-\alpha'-\beta'-\alpha \pm \sqrt{(\alpha'+\beta'+\alpha)^2-4(\alpha\beta+\alpha'\beta')} & \text{if} \quad \beta<\beta_c\\ -\alpha'-\beta'-\alpha \pm i\sqrt{4(\alpha\beta+\alpha'\beta')-(\alpha'+\beta'+\alpha)^2} & \text{if} \quad \beta>\beta_c\\ -\alpha'-\beta'-\alpha & \text{if} \quad \beta=\beta_c\end{cases}. \tag{II.43}$$

C Computation of the volatility induced by Gaussian shocks on productivity factors

If we consider shocks on productivity factors $z_i(t) = z_i + \xi_i(t)$ with $\xi_i(t)$ a Gaussian white noise, we can linearize the dynamics of the naive model in both small deviations from equilibrium and small shocks. The stochastic equation that we retrieve reads

$$\frac{\mathrm{d}\mathbf{U}(t)}{\mathrm{d}t} = \mathbb{D}\mathbf{U}(t) + \mathbf{\Xi}(t), \tag{II.44}$$

with a noise $\mathbf{\Xi}$ of the form

$$\mathbf{\Xi}(t) = \begin{pmatrix}-\frac{\alpha+\alpha'}{z_i}\mathbf{p}_{\mathrm{eq}}\circ\boldsymbol{\xi}(t)\\ \frac{\beta-\beta'}{z_i}\boldsymbol{\gamma}_{\mathrm{eq}}\circ\boldsymbol{\xi}(t)\end{pmatrix} \underset{\varepsilon\to 0}{\sim} \begin{pmatrix}-\frac{\alpha+\alpha'}{\varepsilon\rho_N}(\boldsymbol{\ell}_N\cdot\mathbf{V})\mathbf{r}_N\circ\boldsymbol{\xi}(t)\\ \frac{\beta-\beta'}{(\boldsymbol{\ell}_N\cdot\mathbf{V})\rho_N}\mathbf{l}_N\circ\boldsymbol{\xi}(t)\end{pmatrix}, \tag{II.45}$$

with $\mathbf{r}_N$ (resp. $\boldsymbol{\ell}_N$) the right (resp. left) eigenvector of $\mathbf{M}$ associated to ε. The correlations of this noise are slightly more complicated than in the main text of this chapter

$$\langle \Xi_i(t)\Xi_j(s)\rangle = \sigma^2 G(|t-s|) \times \begin{cases} \delta_{ij}\left(\frac{(\alpha+\alpha')(\boldsymbol{\ell}_N\cdot\mathbf{V})}{\rho_N}\right)^2 r_{N,i}r_{N,j}\varepsilon^{-2} & \text{if} \quad i,j\leq n \\ \delta_{ij}\left(\frac{\beta-\beta'}{(\boldsymbol{\ell}_N\cdot\mathbf{V})\rho_N}\right)^2 l_{N,i}l_{N,j} & \text{if} \quad i,j>n \\ -\delta_{i,j-n}\frac{(\beta-\beta')(\alpha+\alpha')}{\rho_N^2} r_{N,i}l_{N,j}\varepsilon^{-1} & \text{if} \quad i\leq n,\ j>n \\ -\delta_{i-n,j}\frac{(\beta-\beta')(\alpha+\alpha')}{\rho_N^2} l_{N,i}r_{N,j}\varepsilon^{-1} & \text{if} \quad i>n,\ j\leq n \end{cases}. \tag{II.46}$$

For an undirected network and in the limit $\varepsilon \to 0$, the matrix $\mathbb{D}$ yields two eigenvalues $\sigma_N^{\pm} = k^{\pm}\varepsilon \to 0$ with associated eigenvectors $\boldsymbol{\Sigma}_N^{\pm} = (\mathbf{e}_N, \boldsymbol{\nu}^{\pm}\varepsilon)^{\top}$ where $\mathbf{e}_N$ is the Perron-Frobenius eigenvector of $\mathbf{M}$. We assume $\beta < \beta_c$ so that the marginal eigenvalues are real, as well as their eigenvectors. It follows that, at leading order in ε, the volatility of the marginal components of $\mathbf{U}(t)$ behaves as $\varepsilon^{-3/2}$. Indeed

$$\left\langle u_N^{\pm}(t)^2 - \left\langle u_N^{\pm}(t)\right\rangle^2 \right\rangle = \frac{\sigma^2}{\left(k^{\pm}\right)^2\varepsilon^3}\left(\frac{(\alpha+\alpha')(\boldsymbol{e}_N\cdot\mathbf{V})}{\rho_N}\right)^2 \mathscr{H}\left(\mathbf{e}_N\right)\int_0^{\infty} d\tau e^{-\varepsilon\tau} G\left(\frac{\tau}{\nu^{\pm}}\right),$$

where $\mathscr{H}$ represents the inverse participation ratio. To retrieve the volatility as $\varepsilon^{-1/2}$ we may rescale $\delta p_i(t)$ (resp. $\delta\gamma_i(t)$) by $p_{eq,i}$ (resp. $\gamma_{eq,i}$). Denoting by $\boldsymbol{\epsilon}_i$ the ith canonical vector of $\mathbb{R}^{2N}$, we have

$$\begin{aligned}
\mathrm{Var}\left(\frac{\delta p_i(t)}{p_{eq,i}}\right) &= p_{eq,i}^{-2}\mathrm{Var}\left(\sum_{\substack{k=1\\ \tau=\pm}}^{N} u_k^{\tau}(t)(\boldsymbol{\Sigma}_k^{\pm}\cdot\boldsymbol{\epsilon}_i)\right) \\
&\underset{\substack{\varepsilon\to 0\\ \varepsilon t\ll 1}}{\approx} \frac{\varepsilon^2}{e_{N,i}^2(\mathbf{e}_N\cdot\mathbf{V})^2}\mathrm{Var}\left(u_N^+(t)e_{N,i} + u_N^-(t)e_{N,i}\right) \\
&= \frac{\varepsilon^2}{(\mathbf{e}_N\cdot\mathbf{V})^2}\left[\mathrm{Var}\left(u_N^+(t)\right) + \mathrm{Var}\left(u_N^-(t)\right) + 2\mathrm{Cov}\left(u_N^+(t), u_N^-(t)\right)\right] \\
&\propto \frac{1}{\varepsilon}; \\
\mathrm{Var}\left(\frac{\delta\gamma_i(t)}{\gamma_{eq,i}}\right) &= \gamma_{eq,i}^{-2}\mathrm{Var}\left(\sum_{\substack{k=1\\ \tau=\pm}}^{N} u_k^{\tau}(t)(\boldsymbol{\Sigma}_k^{\pm}\cdot\boldsymbol{\epsilon}_{i+N})\right) \\
&\underset{\substack{\varepsilon\to 0\\ \varepsilon t\ll 1}}{\approx} \frac{(\mathbf{e}_N\cdot\mathbf{V})^2}{e_{N,i}^2}\mathrm{Var}\left(u_N^+(t)\nu^+\varepsilon e_{N,i} + u_N^-(t)\nu^-\varepsilon e_{N,i}\right) \\
&= (\mathbf{e}_N\cdot\mathbf{V})^2\varepsilon^2\left[(\nu^+)^2\mathrm{Var}\left(u_N^+(t)\right) + (\nu^-)^2\mathrm{Var}\left(u_N^-(t)\right)\right. \\
&\qquad \left. +2\nu^+\nu^-\mathrm{Cov}\left(u_N^+(t), u_N^-(t)\right)\right] \\
&\propto \frac{1}{\varepsilon}.
\end{aligned}$$

D Elements of analytical perturbation theory

In this appendix, we will present some useful concepts related to analytical perturbation theory of matrices and operators. These ideas have been lifted almost *verbatum* from [105] and are here for completeness. We introduce such concepts to have an abstract approach to the holomorphic perturbation $\mathbb{D}(\epsilon)$.

Let us study the local behavior of the spectrum of $A(z)$, a meromorphic operator-valued function defined on $G \subset \mathbb{C}$, around a point $z_0 \in G$. If z_0 is a pole of order k of A then the same results apply to $B(z) := (z - z_0)^k A(z)$.

D.1 Characteristic polynomial

Definition II.1. *Let $A(z)$ be meromorphic in G. We call characteristic polynomial of $A(z)$ the quantity*

$$\chi(\lambda, A(z)) = \det(\lambda I_n - A(z)) := \lambda^n + a_1(z)\lambda^{n-1} + \cdots + a_N(z)$$

This polynomial of $G[\lambda]$ is normalized with scalar meromorphic functions as coefficients $a_i(z)$. If A is holomorphic in G we say that $\chi \in \mathscr{H}_G[\lambda]$. Furthermore, if at some point $z_0 \in G$ the equation $a_1(z_0) = \ldots = a_N(z_0) = 0$ holds, we say that $\chi \in \mathscr{H}_G^{z_0}[\lambda]$.

After this definition, a straightforward consequence of the fundamental theorem of polynomial factorization allows stating the following

Theorem II.1. *One can factorize χ such that*

$$\chi(\lambda, A(z)) = \prod_{\rho=1}^{r} p_\rho^{m_\rho} \tag{II.47}$$

where each p_ρ are normalized and irreducible elements of $G[\lambda]$. The poles of their coefficients belong to the set of poles of A. Furthermore, if $\chi \in \mathscr{H}_G[\lambda]$ (resp. $\chi \in \mathscr{H}_G^{z_0}[\lambda]$) so do every prime factors.

Proof. The first point is a straightforward consequence of the fundamental theorem of algebra. The second point is easily checkable when one expands the r.h.s of Eq. (II.47). The very last point is the trickiest. Assuming $\chi \in \mathscr{H}_G^{z_0}[\lambda]$, one has

$$\chi(\lambda, A(z_0)) = \lambda^n$$

For the r.h.s of Eq. (II.47) to reproduce this, each prime factors must have vanishing coefficients at z_0 since they are normalized. □

We will now introduce the concepts of simple and multiple points.

D.2 Simple and multiple points

The dotted set $G \setminus S_A$ (S_A being the set of poles of A) can be split into a set of simple points and a set of multiple points. First, we state the following general theorem before formulating Theorem II.3.

Theorem II.2. *Let p and q be normalized polynomial from $\mathscr{M}[\lambda]$ that are relatively prime in $\mathscr{M}[\lambda]$. Then, except for a set $H \subset G$, isolated and closed in G, the polynomial p and q are relatively prime in $\mathbb{C}[\lambda]$ for all $z \in G \setminus (S_p \cup S_q)$, i.e, for all $z \in G \setminus (S_p \cup S_q \cup H)$, p and q are relatively prime.*

Proof. Let $\deg p \leq \deg q > 0$. Since p and q are relatively prime, the remainder of the euclidean division of p by q is a polynomial p_r of degree 0, that is $f(z)$ a non-identically vanishing meromorphic function on G. Let $E = \bigcup_\rho (S_{p_\rho} \cup S_{q_\rho})$ the union of all poles of p_ρ and q_ρ, polynomials generated by Euclide's algorithm. E is an enumerable union of isolated and closed sets in G, it is then itself isolated and closed in G. Let N be the set of all roots of f. Then, for $N = f^{-1}\{0\}$, N is closed. Furthermore, since f is holomorphic on $G \setminus S_{p_r}$ and non identically vanishing, N is isolated. Let $z_0 \in G \setminus E$ and let λ_0 denote a common root of $p(\lambda, z_0)$ and $q(\lambda, z_0)$. From Euclide's algorithm it follows that

$$p_1(\lambda_0, z_0) = p_2(\lambda_0, z_0) = \cdots = p_{r-1}(\lambda_0, z_0) = f(z_0) = 0$$

ensuring that z_0 must be a root of $f(z)$. Hence, for all $z \in G \setminus (E \cup N)$, p and q have no common root. □

This theorem will be of help in the proof of the following

Theorem II.3. *Let p be a normalized and irreducible polynomial from $\mathscr{H}_G[\lambda]$. The set of all poles of coefficients of p is denoted by S_p. For all $z_0 \in G \setminus S_p$, the polynomial $p = p(\lambda, z_0)$ can be considered as a polynomial from $\mathbb{C}[\lambda]$. Then, except for an isolated and closed set in G, $p(\lambda, z_0)$ has only simple roots for all $z_0 \in G \setminus S_p$.*

Proof. Let us prove the assertions by induction on the degree of p. The case $\deg p = 1$ is trivial. Let us consider p such that $\deg p > 1$ and let us denote $q(\lambda, z) = \frac{\partial p}{\partial \lambda}(\lambda, z)$. Since p is irreducible, $(p, q) = 1$ meaning that p and q are relatively prime. From Theorem II.2, we know that p and q have no common roots, except for a closed and isolated subset of G. This means that, except for a closed and isolated subset of G, p only has simple roots for $z \in G \setminus S_p$. □

We can apply this theorem to the characteristic polynomial. The prime factors $p_\rho(\lambda, z_0)$ have multiple roots with respect to λ for at most an enumerable set of points z_0 from G. We define the polynomial q as

$$q(\lambda, z) = \prod_{\rho=1}^{r} p_\rho(\lambda, z)$$

Definition II.2. *The point $z_0 \in G \setminus S_A$ is called a* multiple point *if $q(\lambda, z_0)$ has at least one multiple root with respect to λ. Conversely, the point z_0 is called* simple *if $q(\lambda, z_0)$ has only simple roots with respect to λ.*

To finish this section, we will state a lemma, which will be of importance when dealing with the perturbed behavior of the spectrum around simple points.

Lemma II.1. *The set M of all multiple points is isolated and in G closed, i.e, M is enumerable and any accumulation point of M is to be found on ∂G.*

Proof. This is a straightforward consequence of Theorem II.3. □

D.2.1 Local behavior of the eigenvalues in the neighborhood of simple points

Let z_0 be a holomorphic point of $A(z)$ and let z_0 be simple. Recalling that

$$q(\lambda, z) = \prod_{\rho=1}^{r} p_\rho(\lambda, z)$$

From Lemma II.1, there exists an ϵ to that every point $z \in \mathscr{D}(z_0, \epsilon)$ is a simple point. This means that for each $\rho = 1, \cdots, r$, there exists *different* holomorphic function elements $\lambda_{\rho\sigma}(z)$ with $\sigma = 1, \cdots, g_\rho$ (with $g_\rho = \deg p_\rho$) such that

$$p_\rho(\lambda, z) = \prod_{\sigma=1}^{g_\rho} (\lambda - \lambda_{\rho\sigma}(z))$$

Altogether, one obtains different holomorphic eigenvalue elements over $|z - z_0| < \epsilon$ and one has

$$\chi(\lambda, A(z)) = \prod_{\rho=1}^{r} \prod_{\sigma=1}^{g_\rho} (\lambda - \lambda_{\rho\sigma}(z))$$

Each perturbed eigenvalue has a holomorphic dependency on z.

D.3 Splitting behavior of eigenvalues in the neighborhood of multiple points

Let z_0 be a holomorphic point of $A(z)$ and let it be multiple. The behavior of eigenvalues in the vicinity of z_0 can be very complicated and splitting may occur. Let λ_0 be a fixed root of $q(\lambda, z_0)$ with multiplicity $m > 1$. The multiplicity of λ_0 with respect to $p_\rho(\lambda, z_0)$ is denoted by n_ρ such that $\sum_\rho n_\rho = m$, and there is at least one $n_\rho > 0$. Let us state the following admitted theorem (the proof is too long and out of scope for our discussion).

Theorem II.4. *Let $p \in \mathscr{M}_G[\lambda]$ be normalized, let $z_0 \in G \backslash S_p$ and $p(\lambda, z_0) = \prod_{\rho=1}^{r} (\lambda - \lambda_0)^{k_\rho}$. Then, there is a neighborhood of z_0, for instance a disc $K = \mathscr{D}(z_0, \epsilon)$ such that the following properties hold. There exist r polynomials $q_1(\mu, z), \ldots, q_r(\mu, z)$ belonging to $\mathscr{H}_K^{z_0}[\mu]$ with $\deg q_\rho = k_\rho$ such that*

$$p(\lambda, z) = \prod_{\rho=1}^{r} q_\rho(\lambda - \lambda_\rho, z)$$

is a decomposition of p within $\mathscr{H}_K[\lambda]$.

We apply this theorem to each factors of q. We choose ϵ such that $\mathscr{D}(z_0, \epsilon)$ is common for all p_ρ (i.e $\epsilon = \min_\rho \epsilon_\rho$ with obvious notations), and such that this dotted disc contains only simple points (possible from Lemma II.1). The decomposition of Theorem II.4 for $p_\rho(\lambda, z)$ contains a factor corresponding to the root λ_0. Let us denote this factor by $q_\rho(\lambda - \lambda_0, z)$ where $\deg q_\rho = n_\rho$ and $q_\rho(\mu, z) \in \mathscr{H}_K^{z_0}[\mu]$. We can decompose this polynomial into prime factors with respect to $\mathscr{H}_K[\mu]$

$$q_\rho(\lambda - \lambda_0, z) = \prod_{\alpha}^{k_\rho} q_{\rho\alpha}(\lambda - \lambda_0, z)$$

with $q_{\rho\alpha} \in \mathscr{H}_K^{z_0}[\mu]$ and irreducible with respect to $\mathscr{H}_K[\mu]$. Since p_ρ is irreducible with respect to $\mathscr{M}_G[\lambda]$ and that q_ρ are prime factors of p, no multiple factors can occur among the $q_{\rho\alpha}$. Denoting

$\deg q_{\rho\alpha} = g_{\rho\alpha}$ we then have $\sum_{\alpha=1}^{k_\rho} = n_\rho$. Let us now state a theorem that will give us the behavior of roots of $q_{\rho\alpha}$.

Theorem II.5. *Let $p(\mu, z) \in \mathscr{H}_K^{z_0}[\mu]$ where $K = \mathscr{D}(z_0, \epsilon)$ and $\deg p = g$ and p irreducible in $\mathscr{H}_K^{z_0}[\mu]$ (hence also irreducible with respect to $\mathscr{H}_K[\mu]$). Furthermore, for all $z \in K \setminus \{z_0\}$, $p(\mu, z)$ is assumed to have only simple roots with respect to μ. Then p defines a unique g-values algebroid function $\mathfrak{P}$ over K where only z_0 is a singular point, namely a branching point of order g. As $z \to z_0$, the function $\mathfrak{P}$ assumes the unique finite limit 0. Furthermore, $\mathfrak{P}$ is represented over K by a convergent Puiseux series of the form*

$$\sum_{\rho=0}^{\infty} a_\rho (z - z_0)^{\rho/g}, \quad a_0 = 0, \quad z \in K$$

that is, if one denotes by $\lambda_1(z), \ldots, \lambda_g(z)$ the values of $\mathfrak{P}$ over $z \neq z_0$, then (with suitable ordering)

$$\lambda_\sigma(z) = \sum_{\rho=0}^{\infty} a_\rho \left[\zeta^\sigma (z - z_0)^{1/g}\right]^\rho, \quad \sigma = 1, \ldots, g$$

where $(z - z_0)^{1/g}$ denotes a fixed root and ζ a g-th primitive root of unity.

We can now describe the situation as follows. Every polynomial $q_{\rho\alpha}(\lambda - \lambda_0, z)$ represents a branch $\mathfrak{H}_{\rho\alpha}$ of $\mathfrak{P}_\rho$ with the only singularity z_0 which is a branching point of $\mathfrak{H}_{\rho\alpha}$ of order $g_{\rho\alpha}$ with the unique finite limit λ_0 as $z \to z_0$. For $z \neq z_0$ the values of the branch are denoted by $\lambda_{\rho\alpha\sigma}(z)$ for $\sigma = 1, \ldots, g_{\rho\alpha}$ which are holomorphic function elements of $\mathfrak{H}_{\rho\alpha}$. Furthermore, they have the property $\lambda_{\rho\alpha\sigma} \to \lambda_0$ as z approaches z_0.
The family $\{\lambda_{\rho\alpha\sigma}\}$ is called the (z_0, λ_0)-group of perturbed eigenvalues. One can formulate the following results

- An eigenvalue λ_0 of $A(z_0)$ always splits under the perturbation $A(z)$ if it is a multiple root of $q(\lambda, z_0)$.
- If z_0 is multiple, then there is at least one eigenvalue λ_0 of $A(z_0)$ which splits under the perturbation $A(z)$.
- If z_0 is simple, then there is no splitting for the eigenvalues of $A(z_0)$ under the perturbation $A(z)$.

If the operator-valued function $A(z)$ is considered on the restricted region K, the eigenvalues of each branch $\mathfrak{H}_{\rho\alpha}$ form K-cycles of eigenvalues. In this way, we obtain a decomposition of the (z_0, λ_0)-group into several K-cycles. The eigenvalues $\lambda_{\rho\alpha\sigma}(z)$, $\sigma = 1, \ldots, g_{\rho\alpha}$ of a fixed K-cycle are given over K according to Theorem II.5, by a Puiseux series of the form

$$\lambda_{\rho\alpha\sigma}(z) = \lambda_0 + \sum_{x=1}^{\infty} a_{\rho\alpha x} \left[(z - z_0)^{1/g_{\rho\alpha}}\right]^x$$

where the $g_{\rho\alpha}$ different eigenvalues are obtained if $(z - z_0)^{1/g_{\rho\alpha}}$ runs through all the values of the root.

Finally, to end this appendix, we will give two definitions suggested by the previous analysis.

Definition II.3. *Let $z_0 \in G$ be a multiple point for the perturbation $A(z)$. Let λ_0 be a root of $q(\lambda, z_0)$. Then we have two situations*

- *If λ_0 is a multiple root of $q(\lambda, z_0)$, then the point $(z_0, \lambda_0$ is called a* splitting *point of the perturbation,*
- *If λ_0 is a simple root of $q(\lambda, z_0)$, then the point $(z_0, \lambda_0$ is called a* normal *point.*

CHAPTER III

Dynamical mean-field theory: the proverbial firm

Abstract

Even if interactions are key to understand the properties of complex systems, they usually make analytical computations complicated and painful. However, when the number N of interacting agents grows very large, certain systems exhibit some universality and can be described using a small amount of parameters. This universality translates into equations on representative agents, which feel overall interactions as a *mean field*. When applied to dynamical processes, such methods are called dynamical mean-field theories. In this chapter, we try to obtain dynamical mean-field theories to study the economic system presented in Chapter II. More generally, such approach seems to be interesting for economics as economic models often consider "representative" agents which aim at describing generic behaviors obtained after aggregation of granular units. Dynamical mean-field theories could allow specifying such aggregation processes.

1 Dynamical mean-field theory

Solving high-dimensional differential equations is in general a complicated task. When equations are coupled and non-linear, very little can be said in general about their properties, such as stability or the existence of limit cycles. Pioneer of the science of complex systems, Robert May [98] showed that the question of stability for a random N-dimensional linear dynamical system of the form

$$\frac{\mathrm{d}\mathbf{x}}{\mathrm{d}t} = \mathbf{A}\mathbf{x}, \tag{III.1}$$

only depends upon parameters relative to the distribution of the matrix elements A_{ij}. More precisely, May showed the following bound for stability. Considering that A_{ij} are IID random variables such that they are set to 0 with probability $1-p$, or drawn, with probability p, from a centered distribution of variance σ^2, the system is stable if $N < (\sigma^2 p)^{-1}$. In the context of computational neurosciences, Sompolinsky, Crisanti and

Sommers [106] showed some years later that a system of N neurons, modeled by a local field $h_i(t)$ and interacting through synaptic impulses $S_i(t) = \tanh gh_i(t)$ as

$$\frac{\mathrm{d}h_i(t)}{\mathrm{d}t} = -h_i(t) + \sum_{j\neq i} J_{ij}S_j(t), \quad J_{ij} = -J_{ji} \hookrightarrow \frac{J}{\sqrt{N}}\mathsf{N}(0,1)\,, \tag{III.2}$$

can exhibit chaotic behavior if the aggregate variable gJ is greater than 1, whereas a zero fixed-point exists otherwise.

In both cases, the specific nature of interactions (matrices $\mathbf{A}$ or $\mathbf{J}$) does not matter in the large size limit $N \to \infty$, and the systems exhibit some universality which only depends on a few parameters. In the second case, the authors derive a *self-consistent* (in the large size limit) equation for a single neuron

$$\frac{\mathrm{d}h}{\mathrm{d}t} = -h(t) + \eta(t), \tag{III.3}$$

where $\eta(t)$ is a Gaussian white noise of zero mean and covariance

$$\langle \eta(t)\eta(t+\tau)\rangle = J^2\mathbb{E}\left[N^{-1}\sum_j S_j(t)S_j(t+\tau)\right]. \tag{III.4}$$

The brackets $\langle(\cdot)\rangle$ denote the average over the Gaussian distribution of $\eta(t)$, while $\mathbb{E}[(\cdot)]$ the average over the distribution of $\mathbf{J}$. Eq. (III.3) therefore describes the behavior of an *average* neuron with interactions-induced fluctuations $\eta(t)$. The equivalence between Eqs. (III.2) and (III.3), or equivalently that between averages $\langle(\cdot)\rangle$ and $\mathbb{E}[(\cdot)]$, has been proven in [107] (in the context of spin-glasses which is analogous), and therefore Eq. (III.3) provides a faithful description of the system as N grows very large.

These equations are called *dynamical mean-field theories* (DMFT) and can provide faithful representations for large systems with complex interactions. Such theories might be useful for economics, which often uses the "representative" agent approximation. However, the actual derivation might be cumbersome and often depends on the actual model. As we mentioned in Chapter II, the behavioral rules that we postulate for prices and productions adjustments lead to equations which strongly resemble generalized Lotka-Volterra equations, for which DMFT has been used to study stability, attractors and chaotic behavior [108, 100, 109]. For completeness, we present here a rapid derivation of the DMFT equations associated with the generalized Lotka-Volterra model using the cavity method. For a full and detailed account, see [108] on which we heavily rely for the following explanation.

Consider an ecosystem which consists of S interacting species. Each species has a population of $N_i(t)$ which we assume to be continuous for simplicity. They reproduce at a rate r_i, and have carrying capacity [1] K_i, which we both set to 1 for simplicity. Species i and j interact through the matrix elements α_{ij} which account for cooperation ($\alpha_{ij} > 0$)

[1] The carrying capacity refers to the maximum population that can be sustained by an environment given the available resources.

or competition ($\alpha_{ij} < 0$). In the DMFT framework, the matrix elements α_{ij} are chosen to be IID random variables such that

$$\overline{\alpha_{ij}} = \mu/S, \quad \overline{(\alpha_{ij} - \overline{\alpha_{ij}})^2} = \sigma^2/S, \quad \overline{(\alpha_{ij} - \overline{\alpha_{ij}})(\alpha_{ji} - \overline{\alpha_{ji}})} = \gamma\sigma^2/S,$$

where $\overline{(\cdot)}$ denotes the average over the distribution of elements. The parameter γ measures the amount of symmetry of matrix $\boldsymbol{\alpha}$. The generalized Lotka-Volterra equations read

$$\frac{\mathrm{d}N_i}{\mathrm{d}t} = N_i \left(1 - N_i(t) - \sum_{j \neq i} \alpha_{ij} N_j(t) + h_i(t) \right), \tag{III.5}$$

where $h_i(t)$ is an external field necessary to define the responses of the system to perturbations. The method used in [108, 94] to derive the DMFT equations is called the *cavity method*. Roughly speaking, it amounts to adding a new species to a system of size S, deriving equations linking observables in the cases of size S and $S+1$, and equating the distributions of these observables in the large size limit. More precisely, here are the different steps to obtain self-consistent equations

1. Draw a $S \times S$ interaction matrix $\boldsymbol{\alpha}$, initial conditions $N_i(0)$ and let the system evolve.

2. Upon adding a new species $i = 0$ (with initial condition $N_0(0)$ and interactions α_{i0}, α_{0i}), we expect the subsequent perturbation on the old trajectories of N_i to be small (typically of order S^{-1}). The new species modifies the field $h_j(t)$ into $\widetilde{h}_j(t) = h_j(t) - \alpha_{j0} N_0(t)$, and we use linear response theory to relate unperturbed trajectories $N_i(t)$ to perturbed trajectories $\widetilde{N_i}(t)$, i.e.

$$\widetilde{N_i}(t) = N_i(t) - \sum_{j=1}^{S} \int_0^t ds \left. \frac{\delta N_i(t)}{\delta h_j(s)} \right|_{h=0} \alpha_{j0} N_0(s).$$

   We will denote by $\chi_{ij}(t,s)$ the response function $\left. \frac{\delta N_i(t)}{\delta h_j(s)} \right|_{h=0}$.

3. We can plug these expressions into the equation on N_0

$$\frac{\mathrm{d}N_0}{\mathrm{d}t} = N_0 \left(1 - N_0 - \sum_j \alpha_{0j} \widetilde{N_j} + h_0(t) \right),$$

   and carefully evaluate the interaction terms using both the law of large numbers and the central limit theorem. For instance, decomposing $\alpha_{ij} = \mu/S + \sigma a_{ij}$ (with a_{ij} centered Gaussian of variance $1/S$), one of the interaction terms yields

$$\sigma \sum_i a_{0i} N_i(t) \approx \sigma S \langle a_{0i} N_i(t) \rangle + \sigma \sqrt{S} \sqrt{\langle a_{0i}^2 N_i(t)^2 \rangle} Z \approx \sigma \sqrt{\langle N_i(t)^2 \rangle} Z,$$

   with Z a centered Gaussian random variable.

4. Evaluating all these interaction terms (see [108] for a full account), we get an equation on N_0 where we drop the index 0 since this species can be replaced by any other without changing results

$$\frac{\mathrm{d}N}{\mathrm{d}t} = N\left(1 - \mu m(t) - \sigma\eta(t) + \gamma\sigma^2 \int_0^t \chi(t,s)N(s) + h(t)\right).$$

Here, $\eta(t)$ is a centered Gaussian noise with correlator $C(t,s)$. $C(t,s)$, $m(t)$ and $\chi(t)$ are determined self-consistently through

$$\begin{aligned} m(t) &= \mathbb{E}\left[N(t)\right] \\ C(t,s) &= \mathbb{E}\left[N(t)N(s)\right] \\ \chi(t,s) &= \mathbb{E}\left[\left.\frac{\delta N(t)}{\delta h(s)}\right|_{h=0}\right], \end{aligned}$$

with $\mathbb{E}\left[(\cdot)\right]$ is the average over both noise $\eta(t)$ and initial condition $N(0)$.

Of course, the previous equation is still complex, but a lot can be said on its properties, which was not obvious for the initial Lotka-Volterra equations (see [108]). In the following, we will try to apply this reasoning to Eqs. (II.10) from Chapter II.

2 Mean-field Hawkins-Simons transition

In this section, we start by considering a mean-field approach to the equilibrium equations of Chapter I for constant return to scale. To do so, we will consider that the elements of the network matrix are Gaussian random variables, as in the computations that we presented in the introductory section. However, in contrast with the interaction matrix $\boldsymbol{\alpha}$ of the generalized Lotka-Volterra equations, the network matrix $\mathbf{M}$ has a Z-matrix structure, i.e. a positive diagonal populated by productivity factors and negative off-diagonal elements $-J_{ij}$. This sign structure must be conserved in the limit $N \to \infty$. We therefore model links weights as Gaussian random variables such that

$$\langle J_{ij}\rangle = \mu_J/N \tag{III.6}$$

$$\langle J_{ij}^2\rangle - \langle J_{ij}\rangle^2 = \sigma_J^2/N^\gamma, \tag{III.7}$$

where $\gamma > 1$ ensuring that J_{ij} remains almost surely positive in the large N limit. Furthermore, productivity factors are drawn from a distribution with probability density $P(z)$ such that $P(z) = 0$ if $z \leq 0$.

With this prescription for the network matrix, we start by considering the equilibrium equation on prices for N firms

$$\mathbf{M}_N\mathbf{p}_N = \mathbf{V}, \tag{III.8}$$

where the N subscript denotes the value for N firms. In the same spirit as in Section 4 of Chapter I, we introduce a new firm $i = 0$ with link variables J_{i0} and J_{0i} along with

productivity factor z_0. The new equilibrium equations on prices read (for $i \geq 1$)

$$\sum_{j=0}^{N}(M_{N+1})_{ij}(p_{N+1})_j = \sum_{j=1}^{N}(M_N)_{ij}(p_{N+1})_j - J_{i0}p_0 = V_i = \sum_{j=1}^{N}(M_N)_{ij}(p_N)_j, \quad \text{(III.9)}$$

where we used Eq. (III.8) for the last equality. We can insert these relations into the equilibrium equation for $i = 0$, which yields

$$z_0 p_0 = V_0 + \sum_{j=1}^{N} J_{0j}(p_{N+1})_j$$

$$z_0 p_0 = V_0 + p_0 \sum_{i,j} J_{0j}(M_N^{-1})_{ij}J_{i0} + \sum_{j=1}^{N} J_{0j}(p_N)_j,$$

leading to

$$p_0 = \frac{V_0 + \sum_{j=1}^{N} J_{0j}(p_N)_j}{z_0 - \sum_{i,j} J_{0j}(M_N^{-1})_{ij}J_{i0}}. \quad \text{(III.10)}$$

Assuming that prices are IID samples from a random variable p in the large N limit, one can write

$$\sum_{j=1}^{N} J_{0j}(p_N)_j \approx \mu_J \mathbb{E}[p] + \mathcal{O}\left(N^{(1-\min(\gamma,2))/2}\right), \quad \text{(III.11)}$$

with $\mathbb{E}[(\cdot)]$ the average over the distribution of p. Furthermore, one can approximate $\mathbf{M}_N^{-1}$ as

$$(M_N^{-1})_{ij} = \frac{\delta_{ij}}{z_i} + \frac{J_{ij}}{z_i z_j},$$

since $J_{ij} \to 0$ almost surely. As a consequence, the sum $\sum_{i,j} J_{0j}(M_N^{-1})_{ij}J_{i0}$ at the denominator of Eq. (III.10) only gives vanishing contributions as $N \to \infty$ since the leading term is $\sum_{j=1}^{N} J_{0j}J_{j0}/z_i \approx N^{-1}\mu_J^2\mathbb{E}[z^{-1}] + \mathcal{O}(N^{-1})$. Putting all these ingredients together yields a mean-field self-consistent equation on p

$$p = \frac{V + \mu_J \mathbb{E}[p]}{z}. \quad \text{(III.12)}$$

Introducing $\mu_J^c = \left(\int_0^\infty \mathrm{d}z P(z)/z\right)^{-1}$, we have

$$p = \frac{V\mu_J^c}{z}\left(\mu_J^c - \mu_J\right)^{-1}, \quad \text{(III.13)}$$

where we assumed V constant for simplicity. In the same way, we can get a mean-field equation on production levels by rescaling the baseline work-offer as $L_0 = N\ell_0$, and assuming that preference factors $\theta_i := \theta$ are constant

$$\gamma = \frac{\mu_J \ell_0}{zV} + \frac{\ell_0}{V\mu_J^c}\left(\mu_J^c - \mu_J\right). \quad \text{(III.14)}$$

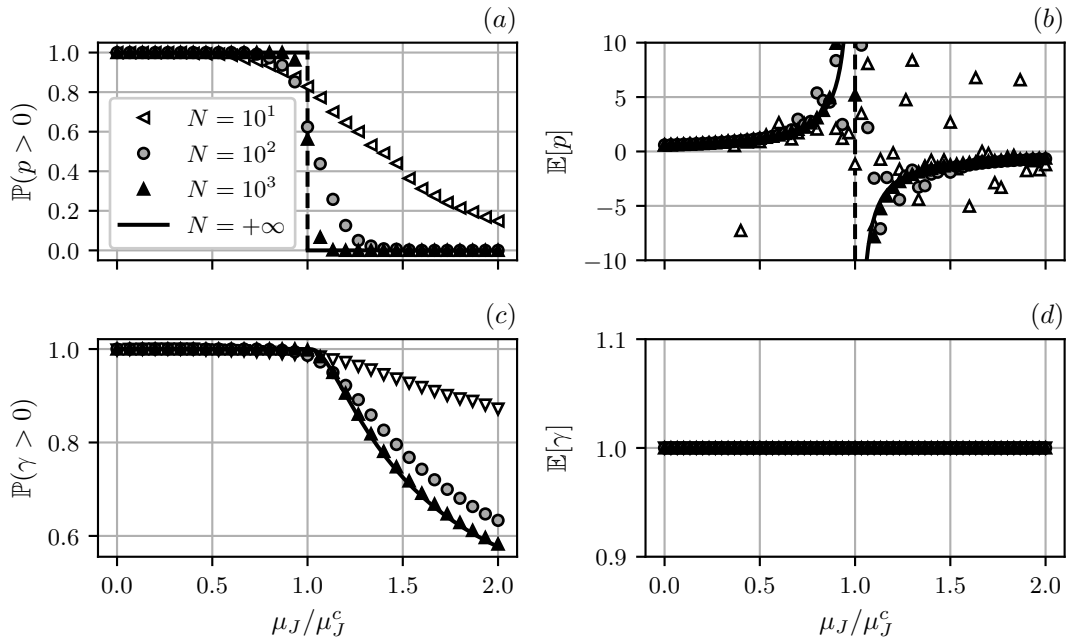


Figure III.1: Statistics of prices and production as a function of μ_J/μ_J^c obtained by inverting the systems $\mathbf{Mp} = \mathbf{V}$ and $\mathbf{M}^\top \boldsymbol{\gamma} = \ell_0/\mathbf{p}$ for $N \in \{10^1, 10^2, 10^3\}$, $z_i \hookrightarrow \mathsf{LN}(1,1)$ and J_{ij} Gaussian of mean μ_J/N and variance σ_J^2/N^γ, $\gamma = 3/2$. Plain dark lines indicate the solutions obtained from Eqs. (III.13) and (III.14). Each dot is obtained by averaging over 500 realizations of $\mathbf{M}$. (a) Probability that prices are positive, (b) empirical mean of prices, (c) probability that productions are positive, (d) empirical mean of productions.

These mean-field equations make the Hawkins-Simons transition plain as day: as soon as $\mu_J > \mu_J^c$, prices become negative (since productivity factors are positive). The interpretation is a lot clearer here as well: μ_J measures the network needs since $\mu_J \approx \sum_i J_{ij}$, whereas μ_J^c measures an average productivity in the network. Similar results are obtained upon studying the statistics of Leontief inverses $(\mathbf{I} - \mathbf{A})^{-1}\,\mathbf{e}$ in [110], with $\mathbf{A}$ the adjacency matrix of the network and $\mathbf{e} = (1, \ldots, 1)^\top$. Figure III.1 shows the probability to have positive prices or productions, along with the associated expectation values as a function of μ_J/μ_J^c and for several values of N.

Finally, one can see that the fluctuations associated with the J_{ij}s are not present in the final equations. This difference from the generalized Lotka-Volterra case comes from the fact that interactions are constrained to obey sign properties in the network matrix. We have not found a way to retrieve fluctuations all the while respecting these constraints. It would be very interesting to find such a regime since in that case the HS transition would be less trivial, see [109] for Lotka-Volterra.

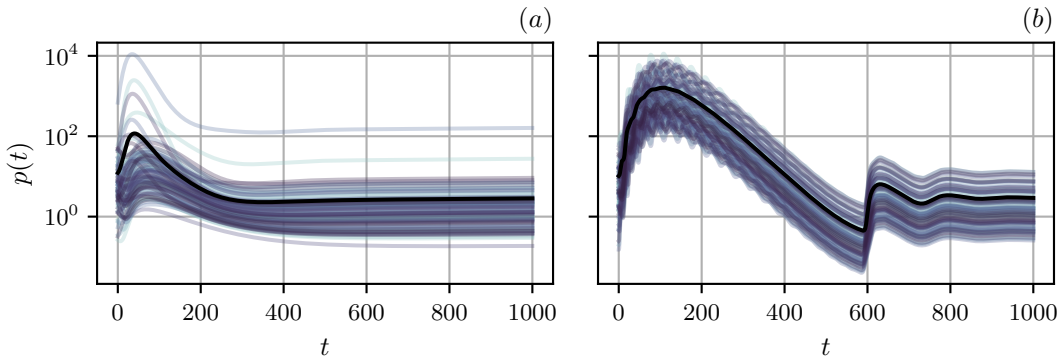


Figure III.2: Trajectories of log-prices under system (III.15) along with the average trajectory in black. (*a*) $\beta < \beta_c$ corresponding to overall exponential dampening. (*b*) $\beta > \beta_c$ corresponding to dampened oscillations.

3 DMFT for firm networks

As in the static case, the immutable sign structure of the network matrix $\mathbf{M}$ makes the DMFT equations associated to Eqs. (II.10) a lot less complex than in the Lotka-Volterra case. Our DMFT equations read (see Appendix A for a sketch of the computations)

$$\frac{\mathrm{d}p}{\mathrm{d}t} = -\alpha\frac{p}{z\gamma}\left(z\gamma - \mu_J\mathbb{E}[\gamma] - \frac{\ell_0}{p}\right) - \frac{\alpha'}{z}\left(zp - \mu_J\mathbb{E}[p] - V\right) \tag{III.15a}$$

$$\frac{\mathrm{d}\gamma}{\mathrm{d}t} = \beta\frac{\gamma}{zp}\left(zp - \mu_J\mathbb{E}[p] - V\right) - \frac{\beta'}{z}\left(z\gamma - \mu_J\mathbb{E}[\gamma] - \frac{\ell_0}{p}\right), \tag{III.15b}$$

where $\mathbb{E}[(\cdot)]$ denotes the average over both the distribution of z and initial conditions. From these equations, one can very easily recover most results from Chapter II. Appendix B will provide details for the results exposed below. Since z is drawn before running the dynamics on prices and productions, these equations are a lot easier to simulate than their Lotka-Volterra counterpart. Figure III.2 shows trajectories for prices under system (III.15) along with the trajectory of the average price $\mathbb{E}[p(t)]$.

3.1 Marginal stability

Considering fluctuations δp and $\delta\gamma$ around the fixed point $(p_{\mathrm{eq}}, \gamma_{\mathrm{eq}})$ defined by Eqs. (III.13) and (III.14), one gets the following linear evolution for the 2-dimensional vector $\mathbf{U}(t) = (\delta p, \delta\gamma)^\top$

$$\frac{\mathrm{d}\mathbf{U}}{\mathrm{d}t} = \begin{pmatrix} -\alpha\frac{\ell_0}{zp_{\mathrm{eq}}\gamma_{\mathrm{eq}}} - \alpha' & -\alpha\frac{p_{\mathrm{eq}}}{\gamma_{\mathrm{eq}}} \\ -\beta'\frac{\ell_0}{zp_{\mathrm{eq}}^2} + \beta\frac{\gamma_{\mathrm{eq}}}{p_{\mathrm{eq}}} & -\beta' \end{pmatrix}\mathbf{U}(t) := \mathbb{D}_{\mathrm{MF}}\mathbf{U}(t). \tag{III.16}$$

One can immediately write the characteristic polynomial $p(\lambda)$ of $\mathbb{D}_{\mathrm{MF}}$

$$p(\lambda) = \lambda^2 + \left(\alpha' + \beta' + \alpha\frac{z}{z+c}\right)\lambda + \alpha\beta + \alpha'\beta', \tag{III.17}$$

with $c = \mu_J \mu_J^c/(\mu_J^c - \mu_J)$ and with associated eigenvalues $\lambda_{1,2}$. A straightforward study (see Appendix B) shows that the fate of the eigenvalues, i.e. whether they are real or complex, is determined by quantities $m_\pm$ depending on time-scales

$$m_\pm = \alpha^{-1}\left(-\alpha' - \beta' \pm 2\sqrt{\alpha\beta + \alpha'\beta'}\right). \tag{III.18}$$

Noticing that

$$\beta_c - \beta = \frac{\alpha}{4}(1 - m_-)(1 - m_+), \tag{III.19}$$

where β_c is defined in Eq. (II.18) (the threshold determining whether the marginal eigenvalue of the system in Chapter II is real or complex), we see a correspondence between the values of $m_\pm$ and the relative values of β_c and β. Since $m_- < 0$, the relative magnitude of β and β_c is determined by the relative magnitude between m_+ and 1. Furthermore, the sign of m_+ is the same as the sign of $(\alpha' - \beta')^2 - 4\alpha\beta$ which was the condition for the stability matrix to have a complex or real spectrum right at the HS transition in Chapter II. Of course, none of this is a coincidence, and we can show for instance that as soon as $m_+ > 1$ the spectrum of $\mathbb{D}_{\mathrm{MF}}$ is almost surely complex below the HS transition (see Appendix B), as it would for the same parameters in Chapter II. Focusing on this case, one can write the real part of the eigenvalues and compute an expectation over z. It yields

$$\mathbb{E}\left[\mathfrak{Re}\left(\lambda_i\right)\right] = -\frac{1}{2}(\alpha' + \beta') - \frac{1}{2}\alpha\,\mathbb{E}\left[\frac{z}{z+c}\right],$$

which can be rearanged into

$$\begin{aligned}\mathbb{E}\left[\mathfrak{Re}\left(\lambda_i\right)\right] = &-\frac{1}{2}(\alpha' + \beta')\left(1 - \frac{\varepsilon}{\mu_J^c}\right)\mathbb{E}\left[\frac{1}{1 + \varepsilon(z - \mu_J^c)/(\mu_J^c)^2}\right] \\ &- \frac{1}{2}(\alpha' + \beta' + \alpha)\frac{\varepsilon}{(\mu_J^c)^2}\mathbb{E}\left[\frac{z}{1 + \varepsilon(z - \mu_J^c)/(\mu_J^c)^2}\right].\end{aligned}$$

where we set $\varepsilon = \mu_J^c - \mu_J > 0$. The previous expression interpolates between the large/low productivity regimes of Chapter II through ε (paramount of the lowest eigenvalue of $\mathbf{M}$), i.e.

- $\varepsilon \to \mu_J^c$ corresponds to the large productivity regime $\mu_J = 0$. It yields

  $$\mathbb{E}\left[\mathfrak{Re}\left(\lambda_i\right)\right] = -\frac{1}{2}(\alpha' + \beta' + \alpha),$$

  which is exactly the real part of the common eigenvalue in the large productivity regime of Chapter II.

- $\varepsilon \to 0^+$ corresponds to the low productivity regime where the HS condition is almost violated. In this case, the first term of $\mathbb{E}\left[\mathfrak{Re}\left(\lambda_i\right)\right]$ yields the average value of the real part of the spectrum of $\mathbb{D}$ for $\varepsilon = 0$ in Chapter II. The second term yields the real part of the marginal eigenvalue.

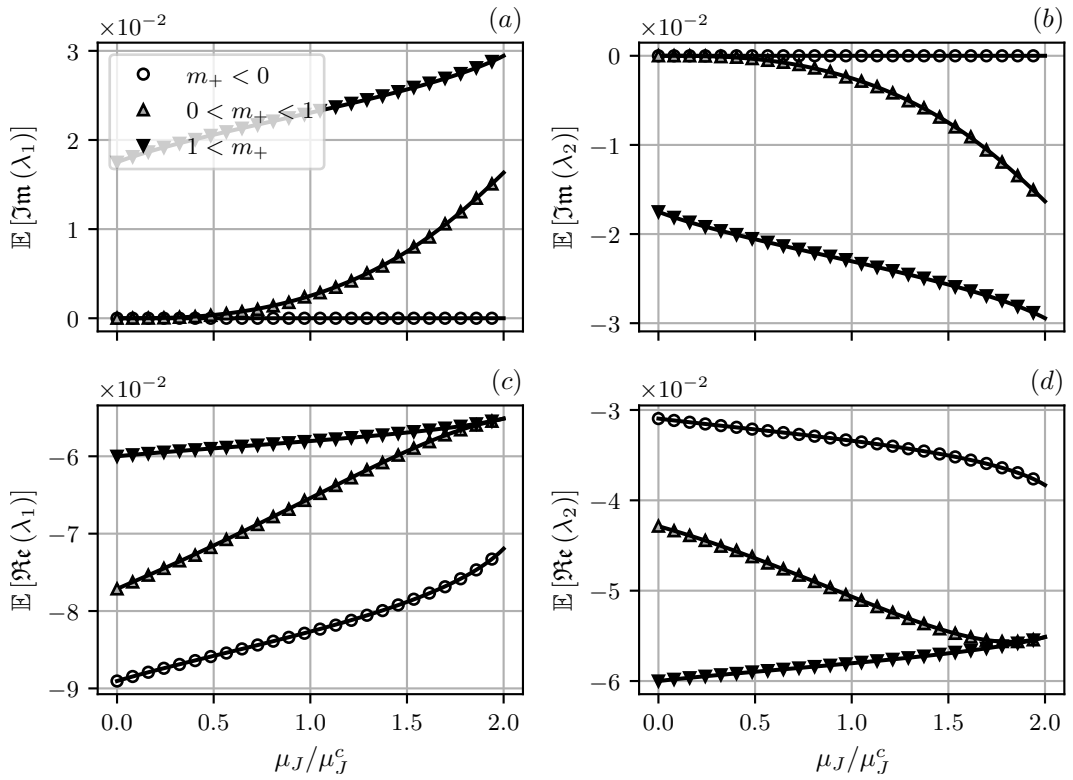


Figure III.3: Simulated eigenvalues of the matrix $\mathbb{D}_{\text{MF}}$ with respect to μ_J/μ_J^c and the value of m_+. The expectation value is taken over 500 realizations of $z \hookrightarrow \mathsf{LN}(1,1)$. $(a)-(b)$ display the imaginary part of λ_1 and λ_2 respectively. $(c)-(d)$ display the real part of λ_1 and λ_2 respectively

In opposition to the network model in Chapter II, we can get the eigenvalues of $\mathbb{D}_{\text{MF}}$ for any value of ε. We therefore fully characterize the interpolation between the plateauing eigenvalues (as $\varepsilon \to \infty$) and the marginal stability (as $\varepsilon \to 0$) of the previous chapter. Figure III.3 shows the real and imaginary parts of the eigenvalues $\lambda_{1/2}$ of $\mathbb{D}_{\text{MF}}$ along with the analytical solution from Appendix B.

3.2 Non-linear study

3.2.1 General features

Interestingly, Eqs. (III.15) can also be studied in their non-linear form. For simplicity, we will dispose of the expectation values $\mathbb{E}[p]$, $\mathbb{E}[\gamma]$ by choosing homogeneous productivity $P(z) = \delta(z - z_\star)$ and initial conditions $P(p(0), \gamma(0)) = \delta(p(0) - p_0)\delta(\gamma(0) - \gamma_0)$. Our

simplified equations now read

$$\frac{\mathrm{d}p}{\mathrm{d}t} = -\alpha \frac{p}{z_\star \gamma}\left(\varepsilon\gamma - \frac{\ell_0}{p}\right) - \frac{\alpha'}{z_\star}\left(\varepsilon p - V\right) \tag{III.20a}$$

$$\frac{\mathrm{d}\gamma}{\mathrm{d}t} = \beta \frac{\gamma}{z_\star p}\left(\varepsilon p - V\right) - \frac{\beta'}{z_\star}\left(\varepsilon\gamma - \frac{\ell_0}{p}\right), \tag{III.20b}$$

with $\varepsilon = z_\star - \mu_J$. We can define new variables $u = p/p_{\mathrm{eq}}$ and $g = \gamma/\gamma_{\mathrm{eq}}$ with $p_{\mathrm{eq}} = V/\varepsilon$ and $\gamma_{\mathrm{eq}} = \ell_0/V$, along with a new time $\tau = |\varepsilon|t/z_\star$ to get

$$\frac{\mathrm{d}u}{\mathrm{d}\tau} = \mathrm{sgn}\,(\varepsilon)\left[-\alpha\frac{u}{g}\left(g - \frac{1}{u}\right) - \alpha'\left(u - 1\right)\right] \tag{III.21a}$$

$$\frac{\mathrm{d}g}{\mathrm{d}\tau} = \mathrm{sgn}\,(\varepsilon)\left[\beta\frac{g}{u}\left(u - 1\right) - \beta'\left(g - \frac{1}{u}\right)\right]. \tag{III.21b}$$

We finally introduce the vector field $\mathbf{F}(u, g)$ to write the previous equations in vector form

$$\frac{\mathrm{d}}{\mathrm{d}t}\begin{pmatrix} u \\ g \end{pmatrix} = \mathrm{sgn}\,(\varepsilon)\,\mathbf{F}(u, g). \tag{III.22}$$

We can see from the previous equation that changing the sign of ε amounts to changing the direction of the arrow of time, i.e. $\varepsilon \to -\varepsilon$ is equivalent to $t \to -t$. Consequently, a stable system for $\varepsilon > 0$ will be unstable whenever the HS condition is violated. We can therefore only consider the case where $\varepsilon > 0$. Figure III.4 shows the vector field $\mathbf{F}$ along with possible trajectories from Eq. III.22.

A new feature that we can deduce from Eq. (III.22) is the non-existence of limit-cycles in this system. This point is not obvious and requires the following theorem

Theorem III.1 (Dulac-Bendixon's criterion)**.** *Let* $\mathbf{x} = (x_1, x_2) \in \mathbb{R}^2$ *evolve according to*

$$\dot{\mathbf{x}} = \mathbf{F}(x_1, x_2).$$

Let Ω *be a simply-connected domain in* $\mathbb{R}^2$*. If there exists a positive scalar function* $\mu \in \mathcal{C}^1(\mathbb{R}^2)$ *such that*

$$\nabla \cdot (\mu\mathbf{F})$$

keeps a constant sign over Ω*, then the dynamical system does not have any closed trajectory lying in* Ω*.*

For any function μ, we have the following computation in the case of the vector field from Eq. (III.22)

$$\begin{aligned}\nabla \cdot (\mu\mathbf{F}) = -\mu(\alpha + \beta + \beta') - \frac{g - u^{-1}}{g}\left[\beta' g\partial_g\mu + \alpha u\partial_u\mu\right] \\ + \frac{u - 1}{u}\left[\beta'\mu + \beta g\partial_g\mu - \alpha' u\partial_u\mu\right].\end{aligned}$$

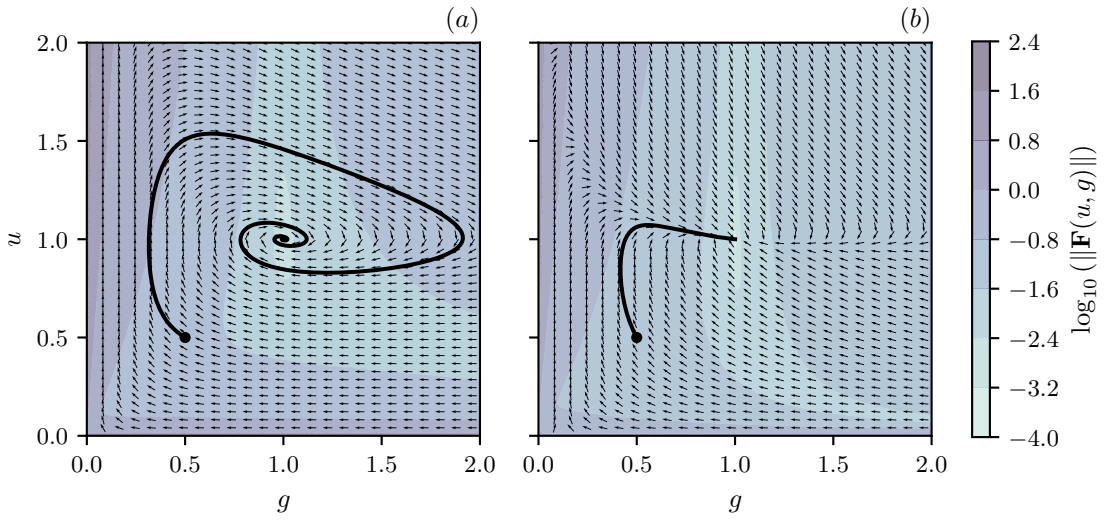


Figure III.4: Trajectories in the plane (u, g) (black curves) starting from initial condition $(0.5, 0.5)$ (black dots). The equilibrium of the system is the point $(u, g) = (1, 1)$. Small arrows represent the direction of the vector field $\mathbf{F}$, whereas the color gradient represents its magnitude. (a) $m_+ > 1$ equivalent to $\beta > \beta_c$ for which we see a stable spiraling trajectory towards equilibrium. (b) $m_+ < 0$ equivalent to $\beta < \beta_c$ for which we see a stable exponentially decaying trajectory towards equilibrium.

If one chooses

$$\mu(u, g) = u^k g^q, \quad k = \frac{\beta\beta'}{\alpha\beta + \alpha'\beta'}, \quad q = -\frac{\alpha\beta}{\alpha\beta + \alpha'\beta'},$$

the divergence simplifies to

$$\nabla \cdot (\mu \mathbf{F}) = -\mu(\alpha + \beta + \beta'), \tag{III.23}$$

and remains negative for $u, g > 0$. Taking Ω to be the strictly positive quadrant of $\mathbb{R}^2$, μ verifies every criterion of the previous theorem, which renders limit cycles impossible in the region $p, \gamma > 0$.

In this simplified case, we proved two important features. First, any stable trajectory for a given $\varepsilon > 0$ would become unstable as $\varepsilon \to -\varepsilon$. Second, since no limit cycle is possible, trajectories are bound to be unstable in the quarter plane $p, \gamma > 0$ as soon as $\varepsilon < 0$. The need to improve the model of Chapter II is made even clearer by this DMFT approach.

3.2.2 An exactly solvable case

Taking $\alpha' = \beta$, we can fully solve the previous equations. It is easy to show that the aggregate variable $h = ug$ obeys the linear equation

$$\dot{h} = -(\alpha + \beta')(h(t) + 1), \tag{III.24}$$

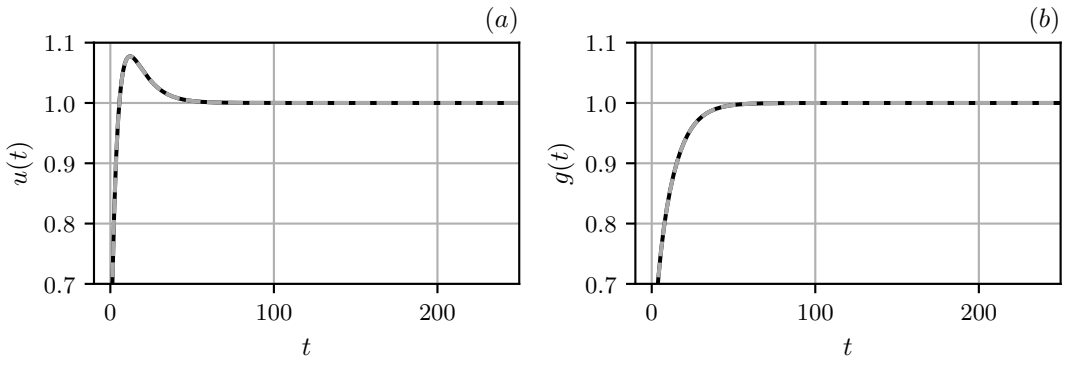


Figure III.5: Simulated trajectories (plain black lines) for variables (*a*) $u(t)$ and (*b*) $g(t)$ along with the exact formulas (dashed gray lines) inferred from Eqs. (III.25) and (III.27).

which yields

$$h(t) = 1 - C\exp\big(-(\alpha+\beta')t\big), \tag{III.25}$$

with $C = 1 - u_0 g_0$. We can express this back into the equation on u to find

$$\dot{u} = -u(\alpha + \alpha' - \alpha/h(t)) + \alpha'. \tag{III.26}$$

This equation is very simple and solves as

$$u(t) = \Big(C - e^{t(\alpha+\beta')}\Big)^{\frac{\alpha}{\alpha+\beta'}} \left(K e^{-(\alpha+\alpha')t} + \frac{\alpha'\Big(C - e^{t(\alpha+\beta')}\Big)^{\frac{\beta'}{\alpha+\beta'}}}{C(\alpha+\alpha')} H(t) \right), \tag{III.27}$$

with K an integration constant and

$$H(t) = {}_2F_1\left(1, \frac{\alpha'}{\alpha+\beta'} + 1; \frac{\alpha+\alpha'}{\alpha+\beta'} + 1; \frac{e^{(\alpha+\beta')t}}{C}\right).$$

In this case, the relaxation is exponential-like as highlighted in Figure III.5.

4 Conclusion

Dynamical mean-field theories provide a natural way to take the "representative" limit in large interacting complex systems. Applying this framework to the equations of our weakly out-of-equilibrium dynamics from Chapter II, we were able to show that most results for which computations revealed cumbersome could be recovered easily. Furthermore, we were also able to infer new results such as the absence of limit cycles, which would have been difficult to obtain within the full model of Chapter II. The definitive absence of bounded dynamics whenever the HS transition is violated is yet another argument in favor of developing a much more consistent model for dynamics in firm networks.

Key takeaways

- **Dynamical Mean-Field Theories (DMFT)** aim a reducing the complexity of a system down to a few universal parameters. These theories seem to be a good avenue for thinking about representative agents in economics or social sciences.
- **Mean-field network economies**: applied to the model of Chapter II, DMFT allows to retrieve most results from the study with N firms. Furthermore, it also allows to prove two key features of the model from Chapter II:
  - ⋆ There is no limit cycle in the region $p, \gamma > 0$.
  - ⋆ There is no bounded trajectory in the region $p, \gamma > 0$ whenever the HS condition is violated.

  Both features firmly motivate the sharpening from the model of Chapter II by including more realistic features.
- **Heterogeneity on** J_{ij} plays no role in the firm network setting because of the positivity constraint $J_{ij} \geq 0$.

A Sketch of the derivation of the DMFT equations

In this appendix, we sketch the computations leading to the DMFT equations (III.15). We will remain brief as most terms do not contribute in the limit $N \to \infty$ for the particular scaling chosen for the matrix elements J_{ij}

$$\langle J_{ij} \rangle = \mu_J / N \tag{III.28}$$

$$\langle J_{ij}^2 \rangle - \langle J_{ij} \rangle^2 = \sigma_J^2 / N^\gamma, \ \gamma > 1. \tag{III.29}$$

We recall the system of equations from Chapter II

$$z_i \gamma_i(t) \frac{\mathrm{d}p_i}{\mathrm{d}t} = -\alpha p_i(t) \left(\sum_j M_{ji} \gamma_j(t) - C_i(t) \right) - \alpha' \gamma_i(t) \left(\sum_j M_{ij} p_j(t) - V_i \right) + h_i^p(t)$$

$$z_i p_i(t) \frac{\mathrm{d}\gamma_i}{\mathrm{d}t} = \beta \gamma_i(t) \left(\sum_j M_{ij} p_j(t) - V_i \right) - \beta' p_i(t) \left(\sum_j M_{ji} \gamma_j(t) - C_i(t) \right) + h_i^\gamma(t),$$

to which we added external fields $h_i^{p,\gamma}$. For simplicity, we assume that preference factors $\theta_i := \theta$ are constant and $L_0 = N\ell_0$, such that $C_i(t) = \ell_0 / p_i(t)$. Upon adding a new firm $i = 0$, the external field acting on prices $i > 0$ is modified as

$$\widetilde{h}_i^p(t) = h_i^p(t) - \alpha p_i(t) M_{0i} \gamma_0(t) - \alpha' \gamma_i(t) M_{i0} p_0(t), \tag{III.30}$$

A similar expression can be written for $\widetilde{h}_i^\gamma(t)$. We assume that the perturbation induce by the new firm is small enough such that responses are linear, i.e. the perturbed price $\widetilde{p}_i(t)$ $(i > 0)$ can be written as

$$\begin{aligned} \widetilde{p}_i(t) = p_i(t) &- \sum_{j=1}^N \int_0^t ds \chi_{ij}^{pp}(t,s) \left(\alpha p_j(s) M_{0j} \gamma_0(s) + \alpha' \gamma_j(s) M_{j0} p_0(s) \right) \\ &+ \sum_{j=1}^N \int_0^t ds \chi_{ij}^{p\gamma}(t,s) \left(-\beta' p_j(s) M_{0j} \gamma_0(s) + \beta \gamma_j(s) M_{j0} p_0(s) \right), \end{aligned} \tag{III.31}$$

where we defined response functions

$$\chi_{ij}^{uv}(t,s) := \left. \frac{\delta u_i(t)}{\delta h_j^v(s)} \right|_{h=0}, \tag{III.32}$$

for $u, v \in \{p, \gamma\}$. Once again, a similar equation can be written for the perturbation of productions. Injecting these perturbed forms into the equations for the new firm $i = 0$, one readily sees that one must compute the large N behavior of the two quantities

$$\sum_{j=0}^N M_{0j} \widetilde{p}_j(t), \quad \sum_{j=0}^N M_{j0} \widetilde{\gamma}_j(t).$$

We will focus on the first one since computations are essentially similar. From Eq. (III.31), we have a term reading

$$\sum_{j=0}^N M_{0j} p_j(t) = z_0 p_0(t) - \sum_{j=1}^N J_{0j} p_j(t),$$

which we express using the indepedance between J_{0j} and p_j along with the IID approximation for prices

$$\sum_{j=0}^{N} M_{0j} p_j(t) = z_0 p_0(t) - \mu_J \mathbb{E}[p(t)] + \mathcal{O}(N^{(1-\min(\gamma,2))/2}).$$

The average $\mathbb{E}[(\cdot)]$ is taken over z_i, the matrix $\mathbf{J}$ and initial conditions. Note that, in contrast with the Lotka-Volterra case, no ensemble noise remains because of the sign structure of $\mathbf{J}$ encoded in γ. The other terms from $\sum_{j=0}^{N} M_{0j}\widetilde{p}_j(t)$ can be treated in a similar way, and we will only give one example. We have a term proportional to

$$\begin{aligned}\sum_{j=0}^{N} M_{0j} \sum_{k=1}^{N} \int_0^t ds \chi_{jk}^{pp}(t,s) p_k(s) M_{0k} \gamma_0(s) = z_0 \int_0^t ds \gamma_0(s) \sum_{k=1}^{N} \chi_{0k}^{pp}(t,s) M_{0k} p_k(s) \\ + \int_0^t ds \gamma_0(s) \sum_{j,k=1}^{N} J_{0j} J_{0k} \chi_{jk}^{pp}(t,s) p_k(s).\end{aligned}$$

As it turns out, only diagonal response functions $\chi_{ii}^{\alpha\alpha}$ contribute in the large N limit. First, we can compute the single-time response $\chi_{ij}^{\alpha\beta}(t,t)$ in the following way. We start by computing the time evolution of the response function. We take the functional derivative of the equation on prices with respect to $h_j^{\alpha}(s)$. We set all external fields to 0, thus yielding

$$\begin{aligned}\frac{\partial}{\partial t}\chi_{ij}^{p\alpha} = &-\frac{\alpha'}{z_i}\sum_k M_{ik}\chi_{kj}^{p\alpha} - \frac{\alpha p_i}{z_i\gamma_i}\left(\sum_k M_{ki}\chi_{kj}^{\gamma\alpha} + \frac{\ell_0}{p_i^2}\chi_{ij}^{p\alpha}\right) \\ &- \frac{\alpha}{z_i}\left(\gamma_i^{-1}\chi_{ij}^{p\alpha} - \frac{p_i}{\gamma_i^2}\chi_{ij}^{p\alpha}\right)\left(\sum_k M_{ki}\gamma_k - C_i\right) \\ &+ \frac{1}{z_i\gamma_i}\delta_{ij}\delta_{p\alpha}\delta(t-s).\end{aligned}$$

We then integrate this relation over t between $s-\tau$ and s and use the fact that responses are causal, i.e. ($\chi_{ij}^{p\alpha}(t,s) = 0$ for $t < s$), to get (for $\tau \to 0^+$)

$$\chi_{ij}^{p\alpha}(s,s) = \frac{\delta_{ij}\delta_{p\alpha}}{z_i\gamma_i(s)}. \tag{III.33}$$

Non-diagonal single-time responses (cross-fields or cross-firms) are therefore sub-dominant, and we actually expect them to remain sub-dominant as $t \neq s$. Note that this point is rather intuitive since non-diagonal responses are obtained after one "correlation loop". Using this fact, we can revert to the time evolution of non-diagonal responses and only consider contributions from diagonal responses

$$\frac{\partial}{\partial t}\chi_{i\neq j}^{p\neq\alpha} \sim -\frac{\alpha'}{z_i} J_{ij}\chi_{jj}^{pp}, \tag{III.34}$$

implying

$$\chi_{i\neq j}^{p\neq\alpha} \sim J_{ij} \sim N^{-1}. \tag{III.35}$$

Coming back to the perturbations on prices, we can simplify our computation

$$\begin{aligned}\sum_{j=0}^{N} M_{0j} \sum_{k=1}^{N} \int_0^t ds \chi_{jk}^{pp}(t,s) p_k(s) M_{0k}\gamma_0(s) &\sim \int_0^t ds\gamma_0(s) \sum_{j=1}^{N} J_{0j}^2 \chi_{jj}^{pp}(t,s) p_j(s) \\ &= \mathcal{O}\left(N^{(1-\min(\gamma,2)/2}\right).\end{aligned}$$

The other terms can be treated in the same way, and we see that the only nontrivial contributions in the initial sums are

$$\sum_{j=0}^{N} M_{0j}\widetilde{p}_j(t) \underset{N\to\infty}{\sim} z_0 p_0 - \mu_J \mathbb{E}[p(t)] \tag{III.36}$$

$$\sum_{j=0}^{N} M_{j0}\widetilde{\gamma}_j(t) \underset{N\to\infty}{\sim} z_0 \gamma_0 - \mu_J \mathbb{E}[\gamma(t)]. \tag{III.37}$$

Injecting these behaviors into the equation on the new firm $i = 0$ and dropping the index 0 yields system (III.15)

$$\frac{\mathrm{d}p}{\mathrm{d}t} = -\alpha \frac{p}{z\gamma}\left(z\gamma - \mu_J \mathbb{E}[\gamma(t)] - \frac{\ell_0}{p}\right) - \frac{\alpha'}{z}\left(zp - \mu_J \mathbb{E}[p(t)] - V\right) \tag{III.38a}$$

$$\frac{\mathrm{d}\gamma}{\mathrm{d}t} = \beta \frac{\gamma}{zp}\left(zp - \mu_J \mathbb{E}[p(t)] - V\right) - \frac{\beta'}{z}\left(z\gamma - \mu_J \mathbb{E}[\gamma(t)] - \frac{\ell_0}{p}\right). \tag{III.38b}$$

B Linear study of the DMFT equations

In this appendix, we provide the computations for the linear study.

B.1 Purely complex spectrum for $\mathbb{D}_{\mathrm{MF}}$

As we explained in Chapter II, the relaxation time of the system is given by

$$\tau_r = 1/|\min(\mathfrak{Re}\,(\lambda_1)\,, \mathfrak{Re}\,(\lambda_2))|.$$

The expressions $\mathfrak{Re}\,(\lambda_i)$ depend on the parameters of the model that can make the spectrum of $\mathbb{D}_{\mathrm{MF}}$ either purely real or purely complex. To properly express τ_r, we therefore need to characterize the conditions yielding real or complex spectra. We have

$$\begin{aligned}\mathbb{P}\left(\lambda_{1/2} \in \mathbb{C}\setminus\mathbb{R}\right) &= \mathbb{P}\left(\mathrm{Tr}\left(\mathbb{D}_{\mathrm{MF}}\right)^2 - 4\det \mathbb{D}_{\mathrm{MF}} < 0\right)\\ &= \mathbb{P}\left(\frac{z}{z+c} \in [m_-, m_+]\right),\end{aligned}$$

with

$$m_\pm = \frac{1}{\alpha}\left(-\alpha' - \beta' \pm 2\sqrt{\alpha\beta + \alpha'\beta'}\right),$$

and $c = \mu_J\mu_J^c/(\mu_J^c - \mu_J)$ as defined in the main sections.

B.1.1 Below the transition $\mu_J < \mu_J^c$

In this case, $c > 0$, and one readily sees that the $z/(z+c) > 0$ (since we chose $z > 0$). We can carry out the computation

$$\mathbb{P}\left(\frac{z}{z+c} \in [m_-, m_+]\right) = \mathbb{P}\left(\frac{z}{z+c} \le m_+\right) = \begin{cases} 0 & , \quad m_+ < 0 \\ \mathbb{P}\left(z \in \left[0, \frac{cm_+}{1-m_+}\right]\right) & , \quad 0 < m_+ < 1 \\ 1 & , \quad 1 < m_+ \end{cases}.$$

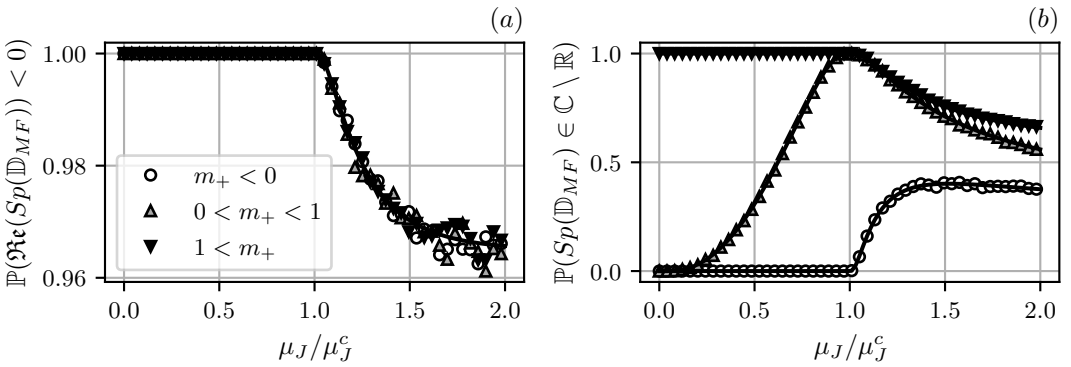


Figure III.6: (a) Probability that the matrix $\mathbb{D}_{\mathrm{MF}}$ is stable. We see that below the transition, equilibrium is always stable. (b) Probability that the spectrum of $\mathbb{D}_{\mathrm{MF}}$ is purely complex. In the case $0 < m_+ < 1$, the system naturally interpolates between real and complex spectrum as it gets closer to the HS transition.

As mentioned in the text, we retrieve a purely complex real (resp. purely complex) whenever $m_+ < 0$ (resp. $m_+ > 1$). Since $m_+ < 0$ corresponds to $(\alpha' - \beta')^2 < 4\alpha\beta$ and $\beta > \beta_c$, we expect a real spectrum whenever $\varepsilon \to \infty$ and $\varepsilon \to 0^+$ by analogy with Chapter II. If now $m_+ > 1$ the spectrum is expected to be complex in this regime since inequalities on β are reversed. In the intermediate case, $0 < m_+ < 1$, we have a real spectrum for $\varepsilon \to \infty$ and a complex one for $\varepsilon \to 0$. The probability $\mathbb{P}\left(z \in \left[0, \frac{cm_+}{1-m_+}\right]\right)$ interpolates between these two cases since $c \underset{\varepsilon\to\infty}{\longrightarrow} 0$ and $c \underset{\varepsilon\to 0^+}{\longrightarrow} \infty$.

B.1.2 Above the transition $\mu_J > \mu_J^c$

In this case, $c < 0$ which can make $z/(z+c)$ negative as well. Careful evaluation shows that

$$\mathbb{P}\left(\frac{z}{z+c} \in [m_-, m_+]\right) = \begin{cases} \mathbb{P}\left(z \in \left[\frac{cm_+}{1-m_+}, \frac{cm_-}{1-m_-}\right]\right) & , \quad m_+ < 0 \\ \mathbb{P}\left(z \leq \frac{cm_-}{1-m_-}\right) & , \quad 0 < m_+ < 1\,. \\ 1 - \mathbb{P}\left(z \in \left[\frac{cm_+}{1-m_+}, \frac{cm_-}{1-m_-}\right]\right) & , \quad 1 < m_+ \end{cases}$$

The interpretation is not as straightforward as in the case $\mu_J < \mu_J^c$, but we can still see that cases $m_+ > 1$ and $m_+ < 0$ are complementary.

B.2 Stable equilibrium

In the same way, we can compute the probability to have a stable equilibrium. To do so, we use the following straightforward string of equivalences

$$\mathfrak{Re}\left(\mathrm{Sp}\left(\mathbb{D}_{\mathrm{MF}}\right)\right) < 0 \Longleftrightarrow \mathrm{Tr}\left(\mathbb{D}\right) < 0 \Longleftrightarrow \frac{z}{z+c} \geq -\frac{\alpha' + \beta'}{\alpha},$$

which holds regardless of the position of μ_J with respect to the transition. We can then compute the following probabilities for $c < 0$

$$\begin{aligned}
\mathbb{P}\left(\frac{z}{z+c} \geq -\frac{\alpha'+\beta'}{\alpha} \bigcap \frac{z}{z+c} \in [m_-, m_+]\right) &= \mathbb{P}\left(\frac{z}{z+c} \in \left[-\frac{\alpha'+\beta'}{\alpha}, m_+\right]\right) \\
&= \mathbb{P}\left(\frac{z}{z+c} \leq m_+\right) - \mathbb{P}\left(z \in \left[-c\frac{\alpha'+\beta'}{\alpha+\beta'+\alpha}, -c\right]\right) \\
\mathbb{P}\left(\frac{z}{z+c} \geq -\frac{\alpha'+\beta'}{\alpha} \bigcap \frac{z}{z+c} \notin [m_-, m_+]\right) &= \mathbb{P}\left(\frac{z}{z+c} \geq -\frac{\alpha'+\beta'}{\alpha} \bigcap \frac{z}{z+c} < m_-\right) \\
&\quad + \mathbb{P}\left(\frac{z}{z+c} \geq -\frac{\alpha'+\beta'}{\alpha} \bigcap \frac{z}{z+c} > m_+\right) \\
&= \mathbb{P}\left(\frac{z}{z+c} > m_+\right).
\end{aligned}$$

For $c > 0$, the latter one remains unchanged while the former becomes

$$\mathbb{P}\left(\frac{z}{z+c} \geq -\frac{\alpha'+\beta'}{\alpha} \bigcap \frac{z}{z+c} \in [m_-, m_+]\right) = \mathbb{P}\left(\frac{z}{z+c} \in [m_-, m_+]\right).$$

Finally

$$\begin{aligned}
\mathbb{P}(\mathfrak{Re}\left(\mathrm{Sp}\left(\mathbb{D}_{\mathrm{MF}}\right)\right) < 0) &= \mathbb{P}\left(\frac{z}{z+c} > m_+\right) + \mathbb{P}\left(\frac{z}{z+c} \leq m_+\right) - \mathbb{P}\left(z \in \left[-c\frac{\alpha'+\beta'}{\alpha+\beta'+\alpha}, -c\right]\right) \\
&= \begin{cases} 1 & , \quad \mu_J < \mu_J^c \\ 1 - \mathbb{P}\left(z \in \left[-c\frac{\alpha'+\beta'}{\alpha+\beta'+\alpha}, -c\right]\right) & , \quad \mu_J > \mu_J^c \end{cases}.
\end{aligned}$$

We can see that below the transition, the system is almost surely locally stable.

B.3 Expectation of eigenvalues

Using previous results, we can write the expectation values of $\lambda_{1/2}$. We will only write out the results below the HS transition, but the other case can be obtained in the same way. We have for the real parts

$$\mathbb{E}\left[\mathfrak{Re}\left(\lambda_{1/2}\right)\right] = \mathbb{E}\left[\mathfrak{Re}\left(\lambda_{1/2}\right)\mathbb{1}\left(\frac{z}{z+c} \in [m_-, m_+]\right)\right] + \mathbb{E}\left[\mathfrak{Re}\left(\lambda_{1/2}\right)\mathbb{1}\left(\frac{z}{z+c} \notin [m_-, m_+]\right)\right].$$

Denoting by $\mathrm{D}z = P(z)\mathrm{d}z$, we have the different cases

- Case $m_+ < 0$

$$\mathbb{E}\left[\mathfrak{Re}\left(\lambda_{1/2}\right)\right] = \frac{1}{2}\left(-\alpha'-\beta'-\int_0^\infty \mathrm{D}z\left(\alpha\frac{z}{z+c} \mp \sqrt{4(\alpha\beta+\alpha'\beta') - \left(\alpha'+\beta'+\alpha\frac{z}{z+c}\right)^2}\right)\right)$$

- Case $0 < m_+ < 1$

$$\mathbb{E}\left[\mathfrak{Re}\left(\lambda_{1/2}\right)\right] = -\frac{1}{2}(\alpha' + \beta')\mathbb{P}\left(\frac{z}{z+c} \in [m_-, m_+]\right) - \frac{1}{2}\alpha \int_0^{\frac{cm_+}{1-m_+}} \mathrm{D}z \frac{z}{z+c}$$
$$+ \frac{1}{2}\left(-\alpha' - \beta' - \int_{\frac{cm_+}{1-m_+}}^{\infty} \mathrm{D}z \left(\alpha \frac{z}{z+c} \mp \sqrt{4(\alpha\beta + \alpha'\beta') - \left(\alpha' + \beta' + \alpha \frac{z}{z+c}\right)^2}\right)\right)$$

- Case $1 < m_+$

$$\mathbb{E}\left[\mathfrak{Re}\left(\lambda_{1/2}\right)\right] = -\frac{1}{2}(\alpha' + \beta') - \frac{1}{2}\alpha \int_0^{\infty} \mathrm{D}z \frac{z}{z+c}$$

The imaginary part can be obtained in the same way. See Figure III.3 for a comparison between simulated expectation values and the previous analytical results in the case where z follows a log-normal distribution.

Conclusion of Part I

The central proposition of this part is that the standard economic equilibrium may actually be dynamically unattainable. Correspondingly, the "small shock, large business cycles" paradox (i.e. aggregate fluctuations much too large to be explained by exogenous shocks alone, see e.g. [9] and [10]) would be chiefly explained by *out-of-equilibrium* effects. Indeed, in such out-of-equilibrium situations, the dynamics is mostly of endogenous origin and cannot be accounted for by traditional equilibrium arguments, like those of e.g. [35] and [13, 41, 111]. From a conceptual point of view, our point is the following: economic equilibrium requires so much cooperation between rational, forward-looking agents, that the only way such equilibrium can plausibly be achieved is through some kind of adjustment process, that inevitably takes some time to complete. Such a situation requires a richer modelling framework where out-of-equilibrium dynamics is an integral part of the description: we do not only need to describe the final equilibrium state, but also the path to equilibrium, which may in fact never converge.

We started making our case by showing that the notion of economic equilibrium can be itself ill-defined. Competitive equilibrium is the perfect balancing of economic fluxes, summarized by *market clearing* (production is either bought or consumed) and *zero profits* (competition inevitably drive profits towards zero). This last condition is different from the standard definition, where profits are maximized at equilibrium (except for constant return to scale, where the two coincide). This new definition allows anticipating on Part II, where causality imposes to minimize costs rather than maximize profits in order to compute exchanged quantities. These two conditions translate into equations on equilibrium prices and productions (independent of any dynamical process). As argued in [24], admissible economic equilibrium, i.e. one with positive prices and productions, can only be achieved if firms are efficient enough in converting inputs into outputs. We unveiled a quantity ε measuring this efficiency relative to the amount of cooperation needed from the network: as long as $\varepsilon > 0$ firms are efficient enough and equilibrium is properly defined, whereas when $\varepsilon < 0$ network needs are too important and equilibrium disappears. An illustration of this transition is given on Figure III.7. As we discussed in Chapter I, a possibly nonexistent equilibrium invalidates the central hypothesis of most economic models, and makes out-of-equilibrium modelling a necessity.

We then proposed a minimal model for weakly out-of-equilibrium dynamics in firm networks. We based it on a set of heuristic rules describing the behavior of agents faced with non-balancing fluxes. The general idea behind these rules is that agents act

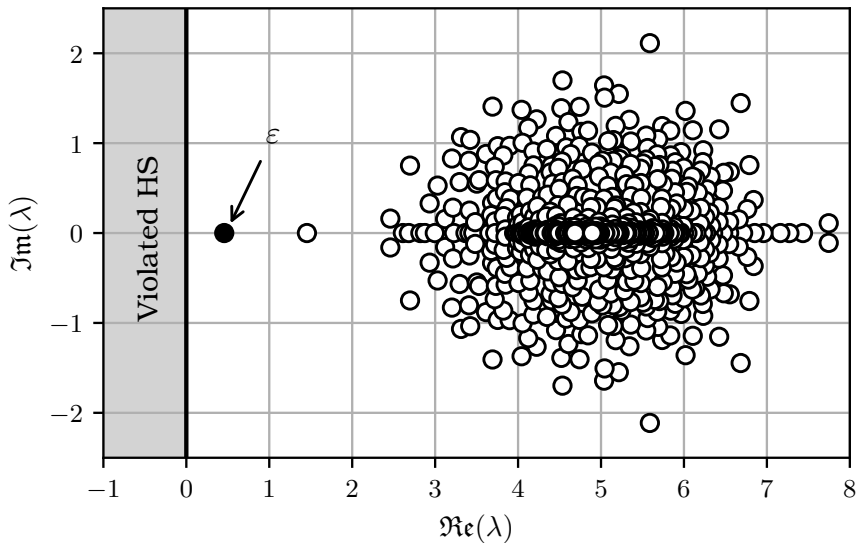


Figure III.7: Eigenvalues λ of the network matrix $M_{ij} = z_i\delta_{ij} - J_{ij}$ for $z_i \hookrightarrow \mathsf{U}(6,8)$ and J_{ij} the adjacency matrix of an input-output network inferred from FACTSET data [76]. Links correspond to an existing supplier-buyer relationship between 2012 and 2015. Productivity factors are chosen uniform only to illustrate the HS transition.

to reduce imbalances with respect to equilibrium, as though these deviations acted as frictions. These imbalances are measured through profits $\pi_i(t)$ – gains minus losses – and excess production $\mathscr{E}_i(t)$ – supply minus demand – and serve as proxies for the distance to equilibrium. Prices and productions are adjusted through linear responses to these imbalances

$$\log\left(\frac{p_i(t+\delta t)}{p_i(t)}\right) = \left(-\alpha\frac{\mathscr{E}_i(t)}{y_i(t)} - \alpha'\frac{\pi_i(t)}{p_i(t)y_i(t)}\right)\delta t$$
$$\log\left(\frac{y_i(t+\delta t)}{y_i(t)}\right) = \left(\beta\frac{\pi_i(t)}{p_i(t)y_i(t)} - \beta'\frac{\mathscr{E}_i(t)}{y_i(t)}\right)\delta t$$

For instance, faced with excess demand, a firm will increase its production. Inverse timescales α, α', β, β' measure the strength of the response to imbalances. Interestingly, the HS transition transfers into a dynamical transition for this adjustment process. As $\varepsilon \to 0$, the economy becomes less and less resilient to shocks as its relaxation time diverges with ε^{-1}. Intuitively, if the relaxation time of the economy is much slower than the typical time between shocks, they will tend to accumulate rather than vanish. This lingering of shocks provides a nice mechanism for excess volatility in firm networks. Furthermore, even if economic equilibrium exists, it might not be dynamically attainable since the time needed to reach it might be unrealistically high. As a consequence, equilibrium is effectively nonexistent, which further strengthen our view on the necessity of out-of-equilibrium modelling.

However, the results obtained in Chapter II have to be mitigated. Indeed, upon simulating our system, we found no bounded trajectories (specifically limit cycles) as soon as $\varepsilon < 0$. Even if divergent economies – exploding prices and plummeting productions – can make sense, we did not expect it to be the only possibility as soon as the HS conditions were violated. Turning to *dynamical mean-field theory*, we were able to prove that the no-equilibrium region could not yield any bounded trajectories, and that our model for weakly out-of-equilibrium dynamics was in fact too "naive". By resorting to a toy-model, we stripped out too much of the inherent complexity involved in the interactions between firms and therefore overlooked essential constraints, some of which were discussed in the concluding sections of Chapter II.

The next step for this work is therefore to factor in this missing complexity. In the next part, we present the central model of this manuscript: a macroeconomic agent-based model following the same behavioral rules as in Chapter II, but abiding to essential constraints such as causality or conservation of goods.

Part II

Macroeconomic agent based modelling

Foreword

The second part of this thesis is devoted to macroeconomic agent-based modelling. We will heavily draw onto notions and results from previous chapters since we generalize the model presented in the first part.

In both Chapter IV and Chapter V, we devise Agent-Based Models (ABMs) to account for the *out-of-equilibrium* dynamics of a single firm (Chapter IV), or N firms (Chapter V), adjusting prices and productions across time. In ABMs, the constitutive entities (agents) go through a series of actions constituting a fundamental *time-step* of the model. As time goes by, agents loop through these actions until some time-horizon is reached. This approach is of course very versatile since virtually any system can be simulated, provided enough computational power is available. Factoring in essential realistic features, our ABMs are based on the same behavioral assumptions about reactions to imbalances as in Part I. We will see that a rich phenomenology of behavior emerges, such as sustained endogenous oscillations of prices and productions.

Chapter VI will serve as a conclusion to the first two parts of this thesis. It will summarize the different explanations to the "small shocks, large business cycles" puzzle in terms of out-of-equilibrium effects. It will also discuss some key economic features that should be included in the models as well as perspectives for generalizations.

CHAPTER IV

A SIMPLIFIED APPROACH

Abstract

In this chapter, we present a simple representative model for out-of-equilibrium dynamics in a primitive economy consisting of one firm and one household. The idea of this chapter is to introduce the general concept of Agent-Based Models, along with some of the analytical methods that one may use to approach them. It also serves as an introduction to the next chapter, which will present a much more complex framework although based on the same principles. We will also introduce the concept of conewise linear dynamics, central in the model of Chapter V.

1 A causal mass-conserving economy

Chronologically, this project came after the work of Chapter V was submitted to publication. We wanted to reduce the model of the next chapter to gain a deeper understanding of the equations, while still factoring in some complexity missing from Chapter II. To that end, we decided to take a well known economic model and endow it with the same dynamics as in Chapter V. As in [112, Chapter 2], we consider a single-firm single-household economy. The firm produces a quantity y of goods using only manpower ℓ through the production function

$$y = z\ell^b, \tag{IV.1}$$

where $z > 0$ is a technological productivity factor and b accounts for return to scale. The firm sells this production to the household at some price p, and pays workers for their labor at wage p_0. For its part, the household seeks to maximize some utility function [1]

$$U = \log C - \frac{1}{1+\varphi}\left(\frac{\ell}{\ell_0}\right)^{1+\varphi}, \tag{IV.2}$$

where the log-consumption corresponds to the limit $\sigma \to 1^-$ in [112]. The household is subject to the budget constraint

$$pC \leq p_0\ell + S, \tag{IV.3}$$

[1] Unlike [112], we disregard inter-temporal effects in the utility maximization.

where S denotes possible savings. We do not take bonds nor debts into account here. From this very simple static framework, we will move to a time-dependent description by allowing prices, production etc. to adjust throughout time. We will use update rules similar to those of Chapter II, but we will factor in essential ingredients that were missing from Chapter II: imbalances and causality.

1.1 Imbalances

Accounting for imbalances, we enforce the general rule that neither sales nor manpower can exceed available supply (where supply refers to the available pool of workers in the case of manpower). If supply of goods is plentiful, then demands will be satisfied. However, if demands exceed available supply, the firm will only sell what is available. The flow of goods going from the firm to the household must therefore be computed with care. Instead of a single consumed quantity $C(t)$ considered in Chapter II, we need to introduce the amount of goods *demanded* by the household, $C^{\mathrm{d}}(t)$, that can only be smaller or equal to the quantity actually exchanged, $C(t)$. We also keep track of the firm's inventory, denoted by $I(t)$, to which we successively add goods that the firm did not manage to sell (if supply exceeds demands), and subtract those that perished. In this highly simplified setting, it is straightforward to relate realized and demanded consumption. Indeed, firm's supply and demand, $\mathscr{S}(t)$ and $\mathscr{D}(t)$, are given by

$$\mathscr{S}(t) = y(t) + I(t) \tag{IV.4}$$

$$\mathscr{D}(t) = C^{\mathrm{d}}(t), \tag{IV.5}$$

which implies

$$C(t) = C^{\mathrm{d}}(t) \min\left(1, \frac{\mathscr{S}(t)}{\mathscr{D}(t)}\right) = \min\left(C^{\mathrm{d}}(t), y(t) + I(t)\right). \tag{IV.6}$$

Similarly, the manpower ℓ^{d} required by the firm to produce may not be equal to the total maximum amount of work ℓ^{s} provided by the household. Consequently, realized working hours are capped in the same way as consumption is, i.e.

$$\ell(t) = \ell^{\mathrm{d}}(t) \min\left(1, \frac{\ell^{\mathrm{s}}(t)}{\ell^{\mathrm{d}}(t)}\right) = \min\left(\ell^{\mathrm{d}}(t), \ell^{\mathrm{s}}(t)\right), \tag{IV.7}$$

where supply of work $\ell^{\mathrm{s}}(t)$ is fixed by the household (see below).

Finally, since the number of hired employees may be slightly smaller than expected, firms may produce less than anticipated. We will therefore make the distinction between production *target* $\widehat{y}(t)$ (used to estimate manpower needs $\ell^{\mathrm{d}}(t)$) and real production $y(t)$, such that $y(t) \leq \widehat{y}(t)$.

1.2 Causality

Implementing causality in the dynamics also means dissecting the firms' decision process. Clearly, goods can only be sold at time t after they have been produced at time $t-1$, and

prices may change (if only slightly) between these two times. More importantly, the firm only have partial information about the amount of goods it will be able to buy and sell when it plans for the next production cycle. Likewise, the number of employees it will be able to hire is not known precisely, because it depends on the amount of work deemed acceptable by the households. It is at this stage that we will introduce a heuristic rule that allows firms to plan for the next production round by making more or less informed guesses about these unknown quantities. In the present work, we assume that firms base their estimate on what happened in the previous time step, although more complicated and more general rules can already be imagined.

1.3 Decision process

As hinted at in the last paragraph, causality requires dissecting firms' decision process. Each time-step is therefore sliced into three epochs – *planning*, *hiring* and *producing* – over which the firm will loop. Intuitively, one time-step can be thought of as a quarter during which the firm will carry out several non-instantaneous tasks.

1.3.1 Planning

In this phase, firms will plan their production by setting a target production $\widehat{y}(t)$ with a similar heuristics as in Chapter II. However, since causality forbids the use of yet to be disclosed information, the firm must forecast future profits and production surplus in order to set out a production target.

Forecasts We will assume that forecasts, denoted by $\mathbb{E}_t[\,\cdot\,]$, are computed using demands from the preceding time-step, i.e. firms assume that, through their dynamical adjustment of prices and productions, they are now able to meet past observed demands. As a consequence

$$\mathbb{E}_t[C] = C^{\mathrm{d}}(t-1) \tag{IV.8}$$

$$\mathbb{E}_t[\ell] = \ell^{\mathrm{d}}(t-1), \tag{IV.9}$$

so that expected profits and surplus read

$$\mathbb{E}_t[\pi] = C^{\mathrm{d}}(t-1)p(t) - p_0(t)\ell^{\mathrm{d}}(t-1) \tag{IV.10}$$

$$\mathbb{E}_t[\mathscr{E}] = y(t) + I(t) - C^{\mathrm{d}}(t-1). \tag{IV.11}$$

Note that the supply part of $\mathbb{E}_t[\mathscr{E}]$, i.e. $y(t) + I(t)$ is known for the current period since production and compilation of inventories already occured (see below).

Setting targets Using these forecasts, the firm sets a production target $\widehat{y}(t+1)$ through the update rule

$$\log\left(\frac{\widehat{y}(t+1)}{y(t)}\right) = 2\beta\frac{\mathbb{E}_t[\pi]}{\mathbb{E}_t[\mathscr{G}] + \mathbb{E}_t[\mathscr{L}]} - 2\beta'\frac{\mathbb{E}_t[\mathscr{E}]}{\mathbb{E}_t[\mathscr{S}] + \mathbb{E}_t[\mathscr{D}]}, \tag{IV.12}$$

with $\mathscr{G}$ and $\mathscr{L}$, the gains and losses of the firm such that $\pi = \mathscr{G} - \mathscr{L}$. Note that the update rule is slightly different from that of Chapter II. The normalization of each term is chosen such that the update factors stay between -1 and 1. In addition, since at equilibrium gains equal losses and supply equals demand, the denominator yields a factor of two, which cancels out with the one in front of the inverse time-scales.

Posting demands Now that a production target has been set, the firm computes the optimal working hours that minimize costs while allowing to reach the target. Such process is described in Chapter I and yields

$$\ell^{\mathrm{d}}(t) = (\widehat{y}(t+1)/z)^{1/b}\,. \tag{IV.13}$$

The subsequent demand of work $\ell^{\mathrm{d}}(t)$ is posted to the household. In parallel, the household posts its consumption demand $C^{\mathrm{d}}(t)$ and available man-power $\ell^{\mathrm{s}}(t)$ by optimizing the expected utility

$$\mathbb{E}_t[\mathcal{U}] = \log C^{\mathrm{d}}(t) - \frac{1}{1+\varphi}\left(\frac{\ell^s(t)}{\ell_0}\right)^{1+\varphi}, \tag{IV.14}$$

under the expected budget constraint $p(t)C^{\mathrm{d}}(t) = p_0(t)\ell^{\mathrm{s}}(t) + S(t)$, where $S(t)$ is a leftover budget from previous periods. We also introduced the baseline work offer ℓ_0: if $\varphi \to \infty$, the household refuses to work more than ℓ_0. In this chapter and the next, we consider the household to be optimistic, i.e. it assumes that it will consume and work as much as it intends.

1.3.2 Hiring

Now that demands have been posted, the firm can hire workers and pay the household, which in turn consumes goods.

Hiring and wage payment The hiring process only needs to comply with the available workforce. If the overall workforce is smaller than the firm's demand, the firm will only be able to hire a fraction of what it needs, and the household will be fully employed. If now the available workforce is enough, the household will satisfy the firm's demand but will be partially unemployed. This traduces into

$$\ell(t) = \min\left(\ell^{\mathrm{d}}(t), \ell^{\mathrm{s}}(t)\right). \tag{IV.15}$$

After being hired, the household is paid and has an available budget of

$$B(t) = p_0(t)\ell(t) + S(t). \tag{IV.16}$$

The firm offers a certain quantity to buy $C^{\mathrm{o}}(t)$

$$C^{\mathrm{o}}(t) = C^{\mathrm{d}}(t)\min\left(1, \frac{\mathscr{S}(t)}{\mathscr{D}(t)}\right), \tag{IV.17}$$

that the household consumes according to the previous budget

$$C(t) = C^{\mathrm{o}}(t) \min\left(1, \frac{B(t)}{p(t)C^{\mathrm{o}}(t)}\right). \tag{IV.18}$$

Finally, the household updates its leftover savings by the amount that might be left after consumption

$$S(t+1) = B(t) - p(t)C(t). \tag{IV.19}$$

Price and wage updating After paying wage to its workers, the firm can compute its losses $\mathscr{L}(t) = p_0(t)\ell(t)$. In addition, the household has spent money by consuming goods, and the firm can also compute its gains $\mathscr{G}(t) = p(t)C(t)$. Realized profits and realized production surplus therefore read

$$\pi(t) = p(t)C(t) - p_0(t)\ell(t) \tag{IV.20}$$

$$\mathscr{E}(t) = y(t) + I(t) - C^{\mathrm{d}}(t). \tag{IV.21}$$

The firm adjusts its selling price for the next period with a rule similar to that of Chapter II

$$\log\left(\frac{p(t+1)}{p(t)}\right) = -2\alpha\frac{\mathscr{E}(t)}{\mathscr{S}(t)+\mathscr{D}(t)} - 2\alpha'\frac{\pi(t)}{\mathscr{G}(t)+\mathscr{L}(t)}. \tag{IV.22}$$

Furthermore, the wage $p_0(t)$ is not constant anymore and reacts to tensions in the labor market

$$\log\left(\frac{p_0(t+1)}{p_0(t)}\right) = -2\omega\frac{\ell^{\mathrm{s}}(t) - \ell^{\mathrm{d}}(t)}{\ell^{\mathrm{s}}(t) + \ell^{\mathrm{d}}(t)} := -2\omega\frac{\mathscr{E}_0(t)}{\ell^{\mathrm{s}}(t) + \ell^{\mathrm{d}}(t)}, \tag{IV.23}$$

where ω is an inverse timescale (paramount to α, β, α', β') measuring the speed of wage adjustment, and where we defined the excess work $\mathscr{E}_0(t) = \ell^{\mathrm{s}}(t) - \ell^{\mathrm{d}}(t)$. This heuristics is of course in the same spirit as those on prices/productions. We will discuss it further in Chapter V and it implements a "Philip's curve" at each time-step.

Rescaling Conventionally, we rescale every monetary quantities by the value of the wage to avoid exponential growth or decay conveyed by inflation/deflation effects. Note that this step is not part of the firm's decision process *per se*, but is mostly for numerical convenience. The rescaling is as follows

$$\begin{aligned} p(t+1) &\longleftarrow \frac{p(t+1)}{p_0(t+1)} \\ S(t+1) &\longleftarrow \frac{S(t+1)}{p_0(t+1)} \\ p_0(t+1) &\longleftarrow 1. \end{aligned}$$

1.3.3 Producing

After the hiring phase, the firm is able to produce and compile its inventories. This phase is a lot less cumbersome than the corresponding one in Chapter V since inventories are only compiled for the unique good and production only takes work into account.

Production Given working hours $\ell(t)$ provided by the household, the firm produces a quantity $y(t+1)$ that will be sold during the next period

$$y(t+1) = z\ell(t)^b \leq \widehat{y}(t+1). \tag{IV.24}$$

Note that, in an economy whose production is only work-dependent, the distinction between the different production functions of Chapter I becomes irrelevant (up to a redefinition of the productivity factor).

Inventories Compiling inventories is simple here and amounts to storing leftover goods that have not been consumed by the household

$$I(t+1) = e^{-\sigma}\left(\mathscr{S}(t) - C(t)\right). \tag{IV.25}$$

We introduced a depreciation factor $e^{-\sigma}$ to interpolate between non-perishable ($\sigma = 0$) and instantaneously perishable goods ($\sigma = \infty$).

1.4 Laying down the equations

The previous steps can be rewritten into a discrete dynamical system linking times $t+1$, t and $t-1$. It reads

$$\widehat{y}(t+1) = y(t)\exp\left[2\beta\frac{\mathbb{E}_t[\pi]}{\mathbb{E}_t[\mathscr{G}] + \mathbb{E}_t[\mathscr{L}]} - 2\beta'\frac{\mathbb{E}_t[\mathscr{E}]}{\mathbb{E}_t[\mathscr{S}] + \mathbb{E}_t[\mathscr{D}]}\right] \tag{IV.26}$$

$$y(t+1) = z\left(\min(\ell^{\mathrm{s}}(t), \ell^{\mathrm{d}}(t)\right)^b \tag{IV.27}$$

$$p(t+1) = p(t)\exp\left[-2\alpha\frac{\mathscr{E}(t)}{\mathscr{S}(t) + \mathscr{D}(t)} - 2\alpha'\frac{\pi(t)}{\mathscr{G}(t) + \mathscr{L}(t)} + 2\omega\frac{\mathscr{E}_0(t)}{\ell^{\mathrm{s}}(t) + \ell^{\mathrm{d}}(t)}\right] \tag{IV.28}$$

$$I(t+1) = e^{\sigma}\left(\mathscr{S}(t) - C(t)\right) \tag{IV.29}$$

$$S(t+1) = \left(B(t) - p(t)C(t)\right)\exp\left[2\omega\frac{\mathscr{E}_0(t)}{\ell^{\mathrm{s}}(t) + \ell^{\mathrm{d}}(t)}\right] \tag{IV.30}$$

where prices and savings are rescaled by wages which are therefore set to 1. These constitutive equations are consistent in the sense that these five variables are enough to describe the entire system. Of course, there is little to no hope to get any analytical tractability out of this system: it is non-linear, intricately coupled, second-order recursive. Furthermore, the form of the equations actually depends on the relative magnitude of the state variables. For instance, if labor supply exceeds labor demand then $y(t+1) = z(\ell^{\mathrm{d}}(t))^b$, whereas $y(t+1) = z(\ell^{\mathrm{s}}(t))^b$ if it were the other way around. This adds another layer of complexity since the system will act differently depending on the position of the state variables in state space. We will see in Section 3 that one can give (to some extent) a characterization of the behavior of the system at linear level.

1.5 Absence of HS transition

In this model, competitive equilibrium equations are fairly simple and immediately yield

$$p_{\mathrm{eq}} = \frac{\ell_0^{1-b}}{z} \tag{IV.31}$$

$$\gamma_{\mathrm{eq}} = \ell_0^b. \tag{IV.32}$$

Provided that z is strictly positive (which should always be the case), equilibrium price and production will always be positive. This model therefore does not have any analogous of the HS transition that we presented in Part I. As a consequence, z actually plays very little role in the dynamics, and we will set it to $z = 1$. Finally, the absence of HS transition highlights that this model is not some representative mean-field limit of the model in Chapter II. To retrieve the HS transition, one could impose that the firm needs a fraction of its own production as an input. This self-interaction would effectively shift the productivity factor $z \to z - q$, and allow for negative equilibrium prices while keeping $z > 0$. We disregard such a possibility here.

2 Short numerical survey

Since very little can be said *a priori* about the dynamics of this model, we will resort to numerical simulations in the same way as we will in Chapter V. We classify the different dynamical behaviors that we obtain into a phase diagram, i.e. a graphical representation associating a specific phase to the parameters generating it. As for those presented in Chapter V, we choose $\alpha = \alpha' = \beta = \beta'$ for simplicity. We also set $z = 1$ (since this parameter is just a scaling factor in this model), $\ell_0 = 1$, $\varphi = 1$ and $b = 1$. Figure IV.1 shows four different phase diagrams in the parameter plane (α, ω), for $\sigma = \{0, \infty\}$ and different initial perturbations of equilibrium. To obtain these phase diagram, we run the dynamics for $T = 10000$ time-steps with the prescribed initialization and parameters. We then classify the different asymptotic behaviors. The different phases obtained are

- **Collapse**: the price blows up exponentially while production plummets, i.e. the economy collapses.
- **Competitive equilibrium**: price and production converge to the equilibrium defined in Chapter I, i.e. the economy is stable. The type of dynamics for the relaxation depends on the parameters of the model and can be rather complex (see Figure IV.2-(a, b) and Section 3).
- **Deflationary equilibrium**: the rescaled price converges towards a value different from competitive equilibrium. In this phase, a fraction of the household is unemployed $\ell_\infty^{\mathrm{s}} > \ell_\infty^{\mathrm{d}}$, and the wage decreases at constant rate.
- **Inflationary equilibrium**: the rescaled price converges towards a value different from competitive equilibrium. In this phase, the household is fully employed $\ell_\infty^{\mathrm{s}} < \ell_\infty^{\mathrm{d}}$, and the wage increases at constant rate.

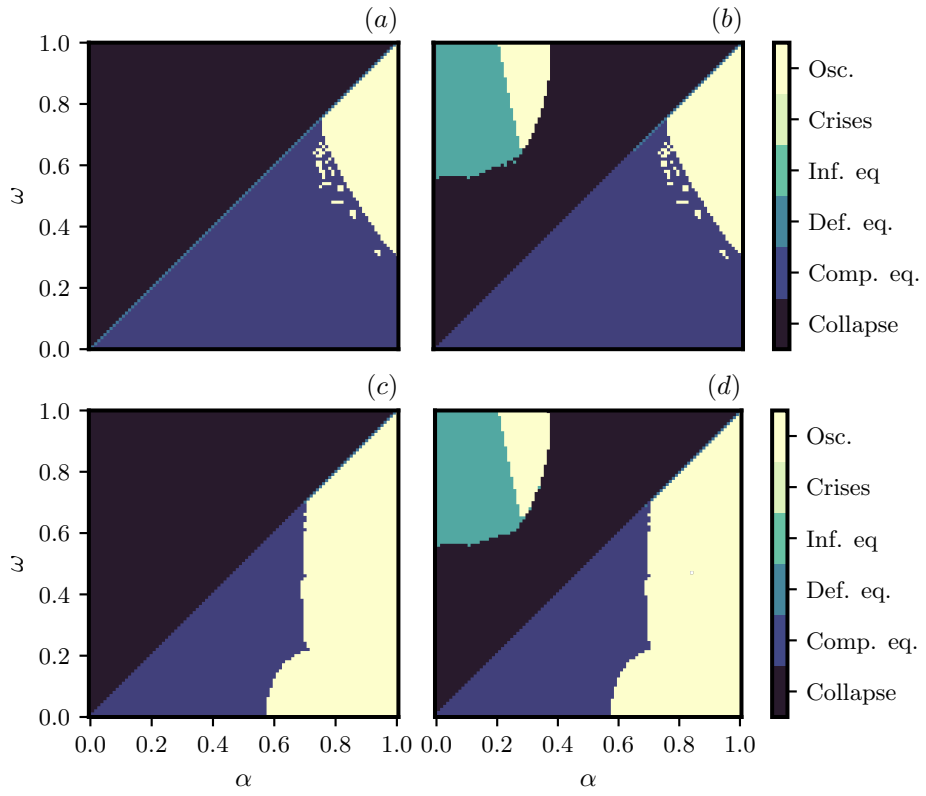


Figure IV.1: Phase diagram in the plane (α, ω) obtained by classifying the different asymptotic behaviors of the system after an initial perturbation. For each plot, we chose $\alpha = \alpha = \beta = \beta'$ along with $z = 1$, $b = 1$, $\varphi = 1$, $\ell_0 = 1$ and an initial perturbation $\gamma(0) = \gamma_{\text{eq}}(1+\delta), \widehat{\gamma}(t+1) = \gamma_{\text{eq}}(1+\delta)$ with $\delta = 10^{-5}$. (a) $\sigma = 0$ and $p(0) = p_{\text{eq}}(1+\delta)$. (b) $\sigma = 0$ and $p(0) = p_{\text{eq}}(1-\delta)$. (c) $\sigma = \infty$ and $p(0) = p_{\text{eq}}(1+\delta)$. (d) $\sigma = \infty$ and $p(0) = p_{\text{eq}}(1-\delta)$. Whenever the system is initialized with a downward perturbation on prices, we see the emergence of an additional inflationary/oscillatory region.

- **Crises**: price and production start converging towards competitive equilibrium but are violently destabilized when getting too close. This creates a series of price spikes (and production falls) more or less spaced out in time.

- **Oscillations**: price and production enter limit cycles of various nature. The economy remains bounded but is unstable. Cycles can be rather ordered or exhibit more chaotic patterns (see Figure IV.2-(c, d)).

The precise nature of the different phases will be discussed at length in Chapter V since we retrieve most of the same behaviors. However, we already have an improvement from the model presented in Chapter II with the emergence of a large region of parameter space where sustained oscillations occur (see Figure IV.2 for examples of oscillatory patterns).

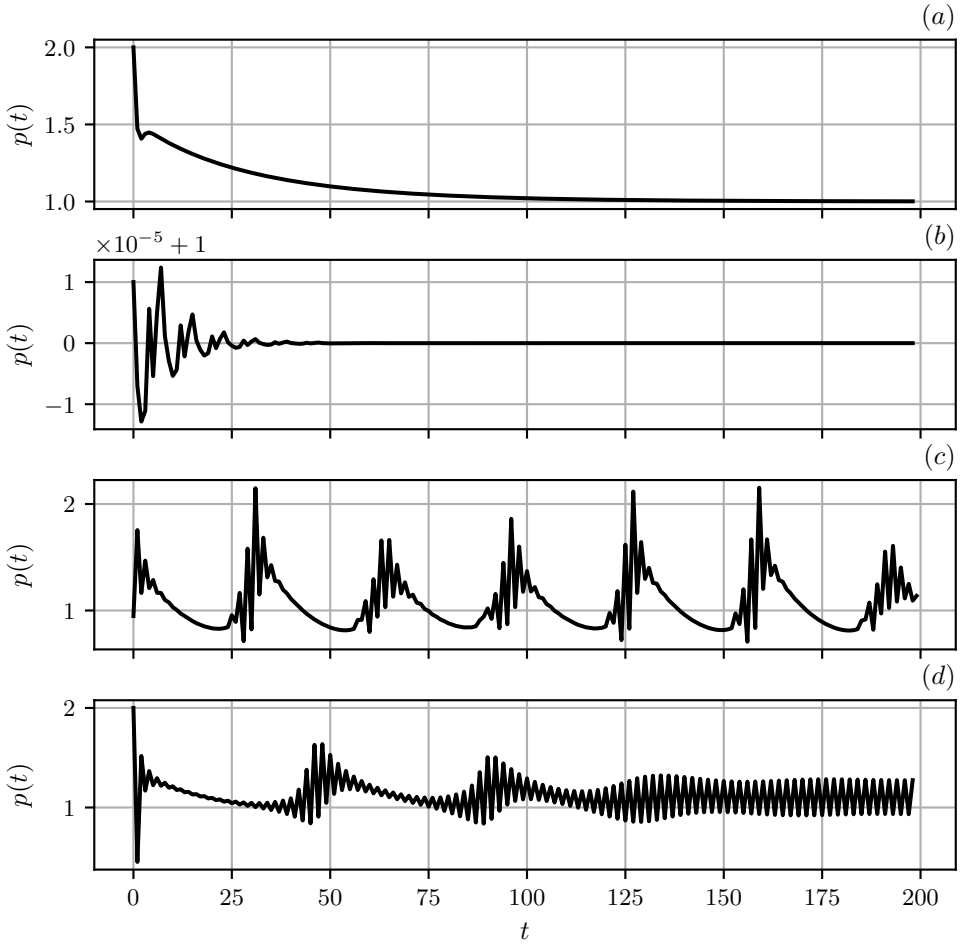


Figure IV.2: Some price trajectories generated by the model. We chose $\alpha = \alpha' = \beta = \beta'$, $z = 1$, $\ell_0 = 1$ and $\varphi = 1$ for each trajectory. (a) Simple exponential relaxation for $\alpha = 0.2$, $\omega = 0.1$, $\sigma = \infty$ and $b = 1$. (b) Complex damped oscillations for $\alpha = 0.8$, $\omega = 0.1$, $\sigma = 0$ and $b = 1$. (c) Sustained oscillations with smooth excursions for $\alpha = 0.8$, $\omega = 0.7$, $\sigma = 0$ and $b = 1$. (d) Sustained oscillations with dampening modulations for $\alpha = 0.8$, $\omega = 0.75$, $\sigma = 0.1$ and $b = 0.95$. Initial conditions: $p(0) = 2p_{\text{eq}}$, $\gamma(0) = 2\gamma_{\text{eq}}$, $\widehat{\gamma}(1) = 2\gamma_{\text{eq}}$ for $(a) - (c)$; $p(0) = p_{\text{eq}}(1 + \delta)$, $\gamma(0) = \gamma_{\text{eq}}(1 + \delta)$, $\widehat{\gamma}(1) = \gamma_{\text{eq}}(1 + \delta)$ with $\delta = 0^{-5}$ for $(b) - (d)$; the remaining variables are initialized with the associated equilibrium values.

In Figure IV.1-(a, c), oscillatory patterns can be observed for large values of α. Intuitively, the firm's reactions to imbalances are too strong and lead to overshoots/undershoots in the update of price and production, therefore generating oscillatory patterns. In the following, we will see that oscillations can also emerge when the economy switches from one region of state space to another, where dynamical equations have different outputs due to shortages. This feature is also linked to the appearance of the two inflationary/oscillatory regions in

the upper left corner of the diagrams whenever the price is initialized with a downward perturbation on equilibrium. Such a perturbation increases consumption demand and puts the system in a situation where supply is not enough to meet demand. This will be discussed at length in the next section. Finally, inflationary equilibria can be observed in this model, whereas they are not present in the model of Chapter V to the best of our knowledge. The nature of these equilibria is still rather elusive, and an attempt to properly characterize them is underway. However, in Chapter V, large regions of parameters space were found to display oscillations with persistent inflation, i.e. $\ell^{\mathrm{s}}(t) < \ell^{\mathrm{d}}(t)$.

The transition lines between the different phases in Figure IV.1 are tricky to assess analytically since they are of various origins. The diagonal transition line between collapsing and bounded dynamics (competitive equilibrium or oscillations) corresponds to a linear stability/instability transition of equilibrium in some regions of space, as we will see below. However, the transition between competitive equilibrium and oscillatory patterns (below the diagonal) is related to the invariance or non-invariance of some specific regions of space, and is therefore a lot harder to pinpoint.

3 Conewise dynamics and geometric study

In this section, we will study the dynamics of the system close to competitive equilibrium. Even at linear level, the system remains rather non-trivial since competitive equilibrium is a *cusp* of the dynamics, as we will see below. In the following, we will denote by $\boldsymbol{\epsilon}_i$ the i-th column vector of the canonical basis of $\mathbb{R}^5$.

3.1 Shortages close to equilibrium

One of the new features of this model is that it accounts for imbalances in goods, work and budget. Mathematically, these imbalances translate into constraint factors of the form $\min(1, a(t)/b(t))$ such that $a_{\mathrm{eq}} = b_{\mathrm{eq}}$. For instance, the budget constraint factor is obtained by taking $a(t) = B(t)$ and $b(t) = p(t)C^{\mathrm{o}}(t)$. Considering small perturbations $\delta(\cdot)$ around the equilibrium values of a and b, the constraint factor can be linearly approximated by

$$\min\left(1, \frac{a(t)}{b(t)}\right) \approx \min\left(1, 1 + \frac{\delta a(t) - \delta b(t)}{b_{\mathrm{eq}}}\right) = 1 + \min\left(0, \frac{\delta a(t) - \delta b(t)}{b_{\mathrm{eq}}}\right).$$

We see that the $\min(0, \cdot)$ function cannot be disregarded even close to equilibrium, and its output depends on the sign of $\delta a(t) - \delta b(t)$. Indeed, competitive equilibrium coincides with a non-differentiable point for constraint factors, i.e a cusp of the dynamics. To make proper sense, the perturbative analysis around equilibrium must be performed in restrictions of space where $\delta a(t) - \delta b(t)$ keeps a constant sign. Take for instance the production level $\gamma(t+1) = \ell(t)^b$ (with $z = 1$). We can write its evolution as

$$\delta\gamma(t+1) = \delta\widehat{\gamma}(t+1) + b\frac{\gamma_{\mathrm{eq}}}{\ell_{\mathrm{eq}}}\min(0, \delta\mathscr{E}_0^{\mathrm{o}}), \tag{IV.33}$$

which can take two different forms:

- if enough work was supplied to reach the target of production, i.e. $\delta\mathscr{E}_0(t) > 0$, then

$$\delta\gamma(t+1) = \delta\widehat{\gamma}(t+1),$$

- otherwise, i.e. $\delta\mathscr{E}_0(t) < 0$, production is capped by available work

$$\delta\gamma(t+1) = \delta\widehat{\gamma}(t+1) + b\frac{\gamma_{\mathrm{eq}}}{\ell_{\mathrm{eq}}}(\delta\ell^{\mathrm{s}}(t) - \delta\ell^{\mathrm{d}}(t)).$$

In either region $\delta\mathscr{E}_0 \gtrless 0$ the dynamics linearly depends on the perturbations, but the linear dependency differs depending on the region. Of course, the same applies for good and budget shortages. The expression of the dynamics depends on the sign of the three perturbations $\delta\mathscr{E}(t)$ (good shortages), $\delta\mathscr{E}_0(t)$ (work shortage) and $\delta h(t) = -\delta\mathscr{E}_0(t) + \min(0, \delta\mathscr{E}_0) - p_{\mathrm{eq}}\min(0, \delta\mathscr{E})$ (budget shortages).

In Appendix A, we provide the computations for the complete linearization of the dynamics. We show that the system can be described through the evolution of a vector $\mathbf{U}(t)$ encapsulating perturbations on past and present targets along with present prices, productions, stocks and savings

$$\mathbf{U}(t) = \begin{pmatrix} \delta\widehat{\gamma}(t+1) \\ \delta\gamma(t) \\ \delta p(t) \\ \delta I(t) \\ \delta S(t) \\ \delta\widehat{\gamma}(t) \end{pmatrix}. \tag{IV.34}$$

The stability matrix $\mathbb{D}(t)$ of the system is of the form

$$\mathbb{D}(t) = \mathbb{F}\mathbb{E}(t), \tag{IV.35}$$

where $\mathbb{F} \in \mathcal{M}_{6,10}$ is fixed and $\mathbb{E}(t) \in \mathcal{M}_{10,6}$ is a matrix that depends on the signs of the quantities $\delta\mathscr{E}, \delta\mathscr{E}_0, \delta h$. At linear level, these quantities can be expressed as the overlaps between the state vector $\mathbf{U}(t)$ and three vectors $\mathbf{c}_g, \mathbf{c}_w, \mathbf{c}_h(t)$, i.e.

$$\begin{aligned} \delta\mathscr{E}(t) &= \mathbf{c}_g^\top \mathbf{U}(t) \\ \delta\mathscr{E}_0(t) &= \mathbf{c}_w^\top \mathbf{U}(t) \\ \delta h(t) &= \mathbf{c}_h(t)^\top \mathbf{U}(t), \end{aligned}$$

where

$$\begin{aligned} \mathbf{c}_g &= \left(0, z, \frac{C_{\mathrm{eq}}}{p_{\mathrm{eq}}}, 1, -\frac{C_{\mathrm{eq}}}{k\ell_0}, 0\right) \\ \mathbf{c}_w &= \left(-\frac{\ell_{\mathrm{eq}}}{b\gamma_{\mathrm{eq}}}, 0, 0, 0, -\frac{1}{1+\varphi}, 0\right). \end{aligned}$$

Note that $\mathbf{c}_h$ is itself time dependent, since it also depends on the signs of $\delta\mathscr{E}, \delta\mathscr{E}_0$. One can therefore partition $\mathbb{R}^6$ into at most eight regions $\mathcal{C}_{\pm,\pm,\pm}$ where $\delta\mathscr{E}$, $\delta\mathscr{E}_0$, $\delta h(t)$ keep a constant sign

$$\mathcal{C}_{\pm,\pm,\pm} = \left\{\mathbf{x} \in \mathbb{R}^6,\ \text{sgn}\left(\mathbf{c}_g^\top \mathbf{x}\right) = \pm 1,\ \text{sgn}\left(\mathbf{c}_w^\top \mathbf{x}\right) = \pm 1,\ \text{sgn}\left(\mathbf{c}_h^\top \mathbf{x}\right) = \pm 1\right\}. \quad \text{(IV.36)}$$

These regions are convex cones within which the evolution of $\mathbf{U}(t)$ is determined by a single value $\mathbb{D}(t)$. Such a situation is generically called *conewise linear dynamics*, and can yield highly complex dynamics, as we will see. To be more precise, our situation is not exactly conewise linear since $\mathbf{c}_h$ also depends on the position, and therefore the cones themselves depends on the position in space. However, we will still refer to this type of dynamics as conewise linear for clarity purposes. In the next section, we will give the explicit form of $\mathbb{D}(t)$ in the different cones.

3.2 Exchange matrices

As we said before (see Appendix A), the dynamical matrix $\mathbb{D}(t)$ is of the form $\mathbb{D}(t) = \mathbb{F}\mathbb{E}(t)$ with $\mathbb{F}$ fixed and $\mathbb{E}(t)$ a conewise constant function with block form

$$\mathbb{E}(t) = \begin{pmatrix} \mathbb{S}(t) & \mathbf{0}_5 \\ \mathbf{I}_5 - \boldsymbol{\epsilon}_5 \boldsymbol{\epsilon}_5^\top & 0 \end{pmatrix}, \quad \text{(IV.37)}$$

with $\mathbf{I}_5$ the identity of $\mathcal{M}_{5,5}$. The shortage matrix $\mathbb{S}(t)$ can take 5 different values determined by the form of the update of savings

$$\delta S(t+1) = \delta h(t) - \min(0, \delta h), \quad \text{(IV.38)}$$

stocks

$$\delta I(t+1) = e^{-\sigma}\left(\delta\mathscr{E}(t) - \min(0, \delta\mathscr{E}) - \frac{C_{\text{eq}}}{B_{\text{eq}}}\min(0, \delta h)\right), \quad \text{(IV.39)}$$

production levels,

$$\delta\gamma(t+1) = \delta\widehat{\gamma}(t+1) + b\frac{\gamma_{\text{eq}}}{\ell_{\text{eq}}}\min(0, \delta\mathscr{E}_0), \quad \text{(IV.40)}$$

and finally prices through profits

$$\delta\pi(t) = \delta S(t) - \delta h(t) + \min(0, \delta h). \quad \text{(IV.41)}$$

The previous equations are obtained in Appendix A. We will detail the different values $\mathbb{S}_i$ taken by $\mathbb{S}(t)$ along with their interpretations below. Finally, each situation is also described graphically on Figure IV.3 where we look at a projection of the state space onto the plane $(\mathbf{c}_g, \mathbf{c}_w)$. The labeling of the different situations below corresponds to the one on Figure IV.3. To each matrix $\mathbb{S}_i$, we naturally associate the corresponding stability matrix $\mathbb{D}_i$, along with the cone $\mathcal{C}_i$ within which they are active.

(*a*) **Plentiful supply, partial unemployment:** In this situation $\delta\mathscr{E}(t) > 0$ as well as $\delta\mathscr{E}_0(t) > 0$: there is enough supply to satisfy demand, and the household is not fully employed since $\delta\ell^{\mathrm{s}}(t) > \delta\ell^{\mathrm{d}}(t)$. In this case, the household will be faced with a shortage of budget. Indeed, since it is employed for $\ell_{\mathrm{eq}} + \delta\ell^{\mathrm{d}}(t) < \ell_{\mathrm{eq}} + \delta\ell^{\mathrm{s}}(t)$ hours, its expected budget (computed optimistically by assuming full employment) will be lower that its realized counterpart. Furthermore, its consumption demand will be met since supply is plentiful and the household will be unable to consume it all. In this case, $\delta h = -\delta\mathscr{E}_0 < 0$, i.e. $\mathbf{c}_h = -\mathbf{c}_w$, which is expected from the previous discussion. Furthermore, no money will be saved $\delta S(t+1) = 0$ since the budget will be entirely used to consume as much as possible. The firm will profit from the goods consumed thanks to the household possible savings $\delta\pi(t) = \delta S(t)$ and will store the leftover supply

$$\delta I(t+1) = e^{-\sigma}\left(\delta\mathscr{E}(t) + \frac{C_{\mathrm{eq}}}{B_{\mathrm{eq}}}\delta\mathscr{E}_0(t)\right),$$

where the last term comes from goods that could not be consumed due to budget shortage. Finally, the production target is reached $\delta\gamma(t+1) = \delta\widehat{\gamma}(t+1)$ since enough work was provided. The subsequent matrix will be called $\mathbb{S}_0$ and reads

$$\begin{aligned}\mathbb{S}_0 = (\boldsymbol{\epsilon}_1 + \boldsymbol{\epsilon}_2)\boldsymbol{\epsilon}_1^\top + \boldsymbol{\epsilon}_3\left(\boldsymbol{\epsilon}_3 - \alpha\frac{p_{\mathrm{eq}}}{z\gamma_{\mathrm{eq}}}\mathbf{c}_g + \omega\frac{p_{\mathrm{eq}}}{\ell_{\mathrm{eq}}}\mathbf{c}_w - \alpha'\frac{1}{z\gamma_{\mathrm{eq}}}\boldsymbol{\epsilon}_5\right)^\top \\ + e^{-\sigma}\boldsymbol{\epsilon}_4\left(\mathbf{c}_g + \frac{C_{\mathrm{eq}}}{B_{\mathrm{eq}}}\mathbf{c}_w\right)^\top.\end{aligned} \tag{IV.42}$$

(*b*) **Plentiful supply, full employment:** In this situation $\delta\mathscr{E}(t) > 0$ still but now $\delta\mathscr{E}_0(t) < 0$, i.e. firms cannot hire as much as needed and the household is fully employed. There is no budget shortage in this case since the consumption demand is satisfied (plentiful supply) and the household work as much as it expected. Here $\mathbf{c}_h = 0$. As before no money is saved $\delta S(t+1) = 0$, and profits come from consumption thanks to savings $\delta\pi(t) = \delta S(t)$. The firm will stock less than in the previous case since the household consumes more

$$\delta I(t+1) = e^{-\sigma}\delta\mathscr{E}(t).$$

However, since the firm did not get the amount of work needed, the actual production level is lower that the targeted value

$$\delta\gamma(t+1) = \delta\widehat{\gamma}(t+1) + b\frac{\gamma_{\mathrm{eq}}}{\ell_{\mathrm{eq}}}\delta\mathscr{E}_0(t).$$

The subsequent matrix is called $\mathbb{S}_w$ and reads

$$\begin{aligned}\mathbb{S}_w = \boldsymbol{\epsilon}_1\boldsymbol{\epsilon}_1^\top + \boldsymbol{\epsilon}_2\left(\boldsymbol{\epsilon}_1 + b\frac{\gamma_{\mathrm{eq}}}{\ell_{\mathrm{eq}}}\mathbf{c}_w\right)^\top + \boldsymbol{\epsilon}_3\left(\boldsymbol{\epsilon}_3 - \alpha\frac{p_{\mathrm{eq}}}{z\gamma_{\mathrm{eq}}}\mathbf{c}_g + \omega\frac{p_{\mathrm{eq}}}{\ell_{\mathrm{eq}}}\mathbf{c}_w - \alpha'\frac{1}{z\gamma_{\mathrm{eq}}}\boldsymbol{\epsilon}_5\right)^\top \\ + e^{-\sigma}\boldsymbol{\epsilon}_4\mathbf{c}_g^\top.\end{aligned} \tag{IV.43}$$

(*c*) **Good shortage, full employment:** In this situation, $\delta\mathscr{E}_0(t) < 0$ as well as $\delta\mathscr{E}(t) < 0$. Since the household is fully employed, there is no budget shortage. However, the firm cannot fulfill the household's demand and the latter is frustrated in its consumption. Here $\mathbf{c}_h = -p_{\text{eq}}\mathbf{c}_g$. Money will be saved

$$\delta S(t+1) = -p_{\text{eq}}\delta\mathscr{E}(t),$$

and the firm will make less profits than they would have with plentiful supply

$$\delta\pi(t) = \delta S(t) + p_{\text{eq}}\delta\mathscr{E}(t).$$

Since the firm tries to fulfill the household's demand as much as possible, it will completely empty its supply and no good will be stored $\delta I(t+1) = 0$. Finally, since work was not sufficient as before, the production target will not be reached

$$\delta\gamma(t+1) = \delta\widehat{\gamma}(t+1) + b\frac{\gamma_{\text{eq}}}{\ell_{\text{eq}}}\delta\mathscr{E}_0(t).$$

The subsequent matrix is called $\mathbb{S}_{g,w}$ and reads

$$\begin{aligned}\mathbb{S}_{g,w} = \boldsymbol{\epsilon}_1\boldsymbol{\epsilon}_1^\top + \boldsymbol{\epsilon}_3\left(\boldsymbol{\epsilon}_3 - \alpha\frac{p_{\text{eq}}}{z\gamma_{\text{eq}}}\mathbf{c}_g + \omega\frac{p_{\text{eq}}}{\ell_{\text{eq}}}\mathbf{c}_w - \alpha'\frac{1}{z\gamma_{\text{eq}}}(\boldsymbol{\epsilon}_5 + p_{\text{eq}}\mathbf{c}_g)\right)^\top \\ - p_{\text{eq}}\boldsymbol{\epsilon}_5\mathbf{c}_g^\top + \boldsymbol{\epsilon}_2\left(\boldsymbol{\epsilon}_1 + b\frac{\gamma_{\text{eq}}}{\ell_{\text{eq}}}\mathbf{c}_w\right)^\top.\end{aligned} \tag{IV.44}$$

(*d*) **Good shortage, partial unemployment:** This final situation with $\delta\mathscr{E}_0(t) > 0$ and $\delta\mathscr{E}(t) < 0$ is more intricate. Since $\delta\mathscr{E}_0(t) > 0$ the household works less than it expected, and therefore overestimates its budget before consuming. Consequently, a budget shortage can occur. However, since there is a good shortage, the amount of goods offered by the firm can be low enough so that the household is still able to consume them entirely, regardless of the unanticipated low budget. We have $\delta h(t) = -\delta\mathscr{E}_0(t) - p_{\text{eq}}\delta\mathscr{E}(t)$, so that $\mathbf{c}_h = -\mathbf{c}_w - p_{\text{eq}}\mathbf{c}_g$, and the following situations can occur:

(*i*) **Budget shortage:** If budget is still short in spite of the low offer in goods, i.e. $\delta h(t) < 0$, the household will not save anything $\delta S(t+1) = 0$. The firm will profit from the savings' expenses $\delta\pi(t) = \delta S(t)$, will store the left over supply

$$\delta I(t+1) = e^{-\sigma}\frac{C_{\text{eq}}}{B_{\text{eq}}}\left(\mathbf{c}_w + p_{\text{eq}}\mathbf{c}_g\right),$$

and will reach its target production $\delta\gamma(t+1) = \delta\widehat{\gamma}(t+1)$. The subsequent matrix is called $\mathbb{S}_{g,b}$ and yields

$$\begin{aligned}\mathbb{S}_{g,b} = (\boldsymbol{\epsilon}_1 + \boldsymbol{\epsilon}_2)\boldsymbol{\epsilon}_1^\top + \boldsymbol{\epsilon}_3\left(\boldsymbol{\epsilon}_3 - \alpha\frac{p_{\text{eq}}}{z\gamma_{\text{eq}}}\mathbf{c}_g + \omega\frac{p_{\text{eq}}}{\ell_{\text{eq}}}\mathbf{c}_w - \alpha'\frac{1}{z\gamma_{\text{eq}}}\boldsymbol{\epsilon}_5\right)^\top \\ + e^{-\sigma}\frac{C_{\text{eq}}}{B_{\text{eq}}}\boldsymbol{\epsilon}_4\left(\mathbf{c}_w + p_{\text{eq}}\mathbf{c}_g\right)^\top.\end{aligned} \tag{IV.45}$$

(*ii*) **No budget shortage:** Here, the shortage of goods is so important that the firm offers a small enough quantity such that the household is not inconvenienced by its low budget, i.e. $\delta h(t) > 0$. The household will then save some amount of money

$$\delta S(t+1) = -\delta \mathscr{E}_0(t) - p_{\text{eq}} \delta \mathscr{E}(t) > 0.$$

The firm will empty its stocks $\delta I(t+1) = 0$ and make less profits than in the previous situation

$$\delta \pi(t) = \delta S(t) + \delta \mathscr{E}_0(t) + p_{\text{eq}} \delta \mathscr{E}(t).$$

As before, the production target is reached. The subsequent matrix is called $\mathbb{S}_g$ and yields

$$\mathbb{S}_g = (\boldsymbol{\epsilon}_1 + \boldsymbol{\epsilon}_2)\boldsymbol{\epsilon}_1^\top + \boldsymbol{\epsilon}_3 \left(\boldsymbol{\epsilon}_3 - \alpha \frac{p_{\text{eq}}}{z\gamma_{\text{eq}}} \mathbf{c}_g + \omega \frac{p_{\text{eq}}}{\ell_{\text{eq}}} \mathbf{c}_w - \alpha' \frac{1}{z\gamma_{\text{eq}}} \left(\boldsymbol{\epsilon}_5 + \mathbf{c}_w + p_{\text{eq}} \mathbf{c}_g \right) \right)^\top - \boldsymbol{\epsilon}_5 \left(\mathbf{c}_w + p_{\text{eq}} \mathbf{c}_g \right)^\top. \tag{IV.46}$$

3.3 Equilibrium stability and transition lines

In conewise linear systems, the question of stability does not have a straightforward answer [113, 114]. Since the dynamics can switch from one cone to another, the state vector $\mathbf{U}(t)$ is given by a time-ordered product of matrices applied to $\mathbf{U}(0)$. To assess the stability of this system, one would need to know the eigenvalues of this product, which is a notoriously difficult task. As an introduction, Figure IV.4-(*a*) reproduces the phase diagram of Figure IV.1-(*c*) (obtained for $\sigma = \infty$ and an initial upward deviation from equilibrium) over which we overlaid two transition lines associated with the matrix $\mathbb{D}_0$:

- the ARK1 line refers to the asymptotically rank-one transition discussed in Section 3.3.1. On the left of this line, the matrix $\mathbb{D}_0$ possesses an invariant cone $\mathcal{K}$, i.e. such that $\mathbb{D}_0 \mathcal{K} \subset \mathcal{K}$.

- the stable transition refers to the escape of at least one eigenvalue from the unit circle. On the left of this line, a linear dynamics governed by $\mathbb{D}_0$ would be convergent.

As we see on Figure IV.4-(*a*), even if equilibrium is stable under $\mathbb{D}_0$, there is an entire region of spontaneous oscillations occurring for small enough ω. However, as soon as $\mathbb{D}_0$ possesses an invariant cone, the system is able to reach equilibrium. As we will see, equilibrium stability is by no means a token of convergence in conewise linear systems, and one needs to study the invariance properties of the matrices $\mathbb{D}_i$.

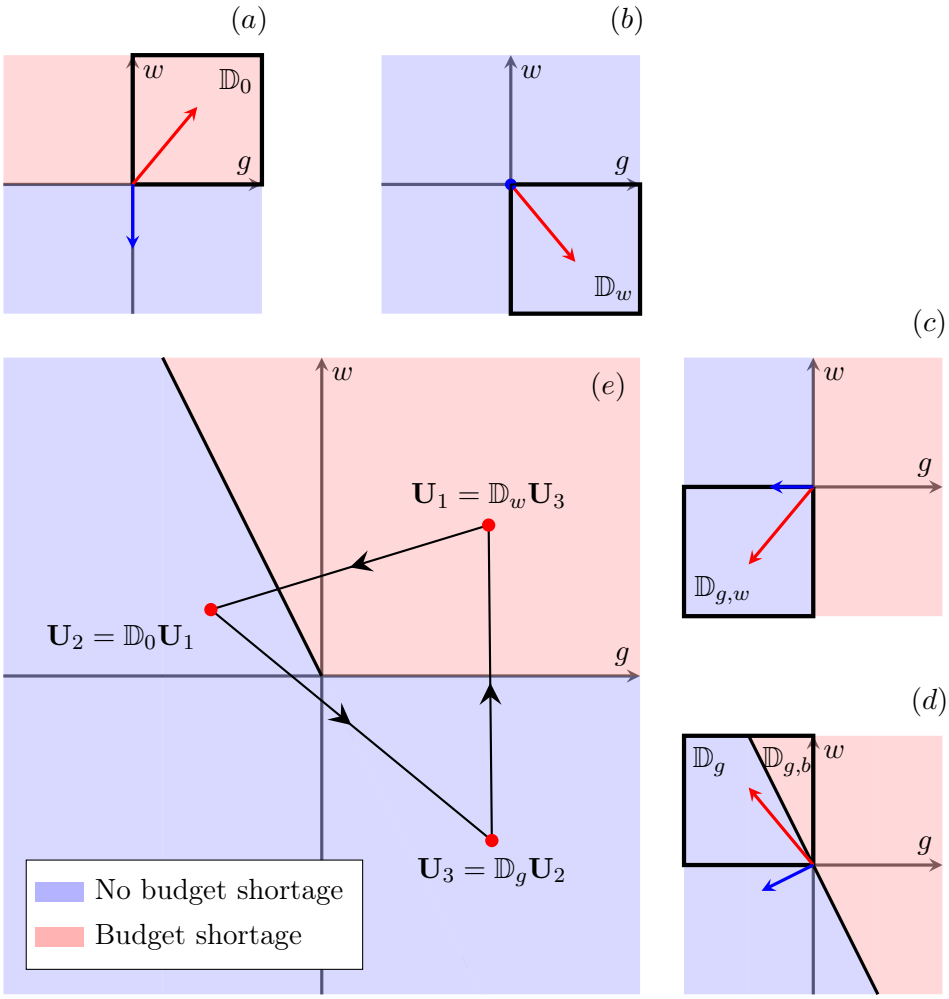


Figure IV.3: Schematic representation of the different cones in the plane spanned by $(\mathbf{c}_g, \mathbf{c}_w)$. The red arrows correspond to the position of $\mathbf{U}$ in the plane $(\mathbf{c}_g, \mathbf{c}_w)$ and the blue arrows correspond to the vector $\mathbf{c}_h$. The subplots $(a) - (b) - (c) - (d)$ correspond to the different situations described in Section 3.2. (e) provides a fictitious evolution of the vector $\mathbf{U}$ (red dots) that loops over the three regions governed by $\mathbb{D}_0, \mathbb{D}_g$ and $\mathbb{D}_w$. Finally, the color code highlights the regions where budget shortage occurs or not.

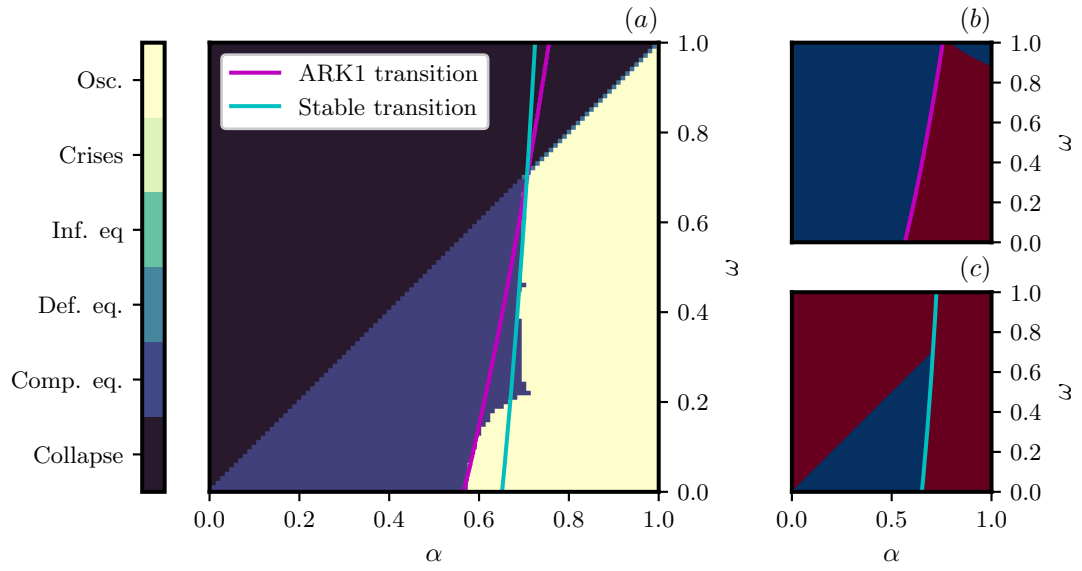


Figure IV.4: (a) Phase diagram of Figure IV.1-(c) obtained for $\sigma = \infty$ and an upward initial perturbation applied to equilibrium prices, productions and targets. (b) Regions (in blue) in parameter plane (α, ω) for which $\mathbb{D}_0$ is asymptotically rank-one (ARK1) along with the pink transition line overlaid on (a). (c) Regions (in blue) in parameter plane (α, ω) for which $\mathbb{D}_0$ is stable along with the cyan transition line overlaid on (a).

3.3.1 Cone invariance

Since within one cone the dynamics is linear (and therefore fully determined by the eigenpairs of the associated matrix), a natural question to ask is under which condition will a cone be stable under this linear dynamics [2]. To the best of our knowledge, given a cone $\mathcal{C}$ and a matrix $\mathbb{A}$, there does not exist any straightforward criterion for $\mathcal{C}$ to be stable under $\mathbb{A}$. However, there exist some conditions for the existence of a stable cone under $\mathbb{A}$. First, we recall the generalization of the Perron-Frobenius theorem

Theorem IV.1 (Perron-Frobenius)**.** *Let a proper cone $\mathcal{C}$ be strictly invariant for a non zero matrix $\mathbb{A}$. Then the following facts hold*

(i) the spectral radius $\rho(\mathbb{A})$ [3] is a simple positive eigenvalue of $\mathbb{A}$ and $|\lambda| < \rho(\mathbb{A})$ for any other eigenvalue λ of $\mathbb{A}$;

(ii) int$(\mathcal{C})$ [4] contains the unique leading eigenvector v associated with $\rho(\mathbb{A})$;

[2] A cone $\mathcal{C}$ is stable under $\mathbb{A}$ if $\mathbb{A}\mathcal{C} \subset \mathcal{C}$.

[3] The spectral radius $\rho(\mathbb{A})$ of a $N \times N$ matrix $\mathbb{A}$ is defined as $\rho(\mathbb{A}) = \max\{|\lambda_1|, \dots, |\lambda_N|\}$ where λ_i is the i-th eigenvalue of $\mathbb{A}$.

[4] For a subset A of a topological space X, the set int$A$ is a subset of X included in A defined as the union of all open sets contained in A.

(iii) the secondary eigenvectors and generalized eigenvectors of $\mathbb{A}$ *do not belong to* $\mathcal{C}$*.*

This theorem provides some properties whenever an invariant cone exists, but does not ensure the existence of such a cone. For the existence of invariant cones, we need the following definition

Definition IV.1. *A matrix* $\mathbb{A}$ *is said to be asymptotically rank-one if the following conditions hold*

(i) $\rho(\mathbb{A}) > 0$*;*

(ii) exactly one between $\rho(\mathbb{A})$ *and* $-\rho(\mathbb{A})$ *is an eigenvalue of* $\mathbb{A}$ *and, moreover, it is a simple eigenvalue;*

(iii) $|\lambda| < \rho(\mathbb{A})$ *for any other eigenvalue* λ *of* $\mathbb{A}$*.*

Intuitively, such matrices will behave as a projector onto the eigenvector associated with $\pm\rho(\mathbb{A})$ whenever they are raised to a large power. As a consequence, we have the following theorem (see [115])

Theorem IV.2. *A matrix* $\mathbb{A}$ *is asymptotically rank-one if and only if* $\mathbb{A}$ *or* $-\mathbb{A}$ *admits an invariant proper cone.*

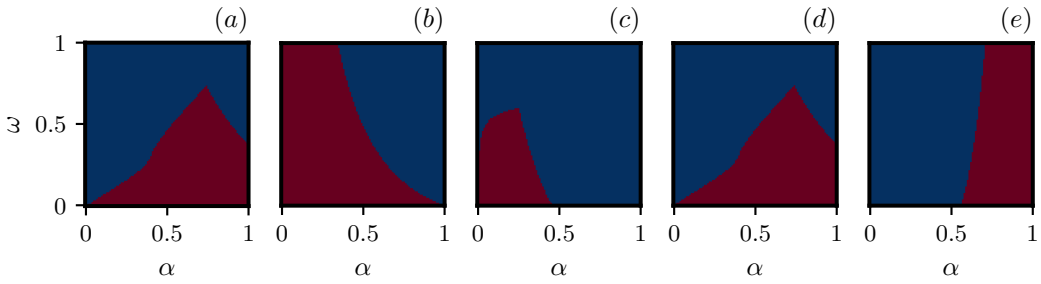
To ensure the existence of an invariant cone, we can therefore use the rank-one characterization, which we can easily check numerically. Figure IV.5 shows the different regions where matrices $\mathbb{D}_i$ are asymptotically rank-one. Of course, the previous theorem does not say anything about the features of the invariant cone $\mathcal{C}$ but, together with Perron-Frobenius theorem, we know that it must contain the eigenvector v associated with $\pm\rho(\mathbb{A})$. Finally, if v is also contained within some cone of the dynamics, we can deduce that the dynamics will leave at least part of this cone invariant.

To summarize, let us take $\mathbb{A} = \mathbb{D}_0$ and consider the dynamics associated with the plentiful supply and partial unemployment cone $\mathcal{C}_0$. If $\mathbb{D}_0$ is asymptotically rank-one, then there exists a cone $\mathcal{K}$ invariant under $\mathbb{D}_0$. Furthermore, the eigenvector v associated with $\pm\rho(\mathbb{D}_0)$ is contained within $\mathcal{K}$. If also $v \in \mathcal{C}_0$, then $\mathbb{D}_0$ will leave $\mathcal{K} \cap \mathcal{C}_0$ invariant and the dynamics will be trivial in this region. Since we do not know the exact nature of $\mathcal{K}$, we cannot say for certain whether $\mathcal{K} \cap \mathcal{C}_0 = \mathcal{C}_0$ (i.e. $\mathcal{C}_0 \subset \mathcal{K}$), which would imply that $\mathcal{C}_0$ itself is invariant, but we know that $\mathcal{C}_0$ is at least partially invariant.

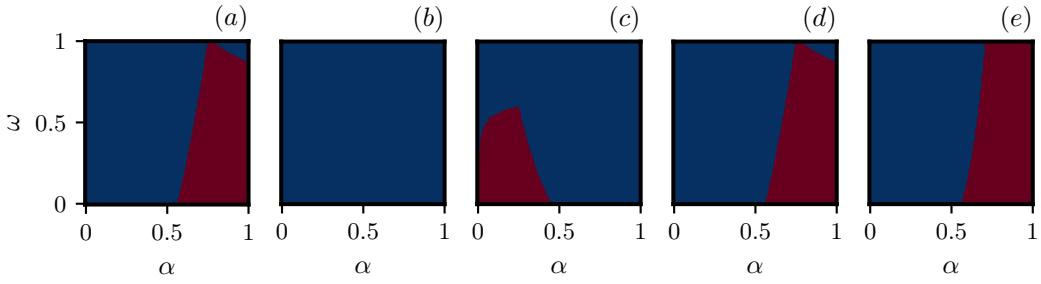
On Figure IV.4, we can see that the dynamics is less stable whenever $\mathbb{D}_0$ is not asymptotically rank-one. This suggests that the oscillatory patterns come from excursions in different cones where matrices are less stable than $\mathbb{D}_0$.

3.3.2 Matrix stability

Since the dynamics may leave some of the cones invariant, it is interesting to study the spectral properties of the different matrices $\mathbb{D}_i$. In this section, we will focus on the matrix



(i) $\sigma = 0$



(ii) $\sigma = \infty$

Figure IV.5: Regions in the parameter plane (α, ω) where matrices $\mathbb{D}_i$ are asymptotically rank-one (in blue) for $\sigma = 0$ (top) and $\sigma = \infty$ (bottom). (a) $\mathbb{D}_0$, (b) $\mathbb{D}_w$, (c) $\mathbb{D}_{g,w}$, (d) $\mathbb{D}_{g,b}$, (e) $\mathbb{D}_g$. We chose $\alpha = \alpha' = \beta = \beta'$, $z = 1$, $\ell_0 = 1$, $b = 1$ and $\varphi = 1$.

$\mathbb{D}_0$, but computations are very similar for other matrices. Assuming that the matrix $\mathbb{D}_0$ leaves the cone $\mathcal{C}_0$ invariant, the dynamics on $\mathbf{U}$ is trivial and one has

$$\mathbf{U}(t) = \mathbb{D}_0^t \mathbf{U}(0). \tag{IV.47}$$

The system is therefore stable if all the eigenvalues of $\mathbb{D}_0$ are contained within the unit circle. It is not hard to compute the characteristic polynomial of $\mathbb{D}_0$, but it is a bit lengthy and we will therefore not show the computation. For simplicity, let us consider the case $\alpha = \alpha' = \beta = \beta'$ and $\sigma = \infty$. The characteristic polynomial χ_0 of $\mathbb{D}_0$ is expressed as follows

$$\chi_0(\lambda) = \lambda^3 \left(\lambda^3 + \lambda^2(\alpha(\omega + 3) - 2) + \lambda\left(3\alpha^2 - 2\alpha\omega - 3\alpha + 1\right) - 2\alpha^2\right). \tag{IV.48}$$

From this expression, one could use the cubic roots' formula to get the eigenvalues. However, the final expressions would be hard to interpret in terms of stability. We will therefore give some conditions for the existence of roots lying right onto the unit circle by studying $\widetilde{\chi_0} = \chi_0/\lambda^3$ directly. There are different possibilities.

$\lambda_0 = 1$ is a root In this case, we have the equation $\widetilde{\chi_0}(1) = 0$ which translates into the relation

$$\alpha = \omega. \tag{IV.49}$$

In the general case, the relationship would have been $\alpha\beta = \beta'\omega$ independent of both α' and σ. With Eq. (IV.49), we easily retrieve the diagonal transition from the collapsing regions and the bounded dynamics region in Figure IV.1.

$\lambda_0 = -1$ is a root With the same reasoning, we have the following relationship

$$\omega = \frac{4 - 6\alpha + 5\alpha^2}{3\alpha}. \tag{IV.50}$$

This condition is less restrictive than the one obtained for the case $\lambda = 1$, and therefore does not play a role in the stability of $\mathbb{D}_0$.

Two complex roots on the unit circle If we assume that $\widetilde{\chi}_0$ has two complex roots $\lambda_1/\bar{\lambda}_1$ and one real root λ_0, we have the following factorization

$$\widetilde{\chi}_0(\lambda) = (\lambda - \lambda_0)(\lambda - \lambda_1)(\lambda - \bar{\lambda}_1),$$

which we can expand

$$\widetilde{\chi}_0(\lambda) = \lambda^3 - (\lambda_0 + 2\mathfrak{Re}\,(\lambda_1))\lambda^2 + \lambda_0(\lambda_0 + 2\mathfrak{Re}\,(\lambda_1))\lambda - \lambda_0,$$

and where we used $|\lambda_1| = 1$. We immediately see that in this case, the constant term of $\widetilde{\chi}_0$ must be the opposite of the root λ_0, i.e. $-a_0$ is a root. We can write

$$\widetilde{\chi}_0(\lambda) = (\lambda + a_0)P(\lambda) + Q(\lambda),$$

such that $Q = 0$ whenever two complex roots lie on the unit circle. Since $\deg Q < \deg(\lambda + a_0) = 1$, Q is a real number. Solving $Q = 0$ yields the relationship

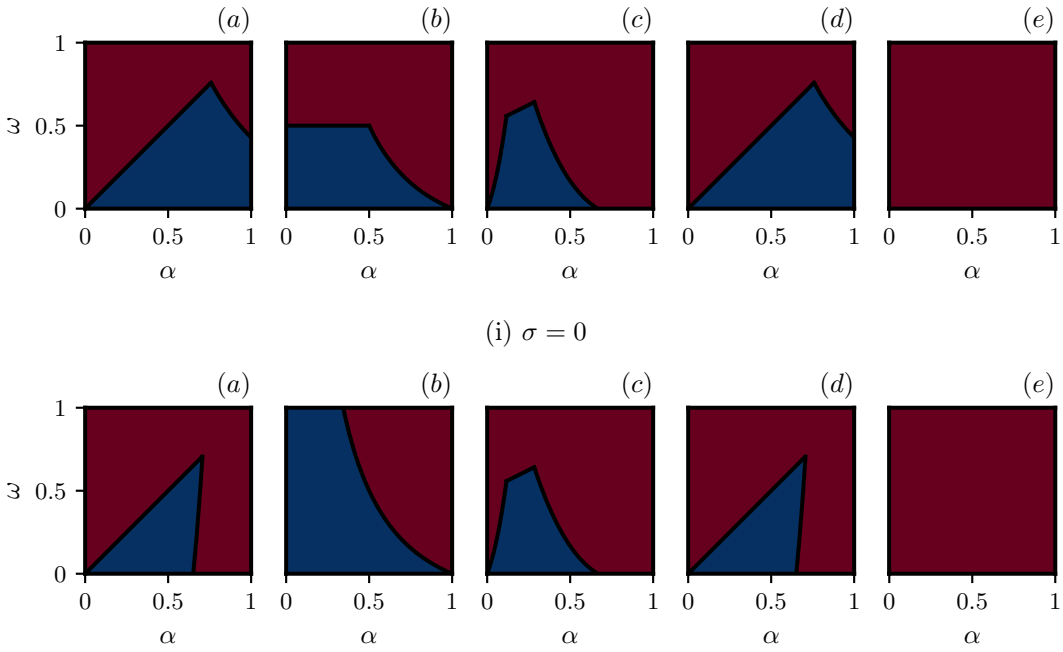
$$\omega = \frac{3 - 2\alpha - 4\alpha^2}{2(\alpha - 1)}. \tag{IV.51}$$

As we said, Eq. (IV.50) turns out to be irrelevant and the stability of the matrix $\mathbb{D}_0$ is solely determined by the position of α or ω with respect to the lines (IV.49) and (IV.51). The different regions in the plane (α, ω) where matrices $\mathbb{D}_i$ are stable are shown in blue on Figure IV.6 for different values of the perishability parameter σ. Together with the asymptotically rank-one condition as shown on Figure IV.5, one can devise an approximate region where equilibrium is stable, and the dynamics determined by $\mathbb{D}_0$.

3.3.3 Sequence stability

Of course, the situation where cones are not stable is a lot more complex to tackle. In full generality, the solution to the conewise linear system can be written as

$$\mathbf{U}(t) = \mathbb{M}(t)\mathbf{U}(0), \tag{IV.52}$$



(i) $\sigma = 0$

(ii) $\sigma = \infty$

Figure IV.6: Regions in the parameter plane (α, ω) where matrices $\mathbb{D}_i$ are stable (in blue) for $\sigma = 0$ (top) and $\sigma = \infty$ (bottom). (a) $\mathbb{D}_0$, (b) $\mathbb{D}_w$, (c) $\mathbb{D}_{g,w}$, (d) $\mathbb{D}_{g,b}$, (e) $\mathbb{D}_g$. We chose $\alpha = \alpha' = \beta = \beta'$, $z = 1$, $\ell_0 = 1$, $b = 1$ and $\varphi = 1$. The solid black lines indicate the analytical values of the transition lines such as Eqs. (IV.49) or (IV.51).

with $\mathbb{M}(t)$ a matrix accounting for the different cones visited by the dynamics

$$\mathbb{M}(t) = \mathcal{T} \prod_{\mathcal{K} \in \vec{\mathcal{C}}} \mathbb{D}_{\mathcal{K}}^{\tau_{\mathcal{K}}}. \tag{IV.53}$$

The operator $\mathcal{T}$ denotes the time ordered product,$\vec{\mathcal{C}}$ a cone sequence with elements $\mathcal{K}$ and $\tau_{\mathcal{K}}$ the occupation time of cone $\mathcal{K}$ such that $\sum_{\mathcal{K} \in \vec{\mathcal{C}}} \tau_{\mathcal{K}} = t$. The stability of the system can therefore be assessed using Lyapunov analysis. The system is stable if the maximum Lyapunov exponent $\lambda_{\max}$ is negative, where

$$\lambda_{\max} = \lim_{t \to \infty} t^{-1} \ln \|\mathbb{M}(t)\|, \tag{IV.54}$$

and with $\|(\cdot)\|$ a matrix norm. Whereas the analytical computation of $\lambda_{\max}$ seems out of reach in full generality, the case of a periodic cone sequence yields some simplifications.

Assume for concreteness that the system visits the no-good/no-work shortage region $\mathcal{C}_0$, then hops over to the work shortage region $\mathcal{C}_w$ and ends up in the good/work shortage region $\mathcal{C}_{g,w}$ before going around again. The effective matrix can be written as (assuming

that one starts in $\mathcal{C}_0$ at $t = 0$)

$$\begin{aligned}\mathbb{M}(3T) &= (\mathbb{D}_{g,w}\mathbb{D}_w\mathbb{D}_0)^T \\ \mathbb{M}(3T+1) &= \mathbb{D}_0\,(\mathbb{D}_{g,w}\mathbb{D}_w\mathbb{D}_0)^T \\ \mathbb{M}(3T+2) &= \mathbb{D}_w\mathbb{D}_0\,(\mathbb{D}_{g,w}\mathbb{D}_w\mathbb{D}_0)^T\,,\end{aligned}$$

and the maximal Lyapunov exponent reads

$$\lambda_{\max} = \log\rho\left((\mathbb{D}_{g,w}\mathbb{D}_w\mathbb{D}_0)^{1/3}\right). \tag{IV.55}$$

Note that, by shifting the origin of time, we would have considered cyclic permutations of the matrix $\mathbb{M}(3T)$ in the previous expression, which does not change the eigenvalues. One can therefore study the product $\mathbb{D}_{g,w}\mathbb{D}_w\mathbb{D}_0$ to assess the stability of the system. Figure IV.7 shows four examples of converging dynamics with different cone sequence, one of which involves a product of 44 matrices!

Interestingly, some situations arise where each individual matrix involved in the product is unstable, but the product itself is not. In this situation, the time spent in the cones yielding unstable matrices must be "small" in order for the dynamics to converge, i.e. unstable cones must be very repulsive. The study of the time spent in the cones seems however out of reach for this model, but will be discussed in Part III in the context of random conewise linear systems.

4 Conclusion

In this introductory chapter, we start with a very simple economic model consisting of one firm and one household. The firm produces some good which is sold to the household and, in turn, the household provides manpower to the firm. The equilibrium description of this economy is well known. Equilibrium prices and productions are given by

$$p_{\text{eq}} = \frac{\ell_0^{1-b}}{z}\ ,\ \gamma_{\text{eq}} = \ell_0^b, \tag{IV.56}$$

where $z > 0$ is the productivity factor of the firm, ℓ_0 the equilibrium available workforce and b the return to scale parameter. We see immediately that there is no equivalent to the HS transition in this model, so that equilibrium always exists and is well-defined. We then moved to a dynamical picture by allowing prices, productions etc. to vary and adjust throughout time. We used adjustment rules similar (up to normalization) to the heuristics from Chapter II, but we factored in essential constraints, which were missing from the model of Chapter II. The first constraint was to properly account for imbalances:

- the firm cannot sell more than the available supply (taking possible inventories into account);
- the household cannot work more than the available workforce, or consume more than what is allowed by its budget (we do not consider loans or debts in this model).

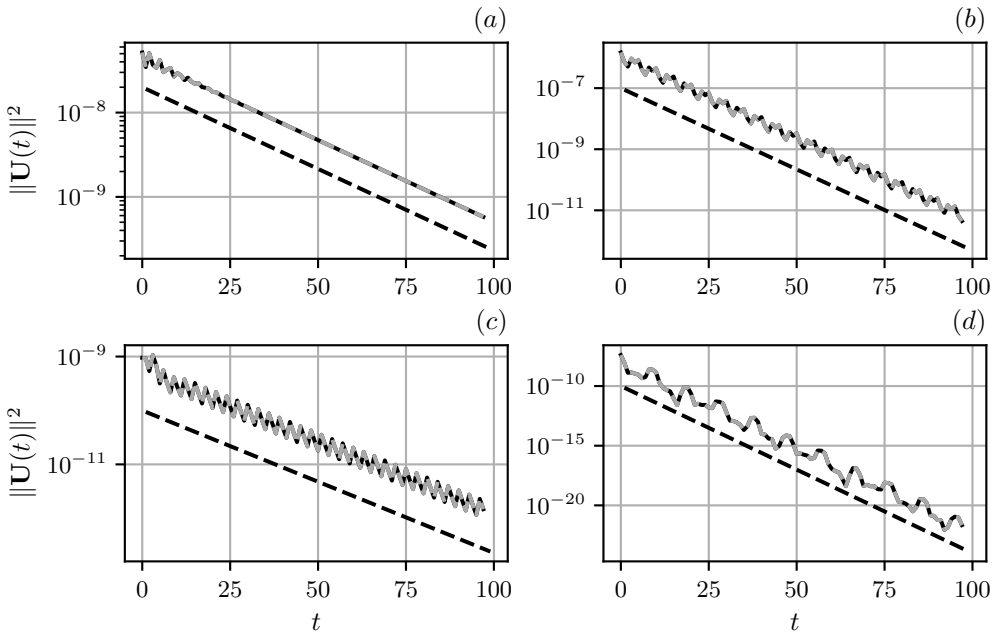


Figure IV.7: Non-linear dynamics close to equilibrium (solid black lines) compared with the associated conewise linear dynamics (dashed gray lines). The dashed black line shows the decay rate predicted by the Lyapunov exponent of the system. (a) Simple case where $\mathcal{C}_0$ is stable and the dynamics is governed solely by $\mathbb{D}_0$. We chose $\alpha = \alpha' = \beta = \beta' = 0.6$, $\omega = 0.5$, $\sigma = \infty$, $z = 1$, $b = 0.95$, $\ell_0 = 2$ and $\varphi = 1$. (b) The effective matrix is given by $\mathbb{M} = (\mathbb{D}_{g,w}\mathbb{D}_{g,b}\mathbb{D}_w)^{1/3}$ and the system loops through the three associated cones. We chose $\alpha = \alpha' = \beta = \beta' = 0.6$, $\omega = 0.2$, $\sigma = \infty$, $z = 1$, $b = 1$, $\ell_0 = 1$ and $\varphi = 1$. (c) The effective matrix is $\mathbb{M} = \left(\mathbb{D}_0^2\mathbb{D}_{g,w}\mathbb{D}_0\mathbb{D}_{g,w}\right)^{1/5}$. We chose $\alpha = 0.66$, $\alpha' = 0.24$, $\beta = 0.9$, $\beta' = 0.9$, $\omega = 0.3$, $\sigma = \infty$, $z = 1$, $b = 1$, $\ell_0 = 1$ and $\varphi = 1$. (d) The effective matrix is $\mathbb{M} = \left(\mathbb{D}_0^4\mathbb{D}_{g,w}^5\mathbb{D}_w\mathbb{D}_{g,b}\mathbb{D}_{g,w}^4\mathbb{D}_0^4\mathbb{D}_w\mathbb{D}_{g,w}^4\mathbb{D}_{g,b}\mathbb{D}_0^3\mathbb{D}_w\mathbb{D}_{g,b}\mathbb{D}_{g,w}^4\mathbb{D}_0^4\mathbb{D}_w\mathbb{D}_{g,b}\mathbb{D}_{g,w}^3\mathbb{D}_g\right)^{1/44}$. We chose $\alpha = 0.66$, $\alpha' = 0.24$, $\beta = 0.9$, $\beta' = 0.9$, $\omega = 0.1$, $\sigma = 0.1$, $z = 1$, $b = 0.95$, $\ell_0 = 2$ and $\varphi = 1$. The initial perturbation is chosen to be an upward perturbation of magnitude $\delta = 10^{-5}$ relative to equilibrium applied on prices, productions and targets for $(a) - (c) - (d)$. For (b), we used a downward (resp. upward) perturbation on prices and productions (resp. targets) of magnitude $\delta = 10^{-5}$.

With these prescriptions, the model is conservative in the sense that no goods nor money are generated without reason. The second constraint was to properly account for causality:

- goods cannot be sold before being produced;
- manpower cannot be used to produce before it is available;
- information cannot be used before being disclosed.

These prescriptions are a bit more subtle to implement in the model. To that effect, we needed to depart from the ODE description of Chapter II. We therefore devised a series of steps that the firm and the household loop over throughout time. This kind of model is generically referred to as *Agent-Based Model* (ABM). The description of the dynamics is given by specific actions taken by different agents (here the firm and the household). In our model, each time step is broken down into three epochs: planning, hiring and producing. During the planning phase, the firm sets out a production target by trying to forecast the amount of goods sold and workforce hired. During the hiring phase, the firm hires workers and pays them. The production phase may then occur since workforce has been provided.

The dynamical model that we obtain can be simulated and yields a rich variety of behaviors. In anticipation with Chapter V, we provided a succinct description of the different phases that can be reached asymptotically by this dynamics. Right away, we observe a clear improvement from the phenomenology of Chapter II: entire regions of parameter space do not allow the dynamics to converge towards competitive equilibrium, even though it is always well-defined. Furthermore, sustained oscillatory patterns (whether they are limit cycles or more chaotic) can be observed.

Finally, a large part of this chapter was devoted to the linear analysis of this ABM. We showed that accounting for imbalances introduced an additional layer of complexity. Close to equilibrium, the evolution of the model is *conewise linear*. We can identify five disjoint cones in state space, each corresponding to a specific economic situation in the model, within which the dynamics is governed by a single stability matrix. However, stability matrices are different across cones. As a consequence, the stability of equilibrium cannot be accounted for by traditional arguments regarding the spectrum of each individual matrices. One needs to understand how regions interact with one another. This conewise dynamics leads to situations where individual matrices can all be unstable but the system still manages to reach equilibrium by rapidly switching from cones to cones. This behavior (along with the sustained oscillations observed in this model) can be a satisfying answer to the "small shocks, large business cycles" puzzle. After an initial perturbation, even though the economy manages to reach back equilibrium, its trajectory visits regions of booms or recessions.

In the next chapter, we will augment this model by considering a network of firms rather that a representative one. On top of the already rich phenomenology reported in this chapter, we will see the effects of the Hawkins-Simons transition on the dynamics.

Key takeaways

- **Agent-Based Models (ABMs)** are models for which actions taken by agents (constitutive entities of the model) are prescribed and looped over throughout time. These models allow for intricate descriptions since agents can all be different from one another (both in their descriptions and actions).
- **Imbalances & causality** are two essential constraints missing from Chapter II. Accounting for them, we needed to (1) depart from the ODE description of Chapter II and resort to Agent Based Modelling, (2) impose by hand constraint factors to prevent creation of goods/money.
- **Asymptotic behaviors** are very rich in this model. From a generic initial condition six different outcomes are possible: collapsing, competitive equilibrium, deflationary/inflationary equilibria, crises and oscillations. Even though equilibrium is always well defined, it is seldom reached in practice.
- **Conewise linear systems** are systems for which the linear stability matrix depends on the region of space. Let $\mathcal{C}_1, \mathcal{C}_2$ be two space-partitioning disjoint cones and $\mathbb{D}_1, \mathbb{D}_2$ two matrices. If

$$\mathbf{U}(t+1) = \mathbb{D}_i \mathbf{U}(t)\,, \quad \mathbf{U}(t) \in \mathcal{C}_i,$$

  then $\mathbf{U}(t)$ follows a conewise linear dynamics. For such systems, the stability of the origin cannot be understood solely by studying the spectrum of each individual $\mathbb{D}_i$.

A Linearization

For a generic variable $x(t)$, with associated equilibrium value $x_{\rm eq} > 0$, we will write the perturbation $\delta x(t)$ around equilibrium as $x(t) = x_{\rm eq} \exp \delta x(t)/x_{\rm eq}$. For quantities with an equilibrium value of zero (such as savings, inventories, production surplus or profits), we will identify said quantity with the associated perturbation, i.e. $x(t) \to \delta x(t)$. When there is no ambiguity, we will drop the time dependency for clarity. Furthermore, we will implicitly consider monetary quantities as being rescaled by wages, which are therefore set to 1. We will finally use the equilibrium relationships

$$\begin{aligned} p_{\rm eq} C_{\rm eq} &= B_{\rm eq} = \ell_{\rm eq} \\ z\gamma_{\rm eq} &= C_{\rm eq} \\ \mu_{\rm eq} &= 1. \end{aligned}$$

A.1 Goods and labor constraints

As we explained in the main section of this chapter, the constraints imposed by imbalances are perfectly satisfied at equilibrium. For instance, since $\mathscr{S}_{\rm eq} = \mathscr{D}_{\rm eq} = z\gamma_{\rm eq}$, we have trivially, $\min(1, \mathscr{S}_{\rm eq}/\mathscr{D}_{\rm eq}) = 1$. Close to equilibrium, we therefore have

$$\min\left(1, \frac{\mathscr{S}}{\mathscr{D}}\right) = 1 + \min\left(0, \frac{\mathscr{E}}{\mathscr{D}}\right) \approx 1 + \min\left(0, \frac{\delta\mathscr{E}}{z\gamma_{\rm eq}}\right).$$

The same holds for labor constraints

$$\min\left(1, \frac{\ell^{\rm s}}{\ell^{\rm d}}\right) \approx 1 + \min\left(0, \frac{\delta\mathscr{E}_0}{\ell_{\rm eq}}\right),$$

and we see that, even at linear level, one still has to take into account the position of the state variables in state space. A similar but more complex condition holds for the budget constraint, and we will detail it in the next section.

A.2 Household

The household sets consumption demand $C^{\rm d}$ and labor supply $\ell^{\rm s}$ by optimizing an expected utility function under expected budget constraint. These two quantities read (see Chapter I)

$$\begin{aligned} C^{\rm d} &= \frac{\ell_0}{\mu p} \\ \ell^{\rm s} &= \ell_0 \mu^{1/\varphi} \\ 1 &= \mu^k + \frac{S}{\ell_0}\mu, \end{aligned}$$

where μ is a Lagrange multiplier that depends on savings S, and where $k = 1 + 1/\varphi$ with φ the Frisch index [81]. One can linearize the last equation to relate the perturbation on μ to that of savings

$$\delta\mu = -\frac{\mu_{\rm eq}}{k\ell_0}\delta S, \tag{IV.57}$$

and revert it back into C^{d} and ℓ^{s}

$$\delta C^{\mathrm{d}} = \frac{C_{\mathrm{eq}}\mu_{\mathrm{eq}}}{k\ell_0}\delta S - \frac{C_{\mathrm{eq}}}{p_{\mathrm{eq}}}\delta p \tag{IV.58}$$

$$\delta \ell^{\mathrm{s}} = -\frac{\ell_{\mathrm{eq}}\mu_{\mathrm{eq}}}{\varphi k\ell_0}\delta S. \tag{IV.59}$$

The firm satisfies the household demand if supply is plentiful. The firm therefore offers a quantity to consume $C_{\mathrm{eq}} \exp \delta C^{\mathrm{o}}/C_{\mathrm{eq}}$, such that

$$\delta C^{\mathrm{o}} = \delta C^{\mathrm{d}} + \frac{C_{\mathrm{eq}}}{z\gamma_{\mathrm{eq}}} \min\left(0, \delta\mathscr{E}\right). \tag{IV.60}$$

In turn, the household is able to consume this quantity if its budget is plentiful. The perturbation on budget reads

$$\delta B = \delta S + \delta\ell = \delta S + \delta\ell^{\mathrm{d}} + \min\left(0, \delta\mathscr{E}_0\right). \tag{IV.61}$$

The budget constraint is satisfied at equilibrium, and we can therefore rewrite it as

$$\min\left(1, \frac{B}{pC^{\mathrm{o}}}\right) \approx 1 + \min\left(0, \frac{\delta B - \delta(pC^{\mathrm{o}})}{p_{\mathrm{eq}}C_{\mathrm{eq}}}\right).$$

The numerator $\delta h = \delta B - \delta(pC^o)$ can be simplified as follows

$$\begin{aligned}
\delta h &= \delta S + \delta\ell^{\mathrm{d}} + \min\left(0, \delta\mathscr{E}_0\right) - p_{\mathrm{eq}}\delta C^{\mathrm{o}} - C_{\mathrm{eq}}\delta p \\
&= \delta S + \delta\ell^{\mathrm{d}} + \min\left(0, \delta\mathscr{E}_0\right) - \frac{p_{\mathrm{eq}}C_{\mathrm{eq}}}{z\gamma_{\mathrm{eq}}} \min\left(0, \delta\mathscr{E}\right) - C_{\mathrm{eq}}\delta p - p_{\mathrm{eq}}\delta C^{\mathrm{d}} \\
&= \delta S + \delta\ell^{\mathrm{d}} + \min\left(0, \delta\mathscr{E}_0\right) - \frac{p_{\mathrm{eq}}C_{\mathrm{eq}}}{z\gamma_{\mathrm{eq}}} \min\left(0, \delta\mathscr{E}\right) - \frac{p_{\mathrm{eq}}C_{\mathrm{eq}}}{k\ell_0}\delta S \\
&= \frac{1}{1+\varphi}\delta S + \delta\ell^{\mathrm{d}} + \min\left(0, \delta\mathscr{E}_0\right) - \frac{p_{\mathrm{eq}}C_{\mathrm{eq}}}{z\gamma_{\mathrm{eq}}} \min\left(0, \delta\mathscr{E}\right) \\
&= -\delta\mathscr{E}_0 + \min\left(0, \delta\mathscr{E}_0\right) - p_{\mathrm{eq}} \min\left(0, \delta\mathscr{E}\right),
\end{aligned}$$

where we used the equilibrium relationships along with the definition of $\delta\ell^{\mathrm{s}}$ and δC^{d}. The perturbation on realized demand can therefore be written as

$$\delta C = \delta C^{\mathrm{d}} + \min\left(0, \delta\mathscr{E}\right) + \frac{C_{\mathrm{eq}}}{B_{\mathrm{eq}}} \min\left(0, \delta h\right), \tag{IV.62}$$

and the household computes its savings for the next period

$$\delta S(t+1) = \delta h(t) - \min\left(0, \delta h\right), \tag{IV.63}$$

where the wage rescaling does not intervene since it would yield a second order perturbation.

A.3 Firms

The firm sets a consumption target by forecasting future profits and production surplus. Both expectations are computed using previous demands and read, close to equilibrium

$$\delta\mathbb{E}_t[\mathscr{E}] = z\delta\gamma(t) + \delta I(t) - \delta C^{\mathrm{d}}(t-1) \tag{IV.64}$$

$$\delta\mathbb{E}_t[\pi] = \delta(p(t)C^{\mathrm{d}}(t-1)) - \delta\ell^{\mathrm{d}}(t-1). \tag{IV.65}$$

The target is set as

$$\delta\widehat{\gamma}(t+1) = \delta\gamma(t) + \beta\frac{\delta\mathbb{E}_t[\pi]}{zp_{\text{eq}}} - \beta'\frac{\delta\mathbb{E}_t[\mathscr{E}]}{z}, \tag{IV.66}$$

and work demands can be computed

$$\delta\ell^{\text{d}}(t) = \frac{\ell_{\text{eq}}}{b\gamma_{\text{eq}}}\delta\widehat{\gamma}(t+1). \tag{IV.67}$$

After hiring the household, the firm can compute real production surplus and profits

$$\delta\mathscr{E} = z\delta\gamma + \delta I - \delta C^{\text{d}} \tag{IV.68}$$

$$\delta\pi = \delta(pC) - \delta\ell. \tag{IV.69}$$

One can expand and rewrite profits so that they read

$$\delta\pi = \delta S - \delta h + \min(0, \delta h). \tag{IV.70}$$

The firm then updates its price for the next period

$$\delta p(t+1) = \delta p(t) - \alpha\frac{p_{\text{eq}}}{z\gamma_{\text{eq}}}\delta\mathscr{E} - \alpha'\frac{1}{z\gamma_{\text{eq}}}\delta\pi + \omega\frac{p_{\text{eq}}}{\ell_{\text{eq}}}\delta\mathscr{E}_0, \tag{IV.71}$$

produces

$$\delta\gamma(t+1) = \delta\widehat{\gamma}(t+1) + b\frac{\gamma_{\text{eq}}}{\ell_{\text{eq}}}\min(0, \delta\mathscr{E}_0), \tag{IV.72}$$

and compiles its inventories

$$\delta I(t+1) = e^{-\sigma}(\delta\mathscr{S} - \delta h) = e^{-\sigma}\left(\delta\mathscr{E} - \min(0, \delta\mathscr{E}) - \frac{C_{\text{eq}}}{B_{\text{eq}}}\min(0, \delta h)\right). \tag{IV.73}$$

A.4 Forecasting and exchanging

We will now summarize the previous relationships into the linear evolution of a vector $\mathbf{U}(t)$. The information-optimal vector (in the sense of the number of variables carried) is

$$\mathbf{U}(t) = \begin{pmatrix} \delta\widehat{\gamma}(t+1) \\ \delta\gamma(t) \\ \delta p(t) \\ \delta I(t) \\ \delta S(t) \\ \delta\widehat{\gamma}(t) \end{pmatrix}. \tag{IV.74}$$

To get to a linear evolution of $\mathbf{U}$, it is easier to break down the period $t \to t+1$ into two linear actions: forecasting and exchanging. The forecasting step sets the target, and the exchanging step updates prices, productions, savings and inventories.

A.4.1 Forecasting

This step implements Eq. (IV.66). We introduce the intermediate vector $\widetilde{\mathbf{U}}$

$$\widetilde{\mathbf{U}}(t) = \begin{pmatrix} \delta\widehat{\gamma}(t) \\ \delta\gamma(t) \\ \delta p(t) \\ \delta I(t) \\ \delta S(t) \\ \delta\widehat{\gamma}(t-1) \\ \delta\gamma(t-1) \\ \delta p(t-1) \\ \delta I(t-1) \\ \delta S(t-1) \end{pmatrix}, \tag{IV.75}$$

and a matrix $\mathbb{F} \in \mathcal{M}_{6,10}(\mathbb{R})$ such that

$$\mathbf{U}(t) = \mathbb{F}\widetilde{\mathbf{U}}(t). \tag{IV.76}$$

The matrix $\mathbb{F}$ has the block form

$$\mathbb{F} = \begin{pmatrix} \mathbb{F}_1 & \mathbb{F}_2 \\ \boldsymbol{\epsilon}_1^\top & 0_5^\top \end{pmatrix}, \tag{IV.77}$$

with $\boldsymbol{\epsilon}_1 = (1,0,0,0,0)^\top \in \mathbb{R}^5$, $0_5 = (0,0,0,0,0)^\top \in \mathbb{R}^5$ and where $\mathbb{F}_{1/2} \in \mathcal{M}_{5,5}(\mathbb{R})$ can be deduced from Eq. (IV.66)

$$\mathbb{F}_1 = \begin{pmatrix} -\frac{\beta}{b} & 1-\beta' & \beta\frac{C_{\text{eq}}}{zp_{\text{eq}}} & -\frac{\beta'}{z} & 0 \\ 0 & 1 & 0 & 0 & 0 \\ 0 & 0 & 1 & 0 & 0 \\ 0 & 0 & 0 & 1 & 0 \\ 0 & 0 & 0 & 0 & 1 \end{pmatrix}, \quad \mathbb{F}_2 = \begin{pmatrix} 0 & 0 & -(\beta'+\beta)\frac{C_{\text{eq}}}{zp_{\text{eq}}} & 0 & (\beta'+\beta)\frac{C_{\text{eq}}}{zk\ell_0} \\ 0 & 0 & 0 & 0 & 0 \\ 0 & 0 & 0 & 0 & 0 \\ 0 & 0 & 0 & 0 & 0 \\ 0 & 0 & 0 & 0 & 0 \end{pmatrix}. \tag{IV.78}$$

One can check that the first line of $\mathbb{F}$ implements Eq. (IV.66) while the other lines ensure the reduction of size going from $\widetilde{\mathbf{U}}$ to $\mathbf{U}$.

A.4.2 Exchanging

Conversely, the exchange phase allows one to go from $\mathbf{U}$ to $\widetilde{\mathbf{U}}$ through a matrix $\mathbb{E}(t) \in \mathcal{M}_{6,10}(\mathbb{R})$ such that

$$\widetilde{\mathbf{U}}(t) = \mathbb{E}(t)\mathbf{U}(t-1) := \begin{pmatrix} \mathbb{S}(t) & 0_5 \\ I_5 - \boldsymbol{\epsilon}_1\boldsymbol{\epsilon}_1^\top & \boldsymbol{\epsilon}_1 \end{pmatrix} \mathbf{U}(t-1), \tag{IV.79}$$

with I_5 the identity matrix in $\mathcal{M}_5(\mathbb{R})$ and $\mathbb{S}(t) \in \mathcal{M}_{5,5}(\mathbb{R})$. This last matrix accounts for Eqs. (IV.73), (IV.71), (IV.72) and (IV.73). The time dependency comes from the fact that the form of the update relationships can vary regarding the position of the state vector $\mathbf{U}(t) \in \mathbb{R}^6$. This point is discussed in details in the main sections of this chapter.

CHAPTER V

Out-of-equilibrium dynamics and excess volatility in firm networks

Abstract

In this chapter, we merge models from Chapter II and Chapter IV, and devise an ABM for interacting firms. We discuss the different steps of the decision process of firms, along with possible generalizations. We then provide a general numerical study of this ABM. We highlight that the model is able to generate spontaneous oscillations of endogenous origin, even if firms are individually trying to reduce imbalances. This provides yet another possible avenue of explanation to the "small shocks, large business cycles" puzzle.

Adapted from: [1] Théo Dessertaine, José Moran, Michael Benzaquen, and Jean-Philippe Bouchaud. *Out-of-equilibrium dynamics and excess volatility in firm networks.* Journal of Economic Dynamics and Control, 138:104362, 2022.

1 A fully consistent approach

In the previous chapter, we devised a model with an already rich phenomenology. Accounting for natural constraints such as causality and imbalances, we saw a clear improvement from the naive model of Chapter II, with the appearance of non-trivial dynamical outcomes such as oscillatory patterns. As we will detail below, these cycles provide another possible explanation to the "small shocks, large business cycles" puzzle. However, in the previous chapter and in contrast with Chapter II, we moved to a representative firm as in [112, Chapter 2]. Consequently, network effects such as the HS transition that we extensively discussed in Chapter II were completely absent from the phenomenology of the previous model. In this chapter, we again adopt a granular description of the firm sector as in Chapter I.

Recall that firms interact through supplier-buyer relationships. The underlying input-output network is a weighted graph: link weights J_{ij} are non zero if j supplies to i, and their magnitude measures the amount of goods j needed by i to produce one unit

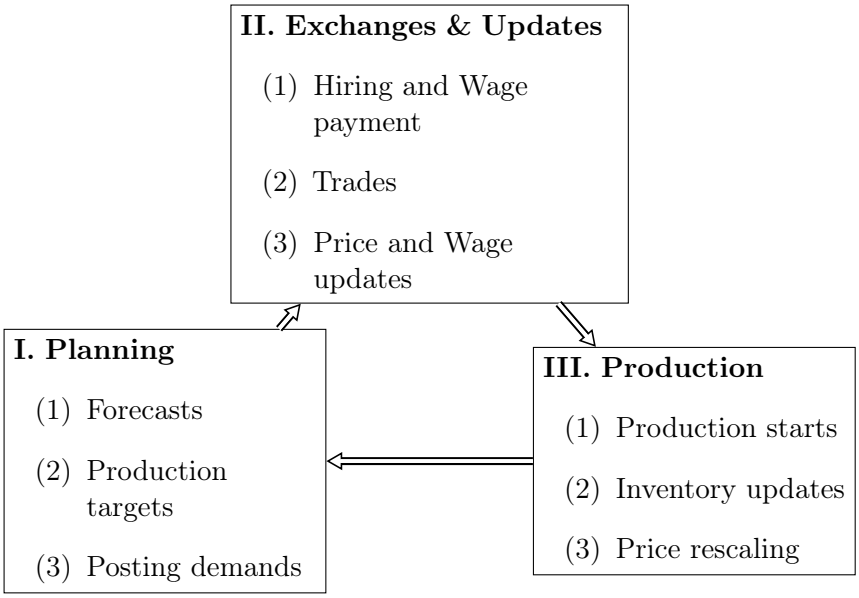


Figure V.1: Time-line of the model.

of good. Conventionally, we denoted by $j = 0$ the household sector and therefore J_{i0} measures the amount of work needed by i to produce. Throughout this chapter, we will use the Leontief production function

$$y_i = z_i \min \left[\min_j \left(\frac{x_{ij}}{J_{ij}} \right), \frac{\ell_i}{J_{i0}} \right]^b, \tag{V.1}$$

with z_i firms' technological productivity factors, x_{ij} the amount of goods exchanged, $\ell_i := x_{i0}$ the amount of manpower provided and b the return to scale parameter. Finally, in Chapter I we also introduced the *network matrix* (or production matrix) $\mathbf{M}$ such that

$$M_{ij} = z_i \delta_{ij} - J_{ij}. \tag{V.2}$$

We recall that the Hawkins-Simons (HS) transition refers to the disappearance of positive equilibrium prices and productions whenever the smallest eigenvalue ε of $\mathbf{M}$ becomes negative. In Chapter II, we related this transition to a critical slow down of the dynamics close to equilibrium: as $\varepsilon \to 0^+$, the economy needed a time inversely proportional to ε to recover from a shock. However, within the framework of Chapter II, we could not obtain any bounded economic trajectory as soon as $\varepsilon < 0$. In this chapter, we will merge the models of Chapter II and Chapter IV and devise an agent-based model over an interacting network of firms.

1.1 Time-line of the model

In order to keep all causal constraints satisfied, one must carefully set up a consistent chronology for the actions of firms and households. The resulting time-line of the model

is schematized in Figure V.1. Each time-step δt ($\delta t = 1$ hereafter) is conveniently sliced in three successive "epochs", represented as boxes in Figure V.1. At the end of time step $t-1$, goods have been produced and are available for consumption at t in quantities $y_i(t)$ and prices $p_i(t)$.

1.1.1 Planning

At any given time, firms must plan how much to produce for the following period. To capture this, we keep exactly the same adjustment rule as in the naive version of our model in Chapter II, Eq. (II.3b), but using now the *expected* profits $\mathbb{E}_t[\pi_i]$ and excess productions $\mathbb{E}_t[\mathscr{E}_i]$ at the end of the period, which we specify below.

Thus, the *target* production for time $t+1$, $\widehat{y}_i(t+1)$, is set using

$$\log\left(\frac{\widehat{y}_i(t+1)}{y_i(t)}\right) = 2\beta\frac{\mathbb{E}_t[\pi_i(t)]}{\mathbb{E}_t[\mathscr{G}_i(t)]+\mathbb{E}_t[\mathscr{L}_i(t)]} - 2\beta'\frac{\mathbb{E}_t[\mathscr{E}_i(t)]}{\mathbb{E}_t[\mathscr{S}_i(t)]+\mathbb{E}_t[\mathscr{D}_i(t)]}, \tag{V.3}$$

where $\mathscr{G}_i(t)$ denotes the proceeds of the sales ("gains"), $\mathscr{L}_i(t)$ the production costs ("losses"), $\mathscr{D}_i(t)$ the overall demand for good i and $\mathscr{S}_i(t)$ the supply of good i, which is already known to the firm at time t, hence $\mathbb{E}_t[\mathscr{S}_i(t)] \equiv \mathscr{S}_i(t)$.

Once the target productions for $t+1$ are decided, the corresponding quantities $\widehat{x}_{ij}$ are computed according to (see Chapter I)

$$\widehat{x}_{ij} = J_{ij}\widehat{\gamma}_i(t+1), \tag{V.4}$$

in the Leontief framework. Firm i then posts its demands x_{ij}^{d} for inputs j for delivery at time t, taking into account their current available stock I_{ij} of said inputs, with the rule

$$x_{ij}^{\mathrm{d}} = \begin{cases} \max\left(0, \widehat{x}_{ij} - I_{ij}\right) & i = 1,\dots,N;\ j = 1,\dots,N \\ \widehat{x}_{i0} & i = 1,\dots,N;\ j = 0. \end{cases} \tag{V.5}$$

Thus, if stocks are plentiful, the firm will prefer drawing from them instead of buying new inputs. Of course one cannot store work, and work demands are equal to their optimal counterpart. In the meantime, households calculate their own consumption target for good i as detailed below, and they also decide, given offered wages, how much labor they are willing to supply, a quantity we call $L^{\mathrm{s}}(t)$ that now may not correspond to full employment (in contrast with Chapter II).

1.1.2 Exchanges & price/wage updates

At this point, firms start hiring workers from the job market, albeit without exceeding the total supply of work L^{s}, i.e.

$$\ell_i(t) = \ell_i^{\mathrm{d}}(t)\min\left(1, \frac{L^{\mathrm{s}}(t)}{L^{\mathrm{d}}(t)}\right); \qquad L^{\mathrm{d}}(t) := \sum_i \ell_i^{\mathrm{d}}(t), \tag{V.6}$$

where ℓ_i is the real amount of work contracted by firm i. Workers are paid the same wage $p_0(t)$ independently of their employer. [1] Conventionally, we prescribe that wages are paid immediately upon hiring – regardless of any technical unemployment in the future caused by shortages of inputs – which allows the household to compute its available budget for the present period:

$$B(t) = S(t) + p_0(t) \sum_i \ell_i(t), \tag{V.7}$$

with $S(t)$ the household's savings. The household's demands for goods $C_i^{\mathrm{d}}(t)$ are computed in section 1.3.

Trading can now start, whereby firms sell their production and buy the goods they need, in a way to satisfy the constraint that the total amount of goods sold cannot exceed production plus inventory, i.e.

$$C_i(t) + \sum_j x_{ji}(t) \leq \mathscr{S}_i(t) := y_i(t) + I_{ii}(t). \tag{V.8}$$

If demand exceeds supply, buyers are satisfied proportionally to their posted demand, and so quantities x that are effectively exchanged are given by

$$x_{ji}(t) = x_{ji}^{\mathrm{d}}(t) \min\left(1, \frac{\mathscr{S}_i(t)}{\mathscr{D}_i(t)}\right); \qquad \mathscr{D}_i(t) := C_i^{\mathrm{d}}(t) + \sum_j x_{ji}^{\mathrm{d}}(t), \tag{V.9}$$

where $\mathscr{D}_i(t)$ is the total demand for good i at time t. The equation for $C_i(t)$ is slightly more convoluted because we do not give households access to debt, see Eq. (V.33) below.

At this point, firms have an exact knowledge of their earnings and expenses. Their profit at round t may now be computed

$$\pi_i(t) = p_i(t) \left(\sum_j x_{ji}(t) + C_i(t) \right) - \left(\sum_j p_j(t) x_{ij}(t) + p_0(t) \ell_i(t) \right) := \mathscr{G}_i(t) - \mathscr{L}_i(t), \tag{V.10}$$

and they also know how much excess supply or demand they actually registered

$$\mathscr{E}_i(t) = \mathscr{S}_i(t) - \mathscr{D}_i(t). \tag{V.11}$$

Realized profits and supply/demand imbalances then generate price updates. We describe them exactly as in Eq. (II.3a) from Chapter II, which now reads

$$\log\left(\frac{p_i(t+1)}{p_i(t)}\right) = -2\alpha \frac{\mathscr{E}_i(t)}{\mathscr{S}_i(t) + \mathscr{D}_i(t)} - 2\alpha' \frac{\pi_i(t)}{\mathscr{G}_i(t) + \mathscr{L}_i(t)}, \tag{V.12}$$

and where all quantities are now known. [2]

[1] Extending the model to firm-dependent wages would be interesting but requires one to move beyond a representative agent description of the household sector.

[2] Since markets do not clear and profits are non zero, we choose symmetric normalization factors involving the average of supply and demand for the first term, and the average of sales and costs for the second.

Prices are updated due to tension between supply and demand, which is in our framework a natural channel for inflation or deflation. By the same token, tensions on the job market are bound to lead to wage updates, which we postulate to be of the same form as for price updates, namely

$$\log\left(\frac{p_0(t+1)}{p_0(t)}\right) = 2\omega\,\frac{L^{\mathrm{d}}(t) - L^{\mathrm{s}}(t)}{L^{\mathrm{d}}(t) + L^{\mathrm{s}}(t)}, \tag{V.13}$$

meaning that excess demand of labor increases wages, and vice-versa. This rule implements a Phillips curve at each time step (see [89] and [116]). One could also use an asymmetric update rule, accounting for the fact that lowering nominal wages is more difficult than raising them. Finally, one could also consider adding a direct coupling between the inflation of the price of goods and wages, as an extra term in the right hand side of Eq. (V.13).

1.1.3 Production

The last epoch corresponds to the start of production. Firm i uses the workforce ℓ_i, along with available quantities x^{a}_{ij} that depend on exchanges x, optimal inputs $\widehat{x}$ and inventories I, as

$$x^{\mathrm{a}}_{ij}(t) = x_{ij}(t) + \min\left(I_{ij}, \widehat{x}_{ij}\right). \tag{V.14}$$

Indeed, if the inventory I allows to provide for optimal input $\widehat{x}$, then no demand is posted (see Eq. (V.5)): $x = 0$ and $x^{\mathrm{a}} = \widehat{x}$. Otherwise, the firm acquired a quantity x that now adds to available stocks, and so $x^{\mathrm{a}} = x + I \leq \widehat{x}$. Note that labor cannot be stored, and therefore $I_{i0} = 0$ at all times.

Now that all of the available inputs x^{a}_{ij} and labor ℓ_i are known, the outputs are determined by the firms' production functions, which in the Leontief case with $b = 1$ entails:

$$y_i(t+1) = z_i(t)\min\left[\min_j\left(\frac{x^{\mathrm{a}}_{ij}(t)}{J_{ij}}\right), \frac{\ell_i(t)}{J_{i0}}\right]. \tag{V.15}$$

The firms' inventories of their own production is also updated, as

$$I_{ii}(t+1) = e^{-\sigma_i}\left(y_i(t) + I_{ii}(t) - \sum_j x_{ji}(t)\right), \tag{V.16}$$

where the decay factor σ_i measures the perishability of good i. For durable goods, $\sigma_i \ll 1$ and $e^{-\sigma_i} \approx 1$, whereas $\sigma_i \gg 1$ and $e^{-\sigma_i} \ll 1$ for perishable goods.

Furthermore, in the Leontief framework total production is limited by the scarcest input, which is therefore depleted during production, leaving a fraction of the other inputs unused. We denote by

$$j^\star(i) = \arg\min_j\left(\frac{x^{\mathrm{a}}_{ij}}{J_{ij}}\right),$$

so that we can write the fraction of inputs $k \neq j^\star(i)$ effectively used as

$$x^{\mathrm{u}}_{ik}(t) = \frac{J_{ik}}{J_{ij^\star(i)}} x^{\mathrm{a}}_{ij^\star(i)}. \tag{V.17}$$

The unused inputs add to firm inventories, and their update may be written using Eq. (V.14), as

$$I_{ik}(t+1) = e^{-\sigma_k} \left(x^{\mathrm{a}}_{ik} - x^{\mathrm{u}}_{ik} \right). \tag{V.18}$$

Finally, for numerical purposes, it is convenient to rescale new prices $p_i(t+1)$ by the new wage $p_0(t+1)$ to avoid exponential growth (or decay) of prices induced by inflation (or deflation), effectively measuring prices in units of wages. We therefore set: [3]

$$p_i(t+1) \longrightarrow \frac{p_i(t+1)}{p_0(t+1)}; \qquad p_0(t+1) \longrightarrow 1. \tag{V.19}$$

This concludes the third and last epoch of the time step. The process is then repeated at time $t+1$, with productions $y_i(t+1)$ and prices $p_i(t+1)$.

To close the model, we now need to specify how firms estimate their future profits/losses and excess/deficit production. The behavior of households must also be spelled out, to allow for the determination of the demand of goods and the supply of labor.

1.2 Expected profits and imbalances

We may write the expected profit of firm i as

$$\mathbb{E}_t[\pi_i] = p_i(t) \left(\sum_j \mathbb{E}_t[x_{ji}] + \mathbb{E}_t[C_i] \right) - \left(\sum_j p_j(t) \mathbb{E}_t[x_{ij}] + p_0(t) \mathbb{E}_t[\ell_i] \right), \tag{V.20}$$

showing that in the planning phase firms must estimate future goods and labor demand, which we will denote generically as $\mathbb{E}_t[x]$. Similarly, the expected excess production is also a function of $\mathbb{E}_t[x]$:

$$\mathbb{E}_t[\mathscr{E}_i] = y_i(t) + I_{ii}(t) - \sum_j \mathbb{E}_t[x_{ji}] - \mathbb{E}_t[C_i]. \tag{V.21}$$

The simplest assumption we can adopt is that firms are "sticky", and estimate all future demands to be equal to their last observation (which follows the rationale that firms produce in order to meet total demand), i.e.

$$\mathbb{E}_t[x] = x^{\mathrm{d}}(t-1). \tag{V.22}$$

However, some immediate generalizations come to mind. For example, firms may also factor in *realized* quantities $x(t-1)$ in their estimate, and set as a learning rule

$$\mathbb{E}_t[x] = \lambda x^{\mathrm{d}}(t-1) + (1-\lambda) x(t-1), \tag{V.23}$$

[3] Note that profits and savings should also be appropriately rescaled, when necessary, e.g. $S(t+1) \to S(t+1)/p_0(t+1)$, etc.

where $\lambda \in [0,1]$ is a parameter interpolating between the two behaviors. Our "sticky" assumption that will be used henceforth thus corresponds to $\lambda = 1$.

Another possible generalization is that firms use a more sophisticated learning rule that allows them to estimate $\mathbb{E}_t[x]$ using time-series analysis, the simplest of which is "constant gain learning" (equivalent to computing the exponential moving average) of past realized demands. This is similar to the AR1 estimation of economic growth used by the agents of [65] in their decision-making process. Trend-following, extrapolative rules may also be considered.

1.3 Household demand and labor

1.3.1 Work-elastic households

As in standard macroeconomic models, we assume that households are represented by a single representative agent with a certain disutility for work, who seeks to maximize the following utility function [4]

$$\mathcal{U}(t) = \sum_j \theta_j \log C_j(t) - \frac{\Gamma}{1+\varphi}\left(\frac{L(t)}{L_0}\right)^{1+\varphi}, \tag{V.24}$$

where $L(t) = \sum_j \ell_j(t) := \sum_j x_{j0}(t)$ is the total amount of work provided by the representative household. The so called Frisch elasticity index φ, after the eponymous author of [81], gives a measure of the convexity of the disutility of work, L_0 is the scale of the amount of work that the household is able to provide and Γ is a parameter that can be set to unity without loss of generality. In the limit $\varphi \to \infty$, households are indifferent to the amount of work provided $L(t) < L_0$, but refuse to work more than L_0. With an utility function of this form, the household may then compute its optimal demand for good i, $C_i^{\mathrm{d}}(t)$ which it will set as a consumption target for period t, and the optimal amount of labor $L^{\mathrm{s}}(t)$ it is willing to provide to firms.

1.3.2 The optimization sequence

To compute the aforementioned quantities, the household needs to know its current savings $S(t)$ and anticipate its income for the next period. The expected utility is estimated with optimistic forecasts (i.e. consumption demand will be met and offered labor will be fully utilized). Wage $p_0(t)$ and prices $p_i(t)$, on the other hand, are all known before the "Exchange and Update" stage, see Section 1.1.2. Hence,

$$\mathbb{E}_t[\mathcal{U}] = \sum_i \theta_i \log C_i^{\mathrm{d}}(t) - \frac{1}{1+\varphi}\left(\frac{L^{\mathrm{s}}(t)}{L_0}\right)^{1+\varphi}, \tag{V.25}$$

[4] We restrict to a "myopic" optimization here, that does not take into account the long-term forecasts and desires of the household. Inter-temporal effects would require to add interest rates, which we completely disregard in the present study.

with an expected budget constraint that reads

$$\sum_i p_i(t) C_i^{\mathrm{d}}(t) = p_0(t) L^{\mathrm{s}}(t) + S(t) := \mathbb{E}_t[B], \tag{V.26}$$

where $\mathbb{E}_t[B]$ is the expected (or in fact hoped for!) budget. For convenience, we denote as $W_0(t) = p_0(t) L_0$ the wage associated to L_0 work-hours.

The household optimizes its expected utility while enforcing the budget constraint using a Lagrange multiplier $\mu(t)/W_0$, so that [5]

$$C_i^{\mathrm{d}}(t) = L_0 \frac{\theta_i}{\mu(t)} \frac{p_0(t)}{p_i(t)} \tag{V.28a}$$

$$L^{\mathrm{s}}(t) = L_0 \, \mu(t)^{1/\varphi}. \tag{V.28b}$$

In order to find $\mu(t)$, one must enforce Eq. (V.26). We find the following equation on $\mu(t)$:

$$\mu^k(t) + \frac{S(t)}{W_0(t)} \mu(t) = \bar{\theta}, \tag{V.29}$$

with $k = 1 + 1/\varphi$ and $\bar{\theta} = \sum_i \theta_i$. For instance, if $\varphi = \infty$ (constant work offer $L^{\mathrm{s}}(t) = L_0$), we have

$$\mu(t) = \frac{\bar{\theta} W_0(t)}{W_0(t) + S(t)}. \tag{V.30}$$

When $\varphi = 1$ (a common value found in the literature and corresponding to a quadratic work-disutility), we have

$$\mu(t) = \frac{1}{2W_0(t)} \left(\sqrt{S(t)^2 + 4\bar{\theta} W_0(t)^2} - S(t) \right). \tag{V.31}$$

Note, interestingly, that high savings lead to reduced labor supply. Also, because of possible involuntary unemployment, the household may want to consume more than it is able to spend when $L^{\mathrm{d}}(t) < L^{\mathrm{s}}(t)$.

A final word on the scaling behavior of these quantities with N is in order. For large N we expect that the size of the household sector will also be of order N. Noting that $\bar{\theta}$ is also of order N, one finds the following coherent scaling laws if we choose $L_0 \sim \sqrt{N}$:

$$\mu \sim \sqrt{N}; \qquad L^{\mathrm{s}} \sim N; \qquad C_i^{\mathrm{d}}(t) \sim 1, \tag{V.32}$$

meaning that total work-hours and total consumption are proportional to the size of the population, as it should be.

[5] Although not necessary for the present model, it is important to allow for confidence effects, which can lead to endogenous crises (see e.g. [67]). One possibility is to couple the consumption propensity to the unemployment level, taken as a proxy of consumer confidence, i.e.:

$$\log\left(\frac{\theta_i(t)}{\theta_i^0}\right) = 2\omega' \frac{L^{\mathrm{d}}(t) - L^{\mathrm{s}}(t)}{L^{\mathrm{d}}(t) + L^{\mathrm{s}}(t)}, \tag{V.27}$$

where θ_i^0 are the baseline values for consumption preferences. In the following, we will fix $\omega' = \omega$.

1.3.3 Savings update

Because we do not allow households to borrow in the present version of the model, real consumption must be adjusted in the case of partial unemployment. In this case, the available budget is necessarily smaller than what was hoped, leading to a realized consumption:

$$C_i^{\mathrm{r}}(t) = C_i(t) \min\left(1, \frac{B(t)}{\sum_j p_j(t) C_j(t)}\right); \qquad C_i(t) = C_i^{\mathrm{d}}(t) \min\left(1, \frac{\mathscr{S}_i(t)}{\mathscr{D}_i(t)}\right), \tag{V.33}$$

with $B(t)$ their available budget computed in Eq. (V.7) . The difference between $C_i(t)$ and $C_i^{\mathrm{r}}(t)$, if positive, is added to the inventory $I_{ii}(t)$ of firm i. The households' savings are then updated as:

$$S(t+1) = B(t) - \sum_i p_i(t) C_i^{\mathrm{r}}(t). \tag{V.34}$$

1.4 Discussion

The above steps look rather tedious and considerably more complex than the simple logic behind the model of Chapter II. Nonetheless, they are quite natural when one decomposes all the stages of a real production process. But more importantly, we have found that short-circuiting any of these steps leads to inconsistent dynamics with spurious instabilities, reflecting that natural constraints are in fact violated. Furthermore, the approach of behavior modelling as a series of actions or sequence of events is a typical feature of ABMs, where the ordering of these events is done in a coherent way as to ensure causality.

An important difference with the naive version of Chapter II is the large number of update rules that necessarily involve cusps, such as those involving taking the maximum or minimum of two expressions, see section 2.2 below. Furthermore, the number of thumb rules used by firms and households to aid their decision has increased, and so has the number of parameters that are needed to describe a given instance of our toy economy.

Therefore, and in spite of the fact that the naive model allows a fair understanding of certain regions of the parameter-space of the full model, we cannot reasonably attempt an exhaustive description using analytical tools only. We therefore resort to a numerical exploration of its properties. We also provide open access to a simulation tool [5] that allows the reader to explore different configurations here: `https://yakari.polytechnique.fr/dash`.

2 A numerical study

The following section is a numerical investigation of the very rich phenomenology of the above model, supplemented with some analytical results when possible. Because of the relatively large number of parameters, we only investigate here some specific "cuts" in

parameter space, but we believe that these cuts are representative of all the possible dynamical classes that the model can generate.

To facilitate reading this section, we will first recall the different parameters that can be adjusted. We will then explore the different types of dynamical trajectories that can be observed in our toy economy, and classify them into different "phases". This idea comes from physics, where the macroscopic properties of a system can be split into different parameter regions where its aggregate behavior is qualitatively the same. These regions only depend on the values taken by a handful of parameters that describe the system; an eloquent example is that of water, which depending on the pressure or temperature can be in either the liquid, solid or gas phase.

We will therefore present the following "phase diagrams" that summarize the influence of the parameters on the broad dynamical behavior of our model, an idea that was already advocated for economic Agent-Based Modelling in [61].

2.1 Summary of parameters

The different parameters introduced in the previous sections may be split into two categories: static parameters, describing the production network and the production function, and dynamic parameters, describing the evolution of prices, labor and outputs. We provide an overview of them along with typical values we assign to them in our simulations below.

Static parameters

1. Number of firms N – here $N = 100$.

2. Type of network – here a random regular directed network, see [97, 117], where each firm has the same number of clients and suppliers $d = 15$.

3. Constant Elasticity of Substitution production function – here a Leontief production function ($q = 0^+$) with a return to scale parameter $b = 0.95$. [6]

4. The smallest eigenvalue ε of the network matrix $\mathbf{M}$, which for large values corresponds to a stable economy.

5. Firm inter-linkages J_{ij}, which we take to be 1 when firms i and j are linked and 0 otherwise.

6. Firm productivity factors z_i, first set to 1 and then adapted to adjust ε to take the required value. [7]

[6] Choosing b slightly below unity helps stabilizing the dynamics and also prevents the relaxation time from diverging as the smallest eigenvalue of the production matrix $\varepsilon \to 0$. Arguments to this effect are detailed in Chapter I.

[7] Modifying the productivity factors as $z' = z + \varepsilon - \min \mathrm{Sp}\,(\mathbf{M})$ makes the minimum eigenvalue of $\mathbf{M}$ equal to ε.

7. Baseline household consumption preferences θ_i^0, modeled by IID uniform random variables rescaled to have $\sum_i \theta_i^0 = 1$.

8. Work disutility Frisch index, set to $\varphi = 1$ (quadratic disutility of labor) and scale of workforce set to $L_0 = 1$.

9. The behavioral extrapolation parameter λ, defined in Eq. (V.23), is set to 1.

Note that we shall also simulate our model on more realistic models of firm networks, including actual input-output networks constructed from the FACTSET database [76], see Section 3.

Dynamic parameters

1. Parameters describing restoring forces: $\alpha, \alpha', \beta, \beta'$, (see Eqs. (V.3)-(V.12)). We restrict ourselves to the case $\beta' = \alpha' = \beta = \alpha$ and scan for varying values of α.

2. Phillips curve parameter ω, relating wages to tensions in the job market (see Eq. (V.13)).

3. Confidence parameter, relating consumption propensities to unemployment: ω' (see Eq. (V.27)). For this study, we take $\omega' = \omega$.

4. Perishability parameters σ_i describing the speed of decay of good i, all taken as $\sigma_i = \sigma$ except when otherwise indicated.

These choices therefore reduce the number of parameters to explore to four: ε (network stability), α (strength of restoring forces), ω (Phillips curve parameter) and σ (perishability). We will now show how varying them may lead to a very rich phenomenology.

2.2 Perturbations around equilibrium and cone-wise linear dynamics

Similarly to what was presented in Chapter IV, the cusps of the full model, imply that perturbative analysis produces at best piecewise-linear equations. [8]

To be precise, let us attempt to linearize the different update rules by writing $\delta x(t) = x(t) - x_{\text{eq}}$ for the perturbed value of any quantity x and expanding the different equations to lowest order in $\delta(\cdot)$. When applied to the flows of goods x_{ji} one gets:

$$\delta x_{ji}(t) = \delta x_{ji}^{\text{d}}(t) + \frac{x_{eq,ji}}{z_i \gamma_{\text{eq},i}} \min\left(0, \delta \mathscr{S}_i(t) - \delta \mathscr{D}_i(t)\right). \tag{V.35}$$

Depending on the sign of $\delta \mathscr{S}_i(t) - \delta \mathscr{D}_i(t)$, the flow of exchanged goods is characterized by two different linear equations, rendering the system piecewise-linear. The same feature also holds for exchanged work (replacing $\delta \mathscr{S}_i(t) - \delta \mathscr{D}_i(t)$ by $\delta L^{\text{s}}(t) - \delta L^{\text{d}}(t)$) and realized

[8] This, as the general time-line framework outlined in Section 1.1, is a feature common to other ABMs, such as Mark-0 [61], or the ABM recently developed in [118].

consumption (where the switch depends on $\delta\mathscr{S}_i(t) - \delta\mathscr{D}_i(t)$ as well as on the budget constraint, which is more cumbersome to write, see Eq. (V.33)). These non-vanishing cusps mean, perhaps surprisingly, that there does not exist a limiting case where the full model would boil down to the "naive" model of Chapter II.

Linearizing around equilibrium yields piecewise-linear dynamics that can be described by the evolution of a $(N^2 + 4N + 1)$-dimensional state vector that we denote by $\mathbf{U}(t)$. This vector encodes perturbations on stocks $\delta I_{ij}(t)$ (stacking the columns of the $N \times N$ stocks-matrix in an N^2-dimensional vector), current production targets $\delta\widehat{\gamma}_i(t+1)$, past targets $\delta\widehat{\gamma}_i(t)$, production levels $\delta\gamma_i(t)$, prices $\delta p_i(t)$, and finally household's savings $\delta S(t)$. A detail account of the linearization procedure is given in Appendix A.

In Appendix A, we also provide a characterization of the different regions of space over which the dynamics is linear. In this paragraph, we will disregard the piece-wise effects coming from the budget shortage condition for clarity purposes, and focus exclusively on work/good shortages. See however Appendix B for a detailed account. To study possible switches in the conditions defining regions of plentiful/shortage of goods and work, let us define two vectors $\mathbf{c}_{g,i}$ and $\mathbf{c}_w$ such that

$$\mathbf{c}_{g,i}^\top \mathbf{U}(t) = \delta\mathscr{S}_i(t) - \delta\mathscr{D}_i(t), \quad \mathbf{c}_w^\top \mathbf{U}(t) = \delta L^{\mathrm{s}}(t) - \delta L^{\mathrm{d}}(t). \tag{V.36}$$

Each vector defines a hyperplane $\mathcal{C}_i = \{\mathbf{c}_{g,i}\}^\perp$ (resp. $\mathcal{C}_w = \{\mathbf{c}_w\}^\perp$) separating state space into two regions:

- the no shortage region for i, $\mathcal{C}_i^+$ (resp. $\mathcal{C}_w^+$) where $\mathbf{c}_{g,i}^\top \mathbf{U}(t) > 0$ (resp. $\mathbf{c}_w^\top \mathbf{U}(t) > 0$) where i's supply is enough to cope with demand (resp. work offer is enough to cope with work demands);
- the shortage region for i, $\mathcal{C}_i^-$ (resp. $\mathcal{C}_w^-$) where $\mathbf{c}_{g,i}^\top \mathbf{U}(t) < 0$ (resp. $\mathbf{c}_w^\top \mathbf{U}(t) < 0$) where i's supply is not enough to cope with demand (resp. work offer is not enough to cope with work demands).

The intersection of these half-spaces defines regions of space called *cones* in which the linearized dynamics is fully characterized by a single stability matrix. Calling $S \subseteq [\![1, N]\!]$, the set of firms with a shortage of goods, we define stability matrices in each cone as follows

$$\begin{aligned}
\mathbf{U}(t) \in \bigcap_{s\in S} \mathcal{C}_s^- \cap \bigcap_{s'\in[\![1,N]\!]\setminus S} \mathcal{C}_{s'}^+ \cap \mathcal{C}_w^+ &\iff \mathbf{U}(t+1) = \mathbb{D}_S \mathbf{U}(t), \\
\mathbf{U}(t) \in \bigcap_{s\in S} \mathcal{C}_s^- \cap \bigcap_{s'\in[\![1,N]\!]\setminus S} \mathcal{C}_{s'}^+ \cap \mathcal{C}_w^- &\iff \mathbf{U}(t+1) = \mathbb{D}_{S,w} \mathbf{U}(t).
\end{aligned} \tag{V.37}$$

If $S = \emptyset$ (no shortages), we call $\mathbb{D}_0$ and $\mathbb{D}_{0,w}$ the stability matrices without/with work shortage; and if $S = [\![1, N]\!]$ (all firms have shortages), we call them $\mathbb{D}_N$ and $\mathbb{D}_{N,w}$. Figure V.2 illustrates the previous construction in a schematic 2-dimensional space.

Although the dynamics inside each cone is linear, knowledge of the eigenvalues of the stability matrices is in general not sufficient to conclude on the stability of the entire system. Indeed, knowing whether a cone is preserved or not by its stability matrix is

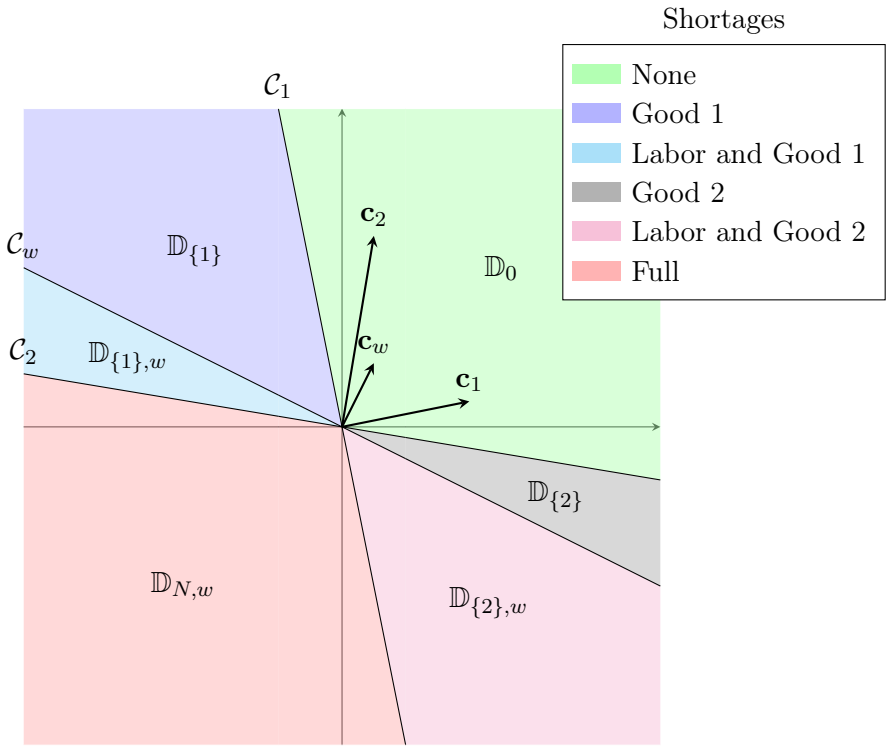


Figure V.2: Example of the cone-separation for a schematic two dimensional space. Solid black lines represent the hyperplanes $\mathcal{C}_{1,2,w}$ separating shortage/no-shortage cones, they are orthogonal to cone vectors $\mathbf{c}_{g,1,2}, \mathbf{c}_w$. Shaded areas represent the different cones of possible shortages along with the associated stability matrices. Note that for the given configuration of vectors, the matrices $\mathbb{D}_N$ and $\mathbb{D}_{0,w}$ cannot exist.

essential to understand the dynamics. If the linear dynamics corresponding to the stability matrix inside a cone preserves it, meaning that any trajectory starting in the cone will always be contained within it, the dynamics becomes trivial. On the other hand when this is not the case, a trajectory may switch back and forth between different cones, and it will therefore be described by a product of stability matrices. It is said product that one most study in order to conclude on the overall stability of the system. This can lead to quite complicated trajectories, where for example two different cones have stability matrices that are such that a trajectory starting in one inevitably ends up in the other and vice versa, leading to a pseudo-oscillation that can be stable in the long run. To our knowledge, the mathematical tools needed to account for these interesting cone-wise linear dynamics are not available in the general case.

2.3 Phase diagrams and dynamical classes

For each set of values of the parameters (α, ω, σ, ε), we start from a random perturbation about equilibrium of relative magnitude $\delta = 10^{-3}$, taking e.g. $p_i(t) = p_{\mathrm{eq},i}(1 + \delta u)$ with u

uniform in $[-1, 1]$. [9] We then run the dynamics for $T = 20000$ time-steps and consider only the last 2500 to classify the trajectory into one of several classes that are detailed below.

The trajectories we will use to classify the behavior of our model are those of relative price differences $\overline{\delta p}(t) := p(t)/p_{\mathrm{eq},i} - 1$. [10] In order to provide more vivid illustrations of some of these dynamical types, we have made firms slightly heterogeneous in their values of the parameters α and σ. In the figure captions below, the notation $\alpha, \sigma \in [A, B]$ means that these quantities are chosen uniformly in $[A, B]$, independently for each firm. Finally, for all price trajectories reported below, we highlight one firm at random to make the time-series more readable.

In general, we observe five classes of behavior (or "phases"): convergence towards the competitive equilibrium, convergence towards deflationary equilibria, crises, business-cycle like oscillations or chaotic oscillations and economic collapse, where the economy crashes after a finite number of time steps. Different phase diagrams corresponding to this classification can be seen in Figure V.3 with ε in $[100, 1, 0, 01, -5]$, and the study and description of these phases is detailed in the sections below.

Note that the boundaries of the phase diagrams depend on the network of interactions, especially as $\varepsilon \to 0$. If $\varepsilon \gg 1$, then productivity factors are very large, and network effects can safely be neglected. However, as $\varepsilon \to 0$, these network effects become more and more important and the specific type of network will play a role. The regular network chosen in this section is thus only meant to illustrate the different *classes* of dynamical trajectories that can be generated by the model. But such classes are in fact generic and appear for a broad family of networks, and are a consequence of the non-linear update rules followed by firms.

Before delving into the description of each of these classes, we note in particular that (see Figure V.3):

- All the different classes appear for values of parameters α, ω, σ, ε of order unity, meaning that interesting dynamical behavior do not require uncanny values of the parameters.

- The region where the competitive equilibrium is reached shrinks as the economy approaches the instability $\varepsilon \to 0$ from above. When $\varepsilon < 0$, there is no admissible equilibrium and only deflationary equilibria or cycles/chaos can be attained.

- For a fixed perishability σ one observes the following succession of phases as the restoring parameter α is increased: collapse when α is too small, followed by deflationary equilibria, then competitive equilibrium and finally cycles and chaos for large α, corresponding to firms that overreact to imbalances.

[9] When $\varepsilon < 0$ and no competitive equilibrium can be defined, we start from random initial conditions between 1 and 2 for prices and productions.

[10] The trajectories of produced quantities are qualitatively similar within each phase, except that, as expected, high prices correspond to production troughs, and vice versa.

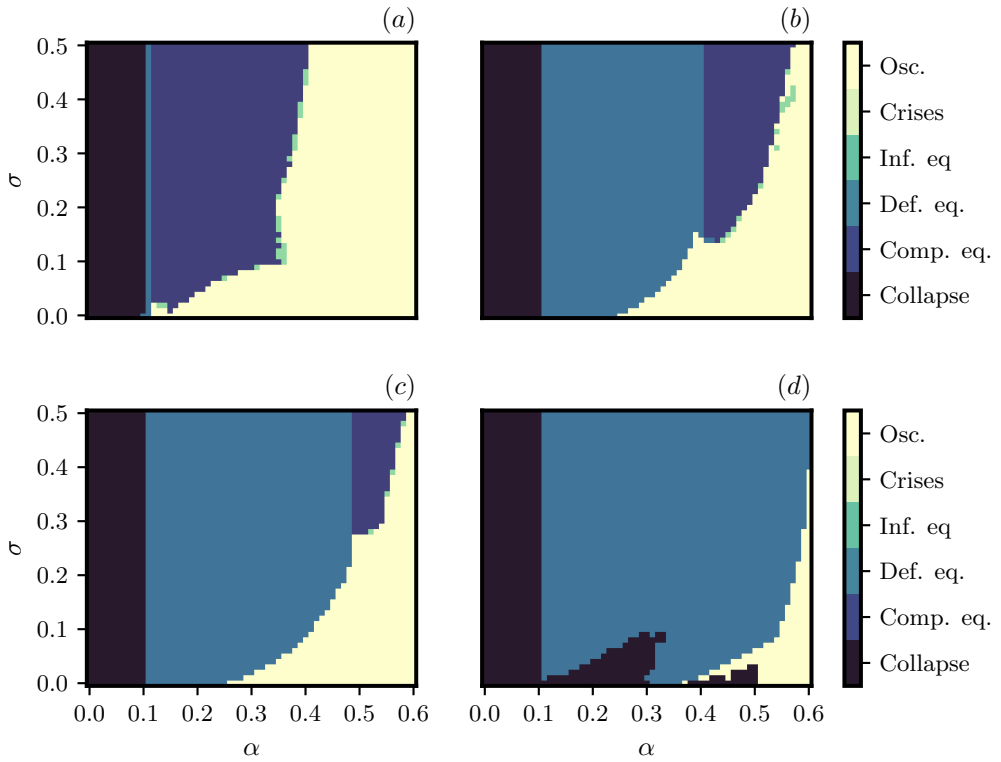


Figure V.3: Phase diagrams in the plane restoring forces, perishability (i.e. (α, σ)), all for the same network economy, $\omega = 0.1$ and different values of ε: (a) $\varepsilon = 100$, (b) $\varepsilon = 1$, (c) $\varepsilon = 0.01$, (d) $\varepsilon = -5$. The color code is explained in the legends. The region where the competitive equilibrium state is stable shrinks when ε decreases, and disappears when $\varepsilon < 0$ as deflationary equilibria and cycles/chaos take over. One also observes large regions with cycles/chaos, and crises when $\varepsilon > 0$. Finally, when restoring forces are to0 weak (small α) the economy crashes.

- At the boundary between competitive equilibrium and cycles and chaos, one observes intermittent crises, similar to the ones described in [61, 62] – see below.

2.3.1 Economic collapse

Starting from $\alpha = 0$ and increasing its value, the model finds itself in a collapse phase first, where prices diverge exponentially and productions plummet to zero. As α grows we reach a critical value α_c corresponding to a transition from the collapse phase to one where the economy is able to stabilize (either in a deflationary or competitive equilibrium).

This transition, which can be observed in Figure V.3, appears to be independent of both ε and σ. The fact that α_c is independent of ε means that the economy collapses when prices are too slow to adjust, regardless of the nature of the firm network. The

exact value of α_c in Figure V.3 can be computed to be:

$$\alpha_c = \omega \frac{\beta'}{\beta} \tag{V.38}$$

(i.e. $\alpha_c = \omega$ whenever $\alpha = \alpha' = \beta = \beta'$), where ω is the Phillips curve parameter relating wages to unemployment (see Eq. (V.13)).

This value is obtained by diagonalizing the stability matrix of the system $\mathbb{D}_0$ in the no shortage cone $\delta\mathscr{S}_i(t) - \delta\mathscr{D}_i(t) > 0$ for all firms i (see Section 2.2), which happens to be stable under the quasi-linear dynamics. The computation is detailed in Appendix C and Appendix D.

This collapse transition may also be observed along the diagonal $\omega = \alpha$ of the plots in Figure V.11 below, as well as along the parabola on Figure V.13. (Note however that an additional wedge where the economy diverges appears for small ω which will be discussed in Section 2.7.2.)

2.3.2 Competitive equilibrium

The most natural behavior one could expect is for the economy to converge to a competitive equilibrium, where all profits are zero and markets clear, as classically assumed in economics models. This is indeed what happens, but, interestingly, it requires α to be neither too small, nor too large, i.e. when restoring forces are strong enough to stabilize the system but not too strong to avoid overshoots and the corresponding impossibility for the economy to coordinate. Perishability σ should also be large enough, see Figure V.3. Finally, as returns to scale diminish (i.e. as the parameter b decreases), the region where competitive equilibrium can be attained becomes more extended (see Figure V.5 below).

In order to give some economic meaning to the phase where competitive equilibrium is reached, let us focus on the case $\varepsilon = 1$, i.e. a firm network of moderate average productivity, relatively far from the Hawkins-Simons instability. Choosing the unit time scale of the model to be a quarter (3 months, a reasonable period for firms to adjust prices and production). Competitive equilibrium cannot be reached when $\alpha < \alpha_d(\varepsilon = 1) \approx 0.395$. Such a value of α means that a firm facing a production imbalance of say 10% will decrease – say – prices by $e^{-0.395\times 10\%} \approx 3.8\%$ over the next quarter. Attempting to reduce it much faster leads to oscillation and chaos. For example, when $\sigma = \log 2 \approx 0.69$, corresponding to half-life of goods of a quarter, α should remain smaller than ≈ 0.55 to avoid falling in the yellow region of Figure V.3. Note that when σ drops below ≈ 0.3, competitive equilibrium is unattainable.

Note further that within the competitive equilibrium phase, convergence can either be purely exponential, or correspond to damped oscillations or even damped chaos, see Figure V.4. The precise nature of the relaxation depends on the relative values of α, α', β and β'.

2.3.3 Deflationary equilibrium

An interesting feature of our model is the appearance of a different kind of equilibrium, corresponding to stationary points where profits and excess demand are non-zero, but

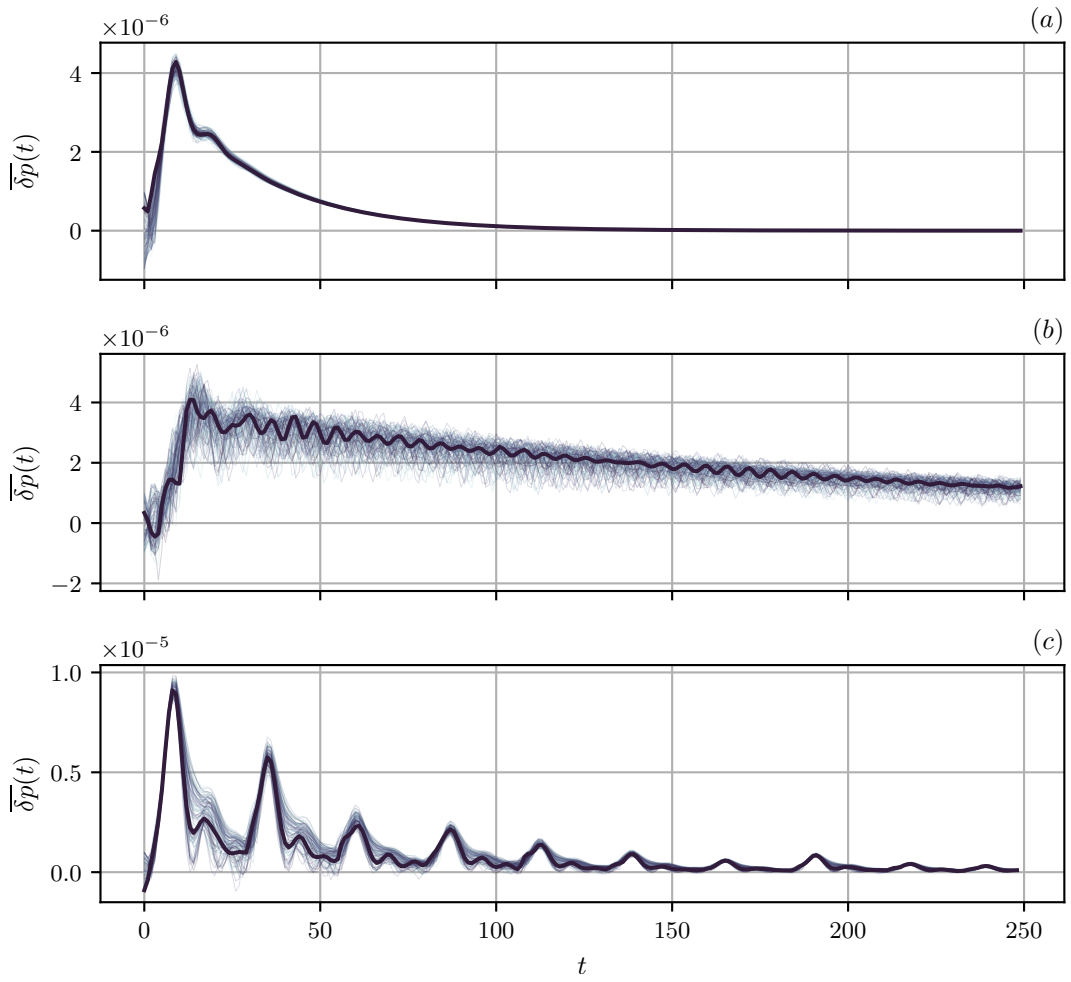


Figure V.4: Relaxation towards competitive equilibrium after a perturbation of magnitude $\delta = 10^{-3}$ for a variety of firms. (a) Exponential relaxation for $\varepsilon = 10$, $\omega = \omega' = 0.1$, $\alpha = \alpha' = \beta = \beta' \in [0.3, 0.35]$ and $\sigma \in [0.5, 0.6]$. (b) Damped oscillations for $\varepsilon = 1$, $\omega = \omega' = 0.1$, $\alpha = \alpha' = \beta = \beta' \in [0.4, 0.45]$ and $\sigma \in [0.2, 0.6]$. (c) Damped chaotic oscillations for $\varepsilon = 100$, $\omega = \omega' = 0.1$, $\alpha = \alpha' = \beta = \beta' \in [0.25, 0.3]$ and $\sigma \in [0.2, 0.6]$. The dark lines correspond to one randomly picked firm

equal to a constant value. We call them "deflationary" equilibria because prices synchronize with the (negative) inflation rate determined by the downward evolution of wages, induced by chronic unemployment (i.e. $L^{\mathrm{s}} > L^{\mathrm{d}}$).

Figure V.7 shows an example of the convergence of inflation-adjusted prices towards their stationary values. Note that in real terms, the stationary price level is above the equilibrium value. Throughout our simulations we have found these equilibria to be rather stable. For a fixed value of ω, the transition between deflationary equilibria and

competitive equilibrium occurs at a value $\alpha_d(\varepsilon)$ which is difficult to compute analytically. We can nevertheless locate this transition numerically by simulating the stability matrix in the no-shortage cone mentioned in the previous subsection. Results are reported in Figure V.5.

In contrast with the competitive equilibrium, which is independent of the dynamical parameters $\alpha, \alpha', \beta, \beta'$, deflationary equilibria are characterized by prices and production levels that depend on the parameters of the dynamics. Explicit expressions for the stationary prices/productions are, however, difficult to compute analytically as we expose now. Since real prices (i.e. deflated by wage) reach a stationary value p_i^∞, we deduce from Eq. (V.12) and the subsequent wage rescaling that

$$p_i^\infty = p_i^\infty \exp\left(-2\alpha'\overline{\pi}_i^\infty - 2\alpha\overline{\mathscr{E}}_i^\infty + 2\omega\overline{\mathscr{E}}_0^\infty\right), \tag{V.39}$$

where $\overline{\pi} = (\mathscr{G} - \mathscr{L})/(\mathscr{G} + \mathscr{L})$, $\overline{\mathscr{E}} = (\mathscr{S} - \mathscr{D})/(\mathscr{S} + \mathscr{D})$, $\overline{\mathscr{E}}_0 = (L^{\mathrm{s}} - L^{\mathrm{d}})/(L^{\mathrm{s}} + L^{\mathrm{d}})$ and the superscript ∞ denotes associated stationary values. Furthermore, targets and productions also reach stationary values $\widehat{y}_i^\infty$ and y_i^∞, which can be linked through Eq. (V.3)

$$\widehat{\gamma}_i^\infty = \gamma_i^\infty \exp\left(2\beta\mathbb{E}_\infty[\overline{\pi}_i] - 2\beta'\mathbb{E}_\infty[\overline{\mathscr{E}}_i]\right). \tag{V.40}$$

We therefore have a set of equations linking stationary values of prices, targets and productions to stationary imbalances and expectations:

$$\begin{aligned} \alpha\overline{\mathscr{E}}_i^\infty + \alpha'\overline{\pi}_i^\infty &= \omega\frac{L^{\mathrm{s},\infty} - L^{\mathrm{d},\infty}}{L^{\mathrm{s},\infty} + L^{\mathrm{d},\infty}} \quad (>0), \\ \beta\mathbb{E}_\infty[\overline{\pi}_i] - \beta'\mathbb{E}_\infty[\overline{\mathscr{E}}_i] &= \frac{1}{2}\ln\frac{\widehat{y}_i^\infty}{y_i^\infty}. \end{aligned} \tag{V.41}$$

We can try to further simplify these equations by assuming that $\mathscr{E}_i^\infty > 0$ for all firms (i.e no good shortages). Since the system is at deflationary equilibrium we also have $\mathscr{E}_0^\infty > 0$ (i.e available workforce is greater than demands). As no shortages occur, we therefore have $\widehat{y}_i^\infty = y_i^\infty$. Furthermore, households demand C_i^∞ are always satisfied by firms, but the household systematically overestimates its budget $\mathbb{E}_\infty[B]$ since $L^{\mathrm{s},\infty} > L^{\mathrm{d},\infty}$ so that: (1) the household voids its available budget and no savings are made $S^\infty = 0$, (2) realized consumption is given by

$$C_i^{\mathrm{r},\infty} = C_i^{\mathrm{d},\infty}\frac{B_\infty}{\mathbb{E}_\infty[B]} \equiv C_i^{\mathrm{d},\infty}\frac{L^{\mathrm{d},\infty}}{L^{\mathrm{s},\infty}}.$$

Note also that since $S^\infty = 0$, work offer is equal to the competitive equilibrium value. On the firms' side, since no shortages occur, forecasts are correct (except for consumption forecasts)

$$\begin{aligned} \mathbb{E}_\infty[\ell_i] &:= \ell_i^{\mathrm{d},\infty} = \ell_i^\infty \\ \mathbb{E}_\infty[x_{ij}] &:= x_{ij}^{\mathrm{d},\infty} = x_{ij}^\infty, \end{aligned}$$

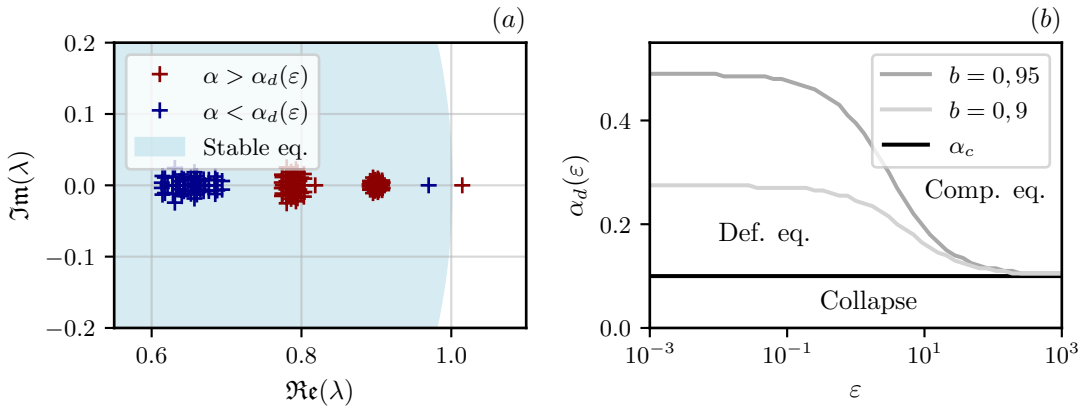


Figure V.5: (a) Eigenvalues λ of the stability matrix for $\varepsilon = 10$ in the no-shortage cone where $\delta\mathscr{S}_i(t) - \delta\mathscr{D}_i(t) > 0$ for all i. Here, $\sigma = \infty$, $\alpha = \alpha' = \beta = \beta' \in \{0.12, 0.25\}$ and $\omega = 0.1$. For $\alpha_c < \alpha < \alpha_d(\varepsilon)$, competitive equilibrium is not stable and the non-linear dynamics converges to a deflationary equilibrium. (b) α_d as a function of ε (in log-scale on the x-axis) for different values of the return-to-scale parameter b. The horizontal plain dark line corresponds to $\alpha_c = \omega = 0.1$, which is independent of ε. The labelled areas correspond to the different phases of Figure V.3 for $b = 0.95$. As b decreases, one can see that the area below $\alpha_d(\varepsilon)$ tend to decrease i.e. the region where competitive equilibrium is reached becomes larger. As mentioned in footnote 6, decreasing return to scale tend to stabilize the dynamics. Note that the values of $\alpha_d(\varepsilon = 100)$, $\alpha_d(\varepsilon = 10)$ and $\alpha_d(\varepsilon = 1)$ are consistent with values observed on the phase diagrams of Figure V.3 for which $b = 0.95$. Finally, as $\varepsilon \to 0$, one can see in Figure V.3 that the smallest σ over which this transition exists gets larger. As a consequence, for small ε, the region labelled "competitive equilibrium" only exists for large enough σ.

and no stocks of inputs are kept $I_{ij}^{\infty} = 0$, $i \neq j$. However, since the household cannot consume everything offered, some of the production is stored but we will assume $\sigma = \infty$ for simplicity so that $I_{ii}^{\infty} = 0$. Finally, using previous results we can write the error that firms made in forecasting imbalances

$$\begin{aligned}
\mathbb{E}_{\infty}[\mathscr{E}_i] &= \mathscr{E}_i^{\infty} \\
\mathbb{E}_{\infty}[\pi_i] &= \pi_i^{\infty} + p_i^{\infty} C_i^{\mathrm{d},\infty} \left(1 - \frac{L^{\mathrm{s},\infty}}{L^{\mathrm{d},\infty}}\right),
\end{aligned}$$

and we see that they systematically overestimate profits. From here one could continue and plug this relationships into Eqs. (V.41) but the subsequent equations would not be very helpful. We can however see that such equilibrium is very peculiar: by systematically overestimating profits, firms should have higher production target and therefore work demands which would contribute to bridge the gap between L^{s} and L^{d}.

Actually, these deflationary equilibria make little economic sense in the long run, because (a) the stationary level of production tends to be extremely small compared to

equilibrium values and (b) forecasts of consumption (for households) and profits (for firms) systematically overshoot their realized counterparts. One expects that in such situations, like in the case of economic collapse, the influence of monetary and fiscal policies cannot be neglected. Furthermore, we expect that when biases are strong and systematic, agents would soon adapt and change their forecasting rules accordingly. Such an extension is however beyond the scope of the present paper, but a natural conjecture is that firms would react more strongly to imbalances (i.e. increase the coefficients $\alpha, \alpha', \beta, \beta'$), which would drive the system back in the competitive equilibrium phase or in the oscillatory phase.

We finally point out that we have not found, within the present specification of the model and in contrast with Chapter IV, inflationary equilibria where the demand for labor exceeds the supply. We have found that introducing precautionary savings used to buy interest rate paying bonds leads to new phenomena, including a whole region where *inflationary* equilibria are now found. However, we have observed that large regions of parameter space can display oscillations accompanied by inflation, i.e. oscillations for which $L^{\mathrm{s}}(t) < L^{\mathrm{d}}(t)$ consistently. These regions are characterized by quicker adjustment speeds for productions i.e. $\beta, \beta' > \alpha, \alpha'$. Further characterization is still underway.

2.3.4 Oscillatory dynamics

Owing to the strongly non-linear dynamics defining the model, it is natural to expect that some choices of the parameters lead – as in generic dynamical systems – to oscillations or to chaotic dynamics, which is indeed what we observe in a whole region of parameter space – in short, when firms tend to over-react and adjust prices/productions too quickly in the face of imbalances (i.e. α "large") or when goods do not quickly perish (i.e. σ "low"). Both situations can of course occur at the same time but lead to different signatures. For large α, the economy constantly over/undershoot leading to sharp oscillations. For low σ, oscillations are smoother and determined by the slow depletion of stocks (see Section 2.6 for an in-depth discussion).

The first interesting oscillatory behavior is that of spontaneously emerging business cycles, as shown in Figure V.6. They can be either synchronized (Figure V.6-a) or completely unsynchronized (Figure V.6-b), depending on the values of ω and ε, and the relative values of α and β'. Chaotic oscillations also emerge (see Figure V.6-(c)).

We stress that such persistent oscillations, observed in rather large portions of the phase diagram, are not due to external perturbations, absent in these simulations (compared with Chapter II where small external shocks are amplified by the proximity of an instability). Rather, this is a region of the phase diagram where the volatility of the economy is purely endogenous (see [66] for similar observations).

This provides yet another scenario to explain the "small shock, large business cycle" puzzle described by [10], different from the proximity of an unstable point, as in Chapter II. Volatility may be high because of the existence of self-sustained oscillations/chaos, as reported here and in many previous work in which a dynamical systems approach to economics was advocated, see e.g. [42, 29, 119, 43, 120] and also [56, 32, 61, 121] in the context of ABMs.

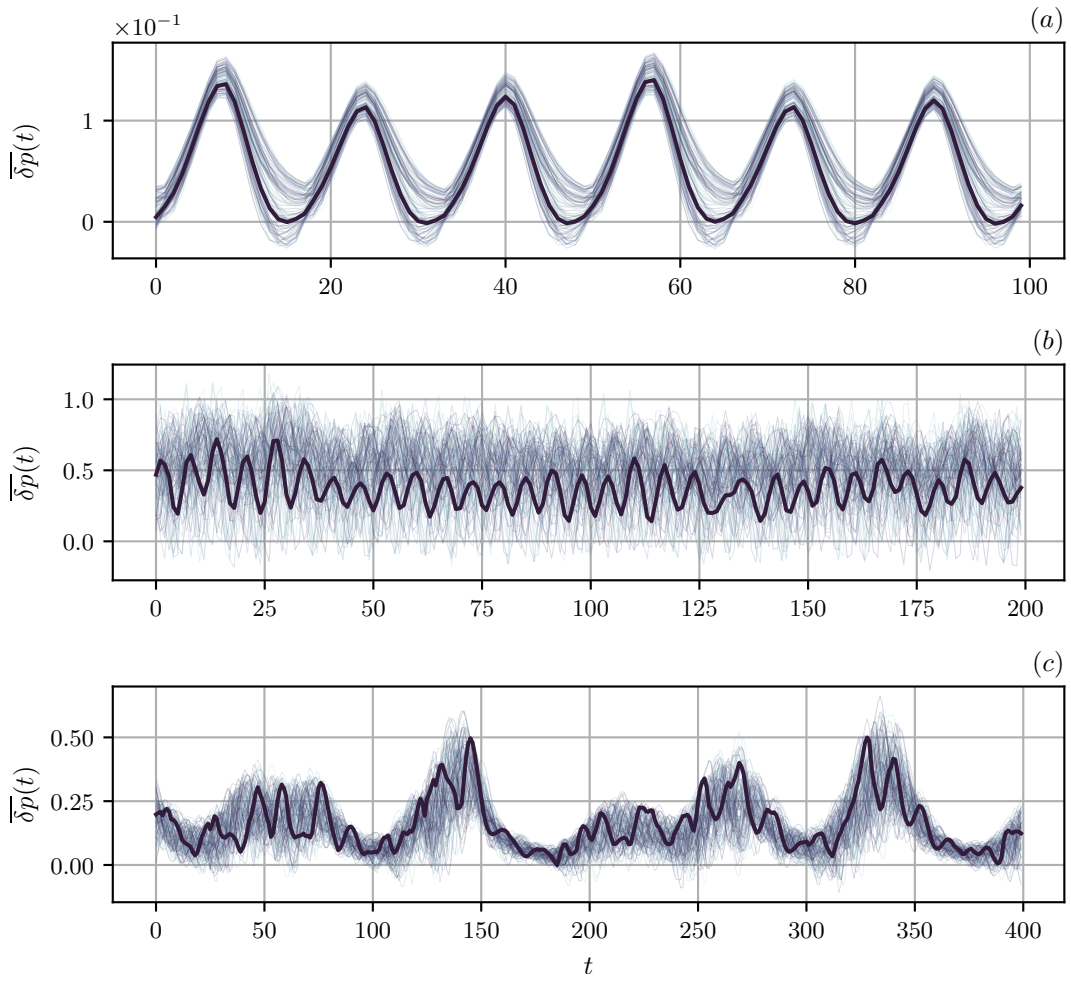


Figure V.6: Different types of price (or production) oscillations around equilibrium after an initial perturbation of magnitude $\delta = 10^{-3}$ from equilibrium. (a) Synchronized business cycles for $\varepsilon = 100$, $\omega = \omega' = 0.05$, $\alpha = \alpha' = \beta = \beta' \in [0.2, 0.25]$, $\sigma \in [0.1, 0.4]$. (b) unsynchronized oscillations for $\varepsilon = 100$, $\omega = \omega' = 0.1$, $\alpha = \alpha' = \beta \in [0.25, 0.4]$, $\sigma = 0.2$; $\beta' = 1.3\alpha$. (c) Chaotic oscillations for the same parameters except $\varepsilon = 1$ and $\beta' = 0.2\alpha$. The dark lines correspond to one randomly picked firm.

2.3.5 Intermittent crises

This additional dynamical class is represented in Figure V.7-(a). Here, a fast relaxation to equilibrium is followed by spontaneous destabilization. The system enters a cycle of price inflation and plummeting production. This is most likely due to a switch between different cones, characterized by different stability matrices, as discussed in Section 2.2. The first matrix is stable, whereas the second has at least one eigenvalue out of the unit circle, and therefore an unstable direction.

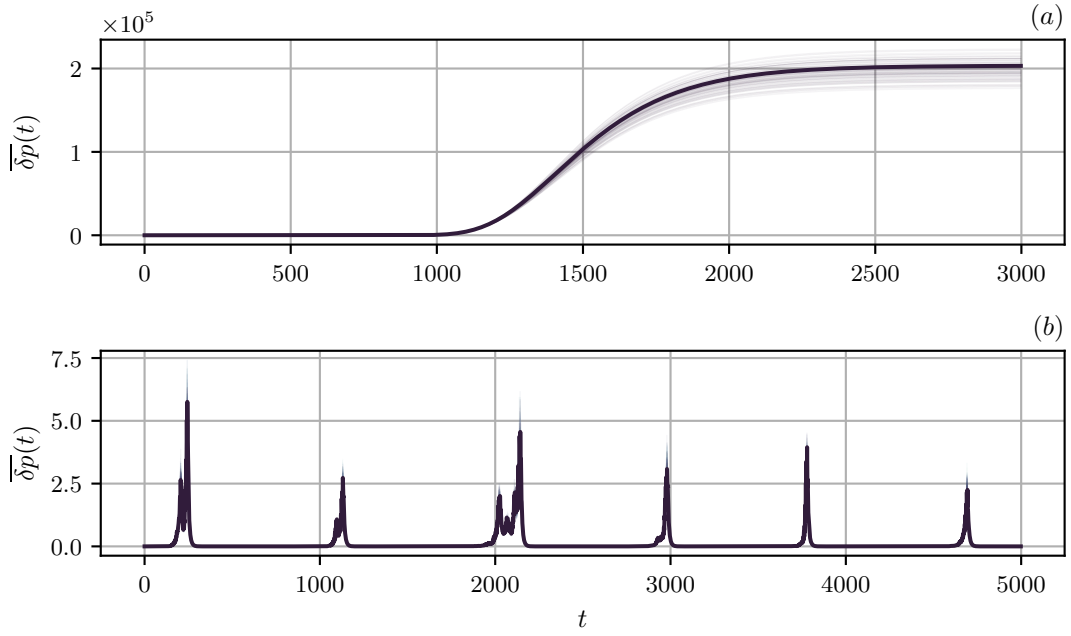


Figure V.7: (a) Example of a deflationary equilibrium with $\varepsilon = 1$ and heterogeneous productivity factors. Note that we show here real prices (deflated by wages), which reach unreasonable values 10^5 higher than at equilibrium. We choose here $\omega = \omega' = 0.1$, $\alpha = \alpha' = \beta = \beta' \in [0.25, 0.3]$ and $\sigma = 0.6$. (b) Crises-like price pattern for $\varepsilon = 100$, $\omega = \omega' = 0.1$, $\alpha = \alpha' = \beta = \beta' = 05$, $\sigma = \infty$. The dark line corresponds to one randomly picked firm.

Non-linear saturation effects then take over and quell the dynamics, and the system flows back towards equilibrium before the next crisis appears. These acute endogenous crises are one of the most interesting aspects of our model; they also appear in the Agent-Based Models of [61] and [64] where they result from a generic synchronization mechanism, as made explicit by [122].

2.4 Critical slow-down and SOC driven instability

2.4.1 Diverging relaxation time for $\varepsilon > 0$

Figure V.9 displays the relaxation time τ_r as a function of α for fixed values of $\varepsilon = 1$, $\omega = 0.1$ and $\sigma = 1$. Whenever $\alpha \to \alpha_d^{\pm}$ or $\alpha \to \alpha_c^{+}$, we observe that the relaxation time τ_r diverges continuously and the economy experiences a *second-order* transition known as a *critical slow-down* in the field of dynamical systems. Interestingly, and in contrast with the results of Chapter II, a slow-down of the dynamics, and therefore the associated increase in the aggregate volatility, can happen for values of ε greater than 0.

As an illustration, if we take $\varepsilon \to \infty$, one finds $\alpha_d = \alpha_c$ as given by Eq. (V.38). If

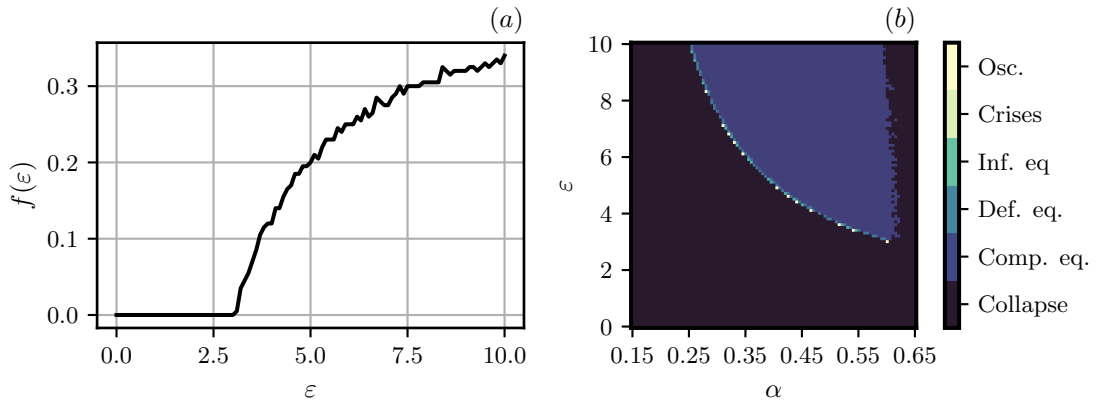


Figure V.8: (*a*) Function $f(\varepsilon) := \alpha_o(\varepsilon, \infty) - \alpha_d(\varepsilon, \infty)$ extracted from the phase diagram displayed in (*b*). We see the behavior described in Eq. (V.42). (*b*) Phase diagram in the plane (α, ε) for $b = 1$, $\sigma = \infty$ and $\omega = 0$. We observe that the region where competitive equilibrium can be reached shrinks as $\varepsilon \to 0$, and actually vanishes for a value $\varepsilon_c(\sigma = \infty) \approx 3$

.

we now set $\alpha = \alpha_c + \delta$ with $\delta \ll \alpha_c$, it is not hard to show that the largest eigenvalue of $\mathbb{D}_0$ is given by $1 - \delta/(3(1+\omega)) + O(\delta^2)$. If $\delta > 0$, the matrix $\mathbb{D}_0$ is stable (the system lies above the collapse transition), whereas for $\delta < 0$, the system becomes unstable. The relaxation time is then of order δ^{-1}, and indeed diverges close to the collapse/competitive transition. The same behavior holds for generic values of ε, when $\alpha = \alpha_d(\varepsilon) + \delta$ as we can clearly see on Figure V.9.

Furthermore, the type of equilibrium reached by the economy does not qualitatively influence the slow-down. Whenever $\varepsilon < \infty$ (such that $\alpha_c \neq \alpha_d$), if $\alpha \to \alpha_c^+$ and $\alpha \to \alpha_d^-$, the time needed to reach *deflationary* equilibrium diverges, while whenever $\alpha \to \alpha_d^+$ it is the time needed to reach *competitive* equilibrium that diverges as illustrated on Figure V.9.

Finally, whenever $\alpha \to \alpha_o^-$ (where $\alpha_o(\varepsilon, \sigma)$ denotes the value of α for which the economy enters the region of oscillations), the relaxation time experiences a *first-order* transition, in opposition with the second-order transition close to α_c, α_d. For $\alpha > \alpha_o$, equilibrium is never reached, which corresponds to $\tau_r = \infty$. However, as $\alpha \to \alpha_o^-$, Figure V.9 indicates that τ_r converges to a *finite* value τ_r^o. As it crosses the transition line α_o the relaxation time jumps *discontinuously* from $\tau_r^o < \infty$ to an infinite value, where the discontinuous nature of the jump is a token of a first-order transition.

2.4.2 Forced slow-down when $\varepsilon \to 0^+$

For a fixed value of σ, let us now focus on the region where competitive equilibrium can be reached. With the notation introduced in the previous sections, this interval is $]\alpha_d(\varepsilon, \sigma), \alpha_o(\varepsilon, \sigma)[$. As $\varepsilon \to 0$, this interval shrinks down, i.e. $\alpha_o(\varepsilon, \sigma) - \alpha_d(\varepsilon, \sigma) :=$

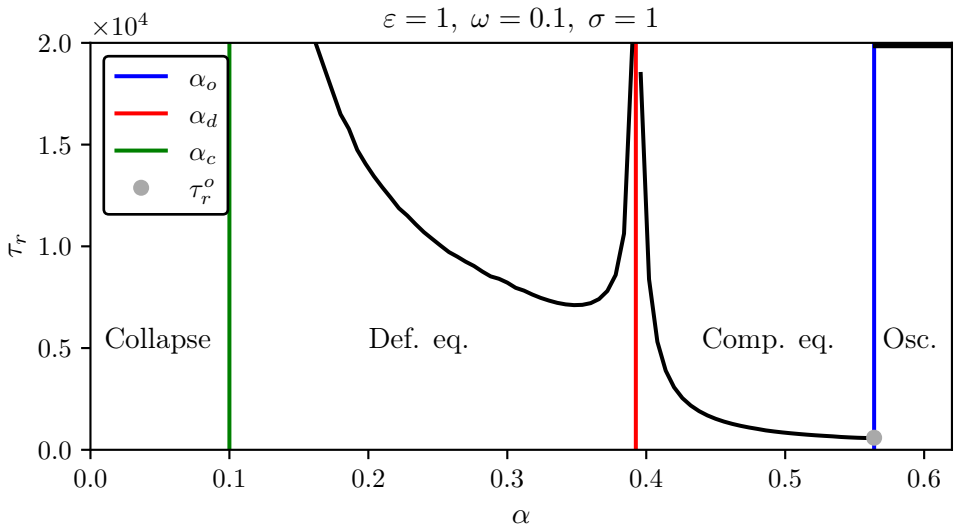


Figure V.9: Relaxation time τ_r (gray line) as a function of the adjustment speed α for $\varepsilon = 1,\ \omega = 0.1,\ \sigma = 1$. We ran the model for $T = 2 \times 10^4$ time-steps and defined τ_r as $\tau_r = \inf\{t \in [0, T],\ \|\mathbf{p}(t) - \mathbf{p}(T)\|_2 < 10^{-8}\}$ (if the previous set is empty, $\tau_r > T$ and not displayed on the plot). We can see that on either side of the transition line $\alpha_d(\varepsilon, \sigma)$ (shown on the red vertical line) and on the right of the transition line α_c (shown on the green vertical line), the relaxation time of the economy diverges continuously featuring a second-order transition (regardless of the type of equilibrium reached). Furthermore, as α gets closer to the left of the transition line α_o (shown on the blue vertical line), the relaxation time reaches a finite value τ_r^o before jumping to an infinite value whenever $\alpha > \alpha_o$, therefore displaying a first-order transition.

$f(\varepsilon) \to 0$, as illustrated on Figure V.8. More precisely, numerical simulations show that there exists a value ε_c (depending on σ, b and ω) such that

$$f(\varepsilon) = \begin{cases} 0, & \text{for } \varepsilon \leq \varepsilon_c \\ r(\varepsilon - \varepsilon_c), & \text{for } \varepsilon \to \varepsilon_c^+ \end{cases}, \tag{V.42}$$

where $r = f'(\varepsilon_c^+)$, see Figure V.8-(a). As $\varepsilon \to \varepsilon_c^+$, the values of α for which competitive equilibrium can be reached are forced to be such that $\alpha \approx \alpha_d + f(\varepsilon)$ with $f(\varepsilon) \ll \alpha_d(\varepsilon)$. By the same argument as in the previous section, the relaxation time will scale as $f(\varepsilon)^{-1} \sim 1/(\varepsilon - \varepsilon_c)$. Consequently, through the self-organized criticality mechanism from Part I which drives ε towards 0, the system is bound to reach ε_c at some point. Therefore, any economy sitting in the region where competitive equilibrium can be reached will be forced to experience a critical slow-down leading to aggregate volatility.

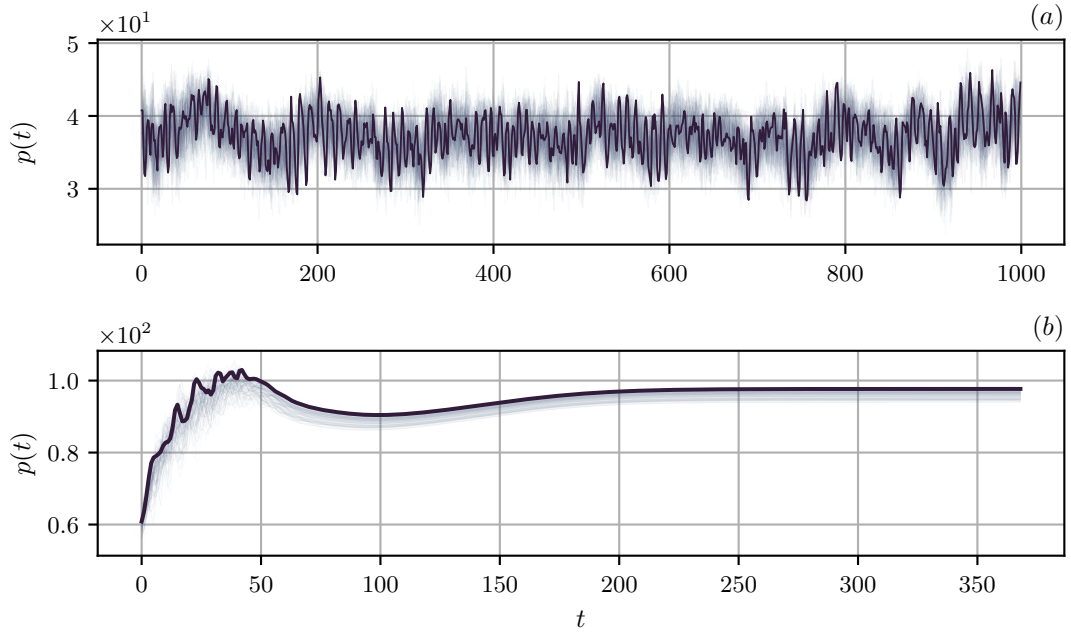


Figure V.10: Different possible price (or production) dynamics in the unstable phase $\varepsilon = -5$, for initial conditions for prices and productions randomly chosen between 1 and 2. (a) Rapid oscillations for $\omega = \omega' = 0.01$, $\alpha = \alpha' = \beta = \beta' = 0.45$, $\sigma = 0.2$. (b) Deflationary equilibrium for $\omega = \omega' = 0.02$, $\alpha = \alpha' = \beta \in [0.4, 0.45]$, $\sigma \in [0.2, 0.8]$. The dark lines correspond to one randomly picked firm.

2.5 The low-productivity phase $\varepsilon < 0$

A weakness of the naive model of Chapter II was that it can only produce divergent trajectories whenever $\varepsilon < 0$, i.e. in the low productivity phase. As illustrated in Figure V.10, our full model produces instead a wide range of interesting behavior in this case, from deflationary equilibria to oscillations. Of course, since there is no well-defined equilibrium, the convergent phase is now proscribed. However, an important message is that a viable economy can exist *even if the Hawkins-Simon condition is violated*, but at the expense of either substantial stationary imbalances or oscillatory/chaotic behavior.

2.6 The role of perishability

Finally, we illustrate here the crucial role of inventories in determining the type of dynamics we observe. As shown in the phase diagrams of Figure V.11 in the (α, ω) plane at fixed σ, goods that perish immediately ($\sigma = \infty$) lead to simple relaxation towards equilibrium (deflationary/competitive) or to a collapse. In a sense, this limit is as close as possible to the model of Chapter II where all inventory effects were overlooked.

On the other hand, non-perishable goods lead to oscillating, highly volatile economies. Intuitively, if firm i has a stock I_{ik} of good k, it will decrease its demand to firm k, leading

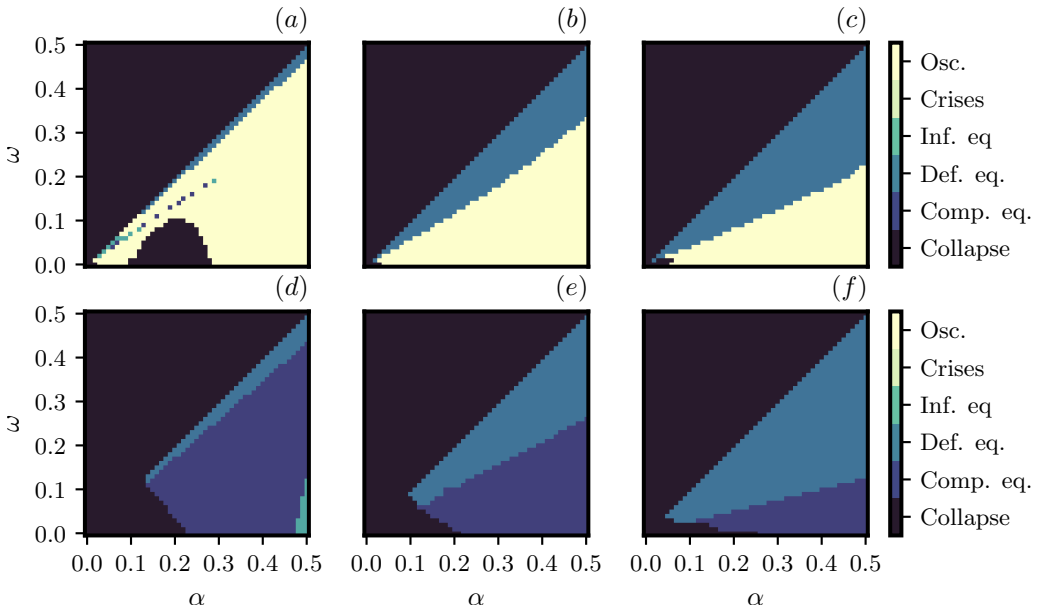


Figure V.11: Phase diagrams for non-perishable ($\sigma = 0$, top row $(a) - (b) - (c)$) and immediately perishable ($\sigma = \infty$, bottom row $(d) - (e) - (f)$) goods in the α, ω plane, for different values of ε: $(a) - (d)$ $\varepsilon = 100$, $(b) - (e)$ $\varepsilon = 10$, $(c) - (f)$ $\varepsilon = 1$.

to a decrease of its production. This lasts until all stocks are exhausted. A phase of booming demands and increase in production follows, firms' stocks begin to pile up again and the economy enters another cycle. This is similar to the well-known "bull-whip effect" suggested by [123], where inventories are known to lead to instability effects.

2.7 Sensitivity to initial conditions

The phase diagrams of Figure V.3 and Figure V.11 have been established by classifying the behavior of the system after an initial perturbation around equilibrium of magnitude 10^{-3}. But since our system is non-linear, larger perturbations may lead to different outcomes for the same set of parameters. In this section, we study of the impact of initial conditions on the dynamics.

2.7.1 Basin of attraction of equilibrium

As for any non-linear dynamical system, the basin of attraction of a given fixed point is defined as the set of initial conditions that will allow the system to reach it. The analytical determination of basins of attraction is a notoriously difficult question, especially for high dimensional systems.

As pointed out in Section 2.2, it is possible to linearize the dynamics around equilibrium. The subsequent dynamics is piece-wise linear and described by the evolution of a

$N^2 + 4N + 1$-dimensional vector. As it would be unrealistic to explore separately the effects of a perturbation on each and every component of this vector, we will restrict our study to uniform perturbations on current productions, prices and production targets. We thus parametrize perturbations as

$$p_i(0) = p_{\mathrm{eq},i}(1 + r_p),\ \gamma_i(0) = \gamma_{\mathrm{eq},i}(1 + r_\gamma),\ \widehat{\gamma}_i(1) = \gamma_{\mathrm{eq},i}(1 + r_\gamma), \tag{V.43}$$

where r_p and r_γ are the perturbation radii ranging from -1 (initial values at 0) and $+\infty$. For a given r_p, we scan all values of r_γ and find the largest upward and downward possible perturbation allowing the system to revert back to equilibrium. Beyond this domain, the dynamics may drive the system to another phase.

Figure V.12 shows the approximate regions for which the dynamics reach equilibrium after a perturbation of size (r_p, r_γ). For large ε, the system is able to sustain very large perturbations when $r_p, r_\gamma > 0$. However, whenever either r_p or r_γ is negative, the system can end up in the collapse region. We will discuss this point in the next section.

Finally, as one expects, the basin of attraction drastically shrinks as ε is reduced (Figure V.12-(b)). One can see that the system is still able to cope with large perturbations on production provided that prices are not too far from equilibrium.

The shrinkage of the basin of attraction of the competitive equilibrium state as $\varepsilon \to 0$ again reveals how network effects are crucial to understand the fragility of the economy, since the value of ε is, we recall, determined by productivity on the one hand, and the structure of the input-output network on the other.

2.7.2 Direction of perturbations

On top of the importance of the magnitude of perturbation, the direction of the perturbation matters as well. This is a consequence of the separation of state space in different cones. For a small perturbation around equilibrium, if the system is initialized in the no-shortage cone, the dynamics will behave differently than if it were initialized in the full shortage cone. As an illustration, Figure V.13 shows the phase diagrams in the plane (α, ω) for the same parameters but for different initial perturbations. On the left (a), a small upward perturbation is applied on equilibrium prices and productions but initial targets are set to $\boldsymbol{\gamma}_{\mathrm{eq}}$. This prepares the system in the no-shortage cone since production is higher than in equilibrium and household's demand lower. We see that the collapse region is very well described by the stability of the matrix $\mathbb{D}_0$ defined in Section 2.2, which in this case keeps the trajectory inside the no-shortage cone.

On the other hand, the right plot (b) shows that initializing the system in a mixture of no-shortages/shortages adds an additional wedge of collapsing dynamics (note that the same wedge is present on the diagrams of Figure V.11). Above this line, the matrix $\mathbb{D}_S$ drives the dynamics outside the partial-shortage cones. The system finally reaches the no-shortage cone, which is preserved by $\mathbb{D}_0$ and for which equilibrium is stable. Below this line, the dynamics is thrown into the full-shortage cone, which is preserved by $\mathbb{D}_N$ but where, on the other hand, equilibrium is unstable.

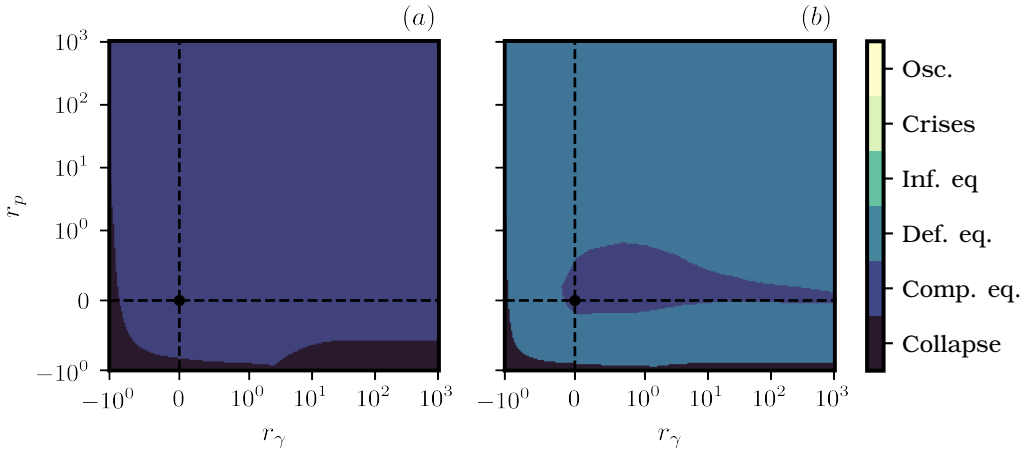


Figure V.12: Approximate basins of attraction of the dynamics for $\alpha = \beta = \beta' = \alpha' = 0.45$, $\omega = 0.1$, $\sigma = \infty$. (a) $\varepsilon = 100$, $\alpha \gg \alpha_d(100) \approx 0.115$ which allows very large perturbations of equilibrium values. (b) $\varepsilon = 1$, $\alpha \gtrsim \alpha_d(1) \approx 0.395$. Large perturbations lead to the system reaching a deflationary equilibrium. Also note that downwards perturbation can lead to deflationary equilibrium. In this case, the system overreacts and blows up to reach a deflationary equilibrium. Dashed black lines separate the regions of positive and negative perturbation on prices or productions. The black dot corresponds to no-perturbation.

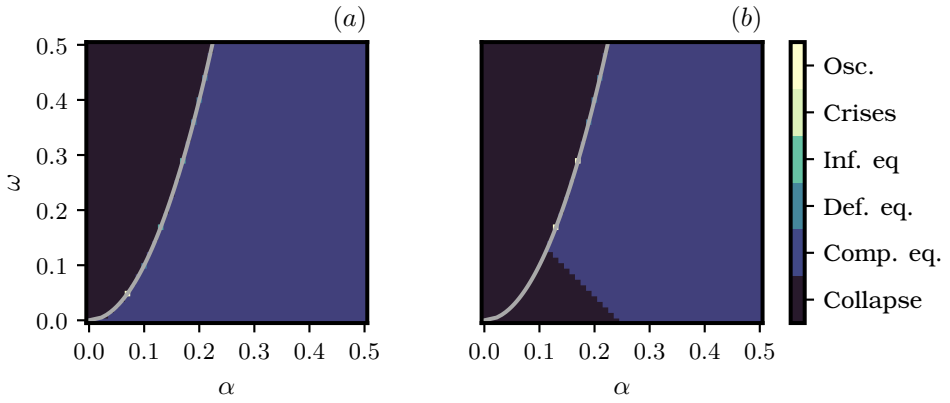


Figure V.13: Phase diagrams (α, ω) for $\varepsilon = 10^4$, $\beta' = 0.1$, $\alpha' = 0.25$, $\sigma = \infty$ and $\alpha = \beta$. (a) The system is initialized in the no-shortage region by applying a small upward perturbation on equilibrium prices and productions of magnitude 10^{-4}. (b) The system is initialized in a mixture of no-shortages and shortages (50%/50%) by applying a perturbation around equilibrium prices and productions. The grey line corresponds to the prediction $\alpha_c = \sqrt{\beta'\omega}$ (here $\alpha = \beta$) for the stability of the matrix $\mathbb{D}_0$. Note here that we fixed values of α' and β' to illustrate another possible shape of the transition around α_c. If we had chosen, as previously, $\alpha = \beta = \alpha' = \beta'$, the transition line would have been the line $\alpha = \omega$, as in Figure V.11.

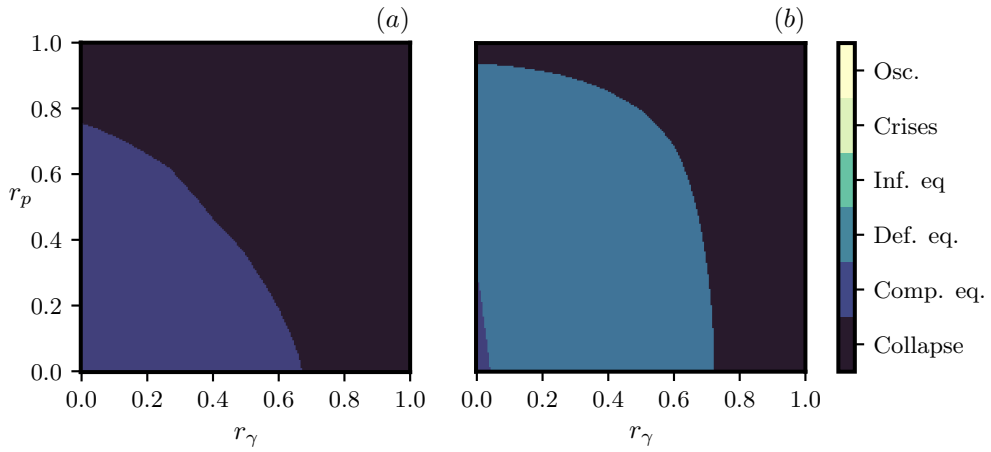


Figure V.14: Approximate basins of attraction of the dynamics for mixed initial conditions (50 % shortages, 50 % mark-ups) for (a) $\varepsilon = 100$ and (b) $\varepsilon = 1$, and $\alpha = \beta = \beta' = \alpha' = 0.45$, $\omega = 0.1$, $\sigma = \infty$.

To further illustrate this effect, we ran the dynamics of our model with mixed initial conditions

$$p_i(0) = p_{\mathrm{eq},i}(1 \pm r_p),\ \gamma_i(0) = \gamma_{\mathrm{eq},i}(1 \pm r_\gamma),\ \widehat{\gamma}_i(1) = \gamma_{\mathrm{eq},i}(1 \pm r_\gamma), \tag{V.44}$$

where we choose $+$ for 50% of the firms and $-$ for the others. This prepares the system in a state where 50% of the firms cannot fulfill demands. In Figure V.14, we show the basin of attraction of equilibrium for perturbations r_p, r_γ ranging from 0 to 1. As we see, large enough shortages can destabilize the dynamics even at large ε.

3 Real world networks

As mentioned at the beginning of Section 2, random regular networks are a crude idealization of real interaction networks. Real networks have been studied extensively (see for instance [73, 75, 74]) and display well identified topological features such as truncated power law distributed in and out vertex degrees. Figure I.1 of Chapter I illustrates the topological discrepancies between regular and real world networks, and highlights similarities with scale-free networks.

To build the network of Figure I.1, we use the FactSet Supply Chain Relationships database to build a supply chain network. The FACTSET dataset [76] contains a list of relational data between firms, stating if firms A and B have a client/supplier relation, if they are in competition or if they have a joint venture. It is built by collecting information from primary public sources such as SEC 10-K annual filings, investor presentations and press releases, and covers about 23, 000 publicly traded companies with over 325, 000 relationships. Since the relationships are inferred from data released to the public, we cannot be sure that it is an exhaustive database of all the relationships between firms, but

the subset of relationships deemed important by the firm themselves. Such links between firms have a finite duration in time and have thus a beginning and end date. For our study, we have chosen the set of client/supplier relationships between the years 2012 and 2015. This allows us to build a graph G where a link $i \to j$ exists whenever i is reported to be a supplier of j or when j is reported to be a client of i. Furthermore, since this graph is not fully connected, we extracted its largest strongly connected component.

Even though phase diagrams are not changed qualitatively if one changes the network, the features of the dynamics within one phase depends on the structure of interactions. As an illustration, we ran our model on the network represented on Figure I.1 for $\varepsilon = 10$ and $\varepsilon = -3$. Results are reported on Figure V.15. While equilibria (whether competitive or deflationary) are reached in a somewhat similar manner as on a regular network, oscillatory patterns are much more disordered due to the in-homogeneity of in and out degrees.

Finally, another effect closely related to network topology is worth mentioning. In the case of random regular networks, firms are always supplied by at least one firm. However it is possible for a firm to use labor as sole input. Upon simulating the dynamics on scale free networks with labor-supplied firms, we found that whenever deflationary equilibria occurred, only a fraction of firms survived while the others saw their prices blow up exponentially and production plummet. Surviving firms are the ones for which going up the supplier network leads only to labor-supplied firms.

4 Conclusion

A numerical investigation of the full model leads to rich phase diagrams, from which we extract the following salient features, with clear economic implications:

- The competitive equilibrium attracts the dynamics *only in a restricted range of parameters*: the speed at which firms adapt to imbalances must neither be too slow nor too fast, and the rate at which goods spoil must be high enough. Diminishing returns to scale also help convergence towards equilibrium.
- When the adaptation speed is too large, or the perishability of goods too low, coordination breaks down and the economy enters a phase with periodic or chaotic business cycles of purely endogenous origin, as was also reported in [66].
- Close to the boundaries between the competitive equilibrium phase and the oscillating phase, one observes a regime of intermittent crises, with long periods of quasi-equilibrium interrupted by bursts of inflation.
- Another class of equilibria exists, with a negative inflation but with stationary real prices and production different from those pertaining to the competitive equilibrium. In particular, markets – including the job market – do not clear in such situations: labor supply is always larger than labor demand. These equilibria are however characterized by persistent discrepancies between forecasts and realized quantities, which presumably make them unstable against simple learning rules.

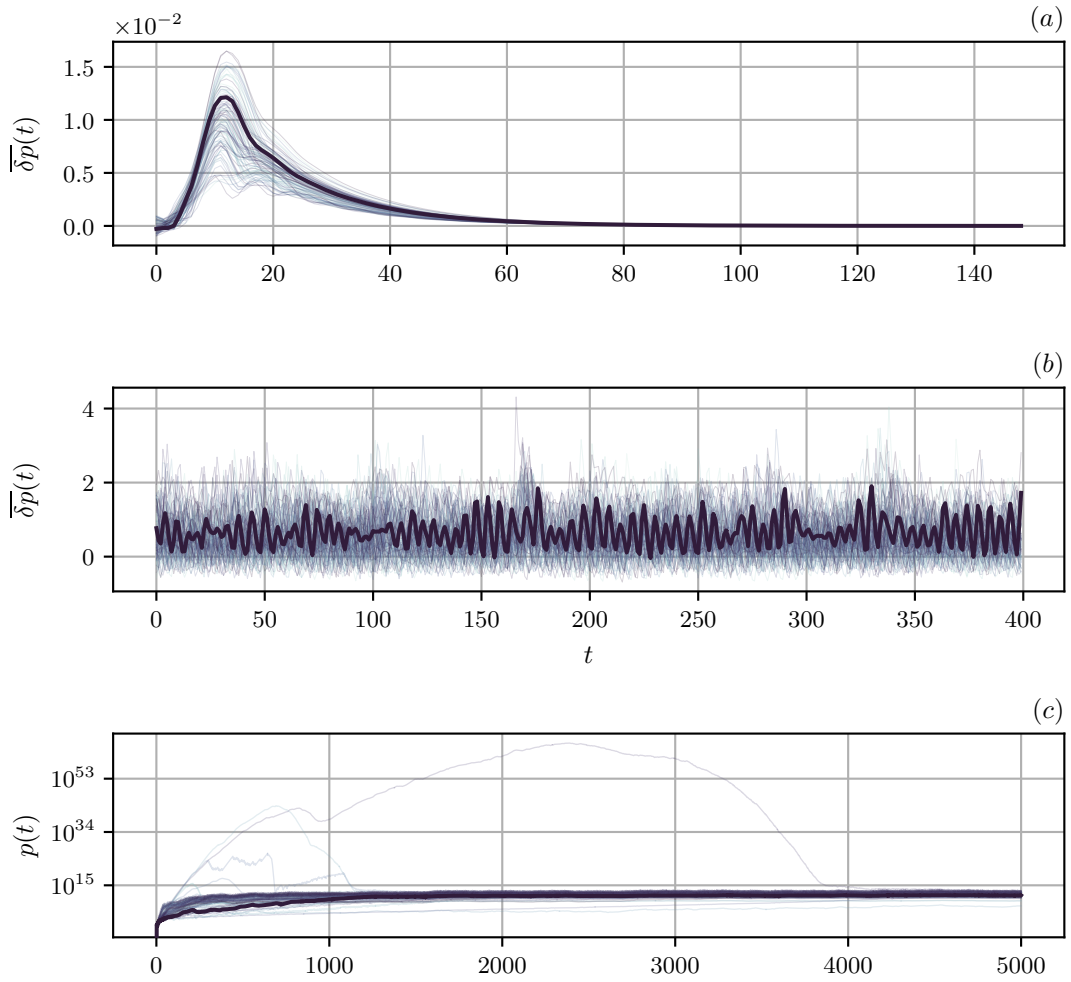


Figure V.15: Example of dynamics on the network of Figure I.1. $(a) - (b)$ Dynamics for $\varepsilon = 10$. (a) Relaxation towards equilibrium. (b) Oscillatory patterns: oscillations are quite disordered relatively to random regular networks. (c) Dynamics for $\varepsilon = -3$. Oscillations with quenched explosions for some firms.

- For *inflationary* equilibria to exist, where labor demand is larger than labor supply, one needs to introduce precautionary savings and interest rates in the model. However, inflation (even though non constant) can be found within the present specifications for quick adjustment speeds on targets.

- Finally, we have checked that the overall shape of the phase diagram is robust to changes of the structure of the network (although see Section 3 for additional information about the dynamics on real input-output networks) and of the specific form of the CES production function that one uses. This means that these results are generic and should hold in realistic situations as well.

This model therefore suggests *two* distinct out-of-equilibrium routes to excess volatility (or "large business cycles"): (a) purely *endogenous* cycles, resulting from over-reactions and non-linearities, or (b) persistence and amplification of *exogenous shocks*, governed by the proximity of a boundary in parameter space where the competitive equilibrium becomes unstable. While scenario (a) may appear at first sight to be more generic, the self-organized criticality scenario proposed long ago by [19] could make (b) plausible as well. Specific empirical work is needed to distinguish between these two scenarios.

It should however be born in mind that many relevant features of the real economy are left out of the present version of the model. In particular, whereas firms are allowed to make losses, we have not accounted to the cost of credit that this would entail, and the impact of monetary policy, increasing or decreasing the interest rate in the face of inflation/deflation.

Nor have we introduced a bankruptcy mechanism when firms go too deep into debt, removing non-competitive firms along the lines of, e.g. [63]. But this would require moving from a static network of firms, as considered throughout this work, to a dynamically evolving network that rewires as some firms go bankrupt and others are created. In fact, another motivation for moving from such a static framework to a rewiring model is to be able to describe possible *cascades of bankruptcies* mediated by the input-output network, much as cascades of defaults can occur in banking networks. We leave this for further investigations.

The household sector also needs to be better described, moving away from the representative household assumption and introducing wage inequalities, confidence effects (as, for example, in [67]) and debt. In fact, our dynamical model can be seen as a hybrid between traditional economic models (describing equilibrium) and Agent Based Models, where extra reasonable but *ad hoc* rules are implemented to account for out-of-equilibrium, dynamical aspects. As we have shown, in some swath of parameters, the classical competitive equilibrium is reached. If reached fast enough, the "adiabatic" assumption used in most standard descriptions will hold, whereas when the relaxation time is long (or even infinite) new phenomena appear.

Finally, an appealing feature of this approach is the possibility to use highly disaggregated data on individual firms and prices (for example through the "Billion Price Project" [124]) to calibrate the model and, hopefully, use it as a powerful descriptive and predictive tool.

Key takeaways

- **Economic equilibrium** can be reached for a restricted range of parameters depending on the distance to the HS transition. Within this range speed of convergence depends on the adjustment parameters as well as ε.
- **Amplification of external shocks** can occur in the same way as in the model of Chapter II. Close to the transition line $\alpha_d(\varepsilon)$, the relaxation time diverges allowing shocks to accumulate in the network. Furthermore, as $\varepsilon \to 0^+$, the size $f(\varepsilon)$ of the region where equilibrium can be reached shrinks down to zero so that the relaxation time (or the volatility of outputs with random exogenous shocks) will behave as $1/f(\varepsilon)$.
- **Endogenous oscillations** emerge for economically sound value of parameters. When perishability is too low, firms tend to accumulate inventories and demands are reduced. As inventories are depleted, demands get boosted back up. When reactions to imbalances are too fast, firms tend to overshoot/undershoot production targets or prices resulting in never-ending adjustments. The fact that this model is able to endogenously generate sustained oscillations offers another avenue of explanation for the excess volatility observed at macroeconomic level.

A Linearization of the model

In this section, we provide computations for the linearization of the ABM presented in the main text. We will implicitly use results from Chapter IV, especially on perturbations of constraint factors.

A.1 Useful relationships at equilibrium

We start by considering equilibrium relationships that will allow for a simplification of computations. Recall that equilibrium relationships on prices $p_{\mathrm{eq},i}$ and production levels $\gamma_{\mathrm{eq},i}$ are given by

$$z_i \gamma_{\mathrm{eq},i} = \sum_j x_{\mathrm{eq},ji} + C_{\mathrm{eq},i} \tag{V.45}$$

$$z_i \gamma_{\mathrm{eq},i} p_{\mathrm{eq},i} = \sum_j p_{\mathrm{eq},j} x_{\mathrm{eq},ij} + x_{\mathrm{eq},i0}. \tag{V.46}$$

At equilibrium, the household has no savings so that its budget is equal to work supply

$$B_{\mathrm{eq}} = L_{\mathrm{eq}} \tag{V.47}$$

$$S_{\mathrm{eq}} = 0 \tag{V.48}$$

$$\mu^k_{\mathrm{eq}} = \bar{\theta} \tag{V.49}$$

$$L_{\mathrm{eq}} = L_0 \tag{V.50}$$

We will assume that $\sum_i \theta_i := \bar{\theta} = 1$, so that $\mu_{\mathrm{eq}} = 1$ for simplicity.

A.2 Notations for linearization

$$\begin{aligned}
p_i(t) &= p_{\mathrm{eq},i} \exp \frac{\delta p_i(t)}{p_{\mathrm{eq},i}} \; ; & \gamma_i(t) &= \gamma_{\mathrm{eq},i} \exp \frac{\delta \gamma_i(t)}{\gamma_{\mathrm{eq},i}} \\
I_{ij}(t) &= \delta I_{ij}(t) \; ; & x^{\#}_{ij}(t) &= x_{\mathrm{eq},ij} \exp \frac{\delta x^{\#}_{ij}(t)}{x_{\mathrm{eq},ij}} \\
C^{\#}_i(t) &= C_{\mathrm{eq},i} \exp \frac{\delta C^{\#}_i(t)}{C_{\mathrm{eq},i}} \; ; & L^{\#}(t) &= L_{\mathrm{eq}} \exp \frac{\delta L^{\#}(t)}{L_{\mathrm{eq}}} \\
S(t) &= \delta S(t) \; ; & \mu(t) &= \exp \delta m(t) \\
B(t) &= B_{\mathrm{eq}} \exp \frac{\delta B(t)}{B_{\mathrm{eq}}} \; ;
\end{aligned} \tag{V.51}$$

A.3 General linearization

A.3.1 Linear optimization by the household

We write the expected budget constraint as

$$L_0 \frac{\bar{\theta}}{\mu(t)} = S(t) + L_0 (\mu(t) f)^{1/\varphi}, \tag{V.52}$$

which we linearize as follows

$$L_0 = \delta S(t) + L_0 + kL_0\delta m(t) \Longleftrightarrow \delta m(t) = -\frac{1}{kL_0}\delta S(t). \tag{V.53}$$

We can then give the expressions for the perturbations of labor supply and consumption demands

$$\frac{\delta C_i^d(t)}{C_{\mathrm{eq},i}} = \frac{1}{kL_0}\delta S(t) - \frac{\delta p_i(t)}{p_{\mathrm{eq},i}} \tag{V.54a}$$

$$\frac{\delta L^{\mathrm{s}}(t)}{L_{\mathrm{eq}}} = -\frac{1}{1+\varphi}\delta S(t), \tag{V.54b}$$

with $C_{\mathrm{eq},i} = L_0\theta_i/p_{\mathrm{eq},i}$.

A.3.2 Linear labor market

We know from the previous section that labor supply is perturbed as Eq. (V.54b). We still have to compute the perturbation on labor demand. Since no stocks have to be taken into account for labor demands $x_{i0}^{\mathrm{d}} = J_{i0}\widehat{\gamma}_i(t+1)^{1/b}$ (see Eq. (V.5)), we can easily compute the perturbation on x_{i0}^{d} and $L^{\mathrm{d}} := \sum_i x_{i0}^{\mathrm{d}}$. It yields

$$\frac{\delta x_{i0}^{\mathrm{d}}(t)}{x_{\mathrm{eq},i0}} = \frac{1}{b}\frac{\delta\widehat{\gamma}_i(t+1)}{\gamma_{\mathrm{eq},i}}, \tag{V.55a}$$

$$\delta L^{\mathrm{d}}(t) = \frac{1}{b}\sum_j \frac{x_{\mathrm{eq},j0}}{\gamma_{\mathrm{eq},j}}\delta\widehat{\gamma}_j(t+1). \tag{V.55b}$$

We now need to compute the actual work provided by the household, taking into account possible work shortages. This is easily obtained and reads:

$$\frac{\delta x_{i0}(t)}{x_{\mathrm{eq},i0}} = \frac{1}{b}\frac{\delta\widehat{\gamma}_i(t+1)}{\gamma_{\mathrm{eq},i}} + \min\left(0, \frac{\delta\mathscr{E}_0(t)}{L_{\mathrm{eq}}}\right), \tag{V.56a}$$

$$\delta L(t) = \delta L^{\mathrm{d}}(t) + \min\left(0, \delta\mathscr{E}_0(t)\right), \tag{V.56b}$$

where the latter is quite natural and similar to Chapter IV.

A.3.3 Linear trade market

Let us now compute perturbations on fluxes of goods. We first need the perturbation of the optimal quantity $\widehat{x}_{ij}(t)$. As for work, this reads:

$$\frac{\delta\widehat{x}_{ij}(t)}{x_{\mathrm{eq},ij}} = \frac{1}{b}\frac{\delta\widehat{\gamma}_i(t+1)}{\gamma_{\mathrm{eq},i}}. \tag{V.57}$$

Now, goods' demands are computed by taking stocks into account

$$x_{ij}^{\mathrm{d}}(t) = \max\left(0, x_{\mathrm{eq},ij} + \delta\widehat{x}_{ij}(t) - \delta I_{ij}(t)\right).$$

Since perturbations are small enough and $x_{\mathrm{eq},ij} > 0$, we can remove the $\max(0,\cdot)$ condition so that

$$\delta x_{ij}^{\mathrm{d}}(t) = \delta\widehat{x}_{ij}(t) - \delta I_{ij}(t). \tag{V.58}$$

Intuitively, removing $\max(0,\cdot)$ amounts to saying that stocks cannot be high enough to entirely take care of production close to equilibrium. Goods are then exchanged according to possible supply shortages which reads

$$\delta x_{ij}(t) = \delta x_{ij}^{\mathrm{d}}(t) + \frac{x_{\mathrm{eq},ij}}{z_j \gamma_{\mathrm{eq},j}} \min\left(0, \delta\mathscr{E}_j(t)\right). \tag{V.59}$$

Finally, available goods for production take into account available stocks

$$x_{ij}^{\mathrm{a}}(t) = x_{ij}(t) + \min\left(I_{ij}(t), \widehat{x}_{ij}(t)\right).$$

The term $\min\left(\delta I_{ij}(t), x_{\mathrm{eq},ij} + \delta\widehat{x}_{ij}(t)\right)$ can be further expressed and always yields $\delta I_{ij}(t)$ close to equilibrium. We can therefore expressed available goods for production in terms of optimal quantities by combining Eq. (V.58) with the previous equation

$$\delta x_{ij}^{\mathrm{a}}(t) = \delta\widehat{x}_{ij}(t) + \frac{x_{\mathrm{eq},ij}}{z_j \gamma_{\mathrm{eq},j}} \min\left(0, \delta\mathscr{E}_j(t)\right). \tag{V.60}$$

A.3.4 Linear retail market and linear household finances

The household consumes goods according to the budget computed upon hiring, whose perturbation reads

$$\delta B(t) = \delta S(t) + \delta L(t). \tag{V.61}$$

Firms reserve some goods for retailing according to shortages of their supply. The perturbation of the offered consumption reads

$$\delta C_i^o(t) = \delta C_i^d(t) + \frac{C_{\mathrm{eq},i}}{z_i \gamma_{\mathrm{eq},i}} \min\left(0, \delta\mathscr{E}_i(t)\right). \tag{V.62}$$

Since the household might have overestimated its budget in its planning, budget shortage may occur. The minimum budget needed to entirely consume $C_i^{\mathrm{o}}(t)$ can be written as

$$\sum_i p_i(t) C_i^o(t) = B_{\mathrm{eq}} \exp \frac{\sum_i \left(C_{\mathrm{eq},i}\delta p_i(t) + p_{\mathrm{eq},i}\delta C_i^o(t)\right)}{B_{\mathrm{eq}}}, \tag{V.63}$$

since this minimum budget has to equate real budget at equilibrium. The budget constraint factor from Eq. (V.33) can therefore be expressed as

$$\min\left(1, \frac{B(t)}{\sum_i p_i(t) C_i^{\mathrm{o}}(t)}\right) = 1 + \frac{1}{B_{\mathrm{eq}}} \min(0, \delta h(t)),$$

where

$$\delta h(t) = -(\delta\mathscr{E}_0(t) - \min\left(0, \delta\mathscr{E}_0(t)\right) - \sum_i \frac{p_{\mathrm{eq},i} C_{\mathrm{eq},i}}{z_i \gamma_{\mathrm{eq},i}} \min\left(0, \delta\mathscr{E}_i(t)\right), \tag{V.64}$$

which generalizes the expression of Chapter IV. We can therefore write the perturbation on the real consumption

$$\delta C_i^r(t) = \delta C_i^d(t) + \frac{C_{\mathrm{eq},i}}{z_i \gamma_{\mathrm{eq},i}} \min\left(0, \delta\mathscr{E}_i(t)\right) + \frac{C_{\mathrm{eq},i}}{B_{\mathrm{eq}}} \min\left(0, \delta h(t)\right). \tag{V.65}$$

The household may then compute its savings for the next period

$$\begin{aligned}
\delta S(t+1) &= \delta B(t) - \delta\left(\sum_i p_i(t)C_i(t)\right) \\
&= \delta S(t) + \delta L^{\mathrm{d}}(t) + \min\left(0, \delta\mathscr{E}_0(t)\right) - \sum_i \delta p_i(t) C_{\mathrm{eq},i} - \sum_i p_{\mathrm{eq},i}\delta C_i(t) \\
&= \delta S(t) + \delta L^{\mathrm{d}}(t) + \min\left(0, \delta\mathscr{E}_0(t)\right) - \sum_i \frac{p_{\mathrm{eq},i}C_{\mathrm{eq},i}}{kL_0}\delta S(t) \\
&\quad - \sum_i \frac{p_{\mathrm{eq},i}C_{\mathrm{eq},i}}{z_i\gamma_{\mathrm{eq},i}} \min\left(0, \delta\mathscr{E}_i(t)\right) - \sum_i \frac{p_{\mathrm{eq},i}C_{\mathrm{eq},i}}{B_{\mathrm{eq}}} \min\left(0, \delta h(t)\right) \\
&= \frac{1}{1+\varphi}\delta S(t) + \delta L^{\mathrm{d}}(t) + \min\left(0, \delta\mathscr{E}_0(t)\right) - \min\left(0, \delta h(t)\right) \\
&\quad - \sum_i \frac{p_{\mathrm{eq},i}C_{\mathrm{eq},i}}{z_i\gamma_{\mathrm{eq},i}} \min\left(0, \delta\mathscr{E}_i(t)\right) \\
&= \delta h(t) - \min\left(0, \delta h(t)\right). \qquad \text{(V.66)}
\end{aligned}$$

Since $S_{\mathrm{eq}} = 0$, rescaling by wages does not affect the previous expression.

A.3.5 Linear imbalances

In this section we will use the notation $\sum_{i\leftarrow j}$ to denote sums over all suppliers j of firm i. Furthermore, we will only show the results from computations since they are quite lengthy.

Forecast We have

$$\begin{aligned}
\delta\mathbb{E}_t[\mathscr{E}_i] = z_i\delta\gamma_i(t) + \delta I_{ii}(t) - \frac{1}{b}\sum_j \frac{x_{\mathrm{eq},ij}}{\gamma_{\mathrm{eq},j}}\delta\widehat{\gamma}_j(t) + \sum_{j\leftarrow i}\delta I_{ji}(t-1) \\
- \frac{C_{\mathrm{eq},i}}{kL_0}\delta S(t-1) + \frac{C_{\mathrm{eq},i}}{p_{\mathrm{eq},i}}\delta p_i(t-1),
\end{aligned} \qquad \text{(V.67)}$$

$$\begin{aligned}
\delta\mathbb{E}_t[\pi_i] &= z_i\gamma_{\mathrm{eq},i}\delta p_i(t) - \sum_j x_{\mathrm{eq},ij}\delta p_j(t) - \frac{p_{\mathrm{eq},i}}{b}\left(z_i\delta\widehat{\gamma}_i(t) - \sum_j \frac{x_{\mathrm{eq},ji}}{\gamma_{\mathrm{eq},j}}\delta\widehat{\gamma}_j(t)\right) \\
&\quad + \sum_{i\leftarrow j} p_{\mathrm{eq},j}\delta I_{ij}(t-1) - p_{\mathrm{eq},i}\sum_{j\leftarrow i}\delta I_{ji}(t-1) \\
&\quad - C_{\mathrm{eq},i}\delta p_i(t-1) + \frac{p_{\mathrm{eq},i}C_{\mathrm{eq},i}}{kL_0}\delta S(t-1).
\end{aligned} \qquad \text{(V.68)}$$

Realized We have

$$\begin{aligned}
\delta\mathscr{E}_i(t) = z_i\delta\gamma_i(t) - \frac{1}{b}\sum_j \frac{x_{\mathrm{eq},ij}}{\gamma_{\mathrm{eq},j}}\delta\widehat{\gamma}_j(t+1) + \sum_{j\leftarrow i}\delta I_{ji}(t) + \delta I_{ii}(t) \\
- \frac{C_{\mathrm{eq},i}}{kL_0}\delta S(t) + \frac{C_{\mathrm{eq},i}}{p_{\mathrm{eq},i}}\delta p_i(t),
\end{aligned} \qquad \text{(V.69)}$$

$$\begin{aligned}\delta\pi_i(t) = z_i\gamma_{\mathrm{eq},i}\delta p_i(t) - \sum_j x_{\mathrm{eq},ij}\delta p_j(t) - \frac{p_{\mathrm{eq},i}}{b}\left(z_i\delta\widehat{\gamma}_i(t+1) - \sum_j \frac{x_{\mathrm{eq},ji}}{\gamma_{\mathrm{eq},j}}\delta\widehat{\gamma}_j(t+1)\right)\\ + \sum_{i\leftarrow j} p_{\mathrm{eq},j}\delta I_{ij}(t) - p_{\mathrm{eq},i}\sum_{j\leftarrow i}\delta I_{ji}(t) + p_{\mathrm{eq},i}\frac{C_{\mathrm{eq},i}}{kL_0}\delta S(t) - C_{\mathrm{eq},i}\delta p_i(t)\\ + \frac{p_{\mathrm{eq},i}C_{\mathrm{eq},i}}{B_{\mathrm{eq}}}\min\left(0,\delta h(t)\right) - \frac{x_{\mathrm{eq},i0}}{L_{\mathrm{eq}}}\min\left(0,\delta\mathscr{E}_0(t)\right)\\ + p_{\mathrm{eq},i}\min\left(0,\delta\mathscr{E}_i(t)\right) - \sum_j \frac{x_{\mathrm{eq},ij}p_{\mathrm{eq},j}}{z_j\gamma_{\mathrm{eq},j}}\min\left(0,\delta\mathscr{E}_j(t)\right).\end{aligned} \tag{V.70}$$

A.3.6 Linear production

Using the Leontief production function and the explicit forms for $x_{\mathrm{eq},ij}$, we have

$$\gamma_i(t+1) = \gamma_{\mathrm{eq},i}\exp\left(b\min\left[\min_j\left(\frac{\delta x^{\mathrm{a}}_{ij}(t)}{x_{\mathrm{eq},ij}}\right), \frac{\delta x_{i0}(t)}{x_{\mathrm{eq},i0}}\right]\right).$$

With the expressions obtained for the different perturbations (Eqs. (V.56a) and (V.59)), it is possible to get the perturbation of the production as a function of the perturbation of the target

$$\delta\gamma_i(t+1) = \delta\widehat{\gamma}_i(t+1) + b\gamma_{\mathrm{eq},i}\min\left\{\min_j\left(\frac{\min\left(0,\delta\mathscr{E}_j(t)\right)}{z_j\gamma_{\mathrm{eq},j}}\right), \frac{\min\left(0,\delta\mathscr{E}_0(t)\right)}{L_{\mathrm{eq}}}\right\}. \tag{V.71}$$

A.3.7 Linear inventories

It is easy to obtain the perturbation for both diagonal and non diagonal stocks

$$\delta I_{ii}(t+1) = e^{-\sigma_i}\left(\delta\mathscr{E}_i(t) - \min\left(0,\delta\mathscr{E}_i(t)\right) - \frac{C_{\mathrm{eq},i}}{B_{\mathrm{eq}}}\min\left(0,\delta h(t)\right)\right) \tag{V.72}$$

$$\begin{aligned}\delta I_{ij}(t+1) = e^{-\sigma_j}x_{\mathrm{eq},ij}\left(\frac{\min\left(0,\delta\mathscr{E}_j(t)\right)}{z_j\gamma_{\mathrm{eq},j}}\right.\\ \left. - \min\left\{\min_k\left(\frac{\min\left(0,\delta\mathscr{E}_k(t)\right)}{z_j\gamma_{\mathrm{eq},j}}\right), \frac{\min\left(0,\delta\mathscr{E}_0(t)\right)}{L_{\mathrm{eq}}}\right\}\right).\end{aligned} \tag{V.73}$$

A.3.8 Linear updates

Finally, updates on prices and production targets can be deduced easily from linear imbalances (both forecast and realized)

$$\delta\widehat{\gamma}_i(t+1) = \delta\gamma_i(t) - \beta'\frac{\delta\mathbb{E}_t[\mathscr{E}_i]}{z_i} + \beta\frac{\delta\mathbb{E}_t[\pi_i]}{z_i p_{\mathrm{eq},i}} \tag{V.74a}$$

$$\delta p_i(t+1) = \delta p_i(t) - \alpha\frac{p_{\mathrm{eq},i}}{z_i\gamma_{\mathrm{eq},i}}\delta\mathscr{E}_i(t) - \alpha'\frac{\delta\pi_i}{z_i\gamma_{\mathrm{eq},i}} + \omega\frac{p_{\mathrm{eq},i}}{L_{\mathrm{eq}}}\delta\mathscr{E}_0(t), \tag{V.74b}$$

where we took wage rescaling into account.

B State space vector, forecast and cones

In this appendix, we detail the geometric structure of the model at linear level. We will use the following notations. Let $\mathbb{M}$ be a square matrix. We denote by $\mathscr{C}_i(\mathbb{M})$ the i-th column of $\mathbb{M}$ (column vector) and by $\mathscr{L}_i(\mathbb{M})$ the i-th row of $\mathbb{M}$ (row vector). Furthermore, we denote by $\otimes$ the Kronecker product. For $\mathbb{A} \in \mathcal{M}_{p,q}$ and $\mathbb{B} \in \mathcal{M}_{n,m}$, then $\mathbb{A} \otimes \mathbb{B} \in \mathcal{M}_{pn,qm}$ is composed of p block rows and q block columns such that block r, s reads $\mathbb{A}_{rs}\mathbb{B}$. Furthermore, we will denote by $\boldsymbol{\epsilon}_i$ the i-th canonical column vector of $\mathbb{R}^N$ and by $\mathbf{E}_{ij} = \boldsymbol{\epsilon}_i \boldsymbol{\epsilon}_j^\top$ the matrices of the canonical basis of $\mathcal{M}_{N\times N}$.

B.1 Two steps dynamics

Similarly to Chapter IV, our dynamics can be decomposed in two steps: forecasts and exchanges. Each step needs different state space vectors. Forecasts will need information on current productions, prices, stocks and savings as well as previous targets, prices, stocks and savings (see Eqs. (V.68)-(V.67)). At time t, the forecast matrix $\mathbb{F}$ will thus act on the intermediate state vector

$$\mathbf{U}_f(t) = \begin{pmatrix} \delta\widehat{\boldsymbol{\gamma}}(t) \\ \delta\boldsymbol{\gamma}(t) \\ \delta\boldsymbol{p}(t) \\ \delta\boldsymbol{I}(t) \\ \delta S(t) \\ \delta\widehat{\boldsymbol{\gamma}}(t-1) \\ \delta\boldsymbol{\gamma}(t-1) \\ \delta\boldsymbol{p}(t-1) \\ \delta\boldsymbol{I}(t-1) \\ \delta S(t-1) \end{pmatrix}, \tag{V.75}$$

and outputs the target $\delta\widehat{\gamma}(t+1)$ along with other relevant quantities for the update step.

The update step only needs the target $\delta\widehat{\gamma}(t+1)$ along with current productions, prices, stocks and savings. Therefore, the exchange matrix $\mathbb{E}$ solely acts on the state vector

$$\mathbf{U}_e(t) = \begin{pmatrix} \delta\widehat{\boldsymbol{\gamma}}(t+1) \\ \delta\boldsymbol{\gamma}(t) \\ \delta\boldsymbol{p}(t) \\ \delta\boldsymbol{I}(t) \\ \delta S(t) \end{pmatrix}. \tag{V.76}$$

Here we consider that the matrix of perturbations on stocks has been flattened row-wise

$$\boldsymbol{\delta I} = \begin{pmatrix} \delta I_{11} \\ \delta I_{21} \\ \vdots \end{pmatrix}. \tag{V.77}$$

We can see that one needs to keep track on the state vector

$$\mathbf{U}(t) = \begin{pmatrix} \delta\widehat{\boldsymbol{\gamma}}(t+1) \\ \delta\boldsymbol{\gamma}(t) \\ \delta\boldsymbol{p}(t) \\ \delta\boldsymbol{I}(t) \\ \delta S(t) \\ \delta\widehat{\boldsymbol{\gamma}}(t) \end{pmatrix} \in \mathbb{R}^{N^2+4N+1}. \tag{V.78}$$

which carries every information. The exchange step may be written as follows

$$\begin{pmatrix} \mathbb{S}(t) & \mathbf{0} \\ \mathbf{P} & \mathbf{Q} \end{pmatrix} \begin{pmatrix} \delta\widehat{\boldsymbol{\gamma}}(t) \\ \delta\boldsymbol{\gamma}(t-1) \\ \delta\boldsymbol{p}(t-1) \\ \delta\boldsymbol{I}(t-1) \\ \delta S(t-1) \\ \delta\widehat{\boldsymbol{\gamma}}(t-1) \end{pmatrix} = \begin{pmatrix} \delta\widehat{\boldsymbol{\gamma}}(t) \\ \delta\boldsymbol{\gamma}(t) \\ \delta\boldsymbol{p}(t) \\ \delta\boldsymbol{I}(t) \\ \delta S(t) \\ \delta\widehat{\boldsymbol{\gamma}}(t-1) \\ \delta\boldsymbol{\gamma}(t-1) \\ \delta\boldsymbol{p}(t-1) \\ \delta\boldsymbol{I}(t-1) \\ \delta S(t-1) \end{pmatrix}. \tag{V.79}$$

where $\mathbb{S}(t) \in \mathcal{M}_{N^2+3N+1,N^2+3N+1}(\mathbb{R})$ encodes the update steps of Eqs. (V.74b), (V.71), (V.72), (V.73), (V.66); and $\mathbf{P}$ and $\mathbf{Q}$ take care of the projection of the $(t-1)$-vectors

$$\mathbf{P} = \begin{pmatrix} \mathbf{0}_N & \mathbf{0}_N & \mathbf{0}_N & \mathbf{0}_{N,N^2} & \vec{0}_N \\ \mathbf{0}_N & \mathbf{I}_N & \mathbf{0}_N & \mathbf{0}_{N,N^2} & \vec{0}_N \\ \mathbf{0}_N & \mathbf{0}_N & \mathbf{I}_N & \mathbf{0}_{N,N^2} & \vec{0}_N \\ \mathbf{0}_{N^2,N} & \mathbf{0}_{N^2,N} & \mathbf{0}_{N^2,N} & \mathbf{I}_{N^2,N^2} & \vec{0}_{N^2} \\ \vec{0}_N^\top & \vec{0}_N^\top & \vec{0}_N^\top & \vec{0}_{N^2}^\top & 1 \end{pmatrix} \in \mathcal{M}_{N^2+3N+1,N^2+3N+1}(\mathbb{R}) \tag{V.80}$$

$$\mathbf{Q} = \begin{pmatrix} \mathbf{I}_N \\ \mathbf{0}_{N^2+3N+1,N} \end{pmatrix} \in \mathcal{M}_{N^2+3N+1,N}(\mathbb{R}). \tag{V.81}$$

The forecast step can then be expressed as

$$\begin{pmatrix} \mathbb{F}_1 & \mathbb{F}_2 \\ \mathbf{Q}^\top & \mathbf{0} \end{pmatrix} \begin{pmatrix} \delta\widehat{\boldsymbol{\gamma}}(t) \\ \delta\boldsymbol{\gamma}(t) \\ \delta\boldsymbol{p}(t) \\ \delta\boldsymbol{I}(t) \\ \delta S(t) \\ \delta\widehat{\boldsymbol{\gamma}}(t-1) \\ \delta\boldsymbol{\gamma}(t-1) \\ \delta\boldsymbol{p}(t-1) \\ \delta\boldsymbol{I}(t-1) \\ \delta S(t-1) \end{pmatrix} = \begin{pmatrix} \delta\widehat{\boldsymbol{\gamma}}(t+1) \\ \delta\boldsymbol{\gamma}(t) \\ \delta\boldsymbol{p}(t) \\ \delta\boldsymbol{I}(t) \\ \delta S(t) \\ \delta\widehat{\boldsymbol{\gamma}}(t) \end{pmatrix}. \tag{V.82}$$

where $\mathbb{F}_1$ and $\mathbb{F}_2$ encode Eq. (V.74a). Finally, the whole process may be written as

$$\mathbf{U}(t+1) = \begin{pmatrix} \mathbb{F}_1 & \mathbb{F}_2 \\ \mathbf{Q}^\top & \mathbf{0} \end{pmatrix} \begin{pmatrix} \mathbb{S}(t) & \mathbf{0} \\ \mathbf{P} & \mathbf{Q} \end{pmatrix} \mathbf{U}(t) = \begin{pmatrix} \mathbb{F}_1\mathbb{S}(t) + \mathbb{F}_2\mathbf{P} & \mathbb{F}_2\mathbf{Q} \\ \mathbf{Q}^\top\mathbb{S}(t) & \mathbf{0} \end{pmatrix} \mathbf{U}(t) \tag{V.83}$$

B.2 Forecast matrices $\mathbb{F}_i$

We will denote by $\mathbb{A}$ the adjacency matrix of the network, i.e. $\mathbb{A}_{ij} = 1$ if j supplies to i. We write forecast matrices as follows

$$\mathbb{F}_1 = \begin{pmatrix} \mathbf{V}_1 & \mathbf{W}_1 & \mathbf{X}_1 & \mathbf{Y}_1 & \mathbf{0} \\ \mathbf{0} & \mathbf{I} & \mathbf{0} & \mathbf{0} & \mathbf{0} \\ \mathbf{0} & \mathbf{0} & \mathbf{I} & \mathbf{0} & \mathbf{0} \\ \mathbf{0} & \mathbf{0} & \mathbf{0} & \mathbf{I} & \mathbf{0} \\ \mathbf{0} & \mathbf{0} & \mathbf{0} & \mathbf{0} & 1 \end{pmatrix} \tag{V.84a}$$

$$\mathbb{F}_2 = \begin{pmatrix} \mathbf{0} & \mathbf{0} & \mathbf{X}_2 & \mathbf{Y}_2 & \mathbf{Z}_2 \\ \mathbf{0} & \mathbf{0} & \mathbf{0} & \mathbf{0} & \mathbf{0} \\ \mathbf{0} & \mathbf{0} & \mathbf{0} & \mathbf{0} & \mathbf{0} \\ \mathbf{0} & \mathbf{0} & \mathbf{0} & \mathbf{0} & \mathbf{0} \\ \mathbf{0} & \mathbf{0} & \mathbf{0} & \mathbf{0} & 0 \end{pmatrix}, \tag{V.84b}$$

where

$$\begin{aligned}
\mathbf{V}_1 &= -\beta' \boldsymbol{\Delta}\left(z_i^{-1}\right) \mathbf{M}_2^\top + \beta' \mathbf{I}_N - \frac{\beta}{b} \boldsymbol{\Delta}\left(z_i^{-1}\right) \mathbf{M}_1^\top \\
\mathbf{W}_1 &= (1-\beta') \mathbf{I}_N \\
\mathbf{X}_1 &= \beta \boldsymbol{\Delta}\left(\frac{\gamma_{\mathrm{eq},i}}{z_i p_{\mathrm{eq},i}}\right) \mathbf{M}_1 \\
\mathbf{Y}_1 &= -\beta' \sum_\ell z_\ell^{-1} \boldsymbol{\epsilon}_\ell^\top \otimes \mathbf{E}_{\ell\ell} \\
\mathbf{X}_2 &= -(\beta+\beta') \boldsymbol{\Delta}\left(\frac{C_{\mathrm{eq},i}}{z_i p_{\mathrm{eq},i}}\right) \\
\mathbf{Y}_2 &= -(\beta'+\beta) \boldsymbol{\Delta}\left(z_i^{-1}\right) \sum_\ell \epsilon_\ell^\top \otimes \left(\epsilon_\ell \mathscr{L}_\ell(\mathbb{A}^\top)\right) \\
&\quad + \beta \boldsymbol{\Delta}\left(z_i^{-1} p_{\mathrm{eq},i}^{-1}\right) \sum_\ell \epsilon_\ell^\top \otimes \boldsymbol{\Delta}\left(\mathscr{L}_l(\mathbb{A})\right) \boldsymbol{\Delta}\left(p_{\mathrm{eq},i}\right), \\
\mathbf{Z}_2 &= (\beta+\beta') \frac{\mathbf{C}_{\mathrm{eq}}}{\mathbf{z} k L_0}
\end{aligned}$$

and where we have defined matrices $\mathbf{M}_{1/2}$ as

$$\begin{aligned}
\mathbf{M}_1 &= \boldsymbol{\Delta}\left(z_i\right) - \boldsymbol{\Delta}\left(\gamma_{\mathrm{eq},i}^{\frac{1-b}{b}}\right) \boldsymbol{J} \\
\mathbf{M}_2 &= \boldsymbol{\Delta}\left(z_i\right) - \frac{1}{b} \boldsymbol{\Delta}\left(\gamma_{\mathrm{eq},i}^{\frac{1-b}{b}}\right) \boldsymbol{J}.
\end{aligned}$$

B.3 Exchanges and cones

In the same way as in Chapter IV, the position of state vector $\mathbb{U}(t)$ in state space conditions the specific exchange matrix that will govern the dynamics. The description of the different regions over which the update matrix is constant is a lot more cumbersome for this model. Not only do they depend on the signs of $\delta\mathscr{E}_i(t), \delta\mathscr{E}_0(t), \delta h(t)$ but one also needs to consider the relative magnitude of the quantities $\delta\mathscr{E}_i(t)$ in Eq. (V.71) and Eq. (V.73), which therefore adds another layer of complexity.

B.3.1 Cone vectors

At linear level, we can express the quantities $\delta\mathscr{E}_i(t), \delta\mathscr{E}_0(t), \delta h(t)$ as overlaps between $\mathbf{U}(t)$ and fixed column vectors $\mathbf{c}_{g,i}, \mathbf{c}_w, \mathbf{c}_h(t)$ such that

$$\mathbf{c}_{g,i}^\top = \left(-\frac{1}{b}\mathscr{L}_i\left(\mathbf{J}\boldsymbol{\Delta}\left(\boldsymbol{\gamma}_{\rm eq}^{(1-b)/b}\right)\right), z_i\boldsymbol{\epsilon}_i, \frac{C_{{\rm eq},i}}{p_{{\rm eq},i}}\boldsymbol{\epsilon}_i, \boldsymbol{\epsilon}_i \otimes \left[\boldsymbol{\epsilon}_i^\top + \mathscr{L}_i(\mathbb{A}^\top)\right], -\frac{C_{{\rm eq},i}}{kL_0}, \vec{0}_N\right)$$
$$\mathbf{c}_w^\top = \left(-\frac{1}{b}\left(\boldsymbol{\Delta}\left(\boldsymbol{\gamma}_{\rm eq}^{(1-b)/b}\right)\mathbf{J}_0\right)^\top, \vec{0}_N, \vec{0}_N, \vec{0}_{N^2}, -\frac{1}{1+\varphi}, \vec{0}_N\right).$$

Some regions of space with a constant stability matrix are similar to those of Chapter IV, but others are much more complex. For a firm i, we will denote by ∂_i^+ the set of suppliers or i, and ∂_i^- the set of buyers of i.

Plentiful supply, partial unemployment Here $\delta\mathscr{E}_0(t) > 0$, i.e. more workforce is available that actual word demands, and every firms have enough supply in goods $\delta\mathscr{E}_i(t) > 0$. In this case, $\mathbf{c}_h = -\mathbf{c}_w$ and therefore $\delta h < 0$ which implies that no savings are made for the next period. This also impacts profits which are lower. The associated matrix is called $\mathbb{S}_0$.

Plentiful supply, full employment Here $\delta\mathscr{E}_0(t) < 0$, i.e. work demands are very high and the household is fully employed, and every firms have enough supply in goods $\delta\mathscr{E}_i(t) > 0$. In this case, $\mathbf{c}_h = 0$ and therefore $\delta h = 0$ which implies that no savings are made for the next period (the household works exactly the amount planned). Productions are capped by work availability and stocks of inputs are made since they were not exhausted due lacking manpower. The associated matrix is called $\mathbb{S}_w$.

Partial (or full) good shortage, full employment Here again $\delta\mathscr{E}_0(t) < 0$, however there are some firms that cannot satisfy demands due to a lack of supply. We call $S \subseteq [\![1, N]\!]$ the subset of firms that are defaulting. In this case

$$\delta h(t) = -\sum_{k\in S}\frac{p_{{\rm eq},k}C_{{\rm eq},k}}{z_k\gamma_{{\rm eq},k}}\delta\mathscr{E}_k(t),$$

rendering $\delta h(t) > 0$. The household therefore saves some money for the next period. Production is capped by either scarcest goods or lack of manpower, and stocks of inputs are replenished. Here the form of the associated stability matrix is still undefined. Indeed, considering one firm i with two defaulting suppliers k, j its perturbation on production reads

$$\delta\gamma_i(t+1) = \delta\widehat{\gamma}_i(t+1) + b\gamma_{{\rm eq},i}\min\left(\frac{\delta\mathscr{E}_k(t)}{z_k\gamma_{{\rm eq},k}}, \frac{\delta\mathscr{E}_j(t)}{z_j\gamma_{{\rm eq},j}}, \frac{\delta\mathscr{E}_0(t)}{L_{\rm eq}}\right),$$

which can have three different outcomes. In general, the number $N(S)$ of possible matrices is given by

$$N(S) = \prod_{\substack{i=1\\ S\cap\partial_i^+\neq\emptyset}}^{N}(1 + |S\cap\partial_i^+|),$$

where $|\mathcal{A}|$ denotes the cardinality of set $\mathcal{A}$. For example, if only firm k is defaulting then

$$N(S) = 2^{|\partial_k^-|}.$$

The associated matrices are called $\mathbb{S}_{g,w}(t)$

Partial (or full) good shortage, partial unemployment Here again $\delta\mathscr{E}_0(t) > 0$ so that manpower is not lacking, however there is still a subset S of firms that cannot answer demands due to a lack of supply. In this case

$$\delta h(t) = -\delta\mathscr{E}_0(t) - \sum_{k\in S} \frac{p_{\mathrm{eq},k}C_{\mathrm{eq},k}}{z_k\gamma_{\mathrm{eq},k}}\delta\mathscr{E}_k(t),$$

and we can have both situations $\delta h(t) \gtrless 0$.

Budget shortage Here $\delta h(t) < 0$. Even though consumption offers are lower than planned, the budget is still too little to consume.

No budget shortage Here $\delta h(t) > 0$. Firms offers are so low that the budget, even though lower than anticipated, is enough to consume.

In both situations $\delta h(t) \gtrless 0$, productions are capped by the scarcest goods and we still end up in a similar situation as before where now the number of possible matrices is

$$\prod_{\substack{i=1\\ S\cap\partial_i^+\neq\emptyset}}^{N} |S\cap\partial_i^+|,$$

since manpower is not lacking. The associated matrices are called $\mathbb{S}_S(t)$ (resp. $\mathbb{S}_{S,b}$) in the case of no budget shortage (resp. budget shortage).

B.4 The matrix $\mathbb{S}_0$

The matrix $\mathbb{S}_0$ associated to the plentiful supply and partial unemployment cone has the structure

$$\mathbb{S}_0 = \begin{pmatrix} \mathbf{I}_N & \mathbf{0} & \mathbf{0} & \mathbf{0} & \vec{0} \\ \mathbf{I}_N & \mathbf{0} & \mathbf{0} & \mathbf{0} & \vec{0} \\ \mathbf{A} & \mathbf{B} & \mathbf{C} & \mathbf{D} & \mathbf{E} \\ \mathbf{F} & \mathbf{G} & \mathbf{H} & \mathbf{I} & \mathbf{J} \\ \vec{0}^\top & \vec{0}^\top & \vec{0}^\top & \vec{0}^\top & 0 \end{pmatrix} \tag{V.85}$$

with

$$\mathbf{A} = \mathbf{\Delta}\left(\frac{p_{\mathrm{eq},i}}{\gamma_{\mathrm{eq},i}}\right)\left(\alpha\mathbf{I} - \left(\frac{\omega\boldsymbol{\gamma}_{\mathrm{eq}}}{bL_{\mathrm{eq}}}\right)\mathbf{e}\left(\mathbf{V}\boldsymbol{\gamma}_{\mathrm{eq}}^{(1-b)/b}\right)^{\top}\right) + \mathbf{\Delta}\left(\frac{p_{\mathrm{eq},i}}{z_i\gamma_{\mathrm{eq},i}}\right)\left(\frac{\alpha'}{b}\mathbf{M}_1^{\top} - \alpha\mathbf{M}_2^{T}\right)$$
$$- \alpha'\left(\frac{p_{\mathrm{eq},\mathbf{C}_{\mathrm{eq}}}}{b\mathbf{z}\boldsymbol{\gamma}_{\mathrm{eq}}B_{\mathrm{eq}}}\right)\left(\mathbf{V}\boldsymbol{\gamma}_{\mathrm{eq}}^{(1-b)/b}\right)^{\top} \tag{V.86}$$

$$\mathbf{B} = -\alpha\mathbf{\Delta}\left(\frac{p_{\mathrm{eq},i}}{\gamma_{\mathrm{eq},i}}\right) \tag{V.87}$$

$$\mathbf{C} = \mathbf{I} - (\alpha - \alpha')\mathbf{\Delta}\left(\frac{C_{\mathrm{eq},i}}{z_i\gamma_{\mathrm{eq},i}}\right) - \alpha'\mathbf{\Delta}\left(\mathbf{z}^{-1}\right)\mathbf{M}_1 \tag{V.88}$$

$$\mathbf{D} = (\alpha' - \alpha)\mathbf{\Delta}\left(\frac{p_{\mathrm{eq},i}}{z_i\gamma_{\mathrm{eq},i}}\right)\sum_k \epsilon_k^{\top} \otimes (\epsilon_k(\epsilon_k^{\top} + \mathscr{L}_k(\mathbb{A}^{\top})))$$
$$- \alpha'\mathbf{\Delta}\left(\mathbf{z}^{-1}\boldsymbol{\gamma}_{\mathrm{eq}}^{-1}\right)\left(\sum_\ell \epsilon_\ell^{\top} \otimes \mathbf{\Delta}\left(\epsilon_k^{\top} + \mathscr{L}_\ell(\mathbb{A})\right)\mathbf{\Delta}\left(p_{\mathrm{eq},i}\right)\right) \tag{V.89}$$

$$\mathbf{E} = \alpha\frac{\mathbf{p}_{\mathrm{eq}}\mathbf{C}_{\mathrm{eq}}}{\mathbf{z}\boldsymbol{\gamma}_{\mathrm{eq}}kL_0} - \omega\frac{\mathbf{p}_{\mathrm{eq}}}{(1+\varphi)L_{\mathrm{eq}}} - \alpha'\frac{\mathbf{p}_{\mathrm{eq}}\mathbf{C}_{\mathrm{eq}}}{\mathbf{z}\boldsymbol{\gamma}_{\mathrm{eq}}(1+\varphi)B_{\mathrm{eq}}} \tag{V.90}$$

$$\mathbf{F} = \sum_i e^{-\sigma_i}\epsilon_i \otimes \left(\epsilon_i\mathbf{o}_i^{\top}\right) \tag{V.91}$$

$$\mathbf{G} = \sum_i e^{-\sigma_i}z_i\epsilon_i \otimes \mathbf{E}_{ii} \tag{V.92}$$

$$\mathbf{H} = \sum_i e^{-\sigma_i}\frac{C_{\mathrm{eq},i}}{p_{\mathrm{eq},i}}\epsilon_i \otimes \mathbf{E}_{ii} \tag{V.93}$$

$$\mathbf{I} = \sum_i e^{-\sigma_i}\mathbf{E}_{ii} \otimes \left(\epsilon_i(\epsilon_i^{\top} + \mathscr{L}_i(\mathbb{A}^{\top})\right) \tag{V.94}$$

$$\mathbf{J} = -\frac{1}{B_{\mathrm{eq}}}\sum_i e^{-\sigma_i}C_{\mathrm{eq},i}\epsilon_i \otimes \epsilon_i \tag{V.95}$$

with

$$\mathbf{o}_i = \mathscr{C}_i(\mathbf{M_2}) - z_i\epsilon_i - \frac{1}{b}\frac{C_{\mathrm{eq},i}}{B_{\mathrm{eq}}}(\mathbf{V}\boldsymbol{\gamma}_{\mathrm{eq}}^{(1-b)/b}) \tag{V.96}$$

C Study of the matrix $\mathbb{D}_0$ in the large productivity limit

We denote by $\mathbb{D}_0$ the dynamical matrix associated to $\mathbb{S}_0$. It reads

$$\mathbb{D}_0 = \begin{pmatrix} \mathbb{F}_1\mathbb{S}(t) + \mathbb{F}_2\mathbf{P} & \mathbb{F}_2\mathbf{Q} \\ \mathbf{Q}^{\top}\mathbb{S}(t) & \mathbf{0} \end{pmatrix} := \left(\begin{array}{ccccc|c} \mathbf{T}_{11} & \mathbf{T}_{12} & \mathbf{T}_{13} & \mathbf{T}_{14} & \mathbf{T}_{15} & \\ \mathbf{I}_N & \mathbf{0} & \mathbf{0} & \mathbf{0} & \vec{0} & \\ \mathbf{A} & \mathbf{B} & \mathbf{C} & \mathbf{D} & \mathbf{E} & \mathbf{0} \\ \mathbf{F} & \mathbf{G} & \mathbf{H} & \mathbf{I} & \mathbf{J} & \\ \vec{0}^{\top} & \vec{0}^{\top} & \vec{0}^{\top} & \vec{0}^{\top} & 0 & \\ \hline & & \mathbf{Q}^{\top} & & & \mathbf{0} \end{array}\right) \tag{V.97}$$

with

$$\mathbf{T}_{11} = \mathbf{V}_1 + \mathbf{W}_1 + \mathbf{X}_1\mathbf{T}\mathbf{A} + \mathbf{Y}_1\mathbf{F} \tag{V.98}$$
$$\mathbf{T}_{12} = \mathbf{X}_1\mathbf{B} + \mathbf{Y}_1\mathbf{G} \tag{V.99}$$
$$\mathbf{T}_{13} = \mathbf{X}_1\mathbf{C} + \mathbf{Y}_1\mathbf{H} + \mathbf{X}_2 \tag{V.100}$$
$$\mathbf{T}_{14} = \mathbf{X}_1\mathbf{D} + \mathbf{Y}_1\mathbf{I} + \mathbf{Y}_2 \tag{V.101}$$

and where we do not give the expression of $\mathbf{T}_{15}$ since it will be irrelevant.

It follows that

$$\mathrm{Sp}\left(\mathbb{D}_0\right) = \{0\}^{N+1} \cup \mathrm{Sp}\begin{pmatrix} \mathbf{T}_{11} & \mathbf{T}_{12} & \mathbf{T}_{13} & \mathbf{T}_{14} \\ \mathbf{I}_N & \mathbf{0} & \mathbf{0} & \mathbf{0} \\ \mathbf{A} & \mathbf{B} & \mathbf{C} & \mathbf{D} \\ \mathbf{F} & \mathbf{G} & \mathbf{H} & \mathbf{I} \end{pmatrix} \tag{V.102}$$

Using notations from Appendix D, we can make the following determinant computation for $N_s = N^2 + 4N + 1$:

$$\begin{aligned}
\det\left(\mu\mathbf{I}_{N_s} - \mathbb{D}_0\right) &= \mu^{N+1}\begin{vmatrix} \mu\mathbf{I}_N - \mathbf{T}_{11} & -\mathbf{T}_{12} & -\mathbf{T}_{13} & -\mathbf{T}_{14} \\ -\mathbf{I}_N & \mu\mathbf{I}_N & \mathbf{0} & \mathbf{0} \\ -\mathbf{A} & -\mathbf{B} & \mu\mathbf{I}_N - \mathbf{C} & -\mathbf{D} \\ -\mathbf{F} & -\mathbf{G} & -\mathbf{H} & \mu\mathbf{I}_{N^2} - \mathbf{I} \end{vmatrix} \\
&= \mu^{N+1}\det\left(\mu\mathbf{I}_{N^2} - \mathbf{I}\right) \\
&\quad \times \left| \begin{pmatrix} \mu\mathbf{I}_N - \mathbf{T}_{11} & -\mathbf{T}_{12} & -\mathbf{T}_{13} \\ -\mathbf{I}_N & \mu\mathbf{I}_N & \mathbf{0} \\ -\mathbf{A} & -\mathbf{B} & \mu\mathbf{I}_N - \mathbf{C} \end{pmatrix} - \begin{pmatrix} \mathbf{T}_{14} \\ \mathbf{0} \\ \mathbf{D} \end{pmatrix} \left(\mu\mathbf{I}_{N^2} - \mathbf{I}\right)^{-1} \begin{pmatrix} \mathbf{F} & \mathbf{G} & \mathbf{H} \end{pmatrix} \right| \\
&= \mu^{N+1}\det\left(\mu\mathbf{I}_{N^2} - \mathbf{I}\right) \\
&\quad \times \begin{vmatrix} \mu\mathbf{I}_N - \mathbf{T}_{11} - \mathbf{T}_{14}\widetilde{\mathbf{F}}(\mu) & -\mathbf{T}_{12} - \mathbf{T}_{14}\widetilde{\mathbf{G}}(\mu) & -\mathbf{T}_{13} - \mathbf{T}_{14}\widetilde{\mathbf{H}}(\mu) \\ -\mathbf{I}_N & \mu\mathbf{I}_N & \mathbf{0} \\ -\mathbf{A} - \mathbf{D}\widetilde{\mathbf{F}}(\mu) & -\mathbf{B} - \mathbf{D}\widetilde{\mathbf{G}}(\mu) & \mu\mathbf{I}_N - \mathbf{C} - \mathbf{D}\widetilde{\mathbf{H}}(\mu) \end{vmatrix} \\
&= \mu^{N+1}\det\left(\mu\mathbf{I}_{N^2} - \mathbf{I}\right)\det\left(\mu\mathbf{I}_N - \mathbf{C} - \mathbf{D}\widetilde{\mathbf{H}}(\mu)\right) \\
&\quad \times \det\Big\{\mu\Big[\mu\mathbf{I}_N - \mathbf{T}_{11} - \mathbf{T}_{14}\widetilde{\mathbf{F}}(\mu) \\
&\qquad - \left(\mathbf{T}_{13} + \mathbf{T}_{14}\widetilde{\mathbf{H}}(\mu)\right)\left(\mu\mathbf{I}_N - \mathbf{C} - \mathbf{D}\widetilde{\mathbf{H}}(\mu)\right)^{-1}\left(\mathbf{A} + \mathbf{D}\widetilde{\mathbf{F}}(\mu)\right)\Big] \\
&\qquad -\mathbf{T}_{12} - \mathbf{T}_{14}\widetilde{\mathbf{G}}(\mu) - \left(\mathbf{T}_{13} + \mathbf{T}_{14}\widetilde{\mathbf{H}}(\mu)\right)\left(\mu\mathbf{I}_N - \mathbf{C} - \mathbf{D}\widetilde{\mathbf{H}}(\mu)\right)^{-1}\left(\mathbf{B} + \mathbf{D}\widetilde{\mathbf{G}}(\mu)\right)\Big\}
\end{aligned} \tag{V.103}$$

where for a generic matrix $\mathbb{M}$ with the right dimension, we define the matrix $\widetilde{\mathbb{M}}$ as

$$\widetilde{\mathbb{M}} = \left(\mu\mathbf{I}_{N^2} - \mathbf{I}\right)^{-1}\mathbb{M}.$$

We also used the block determinant formula

$$\begin{vmatrix} \mathbf{A} & \mathbf{B} \\ \mathbf{C} & \mathbf{D} \end{vmatrix} = \det\mathbf{D}\det\left(\mathbf{A} - \mathbf{B}\mathbf{D}^{-1}\mathbf{C}\right),$$

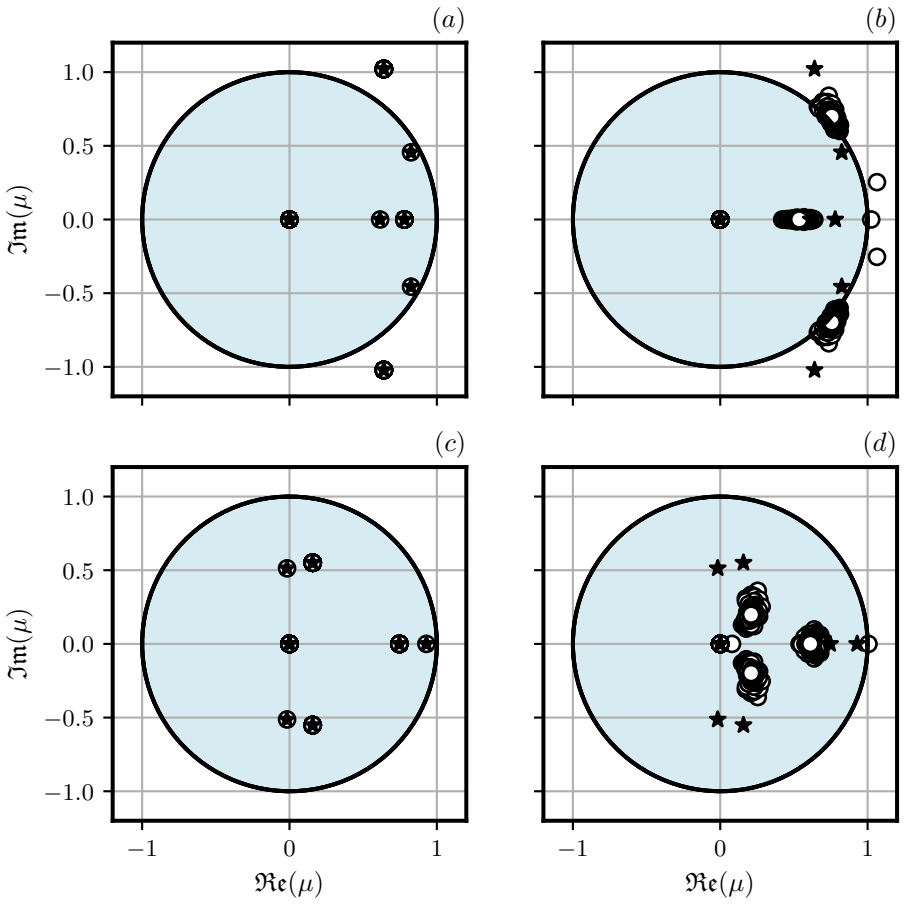


Figure V.16: Eigenvalues μ of $\mathbb{D}_0$ (circles) along with the roots of the polynomial of Eq. (V.104) (black stars). The stability region is represented in light blue. (a) $\varepsilon = 10^4$, $\sigma = 0$. (b) $\varepsilon = 1$, $\sigma = 0$. (c) $\varepsilon = 10^4$, $\sigma = \infty$. (c) $\varepsilon = 1$, $\sigma = \infty$.

for $\mathbf{D}$ an invertible matrix. In Appendix D, we show that, in the large productivity limit $z_i \to \infty$, this characteristic polynomial can be rewritten as

$$\det\left(\mu \mathbf{I}_{N_s} - \mathbb{D}_0\right) = \mu^{N^2+1} \Pi(\mu)^{N-1} \left(\Pi(\mu) + \frac{1}{b}\Xi(\mu)\right). \tag{V.104}$$

One can carry out the same analysis as in Chapter IV to determine stability properties of the matrix $\mathbb{D}_0$ in the large productivity limit. For example, we retrieve a transition line from the simplified model by solving the equation $\Pi(1)+\Xi(1)/b$ i.e. finding the condition on the coefficients such that $\mu = 1$ is a root. We get

$$\alpha\beta = \beta'\omega.$$

D Computational appendix to Appendix C

We present here computations leading to the evaluation of the spectrum of $\mathbb{D}_0$ in the large productivity limit $z_i \to \infty$. We will use the expressions of equilibrium prices and productions in the large productivity limit

$$\boldsymbol{\gamma}_{\text{eq}} = \left(\frac{\boldsymbol{\kappa}}{\mathbf{V}}\right)^b \tag{V.105}$$

$$\mathbf{p}_{\text{eq}} = \frac{\mathbf{V}^b}{\mathbf{z}\boldsymbol{\kappa}^{b-1}}, \tag{V.106}$$

with $\kappa_i = \theta_i L_0$ and we will denote by

$$\mathbf{R} = \frac{1}{L_{\text{eq}}} \left(\frac{\boldsymbol{\kappa}}{\mathbf{V}}\right)^b \left(\mathbf{V}\boldsymbol{\kappa}^{1-b}\right)^\top . \tag{V.107}$$

We will also use the large productivity form of blocks $\mathbf{A}, \mathbf{B}, \mathbf{C}$

$$\mathbf{A} = \frac{1}{b}\boldsymbol{\Delta}\left(\frac{p_{\text{eq},i}}{\gamma_{\text{eq},i}}\right)\left(\boldsymbol{\Delta}\left(\alpha_i'\right) - \boldsymbol{\Delta}\left(\omega + \alpha_i'\right)\mathbf{R}\right) \tag{V.108}$$

$$\mathbf{B} = -\boldsymbol{\Delta}\left(\frac{\alpha_i p_{\text{eq},i}}{\gamma_{\text{eq},i}}\right) \tag{V.109}$$

$$\mathbf{C} = \boldsymbol{\Delta}\left(1 - \alpha_i\right). \tag{V.110}$$

Furthermore, we will assume that inverse time-scales $\alpha_i, \alpha_i', \beta_i, \beta_i'$ are different across firms as subscript i suggests.

D.1 Explicit forms for products of blocks of $\mathbb{D}_0$ and large productivity expressions

D.1.1 Matrix $\mu\mathbf{I}_{N^2} - \mathbf{I}$

The matrix $\mu\mathbf{I}_{N^2} - \mathbf{I}$ is block diagonal with N blocks $\mu\mathbf{I}_N - e^{-\sigma_k}\epsilon_k(\epsilon_k^\top + \mathscr{L}_k(A^\top)) := \mu\mathbf{I}_N - \mathbf{I}_k$. Each block can be inverted and one gets

$$\left(\mu\mathbf{I}_N - \mathbf{I}_k\right)^{-1} = \frac{1}{\mu}\left(\mathbf{I}_N + \frac{\mathbf{I}_k}{\mu - e^{-\sigma_k}}\right),$$

using Sherman-Morison's formula. Finally

$$\left(\mu\mathbf{I}_{N^2} - \mathbf{I}\right)^{-1} = \frac{1}{\mu}\left(\mathbf{I}_{N^2} + \boldsymbol{\Delta}\left(\left(\mu - e^{-\sigma_i}\right)^{-1}\right) \otimes \mathbf{I}_N\mathbf{I}\right). \tag{V.111}$$

Furthermore, the determinant can be expressed as

$$\begin{aligned}
\det\left(\mu\mathbf{I}_{N^2} - \mathbf{I}\right) &= \prod_k \det\left(\mu\mathbf{I}_N - \mathbf{I}_k\right) \\
&= \mu^{N^2}\prod_k \left(1 - \frac{e^{-\sigma_k}(\epsilon_k^\top + \mathscr{L}_k(A^\top))\epsilon_k}{\mu}\right) \\
&= \mu^{N^2-N}\prod_k \left(\mu - e^{-\sigma_k}\right).
\end{aligned}$$

In the following, we will denote by $n_i(\mu)$ the quantity

$$n_i(\mu) = \frac{e^{-\sigma_i}}{\mu - e^{-\sigma_i}}.$$

D.1.2 Products involving I and $(\mu \mathbf{I}_{N^2} - \mathbf{I})^{-1}$

For a generic matrix $\mathbb{M}$ with the right dimension, we define the matrix $\widetilde{\mathbb{M}}$ as

$$\widetilde{\mathbb{M}} = (\mu \mathbf{I}_{N^2} - \mathbf{I})^{-1} \mathbb{M}.$$

We therefore have

$$\begin{aligned}
\mathbf{IH} &= \sum_i (e^{-\sigma_i})^2 \frac{C_{\mathrm{eq},i}}{p_{\mathrm{eq},i}} \epsilon_i \otimes \mathbf{E}_{ii} \\
\widetilde{\mathbf{H}}(\mu) &= \sum_i n_i(\mu) \frac{C_{\mathrm{eq},i}}{p_{\mathrm{eq},i}} \epsilon_i \otimes \mathbf{E}_{ii} \\
\widetilde{\mathbf{G}}(\mu) &= \sum_i n_i(\mu) z_i \epsilon_i \otimes \mathbf{E}_{ii} \\
\widetilde{\mathbf{F}}(\mu) &= \sum_i n_i(\mu) \epsilon_i \otimes \epsilon \mathbf{o}_i^\top.
\end{aligned}$$

D.1.3 Products of D with $\widetilde{(\cdot)}$-matrices

$$\begin{aligned}
\mathbf{D}\widetilde{\mathbf{H}}(\mu) &= -\alpha \boldsymbol{\Delta} \left(n_i(\mu) \frac{C_{\mathrm{eq},i}}{z_i \gamma_{\mathrm{eq},i}} \right) \\
\mathbf{D}\widetilde{\mathbf{G}}(\mu) &= -\alpha \boldsymbol{\Delta} \left(n_i(\mu) \frac{p_{\mathrm{eq},i}}{\gamma_{\mathrm{eq},i}} \right) \\
\mathbf{D}\widetilde{\mathbf{F}}(\mu) &= -\alpha \boldsymbol{\Delta} \left(n_i(\mu) \frac{p_{\mathrm{eq},i}}{z_i \gamma_{\mathrm{eq},i}} \right) \left(\mathbf{M}_2^\top - \boldsymbol{\Delta}(z_i) - \frac{1}{b} \boldsymbol{\Delta} \left(\frac{C_{\mathrm{eq},i}}{B_{\mathrm{eq}}} \right) \mathbf{e} \left(\mathbf{V} \boldsymbol{\gamma}_{\mathrm{eq}}^{(1-b)/b} \right)^\top \right).
\end{aligned}$$

D.1.4 Expression of $(\mu \mathbf{I}_N - \mathbf{C} - \mathbf{D}\widetilde{\mathbf{H}}(\mu))^{-1}$

We denote by $\widetilde{\alpha}_i = \alpha_i (1 + n_i(\mu))$

$$\begin{aligned}
\mu \mathbf{I}_N - \mathbf{C} - \mathbf{D}\widetilde{\mathbf{H}}(\mu) &= \mu \mathbf{I}_N - \boldsymbol{\Delta} \left((1 - \widetilde{\alpha}_i - \alpha_i') \frac{C_{\mathrm{eq},i}}{z_i \gamma_{\mathrm{eq},i}} \right) + \boldsymbol{\Delta} \left(\alpha_i' z_i^{-1} \right) \mathbf{M_1} \\
&\underset{z \to \infty}{\sim} \mu \mathbf{I}_N - \boldsymbol{\Delta} (1 - \widetilde{\alpha}_i) := \boldsymbol{\Delta}_C,
\end{aligned}$$

where we have defined the diagonal matrix $\boldsymbol{\Delta}_C$ by identification.

D.1.5 Expressions involving $\mathbf{Y}_1$

$$
\begin{aligned}
\mathbf{Y}_1\mathbf{F} &= -\boldsymbol{\Delta}\left(\frac{\beta_i' e^{-\sigma_i}}{z_i}\right)\left(\mathbf{M}_2^\top - \boldsymbol{\Delta}\left(z_i\right) - \frac{1}{b}\boldsymbol{\Delta}\left(\frac{C_{\mathrm{eq},i}}{B_{\mathrm{eq}}}\right)\mathbf{e}\left(\mathbf{V}\boldsymbol{\gamma}_{\mathrm{eq}}^{(1-b)/b}\right)^\top\right) \\
&\underset{z\to\infty}{\sim} +\boldsymbol{\Delta}\left(\frac{\beta_i' e^{-\sigma_i}}{b}\right)\frac{L_{\mathrm{eq}}}{B_{\mathrm{eq}}}\mathbf{R} \\
\mathbf{Y}_1\mathbf{G} &= -\boldsymbol{\Delta}\left(\beta_i' e^{-\sigma_i}\right) \\
\mathbf{Y}_1\mathbf{H} &= -\boldsymbol{\Delta}\left(\frac{\beta_i' e^{-\sigma_i} C_{\mathrm{eq},i}}{z_i p_{\mathrm{eq},i}}\right) \\
\mathbf{Y}_1\mathbf{I} &= -\boldsymbol{\Delta}\left(\beta_i'\right)\sum_i \frac{e^{-\sigma_i}}{z_i}\epsilon_i^\top \otimes \epsilon_i \mathbf{e}^\top \\
\mathbf{Y}_1\mathbf{J} &= \frac{1}{B_{\mathrm{eq}}}\boldsymbol{\Delta}\left(\beta_i' e^{-\sigma_i}\frac{C_{\mathrm{eq},i}}{z_i}\right) \\
&\underset{z\to\infty}{\sim} \frac{1}{B_{\mathrm{eq}}}\boldsymbol{\Delta}\left(\beta_i' e^{-\sigma_i}\right)\boldsymbol{\kappa}^b/\mathbf{V}^b \\
\mathbf{Y}_1\widetilde{\mathbf{IF}}(\mu) &= -\boldsymbol{\Delta}\left(\beta_i'\frac{e^{-\sigma_i} n_i(\mu)}{z_i}\right)\left(\mathbf{M_2}^\top - \boldsymbol{\Delta}\left(z_i\right) - \frac{1}{b}\frac{\mathbf{C}_{\mathrm{eq}}}{L_{\mathrm{eq}}}(\mathbf{V}\boldsymbol{\gamma}_{\mathrm{eq}}^{(1-b)/b})^\top\right) \\
&\underset{z\to\infty}{\sim} \frac{1}{b}\boldsymbol{\Delta}\left(\beta_i' e^{-\sigma_i} n_i(\mu)\right)\mathbf{R} \\
\mathbf{Y}_1\widetilde{\mathbf{IG}}(\mu) &= -\boldsymbol{\Delta}\left(\beta_i' e^{-\sigma_i} n_i(\mu)\right) \\
\mathbf{Y}_1\widetilde{\mathbf{IH}}(\mu) &\underset{z\to\infty}{\sim} -\boldsymbol{\Delta}\left(p_{\mathrm{eq},i}^{-1}\right)\boldsymbol{\Delta}\left(\beta_i' e^{-\sigma_i} n_i(\mu)\right)\frac{\boldsymbol{\kappa}^b}{\mathbf{V}^b}.
\end{aligned}
$$

D.1.6 Expressions involving T-matrices

Expressions involving $\mathbf{T}_{11}$

$$
\begin{aligned}
\mathbf{T}_{11} &= \mathbf{I}_N - \boldsymbol{\Delta}\left(\frac{\beta_i}{b} + \beta_i'\right)\boldsymbol{\Delta}\left(\mathbf{z}^{-1}\right)\mathbf{M}_2^\top + \boldsymbol{\Delta}\left(\frac{\beta_i\gamma_{\mathrm{eq},i}}{z_i p_{\mathrm{eq},i}}\right)\mathbf{M}_2\mathbf{A} + \mathbf{Y}_1\mathbf{F} \\
&\underset{z\to\infty}{\sim} \mathbf{I}_N - \boldsymbol{\Delta}\left(\frac{\beta_i}{b} + \beta_i'\right) + \boldsymbol{\Delta}\left(\frac{\alpha_i'\beta_i}{b}\right) - \frac{1}{b}\boldsymbol{\Delta}\left(\beta_i(\omega + \alpha_i') - \beta_i' e^{-\sigma_i}\right)\mathbf{R} \\
&:= \mathbf{I}_N - \boldsymbol{\Delta}\left(\frac{\beta_i}{b} + \beta_i'\right) + \boldsymbol{\Delta}\left(\frac{\alpha_i'\beta_i}{b}\right) - \frac{1}{b}\boldsymbol{\Delta}_{11}\mathbf{R},
\end{aligned}
$$

where we have defined the diagonal matrix $\boldsymbol{\Delta}_{11}$ by identification.

Expressions involving $\mathbf{T}_{12}$

$$
\begin{aligned}
\mathbf{T}_{12} &= -\boldsymbol{\Delta}\left(\beta_i\frac{\gamma_{\mathrm{eq},i}}{z_i p_{\mathrm{eq},i}}\right)\mathbf{M_1}\boldsymbol{\Delta}\left(\alpha_i\frac{p_{\mathrm{eq},i}}{\gamma_{\mathrm{eq},i}}\right) - \boldsymbol{\Delta}\left(\beta_i' e^{-\sigma_i}\right) \\
&\underset{z\to\infty}{\sim} -\boldsymbol{\Delta}\left(\beta_i\alpha_i + \beta_i' e^{-\sigma_i}\right).
\end{aligned}
$$

Expressions involving $\mathbf{T}_{13}$ We denote by $\mathbf{\Delta}_{13}$ the diagonal matrix

$$\mathbf{\Delta}_{13} = \mathbf{\Delta}\left(\beta_i(1-\alpha_i) - \beta_i' e^{-\sigma_i} - \beta_i - \beta_i'\right). \tag{V.112}$$

$$\begin{aligned}
\mathbf{T}_{13} &\underset{z\to\infty}{\sim} \mathbf{\Delta}_{13}\mathbf{\Delta}\left(\frac{\gamma_{\mathrm{eq},i}}{p_{\mathrm{eq},i}}\right)\\
\mathbf{T}_{13}(\mu\mathbf{I}_N - \mathbf{C} - \mathbf{D}\widetilde{\mathbf{H}}(\mu))^{-1}\mathbf{A} &\underset{z\to\infty}{\sim} \frac{1}{b}\mathbf{\Delta}_C^{-1}\mathbf{\Delta}_{13}\left(\mathbf{\Delta}\left(\alpha_i'\right) - \mathbf{\Delta}\left(\omega+\alpha_i'\right)\mathbf{R}\right)\\
\mathbf{T}_{13}(\mu\mathbf{I}_N - \mathbf{C} - \mathbf{D}\widetilde{\mathbf{H}}(\mu))^{-1}\mathbf{B} &\underset{z\to\infty}{\sim} -\mathbf{\Delta}\left(\alpha_i\right)\mathbf{\Delta}_C^{-1}\mathbf{\Delta}_{13}\\
\mathbf{T}_{13}(\mu\mathbf{I}_N - \mathbf{C} - \mathbf{D}\widetilde{\mathbf{H}}(\mu))^{-1}\mathbf{D}\widetilde{\mathbf{F}}(\mu) &\underset{z\to\infty}{\sim} \frac{1}{b}\mathbf{\Delta}\left(\alpha_i n_i(\mu)\right)\mathbf{\Delta}_C^{-1}\mathbf{\Delta}_{13}\mathbf{R}\\
\mathbf{T}_{13}(\mu\mathbf{I}_N - \mathbf{C} - \mathbf{D}\widetilde{\mathbf{H}}(\mu))^{-1}\mathbf{D}\widetilde{\mathbf{G}}(\mu) &\underset{z\to\infty}{\sim} -\mathbf{\Delta}\left(\alpha_i n_\mu(e^{-\sigma_i})\right)\mathbf{\Delta}_C^{-1}\mathbf{\Delta}_{13}.
\end{aligned}$$

Expressions involving $\mathbf{T}_{14}$ We denote by $\mathbf{\Delta}_{14}$ the diagonal matrix

$$\mathbf{\Delta}_{14} = \mathbf{\Delta}\left(n_i(\mu)\left(\beta_i' e^{-\sigma_i} + \alpha_i\beta_i\right)\right).$$

$$\begin{aligned}
\mathbf{T}_{14} &\underset{z\to\infty}{\sim} \mathbf{\Delta}\left(\frac{\beta_i(\alpha_i'-\alpha_i)}{z_i}\right)(\mathbf{e}^\top\otimes\mathbf{I}_N)\\
&\quad - \mathbf{\Delta}\left(\frac{\beta_i\alpha_i'}{z_i p_{\mathrm{eq},i}}\right)\sum_k \epsilon_k\otimes\epsilon_k\mathbf{p}_{\mathrm{eq}}^\top\\
&\quad - \mathbf{\Delta}\left(\beta_i'\right)\sum_i \frac{e^{-\sigma_i}}{z_i}\epsilon_i^\top\otimes\epsilon_i\mathbf{e}^\top + \mathbf{Y}_2\\
\mathbf{T_{14}}\tilde{\mathbf{H}}(\mu) &\underset{z\to\infty}{\sim} -\mathbf{\Delta}_{14}\mathbf{\Delta}\left(\frac{C_{\mathrm{eq},i}}{z_i p_{\mathrm{eq},i}}\right)\\
\mathbf{T_{14}}\tilde{\mathbf{H}}(\mu)(\mu\mathbf{I}_N - \mathbf{C} - \mathbf{D}\widetilde{\mathbf{H}}(\mu))^{-1}\mathbf{B} &\underset{z\to\infty}{\sim} \mathbf{\Delta}\left(\alpha_i\right)\mathbf{\Delta}_C^{-1}\mathbf{\Delta}_{14}\\
\mathbf{T_{14}}\tilde{\mathbf{H}}(\mu)(\mu\mathbf{I}_N - \mathbf{C} - \mathbf{D}\widetilde{\mathbf{H}}(\mu))^{-1}\mathbf{A} &\underset{z\to\infty}{\sim} -\frac{1}{b}\mathbf{\Delta}_C^{-1}\mathbf{\Delta}_{14}\left(\mathbf{\Delta}\left(\alpha_i'\right) - \mathbf{\Delta}\left(\omega+\alpha_i'\right)\mathbf{R}\right)\\
\mathbf{T_{14}}\tilde{\mathbf{H}}(\mu)(\mu\mathbf{I}_N - \mathbf{C} - \mathbf{D}\widetilde{\mathbf{H}}(\mu))^{-1}\mathbf{D}\tilde{\mathbf{G}}(\mu) &\underset{z\to\infty}{\sim} \mathbf{\Delta}\left(\alpha_i n_\mu(e^{-\sigma_i})\right)\mathbf{\Delta}_C^{-1}\mathbf{\Delta}_{14}\\
\mathbf{T_{14}}\tilde{\mathbf{H}}(\mu)(\mu\mathbf{I}_N - \mathbf{C} - \mathbf{D}\widetilde{\mathbf{H}}(\mu))^{-1}\mathbf{D}\tilde{\mathbf{F}}(\mu) &\underset{z\to\infty}{\sim} -\frac{1}{b}\mathbf{\Delta}\left(\alpha_i n_\mu(e^{-\sigma_i})\right)\mathbf{\Delta}_C^{-1}\mathbf{\Delta}_{14}\mathbf{R}\\
\mathbf{T_{14}}\tilde{\mathbf{F}}(\mu) &\underset{z\to\infty}{\sim} \frac{1}{b}\mathbf{\Delta}_{14}\mathbf{R}\\
\mathbf{T_{14}}\tilde{\mathbf{G}}(\mu) &\underset{z\to\infty}{\sim} -\mathbf{\Delta}_{14}.
\end{aligned}$$

D.2 Expression for (V.103)

The characteristic polynomial in Eq. (V.103) can be rewritten as

$$\det\mu\mathbf{I}_{N_s} - \mathbb{D}_0 = \mu^{N^2+1}\det\mathbf{\Delta}\left(\mu - e^{-\sigma_i}\right)\det\left(\mu\mathbf{I}_N - \mathbf{C} - \mathbf{D}\widetilde{\mathbf{H}}(\mu)\right)\det(\mathbb{M}(\mu)), \tag{V.113}$$

thanks to results of the previous sections and identification. In the large productivity limit we saw that

$$\det\left(\mu\mathbf{I}_N - \mathbf{C} - \mathbf{D}\widetilde{\mathbf{H}}(\mu)\right) \sim \det \mathbf{\Delta}_C,$$

therefore yielding further simplifications. The matrix $\mathbb{M}(\mu)$ is expressed through the products of the blocks of $\mathbb{D}_0$. Using the previous sections, this matrix can be decomposed into two terms in the large productivity limit

$$\mathbb{M}(\mu) \sim \mathbf{K}(\mu) + \mathbf{L}(\mu)\frac{\mathbf{R}}{b}, \tag{V.114}$$

where both $\mathbf{K}$ and $\mathbf{L}$ are diagonal matrices

$$\begin{aligned}\mathbf{K}(\mu) = \mu^2\mathbf{I}_N - \mu\left(\mathbf{\Delta}\left(1-\beta_i-\beta_i'+\frac{\alpha_i'\beta_i}{b}\right)+\frac{1}{b}\mathbf{\Delta}_C^{-1}\mathbf{\Delta}\left(\alpha_i'\right)\left(\mathbf{\Delta}_{13}-\mathbf{\Delta}_{14}\right)\right)\\ -\left(-\mathbf{\Delta}\left(\beta_i\alpha_i+\beta_i'e^{-\sigma_i}\right)-\mathbf{\Delta}_{14}+\mathbf{\Delta}\left(\tilde{\alpha}_i\right)\mathbf{\Delta}_C^{-1}(\mathbf{\Delta}_{14}-\mathbf{\Delta}_{13})\right)\end{aligned} \tag{V.115}$$

$$\mathbf{L}(\mu) = -\mu\left[\mathbf{\Delta}_{11}+\mathbf{\Delta}_{14}+\mathbf{\Delta}_C^{-1}\left[\mathbf{\Delta}_{14}-\mathbf{\Delta}_{13}\right]\mathbf{\Delta}\left(\omega+\alpha_i'-\alpha_i n_i(\mu)\right)\right]. \tag{V.116}$$

The diagonal entries of these matrices are rational fractions in μ. Upon multiplying by $\mathbf{\Delta}_C$ and $\mathbf{\Delta}\left(\left(\mu-e^{-\sigma_i}\right)\right)$, we define two diagonal matrices

$$\begin{aligned}\mathbf{\Pi}(\mu) &:= \mathbf{\Delta}\left(\left(\mu-e^{-\sigma_i}\right)\right)\mathbf{\Delta}_C\mathbf{K}(\mu)\\ \mathbf{\Xi}(\mu) &:= \mathbf{\Delta}\left(\left(\mu-e^{-\sigma_i}\right)\right)\mathbf{\Delta}_C\mathbf{L}(\mu).\end{aligned}$$

$\mathbf{\Pi}$ and $\mathbf{\Xi}$ have polynomial entries in μ reading

$$\begin{aligned}\Pi_{ii}(\mu) = (\mu-e^{-\sigma_i})\Bigg[&\mu^3-\mu^2\left(2-\alpha_i-\beta_i'-\frac{\beta_i}{b}+\frac{\alpha_i'\beta_i}{b}\right)\\ &+\mu\left((1-\alpha_i)\left(1-\beta_i'-\frac{\beta_i}{b}\right)+\alpha_i\beta_i+(\beta_i+\beta_i')\frac{\alpha_i'}{b}\right.\\ &\left.+\left(1+\frac{\alpha_i'}{b}\right)\beta' e^{-\sigma_i}\right)\\ &-\alpha_i(\beta_i+\beta_i')-\beta_i'e^{-\sigma_i}\Bigg]\\ +e^{-\sigma_i}\Bigg[&\mu^2\alpha_i+\mu\left(\left(\beta_i'e^{-\sigma_i}+\alpha_i\beta_i'\right)\left(1+\frac{\alpha_i'}{b}\right)-\alpha_i\left(1-\beta_i'-\frac{\beta_i}{b}+\frac{\alpha_i'\beta_i}{b}\right)\right)\\ &-\left(\alpha_i(\beta_i+\beta_i')+e^{-\sigma_i}\beta_i'\right)\Bigg]\end{aligned} \tag{V.117}$$

$$\begin{aligned}\Xi_{ii}(\mu) = -\mu\Big\{(\mu-e^{-\sigma_i})\Big[&-\mu\left(\beta_i(\omega+\alpha_i')-\beta_i'e^{-\sigma_i}\right)\\ &+(1-\alpha_i)\left(\beta_i(\omega+\alpha_i')-\beta_i'e^{-\sigma_i}\right)\\ &-(\omega+\alpha_i')\left(\beta_i(1-\alpha_i)-\beta_i'e^{-\sigma_-}\beta_i-\beta_i'\right)\Big]\\ +e^{-\sigma_i}\Big[&\mu\left(\alpha_i\beta_i+\beta_i'e^{-\sigma_i}\right)+\left(\alpha_i\beta_i+\beta_i'e^{-\sigma_i}\right)(\omega-(1-\alpha_i-\alpha_i'))\\ &+\alpha_i(\beta_i(1-\alpha_i)-\beta_i'e^{-\sigma_i}-\beta_i-\beta_i'-(\beta_i(\omega+\alpha_i')-\beta_i'e^{-\sigma_i}))\Big]\Big\}.\end{aligned} \tag{V.118}$$

The determinant of Eq. (V.103) therefore has the asymptotic form

$$\det\left(\mu\mathbf{I}_{N_s}-\mathbb{D}_0\right) \sim \mu^{N^2+1}\det\left(\mathbf{\Pi}(\mu)+\frac{1}{b}\mathbf{\Xi}(\mu)\mathbf{R}\right). \tag{V.119}$$

Since $\boldsymbol{\Xi}(\mu)\mathbf{R}$ has rank one, we can further express the determinant as

$$\det\left(\mu\mathbf{I}_{N_s} - \mathbb{D}_0\right) \sim \mu^{N^2+1}\left(\prod_i \Pi_{ii}(\mu) + \frac{1}{bL_{\text{eq}}}\sum_i \kappa_i V_i^{1-b}\Xi_{ii}(\mu)\prod_{j\neq i}\Pi_{jj}(\mu)\right). \tag{V.120}$$

If adjustment parameters and stock depreciation parameters are uniform among firms, we finally get

$$\det\left(\mu\mathbf{I}_{N_s} - \mathbb{D}_0\right) \sim \mu^{N^2+1}\Pi(\mu)^{N-1}\left(\Pi(\mu) + \frac{1}{b}\Xi(\mu)\right). \tag{V.121}$$

CHAPTER VI

Summary, discussion and extensions

1 Summary and discussion

What is the origin of macroeconomic fluctuations? Textbook-macroeconomic models picture the world as a succession of equilibria where markets clear perfectly and firms maximize their profits. Each equilibrium is characterized by a different level of productivity or household preferences, themselves driven by exogenous "shocks", which are the primary cause of fluctuations. Drawing an analogy from physics, one may call such an approach "adiabatic", in the sense that the time needed for the system to reach equilibrium is much shorter than the time over which the environment changes, so out-of-equilibrium effects can be neglected. The time evolution of the economy is then *slaved* to the time evolution of the exogenous parameters. This assumption is at the core of DSGE models (see [112]), but also central to the analysis of Acemoglu et al. [13] in their now classic paper on the network origins of aggregate fluctuations.

The central proposition of Part I and Part II of this thesis is that the standard economic equilibrium may actually be dynamically unattainable. Correspondingly, the "small shock, large business cycle" paradox (i.e. aggregate fluctuations much too large to be explained by exogenous shocks alone, see e.g. [9] and [10]) would be chiefly explained by *out-of-equilibrium* effects. Indeed, in such out-of-equilibrium situations, the dynamics is mostly of endogenous origin and cannot be accounted for by traditional equilibrium arguments, like those of e.g. [35] and [13, 41, 111].

From a conceptual point of view, our point is the following: economic equilibrium requires so much cooperation between rational, forward-looking agents, that the only way such equilibrium can plausibly be achieved is through some kind of adjustment process, that inevitably takes some time to complete. [1] We argued that even in cases where equilibrium is eventually reached, this time can be much longer than the evolution time of technology or of any other type of shocks (political, social, geopolitical, sanitary, etc.) that affect the economy, in which case the adiabatic hypothesis is doomed to fail. Such a

[1] This is actually even the case for financial markets where transactions take place at the second time scale. In reality, a large amount of the supply/demand volume is latent and is only slowly revealed, see [125].

situation requires a richer modelling framework where out-of-equilibrium dynamics is an integral part of the description: we do not only need to describe the final equilibrium state, but also the path to equilibrium, which may in fact never converge.

In this concluding chapter, we will summarize the different models and findings presented throughout Part I and Part II. We will also take a critical look at these models and discuss several avenues of extensions.

1.1 Critical network-economies

In Part I, we approached the problem from a physicist's point of view. After defining precisely the notion of *competitive equilibrium* as the clearing of markets and the balancing of gains and losses, we specified the adjustment process mentioned previously. Since firms have no prior notion of equilibrium prices or production, they adjust said quantities by reacting to the variations of two observables of *imbalances*: production surplus $\mathscr{E}(t)$ (measuring the balance between production and demand at time t) and profits $\pi(t)$ (measuring the balance between gains and production costs at time t), which are both zero when competitive equilibrium is attained. The general idea behind the adjustment process is to try to incrementally reduce imbalances. In Chapter II, we hypothesized the following *behavioral rules* for reducing imbalances:

- Faced with excess production, firms will lower prices to prop up demand, and/or reduce production to limit losses.
- Faced with excess demand, on the other hand, firms can consider increasing prices and/or increase production.
- If profits are negative, firms will try to adapt by lowering production and increase prices, with the hope of better compensating production costs.
- When profits are positive, firms may be tempted to increase production but at the same time competition, attracted by the prospect of a profit, should put pressure on prices.

The first three rules are behavioral in essence: given observations of imbalances, firms take specific actions. However, for the last rule, the feedback between profits and prices is the consequence of *effective competition* between firms rather than the modelling of a decision. In any case, all of these rules aim at reducing imbalances, and we further assumed that firms would adjust (log) prices and (log) productions *linearly* according to these rules. Mathematically, this translates into the system

$$\log\left(\frac{p_i(t+\delta t)}{p_i(t)}\right) = \left(-\alpha\frac{\mathscr{E}_i(t)}{y_i(t)} - \alpha'\frac{\pi_i(t)}{p_i(t)y_i(t)}\right)\delta t \tag{VI.1a}$$

$$\log\left(\frac{y_i(t+\delta t)}{y_i(t)}\right) = \left(\beta\frac{\pi_i(t)}{p_i(t)y_i(t)} - \beta'\frac{\mathscr{E}_i(t)}{y_i(t)}\right)\delta t, \tag{VI.1b}$$

where imbalances are measured in terms of total production $y(t)$ for $\mathscr{E}(t)$, and total gains $p(t)y(t)$ for $\pi(t)$. Parameters α, α', β, β' correspond to the *speed* at which firms react in

the face of imbalances. The choice of modelling the dependency between adjustments and imbalances as linear is of course approximate, but it does not affect the point we made further down Chapter II about relaxation time to equilibrium. For instance, one could imagine that faced with a very large excess of production, firms would want to drastically reduce prices, and we could therefore have a quadratic or cubic negative feedback between prices and $\mathscr{E}(t)$. More scenarios can be imagined and one could inspire from the modelling of price returns in financial markets (see for instance [126] for a feedback-driven Langevin-like dynamics on returns).

This model was the setup for illustrating one of the main point of this thesis: even though competitive equilibrium exists, it may not be dynamically attainable. In Chapter I, we introduced the *Hawkins-Simons (HS) transition* in the context of network economies. Given firms' technological productivity factors z_i and an input-output network J_{ij} measuring firm j's importance in i's production, competitive equilibrium is not always well-defined. In [24], authors show [2] that a specific condition needs to be fulfilled by the network matrix $M_{ij} = z_i\delta_{ij} - J_{ij}$ for equilibrium prices and productions to be positive (and therefore make economic sense): the smallest eigenvalue ε of $\mathbf{M}$ must be positive. In essence, this eigenvalue encodes the relative strength between network needs, the J_{ij}s, and abilities to convert inputs into outputs, the z_is. If the latter are too weak, then ε will be negative and an economically admissible equilibrium will cease to exist. As it turns out, the HS transition translates beautifully into a dynamical transition for equations (VI.1). As $\varepsilon \to 0^+$, the relaxation time τ_r of the system diverges as ε^{-1}

$$\tau_r \approx \frac{2\rho_N}{\varepsilon} \times \begin{cases} \left(\alpha' + \beta' + \alpha - \sqrt{(\alpha' + \beta' + \alpha)^2 - 4(\alpha\beta + \alpha'\beta')}\right)^{-1} & \text{if} \quad \beta_c > \beta \\ (\alpha' + \beta' + \alpha)^{-1} & \text{if} \quad \beta_c \leq \beta, \end{cases} \tag{VI.2}$$

where ρ_N is a network-related quantity and β_c is defined in Chapter II. When $\varepsilon \to 0^+$, equilibrium still exists in an economically admissible sense. However, any small deviation from competitive equilibrium will take a time τ_r much larger than typical adjustment times $\sim 1/\alpha$ to be absorbed by the economy. In effect, the economy will never come back to equilibrium again. As a consequence, equilibrium is in essence not dynamically attainable as $\varepsilon \to 0^+$, which forces us to consider economies as intrinsically *out-of-equilibrium* in this limit. Furthermore, as we have shown, the proximity to the critical point $\varepsilon_c = 0$ also gives a natural mechanism for excess volatility. Adding some white noise $\sigma\xi(t)$ with variance σ^2 to system (VI.1), the volatility of prices and productions close to equilibrium would be of order σ^2/ε: marginal stability, which corresponds to a diverging relaxation time, also coincides with an increase in volatility for the associated stochastic system. For this simple feedback-driven dynamics on prices and productions, the "small shock, large business cycles" conundrum is merely due to the economy being in the vicinity of a *critical point* where exogenous shocks linger in the network and end up aggregating.

This last point reignites an old idea by Bak et al. [19], who qualitatively propose such a mechanism to account for excess volatility in large economies. A natural criticism to this mechanism resides in the necessity for the economy to be close to some critical

[2] For generic CES production functions but we restrict ourselves to the Leontief case for this discussion.

point. Why would such a point exist and, if it does, why would the economy sit anywhere close to it? In [20, 19], and then later in the context of network-economies [24], authors explain that complex systems tend to *self-organize* towards such critical points, i.e. the system evolves towards a configuration which is critical or near-critical. In our case, it is easy to argue that large economies are more prone to being critical. Indeed, ε depends on both the amount of firms in the network and their connectivity: if either increases, ε decreases. Since nowadays' economies are so large (around 5 million firms in the United States) and interconnected (truncated power-law behavior of the number of in/out links in the input-output network), one would expect them to be critical.

Of course, nothing prevents economies to be near-critical with a *negative* ε: network needs and inter-connectivity playing an increasingly crucial part today, we actually expect this situation to arise generically. The need of *out-of-equilibrium* modelling is all the more dire in this situation, since equilibrium *does not even exist*. However, our simple model of weakly out-of-equilibrium dynamics breaks down in that region. In Chapter III, we showed that no bounded trajectory with positive prices and productions could exist as soon as $\varepsilon < 0$. The economy systematically collapses with blowing-up prices, and plummeting productions and consumption. Even though such a scenario may certainly exist, we cannot reasonably expect it to be the only possible outcome for a real economy. Driven by the analogy with generalized Lotka-volterra equations, we expected the negative ε phase to yield oscillatory or chaotic behaviors.

We reach here the limits of the toy-modelling approach. In the model of Chapter II, we stripped away a little too much complexity for the economy to make sense when $\varepsilon < 0$. As we explained, the two main constraints that were overlooked are causality and proper management of imbalances. Furthermore, the modelling of the household sector was rather poor compared to the modelling of firms. In Part I, the household offered constant work (and this offer could actually be disregarded altogether) and was paid a constant wage, which is of course too stiff. As Part II is the natural extension of the model of Part I, we will postpone a more in depth critique of the present model to the next section.

1.2 Macroeconomic agent-based modelling

We pointed out that the naive model of Chapter II does not correctly factor in physical constraints: excess demand cannot be satisfied, excess supply must be stored, consumption can only start after goods are produced, wages can only be spent after being paid, etc.

Causality imposes to *dissect* the firms' decision process. As a consequence, we naturally moved to a step-by-step description of adjustments within the framework of Agent-Based Models (ABMs). In such models, agents (here firms or households) carry out a series of actions throughout time, abiding to some rules. We broke down one time step (which can be viewed as a quarter, for instance) of the model into three sub-steps: planning, exchanging, and producing. During the planning phase, firms try to forecast future gains (which are unknown at the time) and set out a target of production. The household also plans its consumption for the next period. During the exchanging phase, firms trade with one another to acquire goods necessary for production. They also hire and pay workers, which in turn consume. Firms can then compute their profits and

measure the excess of production, such that they can adjust prices accordingly. Finally, during the producing phase, firms use goods and labor to actually produce for the next period. They also store the potential left-over supply.

Imbalances management imposes that firms are not able to sell more than their supply, nor is the household capable of providing more workers than the available pool or consuming more than the available budget. These natural constraints modify the equations such that in a situation of under-supply, firms honor their contracts to the best of their capacity and proportionally to the initial demands. Similar equations can be written to account for the possible shortage of workers and budget.

Accounting for all these constraints within a consistent model considerably complicates the resulting equations, but leads to a model that displays a much larger variety of possible dynamical behavior, some very far from the competitive equilibrium. In fact, the dynamics of the model can remain well-behaved even in the region of parameters where equilibrium is inadmissible because some prices and/or productions would be negative, unless some firms are removed from the network.

A numerical investigation of the full model leads to rich phase diagrams, from which we extract the following salient features, with clear economic implications:

- The competitive equilibrium attracts the dynamics *only in a restricted range of parameters*: the speed at which firms adapt to imbalances must neither be too slow nor too fast, and the rate at which goods spoil must be high enough. Diminishing returns to scale also help convergence towards equilibrium.

- When the adaptation speed is too large, or the perishability of goods too low, coordination breaks down and the economy enters a phase with periodic or chaotic business cycles of purely endogenous origin, as was also reported in [66].

- Close to the boundaries between the competitive equilibrium phase and the oscillating phase, one observes a regime of intermittent crises, with long periods of quasi-equilibrium interrupted by bursts of inflation.

- Close to the boundaries between the competitive equilibrium phase and the deflationary equilibrium phase, the relaxation time of the system diverges regardless of the value of ε. Whenever $\varepsilon \to 0$, the region where competitive equilibrium is accessible shrinks down and the relaxation time diverges as well.

- Another class of equilibria exists, with a negative inflation but with stationary real prices and production different from those pertaining to the competitive equilibrium. In particular, markets – including the job market – do not clear in such situations: labor supply is always larger than labor demand. These equilibria are however characterized by persistent discrepancies between forecasts and realized quantities, which presumably make them unstable against simple learning rules.

- For *inflationary* equilibria to exist, where labor demand is larger than labor supply, one needs to introduce precautionary savings and interest rates in the model.

However, whenever $\beta, \beta' > \alpha, \alpha'$, oscillations are accompanied by sustained inflation with $L^{\mathrm{s}}(t) < L^{\mathrm{d}}(t)$ on average.

Our model therefore suggests *two* distinct out-of-equilibrium routes to excess volatility (or "large business cycles"): (a) purely *endogenous* cycles, resulting from over-reactions and non-linearities, or (b) persistence and amplification of *exogenous shocks*, governed by the proximity of a boundary in parameter space where the competitive equilibrium becomes unstable. While scenario (a) may appear at first sight to be more generic, the self-organized criticality scenario proposed long ago by [19] could make (b) plausible as well. Specific empirical work would be needed to distinguish between these two scenarios.

Finally, the linear study of this model revealed that the cause of mechanism (a) could be directly traced to the constraints due to imbalances. We showed that perturbations around competitive equilibrium are not described by a well-defined stability matrix, but rather by a collection of stability matrices whose "activations" depend on the direction of the vector of perturbations in state space. Even close to competitive equilibrium, the economy behaves differently whether the initial shock lowers supplies, or consumption, for instance. This situation, which is generically called conewise linear, is able to easily generate limit cycles of very intricate nature. Since such systems are ubiquitous in economics, a more systematic investigation of their properties would be beneficial.

It should however be borne in mind that many relevant features of the real economy are left out of the present version of the model. In particular, whereas firms are allowed to make losses, we have not accounted to the cost of credit that this would entail, and the impact of monetary policy, increasing or decreasing the interest rate in the face of inflation/deflation. Nor have we introduced a bankruptcy mechanism when firms go too deep into debt, removing non-competitive firms along the lines of, e.g. [63]. But this would require moving from a static network of firms, as considered throughout this work, to a dynamically evolving network that rewires as some firms go bankrupt and others are created. In fact, another motivation for moving from such a static framework to a rewiring model is to be able to describe possible *cascades of bankruptcies* mediated by the input-output network, much as cascades of defaults can occur in banking networks. On the same line of thought, there is no *liquidity* management in this model. Firms buy inputs regardless of previous profits or losses. A more detailed account of this point must be incorporated in the model. The household sector also needs to be better described, moving away from the representative household assumption and introducing wage inequalities, confidence effects (as, for example, in [67]) and debt.

Our dynamical model can be seen as a hybrid between traditional economic models (describing equilibrium) and ABMs, where reasonable but *ad hoc* rules are implemented to account for out-of-equilibrium, dynamical aspects. As we have shown, in some swath of parameters, the classical competitive equilibrium is reached. If reached fast enough, the "adiabatic" assumption used in most standard descriptions will hold, whereas when the equilibrating time is long (or even infinite) new phenomena appear. We hope that the possibility of recovering standard results in some limiting cases will make the ABM approach more palatable to economists, and at the same time elicit the inherent limits of general equilibrium ideas. Conversely, including firm network effects in ABMs such

as Mark-0 [61, 62] along the lines of the present model is certainly worthwhile. Finally, an appealing feature of our approach is the possibility to use highly dis-aggregated data on individual firms and prices (for example through the "Billion Price Project" [124]) to calibrate the model and, hopefully, use it as a powerful descriptive and predictive tool. We look forward to working in that direction in the near future, with access to accounting databases from the French Institute of Statistics.

2 Extensions

2.1 Liquidity, debts and interest rate

We took a rather hard stance at the beginning of Part II by saying that, from now on, our models would incorporate precise imbalances' management. We succeeded in doing so about goods' management. Input goods are converted into outputs using the Leontief production function, and any left-over is stored and used (up to depreciation) during the next period. We also were careful about the household's budget management: it cannot spend more than the available budget, and any left-over budget can be used for the next period. However, we did not take care of any *liquidity* issues at firm level. Liquidity, i.e. the amount of available cash at some point in time, is essential to determine whether firms will be able to pay for the inputs they have to buy in order to fulfill production's targets.

It is here that we can start merging our ABM with existing models such as Mark0 [61, 62, 122]. We will give a brief overview of modifications that such a merging would entail. We first define $\mathcal{L}_i(t)$ as the available liquidity at time t. Liquidity can be negative, and, when so, is interpreted as a firm being indebted. The constitutive accounting equations of Mark0, adapted to our model, are

$$\begin{aligned}
\pi_i(t) &= \sum_j x_{ji}(t)p_i(t) + C_i(t)p_i(t) - \sum_j x_{ij}(t)p_j(t) - \ell_i(t)p_0(t) \\
\mathcal{L}_i(t+1) &= \mathcal{L}_i(t) + \pi_i(t) - \delta\pi_i(t)\Theta\left(\pi_i(t)\right) \\
S(t+1) &= S(t) + B(t) - \sum_i C_i(t)p_i(t) + \delta\sum_i \pi_i(t)\Theta\left(\pi_i(t)\right).
\end{aligned} \tag{VI.3}$$

where household's savings $S(t)$ can also become negative if in debts, and with the budget $B(t) = p_0(t)\sum_i \ell_i(t) + \max\left(0, S(t)\right)$. With this prescription, monetary mass is conserved i.e. $\partial_t\left(S(t) + \sum_i \mathcal{L}_i(t)\right) = 0$. We introduced another parameter δ measuring the fraction of (positive) profits that are redistributed as dividends to the household. With this prescription, no monetary mass is created. However, whenever firms go too much in debts, they go bankrupt and the (negative) liquidity is absorbed by healthier firms and households.

We could go even further and adopt a finer-grained description by adding an explicit variable accounting for debts as in models such as MarkI or MarkI+ [57, 127, 61]. Introducing firm-dependent variables $\mathcal{D}_i(t)$ encoding debt, firms with positive liquidity

can compute their financial need for production $\mathcal{R}_i(t)$ at time t

$$\mathcal{R}_i(t) = \max\left(0, \sum_j x_{ij}^{\mathrm{d}}(t)p_j(t) + \ell_i(t) - \mathcal{L}_i(t)\right). \tag{VI.4}$$

If liquidity is enough to cope with demands in inputs, i.e. $\mathcal{R}_i(t) = 0$, firms do not ask for a loan. Otherwise, the bank, which would be a new agent in the model, can provide a loan up to $\mathcal{R}_i(t) > 0$ with interest rate

$$\rho_i(t) = \rho_0 G(\mathcal{F}_i(t))\left(1 + \xi_i(t)\right), \tag{VI.5}$$

where ρ_0 is the baseline interest rate (set by a central bank), $G(\cdot)$ an increasing function, $\xi_i(t)$ a noise term and $\mathcal{F}_i(t)$ the financial fragility of the firm at time t

$$\mathcal{F}_i(t) = \frac{\mathcal{D}_i(t) + \mathcal{R}_i(t)}{\mathcal{L}_i(t)}. \tag{VI.6}$$

The more financially fragile you are, the higher your interest rate will be through G-function, which is chosen to be $G(u) = 1 + \tanh u$ in MarkI for instance. If firms decide to take a loan, total debt is increased by $\mathcal{R}_i(t)$ (or a fraction of it if the full loan is deemed too high). At each time, firms would pay back a part of the debt $\tau\mathcal{D}_i$ along with the interests $\mathcal{I}_i(t) = \rho_i(t)\mathcal{D}_i(t)$. We would therefore have

$$\begin{aligned}
\pi_i(t) &= \sum_j x_{ji}(t)p_i(t) + C_i(t)p_i(t) - \sum_j x_{ij}(t)p_j(t) - \ell_i(t)p_0(t) - \mathcal{I}_i(t) \\
\mathcal{D}_i(t+1) &= (1-\tau)\left(\mathcal{D}_i(t) + \mathcal{R}_i(t)\right) \\
\mathcal{L}_i(t+1) &= \mathcal{L}_i(t) + \pi_i(t) - \delta\pi_i(t)\Theta\left(\pi_i(t)\right) - \mathcal{I}_i(t) - \tau\mathcal{D}_i(t) \\
S(t+1) &= S(t) + B(t) - \sum_i C_i(t)p_i(t) + \delta\sum_i \pi_i(t)\Theta\left(\pi_i(t)\right),
\end{aligned} \tag{VI.7}$$

along with similar accounting equations for the bank's monetary mass. For these types of accounting schemes, firms with negative liquidity would go bankrupt and their default would be also absorbed by healthy firms.

Finally, the baseline interest rate ρ_0, which is actually time dependent in full generality, is set by the central bank. In DSGE models, the central bank uses a so-called Taylor rule, which takes into account inflation $\Pi(t)$ [112] to adjust baseline interest rates. We will not detail this point here, but it is certainly worth incorporating in our model, and efforts in that direction are currently underway.

2.2 Time-varying networks

One of the very first assumptions that was made in Chapter I and Chapter II, was that we would consider a *static* interaction network throughout the manuscript. We motivated this hypothesis by arguing that the timescale of the intrinsic dynamics of the

network is much larger than those governing prices and productions' variations. However, we then proceeded to show that right before an economically admissible equilibrium disappears, the relaxation time of the system can become arbitrarily large. This of course comes as a contradiction with the assumption that the network evolves more slowly than prices and productions, and we cannot discard this evolution in our description anymore. Furthermore, as we have seen in the previous section, allowing firms to contract loans and manage debts inevitably poses the question of *bankruptcy*. Firms going too much in debt must exit the network, which consequently evolves. Finally, we also explained in Chapter I that the observed configuration of the network is the result of an underlying *competitive* process between firms which "converged" towards this specific configuration. We then factored competition back into our equations in a very weak way through the coupling between prices and profits: as profits grow, the prospect of high profits should attract competition, which would in turn put pressure on prices. Having a dynamical description of the network with firms selling similar goods would account for competition much better than in the present model.

We started investigating in that direction by proposing the following framework. Consider N firms which are distributed among M sectors. Within each sector, firms essentially produce the same good, up to quality considerations. We denote firms by lowercase letters $i \in \{1, \dots, N\}$ and sectors by uppercase letters $S \in \{1, \dots, M\}$. In this framework, firms need specific goods, i.e. specific sectors, in order to produce. The interaction network is therefore an $N \times M$ matrix J_{iS} encoding the amount of goods from sector S that firm i needs to produce. Now, firm i may want to choose one or several firms from this sector as suppliers, and we introduce a "substitutability" matrix a_{ij}, $j \in S$ that measure how easily can good $j \in S$ be used for production with respect to another good $k \in S$. The production function is therefore a nested Leontief production function

$$y_i = z_i \min\left(\min_S\left(\frac{\sum_{k\in S} a_{ik}x_{ik}}{J_{iS}}\right), \frac{\ell_i(t)}{J_{i0}}\right), \tag{VI.8}$$

where x_{ik} denote the exchanged quantities, and $S = 0$ denotes the labor sector. Given a certain production target $\widehat{y}_i(t) = z_i\widehat{\gamma}_i(t)$, we can compute demands using standard Karush-Kunh-Tucker costs optimization

$$x_{ik}^{\mathrm{d}} = \delta_{kk^\star}\frac{J_{iS}}{a_{ik}}\widehat{\gamma}_i, \quad k^\star = \arg\min_{k\in S}\frac{p_k}{a_{ik}}. \tag{VI.9}$$

In that case, firms solely choose that supplier $k^\star \in S$ that minimizes the price-to-usage ratio p_k/a_{ik}. Firms are perfectly rational and competition is fierce: as soon as a firm tries to increase its price, it will lose its buyers (assuming a_{ik} are set to one for simplicity).

At each time, the network can therefore evolve if prices are reshuffled, since firms will switch suppliers. As a way to allow more flexibility in the evolution, we propose two approaches which should be equivalent in the large-time limit. We can first consider that firms exchange a price-dependent quantity with each firm from a supplying sector, i.e. such that

$$x_{ij}^{\mathrm{d}} = \frac{J_{iS}}{a_{ik}}\widehat{\gamma}_i\frac{e^{-\beta_0 p_k/a_{ik}}}{\sum_{j\in S} e^{-\beta_0 p_j/a_{ij}}}. \tag{VI.10}$$

The rationality parameter β_0 interpolates between the previous fully rational decision ($\beta_0 \to \infty$) and an irrational decision ($\beta_0 = 0$) where prices are not taken into account. The interaction network is unchanged throughout time in that case, but the strength of the interaction depends on prices. Note that here the timescale of network variation (more precisely, links' strength variation) is similar to that of prices. The second idea is to consider a more incremental process. Consider a fixed network of interaction at time t. Assume for simplicity that if i needs sector S to produce, it will be fully supplied by one firm j from this sector at the considered time. At time t, with some "small" probability ϕ, choose a random firm i along with a supplying sector S of i. In sector S, choose a random firm k which is not supplying i. Firm i rewires from j to k with probability

$$q_{kj} = \min\left(1, e^{-\beta_0(p_k/a_{ik} - p_j/a_{ij})}\right). \tag{VI.11}$$

In this Metropolis-Hastings-like setup, firms instantly rewire if the price-to-usage ratio is more advantageous, but can also rewire (with a smaller probability) if it is not. The timescale of evolution of the network is of order $\tau_{net} \sim 1/\varphi$ here. We therefore recover models from Part I and Part II on time-scales smaller than τ_{net}.

With the previous dynamics, it is not unlikely that some firms could end up without any buyers (except maybe the household). As said before, for such firms, profits are expected to drop drastically, and they will have to contract some loans if they want to keep producing. If debts are too high, firms go bankrupt and will have to be removed from the network. Bankruptcy can of course occur even if firms still have suppliers. In such a situation, removing the bankrupt firm from the network will force buyers to rewire, therefore creating some kind of shock in the network. Finally, new firms can also enter the network with potentially higher productivity factor z_i, i.e. corresponding to firms with a technological edge. A lot of different models can be considered for network dynamics, but a very prolific one is given in [73] and can be of inspiration for our model.

Key takeaways

- **Excess volatility** can be generated through two mechanisms: (a) the amplification of exogenous shocks through network effects whenever the economy sits close to the Hawkins-Simons transition; (b) the emergence of sustained endogenous oscillations whenever perishability is too low ("bullwhip" effect), or the speed to adjust is too high (constant over/under shoot).
- **Different scenarii** can be found for the same parameters but different initial conditions or, conversely, for different parameters and the same initial conditions. The same model can generate very different outcomes and must therefore be studied in its entirety rather than focusing on regions where equilibrium can be reached.
- **Two main axes of extensions** are (a) the introduction of liquidity, debts and loans and (b) allowing the network to rewire, firms to go bankrupt and new firms to enter the network.

Part III

Complex interactions and random matrices

Foreword

The third and last part of this thesis is devoted to more theoretical studies of conewise linear systems and related topics. Even though the results that we will present can be taken independently of the overall economic context of this thesis, they stemmed from the attempts at understanding some natural economic systems in their simplest form.

In Part II, we devised ABMs which revealed a non-trivial structure close to equilibrium. We showed that economic equilibrium generically coincides with a *cusp* of dynamical price (or production) adjustment processes, since over or under supply situations are not described by the same mathematical relationships. More generally, a dynamical system $\dot{x}_i = f_i(\mathbf{x})$ whose resting point $\mathbf{x}_\star$ coincides with a cusp of its associated vector field $\mathbf{f}$ will yield a *conewise linear system* upon linearization around $\mathbf{x}_\star$. In such a system, the form of the Jacobian matrix depends on the *direction* of the perturbation away from $\mathbf{x}_\star$. In the context of the ABMs of Part II, we saw that, not only was equilibrium cusped in many directions of state space, but the different Jacobian did not have any particular properties facilitating the overall study. In the first chapter of this last part, we present a toy-model of conewise dynamics which involves only two Jacobian matrices, which we choose to be random. We used the same ideas as Robert May in his paper "will a large complex system be stable?" and tried to understand the properties of this system from a statistical point of view, as the size of the matrices diverges. As we will explain in Chapter VII such systems can be either stable or unstable given minute details of the initial perturbation, and display ergodicity breaking.

If the dynamics is bound to remain within a region of constant Jacobian, it becomes linear and therefore trivial. We showed in Chapter IV that a simple condition (the asymptotically rank-one condition) fulfilled by the Jacobian was enough to ensure the existence of an invariant region of space, though the precise nature of this region is not specified. The understanding of this invariance property falls into the more general field of *occupation time* for which the main focus is how long will a property hold for a generic random process. We will see in Chapter VII (and more generally in Chapter VIII) that the occupation time of a single cone, where the Jacobian is fixed, displays a power-law behavior in the large-dimensional limit for a wide class of matrices. In an economic context, persistence or occupation time are notions closely related to that of *economic resilience*, where one would like to estimate the amount of time that an economy spends in recession, for instance.

Finally, the very last chapter tackles a more theoretical problem which stemmed from

the extension of the model of Chapter VII to random matrices with more general structure. We study the mixed-moments of Gaussian elliptic matrices, and give a computationally efficient exact formula for their computation. We map the problem to the partition of Temperley-Lieb algebras into disjoint subsets with constant features. This work is still underway.

CHAPTER VII

Non-self-averaging of maximal Lyapunov exponent in random conewise linear systems

Abstract

We consider a simple model for multidimensional conewise linear dynamics around cusp-like equilibria. We assume that the local linear evolution is either $\mathbf{v}' = \mathbb{A}\mathbf{v}$ or $\mathbb{B}\mathbf{v}$ (with $\mathbb{A}$, $\mathbb{B}$ independently drawn from a rotationally invariant ensemble of symmetric $N \times N$ matrices) depending on the sign of the first component of $\mathbf{v}$. We establish strong connections with the random diffusion persistence problem. When $N \to \infty$, we find that the Lyapunov exponent is non-self-averaging, i.e., one can observe apparent stability and apparent instability for the same system, depending on time and initial conditions. Finite N effects are also discussed and lead to cone trapping phenomena.

Adapted from: [2] Théo Dessertaine and Jean-Philippe Bouchaud. *Non-self-averaging Lyapunov exponent in random conewise linear systems.* Phys. Rev. E, 105:L052104, May 2022.

1 Introduction

The stability of generic equilibrium points is well known to be determined by the largest eigenvalue of the matrix describing the linearized dynamics of small perturbations. However, a large variety of systems exhibit non-linearities even for infinitesimal perturbations. Such a situation arises when the dynamics involves threshold effects or constraints. For example, operational amplifiers in electrical systems involve diodes with voltage thresholds, whereas in neuroscience, simple models of neurons involve a gain function with a threshold over which the considered neuron will fire. For electrical engineering, the question of controlability of switch systems is also crucial. It was shown that, even in the simplest case, numerical assessment of stability and controlability is NP hard [113], see also [114] for a detailed study of a particular class of switch systems. Similar effects

have recently been discussed in the context of out-of-equilibrium macroeconomic models [61, 1]. Economic equilibrium enforces that markets clear, i.e. that firms' supply y equals households' demand c. However, in a dynamical setting, one can be in a situation where demand is – say – larger than supply. In this case, realized consumption c_r is limited by production, i.e. $c_r = \min(c, y)$. Generically, the resulting update rules for firms' production and households' demand will differ when under-supply leads to excess savings, or when over-supply leads to inventories. Hence, even small perturbations away from market clearing will evolve differently in the two regions $c > y$ and $c < y$ (see [1] for a generalization to $n > 1$ firms). A recurrent question in economics is how resilient is the economy to shocks i.e. how well will it recover from – say – a crisis. Within the previous example, the evolution of the economy will be different whether the shock affects consumption or supply. Answering the question of resilience therefore relies on the study of the dynamics within each region as well as the interactions between those.

The situation described above is generically called "cone-wise linear": depending on the *direction* of the perturbation away from equilibrium, the linear stability matrix will not be the same. Even in the simplest case of a planar dynamical system with two cones, the overall dynamics can be highly non trivial and may generate limit cycles, for example. For higher dimensional systems such as considered in [1] (in the context of large economies), it is hard to get an intuition on the possible behaviors generated by such cone-wise dynamics since the amount of interaction is quite high and their form potentially complex. The purpose of the present chapter is to propose a simplified Random Matrix Theory framework to understand some of the phenomenology of these systems in the large-dimension limit, in the spirit of Robert May's celebrated study [98]. We find that the answer to the question "will the system be stable?" is not straightforward, with the emergence of complex non self-averaging behavior.

The simple model we consider in this chapter is the following: let $\mathbf{v}(t) \in \mathbb{R}^N$ be the N-dimensional vector describing the perturbation away from equilibrium. Depending on the sign of the dot-product $\mathbf{v}(t) \cdot \mathbf{e}$, where $\mathbf{e} \in \mathbb{R}^N$ is a *fixed* vector, the linearized dynamics is governed either by matrix $\mathbb{A}$ or by matrix $\mathbb{B}$, chosen to be symmetric $N \times N$ random matrices, independently drawn from $O(N)$ rotationally invariant ensembles with possibly different eigenvalue spectra. [1]. In the present case, the cone structure is simply the two half-spaces separated by the hyperplane $\{\mathbf{e}\}^\perp$. We thus consider the following evolution for $\mathbf{v}(t)$ [2]

$$\mathbf{v}(t+1) = \begin{cases} \mathbb{A}\mathbf{v}(t), & \text{when } v_1(t) > 0 \\ \mathbb{B}\mathbf{v}(t), & \text{when } v_1(t) < 0 \end{cases}, \tag{VII.1}$$

where we have set $\mathbf{e} = (1, 0, \ldots, 0)$ without loss of generality using the rotational invariance of both $\mathbb{A}$ and $\mathbb{B}$. The stability analysis therefore relies on the large-time properties of matrix products of the type $\mathbb{M}(t) = \mathbb{A}^{t-t_{k-1}}\mathbb{B}^{\tau_{k-1}} \cdots \mathbb{A}^{\tau_1}$, with $t_{k-1} := \sum_{i=1}^{k-1} \tau_i$ and

[1] For $\mathbb{X}$ a rotationally invariant random matrix and $\mathbb{O}$ a rotation matrix, $\mathbb{X} \overset{d}{=} \mathbb{O}\mathbb{X}\mathbb{O}^\top$, where $\overset{d}{=}$ denotes the equality in distribution.

[2] The case $v_1(t) = 0$ has a zero probability for generic choices of $\mathbb{A}$ and $\mathbb{B}$, but if it were to happen, one would choose $\mathbb{A}$ or $\mathbb{B}$ with equal probability.

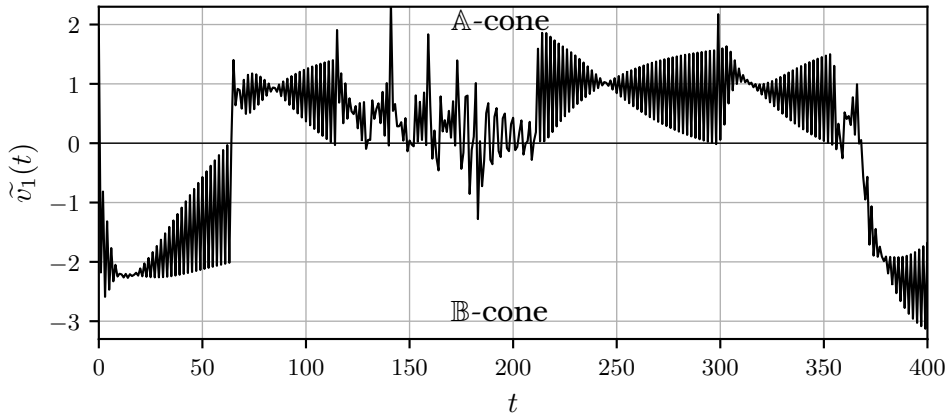


Figure VII.1: Trajectory of the rescaled first component $\widetilde{v_1}(t) = \sqrt{N}v_1(t)/\|\mathbf{v}(t)\| \sim_{N\to\infty} \phi(t)$ (where $\phi(t)$ is defined in Eq. (VII.6)) under the dynamics of Eq. (VII.1) with $\mathbb{A}$ and $\mathbb{B}$ independently drawn GOE matrices with $N = 10^3$, $\nu_{\pm,\mathbb{A}} = \nu_{\pm,\mathbb{B}} = \pm 2$ (where $\nu_{\pm,\mathbb{M}}$ are the lower/upper edges of the matrix $\mathbb{M} = \mathbb{A}, \mathbb{B}$). We see that the dynamics is highly non-trivial with rapid oscillations caused by powers of negative eigenvalues changing sign. Note also that the time spent in each cone varies widely from a single time-step to very long excursions.

$t_{k-1} < t \leq t_k$, and where τ_i are persistence times, i.e. times during which the dynamics leaves $\mathbf{v}(t)$ within the same cone (here the half space). It turns out that in our problem, the probability $Q_0(\tau)$ to remain in a single cone for a time larger or equal to τ decays *algebraically*, i.e. $Q_0(\tau) \sim_{\tau\to\infty} \tau^{-\mu}$, where μ is called the persistence exponent (see [128] for a detailed review). We will see that whenever $\mu < 1$ (which corresponds to natural choices for matrices $\mathbb{A}$ and $\mathbb{B}$, see below), the maximal Lyapunov exponent of the problem, namely

$$\lambda_{\max} = \lim_{t\to\infty} t^{-1} \ln\left(\|\mathbb{M}(t)\mathbf{v}(t=0)\|/\|\mathbf{v}(t=0)\|\right), \tag{VII.2}$$

remains a random quantity even in the large-time limit, and does not converge to its ensemble average value. In some cases one can observe $\lambda_{\max} < 0$, seemingly indicating stability, while in others (or at later times) $\lambda_{\max} > 0$, suggesting instability. This situation departs from the standard Furstenberg-Kesten result [129] for products of random matrices where the maximal Lyapunov exponent self-averages in the large-dimensional limit. In fact, quite non-trivial dynamics can be observed, even for such a simple system, see Figure VII.1.

2 Persistence and intra-cone behavior

To understand the spectral properties of $\mathbb{M}(t)$, we must first characterize the behavior of the persistence times τ_i. Let us consider the evolution of $\mathbf{v}$ within one cone, say $v_1(t) > 0$. As long as $v_1(t) > 0$, the evolution is linear and yields $\mathbf{v}(t) = \mathbb{A}^t\mathbf{v}(0)$. Calling $\boldsymbol{\varepsilon_i}$ the i-th

canonical vector of $\mathbb{R}^N$, we can express the ℓ-th component $v_\ell(t)$ of $\mathbf{v}(t)$ as

$$v_\ell(t) := \boldsymbol{\varepsilon}_{\boldsymbol{\ell}} \cdot \mathbf{v}(t) = \sum_\alpha \left(\mathbb{A}^t\right)_{\ell\alpha} v_\alpha(0).$$

Here, we consider a *fixed* realization of the disorder $\mathbb{A}$. As a consequence, since $\mathbf{v}(0)$ is a Gaussian vector, one immediately sees that $\mathbf{v}(t)$ is also a Gaussian vector whose statistics can be computed easily. Denoting by $\overline{(\,\cdot\,)}$ the average over initial conditions, we get for the mean

$$\begin{aligned}\overline{v_\ell(t)} &= \sum_\alpha \left(\mathbb{A}^t\right)_{\ell\alpha} \overline{v_\alpha(0)} \\ &= 0,\end{aligned}$$

and for the covariance,

$$\begin{aligned}\overline{v_\ell(t)v_{\ell'}(s)} &= \sum_{\alpha,\beta} \left(\mathbb{A}^t\right)_{\ell\alpha} \left(\mathbb{A}^s\right)_{\ell'\beta} \overline{v_\alpha(0)v_\beta(0)} \\ &= \sum_\alpha \left(\mathbb{A}^t\right)_{\ell\alpha} \left(\mathbb{A}^s\right)_{\ell'\alpha} \\ &= \left(\mathbb{A}^t \left(\mathbb{A}^\top\right)^s\right)_{\ell\ell'}.\end{aligned}$$

Once again, these expressions are obtained for a fixed realization of the disorder $\mathbb{A}$. Taking the average over $\mathbb{A}$, one should usually be a bit careful. It is not straightforward that the average over $\mathbb{A}$ will leave the statistics of $\mathbf{v}(t)$ Gaussian. However in our case, we can see that its correlator is actually self-averaging in the limit $N \to \infty$, thanks to the rotational invariance of $\mathbb{A}$ and, as a consequence, the process remains Gaussian for $N \to \infty$ with covariance

$$\overline{v_\ell(t)v_{\ell'}(s)} \underset{N\to\infty}{\sim} \frac{1}{N}\left\langle \mathrm{Tr}\left[\mathbb{A}^t\left(\mathbb{A}^\top\right)^s\right]\right\rangle \delta_{\ell\ell'} \underset{N\to\infty}{\longrightarrow} \tau\left(\mathbb{A}^t\left(\mathbb{A}^\top\right)^s\right) = \left\langle\overline{v_\ell(t)v_{\ell'}(s)}\right\rangle, \quad \text{(VII.3)}$$

where $\langle(\cdot)\rangle$ is the ensemble average of $\mathbb{A}$, and $\tau(\,\cdot\,)$ the normalized trace

$$\tau(\,\cdot\,) = \lim_{N\to\infty} N^{-1}\mathrm{Tr}\,(\cdot)\,.$$

We see that components are uncorrelated and therefore independent in the large N limit since they are Gaussian. Finally, time-wise correlations are given by the *mixed-moments* of matrices $\mathbb{A}$ and $\mathbb{A}^\top$. In the present case where we choose $\mathbb{A}$ symmetric, mixed-moments are nothing more than standard moments $f_{\mathbb{A}}(u)$ of the matrix $\mathbb{A}$, i.e.

$$\left\langle\overline{v_\ell(t)v_{\ell'}(s)}\right\rangle = \delta_{\ell\ell'} f_{\mathbb{A}}(t+s), \quad \text{(VII.4)}$$

with,

$$f_{\mathbb{A}}(t) \underset{t\to\infty}{\sim} K\Gamma(\alpha+1)\,\nu_+^{t+\alpha+1} t^{-\alpha-1}, \quad \text{(VII.5)}$$

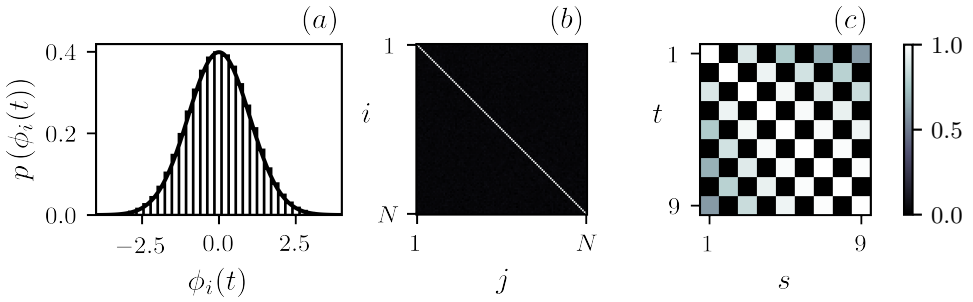


Figure VII.2: Simulations of the vector $\mathbf{v}(t) = \mathbb{M}^t\mathbf{v}(0)$ for $\mathbb{M} \in \mathrm{GOE}(N)$, $\mathbf{v}(0) \hookrightarrow \mathsf{N}(0, \mathbf{I}_N)$, $N = 10^4$ and $t < 10$. The average $\left\langle \overline{(\,\cdot\,)} \right\rangle$ is performed over 5000 realizations of $\mathbb{M}$ and $\mathbf{v}(0)$. (a) Probability distribution of $\phi_i(t)$ overlaid with the density of a Gaussian random variable $\mathsf{N}(0, 1)$. (b) Component-wise covariance matrix $\left\langle \overline{\phi_i(t)\phi_j(t)} \right\rangle$ at time $t = 1$. We see that this covariance matrix is exactly $\mathbf{I}_N$ as predicted by Eq. (VII.31) from Appendix B. (c) Time-wise covariance matrix $\left\langle \overline{\phi_i(t)\phi_i(s)} \right\rangle$ for $t, s < 10$ which coincides with the prediction of Eq. (VII.31) from Appendix B. Note the checkerboard structure coming from the fact that odd moments of GOE matrices are 0.

where K and α relate to the shape of the density of eigenvalues $\rho(\nu)$ of $\mathbb{A}$ near its upper edge ν_+, i.e. $\rho(\nu) \underset{\nu\to\nu_+}{\sim} K|\nu - \nu_+|^\alpha$. See Appendix B for a derivation of the asymptotic behavior of the moments of $\mathbb{A}$. Of course, a similar result holds for the covariance of the sequence of vectors induced by matrix $\mathbb{B}$. In the following, we will assume that the singularity exponent α is the same for $\mathbb{A}$ and $\mathbb{B}$ (but see Appendix D for the general case). Note that the natural case where $\mathbb{A}$ and $\mathbb{B}$ are (shifted) GOE matrices corresponds to $\alpha = 1/2$. For $N \gg 1$, Eq. (VII.4) shows that components $v_\ell(t)$ become independent since the process remains Gaussian. As a consequence, the persistence probability $Q_0(\tau)$ is solely determined by the statistics of the sign of $v_1(t)$.

As it is standard in the study of persistence of Gaussian processes (see [130, 128]), we introduce the rescaled process

$$\phi(t) = v_1(t) / \left\langle \overline{v_1(t)^2} \right\rangle^{1/2}, \tag{VII.6}$$

whose statistics are displayed on Figure VII.2. One obtains the following asymptotic form for the correlator of $\phi(t)$ using Eq. (VII.5) [3]

$$\langle \phi(t)\phi(s) \rangle \underset{t,s\to\infty}{\sim} \left(\frac{2\sqrt{ts}}{t+s} \right)^{\alpha+1}. \tag{VII.7}$$

Interestingly, this is *exactly* the correlator of a well studied problem, namely the random diffusion process with an effective dimension $d = 2(\alpha + 1)$ [131, 132] (see Appendix A

[3] Note that this correlator is independent of the constant K appearing in Eq. (VII.5). Correspondingly, the persistence probability $Q_0(\tau)$ is also independent of K.

for a derivation of the associated correlator). Consider the simple diffusion equation $\partial\phi/\partial t = \Delta\phi$ for a scalar field ϕ on $\mathbb{R}^d$ with random initial conditions having zero mean and short-ranged correlations $\langle\phi(\mathbf{x},0)\phi(\mathbf{x}',0)\rangle = \delta^d(\mathbf{x}-\mathbf{x}')$. The probability that $\phi(\mathbf{0},t)$ does not change sign between time $t=0$ and $t=\tau$, is found to decay asymptotically as $\tau^{-\theta(d)}$, with a dimension-dependent persistence exponent [128, 133]. The connection between these two seemingly unrelated problems boils down to the edge behavior of ρ. As an example with GOE matrices, the square-root singularity of Wigner's semicircle distribution is the same as that of the density of eigenvalues of the three-dimensional Laplacian.

For Gaussian Stationary Processes (GSP), the correlator's asymptotics is related to the persistence decay by the Newell-Rosenblatt theorem [134]. Loosely speaking, a GSP with exponentially decaying correlator $C(t,s) \sim e^{-\lambda|t-s|}$ will have exponentially decaying persistence $Q_0(\tau) \sim e^{-\theta\tau}$, where generically $\theta \neq \lambda$. In the case of Eq. (VII.7), the r.h.s is not stationary but self-similar. If one performs a Lamperti transformation $T = \ln(t)$, the new process $\psi(T) = \phi(\ln(t))$ is asymptotically stationary

$$\langle\psi(T)\psi(S)\rangle \underset{T,S\to\infty}{\sim} (\cosh|T-S|)^{-\alpha-1},$$

and decays exponentially. One can therefore apply the previous theorem: there exists an exponent $\mu(\alpha)$ such that $Q_0(T) \sim e^{-\mu(\alpha)T}$. Reverting back to real time t, the persistence decays algebraically $Q_0(t) \sim t^{-\mu(\alpha)}$. Finally, the asymptotic equivalence of Eq. (VII.7) with the correlator of the random diffusion process does *not* immediately imply equality of persistence exponents. However, in most cases, non-universal corrections to $Q_0(\tau)$, depending on the entire form of the correlator, are sub-leading with respect to the algebraic decay inferred from the asymptotics, and one can equate persistence exponents. Our numerical simulations strongly suggest that this is also the case here, i.e. $\mu(\alpha) = \theta(d)$ with $d = 2(\alpha+1)$, see Figure VII.3-(a). In particular GOE matrices correspond to the random diffusion problem in $d=3$ dimensions. From the results of [133] on the d dependence of θ, we infer that for $\alpha \lesssim 22$, the persistence exponent $\mu = \theta$ is less than unity, corresponding to an infinite mean survival time.

3 Switch process and distribution of the maximal Lyapunov exponent

Now, let us come back to our product of random matrices problem

$$\mathbb{M}(t) = \mathbb{A}^{t-t_{k-1}}\mathbb{B}^{\tau_{k-1}}\cdots\mathbb{A}^{\tau_1}, \quad t_k := \sum_{i=1}^{k}\tau_i. \tag{VII.8}$$

In the large N limit, such products have been extensively studied in the context of free probabilities [135, 136, 137]. However, these methods do not apply here since the different terms in the product are not mutually free. In order to progress, we make the following independent interval hypothesis [130, 138, 128], namely that when the sign of $v_1(t)$

changes, i.e. at times t_k, the current vector $\mathbf{v}(t_k)$ can be considered as independent from the matrix ($\mathbb{A}$ or $\mathbb{B}$) under which it will evolve between t_k and t_{k+1}. Intuitively, since $\mathbb{A}, \mathbb{B}$ are assumed mutually free, i.e. randomly rotated from one another, switching from one to the other erases the effects of the previous matrix. Therefore, persistence times τ_i can be considered as IID random variables with distribution $\mathbb{P}(\tau_i = \tau) := p(\tau) = -\partial_\tau Q_0(\tau)$. (Again, we restrict here to the case where $\mathbb{A}$ or $\mathbb{B}$ share the same upper edge singularity exponent α.) The second consequence of our independence assumption is that the growth of the norm of $\mathbf{v}(t)$ between $t = t_{k-1}$ and $t = t_k$ can be approximated, for large N, as

$$\|\mathbf{v}(t_k)\|^2 = \sum_{a=1}^{N} w_a(t_{k-1})\nu_a^{2\tau_k} \approx \|\mathbf{v}(t_{k-1})\|^2 \int \mathrm{d}\nu \rho_k(\nu)\nu^{2\tau_k} \tag{VII.9}$$

where $w_a = (\mathbf{v}\cdot\mathbf{u}_a)^2$ with $(\nu_a, \mathbf{u}_a)$ the eigenpairs of either $\mathbb{A}$ or $\mathbb{B}$ (depending on which of the two matrices is "active" between t_{k-1} and t_k), and $\rho_k(\nu)$ is the corresponding density of eigenvalues. Note that we implicitly used the asymptotic independence of eigenvectors and eigenvalues for rotationally invariant random matrices. See Appendix C for details about the previous formula. We introduce the notation $g_k(\tau) := \frac{1}{2}\ln\int \mathrm{d}\nu\rho_k(\nu)\nu^{2\tau}$ and use the approximate multiplicative norm process of Eq. (VII.9) to estimate the norm $\|\mathbb{M}(t)\mathbf{v}(t=0)\|$ in the definition of the maximal Lyapunov exponent (VII.2). It yields

$$\log\frac{\|\mathbb{M}(t)\mathbf{v}(0)\|}{\|\mathbf{v}(0)\|} \approx g_k(t-t_{k-1}) + \sum_{i=1}^{k-1} g_i(\tau_i) := \Lambda(\vec{\tau}, t) \tag{VII.10}$$

with $\vec{\tau} = (\tau_1, \ldots, \tau_k)$. The moments of the distribution of the Lyapunov exponent $\lambda_{\max}$ can therefore be expressed as

$$\mathbb{E}\left[\lambda_{\max}^q\right] = \lim_{t\to\infty} t^{-q}\frac{\mathcal{Z}(q,t)}{\mathcal{Z}(0,t)}, \tag{VII.11}$$

where

$$\mathcal{Z}(q,t) = \sum_{k=1}^{\infty}\int_{\vec{\tau}}\prod_i p(\tau_i)\Theta\left(t_k - t\right)\Theta\left(t - t_{k-1}\right)\Lambda^q(\vec{\tau}, t), \tag{VII.12}$$

with $\Theta(\cdot)$ the Heaviside step function. Note that trivially $\mathcal{Z}(0,t) = 1$.

In order to estimate the limit in Eq. (VII.11), we introduce the t-Laplace transform $\widehat{f}(\omega) = \int \mathrm{d}t\, e^{-\omega t} f(t)$ of a generic function f, and use Tauberian analysis [139] to relate the large-time behavior of f to the small ω behavior of $\widehat{f}$. We first consider the case $\mu < 1$, for which $p(t) \sim_{t\to\infty} Ct^{-1-\mu}$ implies $\widehat{p}(\omega) \sim_{\omega\to 0} 1 + C\Gamma(-\mu)\omega^\mu$ (with $\Gamma(\cdot)$ the Euler's gamma function). Now, for (VII.11) to have a finite non-trivial limit, one can make the following *ansatz* for $\mathcal{Z}(q,t) \underset{t\to\infty}{\sim} \mathbb{E}[\lambda_{\max}^q]t^q$. After finding a recursion relation for $\widehat{\mathcal{Z}}(q,\omega)$, one can show that the q-exponential generating function of $\widehat{\mathcal{Z}}$ denoted by $\mathcal{G}_{\widehat{\mathcal{Z}}}(x,\omega)$ verifies the equation

$$\mathcal{G}_{\widehat{\mathcal{Z}}} = \frac{1}{2}\frac{\mathcal{G}_{\widehat{h}_1} + \mathcal{G}_{\widehat{h}_2} + \mathcal{G}_{\widehat{h}_2}\mathcal{G}_{\widehat{\phi}_1} + \mathcal{G}_{\widehat{h}_1}\mathcal{G}_{\widehat{\phi}_2}}{1 - \mathcal{G}_{\widehat{\phi}_1}\mathcal{G}_{\widehat{\phi}_2}}, \tag{VII.13}$$

where $\widehat{\phi}_i(q,\omega)$ (resp. $\widehat{h}_i(q,\omega)$) is the Laplace transform of $t \mapsto p(t)g_i(t)^q$ (resp. $t \mapsto Q_0(t)g_i(t)^q$). See Appendix D for a detailed derivation of Eq. (VII.13).

Using a scaling limit $\omega, x \to 0$ while keeping the ratio $\omega/x = y$ constant, we can show that the probability density of $\lambda_{\max}$, denoted by φ, obeys the following equation

$$\int \mathrm{d}\lambda \, \frac{\varphi(\lambda)}{y-\lambda} = \frac{(y-r_1)^{\mu-1} + (y-r_2)^{\mu-1}}{(y-r_1)^{\mu} + (y-r_2)^{\mu}}, \tag{VII.14}$$

with $r_1 = \ln|\nu_{+,\mathbb{A}}|$, $r_2 = \ln|\nu_{+,\mathbb{B}}|$, and for $y \geq \max(r_1, r_2)$. Finally, using Stieltjes inversion formula, one finds the following density

$$\varphi(\lambda) = |r_2 - r_1| \, \frac{\sin \mu\pi}{\pi} \frac{(z_1 z_2)^{\mu-1}}{z_1^{2\mu} + z_2^{2\mu} + 2(z_1 z_2)^{\mu} \cos(\mu\pi)}, \tag{VII.15}$$

for $z_i = |\lambda - r_i|$. This distribution was first obtained by Lamperti [140] and revisited by Godrèche & Luck [141] in the context of occupation time of renewal stochastic processes. A moment of reflection allows to understand why this distribution appears in our problem as well: when $\mu < 1$, the mean persistence time diverges, which means that the longest persistence time τ_i observed in the interval $[0,t]$ is of order t itself. Hence, Eq. (VII.12) is dominated by long persistence times, for which $g_i(\tau_i) \approx r_i\tau_i$. In other words, our problem indeed boils down to an occupation time problem, at least within our independent interval hypothesis.

Note that when $\lambda \to r_i$ the density $\varphi(\lambda)$ diverges as $\kappa|\lambda - r_i|^{\mu-1}$, reflecting the dominance of long periods where the evolution is given either by matrix $\mathbb{A}$ (contributing to $\lambda \approx \ln|\nu_{+,\mathbb{A}}|$) or by matrix $\mathbb{B}$ (contributing to $\lambda \approx \ln|\nu_{+,\mathbb{B}}|$). Setting $\mu = 1$ in Eq. (VII.14), we see that $\varphi(\lambda) \to \delta(\lambda - m_1)$ with $m_1 = (r_1 + r_2)/2$, rendering the system self-averaging. Figure VII.3 shows the distribution of the Lyapunov exponent for matrices drawn from GOE and the density of Eq. (VII.15) with $\mu = 2\theta(d=3)$ [4]. The agreement with our theoretical prediction is very good. A rigorous hypothesis test is however difficult because of finite N and t effects that cannot be neglected, see below.

In the case where $\mu > 1$ (i.e. $\alpha \gtrsim 22$), the whole small ω analysis of $\widehat{\mathcal{Z}}(q,\omega)$ must be reconsidered (see Appendix D) and leads to the conclusion that the Lyapunov exponent $\lambda_{\max}$ becomes self-averaging and given by

$$\lambda_{\max} = \frac{\mathbb{E}\left[g_{\mathbb{A}}(\tau) + g_{\mathbb{B}}(\tau)\right]}{2\mathbb{E}[\tau]}, \tag{VII.16}$$

with τ distributed according to $p(\tau)$. However, observing this self-averaging regime is not straightforward since for $\alpha \gtrsim 22$, the density of eigenvalues is extremely small close to the upper edge.

[4] Here, the persistence exponent doubles since Wigner's semi-circle distribution is symmetrical and therefore has odd moments equal to zero. As a consequence, $(v_\ell(2s))_s$ and $(v_\ell(2s+1))_s$ are mutually independent and the persistence of the entire system is the square of that of the even or odd process.

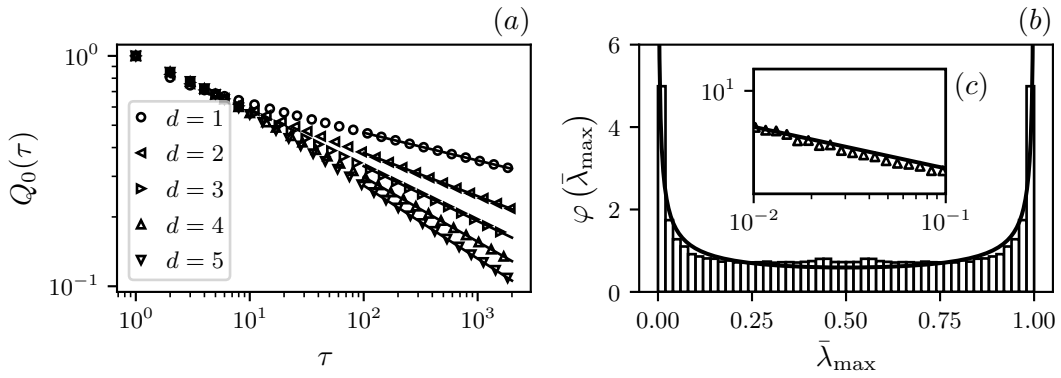


Figure VII.3: (a) Persistence probability of $\phi(t)$ for different effective dimensions d. The spectral distribution ρ is chosen to be a standard symmetric Beta distribution $\mathsf{B}\left(\frac{d}{2}, \frac{d}{2}\right)$ with support $[0, 1]$. The solid lines represent the algebraic decay of the persistence of the random diffusion process $t^{-\theta(d)}$ using the persistence exponents computed in [128, 131]: $\theta(1) = 0.1205$, $\theta(2) = 3/16$, $\theta(3) = 0.2382$, $\theta(4) = 0.2806$, $\theta(5) = 0.3173$. (b) Probability distribution of the normalized Lyapunov exponent $\bar{\lambda}_{\max} = (\lambda_{\max} - r_1)/(r_2 - r_1)$ for GOE matrices $\mathbb{A}$ and $\mathbb{B}$ of size $N \times N$, $N = 10^4$ with $\nu_{+,\mathbb{A}} = 0.05\sqrt{2}$ and $\nu_{+,\mathbb{B}} = 2\sqrt{2}$. The black line shows the density Eq. (VII.15). (c) Zoom on the left-tail of φ showing a very good agreement of the divergence with the predicted exponent $\mu - 1$ (black line).

4 Finite N effects

The previous analysis was conducted in the limit $N \to \infty$, before the large-time limit $t \to \infty$ is taken. As we saw, in this limit, the persistence probability takes the form $Q_0(\tau) \sim \tau^{-\mu}$. However, whenever N is finite, the eigenvalues of the matrices $\mathbb{A}$ and $\mathbb{B}$ do not perfectly sample the respective measures $\rho_{\mathbb{A}}(\nu)$ and $\rho_{\mathbb{B}}(\nu)$. Fluctuations near the edges of the spectrum are thus expected to change the persistence probability. As an example, let us consider matrices $\mathbb{A}$ drawn from GOE. It is well known that at finite N, the maximum eigenvalue of $\mathbb{A}$ (or of $\mathbb{B}$) exhibits fluctuations of order $N^{-2/3}$ around the edge, abiding to the $\beta = 1$ Tracy-Widom distribution F_1 [142]. As a consequence, following the analysis of [131, 143] for the random diffusion problem, we conjecture that the persistence probability at finite, large N writes

$$Q_0(\tau, N) \propto N^{-2\mu/3} h\left(\tau N^{-2/3}\right), \tag{VII.17}$$

where h is a scaling function such that $h(u) \underset{u\to 0}{\sim} u^{-\mu}$ and $h(u) \underset{u\to\infty}{\to} c$, with c a constant. Figure VII.4-(a) shows our numerical results that confirm such a scaling hypothesis, with again $\mu = 2\theta(3)$ for centered GOE matrices. The small u behavior of h recovers the pure power law $\tau^{-\mu}$ in the large N limit, whereas the large u regime shows that, at finite N, $\mathbb{P}(\tau = \infty) = c > 0$. This means that there is a positive probability that the vector $\mathbf{v}(t)$ remains "trapped" forever within a cone. But if the dynamics gets stuck within one cone,

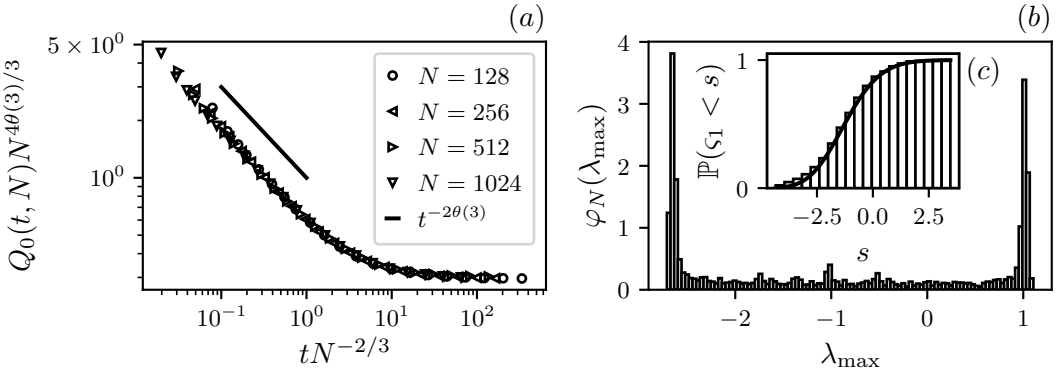


Figure VII.4: (*a*) Scaling form of the persistence probability at finite N for matrices drawn from GOE(N). For GOE, $\alpha = 1/2$ and $d = 3$, however since the eigenvalue density is symmetrical, odd and even times processes are uncorrelated, such that the persistence exponent is $2\theta(3)$. (*b*) Probability distribution φ_N of $\lambda_{\max}$ for finite $N = 128$. We see that the edges of the spectrum are not sharp as in the case $N \to \infty$, but fluctuate around the corresponding values of $\ln|\nu_+|$ (with $\nu_{+,\mathbb{A}} = 0.05\sqrt{2}$ and $\nu_{+,\mathbb{B}} = 2\sqrt{2}$). (*c*) Cumulative distribution of the random variable $\varsigma_1 = (e^{\lambda_{\max}} - \nu_+)N^{2/3}/\gamma$ with $\gamma = \nu_+/2$. We overlay in black the cumulative distribution $F_1(s)$ of the $\beta = 1$ Tracy-Widom distribution.

the associated Lyapunov exponent is simply given by $\lambda_{\max} = \ln|\nu_{\max,N}|$ where $\nu_{\max,N}$ is the largest eigenvalue of either $\mathbb{A}$ or $\mathbb{B}$ for a given finite value of N. As a consequence, the distribution of $e^{\lambda_{\max}}$ will have two peaks of width $N^{-2/3}$ centered around $\nu_{+,\mathbb{A}}$ and $\nu_{+,\mathbb{B}}$. The fluctuations around these peaks are given by Tracy-Widom distributions, as confirmed by our numerical data (see Figure VII.4-(*b*)).

5 Conclusion and extensions

In conclusion, even our highly simplified conewise-linear dynamics exhibits quite non-trivial properties. First, if the large-dimension limit $N \to \infty$ is taken before the large-time limit, we find that for a wide class of random matrices the Lyapunov exponent is non self-averaging, i.e. continues to fluctuate in the large-time limit. Depending on the relative positions of the upper edge of the spectrum of $\mathbb{A}$ and $\mathbb{B}$, one can observe apparent stability and apparent instability for the same system, depending on time and initial conditions. If, on the other hand, N is large but finite, the dynamics eventually gets trapped in one of two half-spaces and the Lyapunov exponent converges to the top (log-)eigenvalue of the corresponding matrix $\mathbb{A}$ and $\mathbb{B}$. So if – say – $\mathbb{A}$ leads to a stable evolution and $\mathbb{B}$ to an unstable explosion, the dynamics of the system, even close to equilibrium, will be either stable or explosive, depending on minute details of the initial perturbation.

Finally, we list here some avenues for the generalizations of the results, some of which are detailed in the technical appendices of this chapter. We can think first of matrices

with more complicated structure such as correlations between coefficients. For example, for non-symmetric Gaussian random matrices with a correlation coefficient ϱ between entries ij and ji ($\varrho = 1$ corresponding to the symmetric case), we have found numerically that the persistence probability $Q_0(\tau)$ decays as a truncated power-law $\tau^{-\mu(\varrho)}e^{-\kappa(\varrho)\tau}$ where $(\mu(\varrho), \kappa(\varrho))$ interpolate between $(\mu, 0)$ ($\varrho = 1$: symmetric case) and $(0, \ln 2)$ ($\varrho = 0$: Ginibre case). For generic ϱ, a non self-averaging behavior occurs up to the time-scale $1/\kappa(\varrho)$. Furthermore, we can think of matrices having outlying eigenvalues in addition to the spectrum supported on a compact set. Take for instance a matrix $\mathbb{A}$ of the form

$$\mathbb{A} = \mathbb{X} + \gamma \frac{\mathbf{u}\mathbf{u}^\top}{\|\mathbf{u}\|^2},$$

with $\mathbb{X}$ a GOE matrix with elements of variance σ^2, $\mathbf{u} \hookrightarrow \mathsf{N}(0, \mathbf{I}_N)$ a random Gaussian vector independent from $\mathbb{X}$ and $\gamma > 0$ a scalar. As γ increases, the spectrum of $\mathbb{A}$ undergoes the well-known BBP transition [144] for a value $\gamma_c = \sigma$. For $\gamma < \gamma_c$, the spectrum of $\mathbb{A}$ is simply given by the bulk of $\mathbb{X}$, whereas whenever $\gamma > \gamma_c$, an outlying eigenvalue $\nu_o = \gamma + \sigma^2/\gamma$ escapes the bulk. In the previous situation, it would be interesting to understand what is the effect of the BBP transition on the persistence probability, and the subsequent Lyapunov exponent. Both previous generalizations are detailed in Appendix F, and Chapter IX is devoted to the study of the mixed-moments of Gaussian elliptic matrices which are of interest for this generalization.

More complicated cone structures could also be considered. The simplest generalization is when the signs of p vector components, say $v_1, v_2, \ldots, v_p$, select which of the 2^p matrices determine the dynamics. In this case, the persistence exponent is simply given by $p\mu$ and the distribution of $\lambda_{\max}$ is a generalization of the Lamperti distribution. Such generalization will be discussed in Chapter VIII, and can be found in [3]. Furthermore, one could also consider mixed switch conditions

$$\mathbf{v}(t+1) = \begin{cases} \mathbb{A}\mathbf{v}(t), & \text{when } v_1(t) > 0 \text{ and } v_2(t) + av_1(t) > 0 \\ \mathbb{B}\mathbf{v}(t), & \text{when } v_1(t) < 0 \text{ and } v_2(t) + av_1(t) > 0 \\ \mathbb{C}\mathbf{v}(t), & \text{when } v_1(t) > 0 \text{ and } v_2(t) + av_1(t) < 0 \\ \mathbb{D}\mathbf{v}(t), & \text{when } v_1(t) < 0 \text{ and } v_2(t) + av_1(t) < 0 \end{cases}, \tag{VII.18}$$

with $a > 0$. Whenever $a = 0$, we retrieve the previous example where cone switching is governed by the signs of v_1 and v_2. Whenever $a \to \infty$, we recover the model of the previous section with matrices $\mathbb{A}$ and $\mathbb{D}$. The persistence exponent therefore depends continuously on a and interpolates between 2μ and μ. However, the precise nature of the relationship $a \mapsto \mu(a)$ is very complex to track down. Indeed, $v_1(t)$ and $v_2(t) + av_1(t)$ are not independent, and the persistence probability therefore does not decouple. Such a situation is of interest for the conewise models of Chapter IV and Chapter V since cone vectors $\mathbf{c}_{g,i}$ and $\mathbf{c}_w$ are not as trivial as the canonical vectors we consider in this chapter.

Finally, small N effects should lead to a breakdown of our strong independence assumption, and generate even more complex types of dynamics, with non-random sequences of visited cones (see Appendix E). In view of the rich phenomenology reported in [1], we believe that such effects would be well worth investigating.

Key takeaways

- **Conewise Linear Systems** are systems for which the linear evolution depends on the direction of the input vector. The simple example of this chapter is a two-cone system with matrices $\mathbb{A}, \mathbb{B}$ such that

$$\mathbf{v}(t+1) = \begin{cases} \mathbb{A}\mathbf{v}(t), & \text{when } v_1(t) > 0 \\ \mathbb{B}\mathbf{v}(t), & \text{when } v_1(t) < 0 \end{cases}.$$

- **Intra-cone behavior**, i.e. the evolution $\mathbf{v}(t+1) = \mathbb{A}\mathbf{v}(t)$, can be mapped onto a centered Gaussian process with covariance

$$\left\langle \overline{v_\ell(t) v_{\ell'}(s)} \right\rangle = \delta_{\ell\ell'} f_{\mathbb{A}}(t+s),$$

  where the average $\left\langle \overline{(\,\cdot\,)} \right\rangle$ is taken over both initial conditions (such that $\mathbf{v}(0)$ is a standard Gaussian vector with independent entries) and the disorder $\mathbb{A}$ (chosen to be orthogonally invariant random matrices), and where $f_{\mathbb{A}}$ refers to the moments of $\mathbb{A}$.

- **Persistence** of $v_1(t)$, i.e. the time for which $v_1(t)$ keeps a constant sign, displays a power-law behavior $Q_0(t) \sim t^{-\mu}$ whenever the matrix $\mathbb{A}$ is symmetric. The exponent μ is characterized by the edge behavior of the spectral density of $\mathbb{A}$, and related to the persistence of diffusive fields in an effective dimension. For non-symmetric matrices, we conjecture an exponential cutoff to the persistence.

- **Stability**, characterized by the maximum Lyapunov exponent $\lambda_{\max}$, depends on the initial conditions and observation time. For symmetric matrices, the system is non-ergodic and the Lyapunov exponent remains random even in the large-time limit, with a distribution given by a Lamperti law

$$\varphi(\lambda) = |r_2 - r_1| \, \frac{\sin \mu\pi}{\pi} \frac{(z_1 z_2)^{\mu-1}}{z_1^{2\mu} + z_2^{2\mu} + 2(z_1 z_2)^{\mu} \cos(\mu\pi)},$$

  for $z_i = |\lambda - r_i|$, $r_1 = \ln|\nu_{+,\mathbb{A}}|$, $r_2 = \ln|\nu_{+,\mathbb{B}}|$.

A Persistence probability for the diffusion equation with random initial conditions

Let us consider a scalar field $\phi(\vec{x}, t)$ over $\mathbb{R}^d$ obeying the diffusion equation

$$\frac{\partial \phi}{\partial t} = \Delta \phi, \tag{VII.19}$$

with initial condition taken to be a Gaussian random field such that

$$\langle \phi(\mathbf{x}, 0) \rangle = 0, \quad \langle \phi(\mathbf{x}, 0)\phi(\mathbf{x}', 0) \rangle = \delta^d(\mathbf{x} - \mathbf{x}'). \tag{VII.20}$$

Assuming that the diffusion may occur in a region of linear size L, i.e. $\|\mathbf{x}\| \leq L$, we want to understand the probability $Q(\tau, L)$ that the field $\phi(\mathbf{x}, t)$ will keep a constant sign up to time τ. The solution to the above equation reads

$$\phi(\mathbf{x}, t) = \int_{\|\mathbf{y}\| \leq L} \mathrm{d}\mathbf{y}\, \mathcal{G}(\mathbf{y} - \mathbf{x}, t)\phi(\mathbf{y}, 0), \tag{VII.21}$$

where $\mathcal{G}$ denotes the Green's function associated to the diffusion equation

$$\mathcal{G}(\mathbf{z}, t) = (4\pi t)^{-d/2} \exp -\|\mathbf{z}\|^2/4t. \tag{VII.22}$$

The persistence probability for this process refers to the amount of time the field ϕ keeps a constant sign at $\mathbf{x} = \mathbf{0}$ [5]. Denoting by $C(t, t')$ the correlator of $\phi(\mathbf{0}, t)$ between times t and t', we can use the explicit solution for ϕ to get

$$C(t, t') := \langle \phi(\mathbf{0}, t)\phi(\mathbf{0}, t') \rangle = \int_{\|\mathbf{y}\| \leq L} \mathrm{d}\mathbf{y}\, \mathcal{G}(\mathbf{y}, t)\mathcal{G}(\mathbf{y}, t'). \tag{VII.23}$$

By rescaling both the field $\psi(t) = \phi(t)/\sqrt{C(t, t)}$ and the time $\tilde{t} = t/L^2$, we can easily obtain the behavior of the correlator $a(\tilde{t}, \tilde{t}')$ for $\psi(\tilde{t})$

$$a(\tilde{t}, \tilde{t}') \sim \begin{cases} \left(\frac{2\sqrt{\tilde{t}\tilde{t}'}}{\tilde{t}+\tilde{t}'}\right)^{d/2} & , \quad \tilde{t}, \tilde{t}' \ll 1 \\ 1 & , \quad \tilde{t}, \tilde{t}' \gg 1 \end{cases}. \tag{VII.24}$$

We will consider the case $L \to \infty$, i.e. $\tilde{t}, \tilde{t}' \ll 1$, but see [128] for the other limit. In this limit, the process is self-similar, i.e. $\psi(\lambda t) \overset{d}{=} \psi(t)$ for $\lambda > 0$. It can therefore be mapped onto a stationary process using the Lamperti transformation $T = \ln t$. In this new variable, the process has the correlator

$$\langle \psi(T)\psi(S) \rangle = (\cosh |T - S|)^{-d/2}, \tag{VII.25}$$

whose exponential decay implies an exponential decay of the associated persistence probability. Reverting back to the original time variable, the persistence $q(\tau)$ of $\psi(t)$ therefore has an algebraic decay with a dimension dependent exponent $q(\tau) \sim \tau^{-\theta(d)}$. There exists no known analytical value for $\theta(d)$, except for $d = 2$ for which $\theta(d) = 3/16$ [131], but several techniques have been developed to estimate them numerically [128, 133].

[5] We choose to look at the point $\mathbf{x} = \mathbf{0}$ since spatial features are irrelevant for the persistence.

B Mapping to a Gaussian process and persistence of $v_1(t)$

In this section, we provide the details of the computation to map the dynamics of Eq. (VII.1) of the main text onto a centered Gaussian process for which Eq. (VII.4) is the particular case for symmetric matrices. Recall that we consider the following conewise-linear system

$$\mathbf{v}(t+1) = \begin{cases} \mathbb{A}\mathbf{v}(t), & \text{when } v_1(t) > 0 \\ \mathbb{B}\mathbf{v}(t), & \text{when } v_1(t) < 0 \end{cases}, \tag{VII.26}$$

where $\mathbb{A}$ and $\mathbb{B}$ are $O(N)$ rotationally invariant random matrices. We assume that the initial condition $\mathbf{v}(0) \in \mathbb{R}^N$ is a centered Gaussian vector of unit variance. For the matrix $\mathbb{M} = \mathbb{A}$ or $\mathbb{B}$, we denote by ρ its spectral density and by $f(t)$ its t-th moment

$$f(t) = \int \mathrm{d}\nu \rho(\nu) \nu^t.$$

Finally, $\langle(\,\cdot\,)\rangle$ will denote the average over the *disorder* $\mathbb{M}$, $\overline{(\,\cdot\,)}$ the average over the initial condition $\mathbf{v}(0)$ and $\tau(\,\cdot\,) = \lim_{N\to\infty} N^{-1}\mathrm{Tr}\,(\cdot)$ the normalized trace.

B.1 Computation of the statistics of $\mathbf{v}(t)$ within one cone in the limit $N \to \infty$

As long as $v_1(t)$ keeps a constant sign, the dynamics is linear and immediately yields

$$\mathbf{v}(t) = \mathbb{M}^t \mathbf{v}(0). \tag{VII.27}$$

Calling $\boldsymbol{\varepsilon_i}$ the i-th canonical vector of $\mathbb{R}^N$, we can express the ℓ-th component $v_\ell(t)$ of $\mathbf{v}(t)$ as

$$v_\ell(t) := \boldsymbol{\varepsilon_\ell} \cdot \mathbf{v}(t) = \sum_\alpha \left(\mathbb{M}^t\right)_{\ell\alpha} v_\alpha(0)$$

Here, we consider a *fixed* realization of the disorder $\mathbb{M}$. As a consequence, since $\mathbf{v}(0)$ is a Gaussian vector, one immediately sees that $\mathbf{v}(t)$ is also a Gaussian vector whose statistics can be computed easily. For the mean, we have

$$\begin{aligned} \overline{v_\ell(t)} &= \sum_\alpha \left(\mathbb{M}^t\right)_{\ell\alpha} \overline{v_\alpha(0)} \\ &= 0 \end{aligned}$$

and for the covariance, we get

$$\begin{aligned} \overline{v_\ell(t) v_{\ell'}(s)} &= \sum_{\alpha,\beta} \left(\mathbb{M}^t\right)_{\ell\alpha} \left(\mathbb{M}^s\right)_{\ell'\beta} \overline{v_\alpha(0) v_\beta(0)} \\ &= \sum_\alpha \left(\mathbb{M}^t\right)_{\ell\alpha} \left(\mathbb{M}^s\right)_{\ell'\alpha} \\ &= \left(\mathbb{M}^t \left(\mathbb{M}^\top\right)^s\right)_{\ell\ell'}. \end{aligned}$$

Once again, these expressions are obtained for a fixed realization of the disorder $\mathbb{M}$. Taking the average over $\mathbb{M}$, one should usually be a bit careful. It is not straightforward that the average over $\mathbb{M}$ will leave the statistics of $\mathbf{v}(t)$ Gaussian. However in our case, we can see its correlator is actually self-averaging in the limit $N \to \infty$ thanks to the rotational invariance of $\mathbb{M}$ and, as a consequence, the process remains Gaussian for $N \to \infty$ with covariance

$$\overline{v_\ell(t)v_{\ell'}(s)} \underset{N\to\infty}{\sim} \frac{1}{N}\left\langle \mathrm{Tr}\left[\mathbb{M}^t\left(\mathbb{M}^\top\right)^s\right]\right\rangle \delta_{\ell\ell'} \underset{N\to\infty}{\longrightarrow} \tau\left(\mathbb{M}^t\left(\mathbb{M}^\top\right)^s\right) = \left\langle \overline{v_\ell(t)v_{\ell'}(s)}\right\rangle. \tag{VII.28}$$

We see that components are uncorrelated and, since they are Gaussian, therefore independent in the large N limit. Finally, time-wise correlations are given by the *mixed-moments* of matrices $\mathbb{M}$ and $\mathbb{M}^\top$.

B.2 The symmetric case: link to random diffusion

If the matrix $\mathbb{M}$ is symmetric, the mixed moment can be easily expressed

$$\tau\left(\mathbb{M}^t\left(\mathbb{M}^\top\right)^s\right) = \tau\left(\mathbb{M}^{t+s}\right) = f(t+s), \tag{VII.29}$$

and amounts to the knowledge of the moments of $\mathbb{M}$. To establish the link with the random diffusion process, we must study the asymptotic behavior of the correlator of $\mathbf{v}(t)$, which boils down to the asymptotics of the moments of $\mathbb{M}$. In the previous section, we have introduced the spectral density ρ of $\mathbb{M}$. As in the main text, we will assume that this density has a compact support $[\nu_-, \nu_+]$ with $\nu_- < \nu_+$. Furthermore, it has a behavior close to the upper edge characterized by a constant K and an exponent α, which we assume greater than -1 for integrability purposes,

$$\rho(\nu) \underset{\nu\to\nu_+}{\sim} K|\nu - \nu_+|^\alpha.$$

With these assumptions, we can use Laplace's method to estimate the large-time behavior of the moments $f(t)$ of ρ. Denoting by $\Delta\nu = \nu_+ - \nu_- > 0$, it yields

$$\begin{aligned}
\nu_+^{-t} f(t) &= \int_{\nu_-}^{\nu_+} \mathrm{d}\nu \rho(\nu) \left(\frac{\nu}{\nu_+}\right)^t \\
&= \int_0^{\Delta\nu} \mathrm{d}\sigma \rho(\nu_+ - \sigma) \left(1 - \frac{\sigma}{\nu_+}\right)^t \\
&= \frac{\nu_+}{t}\int_0^{t\Delta\nu} \mathrm{d}x \rho\left(\nu_+\left(1 - \frac{x}{t}\right)\right)\left(1 - \frac{x}{t}\right)^t \\
&\sim \frac{\nu_+}{t}\int_0^{\infty} \mathrm{d}x K\left|\nu_+ - \nu_+\left(1 - \frac{x}{t}\right)\right|^\alpha e^{-x} \\
&= K\left(\frac{\nu_+}{t}\right)^{\alpha+1}\int_0^\infty \mathrm{d}x e^{-x} x^\alpha \\
&= K\left(\frac{\nu_+}{t}\right)^{\alpha+1}\Gamma(\alpha+1),
\end{aligned}$$

so that we get the asymptotic behavior of the main text

$$f(t) \underset{t\to\infty}{\sim} K\Gamma(\alpha+1)\,\nu_+^{t+\alpha+1} t^{-\alpha-1}. \tag{VII.30}$$

We then introduce (as it is standard in persistence problems), the rescaled process

$$\phi_i(t) = \frac{v_i(t)}{\sqrt{\left\langle \overline{v_i^2(t)} \right\rangle}},$$

with $\phi(t) := \phi_1(t)$ as in the main text. Its correlator is given by

$$\langle \phi_i(t)\phi_j(s)\rangle = \delta_{ij} \frac{f(t+s)}{\sqrt{f(2t)f(2s)}}. \tag{VII.31}$$

Note that $\phi_i(t)$ is a Gaussian random variable with 0 mean and unit variance. Using the asymptotic behavior of Eq. (VII.30), we therefore get

$$\langle \phi(t)\phi(s)\rangle \underset{t,s\to\infty}{\sim} \left(\frac{2\sqrt{ts}}{t+s}\right)^{\alpha+1}, \tag{VII.32}$$

and recover the result stated in the main text. Figure VII.2 shows the statistics of the process $\phi_i(t)$, aligned with the previous theoretical predictions.

C Approximation of the norm-growth of $\mathbf{v}(t)$

The vector $\mathbf{v}(t)$ can be expressed thanks to the initial condition and the effective matrix

$$\mathbf{v}(t) = \mathbb{M}(t)\mathbf{v}(0), \tag{VII.33}$$

with

$$\mathbb{M}(t) = \mathbb{A}^{t-t_{k-1}}\mathbb{B}^{\tau_{k-1}}\cdots\mathbb{A}^{\tau_1},$$

assuming w.l.o.g that $v_1(0) > 0$. Assuming that at time $t_\ell = \sum_{i=1}^{\ell}\tau_i$, one has $v_1(t_\ell) > 0$ (and $v_1(t_\ell - 1) < 0$, we can write

$$\mathbf{v}(t_{\ell+1}) = \mathbb{A}^{\tau_{\ell+1}}\mathbf{v}(t_\ell).$$

Denoting by $(\nu_a, \mathbf{u}_a)$ the eigenpairs associated to $\mathbb{A}$, we can express the norm of $\mathbf{v}(t_{\ell+1})$

$$\|\mathbf{v}(t_{\ell+1})\|^2 = \sum_{a=1}^{N} \nu_a^{2\tau_{\ell+1}} \left(\mathbf{u}_a \cdot \mathbf{v}(t_\ell)\right)^2. \tag{VII.34}$$

Using the IIA approximation of the main text, $\mathbf{v}(t_\ell)$ and $\mathbf{u}_a$ are independent. Furthermore, in the large N limit components of both $\mathbf{v}(t_\ell)$ and $\mathbf{u}_a$ become independent from each other, and the components $u_{a,i}$ can be approximated by centered Gaussian random variables of variance $1/N$. As a consequence

$$\|\mathbf{v}(t_\ell)\|^2 = \sum_{i=1}^{N} v_i^2(t_\ell) \approx N \left\langle \overline{v_1^2(t_\ell)} \right\rangle, \tag{VII.35}$$

and

$$\left(\mathbf{u}_a \cdot \mathbf{v}(t_\ell)\right)^2 := \sum_{i,j} v_i(t_\ell)v_j(t_\ell)u_{a,i}u_{a,j} \approx \sum_i v_i^2(t_\ell)u_{a,i}^2 \approx N \left\langle \overline{v_1^2(t_\ell)} \right\rangle \left\langle u_{a,1}^2 \right\rangle \approx \frac{1}{N}\|\mathbf{v}(t_\ell)\|^2. \tag{VII.36}$$

We can plug this back into Eq. (VII.34) to get

$$\|\mathbf{v}(t_{\ell+1})\|^2 = \|\mathbf{v}(t_\ell)\|^2 \frac{1}{N}\sum_{a=1}^{N} \nu_a^{2\tau_\ell} \approx \|\mathbf{v}(t_\ell)\|^2 \int \mathrm{d}\nu \rho_{\mathbb{A}}(\nu)\nu^{2\tau_\ell}. \tag{VII.37}$$

Of course the same reasoning holds for the matrix $\mathbb{B}$. Using the notation

$$g_k(\tau) := \frac{1}{2}\ln \int \mathrm{d}\nu \rho_k(\nu)\nu^{2\tau},$$

with k denoting either $\mathbb{A}$ or $\mathbb{B}$ depending on which matrix dictates the linear evolution, we can write the norm growth

$$\ln \frac{\|\mathbf{v}(t)\|}{\|\mathbf{v}(0)\|} = g_k(t - t_{k-1}) + \sum_{i=1}^{k-1} g_i(\tau_i). \tag{VII.38}$$

D Distribution of $\lambda_{\max}$

In this appendix, we derive the equation for the q-exponential generating functions of $\widehat{\mathcal{Z}}$ and the density φ of $\lambda_{\max}$. As stated in the text in Eq. (VII.11), the starting point is

$$\mathbb{E}\left[\lambda_{\max}^q\right] = \lim_{t\to\infty} t^{-q}\frac{\mathcal{Z}(q,t)}{\mathcal{Z}(0,t)}, \tag{VII.39}$$

where

$$\mathcal{Z}(q,t) = \sum_{k=1}^{\infty}\int_{\vec{\tau}}\prod_{i=1}^{k} p_i(\tau_i)\Theta\left(t_k - t\right)\Theta\left(t - t_{k-1}\right)\Lambda^q(\vec{\tau},t) := \sum_{k=1}^{\infty}\mathcal{X}_k(q,t), \tag{VII.40}$$

with $t_k = \sum_{i=1}^{k}\tau_i$, $\vec{\tau} = (\tau_1,\ldots,\tau_k)$, $\int_{\vec{\tau}} = \int \mathrm{d}\tau_1\cdots\mathrm{d}\tau_k$ and

$$\Lambda(\vec{\tau},t) = \sum_{i=1}^{k-1} g_i(\tau_i) + g_k\left(t - t_{k-1}\right). \tag{VII.41}$$

The partition function $\mathcal{Z}(q,t)$ corresponds to a grand canonical ensemble partition function. We will denote by $\widehat{f}$ the t-Laplace transform of a generic function f

$$\widehat{f}(\omega) = \int_0^\infty \mathrm{d}t e^{-\omega t} f(t). \tag{VII.42}$$

We also introduce the following quantities

$$\widehat{\phi}_i(\ell,\omega) = \int_0^\infty \mathrm{d}t e^{-\omega t} p_i(t) g_i(t)^\ell, \tag{VII.43}$$

$$\widehat{h}_i(\ell,\omega) = \int_0^\infty \mathrm{d}t p_i(t)\int_0^t \mathrm{d}s e^{-\omega s} g_i(s)^\ell \tag{VII.44}$$

$$= \int_0^\infty \mathrm{d}s e^{-\omega s} g_i(s)^\ell Q_{0,i}(s), \tag{VII.45}$$

$$\widehat{h}_i(0,\omega) := \frac{1-\widehat{p}_i(\omega)}{\omega}, \tag{VII.46}$$

where $\widehat{\phi}_i(0,\omega) := \widehat{p}_i(\omega)$. Finally, note that, unlike in the main text, there is a subscript i on the persistence probabilities. This is the general case where matrices $\mathbb{A}$ and $\mathbb{B}$ can have different edge exponents $\alpha_{\mathbb{A}}$ and $\alpha_{\mathbb{B}}$.

D.1 Canonical ensemble computation

We introduce the following canonical partition function which we will need for the computation of $\mathcal{Z}(q,t)$

$$Z(q,t) = \sum_{k=1}^{\infty} \int_{\vec{\tau}} \prod_{i=1}^{k} p_i(\tau_i) \delta\left(t - t_k\right) \Lambda^q(\vec{\tau}, t) := \sum_{k=1}^{\infty} x_k(q,t). \tag{VII.47}$$

We will express the exponential generating function $G_{\widehat{Z}}(x)$ of $\widehat{Z}$. To do so, we must find a recursive relation on the Laplace transform of Z. Let us start by computing the quantities $\widehat{x}_k(q,\omega)$. We have for x_k

$$x_k(q,t) = \int_{\vec{\tau}} \delta\left(t - t_k\right) \prod_{i=1}^{k} p_i(\tau_i) \left(\sum_{j=1}^{k} g_j(\tau_j) \right)^q,$$

where we have replace the last term in the q-power $g_k\left(t - t_{k-1}\right)$ by $g_k(\tau_k)$ as enforced by the Dirac delta constraint. We can carry out the computation by expanding the q-power using the multinomial theorem

$$\begin{aligned}
&= \int_{\vec{\tau}} \delta\left(t - t_k\right) \prod_{i=1}^{k} p_i(\tau_i) \sum_{\ell_1,\dots,\ell_k} \delta\left(\sum_{i=1}^{k} \ell_i - q \right) \binom{q}{\boldsymbol{\ell}} \prod_{j=1}^{q} g_j(\tau_j)_j^{\ell} \\
&= \sum_{\ell_1,\dots,\ell_k} \delta\left(\sum_{i=1}^{k} \ell_i - q \right) \binom{q}{\boldsymbol{\ell}} \int_{\vec{\tau}} \delta\left(t - t_k\right) \prod_{j=1}^{k} p_j(\tau_j) g_j(\tau_j)^{\ell_j}.
\end{aligned}$$

We can then compute the Laplace transform of x_k

$$\begin{aligned}
\widehat{x}_k(q,\omega) &= \int_0^{\infty} \mathrm{d}t e^{-\omega t} \sum_{\ell_1,\dots,\ell_k} \delta\left(\sum_{i=1}^{k} \ell_i - q \right) \binom{q}{\boldsymbol{\ell}} \int_{\vec{\tau}} \delta\left(t - t_k\right) \prod_{j=1}^{k} p_j(\tau_j) g_j(\tau_j)^{\ell_j} \\
&= \sum_{\ell_1,\dots,\ell_k} \delta\left(\sum_{i=1}^{k} \ell_i - q \right) \binom{q}{\boldsymbol{\ell}} \int_{\vec{\tau}} \prod_{j=1}^{k} p_j(\tau_j) g_j(\tau_j)^{\ell_j} e^{-\omega \tau_j} \\
&= \sum_{\ell_1,\dots,\ell_k} \delta\left(\sum_{i=1}^{k} \ell_i - q \right) \binom{q}{\boldsymbol{\ell}} \prod_{j=1}^{k} \widehat{\phi}_j(\ell_j, \omega).
\end{aligned}$$

To carry out the computation, we need to distinguish between even and odd values of k. Indeed, provided $v_1(0) > 0$, the effective matrix of the system will look like

$$\begin{aligned}
\mathbb{M}(t_{2s}) &= \mathbb{B}^{\tau_{2s}} \mathbb{A}^{\tau_{2s-1}} \cdots \mathbb{B}^{\tau_2} \mathbb{A}^{\tau_1} \\
\mathbb{M}(t_{2s+1}) &= \mathbb{A}^{\tau_{2s+1}} \mathbb{B}^{\tau_{2s}} \cdots \mathbb{B}^{\tau_2} \mathbb{A}^{\tau_1},
\end{aligned}$$

which in turn implies $g_{2s} = g_2$ and $g_{2s+1} = g_1$. As a consequence, we have

$$\begin{aligned}
\widehat{x}_{2s}(q,\omega) &= \sum_{\ell_1,\dots,\ell_{2s}} \delta\left(\sum_{i=1}^{2s} \ell_i - q \right) \binom{q}{\ell_1, \dots, \ell_{2s}} \widehat{\phi}_2(\ell_{2s}, \omega) \prod_{j=1}^{2s-1} \widehat{\phi}_j(\ell_j, \omega) \\
&= \sum_{\ell=0}^{q} \binom{q}{\ell} \widehat{\phi}_2(\ell, \omega) \sum_{\ell_1,\dots,\ell_{2s-1}} \delta\left(\sum_{i=1}^{2s-1} \ell_i - (q - \ell) \right) \binom{q-\ell}{\ell_1, \dots, \ell_{2s-1}} \prod_{j=1}^{2s-1} \widehat{\phi}_j(\ell_j, \omega),
\end{aligned}$$

where the sum over $\ell_1, \ldots, \ell_{2s-1}$ is exactly $\widehat{x}_{2s-1}(q-\ell,\omega)$. A similar fact holds for $\widehat{x}_{2s+1}(q-\ell,\omega)$ and we get

$$\widehat{x}_{2s}(q,\omega) = \sum_{\ell=0}^{q} \binom{q}{\ell} \widehat{\phi}_2(\ell,\omega)\widehat{x}_{2s-1}(q-\ell,\omega), \quad s \geq 1 \tag{VII.48}$$

$$\widehat{x}_{2s+1}(q,\omega) = \sum_{\ell=0}^{q} \binom{q}{\ell} \widehat{\phi}_1(\ell,\omega)\widehat{x}_{2s}(q-\ell,\omega), \quad s \geq 1. \tag{VII.49}$$

These two equations do not account for $\widehat{x}_1(q,\omega)$ but it is easy to compute and reads$\widehat{x}_1(q,\omega) = \widehat{\phi}_1(q,\omega)$. We now introduce odd and even partition functions

$$Z^e(q,t) = \sum_{s=1}^{\infty} x_{2s}(q,t) \tag{VII.50}$$

$$Z^o(q,t) = \sum_{s=0}^{\infty} x_{2s+1}(q,t) \tag{VII.51}$$

$$Z(q,t) = Z^e(q,t) + Z^o(q,t), \tag{VII.52}$$

and sum equations Eqs. (VII.48)-(VII.49) to get the Laplace transforms of Z^e and Z^o

$$\widehat{Z}^e(q,\omega) = \sum_{\ell=0}^{q} \binom{q}{\ell} \widehat{\phi}_2(\ell,\omega)\widehat{Z}^o(q-\ell,\omega) \tag{VII.53}$$

$$\widehat{Z}^o(q,\omega) = \widehat{\phi}_1(q,\omega) + \sum_{\ell=0}^{q} \binom{q}{\ell} \widehat{\phi}_1(\ell,\omega)\widehat{Z}^e(q-\ell,\omega). \tag{VII.54}$$

We recognize exponential convolution equations and we introduce the exponential generating function of a sequence c

$$\mathcal{G}_c(x) = \sum_{q=0}^{\infty} c(q)\frac{x^q}{q!},$$

to solve Eqs. (VII.53)-(VII.54). We get

$$\mathcal{G}_{\widehat{Z}^e} = \mathcal{G}_{\widehat{\phi}_2}\mathcal{G}_{\widehat{Z}^o}$$
$$\mathcal{G}_{\widehat{Z}^o} = \mathcal{G}_{\widehat{\phi}_1} + \mathcal{G}_{\widehat{\phi}_1}\mathcal{G}_{\widehat{Z}^e}$$

and finally

$$\mathcal{G}_{\widehat{Z}^e} = \frac{\mathcal{G}_{\widehat{\phi}_1}\mathcal{G}_{\widehat{\phi}_2}}{1 - \mathcal{G}_{\widehat{\phi}_1}\mathcal{G}_{\widehat{\phi}_2}} \tag{VII.55}$$

$$\mathcal{G}_{\widehat{Z}^o} = \frac{\mathcal{G}_{\widehat{\phi}_1}}{1 - \mathcal{G}_{\widehat{\phi}_1}\mathcal{G}_{\widehat{\phi}_2}}. \tag{VII.56}$$

From these two equations we could continue the computation and get a general recursive formula for $\widehat{Z}(q,\omega)$ but we only need Eqs. (VII.55)-(VII.56) to express the Laplace transform of the grand canonical partition function.

D.2 Grand canonical ensemble computation

The idea for the computation in the grand canonical ensemble is similar to the canonical computation. However, upon summing over t, the constraint $\Theta(t_k - t)\,\Theta(t - t_{k-1})$ does not imply $t - t_{k-1} = \tau_k$ anymore, but only $t_{k-1} \leq t \leq t_k$ i.e $t = t_{k-1} + \tau$, $\tau \in [0, \tau_k]$. Using this, we can compute the Laplace transform of $\mathcal{X}_k$

$$\begin{aligned}
\widehat{\mathcal{X}}_k(q,\omega) &= \int_0^\infty \mathrm{d}t e^{-\omega t} \sum_{\ell_1,\dots,\ell_k} \delta\left(\sum_{i=1}^k \ell_i - q\right) \binom{q}{\boldsymbol{\ell}} \int_{\vec{\tau}} \Theta(t_k - t)\,\Theta(t - t_{k-1}) \prod_{j=1}^k p_j(\tau_j) g_j(\tau_j)^{\ell_j} \\
&= \sum_{\ell_1,\dots,\ell_k} \delta\left(\sum_{i=1}^k \ell_i - q\right) \binom{q}{\boldsymbol{\ell}} \int_{\vec{\tau}} \prod_{j=1}^{k-1} p_j(\tau_j) g_j(\tau_j)^{\ell_j} \\
&\qquad \times \int_0^\infty \mathrm{d}t e^{-\omega t} \Theta(t_k - t)\,\Theta(t - t_{k-1})\, g_k(t - t_{k-1})^{\ell_k} \\
&= \sum_{\ell_1,\dots,\ell_k} \delta\left(\sum_{i=1}^k \ell_i - q\right) \binom{q}{\boldsymbol{\ell}} \int_{\vec{\tau}} \prod_{j=1}^{k-1} p_j(\tau_j) g_j(\tau_j)^{\ell_j} e^{-\omega t_{k-1}} \int_0^{\tau_k} \mathrm{d}\tau e^{-\omega\tau} g_k(\tau)^{\ell_k} \\
&= \sum_{\ell_1,\dots,\ell_k} \delta\left(\sum_{i=1}^k \ell_i - q\right) \binom{q}{\boldsymbol{\ell}} \widehat{h}_k(\ell_k,\omega) \prod_{j=1}^{k-1} \widehat{\phi}_j(\ell_j,\omega).
\end{aligned}$$

As in the canonical computation, we need to distinguish between the parity of k and we have

$$\widehat{\mathcal{X}}_{2s}(q,\omega) = \sum_{\ell=0}^q \binom{q}{\ell} \widehat{h}_2(\ell,\omega) \widehat{x}_{2s-1}(q-\ell,\omega), \quad s \geq 1 \tag{VII.57}$$

$$\widehat{\mathcal{X}}_{2s+1}(q,\omega) = \sum_{\ell=0}^q \binom{q}{\ell} \widehat{h}_1(\ell,\omega) \widehat{x}_{2s}(q-\ell,\omega), \quad s \geq 1. \tag{VII.58}$$

Note that on the r.h.s we have identify the factors $\widehat{x}$ the canonical partition function. For $k = 1$, we also have $\widehat{\mathcal{X}}_1(q,\omega) = \widehat{h}_1(q,\omega)$. Introducing odd and even grand canonical partition functions $\mathcal{Z}^e$ and $\mathcal{Z}^o$, we have

$$\begin{aligned}
\mathcal{G}_{\widehat{\mathcal{Z}}^e} &= \mathcal{G}_{\widehat{h}_2} \mathcal{G}_{\widehat{\mathcal{Z}}^o} \\
\mathcal{G}_{\widehat{\mathcal{Z}}^o} &= \mathcal{G}_{\widehat{h}_1} + \mathcal{G}_{\widehat{h}_1} \mathcal{G}_{\widehat{\mathcal{Z}}^e},
\end{aligned}$$

and using Eqs. (VII.55)-(VII.56) we get for $\mathcal{G}_{\widehat{\mathcal{Z}}} = \mathcal{G}_{\widehat{\mathcal{Z}}^e} + \mathcal{G}_{\widehat{\mathcal{Z}}^o}$

$$\mathcal{G}_{\widehat{\mathcal{Z}}} = \frac{\mathcal{G}_{\widehat{h}_1} + \mathcal{G}_{\widehat{h}_2} \mathcal{G}_{\widehat{\phi}_1}}{1 - \mathcal{G}_{\widehat{\phi}_1} \mathcal{G}_{\widehat{\phi}_2}}. \tag{VII.59}$$

Note that, as in Eqs. (VII.55)-(VII.56), Eqs. (VII.59) are not symmetric upon the interchange $1 \leftrightarrow 2$. This is only due to the fact that we have considered products starting with the matrix $\mathbb{A}$ in the previous analysis. However, these products start either by $\mathbb{A}$ or $\mathbb{B}$ with probability $1/2$, given the initial draw of $v_1(0)$. As a consequence, one should symmetrize Eqs. (VII.59) to get

$$\mathcal{G}_{\widehat{\mathcal{Z}}} = \frac{1}{2} \frac{\mathcal{G}_{\widehat{h}_1} + \mathcal{G}_{\widehat{h}_2} + \mathcal{G}_{\widehat{h}_2} \mathcal{G}_{\widehat{\phi}_1} + \mathcal{G}_{\widehat{h}_1} \mathcal{G}_{\widehat{\phi}_2}}{1 - \mathcal{G}_{\widehat{\phi}_1} \mathcal{G}_{\widehat{\phi}_1}}, \tag{VII.60}$$

as in the main text. We will see however, that this does not matter for the long time behavior of the system.

D.3 Stieltjes transform of $\lambda_{\max}$

Taking $x = 0$ in Eq. (VII.59), we easily get

$$\widehat{\mathcal{Z}}(0,\omega) = \omega^{-1}, \tag{VII.61}$$

which, after Laplace inversion yields

$$\mathcal{Z}(0,t) = 1, \tag{VII.62}$$

and shows that $\lambda_{\max}$ is well normalized. As a consequence, for the limit in Eq. (VII.39) to be well defined, one must have the following asymptotic behavior

$$\mathcal{Z}(q,t) \underset{t\to\infty}{\sim} t^q \mathbb{E}\left[\lambda_{\max}^q\right], \tag{VII.63}$$

which in turns implies in Laplace space

$$\widehat{\mathcal{Z}}(q,\omega) \underset{\omega\to 0^+}{\sim} q!\omega^{-1-q}\mathbb{E}\left[\lambda_{\max}^q\right]. \tag{VII.64}$$

Taking the limit $\omega \to 0^+$ in the r.h.s of Eq. (VII.59), while keeping the ratio $\omega/x = y$ constant, yields

$$\begin{aligned}\mathcal{G}_{\widehat{\mathcal{Z}}}(x,\omega) &\underset{\omega\to 0^+}{\approx} \sum_{q=0}^{\infty} \frac{\left(\omega y^{-1}\right)^q}{q!} q!\omega^{-1-q}\mathbb{E}[\lambda_{\max}^q] \\ &= \frac{y}{\omega}\mathbb{E}\left[\frac{1}{y-\lambda_{\max}}\right].\end{aligned}$$

The last expectation is the Stieltjes transform of $\lambda_{\max}$ and we get

$$\mathcal{G}_{\widehat{\mathcal{Z}}}(x,\omega) \underset{\omega\to 0^+}{\approx} \frac{y}{\omega}\int \mathrm{d}\lambda \frac{\varphi(\lambda)}{y-\lambda}, \tag{VII.65}$$

with φ the density of $\lambda_{\max}$.

D.4 Distribution of $\lambda_{\max}$ in the case where $\alpha_{\mathbb{A}} = \alpha_{\mathbb{B}}$ and $\mathbb{E}[\tau] = +\infty$

In this case, the persistence exponents are the same, i.e. $\mu(\alpha_{\mathbb{A}}) = \mu(\alpha_{\mathbb{B}}) := \mu < 1$ ensuring $\mathbb{E}[\tau] = +\infty$. Note however that the scale factor C_i (such that $p_i(t) \sim C_i t^{-1-\mu}$) could still be different. However, since the correlator of ϕ in Eq. (VII.32) is independent of the constant K such that $\rho(\nu) \sim_{\nu\to\nu_+} K|\nu-\nu_+|^\alpha$, we conclude that $C_{\mathbb{A}} = C_{\mathbb{B}} := C$.

To use Eq. (VII.59) to find the Stieltjes transform of $\lambda_{\max}$, we need to compute the behavior of the Laplace transforms as $\omega \to 0$. We start by linking the long-time behavior of p and g_i to the small-ω behavior of the related Laplace transforms

$$\left.\begin{aligned} p_i(t) &\underset{t\to\infty}{\sim} \frac{C}{t^{1+\mu}} \\ g_i(t) &\underset{t\to\infty}{\sim} r_i t \end{aligned}\right\} \longleftrightarrow \begin{cases} \widehat{p}_i(\omega) \underset{\omega\to 0}{\sim} 1 + C\Gamma(-\mu)\omega^\mu \\ \widehat{\phi}_i(q,\omega) \underset{\omega\to 0}{\sim} r_i^q C\Gamma(q-\mu)\omega^{\mu-q}, \quad q \geq 1 \\ \widehat{h}_i(q,\omega) \underset{\omega\to 0}{\sim} r_i^q C\dfrac{\Gamma(1+q-\mu)}{\mu}\omega^{\mu-q-1}, \quad q \geq 1 \end{cases} \tag{VII.66}$$

Using the same scaling limit $\omega/x = y$ in the e.g.f of $\widehat{\phi}_i$ and $\widehat{h}_i$, we have

$$\mathcal{G}_{\widehat{\phi}_i}(x,\omega) \underset{\omega\to 0^+}{\approx} 1 + C\Gamma(-\mu)\left(\frac{\omega}{y}\right)^{\mu}(y-r_i)^{\mu}$$
$$\mathcal{G}_{\widehat{h}_i}(x,\omega) \underset{\omega\to 0^+}{\approx} C\Gamma(-\mu)\left(\frac{\omega}{y}\right)^{\mu-1}(y-r_i)^{\mu-1}.$$

Plugging these expressions into Eq. (VII.59), we get

$$\int \mathrm{d}\lambda \frac{\varphi(\lambda)}{y-\lambda} = \frac{(y-r_1)^{\mu-1}+(y-r_2)^{\mu-1}}{(y-r_1)^{\mu}+(y-r_2)^{\mu}}, \tag{VII.67}$$

which we can invert using Stieltjes inversion formula

$$\varphi(\lambda) = (r_2-r_1)\frac{\sin\mu\pi}{\pi}\frac{(z_1z_2)^{\mu-1}}{z_1^{2\mu}+z_2^{2\mu}+2(z_1z_2)^{\mu}\cos(\mu\pi)}, \tag{VII.68}$$

with $z_i = |\lambda - r_i|$.

D.5 Self-averaging of $\lambda_{\max}$ for $\mathbb{E}[\tau] < +\infty$

We will consider the case $\alpha_{\mathbb{A}} = \alpha_{\mathbb{B}}$ (the case $\alpha_{\mathbb{A}} \neq \alpha_{\mathbb{B}}$ can be treated in the exact same way). If $\mathbb{E}[\tau] < \infty$ then $\mu > 1$. Let us assume that $\mu \in]1,2[$ in order to carry fewer terms in the Tauberian analysis. The only important feature is that $\mu > 1$ thus ensuring the existence of $\mathbb{E}[\tau]$.

Since the persistence has now a finite first moment, the small-ω behavior of the Laplace transforms are modified. We will denote by $m_\tau = \mathbb{E}[\tau]$ and $m_i = \mathbb{E}[g_i(\tau)]$ (which is finite since $g_i(\tau) \sim_{\tau\to\infty} r_i\tau$). We have the behaviors

$$\left.\begin{aligned} p(t) &\underset{t\to\infty}{\sim} \frac{C}{t^{1+\mu}} \\ g_i(t) &\underset{t\to\infty}{\sim} r_i t \end{aligned}\right\} \longleftrightarrow \begin{cases} \widehat{p}_i(\omega) \underset{\omega\to 0}{\sim} 1 - \omega m_\tau + C\Gamma(-\mu)\omega^{\mu} \\ \widehat{\phi}_i(1,\omega) \underset{\omega\to 0}{\sim} m_i + r_i C\Gamma(1-\mu)\omega^{\mu-1}, \quad q \geq 1 \\ \widehat{\phi}_i(q,\omega) \underset{\omega\to 0}{\sim} r_i^q C\Gamma(q-\mu)\omega^{\mu-q}, \quad q \geq 2 \\ \widehat{h}_i(q,\omega) \underset{\omega\to 0}{\sim} r_i^q C\dfrac{\Gamma(1+q-\mu)}{\mu}\omega^{\mu-q-1}, \quad q \geq 1 \end{cases}, \tag{VII.69}$$

and get for the e.g.f

$$\mathcal{G}_{\widehat{\phi}_i}(x,\omega) \underset{\omega\to 0^+}{\approx} 1 + m_i\frac{\omega}{y} - \omega m_\tau + C\Gamma(-\mu_i)\left(\frac{\omega}{y}\right)^{\mu_i}(y-r_i)^{\mu_i}$$
$$\mathcal{G}_{\widehat{h}_i}(x,\omega) \underset{\omega\to 0^+}{\approx} m_\tau + C\Gamma(-\mu_i)\left(\frac{\omega}{y}\right)^{\mu_i-1}(y-r_i)^{\mu_i-1}.$$

Plugging these into Eq. (VII.59) and keeping only the lowest orders, we get

$$\int \mathrm{d}\lambda \frac{\varphi(\lambda)}{y-\lambda} = \frac{1}{y - \dfrac{m_1+m_2}{2m_\tau}}, \tag{VII.70}$$

which in turn implies that

$$\varphi(\lambda) = \delta\left(\lambda - \frac{m_1+m_2}{2m_\tau}\right). \tag{VII.71}$$

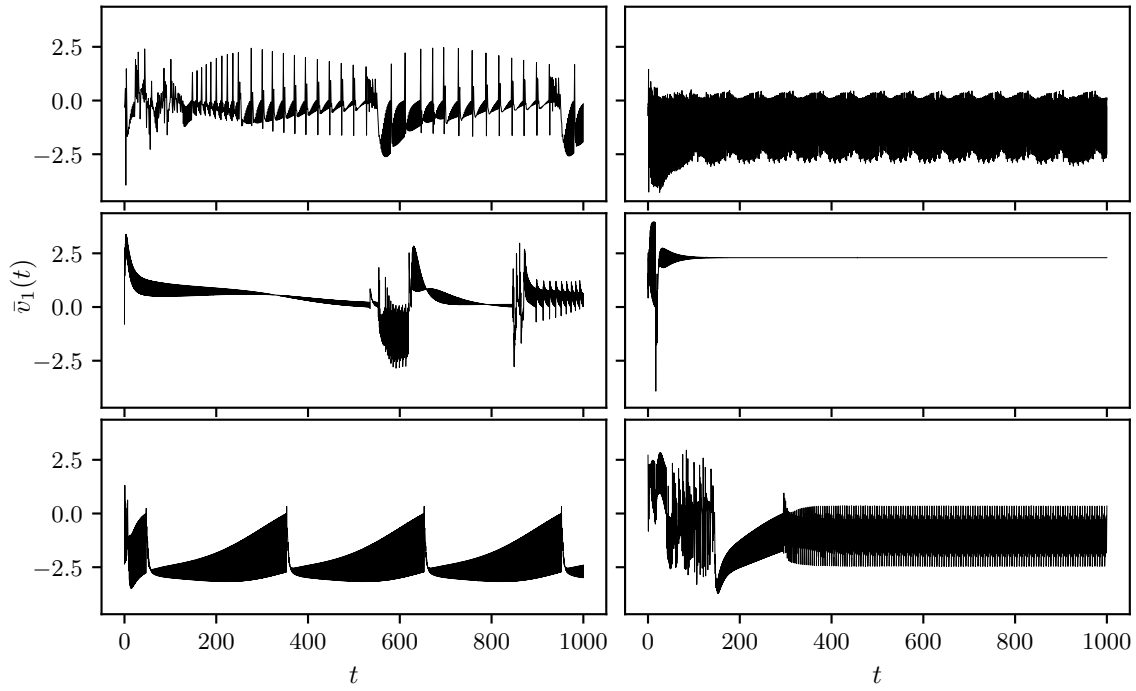


Figure VII.5: Different trajectories for $\bar{v}_1(t) = \sqrt{N}v_1(t)/\|\mathbf{v}(t)\| \sim \phi(t)$ where $\mathbf{v}(t)$ evolves according to Eq. (VII.1) for $N = 2500$ components. The initial condition $\mathbf{v}(0)$ is a Gaussian vector $\mathsf{N}(0, \mathbf{I}_N)$. Matrices $\mathbb{A}$ and $\mathbb{B}$ are drawn from GOE with $\nu_{\pm,\mathbb{A}} = 0.05\sqrt{2}$ and $\nu_{\pm,\mathbb{A}} = 2\sqrt{2}$.

E Trajectories generated by the dynamics in Eq. (VII.1)

On Figure VII.5, we give other examples of the types of complex dynamics that arise from the dynamical equation Eq. (VII.1). The simulations are performed for matrices $\mathbb{A}$ and $\mathbb{B}$ drawn from $GOE(N)$ with $N = 2500$. We chose $\mathbb{A}$ to be a contracting matrix and $\mathbb{B}$ to be expanding. As we can see, the dynamical types observed are quite diverse.

First, the dynamics gets stuck in the $\mathbb{A}$-cone on the middle-right plot. Indeed, since N is finite, the persistence probability $Q_0(\tau)$ reaches a finite limit as $\tau \to \infty$ which indicates a non-zero probability of absorption. Note that here the absorption happens in the contracting cone rendering the system stable.

Second, on the bottom-left and top/bottom-right plots, the dynamics seems to reach limits cycles. As a consequence, the IIA approximation leading to the distribution of $\lambda_{\max}$ is not valid anymore since a "deterministic" sequence of cones is visited over and over. In this situation, $\lambda_{\max}$ should be equal (or at least very close to zero) and one should account for these dynamical type with an additional Dirac delta at zero in the expression of φ.

Finally, we can observe more complex dynamical types on the top/middle-left plots which are reminiscent of the dynamics presented on Figure VII.1 of the main text.

F Extensions

In this final appendix, we consider two extensions related to the properties of matrices $\mathbb{A}$ and $\mathbb{B}$. The generalization of the Lamperti law will be consider in Chapter VIII.

F.1 Gaussian elliptic matrices

We start by considering Gaussian matrices with a slightly more complicated correlation structure. We assume that entries ij and ji are correlated with a coefficient ϱ. Let $\mathbb{S}_+, \mathbb{S}_-$ be two mutually-free $N \times N$ $GOE(N)$ and anti-$GOE(N)$ random matrices. $\mathbb{S}_+$ is a standard $GOE(N)$ matrix thus verifying

$$\mathbb{E}\left[\mathbb{S}_{ij}\right] = 0, \quad \mathbb{E}\left[\mathbb{S}_{ii}^2\right] = \frac{2}{N}, \quad \mathbb{E}\left[\mathbb{S}_{ij}\mathbb{S}_{ji}\right] = \frac{1}{N}, \tag{VII.72}$$

while $\mathbb{S}_-$ is its skew-symmetric counterpart. An Gaussian elliptic random matrix $\mathbb{A}$ of parameter ϱ is obtained through

$$\mathbb{A} = \sqrt{\frac{1+\varrho}{2}}\mathbb{S}_+ + \sqrt{\frac{1-\varrho}{2}}\mathbb{S}_-, \tag{VII.73}$$

and verifies

$$\mathbb{E}\left[\mathbb{A}_{ij}\right] = 0, \quad \mathbb{E}\left[\mathbb{A}_{ii}^2\right] = \frac{1+\varrho}{N}, \quad \mathbb{E}\left[\mathbb{A}_{ij}\mathbb{A}_{ji}\right] = \frac{\varrho}{N}. \tag{VII.74}$$

The parameter ϱ interpolates between the Gaussian Orthogonal Ensemble (symmetric matrices, $\varrho = 1$), the Ginibre ensemble ($\varrho = 0$) and the Anti Gaussian Orthogonal Ensemble (skew-symmetric matrices, $\varrho = -1$). In this case, the correlator of process $\phi(t)$ cannot be simply expressed as the moments of $\mathbb{A}$ and one must evaluate the mixed-moments of $\mathbb{A}$ and $\mathbb{A}^\top$

$$\langle \phi(t)\phi(s)\rangle = \frac{\tau\left((\mathbb{A})^t(\mathbb{A}^\top)^s\right)}{\sqrt{\tau\left((\mathbb{A})^t(\mathbb{A}^\top)^t\right)\tau\left((\mathbb{A})^s(\mathbb{A}^\top)^s\right)}}. \tag{VII.75}$$

In Chapter IX, we show an exact explicit computation of the mixed-moments $\tau\left((\mathbb{A})^t(\mathbb{A}^\top)^s\right)$ by mapping the problem to the enumeration of partitions of Temperley-Lieb algebras. We can therefore give the expression of the mixed moments for t, s even (the case t, s odd is similar, see Chapter IX)

$$\begin{aligned}\tau\left(\mathbb{A}^t\left(\mathbb{A}^\top\right)^s\right) = \sum_{k=0}^{(t\wedge s)/2} \varrho^{(t+s)/2-2k}\frac{(2k+1)^2}{(t/2+k+1)(s/2+k+1)} \\ \times \binom{s}{s/2+k}\binom{t}{t/2+k},\end{aligned} \tag{VII.76}$$

where $t \wedge s = \min(t, s)$.

We can look at some limit cases which are of interest. The cases $\varrho = \pm 1$ are discussed in Chapter IX where it is explained that one recovers the Catalan numbers $C_{(t+s)/2}$ for the symmetric case $\varrho = 1$, or sign-flipping Catalan numbers in the skew-symmetric case $\varrho = -1$.

In the case $\varrho = 0$, which corresponds to matrices drawn from the real Ginibre ensemble, Eq. (VII.76) simplifies greatly to

$$\tau\left(\mathbb{A}^t\left(\mathbb{A}^\top\right)^s\right) = \delta(t-s), \tag{VII.77}$$

and $\phi(t)$ is therefore a Gaussian white noise. The persistence probability thus behaves as

$$Q_0(\tau) = 2^{-\tau}. \tag{VII.78}$$

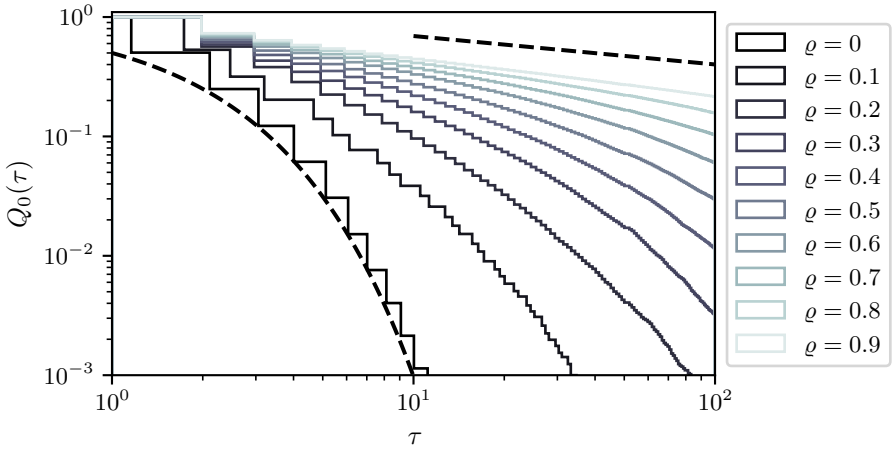


Figure VII.6: Persistence probability for even-time process $\phi(2\ell)$ for Gaussian elliptic matrices. The covariance of ϕ is given by Eq. (VII.76). The dashed line correspond to both limits $\varrho = 0$ (Ginibre matrices; $Q_0(\tau) = 2^{-\tau}$) and $\varrho = 1$ (GOE matrices; $Q_0(\tau) \sim \tau^{-\mu}$).

Intuitively, since Ginibre matrices have a singular value decomposition $\mathbb{A} = \mathbb{O}\Sigma\mathbb{V}^\top$ with $\mathbb{O}$ and $\mathbb{V}$ *independent*, the action of matrix $\mathbb{A}$ on $\mathbf{v}(t)$ completely erases previous effects. Indeed, take for instance the first time steps of the dynamics $\mathbf{v}(2) = \mathbb{O}\Sigma\mathbb{V}^\top\mathbb{O}\Sigma\mathbb{V}^\top\mathbf{v}(1)$. The elements of $\mathbb{V}^\top\mathbb{O}$ are

$$(\mathbb{V}^\top\mathbb{O})_{kl} = \sum_i \mathbb{V}_{ik}\mathbb{O}_{il} \approx N\langle\mathbb{V}_{ik}\mathbb{O}_{il}\rangle \approx N\langle\mathbb{V}_{ik}\rangle\langle\mathbb{O}_{il}\rangle \approx 0,$$

where we used that components of columns of orthogonal matrices are asymptotically independent. Therefore, the innermost matrix $\mathbb{V}^\top\mathbb{O}$ of $\mathbf{v}(2)$ is, roughly speaking, zero on average which "reshuffles" $\mathbf{v}(t)$.

In the generic case $\varrho \in]0, 1[$, we can see numerically on Figure VII.6 that the persistence has an exponential cutoff $\kappa(\varrho)$ such that

$$Q_0(\tau) \underset{\tau\to\infty}{\sim} \tau^{-\mu(\varrho)} e^{-\kappa(\varrho)\tau}. \tag{VII.79}$$

The precise expression of the cutoff seems hard to tackle analytically. Even though the asymptotics of the correlator can be computed analytically using a saddle-point method (see Chapter IX), no known results on the link between correlator's asymptotics and persistence decay can be applied, to the best of our knowledge.

F.2 Outlying eigenvalues

In this section, let us consider the case of a symmetric $N \times N$ $O(N)$-invariant random matrix of the form

$$\mathbb{A} = \mathbb{O}\begin{pmatrix} \nu_o & & & & & \\ & \ddots & & & & \\ & & \nu_o & & & \\ & & & \nu_1 & & \\ & & & & \ddots & \\ & & & & & \nu_{(1-q)N} \end{pmatrix}\mathbb{O}^\top, \tag{VII.80}$$

where $(\nu_i)_{i=1,\cdots,(1-q)N}$ are the eigenvalues of a matrix $\mathbb{M}$ whose spectral measure $\rho_{\mathbb{M}}$ is compactly supported on $[\![\nu_-,\nu_+]\!]$, $0 \leq \nu_- < \nu_+$ as $N \to \infty$, $\nu_o > 0$ [6] is an isolated eigenvalue repeated qN times and $\mathbb{O}$ an orthogonal matrix. With this form, we can write the spectral measure of $\mathbb{A}$ as $N \to \infty$

$$\begin{aligned}\frac{1}{N}\sum_k \delta(\nu-\nu_k) &= \frac{1}{N}\sum_{i=1}^{(1-q)N}\delta(\nu-\nu_i) + q\delta(\nu-\nu_0)\\ &\to (1-q)\rho_{\mathbb{M}}(\nu) + q\delta(\nu-\nu_0) := \rho_{\mathbb{A}}(\nu).\end{aligned}$$

The computation of the moments of $\mathbb{A}$ in the large-dimension limit is straightforward and yields

$$f_{\mathbb{A}}(t) = (1-q)f_{\mathbb{M}}(t) + q\nu_0^t. \tag{VII.81}$$

Now, in order to estimate the asymptotic behavior of the correlator of $\phi(t)$ under the dynamics governed by $\mathbb{A}$, one needs to consider the relative position between ν_o and the upper edge ν_+ of the spectrum of $\mathbb{M}$. We have the asymptotic behaviors:

- if $\nu_o < \nu_+$, i.e. ν_0 is lost in the bulk of $\mathbb{M}$ or lies below the lower edge, the asymptotic behavior of $\mathbb{M}$ is transmitted to $\mathbb{A}$

$$f_{\mathbb{M}}(t) \underset{t\to\infty}{\sim} (1-q)K\Gamma(\alpha+1)\nu_+^{t+\alpha+1}t^{-\alpha-1}. \tag{VII.82}$$

- if $\nu_o \geq \nu_+$, i.e. ν_o is an outlying eigenvalue, which escaped the bulk rightward, the asymptotic behavior is governed by the outlier

$$f_{\mathbb{A}}(t) \underset{t\to\infty}{\sim} q\nu_o^t. \tag{VII.83}$$

Consequently for the correlator of $\phi(t)$, the asymptotic behavior is rather different

$$\langle\phi(t)\phi(s)\rangle \underset{t,s\to\infty}{\sim} \begin{cases}\left(\frac{2\sqrt{ts}}{t+s}\right)^{\alpha+1}, & \text{when } \nu_o < \nu_+\\ 1, & \text{when } \nu_o \geq \nu_+\end{cases}. \tag{VII.84}$$

The persistence probability thus also depends on the relative positions between ν_o and ν_+

$$Q_0(\tau) \underset{\tau\to\infty}{\sim} \begin{cases}\tau^{-\mu(\alpha)}, & \text{when } \nu_o < \nu_+\\ c, & \text{when } \nu_o \geq \nu_+\end{cases}, \tag{VII.85}$$

where $c \in [0,1]$ is a constant. We therefore expect the same *cone-trapping* phenomenon as in the finite N case if dynamical matrices $\mathbb{A}$ and $\mathbb{B}$ both have outlying eigenvalues. The probability density function of $\lambda_{\max}$ will be given by a sum of two Dirac deltas

$$\varphi(\lambda) = \frac{\delta(\lambda - \ln|\nu_{o,\mathbb{A}}|) + \delta(\lambda - \ln|\nu_{o,\mathbb{B}}|)}{2}. \tag{VII.86}$$

Even though, the construction of Eq. (VII.80) might seem a bit *ad-hoc*, it is actually easily achieved by a well-known set of random matrices. Consider a $N \times T$ random matrix $\mathbb{H}$ whose

[6] We only consider the case where ν_o, ν_- and ν_+ are positive for simplicity.

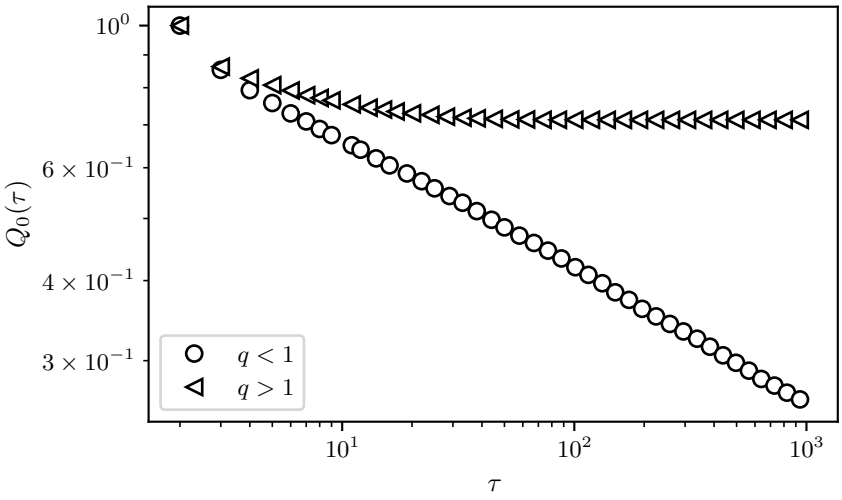


Figure VII.7: Persistence probability for $v_1(t) = (\mathbb{A}^t \mathbf{v}(0)_1$ for $\mathbb{A} = 2\lambda_- \mathbb{1} - \mathbb{W}$, with $\mathbb{W}$ a white Wishart of parameter q and $\lambda_- = (1-q)^2$. We see that when $q > 1$, we recover a power-law decay dictated by the square-root singularity of the Marcenko-Pastur distribution, whereas $q < 1$ shows a plateau of the persistence and therefore a non-zero probability to remain trap within one cone.

entries are time observations of random quantities $H_{it} = x_i^t$. The *sample-covariance* matrix of these observations, namely

$$\mathbb{E} = \frac{1}{T} \mathbb{H}\mathbb{H}^\top \tag{VII.87}$$

is called a Wishart matrix. If in addition, the true covariance matrix $\mathbb{C}$ of the observations is the identity $\mathbb{C} = \mathbb{1}$, then $\mathbb{E} := \mathbb{W}$ is called a white Wishart. It is well-known that the spectral distribution of white Wishart matrices converges towards the Marcenko-Pastur distribution ρ_{MP}

$$\rho_{MP}(\nu) = \frac{\sqrt{[(\nu_+ - \nu)(\nu - \nu_-)]_+}}{2\pi q \nu} + \frac{1-q}{q} \delta(\nu) \Theta(q-1), \tag{VII.88}$$

whenever $T, N \to \infty$ such that $q = N/T$ is fixed and where $\nu_\pm = (1 \pm q)^2$. We therefore see that, when the number of observables N is larger than the number of observations T, $N - T := N(1 - q^{-1})$ eigenvalues are equal to 0 and one recovers the previous construction with the exchange $q \to q^{-1}$ and $\nu_o = 0$. The matrix $\mathbb{A} = \alpha \mathbb{1} - \mathbb{W}$ has an outlying eigenvalue $\nu_o = \alpha$. The prediction of a plateauing persistence probability for $q < 1$ is confirmed by numerical simulations displayed on Figure VII.7.

In the case of the rank-one BBP transition, a single eigenvalue pops out of the bulk as soon as $\gamma > \gamma_c$ where γ is such that

$$\mathbb{A} = \mathbb{M} + \gamma \frac{\mathbf{u}\mathbf{u}^\top}{\|\mathbf{u}\|^2}, \tag{VII.89}$$

with $\mathbf{u}$ a Gaussian random vector. However, in the large N limit, this eigenvalue will not contribute to the spectrum of $\mathbb{A}$ since it has a weight N^{-1}. Consequently, the BBP transition affects the persistence only at finite N.

CHAPTER VIII

Occupation time of a renewal process coupled to a discrete Markov chain

Abstract

A semi-Markov process is one that changes states in accordance with a Markov chain but takes a random amount of time between changes. We consider the generalization to semi-Markov processes of the classical Lamperti law for the occupation time of a two-state Markov process. We provide an explicit expression in Laplace space for the distribution of an arbitrary linear combination of the occupation times in the various states of the process. We discuss several consequences of this result. In particular, we infer the limiting distribution of this quantity rescaled by time in the long-time scaling regime, as well as the finite-time corrections to its moments.

From: [3] Théo Dessertaine, Claude Godrèche, and Jean-Philippe Bouchaud. *Occupation time of a renewal process coupled to a discrete Markov chain.* Journal of Statistical Mechanics: Theory and Experiment, 2022(6):063204, June 2022.

1 Introduction

Studies of the occupation time of stochastic processes have a long history, starting with the investigation by Lévy of the fraction of time spent by Brownian motion above zero or of the fraction of time where the first player is ahead of the second, in repeated coin toss [145]. The limiting density of this fraction of time is the U-shaped arcsine law, with a minimum at 1/2 and infinite tails at 0 and 1 (see [146, 147] for a summary of [145]). These founding investigations were followed by many subsequent studies [146, 148, 149, 150, 151, 152] and the topic is now a classic in probability theory (see [153, 154] for reviews).

Only lately was this topic revisited in the physics community, motivated, in particular, by studies on phase persistence for self-similar coarsening systems, such as breath figures [155], Ising spin systems quenched from high temperature to zero temperature (or more generally to a temperature below the critical temperature) [156, 157], the diffusion equation evolving from a random initial condition [158, 159], to name but a few. The statistics of the occupation time for Ising spins systems, the voter model and diffusive

persistence were addressed in [160], while [161] is entirely devoted to this last subject. However, obtaining a complete solution to the question of the statistics of the occupation time for these extended systems is currently out of reach. Partial analytical studies, as well as numerical or approximate theoretical treatments, allow nevertheless to make progress [160, 161, 162, 163, 164, 165]. A noticeable series of works on the occupation time of the voter model [166, 167, 168, 169, 170] was a source of inspiration for the endeavor made in [160] on this topic. A study on the same issues was further continued in [171].

The above mentioned works [160, 161] were followed by investigations on the statistics of the occupation time for simpler systems, more amenable to exact analysis, and closer to the main stream of probabilistic studies [163, 172, 173, 174, 175, 176, 177, 178]. We refer the reader to [128] for subsequent references and to [179, 180, 181, 182, 183, 184] for more recent works.

The study presented below belongs to the same vein and gives a generalization to multi-state Markov processes of the Lamperti law for the occupation time of a two-state Markov process [150], a problem also considered in [185, 186, 187]. Our motivation comes from a recent work [2] on cone-wise linear dynamics in large dimensions. Each "cone" is characterized by a stability matrix chosen to be from the Gaussian Orthogonal Ensemble. The selected cone is determined by the direction of the dynamically evolving vector with respect to a fixed set of vectors. Because of the random nature of the stability matrix, the cone-switching process can be described, for large dimensions, as a semi-Markov process, with a power-law distribution of switching times [2]. The dynamical system investigated in [2] is among the few known examples where the Lyapounov exponent is not self-averaging (see e.g., [196] for a similar mechanism in the context of Pomeau-Manneville maps).

We consider an irreducible Markov chain $\alpha_1, \alpha_2, \ldots$, with discrete state space $\{a_j, j = 1, 2, \ldots, q\}$, and transition matrix

$$\mathbb{P}_{ij} = \mathbb{P}(\alpha_{n+1} = a_j | \alpha_n = a_i). \tag{VIII.1}$$

In addition, we consider a sequence of time intervals $\tau_1, \tau_2, \ldots$, which represent the time spent in the states $\alpha_1, \alpha_2, \ldots$ More specifically, the jumps occur at the random epochs of time $t_1, t_2, \ldots$, from some time origin $t_0 = 0$. The intervals of time between jumps, $\tau_1 = t_1, \tau_2 = t_2 - t_1, \ldots$, are independent and identically distributed random variables with a common density $\rho(\tau)$, thus forming a renewal process [188, 189, 190, 191]. The process defined by the pairs $(\alpha_n, t_n), n = 1, 2, \ldots$, is known as a Markov renewal process in the mathematical literature, while the process defined as

$$\alpha(t) = \alpha_n, \qquad t_n < t < t_{n+1} \tag{VIII.2}$$

is a simple example of a semi-Markov process [145, 192, 152, 193, 194]. The latter is not Markovian except at the epochs of jumps. As set forth in [194], a semi-Markov process is one that changes states in accordance with a Markov chain but takes a random amount of time between changes. If the latter is exponentially distributed, the process becomes an ordinary Markov chain in continuous time.

The purpose of this chapter is to investigate the statistics of the sum

$$S_t = \int_0^t \mathrm{d}u\, \alpha(u) = \alpha_1\tau_1 + \cdots + \alpha_{N_t}\tau_{N_t} + \alpha_{N_t+1}\Big(t - \sum_{i=1}^{N_t}\tau_i\Big), \tag{VIII.3}$$

where N_t is the random number of jumps between 0 and t. More precisely, we will investigate the limiting distribution $f_M(x)$ of the fraction $M_t = S_t/t$ in the long-time limit, where

$$M = \lim_{t\to\infty} M_t = \lim_{t\to\infty} \frac{S_t}{t} = \lim_{t\to\infty} \frac{1}{t}\int_0^t \mathrm{d}u\, \alpha(u),$$

that is, the distribution of the temporal mean of $\alpha(t)$, when the density $\rho(\tau)$ has a power-law tail (VIII.7), with index $\theta < 1$.

There are several possible interpretations to the quantities S_t or M_t. The first one is in terms of occupation times. To simplify, consider the case where the number of states is $q = 2$ with $a_1 = 0$ and $a_2 = 1$. Then S_t is the occupation time of state a_2 (i.e., the time spent in this state), up to time t. More generally, S_t is the linear combination of the occupation times of the process in the various states $a_1, \ldots, a_q$,

$$S_t = a_1 T_t^{(1)} + a_2 T_t^{(2)} + \cdots + a_q T_t^{(q)}, \tag{VIII.4}$$

where $T_t^{(j)}$ is the occupation time in state a_j (i.e., the time spent in this state), up to time t, with

$$\sum_{j=1}^{q} T_t^{(j)} = t.$$

Equivalently, M_t is the mean of $a_1, a_2, \ldots, a_q$ weighted by the fractions of time $T_t^{(1)}/t$, $T_t^{(2)}/t$, $\ldots, T_t^{(q)}/t$, spent in these various states.

A second interpretation is in terms of a one-dimensional random walk in continuous time. Let $\alpha_1, \alpha_2 \ldots$ be the respective positions of the walker during the time intervals $\tau_1, \tau_2, \ldots$, with $\alpha = 1, 2, \ldots, q$. Then $M_t = S_t/t$ is the mean position of this walker up to time t. Alternatively, let $\alpha_1, \alpha_2 \ldots$ be the respective velocities of the walker during the time intervals $\tau_1, \tau_2, \ldots$. Then S_t is the position at time t of this walker and M_t is its mean speed. Likewise, if α is a Potts spin with q states $a_1, \ldots, a_q$, then M_t represents the mean magnetization up to time t.

To anticipate on what follows, a natural question is to know whether the process is ergodic, i.e., whether the distribution of the mean M_t becomes narrow around $\langle\alpha\rangle$ in the long-time limit, or otherwise stated, is self-averaging. As we will see, the answer depends on the nature of the distribution of waiting times $\tau_1, \tau_2, \ldots$. Finally, note that the sum S_t is a particular instance of what is known in the mathematical literature as a renewal-reward process (see e.g., [191, 194] for details).

In the specific case where the distribution of waiting times $\rho(\tau)$ has a power-law tail (VIII.7), with index $\theta < 1$, we find that, within each sector $a_i < x < a_{i+1}$, $(i = 1, 2, \ldots, q)$,

$$f_M(x) = \frac{\sin \pi\theta}{\pi} \frac{\big(\sum_{j\leq i} \pi_j\, \delta_j^{\theta-1}\big)\big(\sum_{j>i} \pi_j\, \delta_j^{\theta}\big) + \big(\sum_{j\leq i} \pi_j\, \delta_j^{\theta}\big)\big(\sum_{j>i} \pi_j\, \delta_j^{\theta-1}\big)}{\big(\sum_{j\leq i} \pi_j\, \delta_j^{\theta}\big)^2 + \big(\sum_{j>i} \pi_j\, \delta_j^{\theta}\big)^2 + 2\cos\pi\theta\big(\sum_{j\leq i} \pi_j\, \delta_j^{\theta}\big)\big(\sum_{j>i} \pi_j\, \delta_j^{\theta}\big)}, \tag{VIII.5}$$

where $\delta_j = |x - a_j|$, and π_j is the $j-$th component of the stationary measure associated with the Markov chain. For x outside the range of values (a_1, a_q), $f_M(x) = 0$. This result is universal with respect to $\rho(\tau)$, i.e., independent of the details of this distribution. The same expression was obtained in [185, 186] as a generalization of the Boltzmann distribution for systems showing weak ergodicity breaking [195] (see also [187]) [1]. For a uniform stationary probability measure over two states, the expression (VIII.5) recovers the classic Lamperti law [150] (see (VIII.25)).

In the context of the present part of the thesis, i.e. for conewise linear systems, (VIII.5) gives the distribution of the Lyapunov exponent when the mean waiting time within each cone is infinite. The study of the present chapter stems for a natural generalization of the system presented in Chapter VII. Indeed, the model of the previous chapter consists in the simple case where the Markov chain encoding the cone structure has the particular form

$$\mathbb{P} = \begin{pmatrix} 0 & 1 \\ 1 & 0 \end{pmatrix},$$

i.e. the system can only jump from the $\mathbb{A}$-cone to the $\mathbb{B}$-cone and *vice versa*. Consider now that our conewise linear systems consists in four different cones $\mathcal{C}_i$ associated with matrices $\mathbb{A}_i$ such that

$$\mathcal{C}_1 = \{\mathbf{x} \in \mathbb{R}^N,\ x_1 > 0 \,\text{and}\, x_2 > 0\}, \quad \mathbb{A}_1 = \left(\begin{array}{cc|c} 1 & 0 & \\ 0 & -1 & \mathbf{0}_{2,N-2} \\ \hline \multicolumn{2}{c|}{\mathbf{0}_{N-2,2}} & \mathbb{1}_{N-2} \end{array}\right),$$

$$\mathcal{C}_2 = \{\mathbf{x} \in \mathbb{R}^N,\ x_1 > 0 \,\text{and}\, x_2 < 0\}, \quad \mathbb{A}_2 = \left(\begin{array}{cc|c} -1 & 0 & \\ 0 & 1 & \mathbf{0}_{2,N-2} \\ \hline \multicolumn{2}{c|}{\mathbf{0}_{N-2,2}} & \mathbb{1}_{N-2} \end{array}\right),$$

$$\mathcal{C}_3 = \{\mathbf{x} \in \mathbb{R}^N,\ x_1 < 0 \,\text{and}\, x_2 > 0\}, \quad \mathbb{A}_3 = \left(\begin{array}{cc|c} 1 & 0 & \\ 0 & -1 & \mathbf{0}_{2,N-2} \\ \hline \multicolumn{2}{c|}{\mathbf{0}_{N-2,2}} & \mathbb{1}_{N-2} \end{array}\right),$$

$$\mathcal{C}_4 = \{\mathbf{x} \in \mathbb{R}^N,\ x_1 < 0 \,\text{and}\, x_2 < 0\}, \quad \mathbb{A}_4 = \left(\begin{array}{cc|c} -1 & 0 & \\ 0 & -1 & \mathbf{0}_{2,N-2} \\ \hline \multicolumn{2}{c|}{\mathbf{0}_{N-2,2}} & \mathbb{1}_{N-2} \end{array}\right).$$

[1] We will come back to [185, 186, 187], which are closely related to the present work, in Section 6.

In this very simple example, the matrix associated to the cone-switching process is

$$\mathbb{P} = \begin{pmatrix} 0 & 1 & 0 & 0 \\ 0 & 0 & 0 & 1 \\ 0 & 0 & 0 & 1 \\ 1 & 0 & 0 & 0 \end{pmatrix},$$

as $\mathbb{A}_1\mathcal{C}_1 \subseteq \mathbb{C}_2$, $\mathbb{A}_2\mathcal{C}_2 \subseteq \mathcal{C}4$, $\mathbb{A}_3\mathcal{C}_3 \subseteq \mathcal{C}_4$ and $\mathbb{A}_4\mathcal{C}_4 \subseteq \mathcal{C}_1$. The associated stationary measure is therefore $\pi = (1/3, 1/3, 0, 1/3)$ and we see that the system can never end up in $\mathcal{C}_3$. Of course, in this trivial example, the time spent in each cone is designed to be $\tau = 1$ exactly, and the associated Lyapounov exponent is 0 which corresponds to the self-averaging behavior described in Eq. (VIII.69) in Appendix VIII. For general matrices $\mathbb{A}_i$, more complex cone-switching structure should be considered which therefore motivates the study of this chapter.

2 Renewal processes: a brief reminder

As mentioned above, jumps (or renewals) occur at the random epochs of time $t_0, t_1, \ldots$. We take the origin of time at $t_0 = 0$. Intervals of time between two jumps, $\tau_1 = t_1, \tau_2 = t_2 - t_1, \ldots$, are IID random variables with common density $\rho(\tau)$. In other words, $\tau_2, \tau_3, \ldots$ are independent copies of the generic waiting time τ_1. The number of jumps which occurred between 0 and t, denoted by N_t, is the random variable for the largest n for which $t_n \leq t$, with

$$t_n = \tau_1 + \cdots + \tau_n.$$

With this definition, if there is no jump between 0 and t, then $N_t = 0$. The probability of such an event, or survival probability (or yet persistence probability), reads:

$$q(t) = \mathbb{P}(\tau_1 > t) = \int_t^\infty \mathrm{d}\tau\, \rho(\tau).$$

The density $\rho(\tau)$ can either be a narrow distribution with all moments finite, in which case the decay of $q(t)$, as $t \to \infty$, is faster than any power law, or a distribution characterized by a power-law tail with index $\theta > 0$

$$q(t) = \int_t^\infty \mathrm{d}\tau\, \rho(\tau) \approx \left(\frac{\tau_0}{t}\right)^\theta, \tag{VIII.6}$$

hence

$$\rho(\tau) \approx \frac{c}{\tau^{1+\theta}}, \tag{VIII.7}$$

where τ_0 is a microscopic time scale and $c = \theta\tau_0^\theta$ is the tail parameter. If $\theta < 1$ all moments of $\rho(\tau)$ are divergent, if $1 < \theta < 2$, the first moment $\langle\tau_1\rangle$ is finite but higher moments are divergent, and so on. In Laplace space, where s is conjugate to τ, for a narrow distribution we have

$$\underset{\tau}{\mathcal{L}}\, \rho(\tau) = \widehat{\rho}(s) = \int_0^\infty \mathrm{d}\tau\, e^{-s\tau}\rho(\tau) \underset{s\to 0}{=} 1 - \langle\tau_1\rangle s + \frac{1}{2}\left\langle\tau_1^2\right\rangle s^2 + \cdots.$$

For a broad distribution, (VIII.6) yields

$$\widehat{\rho}(s) \underset{s\to 0}{\approx} \begin{cases} 1 - A\, s^{\theta} & (\theta < 1) \\ 1 - \langle \tau_1 \rangle s + A\, s^{\theta} & (1 < \theta < 2), \end{cases} \tag{VIII.8}$$

and so on, where $A = c|\Gamma(-\theta)|$. From now on, unless otherwise stated, we will only consider the case $0 < \theta < 1$. When $\theta > 1$, the process becomes ergodic, in the sense that $M = \lim_{t\to\infty} S_t/t$ converges to the ergodic mean, with possibly non trivial corrections when t is large but finite (see Section 5).

The last time interval involved in the sum (VIII.3) is the backward recurrence time $B_t = t - t_{N_t}$, i.e., the length of time measured backwards from t to the last jump before t, where t_{N_t}, the time of occurrence of this last jump, is the sum of a random number of random variables

$$t_{N_t} = \tau_1 + \cdots + \tau_{N_t}.$$

The backward recurrence time has also the interpretation of the age of the current, unfinished, interval at time t. The statistics of the quantities N_t, t_{N_t}, B_t is investigated in detail in [175], which also contains relevant references on renewal processes.

3 Distribution of the sum S_t when $\alpha_1, \alpha_2, \ldots$ are IID random variables

We start our study with the simpler case where the random variables $\alpha_1, \alpha_2, \ldots$ in (VIII.3) are independent and identically distributed with common distribution $f_\alpha(a)$, as a preparation for the more elaborate situation where these random variables form the Markov chain defined in (VIII.1), and also because this case has an interest in itself. The distribution $f_\alpha(a)$ is either a density,

$$f_\alpha(a) = \frac{\mathrm{d}}{\mathrm{d}a}\mathbb{P}(\alpha \le a),$$

for continuous random variables, or is given by

$$f_\alpha(a) = \sum_{j=1}^{q} p_j \delta(a - a_j), \qquad \sum_{j=1}^{q} p_j = 1, \tag{VIII.9}$$

in the discrete case. As we will see, in the long-time scaling regime, the distribution of the fraction $M = \lim_{t\to\infty} S_t/t$ for this latter case is the same as for the Markov renewal process investigated in Section 4.

3.1 The distribution of S_t

The methods used in [175] for the computation of the distribution of the occupation time of a two-state process can be easily extended to the case of the multi-state process at hand.

The joint probability density of S_t and N_t reads

$$f_{S_t,N_t}(t,y,n) = \frac{\mathrm{d}}{\mathrm{d}y}\mathbb{P}(S_t \leq y, N_t = n),$$

from which the density of S_t is obtained by summing upon n

$$f_{S_t}(t,y) = \sum_{n\geq 0} f_{S_t,N_t}(t,y,n).$$

The computation of this density can be made in Laplace space. The transform

$$\widehat{f}_{S_t}(s,u) = \underset{t}{\mathcal{L}}\underset{y}{\mathcal{L}}\, f_{S_t}(t,y)$$

is taken with respect to the two coordinates t and y with conjugate variables s and u. This yields

$$\begin{aligned}\widehat{f}_{S_t}(s,u) &= \sum_{n\geq 0} \underset{t}{\mathcal{L}} \left\langle e^{-uS_t} I(t_n < t < t_n + \tau_{n+1})\right\rangle \\ &= \sum_{n\geq 0} \left\langle e^{-u(\alpha_1\tau_1+\cdots+\alpha_n\tau_n)} e^{u\alpha_{n+1}t_n} \int_{t_n}^{t_n+\tau_{n+1}} \mathrm{d}t\, e^{-st} e^{-u\alpha_{n+1}t} \right\rangle,\end{aligned}$$

where the average is taken upon the τ_i and α_i and $I(.)$ is the indicator random variable of the event inside the parentheses, equal to 1 if this event occurs and 0 otherwise. The expression of the integral is

$$\int_{t_n}^{t_n+\tau_{n+1}} \mathrm{d}t\, e^{-t(s+u\alpha_{n+1})} = e^{-(s+u\alpha_{n+1})t_n} \frac{1 - e^{-(s+u\alpha_{n+1})\tau_{n+1}}}{s+u\alpha_{n+1}},$$

thus

$$\widehat{f}_{S_t}(s,u) = \sum_{n\geq 0} \left\langle e^{-u(\alpha_1\tau_1+\cdots+\alpha_n\tau_n)} e^{-st_n} \frac{1 - e^{-(s+u\alpha_{n+1})\tau_{n+1}}}{s+u\alpha_{n+1}} \right\rangle \tag{VIII.10}$$

$$= \sum_{n\geq 0} \left\langle \widehat{\rho}(s+u\alpha_1)\ldots\widehat{\rho}(s+u\alpha_n) \frac{1-\widehat{\rho}(s+u\alpha_{n+1})}{s+u\alpha_{n+1}} \right\rangle \tag{VIII.11}$$

$$= \sum_{n\geq 0} \langle \widehat{\rho}(s+u\alpha)\rangle^n \left\langle \frac{1-\widehat{\rho}(s+u\alpha_{n+1})}{s+u\alpha} \right\rangle, \tag{VIII.12}$$

where, in the last two lines, the averages are taken upon the α_i only.

We thus finally obtain

$$\widehat{f}_{S_t}(s,u) = \frac{1}{1-\langle\widehat{\rho}(s+u\alpha)\rangle} \left\langle \frac{1-\widehat{\rho}(s+u\alpha)}{s+u\alpha} \right\rangle, \tag{VIII.13}$$

where the averages are taken upon α. For a generic distribution $f_\alpha(a)$, we get

$$\widehat{f}_{S_t}(s,u) = \frac{1}{1-\int \mathrm{d}a\, f_\alpha(a)\widehat{\rho}(s+ua)} \int \mathrm{d}a\, f_\alpha(a)\, \frac{1-\widehat{\rho}(s+ua)}{s+ua}, \tag{VIII.14}$$

while for the particular case of a discrete distribution (see (VIII.9)), (VIII.13) yields

$$\widehat{f}_{S_t}(s,u) = \frac{1}{1-\sum_{j=1}^{q} p_j\, \widehat{\rho}(s+ua_j)} \sum_{j=1}^{q} p_j \frac{1-\widehat{\rho}(s+ua_j)}{s+ua_j}. \tag{VIII.15}$$

3.2 Scaling regime

In the long-time regime where s and u are small and comparable, using (VIII.8), the result (VIII.13) yields

$$\widehat{f}_{S_t}(s,u) \approx \frac{\langle (s+u\alpha)^{\theta-1}\rangle}{\langle (s+u\alpha)^{\theta}\rangle} \approx \frac{1}{s} g(\xi), \qquad \xi = \frac{u}{s}, \tag{VIII.16}$$

where

$$g(\xi) = \frac{\langle (1+\xi\alpha)^{\theta-1}\rangle}{\langle (1+\xi\alpha)^{\theta}\rangle}.$$

If α is a continuous random variable we have

$$g(\xi) = \frac{\int \mathrm{d}a f_\alpha(a)(1+\xi a)^{\theta-1}}{\int \mathrm{d}a f_\alpha(a)(1+\xi a)^{\theta}}, \tag{VIII.17}$$

while for the discrete case (VIII.15) gives

$$g(\xi) = \frac{\sum_j p_j (1+\xi a_j)^{\theta-1}}{\sum_j p_j (1+\xi a_j)^{\theta}}. \tag{VIII.18}$$

The scaling behavior (VIII.16) entails the following properties (see Appendix B of [175] for more details). First, S_t/t possesses a limiting distribution given by

$$f_M(x) = \lim_{t\to\infty} f_{S_t/t}(t,x), \qquad x = \frac{y}{t}.$$

Hence

$$\widehat{f}_{S_t}(s,u) = \int_0^\infty \mathrm{d}t\, e^{-st} \langle e^{-uS_t}\rangle = \int_0^\infty \mathrm{d}t\, e^{-st} \langle e^{-utM}\rangle = \left\langle \frac{1}{s+uM} \right\rangle,$$

so that

$$g(\xi) = \left\langle \frac{1}{1+\xi M} \right\rangle = \int_0^\infty \mathrm{d}x\, \frac{f_M(x)}{1+\xi x}. \tag{VIII.19}$$

This can be inverted as [2]

$$f_M(x) = -\frac{1}{\pi x} \lim_{\epsilon\to 0} \mathfrak{Im} \left(g\left(-\frac{1}{x+\mathrm{i}\epsilon} \right) \right).$$

[2] Setting $\xi = 1/y$ in (VIII.19) yields

$$h(y) = \frac{1}{y}\, g\left(\frac{1}{y}\right) = \int_0^\infty \mathrm{d}x\, \frac{f_M(x)}{x+y},$$

showing that $h(y)$ is the Stieltjes transform of $f_M(x)$ [197].

Furthermore, the moments of M can be obtained, when they exist, by expanding $g(\xi)$ as a Taylor series, since (VIII.19) implies that

$$g(\xi) = \sum_{k\geq 0} (-\xi)^k \left\langle M^k \right\rangle . \tag{VIII.20}$$

We will come back to the moments of M in Section 5.

In the continuous case, the result is

$$f_M(x) = \frac{\sin \pi\theta}{\pi} \frac{I^<_{\theta-1}(x) I^>_\theta(x) + I^<_\theta(x) I^>_{\theta-1}(x)}{I^<_\theta(x)^2 + I^>_\theta(x)^2 + 2\, I^<_\theta(x) I^>_\theta(x) \cos \pi\theta}, \tag{VIII.21}$$

with

$$I^<_\theta(x) = \int_{-\infty}^{x} \mathrm{d}a\, (x-a)^\theta f_\alpha(a), \quad I^>_\theta(x) = \int_x^{\infty} \mathrm{d}a\, (a-x)^\theta f_\alpha(a). \tag{VIII.22}$$

In the discrete case (see (VIII.9)) we have in each sector $a_i < x < a_{i+1}$,

$$I^<_\theta(x) = \sum_{j\leq i} p_j (x-a_j)^\theta, \qquad I^>_\theta(x) = \sum_{j>i} p_j (a_j - x)^\theta, \tag{VIII.23}$$

which results in the expression for $f_M(x)$ given by (VIII.5), up to the replacement of π_j by p_j. Similar results can be found in [185, 186, 187] (see Section 6).

Recently, an interesting parallel with problems related to random matrices has been made. [3] Setting $\xi = 1/y$, the Stieltjes transform takes the generic form

$$\int \frac{d\mu(z)}{y+z} := h(y) = \frac{1}{\gamma} \frac{P'(y)}{P(y)}, \tag{VIII.24}$$

with $P(y) = \int dz f(z)(y+z)^\gamma$, $\gamma = \theta$ and $f = f_\alpha$ and μ the distribution of M in our case. A similar expression for the Stieltjes transform of the measure is found in the context of the Finite Free Convolution in [199] with $\gamma = n \in \mathbb{N}^*$ and f the negative Markov-Krein transform of μ. In the same way, the same expression is obtained in [200] in the case of the rank-one HCIZ integral interpolating between classical and free convolution. In this context, $\gamma = -c$ with c the interpolation parameter, and f the Markov-Krein transform of μ. The precise nature of the connection is still unclear though.

3.3 Examples

Let us take, as a first example, the case where f_α is discrete (see (VIII.9)), with $q = 2$, and $p_1 = p_2 = 1/2$. Then, if $a_1 < x < a_2$, (VIII.21) and (VIII.23) yield

$$f_M(x) = \frac{(a_2 - a_1)\sin \pi\theta}{\pi} \frac{(x-a_1)^{\theta-1}(a_2-x)^{\theta-1}}{(x-a_1)^{2\theta} + (a_2-x)^{2\theta} + 2\cos \pi\theta (x-a_1)^\theta (a_2-x)^\theta}, \tag{VIII.25}$$

[3] Observations made with Pierre Mergny upon noticing the similarities between (VIII.21) and Eq. (10) from [198].

and $f_M(x) = 0$ otherwise, which is the law found by Lamperti [150]. This function has a power-law singularity with negative exponent at both ends, $x \to a_j$ $(j = 1, 2)$,

$$f_M(x) \approx \frac{\sin \pi\theta}{\pi(a_2 - a_1)^\theta} |x - a_j|^{\theta - 1}. \tag{VIII.26}$$

It is U-shaped, as the arcsine law,

$$f_M(x) = \frac{1}{\pi\sqrt{(a_2 - x)(x - a_1)}},$$

to which it reduces when $\theta = 1/2$, as long as $\theta < \theta_c = 0.594612...$, while a local maximum appears at $x = (a_1 + a_2)/2$ when $\theta > \theta_c$ [163, 175].

As a second example, let the random variable α be uniform between -1 and 1. Then, by (VIII.22), we have

$$I_\theta^<(x) = I_\theta^>(-x) = \frac{(1 + x)^\theta}{2(1 + \theta)},$$

and therefore, if $-1 < x < 1$, (VIII.21) implies

$$f_M(x) = \frac{2(1 + \theta) \sin \pi\theta}{\pi\theta} \frac{(1 - x^2)^\theta}{(1 - x)^{2(1+\theta)} + (1 + x)^{2(1+\theta)} + 2 \cos \pi\theta (1 - x^2)^{(1+\theta)}},$$

and $f_M(x) = 0$ otherwise. This function vanishes as a power-law at both ends, $x \to \pm 1$, with a positive exponent

$$f_M(x) \approx \frac{(1 + \theta) \sin \pi\theta}{2^{1+\theta}\pi\theta} (1 \mp x)^\theta,$$

and is always maximum at $x = 0$. Note that (VIII.27) reduces to the arcsine law for $\theta = -1/2$.

Finally, it is easy to see on both expressions (VIII.25) and (VIII.27) that $f_M(x) \to f_\alpha(x)$ for $\theta \to 0$ (complete absence of self-averaging), and that, when $\theta \to 1$, $f_M(x)$ becomes a δ function centered at $\langle\alpha\rangle$, that is, at $(a_2 + a_1)/2$ for the former and at 0 for the latter (ergodicity). The same holds true for the general expressions (VIII.5) and (VIII.21), as can be seen on (VIII.17) and (VIII.18). We will come back to these limits and their interpretations in Section 5 (see also [150, 160, 161, 163, 175, 185, 186]). Figure VIII.1 shows numerical simulations for different continuous distributions for α.

4 Distribution of the sum S_t for a Markov renewal process

We now assume the Markov chain to be irreducible with the associated stationary probability measure $\langle\pi| = (\pi_1, \ldots, \pi_q)$ satisfying

$$\langle\pi| = \langle\pi|\,\mathbb{P}, \quad \sum_{i=1}^{q} \pi_i = 1. \tag{VIII.27}$$

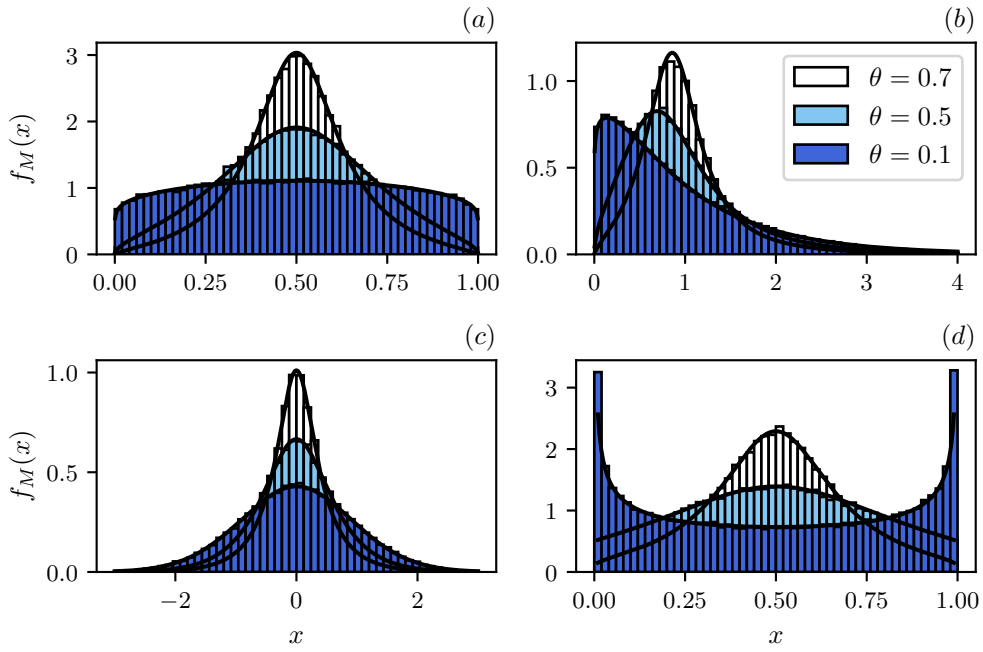


Figure VIII.1: Probability density function $f_M(x)$ for different continuous distributions for α and different values of θ. (a) Uniform distribution on $[0, 1]$. (b) Exponential distribution of parameter 1. (c) Standard Gaussian distribution. (d) Arcsine distribution. We can clearly see the two different limits $\theta \to 0^+$ (M identifies to α) and $\theta \to 1^-$ (M self-averages).

The main results of this section are, first, the exact expression (VIII.31) of the distribution f_{S_t} of the sum S_t in Laplace space, and secondly the scaling form (VIII.33) which leads to the limiting distribution (VIII.5) of the rescaled variable M in real space. This latter expression is the same as that founded for the IID case in Section 3, up to the replacement of π_j by p_j. The difference between the Markov renewal process and the IID case is that the stationary distribution $(\pi_1, \ldots, \pi_q)$ is generated dynamically for the former, while the weights p_i are given a priori for the latter.

4.1 The distribution of the sum S_t

We start again from (VIII.11)

$$\widehat{f}_{S_t}(s,u) = \sum_{n\geq 0} \left\langle \widehat{\rho}(s+u\alpha_1)\ldots\widehat{\rho}(s+u\alpha_n)\frac{1-\widehat{\rho}(s+u\alpha_{n+1})}{s+u\alpha_{n+1}} \right\rangle, \tag{VIII.28}$$

where now the average is upon the configurations $\{\alpha_1, \alpha_2, \ldots, \alpha_{n+1}\}$ of the chain. A realization of such a configuration, with $N_t = n$ fixed, is given by the sequence of values

$$a_{j_1}, a_{j_2}, \ldots, a_{j_{n+1}}, \tag{VIII.29}$$

where each of the indices $j_1, j_2, \dots$ takes the values $1, \dots, q$. Let x_j and y_j denote the quantities appearing in (VIII.15)

$$x_j = \widehat{\rho}(s + ua_j), \qquad y_j = \frac{1 - \widehat{\rho}(s + ua_j)}{s + ua_j}.$$

We also denote by $Q_{j_1} = \mathbb{P}(\alpha_1 = a_{j_1})$ the probability that the first value taken by α be a_{j_1}.

Now (VIII.28) entails

$$\widehat{f}_{S_t}(s,u) = \sum_{n\geq 0} \sum_{j_1,\dots,j_{n+1}} Q_{j_1}\, x_{j_1} \mathbb{P}_{j_1,j_2}\, x_{j_2} \mathbb{P}_{j_2,j_3} \dots x_{j_n} \mathbb{P}_{j_n,j_{n+1}}\, y_{j_{n+1}},$$

or, with matrix notations,

$$\widehat{f}_{S_t}(s,u) = \sum_{n\geq 0} \sum_{j_1,\dots,j_{n+1}} Q_{j_1}\, \Delta^x_{j_1,j_1} \mathbb{P}_{j_1,j_2}\, \Delta^x_{j_2,j_2} \mathbb{P}_{j_2,j_3} \dots \Delta^x_{j_n,j_n} \mathbb{P}_{j_n,j_{n+1}}\, \Delta^y_{j_{n+1},j_{n+1}},$$

where we have introduced the diagonal matrices Δ^x et Δ^y,

$$\Delta^x = \mathrm{diag}(x_1, \dots, x_q), \qquad \Delta^y = \mathrm{diag}(y_1, \dots, y_q).$$

So

$$\widehat{f}_{S_t}(s,u) = \sum_{n\geq 0} \sum_{j_1,j_{n+1}} Q_{j_1} (\Delta^x \mathbb{P})^n_{j_1,j_{n+1}} \Delta^y_{j_{n+1},j_{n+1}} = \sum_{n\geq 0} \langle Q | \, (\Delta^x \mathbb{P})^n \Delta^y \, | R \rangle \,, \qquad \text{(VIII.30)}$$

with

$$|R\rangle = \begin{pmatrix} 1 \\ 1 \\ \vdots \end{pmatrix}, \qquad \langle Q| = (Q_1, \dots, Q_q),$$

so that $\langle Q|R\rangle = 1$. Equation (VIII.30) finally leads to the key result

$$\widehat{f}_{S_t}(s,u) = \langle Q | \, (\mathbb{1} - \Delta^x \mathbb{P})^{-1} \Delta^y \, | R \rangle \,. \qquad \text{(VIII.31)}$$

For $u = 0$, this expression yields

$$\widehat{f}_{S_t}(s,0) = \frac{1 - \widehat{\rho}(s)}{s} \, \langle Q | \, (\mathbb{1} - \widehat{\rho}(s)\mathbb{P})^{-1} \, | R \rangle = \frac{1}{s},$$

showing that f_{S_t} is well normalized.

4.2 Scaling regime

In the long-time regime where s and u are small and comparable, using again (VIII.8), we have

$$\Delta^x \approx \mathbb{1} - A s^\theta \Delta_\theta,$$

with

$$\Delta_\theta = \mathrm{diag}((1+\xi a_1)^\theta, \dots, (1+\xi a_q)^\theta).$$

Likewise

$$\Delta^y \approx A s^{\theta-1} \Delta_{\theta-1}.$$

The matrix $\mathbb{P}$ is dominated by the Perron-Frobenius eigenvalue 1, hence the matrix $(\mathbb{1} - \Delta^x \mathbb{P})^{-1}$ becomes singular when $s \to 0$. The final result reads

$$\widehat{f}_{S_t}(s,u) = \langle Q| \, (\mathbb{1} - \Delta^x \mathbb{P})^{-1} \Delta^y \, |R\rangle \approx \frac{1}{s} \frac{\langle \pi | \Delta_{\theta-1} | R\rangle}{\langle \pi | \Delta_\theta | R\rangle} = \frac{1}{s} g(\xi), \tag{VIII.32}$$

where

$$g(\xi) = \frac{\sum_j \pi_j (1+\xi a_j)^{\theta-1}}{\sum_j \pi_j (1+\xi a_j)^\theta}, \tag{VIII.33}$$

as we now show.

We write

$$\mathbb{1} - \Delta^x \mathbb{P} \approx \mathbb{1} - (\mathbb{1} - A s^\theta \Delta_\theta)\mathbb{P} \approx \mathbb{1} - \mathbb{P} + A s^\theta \Delta_\theta \mathbb{P}.$$

The matrix $\mathbb{M} = \mathbb{1} - \mathbb{P}$ has a zero eigenvalue, with associated (right and left) eigenvectors

$$|R\rangle, \qquad \langle L| = (\pi_1, \pi_2, \dots) = \langle \pi|,$$

i.e.,

$$\mathbb{M}\,|R\rangle = 0 \qquad \langle L|\,\mathbb{M} = 0.$$

For a generic matrix $\mathbb{G}$, it is known that, ϵ being a small parameter,

$$(\mathbb{M} + \epsilon \mathbb{G})^{-1} \approx \frac{1}{\epsilon} \frac{|R\rangle \langle L|}{\langle L|\mathbb{G}|R\rangle}. \tag{VIII.34}$$

Here, using (VIII.34), we get

$$(\mathbb{M} + A s^\theta \Delta_\theta \mathbb{P})^{-1} = \frac{1}{A s^\theta} \frac{|R\rangle \langle L|}{\langle L|\Delta_\theta \mathbb{P}|R\rangle} = \frac{1}{A s^\theta} \frac{|R\rangle \langle L|}{\langle L|\Delta_\theta|R\rangle},$$

since $\mathbb{P}\,|R\rangle = |R\rangle$. Thus

$$\langle Q| \, (\mathbf{1} - \Delta^x \mathbb{P})^{-1} \Delta^y \, |R\rangle \approx \langle Q|R\rangle \frac{1}{s} \frac{\langle L|\Delta_{\theta-1}|R\rangle}{\langle L|\Delta_\theta|R\rangle} = \frac{1}{s} \frac{\langle \pi|\Delta_{\theta-1}|R\rangle}{\langle \pi|\Delta_\theta|R\rangle},$$

which is (VIII.32).

Coming back to (VIII.33) we recognize the expression (VIII.18) found previously, up to the replacement of p_j by π_j, the stationary distribution. As a consequence, the result for the distribution of the mean $M = \lim_{t\to\infty} S_t/t$ is the same as before (up to the replacement of p_j by π_j), i.e., it is given by (VIII.21) and (VIII.23), resulting in (VIII.5). The rationale behind this result is that the chain visits a great many times all accessible states. Of course, as we will see shortly, finite-time behaviors are different for the IID situation of Section 3 and for the Markov case of the present section. Finally, Figure VIII.2 shows examples of simulations of M for two Markov chains and different values of θ.

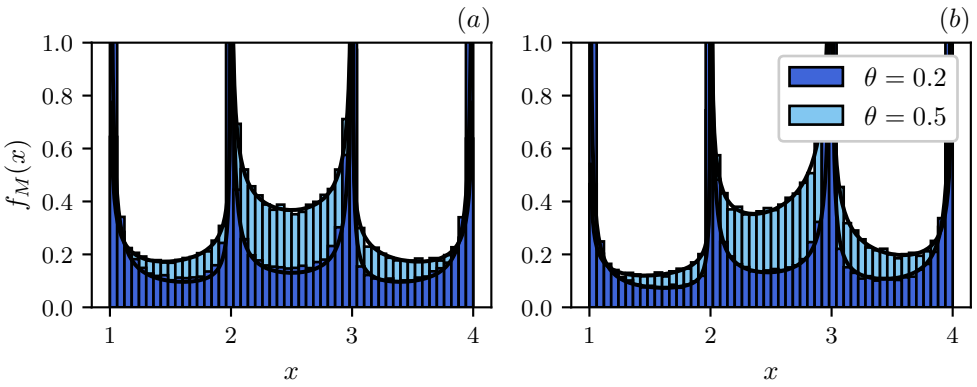


Figure VIII.2: Probability density function $f_M(x)$ for different two different Markov chains on the states $\{1, 2, 3, 4\}$ and values of θ. (a) Deterministic Markov chain defined by $\mathbb{P}_{ij} = \delta_{j,i+1}$ with uniform stationary measure $|\pi\rangle = \frac{1}{4}(1, 1, 1, 1)$. (b) Generic Markov chain with transition matrix

$$\mathbb{P} = \begin{pmatrix} 0.05 & 0.1 & 0.75 & 0.1 \\ 0.25 & 0.25 & 0.25 & 0.25 \\ 0.15 & 0.2 & 0.3 & 0.35 \\ 0.3 & 0.3 & 0.15 & 0.25 \end{pmatrix},$$

and stationary measure $|\pi\rangle = (0.191, 0.217, 0.337, 0.255)$.

5 Moments

5.1 Moments in the long-time regime

The moments of the mean M can be obtained from (VIII.33), as mentioned above (see (VIII.20)). For instance, the first three moments read

$$\langle M \rangle = \langle \alpha \rangle, \qquad \langle M^2 \rangle = \theta \langle \alpha \rangle^2 + (1-\theta)\langle \alpha^2 \rangle,$$
$$\langle M^3 \rangle = \theta^2 \langle \alpha \rangle^3 + \frac{3}{2}\theta(1-\theta)\langle \alpha \rangle \langle \alpha^2 \rangle + \frac{(1-\theta)(2-\theta)}{2}\langle \alpha^3 \rangle. \tag{VIII.35}$$

These results manifest the absence of self-averaging of the process as long as $\theta < 1$. When $\theta \to 0$, M identifies to α (complete absence of self-averaging). For $\theta = 1$, the moments of M are given by powers of $\langle \alpha \rangle$, namely $\langle M^k \rangle = \langle \alpha \rangle^k$. More generally, if $\theta \geq 1$, the system becomes ergodic in the limit of long times, i.e., the limiting distribution $f_M(x)$ is peaked around $\langle \alpha \rangle$, so

$$M = \lim_{t \to \infty} \frac{1}{t} \int_0^t \mathrm{d}u \, \alpha(u) = \langle \alpha \rangle,$$

i.e., the mean is identical to the average (see [185, 186] for similar considerations). For $1 \leq \theta < 2$, for long but finite times, even though the distribution of S_t/t becomes narrow,

the fluctuations of S_t are anomalous. Finally, for $\theta \geq 2$ they are normal and grow as $t^{1/2}$. This phenomenon is analyzed in detail in [175] for the case of two states. The present situation of a multistate Markov chain does not change this picture.

5.2 Finite-time corrections

Coming back to the case where $\theta < 1$, an interesting consequence of the analyses of Section 3 and Section 4 is the possibility of computing the finite-time corrections to the asymptotic formulas (VIII.35), that is, in other words, of answering the question of how fast the fraction M_t converges to its limit M, both for the IID case and for the Markov renewal process. As we will see, this convergence is quite slow, and different for the two processes.

We start from the exact expressions of $\widehat{f}_{S_t}(s,u)$ given respectively by (VIII.13) for the IID case and by (VIII.31) for the Markov renewal case.

For the IID case, taking the derivative of (VIII.13) with respect to u and setting $u = 0$, we have

$$\underset{t}{\mathcal{L}}\,\langle S_t\rangle = \frac{\langle\alpha\rangle}{s^2},$$

yielding the identity, holding for any finite time t,

$$\frac{\langle S_t\rangle}{t} = \langle\alpha\rangle, \tag{VIII.36}$$

which is in line with the result given in (VIII.35) for $\langle M\rangle$. This identity can also be simply obtained by noting that

$$\langle S_t\rangle = \int_0^t \mathrm{d}u\,\langle\alpha(u)\rangle = \langle\alpha\rangle\big(\tau_1 + \cdots + \tau_{N_t} + B_t\big) = \langle\alpha\rangle t.$$

For the Markov renewal process, the identity (VIII.36) no longer holds. We have instead

$$\frac{\langle S_t\rangle}{t} \approx \langle\alpha\rangle + b\,t^{-\theta}, \tag{VIII.37}$$

where the amplitude b of the correction is given by (VIII.40) below, as we now show. We take the derivative of (VIII.31) with respect to u and set $u = 0$, to obtain, after some algebra,

$$\underset{t}{\mathcal{L}}\,\langle S_t\rangle = \frac{1-\widehat{\rho}(s)}{s^2}\,\langle Q|\,(\mathbb{1} - \widehat{\rho}(s)\mathbb{P})^{-1}\Delta^a\,|R\rangle\,, \tag{VIII.38}$$

where

$$\Delta^a = \mathrm{diag}(a_1,\ldots,a_q).$$

Using the spectral decomposition of the matrix $\mathbb{P}$, with eigenvalues λ_i and right and left eigenvectors $|R_i\rangle$ and $\langle L_i|$,

$$\mathbb{P} = \sum_{i=1}^{q} \frac{|R_i\rangle\,\langle L_i|}{\langle L_i|R_i\rangle}\lambda_i,$$

we obtain

$$(\mathbb{1} - \widehat{\rho}(s)\mathbb{P})^{-1} = \sum_{i=1}^{q} \frac{1}{1 - \widehat{\rho}(s)\lambda_i} \frac{|R_i\rangle \langle L_i|}{\langle L_i|R_i\rangle}.$$

In the right side of this equation, the term coming from the Perron eigenvalue $\lambda_1 = 1$ plays a distinct role, so we rewrite it as

$$(\mathbb{1} - \widehat{\rho}(s)\mathbb{P})^{-1} = \frac{1}{1 - \widehat{\rho}(s)} \frac{|R\rangle \langle L|}{\langle L|R\rangle} + \sum_{i=2}^{q} \frac{1}{1 - \widehat{\rho}(s)\lambda_i} \frac{|R_i\rangle \langle L_i|}{\langle L_i|R_i\rangle},$$

leading to the exact result, which is a more explicit expression of (VIII.38),

$$\underset{t}{\mathcal{L}} \langle S_t\rangle = \frac{\langle \alpha\rangle}{s^2} + \frac{1 - \widehat{\rho}(s)}{s^2} \sum_{i=2}^{q} \frac{1}{1 - \widehat{\rho}(s)\lambda_i} \frac{\langle Q|R_i\rangle \langle L_i|\Delta^a|R\rangle}{\langle L_i|R_i\rangle}. \tag{VIII.39}$$

The first order correction is given by

$$\underset{t}{\mathcal{L}} \langle S_t\rangle \approx \frac{\langle \alpha\rangle}{s^2} + As^{\theta-2} \sum_{i=2}^{q} \frac{1}{1 - \lambda_i} \frac{\langle Q|R_i\rangle \langle L_i|\Delta^a|R\rangle}{\langle L_i|R_i\rangle},$$

which, by inversion, yields (VIII.37) with

$$b = \frac{c}{\theta(1-\theta)} \sum_{i=2}^{q} \frac{1}{1 - \lambda_i} \frac{\langle Q|R_i\rangle \langle L_i|\Delta^a|R\rangle}{\langle L_i|R_i\rangle}, \tag{VIII.40}$$

where c is the tail coefficient of $\rho(\tau)$ (see (VIII.7)).

These computations can in principle be extended to higher moments $\langle (S_t/t)^k\rangle$. While they are easy for the IID case, they become increasingly more difficult for the Markov renewal process. In any event, the finite-time corrections are again different for these two cases.

We illustrate this study by the case of a symmetric simple random walk on $q = 4$ sites, with reflecting boundary conditions. The stationary probabilities of this Markov chain are $(\pi_1 = 1/6, \pi_2 = 1/3, \pi_3 = 1/3, \pi_4 = 1/6)$. The random variable α of interest is the position of the walker, which takes the values $a_j = j$ $(j = 1, \ldots, 4)$. With these values, the mean position of the walker is $\langle \alpha\rangle = 5/2$ and the correction amplitude b obtained from (VIII.40) reads

$$b = \frac{c}{\theta(1-\theta)} \Big\{ -\frac{11}{4}, -\frac{5}{4}, \frac{5}{4}, \frac{11}{4} \Big\},$$

according to whether the walker starts at $1, 2, 3, 4$, respectively.

Figure VIII.3-(a) and Figure VIII.3-(b) depict a numerical study of this process. The random time intervals τ are drawn from the distribution $\rho(\tau) = \theta/\tau^{1+\theta}$ for $\tau \geq 1$, with tail coefficient $c = \theta$, corresponding to taking $\tau = U^{-1/\theta}$, where U is uniform between 0 and 1. We choose $\theta = 3/4$, yielding $b = \{-11, -5, 5, 11\}$, according to the initial position of the walker. In Figure VIII.3-(a), the agreement between the simulation points (dots) and

the data coming from a numerical inversion of the exact expressions (VIII.38) or (VIII.39) of f_{S_t} in Laplace space (solid lines) is excellent. In Figure VIII.3-(b), the convergence to the predicted amplitude $b = -5$, for a walker starting at $j = 2$, is demonstrated by plotting the straight line $y = 5 - 15x/4$, together with

$$\left(\frac{5}{2} - \frac{\langle S_t \rangle}{t}\right) t^\theta \approx 5 - \frac{15}{4} t^{\theta-1}, \tag{VIII.41}$$

against $t^{\theta-1}$. Equation (VIII.41) stems from the estimate

$$\frac{\langle S_t \rangle}{t} \approx \frac{5}{2} - \frac{5}{t^\theta} + \frac{15}{4t}, \tag{VIII.42}$$

obtained by expanding (VIII.39) at second order. The data were obtained by a numerical inversion of the exact expressions (VIII.38) or (VIII.39) of f_{S_t} in Laplace space up to time 10^5. The agreement of these finite-time data with the theoretical prediction (VIII.42) is convincing.

Choosing a stable law for the distribution $\rho(\tau)$, with same tail parameter c as above, would yield the same results, as can be seen on (VIII.39) and (VIII.40). In contrast, higher moments of S_t depend on the details of the distribution $\rho(\tau)$.

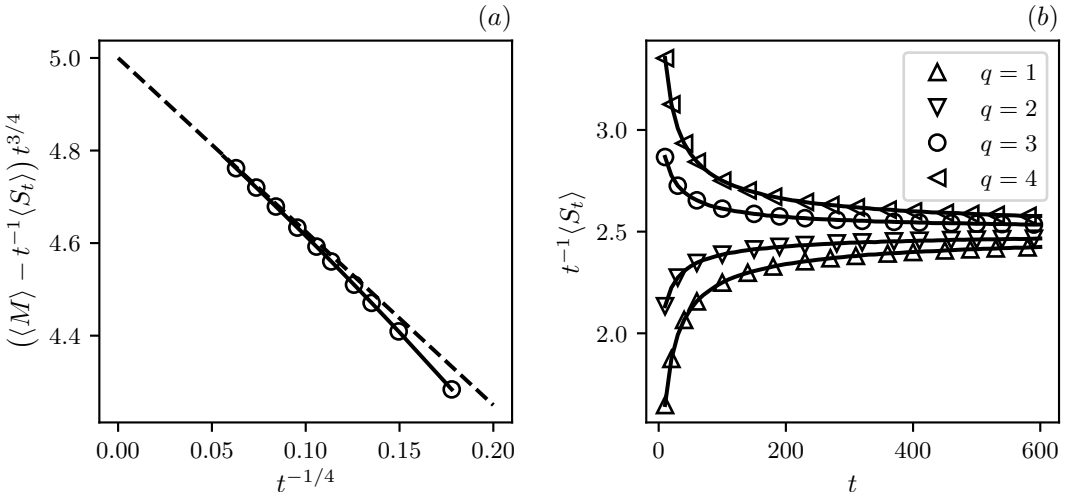


Figure VIII.3: (a) Plot of $\langle S_t \rangle / t$ against time t for the four starting points $1, 2, 3, 4$ of a simple random walker on $q = 4$ sites, with reflecting boundary conditions. Dots: simulation points, solid lines: numerical inversion of the exact Laplace transforms (VIII.38) or (VIII.39). See text for details on $\rho(\tau)$. Here $\theta = 3/4$. (b) Check of the theoretical prediction of the corrections to scaling (VIII.42). Dots: left side of (VIII.41) against $t^{-1/4}$, obtained by a numerical inversion of the exact Laplace transforms (VIII.38) or (VIII.39). Solid line: straight line $y = 5 - 15x/4$.

6 Discussion

The present work is part of the ongoing studies on the generalizations of the law of Lamperti for the occupation time of a two-state Markov process [150]. Reviews in the mathematical literature of this topic can be found in [147, 154]. The purpose of the present work was to extend this law to the specific case of a multistate semi-Markov process. While completing this paper, we became aware of the existence of closely related works, with similar results [187, 153, 185, 186]. These studies are variations around the same theme, with differences, as we now comment.

Reference [187] investigates the Walsh process of index θ, defined as follows. Consider q half-lines H_j, $j = 1, 2, \ldots, q$, with a common endpoint at zero, and a Bessel process (or radial Brownian motion) of dimension $2(1-\theta)$ on these half-lines. When this process arrives at zero, it chooses the half-line H_j with a given probability p_j. Using the inherent scaling properties of Brownian motion, it is shown that the law of the rescaled sum S_t/t obeys (VIII.16), (VIII.18) and (VIII.19). The Walsh process therefore provides an implementation of the IID case of Section 3, at least in the scaling regime (see also [153]).

References [185, 186] are closer in spirit to the present work. The analysis of the process given in these references leads to the expression (VIII.5) of the distribution f_M in the long-time regime, as well as to (VIII.18), (VIII.21) and (VIII.35). Note that these results are already found in the IID case. However the analysis made in [185, 186] does not lead to the explicit expressions of the distribution of the sum S_t in Laplace space, as in (VIII.13) for the IID case and in (VIII.31) for the Markov renewal case, which, in turn, lead to predictions of the finite-time behaviors of these processes, as demonstrated in Section 5.

Key takeaways

- **Renewal processes** are a sequence of intervals of time $\tau_1, \tau_2, \ldots$ representing the time spent in different states $\alpha_1, \alpha_2, \ldots$. The interval of time between the jumps (occurring at time t_i) are IID random variables.
- **Markov Renewal Processes** are defined as the coupled independent evolution of a renewal process (defining the times of jumps between states) and a Markov chain (defining the states). The state of the process is $\alpha(t) = \alpha_n$ for $t_n < t < t_{n+1}$.
- **Power law distribution of intervals** leads to a weak-ergodicity breaking of the observable

  $$M = \lim_{t\to\infty} \frac{1}{t} \int_0^t \mathrm{d}u \alpha(u).$$

  The Stieltjes transform of M is given by

  $$g(\xi) = \frac{\int \mathrm{d}a f_\alpha(a)(1+\xi a)^{\theta-1}}{\int \mathrm{d}a f_\alpha(a)(1+\xi a)^{\theta}},$$

  for f_α the density of states α and θ the exponent (smaller than 1) of the distribution of intervals. In the case of a Markov renewal process, f_α is replaced by the stationary probability of the Markov chain.

A Computation with partition functions

In this appendix, we compute the distribution of the occupation time of a renewal process coupled to a Markov chain using partition functions, in the same spirit as in Chapter VII.

A.1 Setup

Let us then consider a general Markov chain $\{X_n\}_n$ on a discrete state space $\{\alpha_i,\, i \in [\![1, S]\!]\}$ associated with the transition matrix $\mathbb{P}$ such that

$$\mathbb{P}_{ij} = \mathbb{P}\left(X_{n+1} = \alpha_j \,|X_n = \alpha_i\right), \quad \forall i \in [\![1, S]\!],\ \sum_{j=1}^{S} \mathbb{P}_{ij} = 1. \tag{VIII.43}$$

We assume the Markov chain to be irreducible with the associated invariant probability measure $\langle\pi| = (\pi_1, \dots, \pi_S)$ defined through

$$\langle\pi| = \langle\pi|\,\mathbb{P}, \quad \sum_{i=1}^{S} \pi_i = 1. \tag{VIII.44}$$

Furthermore, note that the normalization condition $\forall i \in [\![1, S]\!],\ \sum_{j=1}^{S} \mathbb{P}_{ij} = 1$can be written as $\mathbb{P}\,|e\rangle = |e\rangle$ (or $\langle e|\,\mathbb{P}^\top = \langle e|$), with $|e\rangle = (1, \dots, 1)^\top$. Finally, the initial state is drawn according to a probability vector $|p_0\rangle$. On top of this Markov process, we consider that after having jumped onto a new state, the system will spend a certain amount of time in said state before jumping to the next one. We therefore introduce a *renewal process* $\{t_n\}_n$ for which intervals $\tau_i = t_{i+1} - t_i$ are *independent* and *identically distributed* according to some density $\rho(\tau)$. Our system is then formed by the pairs $\{(X_n, t_n)\}_n$ and we assume the Markov chain and the renewal process to be independent. We want to study the distribution of the *occupation time*

$$M = \lim_{t\to+\infty} \frac{S_t}{t}, \quad S_t = \sum_{i=1}^{N-1} X_i\tau_i + X_N(t - t_{N-1}), \tag{VIII.45}$$

for X_i and τ_i defined above and N a random variable encoding the number of jumps that occurred up to time t.

A.2 Distribution of M

To compute the distribution of M, we will compute all of its moments. We start by computing the moments of S_t/t. To do so, we sum over all possible states' paths $\vec{s}_k = (\alpha_1, \dots, \alpha_k)$, intervals' sequences $\vec{\tau}_k = (\tau_1, \dots, \tau_k)$ and number of jumps k compatible with an observation of the occupation time at time t, i.e. paths such that $\vec{s}$ is unrestricted and $t_{k-1} \le t \le t_k$ for $t_k = \sum_{i=1}^{k} \tau_i$. It therefore yields

$$\mathbb{E}\left[S_t^q\right] = \frac{\displaystyle\sum_{k=1}^{\infty} \int_{\vec{\tau}_k} p\left(\vec{\tau}_k\right) \sum_{\vec{s}_k} p\left(\vec{s}_k\right) \Theta\left(t - t_{k-1}\right) \Theta\left(t_k - t\right) \left(\sum_{i=1}^{k-1} \alpha_i\tau_i + \alpha_k(t - t_{k-1})\right)^q}{\displaystyle\sum_{k=1}^{\infty} \int_{\vec{\tau}_k} p\left(\vec{\tau}_k\right) \sum_{\vec{s}_k} p\left(\vec{s}_k\right) \Theta\left(t - t_{k-1}\right) \Theta\left(t_k - t\right)} := \frac{\mathcal{Z}(q, t)}{\mathcal{Z}(0, t)}, \tag{VIII.46}$$

where we have defined $\mathcal{Z}(q,t)$ through the previous equality and where $\mathcal{Z}(0,t)$ acts as a normalization factor. Furthermore, $p(\vec{\alpha}_k)$ and $p(\vec{\tau}_k)$ refer to the probabilities to have a certain states' path $\vec{s}_k$ and intervals' sequence $\vec{\tau}_k$ given by

$$p(\vec{s}_k) = p_0(s_1)\mathbb{P}_{s_1 s_2}\cdots\mathbb{P}_{s_{k-1}s_k}, \quad p(\vec{\tau}_k) = \prod_{i=1}^{k}\rho(\tau_k), \tag{VIII.47}$$

where we have used the fact that $\{X_n\}_n$ and $\{t_n\}_n$ are respectively a Markov chain and a renewal process. The moments of M are therefore given by

$$\mathbb{E}\left[M^q\right] = \lim_{t\to+\infty} t^{-q}\frac{\mathcal{Z}(q,t)}{\mathcal{Z}(0,t)}. \tag{VIII.48}$$

We evaluate the previous limit by computing the Laplace transforms of the numerator and the denominator. We denote by $\widehat{f}(\omega)$ the Laplace transform of a generic function f. We further introduce $\widehat{\rho}_\ell$ the Laplace transform of the function $\tau \mapsto \rho(\tau)\tau^\ell$ with $\widehat{\rho} := \widehat{\rho}_0$, along with $\widehat{Q}_\ell$ associated with $\tau \mapsto Q(\tau)\tau^\ell$ (where $Q(\tau) = \int_\tau^\infty ds\rho(s)$ is called the *persistence probability*), and where $\widehat{Q}_0(\omega) = (1-\widehat{\rho}(\omega))/\omega$. We further assume that ρ has a power-law behavior $\rho(\tau) \sim_{\tau\to\infty} a\tau^{-1-\theta}$ such that

$$\widehat{\rho}(\omega) \underset{\omega\to 0^+}{\approx} \begin{cases} 1 + a\Gamma(-\theta)\omega^\theta, & 0<\theta<1 \\ 1 - \omega\langle\tau\rangle + a\Gamma(-\theta)\omega^\theta, & 1<\theta \end{cases}, \tag{VIII.49}$$

which in turn implies, if $0<\theta<1$ for $k\geq 1$

$$\begin{aligned} \widehat{\rho}_k(\omega) &\underset{\omega\to 0^+}{\approx} a\Gamma(k-\theta)\omega^{\theta-k} \\ \widehat{Q}_k(\omega) &\underset{\omega\to 0^+}{\approx} a\frac{\Gamma(1+k-\theta)}{\theta}\omega^{\theta-1-k}, \end{aligned} \tag{VIII.50}$$

and finally, if $1<\theta$,

$$\widehat{\rho}_1(\omega) \underset{\omega\to 0^+}{\approx} \langle\tau\rangle - a\Gamma(1-\theta)\omega^{\theta-1}. \tag{VIII.51}$$

A.2.1 Exponential generating function of $\widehat{\mathcal{Z}}$

Let us start by computing the Laplace transform $\widehat{\mathcal{Z}}(0,\omega)$. From Eq. (VIII.46), $\mathcal{Z}(0,t)$ reads

$$\mathcal{Z}(0,t) = \sum_{k=1}^{\infty}\int_{\vec{\tau}_k} p\left(\vec{\tau}_k\right)\sum_{\vec{s}_k} p\left(\vec{s}_k\right)\Theta\left(t-t_{k-1}\right)\Theta\left(t_k-t\right).$$

Using the expression for $p(\vec{s}_k)$, we can easily express

$$\sum_{\vec{s}_k} p\left(\vec{s}_k\right) = \langle e|\left(\mathbb{P}^\top\right)^{k-1}|p_0\rangle = \langle e \mid p_0\rangle = 1, \tag{VIII.52}$$

with $\langle\cdot\mid\cdot\rangle$ the standard scalar product, and where we used the normalization condition for $\mathbb{P}$. We can therefore compute the Laplace transform of $\mathcal{Z}(0,t)$

$$\begin{aligned} \widehat{\mathcal{Z}}(0,\omega) &= \sum_{k=1}^{\infty}\langle e|\left(\mathbb{P}^\top\right)^{k-1}|p_0\rangle\int_0^\infty dte^{-\omega t}\int_{\vec{\tau}_k} p\left(\vec{\tau}_k\right)\Theta\left(t-t_{k-1}\right)\Theta\left(t_k-t\right) \\ &= \frac{1}{\omega}, \end{aligned}$$

which shows that $\mathcal{Z}(0,t)=1$ as expected. In order to compute the generating function of $\widehat{\mathcal{Z}}$, we need to introduce an auxiliary partition functions Z_i defined by

$$Z_i(q,t)=\sum_{k=1}^{\infty}\int_{\vec{\tau}_k} p\left(\vec{\tau}_k\right)\sum_{\vec{s}_k(i)} p\left(\vec{s}_k(i)\right)\delta\left(t-t_k\right)\left(\sum_{j=1}^{k-1}\alpha_j\tau_j+s_i\tau_k\right)^q, \tag{VIII.53}$$

which correspond to intervals' sequences $\vec{\tau}_k$ exactly summing to the observation time t, and states' paths $\vec{s}_k(i)=(s_i,\alpha_{k-1},\dots,\alpha_1)$ ending in state s_i. We encapsulate these auxiliary variables in a vector $|Z\rangle$. Using the Markov property, we write a recursive relation between the terms $x_{k,i}$ of the sum defining Z_i, it reads

$$\begin{aligned}
\widehat{x}_{k,i}(q,\omega) :&= \int_0^{\infty}\mathrm{d}te^{-\omega t}\int_{\vec{\tau}_k} p\left(\vec{\tau}_k\right)\sum_{\vec{s}_k} p\left(\vec{s}_k(i)\right)\delta\left(t-t_k\right)\left(\sum_{j=1}^{k-1}\alpha_j\tau_j+s_i\tau_k\right)^q\\
&=\sum_{\vec{s}_k(i)} p\left(\vec{s}_k(i)\right)\sum_{\vec{\ell}_k}\delta\left(\sum_{i=1}^{k}\ell_i-q\right)\binom{q}{\vec{\ell}_k}\prod_{j=1}^{k}\widehat{\rho}_{\ell_j}(\omega)s_j^{\ell_j}\\
&=\sum_{\ell=0}^{q}\binom{q}{\ell}s_i^{\ell}\widehat{\rho}_{\ell}(\omega)\sum_{\alpha_{k-1}}\mathbb{P}_{\alpha_{k-1}s_i}\sum_{\vec{s}_{k-1}(\alpha_{k-1})} p(\vec{s}_{k-1}(\alpha_{k-1}))\\
&\quad\times\sum_{\vec{\ell}_{k-1}}\delta\left(\sum_{i=1}^{k-1}\ell_i-(q-\ell)\right)\binom{q-\ell}{\vec{\ell}_{k-1}}\prod_{j=1}^{k-1}\widehat{\rho}_{\ell_j}(\omega)s_j^{\ell_j}\\
&=\sum_{\ell=0}^{q}\binom{q}{\ell}s_i^{\ell}\widehat{\rho}_{\ell}(\omega)\sum_{\alpha_{k-1}}\mathbb{P}_{\alpha_{k-1}s_i}\widehat{x}_{k-1,\alpha_{k-1}}(q-\ell,\omega)\\
&=\sum_{\ell=0}^{q}\binom{q}{\ell}s_i^{\ell}\widehat{\rho}_{\ell}(\omega)\sum_{\alpha_{k-1}}\mathbb{P}_{\alpha_{k-1}s_i}\widehat{x}_{k-1,\alpha_{k-1}}(q-\ell,\omega)\\
&=\sum_{\ell=0}^{q}\binom{q}{\ell}s_i^{\ell}\widehat{\rho}_{\ell}(\omega)\left(\mathbb{P}^{\top}\,|\widehat{x}_{k-1}(q-\ell,\omega)\rangle\right)_i.
\end{aligned}$$

The computation above is not valid for $k=1$ but we have $\widehat{x}_{1,i}(q,\omega)=s_i^q\widehat{\rho}_q(q,\omega)p_0(i)$. Summing over k therefore yields

$$\widehat{Z}_i(q,\omega)=s_i^q\widehat{\rho}_q(\omega)p_0(i)+\sum_{\ell=0}^{q}\binom{q}{\ell}s_i^{\ell}\widehat{\rho}_{\ell}(\omega)\left(\mathbb{P}^{\top}\,|\widehat{Z}(q-\ell,\omega)\rangle\right)_i. \tag{VIII.54}$$

We recognize an exponential convolution equation and therefore introduce exponential generating functions $\mathcal{G}_c(x)=\sum_q x^q c_q/q!$. [4] We therefore get

$$\left(\mathcal{G}_{|\widehat{Z}\rangle}\right)_i(x,\omega)=\mathcal{G}_{\widehat{\rho}}(s_ix,\omega)p_0(i)+\mathcal{G}_{\widehat{\rho}}(s_ix,\omega)\left(\mathbb{P}^{\top}\mathcal{G}_{|\widehat{Z}\rangle}\right)_i(x,\omega).$$

With the notation $\Delta_{\widehat{\rho}}$ the diagonal matrix with entries $(\Delta_{\widehat{\rho}})_{ii}=\mathcal{G}_{\widehat{\rho}}(s_ix,\omega)$ and dropping the (x,ω) for clarity, we have a closed form for the e.g.f of $|\widehat{Z}\rangle$

$$\mathcal{G}_{|\widehat{Z}\rangle}=\left(\mathbb{1}-\Delta_{\widehat{\rho}}\mathbb{P}^{\top}\right)^{-1}\Delta_{\widehat{\rho}}\,|p_0\rangle. \tag{VIII.55}$$

[4] Note that the expression in also valid for a vector-valued sequence $|c\rangle$. In this case the associated e.g.f will also be vector-valued with components the e.g.f of the components of $|c\rangle$.

Going back to the initial partition function, one can use the same reasoning to get to the e.g.f. However, since the constraint $\delta(t-t_k)$ is replaced by $\Theta(t-t_{k-1})\,\Theta(t_k-t)$, we need to replace the Laplace transforms $\widehat{\rho}_k$ by $\widehat{Q}_k$. We can write an analogous of equation Eq. (VIII.55) for the partition function $\widehat{\mathcal{Z}}$ using the auxiliary $\widehat{Z}$

$$\widehat{\mathcal{Z}}_i(q,\omega) = s_i^q \widehat{Q}_q(q,\omega) p_0(i) + \sum_{\ell=0}^{q} \binom{q}{\ell} s_i^\ell \widehat{Q}_\ell(\omega) \left(\mathbb{P}^\top \,|\widehat{Z}(q-\ell,\omega)\rangle\right)_i , \tag{VIII.56}$$

and using Eq. (VIII.55), we have

$$\mathcal{G}_{|\widehat{\mathcal{Z}}\rangle} = \Delta_{\widehat{Q}} \left(\mathbb{1} - \mathbb{P}^\top \Delta_{\widehat{\rho}}\right)^{-1} |p_0\rangle . \tag{VIII.57}$$

Finally, the e.g.f of $\widehat{\mathcal{Z}}$ is trivially given by $\langle e|\mathcal{G}_{|\widehat{\mathcal{Z}}\rangle}\rangle$ (one sums over all the possible ending states of states' sequences) and we have

$$\mathcal{G}_{\widehat{\mathcal{Z}}} = \langle e| \Delta_{\widehat{Q}} \left(\mathbb{1} - \mathbb{P}^\top \Delta_{\widehat{\rho}}\right)^{-1} |p_0\rangle . \tag{VIII.58}$$

We will now take the scaling limit $\omega \to 0^+$ while keeping the ratio $\omega/x := y$ constant.

A.2.2 Long-time behavior of $\mathcal{Z}(q,t)$ and Stieltjes transform of M

For Eq. (VIII.48) to be well defined, we must have $\mathcal{Z}(q,t) \underset{t\to\infty}{\approx} t^q \mathbb{E}[M^q]$. Turning to Laplace space, we get $\widehat{\mathcal{Z}}(q,\omega) \underset{\omega\to 0^+}{\approx} q!\mathbb{E}[M^q]\omega^{-1-q}$. Using the scaling $\omega/x := y$, we can express the e.g.f of $\widehat{\mathcal{Z}}$ as follows

$$\begin{aligned}\mathcal{G}_{\widehat{\mathcal{Z}}}(\omega y^{-1},\omega) &\underset{\omega\to 0^+}{\approx} \sum_{q=0}^{\infty} \frac{\left(\omega y^{-1}\right)^q}{q!} q!\omega^{-1-q}\mathbb{E}[M^q] \\ &= \frac{y}{\omega}\mathbb{E}\left[\frac{1}{y-M}\right],\end{aligned}$$

where the last expectation is the Stieltjes transform of M such that

$$\mathcal{G}_{\widehat{\mathcal{Z}}}(\omega y^{-1},\omega) \underset{\omega\to 0^+}{\approx} \frac{y}{\omega}\int \mathrm{d}s \frac{\varphi(s)}{y-s},$$

where φ is the probability density function of M.

A.2.3 Probability density function of M for $0<\theta<1$

Computing the scaling limit of the different e.g.f, we get at leading order in ω

$$\mathcal{G}_{\widehat{\rho}}(s_i\omega y^{-1},\omega) \underset{\omega\to 0^+}{\approx} 1 + a\Gamma(-\theta)\left(\frac{\omega}{y}\right)^\theta (y-s_i)^\theta \tag{VIII.59}$$

$$\mathcal{G}_{\widehat{Q}}(s_i\omega y^{-1},\omega) \underset{\omega\to 0^+}{\approx} -a\Gamma(-\theta)\left(\frac{\omega}{y}\right)^{\theta-1} (y-s_i)^{\theta-1} . \tag{VIII.60}$$

We can therefore compute the r.h.s of Eq. (VIII.58) using perturbation theory for the matrix $\mathbb{1} - \mathbb{P}^\top$

$$\left(\mathbb{1} - \mathbb{P}^\top \Delta_{\widehat{\rho}}\right)^{-1} \underset{\omega\to 0^+}{\approx} -\frac{\omega^\theta}{a\Gamma(-\theta)y^\theta} \frac{|\pi\rangle\langle e|}{\langle e|\,\Delta\left(\left(y-s_i\right)^\theta\right)|\pi\rangle}, \tag{VIII.61}$$

and get

$$\langle e|\,\Delta_{\widehat{Q}}\left(\mathbb{1} - \mathbb{P}^\top \Delta_{\widehat{\rho}}\right)^{-1}|p_0\rangle = \frac{y}{\omega}\frac{\langle e|\,\Delta\left(\left(y-\alpha_i\right)^{\theta-1}\right)|\pi\rangle}{\langle e|\,\Delta\left(\left(y-\alpha_i\right)^{\theta}\right)|\pi\rangle}. \tag{VIII.62}$$

Relating it to the Stieltjes transform of M, we have

$$\int \mathrm{d}s \frac{\varphi(s)}{y-s} = \frac{\sum_j \pi_j (y-\alpha_j)^{\theta-1}}{\sum_j \pi_j (y-\alpha_j)^{\theta}}, \tag{VIII.63}$$

which we can invert by setting $y = x + i\eta$ and taking the limit $\eta \to 0^+$. For $x \notin]\alpha_1, \alpha_S[$, $\varphi(x) = 0$ while for $x \in]\alpha_i, \alpha_{i+1}[$, we get the density

$$\varphi(x) = \frac{\sin\pi\theta}{\pi}\frac{\left(\sum_{j\le i}\pi_j z_j^{\theta-1}\right)\left(\sum_{j>i}\pi_j z_j^{\theta}\right) + \left(\sum_{j\le i}\pi_j z_j^{\theta}\right)\left(\sum_{j>i}\pi_j z_j^{\theta-1}\right)}{\left(\sum_{j\le i}\pi_j z_j^{\theta}\right)^2 + \left(\sum_{j>i}\pi_j z_j^{\theta}\right)^2 + 2\left(\sum_{j\le i}\pi_j z_j^{\theta}\right)\left(\sum_{j>i}\pi_j z_j^{\theta}\right)\cos\pi\theta}, \tag{VIII.64}$$

where $z_j = |x - \alpha_j|$. For a uniform stationary probability measure over two states, we retrieve the density in [141].

A.2.4 Probability density of M for $1 < \theta < 2$

In this case, ρ has a finite first moment and the scaling behavior of the e.g.f is the following

$$\mathcal{G}_{\widehat{\rho}}(s_i\omega y^{-1}, \omega) \underset{\omega\to 0^+}{\approx} 1 - \omega\left(\langle\tau\rangle - \frac{s_i}{y}\right) \tag{VIII.65}$$

$$\mathcal{G}_{\widehat{Q}}(s_i\omega y^{-1}, \omega) \underset{\omega\to 0^+}{\approx} \langle\tau\rangle. \tag{VIII.66}$$

Applying the same procedure as before, we easily get

$$\left(\mathbb{1} - \mathbb{P}^\top \Delta_{\widehat{\rho}}\right)^{-1} \underset{\omega\to 0^+}{\approx} \frac{y}{\omega}\frac{|\pi\rangle\langle e|}{\langle e|\,\Delta\left(y\langle\tau\rangle - s_i\right)|\pi\rangle}. \tag{VIII.67}$$

We can therefore express the Stieltjes transform of M

$$\int \mathrm{d}\lambda \frac{\varphi(\lambda)}{y-\lambda} = \frac{1}{y - \frac{\sum_i \pi_i s_i}{\langle\tau\rangle}}, \tag{VIII.68}$$

which easily gives

$$\varphi(\lambda) = \delta\left(\lambda - \frac{\sum_i \pi_i s_i}{\langle\tau\rangle}\right). \tag{VIII.69}$$

CHAPTER IX

Mixed-moments of Gaussian elliptic matrices

Abstract

We find an explicit formula for the mixed-moments $N^{-1}\mathrm{Tr}\left(\mathbb{X}^t(\mathbb{X}^\top)^s\right)$ in the limit $N \to \infty$ with $t, s \in \mathbb{N}$ and $\mathbb{X}$ a real $N \times N$ Gaussian elliptic random matrix. This formula allows for a numerically efficient way to compute mixed-moments by reducing the exponential complexity of a naive enumeration of non-crossing pairings to a polynomial complexity.

From [4]: Théo Dessertaine and Jean-Philippe Bouchaud. *Explicit computation of mixed-moments of real Gaussian elliptic random matrices.* In preparation.

1 Introduction

The study presented in this chapter stems from the generalization of the simple conewise linear dynamics presented in Chapter VII. One of the problems that we faced was to understand the behavior of the Gaussian process $\mathbf{v}(t) = \mathbb{A}^t\mathbf{v}(0)$ (with $\mathbf{v}(0)$ an initial centered Gaussian vector with IID entries of unit variance) in the large-dimensional limit. We showed that the covariance of the components ij at times t, s was given by

$$\overline{v_i(t)v_j(s)} = (\mathbb{A}^t(\mathbb{A}^\top)^s)_{ij}, \tag{IX.1}$$

where $\overline{(\cdot)}$ denotes the average over initial conditions. Using both self-averaging and rotational invariance of the ensemble of $\mathbb{A}$, the previous expression reduced to

$$\langle v_i(t)v_j(s)\rangle = \delta_{ij}\,\tau\left(\mathbb{A}^t\left(\mathbb{A}^\top\right)^s\right), \tag{IX.2}$$

in the large-dimensional limit. Recall that the linear form $\tau(\cdot)$ is the standard normalized trace from Random Matrix Theory, i.e.

$$\tau(\cdot) = \lim_{N\to\infty}\frac{1}{N}\mathrm{Tr}\,(\cdot)\,. \tag{IX.3}$$

As we explained in Chapter VII, giving an explicit expression for Eq. (IX.2) amounts to computing the mixed-moments of the random matrices $\mathbb{A}$ and $\mathbb{A}^\top$. This is a difficult task since, in this case, these two matrices are not mutually free, i.e. not randomly rotated from one another. In this chapter, we will provide a numerically efficient formula to compute these mixed-moments for Gaussian elliptic matrices. We will present the most general case of computing mixed-moments of such matrices before moving to the two-matrix case.

Before going through this chapter, let us relate this problem to ongoing investigations regarding random matrices. Consider Eq.(IX.1), for a symmetric matrix $\mathbb{A} = \mathbb{O}\Lambda\mathbb{O}^\top$, with $\mathbb{O}$ a random orthogonal matrix and $\Lambda = \boldsymbol{\Delta}(\lambda_i)$ the diagonal matrix of eigenvalues. Using the independence of eigenvectors and eigenvalues for orthogonally invariant matrices, we can perform the average over the Haar measure on the orthogonal group first in Eq. (IX.1)

$$\left\langle \overline{v_i(t)v_j(s)} \right\rangle_{\mathbb{O}} = \left\langle \sum_k \lambda_k^{t+s} \mathbb{O}_{ik}\mathbb{O}_{jk} \right\rangle_{\mathbb{O}} = N^{-1}\delta_{ij} \sum_k \lambda_k^{t+s}, \tag{IX.4}$$

where the last equality is exact. In the large N limit, the rightmost expression converges towards the moment of order $t+s$ of $\mathbb{A}$, and we recover Eq. (IX.2) (in the specific case where $\mathbb{A} = \mathbb{A}^\top$). In this case, the overlap between eigenvectors $\langle \mathbb{O}_{ik}\mathbb{O}_{jl} \rangle_{\mathbb{O}}$ (and more generally $\langle \mathbb{O}_{i_1k_1}\mathbb{O}_{i_2k_2}... \rangle_{\mathbb{O}}$) is completely known and given by the Weingarten functions [201]. Assume now that $\mathbb{A}$ is not symmetric but, say, Gaussian elliptic, i.e. a matrix with some correlation parameter $\varrho \in [-1, 1]$ between entries ij and ji (see below). We can write the singular value decomposition of $\mathbb{A}$ as $\mathbb{A} = \mathbb{O}\Sigma\mathbb{V}^\top$. Both $\mathbb{O}$ and $\mathbb{V}$ are orthogonal matrices, which are not independent for generic values of ϱ. Moreover, the average overlap between left and right eigenvectors is not known analytically for real elliptic matrices (see [202] where the question of overlaps is addressed for complex elliptic matrices). Of course, the result should interpolate between N^{-1} for the symmetric case ($\varrho = 1$) and 0, for the Ginibre case (where it is known that both $\mathbb{O}$ and $\mathbb{V}$ are completely independent). One of the interesting features of the computation that is presented in this chapter is that it bypasses the difficulty of computing the overlaps using self-averaging.

2 Gaussian elliptic matrices

A Gaussian elliptic matrix $\mathbb{X}$ is a random matrix whose entries verify

$$\mathbb{E}[\mathbb{X}_{ij}] = 0, \quad \mathbb{E}\left[\mathbb{X}_{ii}^2\right] = \frac{1+\varrho}{N}, \quad \mathbb{E}[\mathbb{X}_{ij}\mathbb{X}_{ji}] = \frac{\varrho}{N}. \tag{IX.5}$$

The parameter ϱ interpolates between the Gaussian Orthogonal Ensemble, abbreviated $GOE(N)$ (symmetric matrices, $\varrho = 1$), the Ginibre ensemble ($\varrho = 0$) and the Anti Gaussian Orthogonal Ensemble, abbreviated anti-$GOE(N)$ (skew-symmetric matrices, $\varrho = -1$). One can easily build a Gaussian elliptic matrix of parameter ϱ thanks to a linear combination of a $GOE(N)$ matrix $\mathbb{S}_+$ and an anti-$GOE(N)$ matrix $\mathbb{S}_-$. Indeed,

by defining the matrix $\mathbb{X}$ as

$$\mathbb{X} = \sqrt{\frac{1+\varrho}{2}}\mathbb{S}_+ + \sqrt{\frac{1-\varrho}{2}}\mathbb{S}_-, \tag{IX.6}$$

one readily sees that it verifies Eqs. (IX.5).

3 General formula for the mixed-moments

3.1 Moment-cumulant formula

Consider an elliptic matrix $\mathbb{X}$. Using the *moment-cumulant* formula (see [135]), the normalized trace of a product of n terms that are either $\mathbb{X}$ or $\mathbb{X}^\top$ can be expressed as

$$\tau\left(\mathbb{X}^{\epsilon_1}\cdots\mathbb{X}^{\epsilon_n}\right) = \sum_{\pi\in \mathrm{NC}_2(n)} \prod_{(r,s)\in\pi} \kappa_2\left(\mathbb{X}^{\epsilon_r}, \mathbb{X}^{\epsilon_s}\right), \tag{IX.7}$$

where $\mathrm{NC}_2(n)$ denotes the set of all non-crossing pairings of elements of $[\![1,n]\!]$ and $\epsilon_i \in \{1, \top\}$ (in the sense that $\mathbb{X}^{\epsilon_i}$ is either $\mathbb{X}$ or $\mathbb{X}^\top$), see [203, Lemma 4] for a proof of this formula. The cumulant κ_2 is easily computed since $\mathbb{S}_\pm$ are mutually free, implying $\kappa_2(\mathbb{S}_\pm, \mathbb{S}_\mp) = 0$, and we get

$$\begin{aligned}
\kappa_2\left(\mathbb{X}, \mathbb{X}\right) &= \frac{1+\varrho}{2}\kappa_2\left(\mathbb{S}_+, \mathbb{S}_+\right) + \frac{1-\varrho}{2}\kappa_2\left(\mathbb{S}_-, \mathbb{S}_-\right) \\
&= \frac{1+\varrho}{2} - \frac{1-\varrho}{2} \\
&= \varrho \\
&= \kappa_2\left(\mathbb{X}^\top, \mathbb{X}^\top\right), \\
\kappa_2\left(\mathbb{X}, \mathbb{X}^\top\right) &= \frac{1+\varrho}{2}\kappa_2\left(\mathbb{S}_+, \mathbb{S}_+\right) - \frac{1-\varrho}{2}\kappa_2\left(\mathbb{S}_-, \mathbb{S}_-\right) \\
&= \frac{1+\varrho}{2} + \frac{1-\varrho}{2} \\
&= 1 \\
&= \kappa_2\left(\mathbb{X}^\top, \mathbb{X}\right),
\end{aligned}$$

In the product $\prod_{(r,s)\in\pi} \kappa_2\left(\mathbb{X}^{\epsilon_r}, \mathbb{X}^{\epsilon_s}\right)$ from Eq. (IX.7), the different terms can either be 1 or ϱ according to the previous computations. Furthermore, the ϱ contributions correspond to pairs for which $\epsilon_r = \epsilon_s$, i.e. pairs linking the matrix $\mathbb{X}$ or $\mathbb{X}^\top$ with itself. For a non-crossing pairing π, we denote by $\sigma(\pi)$ the quantity $\sigma(\pi) = |\{(r,s) \in \pi,\ \epsilon_r = \epsilon_r\}|$, where $|A|$ denotes the cardinality of set A. We can therefore further simplify Eq. (IX.7)

$$\tau\left(\mathbb{X}^{\epsilon_1}\cdots\mathbb{X}^{\epsilon_n}\right) = \sum_{\pi\in \mathrm{NC}_2(n)} \varrho^{\sigma(\pi)}, \tag{IX.8}$$

and find the result of [203, Lemma 4]. A first fact to notice is that whenever n is odd the set $\mathrm{NC}_2(n)$ is empty since it is not possible to construct pairings across an odd number of elements. Consequently, the mixed moments of an odd number of elliptic terms $\mathbb{X}^{\epsilon_i}$ is always zero, and we will implicitly consider an even number of terms in the following. Finally, we can group consecutive matrices with the same $\epsilon \in \{1, \top\}$ such that

$$\tau\left(\mathbb{X}^{\epsilon_1}\cdots\mathbb{X}^{\epsilon_n}\right) = \tau\left(\mathbb{X}^{r_1}\left(\mathbb{X}^{\top}\right)^{s_1}\cdots\mathbb{X}^{r_k}\left(\mathbb{X}^{\top}\right)^{s_k}\right), \quad \text{with } \sum_{i=1}^{k}(r_i+s_i)=n. \tag{IX.9}$$

In the case where only two blocks can be made, we retrieve the mixed-moments that we needed to compute in Chapter VII.

3.2 The Knights and Ladies of the Round Table

Since τ is invariant under cyclic permutations, it is more natural to represent the non-crossing pairings of Eq. (IX.8) as pairings of elements arranged around a circle. In the following, we will denote by white dots $\circ$ (resp. black dots $\bullet$) matrices $\mathbb{X}$ (resp. $\mathbb{X}^{\top}$). See Figure IX.1 for an example.

In the case where $\varrho = 0$, i.e. the case of Ginibre matrices, the computation of Eq. (IX.8) amounts to solving the mathematical problem historically known as the Knights and Ladies of the Round Table. Imagine that two people want to organize a dinner party. They both invite a group of friends that have never met before. Each person gets randomly seated around the dinner table, and is paired with an invitee from the other friend group. As the two hosts want people to properly hear each other, they try to make no two conversation cross around the table. The question is: from a given seating arrangement, how many ways do the hosts have to pair people as explained? In other more mathematical words, how many non-crossing pairings of two distinct elements (the two groups of friends) can you make? Plugging $\varrho = 0$ in Eq. (IX.8), we immediately see that the only non-zero contributions are those for which $\sigma(\pi) = 0$, i.e. pairings such that $\mathbb{X}$ is always paired with $\mathbb{X}^{\top}$ therefore solving the previous problem. See [204] for a review of the Knights and Ladies problem and the connection to the mixed-moments of Ginibre matrices. In the general case of elliptic matrices, it is much more difficult to get some general formula for Eq. (IX.8) and a systematic study of σ is needed.

4 Explicit formula for $\tau\left(\mathbb{X}^t(\mathbb{X}^{\top})^s\right)$

Let us consider the case $k = 1$ in Eq. (IX.9), i.e. the specific case where $\epsilon_i = 1$ for $i \leq t$ and $\epsilon_i = \top$ otherwise. We will denote by t, s the exponent r_1, s_1 in Eq. (IX.9) with $t + s = n$. We will study the function σ to properly partition the set $\mathrm{NC}_2(t+s)$ and map these partitions onto Temperley-Lieb algebras. Finally, as observed above, $t + s$ must be even implying that t and s must have the same parity (which we are going to assume from now on).

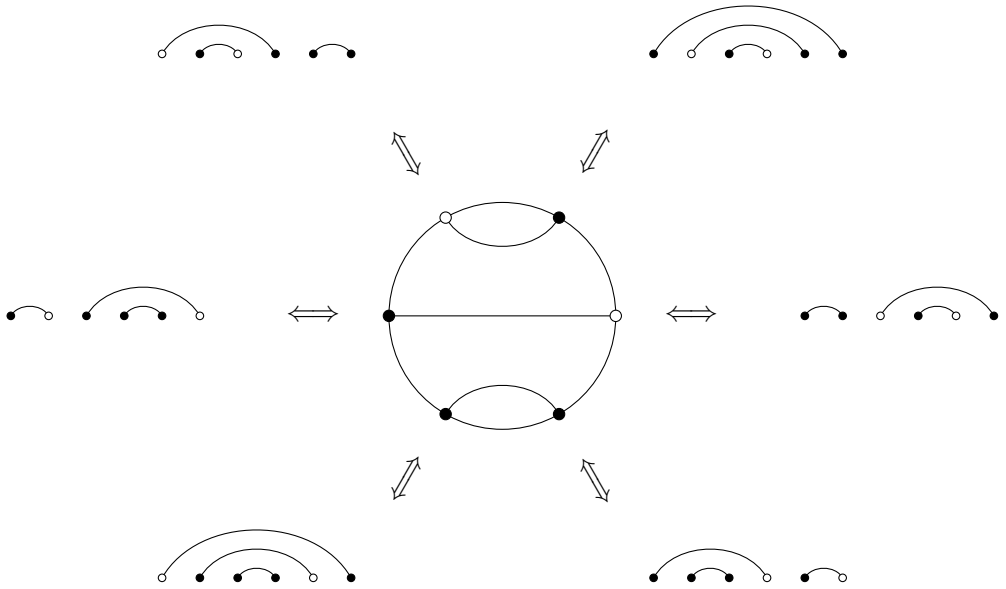


Figure IX.1: An example of a non-crossing pairing involved in the computation of $\tau\left(\mathbb{X}\mathbb{X}^\top\mathbb{X}\left(\mathbb{X}^\top\right)^3\right)$ and yielding a term ϱ. We see that the representation around a circle lifts some of the ambiguity inherent to the line representation.

4.1 Study of σ

Anticipating on the connection with Temperley-Lieb algebras, it makes more sense to study the complementary function to σ, which we denote by $\sigma^c(\pi) = |\{(r,s) \in \pi,\ \epsilon_r \neq \epsilon_r\}|$ and counts the number of pairs $(\circ, \bullet)$. Obviously, the two functions are linked through the relation $\sigma + \sigma^c = (t+s)/2$ where $(t+s)/2 \in \mathbb{N}$ is the number of pairs for a pairing in $\mathrm{NC}_2(t+s)$. It is easy to see that σ and σ^c are both integer-valued piece-wise constant functions, and therefore furnish a natural partitioning of $\mathrm{NC}_2(t+s)$. Furthermore, the number of mixed pairs σ^c is always of the same parity as t and s (since otherwise one would need to pair an odd number of either $\circ$ or $\bullet$), and the maximum number of mixed pairs in given by $t \wedge s := \min(t,s)$. As a consequence, we can partition $\mathrm{NC}_2(t+s)$ in the following way

$$\mathrm{NC}_2(t+s) = \bigsqcup_{k=0}^{(t\wedge s)/2} \mathrm{NC}_2^{2k}(t,s), \quad t,s \in 2\mathbb{N} \tag{IX.10}$$

$$\mathrm{NC}_2(t+s) = \bigsqcup_{k=0}^{(t\wedge s-1)/2} \mathrm{NC}_2^{2k+1}(t,s), \quad t,s \in 2\mathbb{N}+1, \tag{IX.11}$$

where we introduced

$$\mathrm{NC}_2^{\ell}(t,s) = \{\pi \in \mathrm{NC}_2(t+s),\ \sigma^c(\pi) = \ell\}, \tag{IX.12}$$

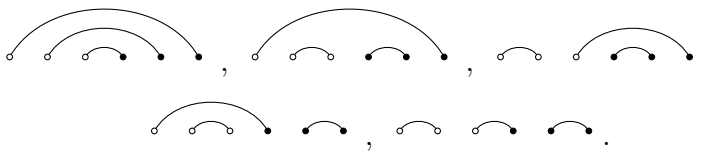
and where $\bigsqcup$ denotes the disjoint union. For simplicity, we will consider the case where $t, s \in 2\mathbb{N}$ in the following. We can finally use the partition from Eq. (IX.10) to rewrite Eq. (IX.8) as

$$\tau\left(\mathbb{X}^t(\mathbb{X}^\top)^s\right) = \sum_{k=0}^{(t\wedge s)/2} \varrho^{(t+s)/2-2k} \left|\mathrm{NC}_2^{2k}(t,s)\right|. \tag{IX.13}$$

We therefore need to study the cardinality of the sets $\mathrm{NC}_2^{2k}(t,s)$ to give an explicit expression.

4.2 Study of the sets $\mathbf{NC}_2^{2k}(t,s)$ and mapping to Temperley-Lieb diagrams

To start studying the sets $\mathrm{NC}_2^{2k}(t,s)$, let us consider an example for $t = 3$ and $s = 3$. There are 5 non-crossing pairings over 6 elements that are represented below

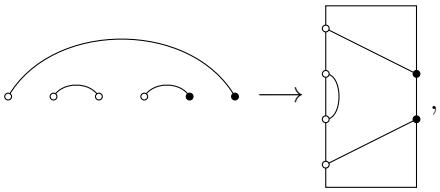


(IX.14)

We naturally arranged (from left to right and top to bottom) partitions by decreasing length of the longest mixed arc $(\circ, \bullet)$. For instance for the first two pairings, the longest mixed arc (or mixed pair) links the leftmost $\circ$ to the rightmost $\bullet$, whereas it links the two innermost $\circ, \bullet$ for the last pairing. Due to the inherent non-crossing pattern, the longest mixed arc naturally cuts the pairing into three regions: the left region, the inner region and the right region. In turn, each of these regions (which can be void), have to be arranged into a non-crossing pairing. One can repeat this process with the second longest mixed arc, the third longest etc. up until the point where one has exhausted the number σ^c of mixed arc. In the example of Eq. (IX.14), there can be either 3 or 1 mixed arc. The case of three mixed arcs is very restricted as the only way to draw them is to symmetrically link $\circ$ with $\bullet$, which only yields one pairing with $\sigma^c = 3$. In the case of one mixed arc, one has more choices available for the endpoints. If $\bullet$ is at the far right, it can be link to either the leftmost or innermost $\circ$, which both yield one pairing. If $\bullet$ is now at the innermost position, it can also be linked to the two previous $\circ$, which also accounts for two pairings. All in all, there are exactly four pairings with $\sigma^c = 1$. This process can be generalized and allows to enumerate the number of pairings with fixed σ^c. In Appendix A, we provide a general derivation leading to the cardinality of the sets $\mathrm{NC}_2^{2k}(t,s)$.

There is however a quicker way to study $\mathrm{NC}_2^{2k}(t,s)$. Indeed, if one rotates the $\circ$-line

by $-\pi/2$ and the $\bullet$-line by $\pi/2$ of any element in $\mathrm{NC}_2(t,s)$, i.e.



(IX.15)

the resulting structure is called a Temperley-Lieb diagram, belonging to the Temperley-Lieb algebra $\mathcal{TL}_{t,s}$. These diagrams connect t $\circ$-elements with s $\bullet$-elements spread over two opposite strands (connections between elements of the same line are allowed). Moreover, the connection pattern has a non-crossing structure. The *rank* of the diagram corresponds to the number of connections between elements belonging to different strands. It is straightforward to see that, the bijective homotopic mapping, geometrically described in Eq. (IX.15), sends elements from $\mathrm{NC}_2^{2k}(t,s)$, with $\sigma^c = 2k$, onto diagrams with rank $2k$. Finally, it is known that the rank function furnishes a simple way to partition $\mathcal{TL}_{t,s}$ into constant-rank subsets (once again isomorphic to $\mathrm{NC}_2^{2k}(t,s)$), and that these subsets have a cardinality given by products of *triangular Catalan numbers* (see [205]). The cardinality of $\mathrm{NC}_2^{2k}(t,s)$ is therefore given by

$$\left|\mathrm{NC}_2^{2k}(t,s)\right| = \frac{(2k+1)^2}{(t/2+k+1)(s/2+k+1)}\binom{t}{t/2+k}\binom{s}{s/2+k}. \tag{IX.16}$$

4.3 Polynomial expression for $\tau\left(\mathbb{X}^t(\mathbb{X}^\top)^s\right)$

As a consequence of the previous analysis, one can rewrite Eq. (IX.8) in the following explicit forms. If $t = 2u$ and $s = 2v$ are even then

$$\tau\left(\mathbb{X}^t(\mathbb{X}^\top)^s\right) = \sum_{k=0}^{u\wedge v} \varrho^{u+v-2k}\frac{(2k+1)^2}{(u+k+1)(v+k+1)}\binom{2u}{u+k}\binom{2v}{v+k}, \tag{IX.17}$$

whereas when $t = 2u+1$ and $s = 2v+1$ are odd, we get

$$\tau\left(\mathbb{X}^t(\mathbb{X}^\top)^s\right) = \sum_{k=0}^{u\wedge v} \varrho^{u+v-2k}\frac{4(k+1)^2}{(u+k+2)(v+k+2)}\binom{2u+1}{u+k+1}\binom{2v+1}{v+k+1}. \tag{IX.18}$$

As the left-hand-side is a little heavy to write, we introduce a sequence of polynomials $P_{t,s} \in \mathbb{N}[X]$ such that $\tau\left(\mathbb{X}^t(\mathbb{X}^\top)^s\right) = P_{t,s}(\varrho)$. This explicit formula is very useful since the number of non-crossing pairings (or equivalently the number of Temperley-Lieb diagrams) involved in the computation of Eq. (IX.8) is equal to $C_{(t+s)/2}$ (the $(t+s)/2$th Catalan number), which rapidly increases as highlighted by the explicit computations below:

$$\tau\left(\mathbb{X}^2(\mathbb{X}^\top)^2\right) = \quad + \quad = 1 + \varrho^2 = P_{2,2}(\varrho) \tag{IX.19}$$

$$\begin{aligned}\tau\left(\mathbb{X}^4(\mathbb{X}^\top)^2\right) = \quad & + \quad + \quad \\ & + \quad + \quad \\ = 3\varrho + 2\varrho^3 &= P_{4,2}(\varrho)\end{aligned} \tag{IX.20}$$

$$\begin{aligned}\tau\left(\mathbb{X}^6(\mathbb{X}^\top)^2\right) = \quad & + \quad \\ & + \quad + \quad \\ & + \quad + \quad \\ & + \quad + \quad \\ & + \quad + \quad \\ & + \quad + \quad \\ & + \quad + \quad \\ = 5\varrho^4 + 9\varrho^2 &= P_{6,2}(\varrho).\end{aligned} \tag{IX.21}$$

In effect, if one were to compute Eq. (IX.8) by enumerating explicitly non-crossing pairings, the complexity of the procedure would be $\mathcal{O}(4^{t+s}/(t+s)^{3/2})$ (using the asymptotics of the Catalan numbers), whereas the proposed formula allows polynomial time $\mathcal{O}(t \wedge s)$ (assuming that each term of the sums Eqs. (IX.18-IX.17) takes $\mathcal{O}(1)$ to compute). Finally, Figure IX.2 shows the excellent agreement between this formula and numerical simulations of mixed-moments. As a final note, one can see that $P_{t,s}$ is symmetric upon the exchange $t \leftrightarrow s$, which accounts for the invariance of τ under both cyclic permutation and transposition.

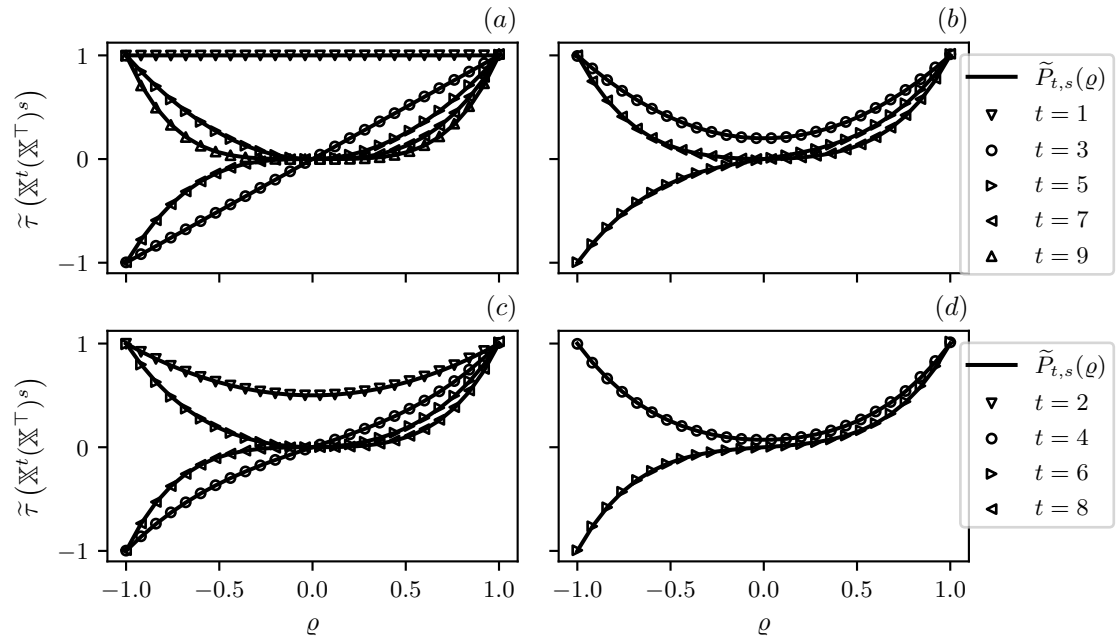


Figure IX.2: Comparison between $\widetilde{\tau}\left(\mathbb{X}^t(\mathbb{X}^\top)^s\right) = \tau\left(\mathbb{X}^t(\mathbb{X}^\top)^s\right)/C_{(t+s)/2}$ and $\widetilde{P}_{t,s} = P_{t,s}/C_{(t+s)/2}$ for $\varrho \in [-1,1]$ and $t+s \leq 10$, $s \leq t$. (a) $s=1$, (b) $s=3$, (c) $s=2$, (d) $s=4$. For each point, we simulated $k=100$ elliptic matrices of size 500×500, and computed the average of the normalized trace of the product $\mathbb{X}^t(\mathbb{X}^\top)^s$. We see an excellent agreement between simulations and theoretical values.

4.4 $GOE(N)$ and anti-$GOE(N)$ matrices: $\varrho = \pm 1$

One must check that $P_{t,s}(1) = C_{(t+s)/2}$ to retrieve the well-known result concerning the moments of $GOE(N)$ matrices, see for instance [135]. Using results from [206], we can use the identity

$$\sum_{k=0}^{u\wedge v} \frac{(2k+1)^2}{(u+k+1)(v+k+1)} \binom{2u}{u+k}\binom{2v}{v+k} = C_{u+v}, \tag{IX.22}$$

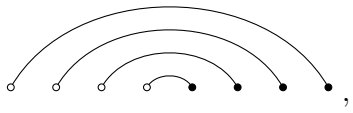
and get the expected result $P_{t,s}(1) = C_{(t+s)/2}$. Furthermore, it is easy to see that the parity of the polynomial function $P_{t,s}$ depends on the parity of t, s and $(t+s)/2$. Indeed, on the one hand, assuming $t,s \in 2\mathbb{N}$, powers of ϱ will have the same parity as $(t+s)/2$. On the other hand if $t,s \in 2\mathbb{N}+1$, they will have an opposite parity from $(t+s)/2$. As a consequence, one can give a more general formula for the mixed-moments of $GOE(N)$ and anti-$GOE(N)$ matrices

$$P_{t,s}(\pm 1) = \begin{cases} (\pm 1)^{(t+s)/2} C_{(t+s)/2}\,, & \text{for } t,s \in 2\mathbb{N} \\ \pm(\pm 1)^{(t+s)/2} C_{(t+s)/2}\,, & \text{for } t,s \in 2\mathbb{N}+1 \end{cases}. \tag{IX.23}$$

One can easily check that these results are coherent with a direct computation of $\tau\left(\mathbb{X}^t(\mathbb{X}^\top)^s\right)$ for $\varrho = \pm 1$.

4.5 Ginibre matrices: $\varrho = 0$

As mentioned above, the Ginibre case is the answer to the Knights and Ladies problem. In our simplified setting, it is easy to see that plugging $\varrho = 0$ in $P_{t,s}$ always yields 0 (there are no solutions to the problem), except when $t = s$ where the only possible pairing is the one connecting $\circ$ and $\bullet$ symmetrically, e.g.



, (IX.24)

in the case $t = s = 4$. As a consequence

$$P_{t,s}(0) = \delta_{t,s}, \tag{IX.25}$$

and this result is reported in [207]. If we come back to the covariance of the Gaussian process of Chapter VII, we see that, in the Ginibre case

$$\langle v_i(t)v_j(s)\rangle = \delta_{ij}\delta_{ts}. \tag{IX.26}$$

Since the process is not correlated in time anymore, the persistence of the sign of $v_1(t)$ is given by $Q_0(\tau) = 2^{-\tau}$.

5 Asymptotics of $\tau\left(\mathbb{X}^t(\mathbb{X}^\top)^s\right)$ as $t, s \to \infty$

The study of the asymptotics of this mixed-moment is relevant in the context of persistence of Gaussian processes whose correlator are exactly given by $\tau\left(\mathbb{X}^t\left(\mathbb{X}^\top\right)^s\right)$. Such processes are of interest in [2] and we have already discussed them in Chapter VII. We will limit this analysis to $\varrho \geq 0$ since the negative counterpart can be easily obtained using the parity of $P_{t,s}$. We will also limit our analysis to $t, s \in 2\mathbb{N}$, $t = 2u$, $s = 2v$, $v \leq u$, but the other case can be obtained in the same way. Finally, we will assume that $u, v \to \infty$ while keeping the ratio $u/v = q \geq 1$ constant.

The polynomial $P_{u,v}(x)$ can be rewritten using an auxiliary polynomial $Q_{u,v}(x)$

$$P_{u,v}(\varrho) = \varrho^{u+v}\, \partial_x(-xQ_{u,v}(x) + \partial_x(x^2 Q_{u,v}(x)))\big|_{x=\varrho^{-1}}, \tag{IX.27}$$

with

$$Q_{u,v}(x) = \sum_{k=0}^{v} \frac{x^{2k}}{(u+k+1)(v+k+1)} \binom{2u}{u+k}\binom{2v}{v+k}. \tag{IX.28}$$

It is easy to give an asymptotic evaluation of $Q_{u,v}$

$$Q_{u,v}(x) \underset{\substack{u,v\to\infty \\ u/v=q}}{\sim} \frac{4^{v(q+1)}}{\pi q^{3/2} v^2} \int_0^1 dy\, g(y;q) e^{v\mathcal{F}(y;x,q)}, \tag{IX.29}$$

where we introduced the following functions

$$\begin{aligned} g(y;q) &= \left[\left(1-y^2\right)\left(1-y^2/q^2\right)\right]^{-1/2}\left[(1+y)\left(1+y/q\right)\right]^{-1} \\ h_\pm(y) &= (1\pm y)\log(1\pm y) \\ \mathcal{F}(y;x,q) &= y\log x^2 - h_+(y) - h_-(y) - q\left(h_+(y/q)+h_-(y/q)\right) \end{aligned} \quad . \tag{IX.30}$$

Note that since x will take the value $1/\varrho$, we will consider that $x \in [1,\infty[$. Furthermore, we will drop the explicit dependency in q and x for clarity. The previous integral can be evaluated via a saddle point approximation. However, one must be careful since the saddle point will be located at 0 and 1 for $\varrho = 1, 0$. In any case, a straightforward computation shows that the saddle point $y_\star$ is given by

$$y_\star = \frac{(q+1)(x^2+1) - \sqrt{(q+1)^2(x^2+1)^2 - 4q(x^2-1)^2}}{2(x^2-1)}. \tag{IX.31}$$

5.1 Case $\varrho \to 1^-$

In this case, we know that $P_{u,v}(\rho)$ must be equivalent to C_{u+v}, and we must therefore recover the Catalan number's asymptotic behavior. $y_\star$ has the following behavior as $x \to 1^+$ (corresponding to the limit $\varrho \to 1^-$ since $x = \varrho^{-1}$)

$$y_\star \underset{x\to 1^+}{\sim} \frac{q}{1+q}(x-1), \tag{IX.32}$$

indicating that the saddle will be located close to 0, as $\varrho \to 1^-$. As a consequence, one must be careful with the saddle point approximation. If the width $(-v\mathcal{F}''(y_\star))^{-1/2}$ of the associated Gaussian is much larger that the saddle point itself, we will have to compute the integral of a half-Gaussian. Conversely, if the width is much smaller, a standard saddle point approximation can be carried out. Assuming that $y_\star \ll (-V\mathcal{F}''(y_\star))^{-1/2}$, we can then further approximate $Q_{u,v}$ as follows

$$Q_{u,v}(x) \underset{\substack{u,v\to\infty \\ u/v=q}}{\sim} \frac{1}{2}\frac{4^{v(q+1)}}{\pi q^{3/2}v^2}\sqrt{\frac{2\pi}{-v\mathcal{F}''(y_\star)}}g(y_\star)e^{v\mathcal{F}(y_\star)}. \tag{IX.33}$$

Note the factor 1/2 that comes from the saddle-point approximation on a *half-Gaussian* since $y_\star \ll (-V\mathcal{F}''(y_\star))^{-1/2}$. Plugging Eq. (IX.31) into Eq. (IX.33), and then Eq. (IX.33) into Eq. (IX.27), we use Mathematica to compute the derivatives and take the limit $\varrho \to 1^-$. Keeping only the highest orders in v yields

$$\begin{aligned} P_{u,v}(\varrho) &\underset{\substack{u,v\to\infty \\ u/v=q}}{\sim} \frac{4^{v(1+q)}}{\sqrt{\pi}q^{3/2}v^2}v^{1/2}\left(\frac{q}{1+q}\right)^{3/2} \\ &= \frac{4^{v+u}}{\sqrt{\pi}(u+v)^{3/2}}, \end{aligned}$$

and we recover the asymptotic behavior of the Catalan numbers as expected.

5.2 Case $0 \ll \varrho \ll 1$

For the generic case of intermediate correlation parameter ϱ, the asymptotics can also be obtained through a saddle point approximation. In this case, $y_\star$ is far enough from the edges of $[0,1]$ so that the standard formula can be applied. One can use Eq. (IX.33) (removing the $1/2$ factor), and differentiate it according to Eq. (IX.27). Keeping only leading order terms, we get

$$P_{u,v}(\varrho) \sim \varrho^{u+v-2} \frac{4^{v(q+1)}}{\pi q^{3/2}} \sqrt{\frac{2\pi}{-v\mathcal{F}''(y_\star)}} g(y_\star)(\mathcal{F}'(y_\star))^2 e^{v\mathcal{F}(y_\star)}. \tag{IX.34}$$

This expression is quite gruesome and does not seem to yield any simplifications at this point. However, numerical simulations shown on Figure IX.3 clearly point towards an exponential cutoff of the rescaled polynomial $\widehat{P}_{v,qv}(\varrho) := P_{v,qv}(\varrho)/\sqrt{P_{v,v}(\varrho)P_{qv,qv}(\varrho)}$ as $v \to \infty$. In the context of persistence of a Gaussian process with correlator $\tau\left(\mathbb{X}^t(\mathbb{X}^\top)^s\right)$, such an exponential cutoff would mean that time-wise correlations are negligible for times larger than said cutoff, which could introduce an exponential cutoff in the persistence of the sign of $v_1(t)$. Furthermore, we also know that this cutoff should interpolate between 0 ($\varrho = 1$; GOE case) and $\ln 2$ ($\varrho = 0$; Ginibre case).

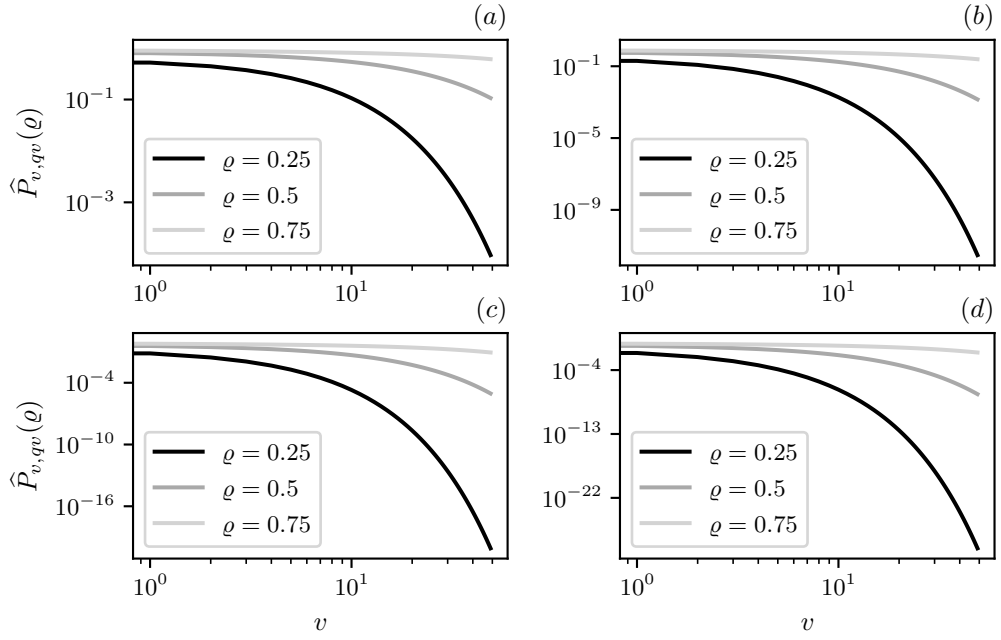


Figure IX.3: Rescaled polynomial $\widehat{P}_{v,qv}(\varrho) := P_{v,qv}(\varrho)/\sqrt{P_{v,v}(\varrho)P_{qv,qv}(\varrho)}$ as a function of v and different values of $0 < \varrho < 1$. (*a*) $q = 2$, (*b*) $q = 3$, (*c*) $q = 4$, (*d*) $q = 5$. We see an exponential decay as v increases. One notices that the closer ϱ is to zero, the faster the exponential decay is. Similarly, the larger q is, the faster the decay will be.

6 Conclusion

In this chapter, we provided an explicit computation for the mixed-moments $\tau(\mathbb{X}^t(\mathbb{X}^\top)^s)$ of Gaussian elliptic matrices $\mathbb{X}$. Our formula can be evaluated in polynomial time which is a significant improvement to the more general formula found in [203] which involves a summation over all possible non-crossing matchings of $t+s$ elements.

Taking this formula as a base case, one could generalize it to compute more complicated mixed-moments with more than one block such as $\tau(X^{t_1}(\mathbb{X}^\top)^{s_1}\mathbb{X}^{t_2}(\mathbb{X}^\top)^{s_2})$. Indeed, considering Eq. (IX.8), we can classify non-crossing matchings on $t_1+t_2+s_1+s_2$ into different categories. Some matchings do not link matrices from the first to the second block: such matchings can be factorized into a non-crossing matching over the first block along with another one over the second. Therefore, the mixed-moment $\tau(X^{t_1}(\mathbb{X}^\top)^{s_1}\mathbb{X}^{t_2}(\mathbb{X}^\top)^{s_2})$ can be expressed as

$$\tau(X^{t_1}(\mathbb{X}^\top)^{s_1}\mathbb{X}^{t_2}(\mathbb{X}^\top)^{s_2}) = \tau(X^{t_1}(\mathbb{X}^\top)^{s_1})\tau(X^{t_2}(\mathbb{X}^\top)^{s_2}) + \sum_{\substack{\text{mixed} \\ \text{non-crossings} \\ \pi}} \varrho^{\sigma(\pi)}. \qquad \text{(IX.35)}$$

We can then study the remaining sum by classifying the mixed non-crossing matchings according to the type of their longest arc, in the same spirit as in Appendix A.

Key takeaways

- **Gaussian elliptic random matrices** are Gaussian random matrices for which elements ij and ji are correlated through a parameter ϱ.
- **Temperley-Lieb diagrams** are non-crossing pairings between points spread across two facing lines. These diagrams can be classified according to their rank, i.e. the number of links from one line to the other.
- **Mixed-moments** of Gaussian elliptic random matrices of the form $\tau(\mathbb{X}^t(\mathbb{X}^\top)^s)$ can be generally expressed as a function of t, s and ϱ in the thermodynamic limit. The expression involves weighted sum over the cardinality of the subspaces partitioning the set of Temperley-Lieb diagrams.

A Study of the sets $\mathbf{NC}_2^{2k}(2t,2s)$

In this Appendix, we will prove the following statement

$$\begin{aligned}\left|\mathrm{NC}_2^{2k}(2t,2s)\right| &= C(t+k+1,t-k+1)C(s+k+1,s-k+1)\\ &= \frac{(2k+1)^2}{(t+k+1)(s+k+1)}\binom{2t}{t+k}\binom{2s}{s+k}\end{aligned} \tag{IX.36}$$

where $C(n,k)$ are triangular Catalan numbers [208], see Table IX.1.

To compute the cardinal of $\mathrm{NC}_2^k(t,s)$, we need to study the properties of mixed pairs $(\circ,\bullet)$. We will order the elements $\circ,\bullet$ on a line such that the leftmost $\circ$ is indexed by t (the innermost by 1), and the rightmost $\bullet$ by s (the innermost by 1), see Figure IX.4 for an illustration.

Consider one mixed pair $(i,j)\in\pi$ where π is a non-crossing pairing. For π to be valid, we must have i and j of the same parity. Indeed, if $i\not\equiv j\,[2]$, the interior set $\{i-1,\dots,1,1,\dots,j-1\}$ is not balanced and since this set is separated from elements $i'>i$ and $j'>j$ (because π is non-crossing and $(i,j)\in\pi$), no pairing of its elements would be possible.

Consider now a non-crossing pairing π with exactly k mixed pairs $\{(i_1,j_1),\dots,(i_k,j_k)$ ordered such that (i_1,j_1) is the inner-most mixed pair and (i_k,j_k) the outer-most i.e

$$1\leq i_1<\cdots<i_k\leq 2t,\quad 1\leq j_1<\cdots<j_k\leq 2s.$$

First-of-all, k must be of the same parity as t and s for balancing purposes. Considering now the ℓ-th mixed pair. The endpoints i_ℓ and j_ℓ must have the same parity as ℓ. Indeed, because of the ordering, the inner-most possibility for (i_ℓ,j_ℓ) is the pair (ℓ,ℓ). Since i_ℓ and j_ℓ must keep the same parity, $i_\ell=\ell+2r$ and $j_\ell=\ell+2s$ for some r,s respecting the ordering. Finally, aside from the parity requirements, the endpoints of the pairs are independent from one another and move freely in the limits of the ordering.

Still considering non-crossing pairings π with exactly k mixed pairs, we can now count how many such pairings there are. Since the number of mixed pairs of π is fixed, π may be written in the following way

$$\pi=\sigma_0\cup\nu_0\cup\left(\bigcup_{\ell=1}^{k}(i_\ell,j_\ell)\cup\sigma_\ell\cup\nu_\ell\right), \tag{IX.37}$$

with σ_ℓ (resp. ν_ℓ) a non-crossing partition over the elements $\{i_\ell+1,\dots,i_{\ell+1}-1\}$ (resp. $\{j_\ell+1,\dots,j_{\ell+1}-1\}$), σ_0 over $\{1,\dots,i_1-1\}$, σ_k over $\{i_k+1,\dots,2T\}$ and ν_0, ν_k defined in the same

n \ k	1	2	3	4	5	6	7
1	1	0	0	0	0	0	0
2	1	1	0	0	0	0	0
3	1	2	2	0	0	0	0
4	1	3	5	5	0	0	0
5	1	4	9	14	14	0	0
6	1	5	14	28	42	42	0
7	1	6	20	48	90	132	132

Table IX.1: Catalan triangle containing the numbers $C(n,k)$

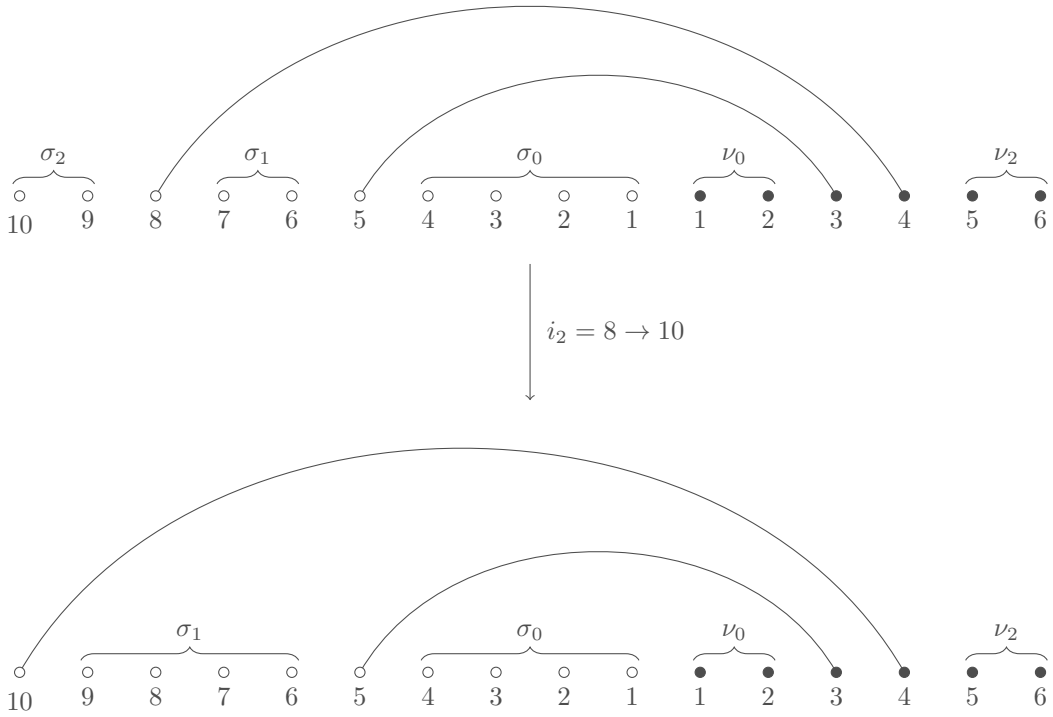


Figure IX.4: Contributions to $\left|\mathrm{NC}_2^2(10,6)\right|$. (Top) partitions with fixed mixed pairs $(8,4)$ and $(5,3)$: $C_1C_1C_2C_1C_0C_1$. (Bottom) partitions with fixed mixed pairs $(10,4)$ and $(5,3)$: $C_0C_2C_2C_1C_0C_1$.

way. We only need to count the number of sub-partitions σ_ℓ, ν_ℓ. For σ_ℓ, there are $C_{(i_{\ell+1}-i_\ell-1)/2}$. Putting all these observations together, we get a formula for $\left|\mathrm{NC}_2^{2k}(2T,2S)\right|$

$$\left|\mathrm{NC}_2^{2k}(2t,2s)\right| = B_{2k}(2t)B_{2k}(2s), \tag{IX.38}$$

and

$$B_{2k}(2r) = \sum_{\substack{1\leq i_1<\cdots<i_2k\leq 2r \\ i_\ell\equiv\ell[2]}} \left(\prod_{\ell=1}^{2k-1} C_{(i_{\ell+1}-i_\ell-1)/2}\right) C_{(t-i_{2k})/2}C_{(i_1-1)/2}, \tag{IX.39}$$

see Figure IX.4 for an illustration of the previous formula. Upon changes of variable to account for the parity constraints $i_\ell \equiv \ell\,[2]$, it is easy to see that $B_{2k}(2t)$ obeys the following recursion relation

$$B_{2k}(2t) = \sum_{\ell=k}^{t} C_{t-\ell} \sum_{s=k-1}^{\ell-1} C_{\ell-s-1}B_{2(q-1)}(2s). \tag{IX.40}$$

We will now show that $B_{2k}(2t) = C(t+k+1, t-k+1)$ $(\star)$ using the identity (see [208])

$$C(r+m,m) = \sum_{s=1}^{m} C(s,s)C(r+m-s, m-s+1), \tag{IX.41}$$

and the fact that $C(n+1, n+1) = C_n$. It is easy to see that the $(\star)$ holds whenever $k = 0$. Assuming that $(\star)$ holds true for any $q \leq k-1$ and $s \leq t-1$, we have

$$\begin{aligned} B_{2k}(2t) &= \sum_{\ell=k}^{t} C_{t-\ell} \sum_{s=k-1}^{\ell-1} C_{\ell-s-1} C(s+k, s-k+2) \\ &= \sum_{\ell=k}^{t} C_{t-\ell} \sum_{s=k-1}^{\ell-1} C(\ell-s, \ell-s) C(s+k, s-k+2) \\ &= \sum_{\ell=k}^{t} C_{t-\ell} \sum_{s=1}^{\ell-k+1} C(s, s) C(\ell+k-s, \ell-k-s+2), \end{aligned}$$

using Eq. (IX.41) with $m = \ell - k + 1$ and $r = 2k - 1$, we have

$$\begin{aligned} &= \sum_{\ell=k}^{t} C_{t-\ell} C(\ell+k, \ell-k+1) \\ &= \sum_{\ell=k}^{t} C(t-\ell+1, t-\ell+1) C(\ell+k, \ell-k+1) \\ &= \sum_{\ell=1}^{t-k+1} C(\ell, \ell) C(t-\ell+k+1, t-\ell-k+2), \end{aligned}$$

and once again with $m = t - k + 1$ and $r = 2k$, we get

$$= C(t+k+1, t-k+1).$$

Finally, using the expression for the numbers $C(n, m)$ we get

$$B_{2k}(2t) = \frac{2k+1}{t+k+1} \binom{2t}{t+k}. \tag{IX.42}$$

Conclusion

In this thesis, we have explored three main avenues to tackle the problem of large macroeconomic fluctuations. The first avenue is built upon the idea of *self-organized criticality*. In this work, we argue that economies are typically close to a point of instability, which naturally increases fluctuations. This point of instability is defined as the tipping point between existence and non-existence of admissible economic equilibrium. Close to the instability, the economy experiences a critical slow-down, which allows shocks to linger and accumulate, therefore producing excess volatility. In this explanation, the economy amplifies exogenous shocks through the proximity with an instability point. The second avenue explores more endogenous origins for the excess volatility by proposing a fully consistent Agent-Based Model (ABM) of interacting firms. Sensible behavioral rules, encoding firms reactions to variations of profits and production surplus, allow for a wide range of aggregate behavior in our ABM. Even though equilibrium may be perfectly well-defined, the economy might not reach it and can either reach different types of equilibria or enter cycles of sustained oscillations. These oscillations can be of different origins depending on the values of the parameters of our ABM. However, they are endogenously generated by the model, without any external driver. This is yet another scenario for explaining macroeconomic fluctuations. Finally, the last avenue is provided by the study of conewise linear systems (CLS). These systems are ubiquitous in economics, and they are able to generate crises-like patterns very easily. We have shown several fascinating properties of CLS in a random setting, i.e. whenever linear evolutions are governed by random matrices. We also looked at more general questions concerning occupation times of random processes. These questions can actually translate to economics since one may wonder for how long an economy could be booming or receding.

The work compiled in this manuscript also advocates for a multidisciplinary approach to economic modelling. We firmly believe that the economy must be dealt with as a complex system evolving through time. The equilibrium-only descriptions must be dropped in favor of more realistic out-of-equilibrium settings, which allow for a much richer phenomenology. Furthermore, the amount of interactions and the number of economic agents should lead to non-trivial emerging behavior. The complex systems approach offers a wide variety of methods and ideas to tackle emerging dynamics and characteristics. We hope that future work in this direction will be carried out, and that the economist's and physicist's communities find common grounds to develop new approaches to economic challenges.

Bibliography

[1] Théo Dessertaine, José Moran, Michael Benzaquen, and Jean-Philippe Bouchaud. Out-of-equilibrium dynamics and excess volatility in firm networks. *Journal of Economic Dynamics and Control*, 138:104362, May 2022.

[2] Théo Dessertaine and Jean-Philippe Bouchaud. Non-self-averaging lyapunov exponent in random conewise linear systems. *Phys. Rev. E*, 105:L052104, May 2022.

[3] Théo Dessertaine, Claude Godrèche, and Jean-Philippe Bouchaud. Occupation time of a renewal process coupled to a discrete markov chain. *Journal of Statistical Mechanics: Theory and Experiment*, 2022(6):063204, June 2022.

[4] Théo Dessertaine and Jean-Philippe Bouchaud. Explicit computation of mixed-moments of real gaussian elliptic random matrices. *In preparation.*

[5] Théo Dessertaine. Network agent-based model web application. `https://yakari.polytechnique.fr/dash`.

[6] U.S. Department of Commerce. Bureau for economic analysis. `https://www.bea.gov/`.

[7] Mauro Gallegati and Domenico Mignacca. Jevons, sunspot theory and economic fluctuations. *History of Economic Ideas*, 2(2):23–40, 1994.

[8] Buiter Willem. The unfortunate uselessness of most 'state of the art' academic monetary economics, 2009.

[9] John H. Cochrane. Shocks. *Carnegie-Rochester Conference Series on Public Policy*, 41:295–364, 1994.

[10] Ben Bernanke, Mark Gertler, and Simon Gilchrist. The financial accelerator and the flight to quality. *The Review of Economics and Statistics*, 78(1):1–15, 1996.

[11] Xavier Gabaix. The Granular Origins of Aggregate Fluctuations. *Econometrica*, 79(3):733–772, 2011.

[12] Xavier Gabaix. Power laws in economics and finance. *Annual Review of Economics*, 1(1):255–294, 2009.

[13] Daron Acemoglu, Vasco Carvalho, Asu Ozdaglar, and Alireza Tahbaz-Salehi. The network origins of aggregate fluctuations. *Econometrica*, 80(5):1977–2016, 2012.

[14] BBC News. What sanctions are being imposed on russia over ukraine invasion? 2022. https://www.bbc.com/news/world-europe-60125659.

[15] Ruediger Bachmann, David Baqaee, Christian Bayer, Moritz Kuhn, Andreas Löschel, Benjamin Moll, Andreas Peichl, Karen Pittel, and Moritz Schularick. What if? The Economic Effects for Germany of a Stop of Energy Imports from Russia. Technical report, 2022.

[16] François Langot and Fabien Tripier. Guerre en ukraine : « un embargo sur le gaz russe coûterait 54 euros par an à chaque français ». *Le Monde*, 2022. https://www.lemonde.fr/idees/article/2022/03/30/guerre-en-ukraine-un-embargo-sur-le-gaz-russe-couterait-54-euros-par-an-a-chaque-francais_6119771_3232.html.

[17] Jean-Philippe Bouchaud. « il faut éviter de sous-évaluer les répercussions économiques d'une diminution de la dépendance au gaz russe ». *Le Monde*, 2022. https://www.lemonde.fr/idees/article/2022/04/18/jean-philippe-bouchaud-il-faut-eviter-de-sous-evaluer-les-repercussions-economiques-d-une-diminution-de-la-dependance-au-gaz-russe_6122586_3232.html.

[18] Daron Acemoglu, Ufuk Akcigit, and William R. Kerr. Networks and the macroeconomy: An empirical exploration. *SSRN Electronic Journal*, 2015.

[19] Per Bak, Kan Chen, Jose Scheinkman, and Michael Woodford. Aggregate fluctuations from independent sectoral shocks: self-organized criticality in a model of production and inventory dynamics. *Ricerche Economiche*, 47(1):3–30, March 1993.

[20] Per Bak. *How nature works: the science of self-organized criticality.* Springer Science & Business Media, 2013.

[21] W. R. Ashby M.D. Principles of the self-organizing dynamic system. *The Journal of General Psychology*, 37(2):125–128, 1947. PMID: 20270223.

[22] Mark R. Gardner and W. Ross Ashby. Connectance of large dynamic (cybernetic) systems: Critical values for stability. *Nature*, 228(5273):784–784, Nov 1970.

[23] Per Bak, Chao Tang, and Kurt Wiesenfeld. Self-organized criticality: An explanation of the 1/f noise. *Phys. Rev. Lett.*, 59:381–384, Jul 1987.

[24] José Moran and Jean-Philippe Bouchaud. May's instability in large economies. *Phys. Rev. E*, 100(3):032307, Sep 2019.

[25] Uri Wilensky. Netlogo. http://ccl.northwestern.edu/netlogo/, Center for Connected Learning and Computer-Based Modeling, Northwestern University, Evanston, IL, 1999.

[26] Uri Wilensky. Netlogo ising model. http://ccl.northwestern.edu/netlogo/models/ising, Center for Connected Learning and Computer-Based Modeling, Northwestern University, Evanston, IL, 1999.

[27] David Weintrop, Seth Tisue, R. Tinker, B. Head, and Uri Wilensky. Netlogo sandpile model. http://ccl.northwestern.edu/netlogo/models/sandpile, Center for Connected Learning and Computer-Based Modeling, Northwestern University, Evanston, IL, 2011.

[28] Jean-Michel Grandmont. Temporary Equilibrium. Working Papers 2006-27, Center for Research in Economics and Statistics, 2006.

[29] Jean-Michel Grandmont. On endogenous competitive business cycles. *Econometrica*, 53(5):995–1045, 1985.

[30] Franklin M. Fisher. *Disequilibrium Foundations of Equilibrium Economics*. Cambridge University Press, Cambridge, 1983.

[31] Jean-Pascal Bénassy. *The Macroeconomics of Imperfect Competition and Nonclearing Markets: A Dynamic General Equilibrium Approach*, volume 1. The MIT Press, September 2005.

[32] Carl Chiarella, Peter Flaschel, and Reiner Franke. *Foundations for a Disequilibrium Theory of the Business Cycle*. Cambridge University Press, Cambridge, 2005.

[33] Herbert Gintis. The Dynamics of General Equilibrium. *The Economic Journal*, 117(523):1280–1309, 2007.

[34] Paul Beaudry, Dana Galizia, and Franck Portier. Putting the cycle back into business cycle analysis. *American Economic Review*, 110(1):1–47, January 2020.

[35] John B. Long and Charles I. Plosser. Real business cycles. *Journal of Political Economy*, 91(1):39–69, feb 1983.

[36] Finn E. Kydland and Edward C. Prescott. Time to build and aggregate fluctuations. *Econometrica*, 50(6):1345, November 1982.

[37] Gerd Gigerenzer, Peter M. Todd, and the ABC Research Group. *Simple heuristics that make us smart*. Oxford University Press, New York, 2002.

[38] Gerd Gigerenzer and Daniel G. Goldstein. Reasoning the fast and frugal way: models of bounded rationality. *Psychological review*, 103 4:650–69, 1996.

[39] Herbert A. Simon. Models of bounded rationality, volume 1: Economic analysis and public policy. 1982.

[40] Herbert Alexander Simon. *Models of bounded rationality: Empirically grounded economic reason*, volume 3. MIT press, 1997.

[41] Vasco M. Carvalho and Alireza Tahbaz-Salehi. Production networks: A primer. *Annual Review of Economics*, 11(1):635–663, 2019.

[42] R. M. Goodwin. A growth cycle. In *Essays in Economic Dynamics*, pages 165–170. Palgrave Macmillan UK, London, 1982.

[43] P. Flaschel. *The Macrodynamics of Capitalism: Elements for a Synthesis of Marx, Keynes and Schumpeter*. Springer, 2008.

[44] A.J. Lotka. Analytical note on certain rhythmic relations in organic systems. *Proceedings of the National Academy of Sciences of the United States of America*, 6(7):410–415, 08 1920.

[45] V. Volterra. Fluctuations in the abundance of a species considered mathematically. *Nature*, 118:558–560, 01 1926.

[46] Ernest Liu and Aleh Tsyvinski. Dynamical Structure and Spectral Properties of Input-Output Networks. NBER Working Papers 28178, National Bureau of Economic Research, Inc, December 2020.

[47] John Von Neumann. The general and logical theory of automata. In *Systems Research for Behavioral Sciencesystems Research*, pages 97–107. Routledge, 2017.

[48] Martin Gardner. The fantastic combinations of john conway's new solitaire game of life. *Sc. Am.*, 223:20–123, 1970.

[49] Jacob Aron. First replicating creature spawned in life simulator. 2010.

[50] Robert T. Wainwright. Life is universal! In *Proceedings of the 7th Conference on Winter Simulation - Volume 2*, WSC '74, page 449–459. Winter Simulation Conference, 1974.

[51] Andrew Adamatzky and Jérôme Durand-Lose. *Collision-Based Computing*, pages 1949–1978. Springer Berlin Heidelberg, Berlin, Heidelberg, 2012.

[52] John H. Holland and John H. Miller. Artificial adaptive agents in economic theory. *The American Economic Review*, 81(2):365–370, 1991.

[53] J.H. Holland. *Emergence: From Chaos to Order*. Popular science / Oxford University Press. Oxford University Press, 2000.

[54] Gérard Ballot, Antoine Mandel, and Annick Vignes. Agent-based modeling and economic theory: where do we stand? *Journal of Economic Interaction and Coordination*, 10(2):199–220, October 2015.

[55] Alan Kirman. Complex economics: Individual and collective rationality. 2010.

[56] Domenico Delli Gatti, Corrado Di Guilmi, Edoardo Gaffeo, Gianfranco Giulioni, Mauro Gallegati, and Antonio Palestrini. A new approach to business fluctuations: heterogeneous interacting agents, scaling laws and financial fragility. *Journal of Economic Behavior & Organization*, 56(4):489–512, 2005.

[57] Domenico Delli Gatti, Edoardo Gaffeo, Mauro Gallegati, Gianfranco Giulioni, and Antonio Palestrini. Emergent macroeconomics: An agent-based approach to business fluctuations. *New Economic Windows*, 6, 01 2008.

[58] Herbert Dawid, Simon Gemkow, Philipp Harting, Sander van der Hoog, and Michael Neugart. The eurace@unibi model: An agent-based macroeconomic model for economic policy analysis. *SSRN Electronic Journal*, 10 2013.

[59] Marco Raberto, Andrea Teglio, and Silvano Cincotti. Debt deleveraging and business cycles. an agent-based perspective. *Economics - The Open-Access, Open-Assessment E-Journal*, 6(27):1–49, 2012.

[60] Giorgio Fagiolo and Andrea Roventini. Macroeconomic Policy in DSGE and Agent-Based Models. *Revue de l'OFCE*, 124(5):67–116, 2012.

[61] Stanislao Gualdi, Marco Tarzia, Francesco Zamponi, and Jean-Philippe Bouchaud. Tipping points in macroeconomic agent-based models. *Journal of Economic Dynamics and Control*, 50:29–61, 2015.

[62] Stanislao Gualdi, Marco Tarzia, Francesco Zamponi, and Jean-Philippe Bouchaud. Monetary policy and dark corners in a stylized agent-based model. *Journal of Economic Interaction and Coordination*, 12(3):507–537, May 2016.

[63] Dhruv Sharma, Jean-Philippe Bouchaud, Marco Tarzia, and Francesco Zamponi. Good speciation and endogenous business cycles in a constraint satisfaction macroeconomic model. *Journal of Statistical Mechanics*, 2021(6):063403, jun 2021.

[64] Dhruv Sharma, Jean-Philippe Bouchaud, Stanislao Gualdi, Marco Tarzia, and Francesco Zamponi. V-, U-, L-, or W-shaped recovery after COVID: Insights from an Agent Based Model. *PLoS ONE*, 16(3):e0247823, 2020.

[65] Sebastian Poledna, Michael Miess, and Cars Hommes. Economic forecasting with an agent-based model. *SSRN Electronic Journal*, 01 2019.

[66] Julius Bonart, Jean-Philippe Bouchaud, Augustin Landier, and David Thesmar. Instabilities in large economies: aggregate volatility without idiosyncratic shocks. *Journal of Statistical Mechanics: Theory and Experiment*, 2014(10):10040, oct 2014.

[67] Federico Guglielmo Morelli, Michael Benzaquen, Marco Tarzia, and Jean-Philippe Bouchaud. Confidence collapse in a multihousehold, self-reflexive DSGE model. *Proceedings of the National Academy of Sciences*, 117(17):9244–9249, April 2020.

[68] Igor Linkov, Benjamin D. Trump, and William Hynes. Resilience strategies and policies to contain systemic threats. 2019.

[69] Wiliam Hynes and Gabriela Ramos. A systemic resilience approach to dealing with covid-19 and future shocks, 2020.

[70] Henrik Salje, Cécile Tran Kiem, Noémie Lefrancq, Noémie Courtejoie, Paolo Bosetti, Juliette Paireau, Alessio Andronico, Nathanaël Hozé, Jehanne Richet, Claire-Lise Dubost, et al. Estimating the burden of sars-cov-2 in france. *Science*, 369(6500):208–211, 2020.

[71] Benjamin Faucher, Rania Assab, Jonathan Roux, Daniel Levy-Bruhl, Cécile Tran Kiem, Simon Cauchemez, Laura Zanetti, Vittoria Colizza, Pierre-Yves Boëlle, and Chiara Poletto. Agent-based modelling of reactive vaccination of workplaces and schools against covid-19. *Nature communications*, 13(1):1–11, 2022.

[72] Alessio Andronico, Cécile Tran Kiem, Juliette Paireau, Tiphanie Succo, Paolo Bosetti, Noémie Lefrancq, Mathieu Nacher, Félix Djossou, Alice Sanna, Claude Flamand, et al. Evaluating the impact of curfews and other measures on sars-cov-2 transmission in french guiana. *Nature communications*, 12(1):1–8, 2021.

[73] Enghin Atalay, Ali Hortaçsu, James Roberts, and Chad Syverson. Network structure of production. *Proceedings of the National Academy of Sciences*, 108(13):5199–5202, 2011.

[74] Andrew B. Bernard and Andreas Moxnes. Networks and trade. *Annual Review of Economics*, 10(1):65–85, 2018.

[75] Vasco M Carvalho, Makoto Nirei, Yukiko U Saito, and Alireza Tahbaz-Salehi. Supply Chain Disruptions: Evidence from the Great East Japan Earthquake. *The Quarterly Journal of Economics*, 136(2):1255–1321, 12 2020.

[76] FactSet. Factset database, 2021.

[77] Guillermo García-Pérez, Antoine Allard, M Ángeles Serrano, and Marián Boguñá. Mercator: uncovering faithful hyperbolic embeddings of complex networks. *New Journal of Physics*, 21(12):123033, 2019.

[78] K. J. Arrow, H. B. Chenery, B. S. Minhas, and R. M. Solow. Capital-labor substitution and economic efficiency. *The Review of Economics and Statistics*, 43(3):225–250, 1961.

[79] Gregory M. Gelles and Douglas W. Mitchell. Returns to scale and economies of scale: Further observations. *The Journal of Economic Education*, 27(3):259–261, 1996.

[80] Keting Shen and John Whalley. Capital-labor-energy substitution in nested ces production functions for china. Working Paper 19104, National Bureau of Economic Research, June 2013.

[81] Ragnar Frisch. A complete scheme for computing all direct and cross demand elasticities in a model with many sectors. *Econometrica*, 27(2):177–196, 1959.

[82] Fiedler, Miroslav, Ptak, and Vlastimil. On matrices with non-positive off-diagonal elements and positive principal minors. *Czechoslovak Mathematical Journal*, 12(3):382–400, 1962.

[83] David Hawkins and Herbert A. Simon. Note: Some conditions of macroeconomic stability. *Econometrica*, 17(3/4):245–248, jul 1949.

[84] Guang Zhang and Wenying Feng. On the number of positive solutions of a nonlinear algebraic system. *Linear Algebra and its Applications*, 422:404–421, 04 2007.

[85] Eugene Paul Wigner. Characteristic vectors of bordered matrices with infinite dimensions i. *Annals of Mathematics*, 62:541–545, 1955.

[86] Eugene P. Wigner. Random matrices in physics. *SIAM Review*, 9(1):1–23, jan 1967.

[87] Pierre Bizeul, Maxime Clenet, and Jamal Najim. Positive solutions for large random linear systems. *ICASSP 2020 - 2020 IEEE International Conference on Acoustics, Speech and Signal Processing (ICASSP)*, pages 8777–8781, 2020.

[88] Claudio Castellano and Romualdo Pastor-Satorras. Relating topological determinants of complex networks to their spectral properties: Structural and dynamical effects. *Phys. Rev. X*, 7:041024, Oct 2017.

[89] A. W. Phillips. The Relation Between Unemployment and the Rate of Change of Money Wage Rates in the United Kingdom, 1861–1957. *Economica*, 25(100):283–299, November 1958.

[90] Daniel Kahneman and Amos Tversky. On the psychology of prediction. *Psychological Review*, 80(4):237–251, 1973.

[91] Amos Tversky and Daniel Kahneman. Judgment under uncertainty: Heuristics and biases. In *Handbook of the Fundamentals of Financial Decision Making*, chapter 15, pages 261–268. Leonard C. MacLean and William T. Ziemba, 1974.

[92] E. Hairer, S.P. Nørsett, and G. Wanner. Solving Ordinary Differential Equations II: Stiff and Differential-algebraic Problems. Springer, 1993.

[93] Giulio Biroli, Guy Bunin, and Chiara Cammarota. Marginally stable equilibria in critical ecosystems. *New Journal of Physics*, 20(8):83051, aug 2018.

[94] Felix Roy, Matthieu Barbier, Giulio Biroli, and Guy Bunin. Complex interactions can create persistent fluctuations in high-diversity ecosystems. *PLOS Computational Biology*, 16(5):e1007827, May 2020.

[95] Pol Antràs, Davin Chor, Thibault Fally, and Russell Hillberry. Measuring the upstreamness of production and trade flows. *American Economic Review*, 102(3):412–416, May 2012.

[96] R. S. MacKay, S. Johnson, and B. Sansom. How directed is a directed network? *Royal Society Open Science*, 7(9):201138, September 2020.

[97] Brendan D McKay. The expected eigenvalue distribution of a large regular graph. *Linear Algebra and its Applications*, 40:203–216, 1981.

[98] Robert M. May. Will a large complex system be stable? *Nature*, 238(5364):413–414, aug 1972.

[99] Yan V. Fyodorov and Boris A. Khoruzhenko. Nonlinear analogue of the may-wigner instability transition. *Proceedings of the National Academy of Sciences*, 113(25):6827–6832, Jun 2016.

[100] Guy Bunin. Ecological communities with lotka-volterra dynamics. *Physical review. E*, 95(4-1):042414, April 2017.

[101] I. Neri and F. L. Metz. Spectra of sparse non-hermitian random matrices: An analytical solution. *Phys. Rev. Lett.*, 109(3):030602, Jul 2012.

[102] Wojciech Tarnowski, Izaak Neri, and Pierpaolo Vivo. Universal transient behavior in large dynamical systems on networks. *Phys. Rev. Research*, 2(2):023333, Jun 2020.

[103] Andrea Marcello Mambuca, Chiara Cammarota, and Izaak Neri. Dynamical systems on large networks with predator-prey interactions are stable and exhibit oscillations. *arXiv:2009.11211 [cond-mat.stat-mech]*, 2020.

[104] K Avrachenkov, J Filar, and P Howlett. *Analytic Perturbation Theory and Its Applications*. Society for Industrial and Applied Mathematics, Philadelphia, PA, 2013.

[105] H Baumgärtel. *Analytic perturbation theory for matrices and operators*. Operator theory. Birkhäuser Verlag, 1985.

[106] H. Sompolinsky, A. Crisanti, and H. J. Sommers. Chaos in random neural networks. *Phys. Rev. Lett.*, 61:259–262, Jul 1988.

[107] Gérard Ben Arous, Amir Dembo, and Alice Guionnet. Cugliandolo-kurchan equations for dynamics of spin-glasses. *Probability theory and related fields*, 136(4):619–660, 2006.

[108] Felix Roy. *Dynamics of populations in large ecosystems.* Theses, Université Paris-Saclay, December 2020.

[109] Tobias Galla. Dynamically evolved community size and stability of random lotka-volterra ecosystems (a). *EPL (Europhysics Letters)*, 123(4):48004, 2018.

[110] Silvia Bartolucci, Fabio Caccioli, Francesco Caravelli, and Pierpaolo Vivo. Inversion-free leontief inverse: statistical regularities in input-output analysis from partial information. 2020.

[111] David Rezza Baqaee and Emmanuel Farhi. The macroeconomic impact of microeconomic shocks: Beyond hulten's theorem. *Econometrica*, 87(4):1155–1203, 2019.

[112] Jordi Galí. *Monetary policy, inflation, and the business cycle: an introduction to the new Keynesian framework and its applications.* Princeton University Press, Princeton, 2015.

[113] Vincent D Blondel and John N Tsitsiklis. Complexity of stability and controllability of elementary hybrid systems. *Automatica*, 35(3):479–489, 1999.

[114] M.K. Camlibel, W.P.M.H. Heemels, and J.M. Schumacher. A full characterization of stabilizability of bimodal piecewise linear systems with scalar inputs. *Automatica*, 44(5):1261–1267, 2008.

[115] James Vandergraft. Spectral properties of matrices which have invariant cones. *Siam Journal on Applied Mathematics*, 16:1208–1222, 1968.

[116] Olivier Blanchard. The phillips curve: Back to the '60s? *American Economic Review*, 106(5):31–34, May 2016.

[117] J. Kim and Van Hanh Vu. Generating random regular graphs. *Combinatorica*, 26(6):683–708, 12 2006.

[118] R Maria del Rio-Chanona, Penny Mealy, Anton Pichler, François Lafond, and J Doyne Farmer. Supply and demand shocks in the COVID-19 pandemic: an industry and occupation perspective. *Oxford Review of Economic Policy*, 36(Supplement_1):S94–S137, 2020.

[119] Steve Keen. From stochastics to complexity in models of economic instability. *Nonlinear Dynamics, Psychology, and Life Sciences*, 1(2):151–172, April 1997.

[120] J. Barkley Rosser. On the complexities of complex economic dynamics. *Journal of Economic Perspectives*, 13(4):169–192, December 1999.

[121] Marco Pangallo. Synchronization of endogenous business cycles. *arXiv:2002.06555 [nlin, q-fin]*, February 2020.

[122] Stanislao Gualdi, Jean-Philippe Bouchaud, Giulia Cencetti, Marco Tarzia, and Francesco Zamponi. Endogenous crisis waves: Stochastic model with synchronized collective behavior. *Phys. Rev. Lett.*, 114(8):088701, Feb 2015.

[123] Jianhua Dai, Shibiao Li, and Shengbo Peng. Analysis on causes and countermeasures of bullwhip effect. *MATEC Web of Conferences*, 100:05018, 01 2017.

[124] Alberto Cavallo and Roberto Rigobon. The billion prices project: Using online prices for measurement and research. *Journal of Economic Perspectives*, 30(2):151–78, May 2016.

[125] Jean-Philippe Bouchaud, J. Doyne Farmer, and Fabrizio Lillo. How markets slowly digest changes in supply and demand. In *Handbook of Financial Markets: Dynamics and Evolution*, chapter 2, pages 57–160. North-Holland, 2009.

[126] Jean-Philippe Bouchaud and Rama Cont. A langevin approach to stock market fluctuations and crashes. *The European Physical Journal B - Condensed Matter and Complex Systems*, 6:543–550, 1998.

[127] Domenico Delli Gatti, Saul Desiderio, Edoardo Gaffeo, Pasquale Cirillo, and Mauro Gallegati. Macroeconomics from the bottom-up. 2011.

[128] Alan J. Bray, Satya N. Majumdar, and G. Schehr. Persistence and First-Passage Properties in Non-equilibrium Systems. *Advances in Physics*, 62(3):225–361, 2013.

[129] H. Furstenberg and H. Kesten. Products of Random Matrices. *The Annals of Mathematical Statistics*, 31(2):457 – 469, 1960.

[130] Satya N. Majumdar, Clément Sire, Alan J. Bray, and Stephen J. Cornell. Nontrivial exponent for simple diffusion. *Phys. Rev. Lett.*, 77:2867–2870, Sep 1996.

[131] Mihail Poplavskyi and Grégory Schehr. Exact persistence exponent for the $2d$-diffusion equation and related kac polynomials. *Phys. Rev. Lett.*, 121:150601, Oct 2018.

[132] T. J. Newman and Z. Toroczkai. Diffusive persistence and the "sign-time" distribution. *Phys. Rev. E*, 58:R2685–R2688, Sep 1998.

[133] T. J. Newman and Will Loinaz. Critical dimensions of the diffusion equation. *Phys. Rev. Lett.*, 86:2712–2715, Mar 2001.

[134] G. F. Newell and M. Rosenblatt. Zero Crossing Probabilities for Gaussian Stationary Processes. *The Annals of Mathematical Statistics*, 33(4):1306 – 1313, 1962.

[135] Marc Potters and Jean-Philippe Bouchaud. *A First Course in Random Matrix Theory: for Physicists, Engineers and Data Scientists*. Cambridge University Press, 2020.

[136] A. Crisanti, G. Paladin, and A. Vulpiani. *Products of Random Matrices: in Statistical Physics*. Springer Series in Solid-State Sciences. Springer Berlin Heidelberg, 2012.

[137] Gabriel Tucci. Asymptotic Products of Independent Gaussian Random Matrices with Correlated Entries. *Electronic Communications in Probability*, 16(none):353 – 364, 2011.

[138] Bernard Derrida, Vincent Hakim, and Reuven Zeitak. Persistent spins in the linear diffusion approximation of phase ordering and zeros of stationary gaussian processes. *Phys. Rev. Lett.*, 77:2871–2874, Sep 1996.

[139] Jacob Korevaar. *Wiener's Theory*, pages 65–115. Springer Berlin Heidelberg, Berlin, Heidelberg, 2004.

[140] John Lamperti. An occupation time theorem for a class of stochastic processes. *Transactions of the American Mathematical Society*, 88(2):380–387, 1958.

[141] C Godrèche and JM Luck. Statistics of the occupation time of renewal processes. *Journal of Statistical Physics*, 104(3):489–524, 2001.

[142] Craig A. Tracy and Harold Widom. Level spacing distributions and the Airy kernel. *Commun. Math. Phys.*, 159:151–174, 1994.

[143] Grégory Schehr and Satya N. Majumdar. Statistics of the number of zero crossings: From random polynomials to the diffusion equation. *Phys. Rev. Lett.*, 99:060603, Aug 2007.

[144] Jinho Baik, Gérard Ben Arous, and Sandrine Péché. Phase transition of the largest eigenvalue for nonnull complex sample covariance matrices. *The Annals of Probability*, 33(5):1643 – 1697, 2005.

[145] Paul Levy. Processus semi-markoviens. In *Proceedings of the International Congress of Mathematicians, 1954, Amsterdam, vol. III*, pages 416–426. Erven P. Noordhoff N. V., Groningen; North-Holland Publishing Co., Amsterdam, 1956.

[146] William Feller. Fluctuation theory of recurrent events. *Trans. Amer. Math. Soc.*, 67:98–119, 1949.

[147] Jim Pitman and Marc Yor. Arcsine laws and interval partitions derived from a stable subordinator. *Proc. London Math. Soc. (3)*, 65(2):326–356, 1992.

[148] M. Kac. On distributions of certain Wiener functionals. *Trans. Amer. Math. Soc.*, 65:1–13, 1949.

[149] D. A. Darling and M. Kac. On occupation times for Markoff processes. *Trans. Amer. Math. Soc.*, 84:444–458, 1957.

[150] John Lamperti. An occupation time theorem for a class of stochastic processes. *Trans. Amer. Math. Soc.*, 88:380–387, 1958.

[151] L. Takács. On a sojourn time problem in the theory of stochastic processes. *Trans. Amer. Math. Soc.*, 93:531–540, 1959.

[152] Harry Kesten. Occupation times for Markov and semi-Markov chains. *Trans. Amer. Math. Soc.*, 103:82–112, 1962.

[153] Jim Pitman. Random weighted averages, partition structures and generalized arcsine laws. *arXiv: Probability*, 2018.

[154] Lancelot F. James. Lamperti-type laws. *Ann. Appl. Probab.*, 20(4):1303–1340, 2010.

[155] Maria Marcos-Martin, Daniel A. Beysens, Jean-Philippe Bouchaud, Claude Godrèche, and I. Yekutieli. Self-diffusion and 'visited' surface in the droplet condensation problem (breath figures). *Physica A-statistical Mechanics and Its Applications*, 214:396–412, 1995.

[156] B. Derrida, A. J. Bray, and C. Godrèche. Nontrivial exponents in the zero temperature dynamics of the 1D Ising and Potts models. *J. Phys. A*, 27(11):L357–L361, 1994.

[157] Alan J. Bray, Bernard Derrida, and Claude Godrèche. Non-trivial algebraic decay in a soluble model of coarsening. *EPL*, 27:175–180, 1994.

[158] Majumdar, Sire, Bray, and Cornell. Nontrivial exponent for simple diffusion. *Physical review letters*, 77 14:2867–2870, 1996.

[159] Derrida, Hakim, and Zeitak. Persistent spins in the linear diffusion approximation of phase ordering and zeros of stationary gaussian processes. *Physical review letters*, 77 14:2871–2874, 1996.

[160] I. Dornic and C. Godrèche. Large deviations and nontrivial exponents in coarsening systems. *J. Phys. A*, 31(24):5413–5429, 1998.

[161] Timothy J. Newman and Zoltán Toroczkai. Diffusive persistence and the "sign-time" distribution. *Physical Review E*, 58, 1998.

[162] J.-M. Drouffe and Claude Godrèche. Stationary definition of persistence for finite-temperature phase ordering. *Journal of Physics A*, 31:9801–9807, 1998.

[163] Andrea Baldassarri, Jean-Philippe Bouchaud, Ivan Dornic, and Claude Godrèche. Statistics of persistent events: An exactly soluble model. *Physical Review E*, 59, 1999.

[164] Zoltán Toroczkai, Timothy J. Newman, and Sankar Das Sarma. Sign-time distributions for interface growth. *Physical review. E, Statistical physics, plasmas, fluids, and related interdisciplinary topics*, 60 2 Pt A:R1115–8, 1999.

[165] J.-M. Drouffe and Claude Godrèche. Temporal correlations and persistence in the kinetic ising model: the role of temperature. *The European Physical Journal B - Condensed Matter and Complex Systems*, 20:281–288, 2001.

[166] J. Theodore Cox and David Griffeath. Occupation time limit theorems for the voter model. *Ann. Probab.*, 11(4):876–893, 1983.

[167] J. Theodore Cox and David Griffeath. Large deviations for some infinite particle system occupation times. In *Particle systems, random media and large deviations (Brunswick, Maine, 1984)*, volume 41 of *Contemp. Math.*, pages 43–54. Amer. Math. Soc., Providence, RI, 1985.

[168] J. Theodore Cox and David Griffeath. Diffusive clustering in the two-dimensional voter model. *Ann. Probab.*, 14(2):347–370, 1986.

[169] Maury Bramson, J. Theodore Cox, and David Griffeath. Occupation time large deviations of the voter model. *Probab. Theory Related Fields*, 77(3):401–413, 1988.

[170] J. T. Cox. Some limit theorems for voter model occupation times. *Ann. Probab.*, 16(4):1559–1569, 1988.

[171] G. Maillard and T. Mountford. Large deviations for voter model occupation times in two dimensions. *Ann. Inst. Henri Poincaré Probab. Stat.*, 45(2):577–588, 2009.

[172] M. Bauer, C. Godrèche, and J. M. Luck. Statistics of persistent events in the binomial random walk: will the drunken sailor hit the sober man? *J. Statist. Phys.*, 96(5-6):963–1019, 1999.

[173] Abhishek Dhar and Satya N. Majumdar. Residence time distribution for a class of Gaussian Markov processes. *Phys. Rev. E (3)*, 59(6):6413–6418, 1999.

[174] G. De Smedt, C. Godrèche, and J. M. Luck. Statistics of the occupation time for a class of Gaussian Markov processes. *J. Phys. A*, 34(7):1247–1269, 2001.

[175] C. Godrèche and J. M. Luck. Statistics of the occupation time of renewal processes. *J. Statist. Phys.*, 104(3-4):489–524, 2001.

[176] C. Godrèche and J. M. Luck. Statistics of the occupation time for a random walk in the presence of a moving boundary. *J. Phys. A*, 34(36):7153–7161, 2001.

[177] Satya N. Majumdar and Alan J. Bray. Large-deviation functions for nonlinear functionals of a Gaussian stationary Markov process. *Phys. Rev. E (3)*, 65(5):051112, 8, 2002.

[178] Golan Bel and Eli Barkai. Occupation times and ergodicity breaking in biased continuous time random walks. *Journal of Physics: Condensed Matter*, 17, 2005.

[179] Florian Angeletti and Hugo Touchette. Diffusions conditioned on occupation measures. *J. Math. Phys.*, 57(2):023303, 16, 2016.

[180] Claude Godrèche. Two-time correlation and occupation time for the brownian bridge and tied-down renewal processes. *Journal of Statistical Mechanics: Theory and Experiment*, 2017:073205, 2017.

[181] Paul C. Bressloff. Stochastically gated local and occupation times of a brownian particle. *Physical review. E*, 95 1-1:012130, 2017.

[182] Theodore W. Burkhardt. Occupation time of a randomly accelerated particle on the positive half axis: results for the first five moments. *J. Stat. Phys.*, 169(4):730–743, 2017.

[183] Wanli Wang, Johannes H. P. Schulz, Weihua Deng, and Eli Barkai. Renewal theory with fat-tailed distributed sojourn times: Typical versus rare. *Physical Review E*, 2018.

[184] Mattia Radice, Manuele Onofri, Roberto Artuso, and Gaia Pozzoli. Statistics of occupation times and connection to local properties of nonhomogeneous random walks. *Phys. Rev. E*, 101(4):042103, 14, 2020.

[185] Adi Rebenshtok and Eli Barkai. Distribution of time-averaged observables for weak ergodicity breaking. *Physical review letters*, 99 21:210601, 2007.

[186] A. Rebenshtok and E. Barkai. Weakly non-ergodic statistical physics. *J. Stat. Phys.*, 133(3):565–586, 2008.

[187] Martin Barlow, Jim Pitman, and Marc Yor. Une extension multidimensionnelle de la loi de l'arc sinus. In *Séminaire de Probabilités, XXIII*, volume 1372 of *Lecture Notes in Math.*, pages 294–314. Springer, Berlin, 1989.

[188] D. R. Cox. *Renewal theory.* Methuen & Co., Ltd., London; John Wiley & Sons, Inc., New York, 1962.

[189] D. R. Cox and H. D. Miller. *The theory of stochastic processes.* John Wiley & Sons, Inc., New York, 1965.

[190] William Feller. *An introduction to probability theory and its applications. Vol. II.* John Wiley & Sons, Inc., New York-London-Sydney, second edition, 1971.

[191] Geoffrey R. Grimmett and David R. Stirzaker. *Probability and random processes.* Oxford University Press, Oxford, 2020. Fourth edition [of 0667520].

[192] W. L. Smith. Regenerative stochastic processes. *Proc. Roy. Soc. London Ser. A*, 232:6–31, 1955.

[193] Erhan Çinlar. Markov renewal theory. *Advances in Appl. Probability*, 1:123–187, 1969.

[194] Sheldon M. Ross. *Stochastic processes*. Wiley Series in Probability and Statistics: Probability and Statistics. John Wiley & Sons, Inc., New York, second edition, 1996.

[195] Jean-Philippe Bouchaud. Weak ergodicity breaking and aging in disordered systems. *Journal De Physique I*, 2:1705–1713, 1992.

[196] Nickolay Korabel and Eli Barkai. Infinite invariant density determines statistics of time averages for weak chaos. *Physical review letters*, 108 6:060604, 2012.

[197] David Vernon Widder. *The Laplace Transform*. Princeton Mathematical Series, vol. 6. Princeton University Press, Princeton, N. J., 1941.

[198] Pierre Mergny. An explicit example for the high temperature convolution: crossover between the binomial law $b(2, 1/2)$ and the arcsine law, 2022.

[199] Adam Marcus, Daniel A. Spielman, and Nikhil Srivastava. Finite free convolutions of polynomials. *Probability Theory and Related Fields*, 182:807 – 848, 2022.

[200] Pierre Mergny and Marc Potters. Rank one hciz at high temperature: interpolating between classical and free convolutions. *SciPost Physics*, 2022.

[201] Don Weingarten. Asymptotic behavior of group integrals in the limit of infinite rank. *Journal of Mathematical Physics*, 19:999–1001, 1978.

[202] Yan V. Fyodorov. On statistics of bi-orthogonal eigenvectors in real and complex ginibre ensembles: Combining partial schur decomposition with supersymmetry. *Communications in Mathematical Physics*, 363:579–603, 2018.

[203] Kartick Adhikari and Arup Bose. Brown measure and asymptotic freeness of elliptic and related matrices. *Random Matrices: Theory and Applications*, 8(02):1950007, 2019.

[204] Todd Kemp, Karl Mahlburg, Amarpreet Rattan, and Clifford Smyth. Enumeration of non-crossing pairings on bit strings. *J. Comb. Theory Ser. A*, 118(1):129–151, jan 2011.

[205] Georgia Benkart and Dongho Moon. *Tensor product representations of Temperley-Lieb algebras and Chebyshev polynomials*, pages 57–80. Rhode Island: American Mathematical Society, 2005.

[206] Martin Aigner. Catalan-like numbers and determinants. *Journal of Combinatorial Theory, Series A*, 87(1):33–51, 1999.

[207] Todd Kemp, Karl Mahlburg, Amarpreet Rattan, and Clifford Smyth. Enumeration of non-crossing pairings on bit strings. *Journal of Combinatorial Theory, Series A*, 118(1):129–151, 2011.

[208] L Carlitz. Sequences, paths, ballot numbers. *Fibonacci Quart*, 10(5):531–549, 1972.

ECOLE
DOCTORALE

Titre : Grandes fluctuations macroeconomiques: criticalité auto-organisée dans les réseaux d'entreprise, modèles basés agents et matrices aléatoires

Mots clés : fluctuations economiques, criticalité auto-organisée, modèles basés agents, systèmes dynamiques, matrices alétoires

Résumé : Quelle est l'origine des fluctuations macroéconomiques ? À la fin du xx^{e}siècle, Ben Bernanke introduisait pour la première fois ce qu'il appela le puzzle des "small shocks, large business cycles" faisant référence à l'apparente incompatibilité entre les petites fluctuations observées aux niveaux granulaires de l'économie ("small shocks") et les larges fluctuations macroéconomiques ("large business cycles"). Par exemple, le PIB des États-Unis montre un taux moyen de croissance annuelle stable autour de 3% mais présente des fluctuations atteignant 2.7%. L'énigme réside dans le fait que la plupart de cette volatilité en excès ne peut être liée à des crises *exogènes* connues, comme les chocs pétroliers ou la crise financière de 2008, et doit donc être d'origine *endogène*, c'est-à-dire générée par l'économie elle-même. De nombreuses explications ont vu le jour, les plus connues impliquant la distribution en loi de puissance des tailles d'entreprises qui se répercuterait aux niveaux agrégés de l'économie, ou bien des effets de réseaux responsables de l'amplification des chocs microscopiques. En revanche, ces explications reposent sur de modèles économiques à l'équilibre représentant le monde comme une succession d'états équilibrés atteints instantanément et sans friction, et qui, tautologiquement, ne prennent pas en compte les effets hors équilibres. Dans cette thèse, les deux premières parties sont consacrées à la recherche de mécanismes hors équilibres pouvant expliquer la volatilité en excès. La troisième partie est dédiée à l'étude plus générale des systèmes linéaires par cônes, omniprésents en économie.
Nous commençons par montrer que l'équilibre au sens économique n'existe par toujours dans les réseaux d'entreprises. Cela a plusieurs conséquences. Premièrement, comme l'équilibre n'est pas toujours bien défini, les modèles économiques devraient être principalement conçus *hors-equilibre*. Deuxièmement, proposant un modèle dynamique minimal et comportemental pour l'ajustement des prix et productions dans un contexte d'interactions inter-entreprises, nous montrons que l'économie subit un *ralentissement critique* au voisinage du point de non-existence de l'équilibre caractérisé par une divergence du temps de relaxation et une accumulation des chocs dans le réseau générant naturellement de la volatilité en excès. Troisièmement, nous argumentons, dans le même esprit que Bak et al., que les économies actuelles sont proches du point de non-existence de l'équilibre à cause du phénomène dit de *criticalité auto-organisée*.
Dans la deuxième partie, nous nous éloignons du modèle minimal et proposons un modèle basé agents pleinement cohérent prenant en considération des éléments économiques plus réalistes. Nous montrons que la multitude de boucles de rétroactions, engendrées par les interactions entre entreprises, génère des oscillations endogènes pour des valeurs économiquement cohérentes des paramètres gouvernant le modèle, donnant alors une autre piste pour expliquer la volatilité en excès. En outre, une étude analytique du modèle révèle que la dynamique reste non triviale au niveau linéaire : la dépendance linéaire des entrées et sorties économiques peut elle-même varier en fonction de la forme des entrées. Ces systèmes, appelés linéaires par cônes, génèrent aisément, même dans les cas les plus simples, des paternes de crises ainsi que des oscillations et sont omniprésents en économie.
Cela mène naturellement à la dernière partie de cette thèse où nous nous intéressons aux propriétés de stabilité de ces systèmes dans un contexte plus général de matrices aléatoires. Nous montrons que les systèmes linéaires par cônes peuvent exhiber des propriétés hautement non triviales comme l'absence de concentration de la mesure de l'exposant de Lyapunov maximum qui gouverne la stabilité du système.

Title : Large macroeconomic fluctuations: self-organized criticality in firm networks, Agent Based Models and random matrices

Keywords : economic fluctuations, self-organized criticality, agent based models, dynamical systems, random matrices

Abstract : What is the origin of macroeconomic fluctuations ? In the late XXth century, Ben Bernanke first introduced the so-called "small shocks, large business cycles" puzzle as the seeming incompatibility between small fluctuations observed at granular levels of the economy (small shocks) and large macroeconomic fluctuations (large business cycles). As an example, the Unites States' GDP displays a steady average yearly growth rate of around 3% but with fluctuations reaching 2.7%. The conundrum is that most of this volatility cannot be linked to known *exogeneous* crises, such as oil shocks or the 2008 financial crisis, and must therefore be of *endogeneous* origin, i.e. generated by the economy itself. Numerous explanations have come to light, the most famous of which involve the power-law distribution of firms' sizes rippling out at aggregate levels of the economy or network effects responsible for amplifying micro-level shocks. However, these explanations rely on equilibrium-only economic models which picture the world as a succession of equilibria instantaneously reached without friction, and which tautologically do not account for out-of-equilibrium effects. In this thesis, the first two parts are devoted to finding mechanisms accounting for the excess volatility through those overlooked out-of-equilibrium effects. The third part is dedicated to studying more general properties of so-called conewise linear systems, which are ubiquitous in economics.
We start by showing that, in firm networks, economic equilibrium does not always exist. This has several consequences. First, since equilibrium can be ill-defined, economic models should be chiefly devised *out-of-equilibrium*. Second, upon proposing a minimal behavioral dynamical model of prices and productions' adjustment with inter-firms interactions, we show that at the onset of equilibrium non-existence, the economy experiences a *critical slowdown* where the relaxation time diverges and shocks start accumulating in the network, naturally generating excess volatility. Third, in the same spirit as Bak et al., we argue that economies generically sits close to the non-existence point through a phenomenon called *self-organized criticality*.
In the second part, we depart from the first minimal model and devise a fully consistent Agent Based Model by factoring in some more realistic economic features. We show that, because of the multiple feedbacks introduced by the interactions between firms, our model is able to generate sustained endogenous business cycles for economically sound values of the parameters governing the model, giving yet another avenue for explaining excess volatility at aggregate levels. Furthemore, an analytical study of the model reveals a non-trivial dynamics even at linear level : the linear dependency between economic inputs and outputs can vary depending on the inputs themselves. Such systems, called conewise linear, can easily generate crises-like patterns and oscillations even in the simplest cases and naturally come to play in economics.
This naturally leads to the last part of this thesis, where we investigate more general stability properties of conewise linear systems in a random matrix theory setting. We show that such system can exhibit highly non-trivial properties, such as the non-self-averaging of the maximal Lyapunov exponent governing the system's stability.

Institut Polytechnique de Paris
91120 Palaiseau, France